

BIOMECHANICAL MODEL OF THE SHOULDER JOINT

This thesis is presented in partial fulfilment of the requirements for the degree of Doctor of Philosophy from the Bioengineering Unit, University of Strathclyde, Glasgow

by

R. John Runciman M.Sc., P.Eng.

September, 1993

Copyright © 1993

Declaration of Author's Rights

The copyright of this belongs to the author under the terms of the United Kingdom Copyright Acts as qualified by University of Strathclyde Regulation 3.49. Due Acknowledgement must always be made of the use of any material contained in, or derived from, this thesis.

ACKNOWLEDGEMENTS

With a project of this magnitude and duration, it is understandable that a large number of people have had a hand in bringing it to a successful conclusion. Some of these people have been directly involved in the work presented in this thesis while others have simply played a part in my adjustment to, and life in Scotland over the last three years.

Nearly five years ago a Canadian student sent a simple letter of request off to a bioengineering department at a Scottish university. To my surprise, I received a warm and detailed response to my enquiry. The letter that I received was from Professor J.P. Paul, and to him I owe a great debt. Without the personal attention that I received to those early enquiries, and in the intervening years, I would certainly not be where I am today.

Dr. A.C. Nicol has played a vital role in both this project and my life here in Scotland. Always interested to discuss a problem or point of view, this project would undoubtedly have followed a much rougher road without his input. Calling upon his years of experience and inter-departmental connections, Sandy has been able to call upon the assistance of other individuals who were ideally suited to whatever task was at hand.

Outside the Bioengineering Unit, Dr. Shaw Dunn at the University of Glasgow and Dr. Garth Johnson at the University of Newcastle upon Tyne have both made vital contributions to this project. Dr. Shaw Dunn taught me the basics of anatomy that were so essential to this project. Dr. Garth Johnson, conducting his own research into shoulder biomechanics, freely shared his research data and knowledge.

To verify the model developed in this thesis an electromyographic analysis of muscle activation was required. Facilities and expertise, unavailable at Strathclyde were found at the Karolinska Institute, Stockholm Sweden. It was there that Dr Gunnar Németh and Professor Ian Goldie gave freely of their valuable time, expertise and resources to ensure that my work at their institution was a success and my time in Sweden enjoyable.

Volunteers are an essential part of many research projects. Eight individuals participated as experimental subjects in this project. Duncan Rand who participated in some of the early experimental sessions, was always willing and eager to assist in the development of the experimental protocol. Pei Lai Cheng and John Watson were also subjects in these early sessions. A special thanks has to be given to John Maclean, William Tierney, Euan Cameron and Shaun Treweek who all participated in the full activity analysis. This involved several days in Stockholm, having wires put into their shoulder muscles and another day in the Bioengineering Unit's motion analysis laboratory. Other volunteers included Mike Kelly who always gave freely of his clinical and bioengineering knowledge, and Carolyn Stewart and Anna Fitzsimmons who assisted in experimental sessions on several occasions.

I also wish to mention some individuals behind the scenes, who have often gone out of their way to help me. In the machine shop, I would like to thank David Robb, Robert Hay and Steve Murray who have always put in their best effort to finish off that "last" piece I required, and also for their impromptu technical lessons that have always proved informative. In the office and upstairs, Ian Tullis, Joan Wilson, Monica McColl and Sadie Smart have always found a moment to assist me even during their busiest times.

I would also like to thank the British Council and the Commonwealth Scholarship Commission for their generous funding of my stay in Scotland and this project.

With a project that has involved as many people as this one has, there always seems to be one individual whose impact and significance overshadows all the rest. To this person who coaxed me to write letters when I would have rather been distracted and to be diligent when I had my fill, I cannot express the full depth of my gratitude. This project would certainly not have happened without you, thank you Donna.

ABSTRACT

A biomechanical model of the glenohumeral joint has been developed to investigate muscle and joint loading during real life three-dimensional activities. Based on a rigid body mechanics approach, the model incorporates algorithms to correct for curved muscle paths and bone geometry, providing realistic muscle orientation over a wide range of limb positions. An optimization routine has been incorporated, minimizing overall maximum muscle stress in the 26 individual muscle elements considered. The model utilizes anatomical muscle and bone data, subject anthropometric data, kinematics measured using a 6 camera Vicon motion analysis system and hand loading measured using a force-plate and mobile six-component strain gauged force transducer developed for this project.

Model stability and sensitivity to input data uncertainties have been investigated. Data used for this was actual subject activity data. Random uncertainties of a known statistical distribution were generated using a Monte Carlo data perturbation technique and superimposed on the subject data. No model instability or unacceptable error magnification was demonstrated in this investigation.

A study of real life three-dimensional activities has been conducted using five male subjects. Normalized, averaged muscle and joint forces were calculated for each activity.

Using the same five subjects, electromyographic (EMG) muscle activation was measured for the same five activities. Both surface and intra-muscular fine wire electrode techniques were used. Eight muscles including infraspinatus, subscapularis and supraspinatus were instrumented. The resulting EMG data was normalized and averaged for each activity.

Muscle activation appears in good agreement with published EMG and our own EMG study. Overall joint compressive and shear forces of up to 7 and 2 times body weight respectively have been calculated.

Results of the study indicate glenohumeral joint forces for athletic activities can be as high as 7 times those forces previously predicted in other studies for simple abduction and flexion.

INTRODUCTION

Arthritis, joint laxity and traumatic injury are all common causes of glenohumeral joint dysfunction. Accurate glenohumeral joint modelling could be a vital tool in the investigation of the causes and progression of these conditions, giving insight into the detailed loading and function of the various shoulder tissues.

Historically, the investigation of shoulder function has been hampered by the inherent complexity, instability and high mobility associated with the joint. To overcome these problems, two-dimensional analysis techniques, contrived loading situations and muscle grouping by function have been used to simplify past shoulder models (Inman et al, 1944, de Luca and Forrest, 1973 and Poppen and Walker, 1978). More recent attempts at modelling shoulder function have included the move to three-dimensional analysis techniques and optimization routines for solving joint indeterminacy (Karlsson and Peterson, 1992 and Van der Helm et al, 1992). Unfortunately, these models still require simplifying assumptions regarding kinematics and loading where these details, essential to the investigation of both normal and pathological joint function, are lost. The aim of this study was to develop a new shoulder model, capable of investigating inter and intra-subject normal or pathological joint function for complex real life three-dimensional activities.

This thesis is organised to take the reader through the development and results of the project. Chapter 1 covers the basics of human shoulder anatomy. Functional considerations of these anatomical shoulder structures are then presented in chapter 2. Chapter 3 reviews previous shoulder biomechanical models and also the general theoretical aspects of joint modelling. Chapter 4 details data and data acquisition required for the shoulder biomechanical model and chapter 5 details the manipulation of this data to model shoulder biomechanics. Model verification and overall project results are presented in chapter 6. Conclusions, a project perspective and prospects for future work are then presented in the final chapter.

CONTENTS

CHAPTER 1. ANATOMY OF UPPER LIMB AND SHOULDER	1
1.1. HARD TISSUES	1
1.2. SOFT TISSUES	2
1.2.1. Passive	2
1.2.2. Active	4
CHAPTER 2. FUNCTIONAL CONSIDERATIONS OF UPPER LIMB AND SHOULDER	8
2.1. DESCRIPTION OF MOTION	8
2.2. JOINT STABILITY	9
2.3. ABDUCTION	11
2.4. FLEXION	13
2.5. OTHER MOVEMENTS	14
CHAPTER 3. BIOMECHANICAL JOINT MODELLING AND RELATED TOPICS	16
3.1. JOINT MODELLING OVERVIEW	16
3.2. BODY SEGMENT KINEMATICS	17
3.2.1. Euler Angle and Floating Axis Techniques	19
3.2.2. Equivalent or Helical Screw Axis Technique	21
3.2.3. Measurement	22
3.3. EXTERNAL BODY SEGMENT AND JOINT LOADING	23
3.3.1. Contact Loading	24
3.3.2. Gravitational Loading	24
3.3.3. Inertial Loading	24
3.4. INTERNAL JOINT LOADS	25
3.4.1. Net Joint Moment	26
3.4.2. Joint Moment Generation	26
3.4.2.1 Muscle Lines of Action	27
3.4.2.2 Muscle Force	28
3.4.3. Joint Contact Forces	31
3.5. SHOULDER MODELS	31
3.6. TOWARDS A NEW SHOULDER MODEL	35

CHAPTER 4. IN PREPARATION FOR A NEW SHOULDER MODEL	36
4.1. ANATOMICAL DATA	36
4.1.1. Trunk	37
4.1.2. Clavicle	38
4.1.3. Scapula	38
4.1.4. Humerus	39
4.1.5. Ulna	39
4.1.6. Radius	40
4.2. BODY SEGMENT PARAMETERS	40
4.3. DETERMINING BODY AND SEGMENT KINEMATICS	41
4.3.1. Measurement Basics	41
4.3.2. Trunk	42
4.3.3. Clavicle	44
4.3.4. Scapula	46
4.3.5. Humerus and Forearm	48
4.4. HAND LOADING	54
4.4.1. The Force Plate	55
4.4.2. The Hand Transducer	56
4.4.2.1 Development and Design	56
4.4.2.2 Hand Loads	58
4.4.2.3 Calibration	60
CHAPTER 5. THE SHOULDER MODEL	65
5.1. MUSCLE WRAPPING	65
5.1.1. Development of a New Technique	65
5.1.1.1 The Dominant Muscle Plane	66
5.1.1.2 Anatomical Assumptions	66
5.1.2. Implementation of the New Technique	67
5.1.2.1 Humeral Head Wrapping	67
5.1.2.2 Humeral Shaft Wrapping	69
5.1.2.3 Humeral Head and Shaft Wrapping	70
5.2. JOINT MOMENTS	71
5.2.1. Moment Equilibrium	71
5.2.1.1 Moments Due to External Loading	72
5.2.1.2 Moments Due to Muscle Action	75

5.2.2. Force Equilibrium	80
5.2.2.1 Forces Due to External Loading	81
5.2.2.2 Forces Due to Muscle Action	81
5.2.2.3 Joint Contact Forces	83
5.3. OPTIMIZATION	84
6. RESULTS AND VERIFICATION	91
6.1. PRELIMINARY STUDY	91
6.1.1. Experimental Procedure	91
6.1.2. Results	92
6.1.3. Discussion	93
6.2. MODEL SENSITIVITY TO INPUT DATA	95
6.2.1. Data Perturbation	95
6.2.2. Reflective Marker Uncertainty	96
6.2.3. Hand Load Uncertainty	97
6.2.4. Subject Geometry	99
6.2.5. Anatomical Muscle Origin and Insertion Uncertainty	100
6.2.6. Combined Input Data Uncertainty	101
6.3 MODEL AND EMG ACTIVITY ANALYSIS	102
6.3.1. EMG Study Materials and Methods	103
6.3.2. Sample EMG Study Results	108
6.3.3. Activity Analysis Materials and Methods	109
6.3.4. Sample Activity Analysis Study Results	111
6.3.5. EMG and Activity Analysis Results and Discussion	111
6.3.5.1 Hand Forces	113
6.3.5.2 Abduction	115
6.3.5.3 Flexion	120
6.3.5.4 Push-up	123
6.3.5.5 Press-up	128
6.3.5.6 Chin-up	131
CHAPTER 7. SUMMARY	135
7.1. CONCLUSIONS	136
7.2. FUTURE WORK	138

REFERENCES	139
APPENDIX A	145
APPENDIX B	147
APPENDIX C	148
APPENDIX D	166
APPENDIX E	169
APPENDIX F	180
APPENDIX G	196

LIST OF ABBREVIATIONS AND SUBSCRIPTS

Abbreviations:

X, Y, Z	... right hand cartesian coordinate system axes
AC	... acromioclavicular joint reflective marker
DHND	... dorsal hand reflective marker
DI	... deltoid insertion reflective marker
ELBO	... elbow reflective marker
ELBO2	... second elbow reflective marker
IA	... scapula inferior angle reflective marker
MS	... scapula medial spine root reflective marker
MJ	... manubriosternal joint reflective marker
PX	... hand transducer X_p axis reflective marker
PY	... hand transducer Y_p axis reflective marker
PZ	... hand transducer Z_p axis reflective marker
T4	... T4 spinous process reflective marker
T12	... T12 spinous process reflective marker
VHND	... ventral hand reflective marker
XP	... xiphoid process reflective marker
[B]	... direction cosine matrix
cm	... centre of mass
cp	... centre of pressure
F	... force
Fg	... force of gravity
Ffp	... force measured by the force plate
Fh	... force applied to the hand
Fp	... force measured by the hand transducer
L	... length
La	... line of action for a muscle
M	... moment
Mfp	... moment measured by the force plate
Mh	... moment applied to the hand
Mp	... moment measured by the hand transducer

Subscripts:

-	... "with respect to"
al	... lower arm
am	... arm reflective markers
au	... upper arm
c	... clavicle
h	... humerus
hh	... humeral head
hs	... humeral shaft
ht	... humeral retrotorsion
lab	... laboratory coordinate system
r	... radius
s	... scapula
st	... static
t	... trunk
tm	... trunk reflective markers
u	... ulna

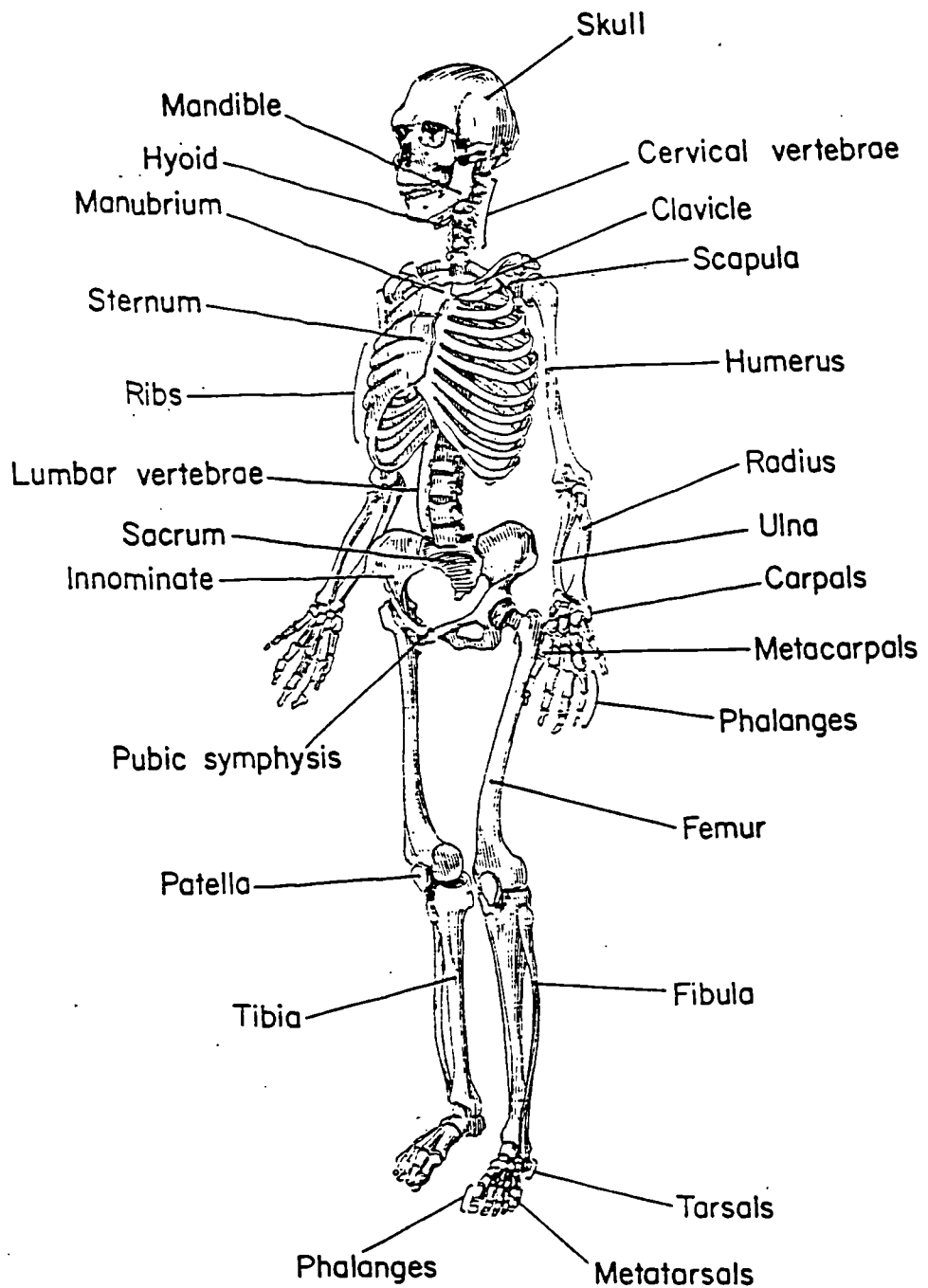


Figure 1.1 The human skeleton in anatomical position (Shipman et al, 1985).

CHAPTER 1. ANATOMY OF UPPER LIMB AND SHOULDER

The human shoulder is a highly mobile, complicated and unstable structure. Under normal conditions it is capable of transmitting large loads over a wide range of positions and directions. This versatility is the result of hard and soft tissue interaction through a series of complex integrated structures. A complete and detailed review of the upper limb and shoulder anatomy is beyond the scope of this work. It is not the aim of this chapter to give the reader a detailed anatomical description of this region as there are many standard texts devoted to this end, but a review of the main points essential to understanding this thesis.

This chapter is organized to review upper limb and shoulder anatomy in generally a proximal to distal order. Hard tissues and joints are considered first, beginning with the thorax and proceeding to forearm and hand. Soft tissues, including ligaments and muscles are reviewed in the second section of the chapter and follow the same convention.

1.1. HARD TISSUES

For this project, five bony structures must be considered; these are:

1. thorax
2. clavicle
3. scapula
4. humerus
5. forearm and hand

Although the thorax, forearm and hand structures are not directly related to the shoulder physically, they are closely linked to shoulder function and as such are included in this review.

The thorax is a collection of bones including: vertebrae, ribs, sternum and manubrium (figure 1.1). Joined together by fibrocartilaginous joints they form essentially a solid structure, although a small amount of relative motion between the bones is possible.

The clavicle is a long "S" shaped bone with articular surfaces at each end (figure 1.2). It forms the only direct link between the thorax and upper limb. Medially it articulates at the cartilaginous sternoclavicular joint, a saddle shaped joint that extends inferiorly allowing articulation with both sternum and first costal cartilage. Laterally, it is flattened superior-inferiorly, passing over the scapula to articulate with the acromion.

The scapula is a flat triangular shaped bone with articulations to the clavicle, humerus and thorax. It has two surfaces, costal and dorsal. The three angles of the bone are called inferior, superior and lateral. The adjacent borders are called the superior, medial and inferior

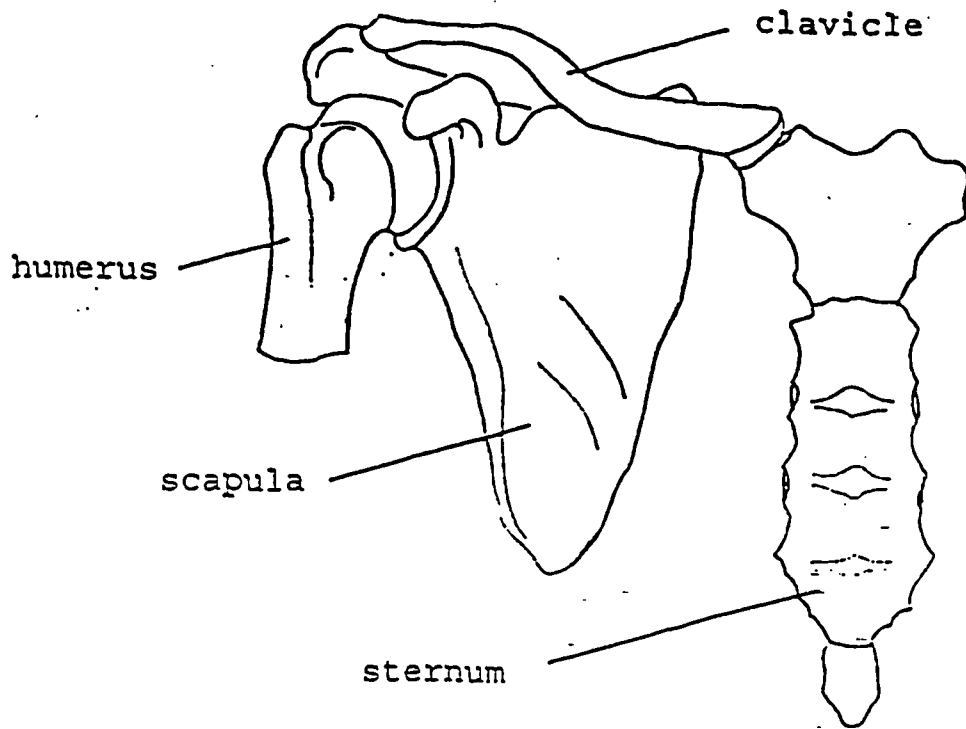


Figure 1.2 Anatomical orientation of sternum, clavicle, scapula and humerus (right side shown).

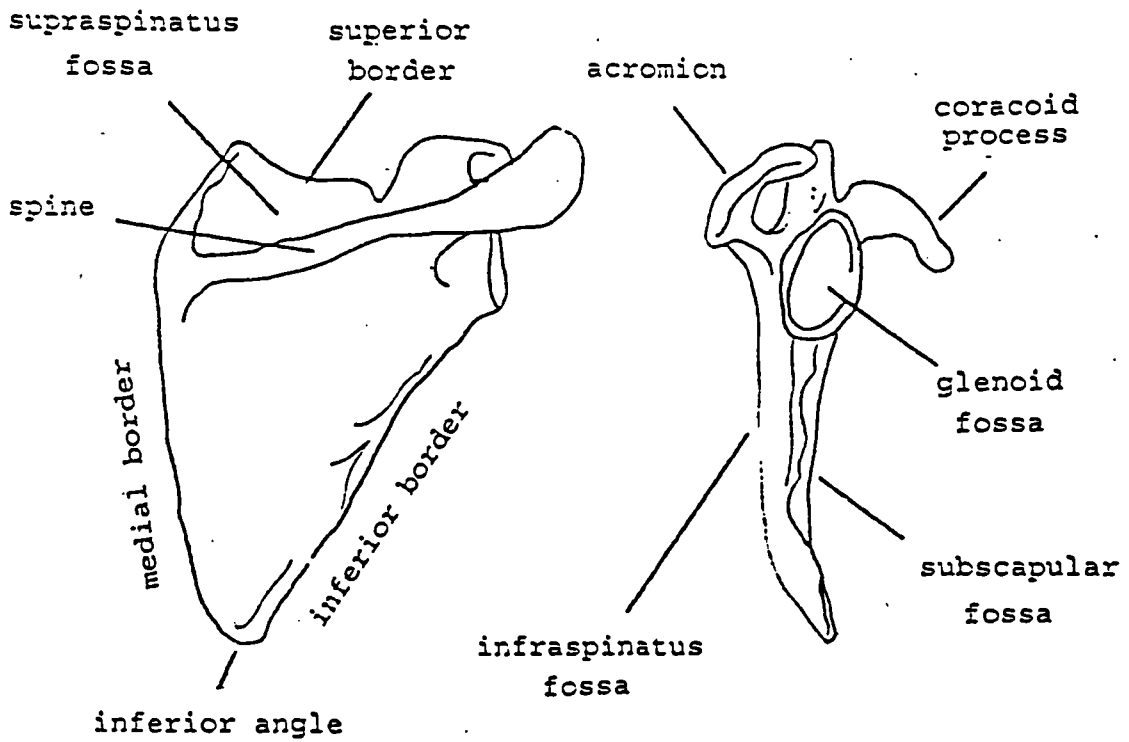


Figure 1.3 Posterior and lateral views of a right scapula.

(figure 1.3). There are three major projections on the scapula. On the dorsal surface is the scapular spine that extends laterally ending in the acromion. Here the scapula articulates with the clavicle through the cartilaginous acromioclavicular joint. At the lateral angle, an expansion forms the glenoid fossa. This shallow socket accepts the spherical humeral head, forming the ball and socket, cartilaginous glenohumeral joint. The third projection, the coracoid process extends from just medial and superior to the glenoid fossa. The third scapular articulation is at the scapulothoracic joint. Although not a true synovial joint it does allow the scapula to glide freely over the thorax.

The humerus forms the long bone of the upper arm. It articulates proximally with the glenoid fossa at the glenohumeral joint and distally, with both of the bones of the forearm at the elbow (figure 1.4). The spherical humeral head centre is offset from the humeral shaft centre line. The articular surface faces posteriorly by approximately 30-40 degrees (Brewer, 1986; Kronberg, 1989). Lateral to the articular surface are two tubercles separated by the bicipital groove. Distally, the articular surface is normally set forward of the humeral shaft centre line. The axis of articulation is skewed slightly, giving rise to the elbow carrying angle. This articular surface is divided into two regions. The trochlea forms a cylindrical cartilaginous joint with the proximal ulna. The capitulum forms a cupped cartilaginous joint with the proximal radius.

The forearm consists of two long bones, the radius and ulna. They articulate with cartilaginous joints at the humerus proximally, carpals distally and each other both proximally and distally (figure 1.5). The hand for the purposes of this work is reviewed as a single entity, joined to the forearm through the carpal articular surfaces.

1.2. SOFT TISSUES

This group can be subdivided by function into passive and active tissues. Passive tissues include: ligaments, joint capsules and fibrous cartilage. Active tissues include the muscles and their associated passive tendons.

1.2.1. Passive

Passive tissues are found at all of the joints associated with the upper limb and shoulder. For review they will be grouped with respect to their associated joint.

The sternoclavicular joint is stabilized by four ligaments and a fibrous capsule. Within the joint capsule is a fibrocartilaginous disc or meniscus that provides congruence between the joint surfaces (Kapandji, 1970).

The acromioclavicular joint is stabilized by three ligaments and a fibrous joint capsule.

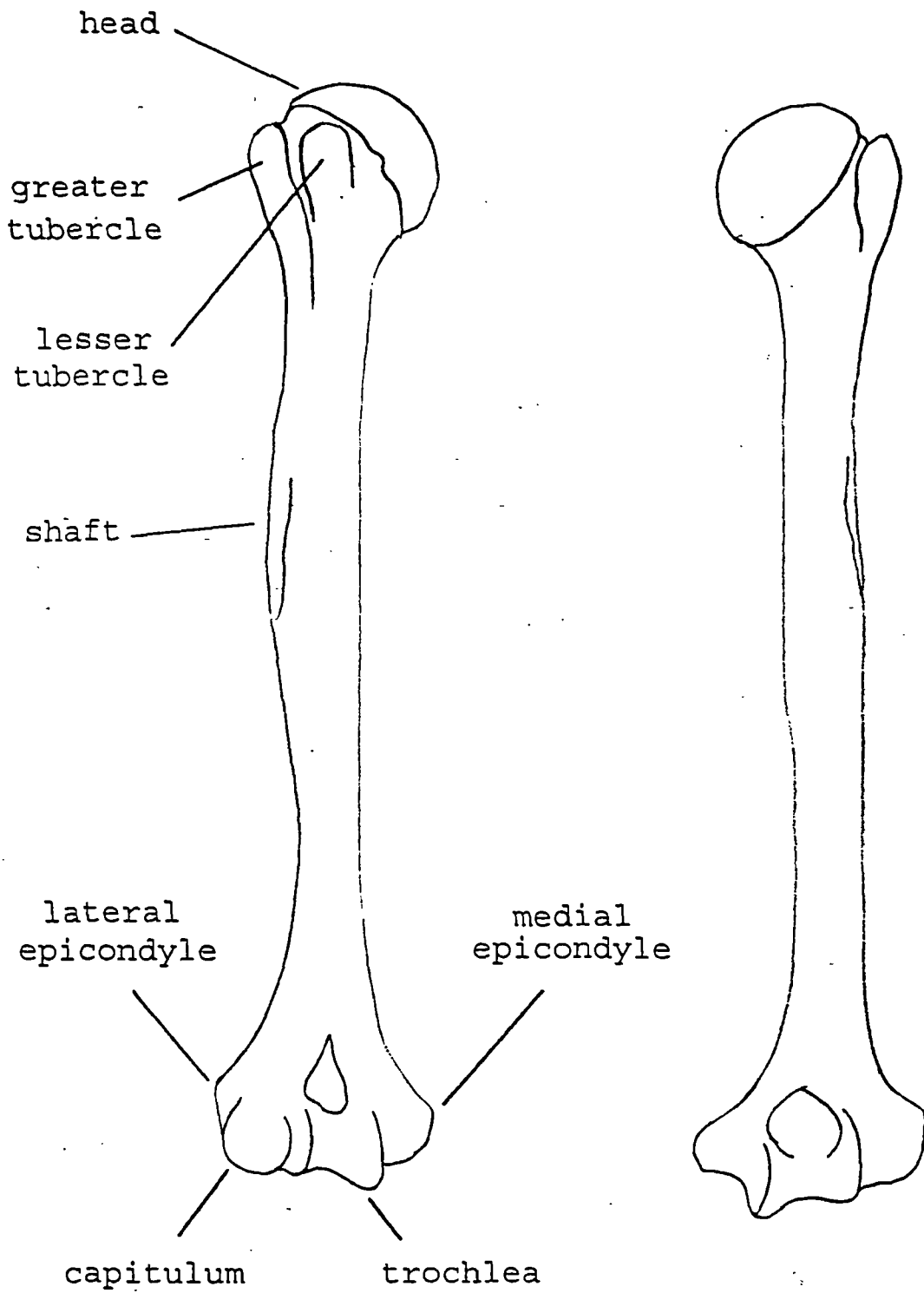


Figure 1.4 Anterior (above left) and posterior (above right) views of a right humerus.

Figure 1.5 Hard tissues of the elbow and forearm, anterior view (Luttgens & Wells, 1982).

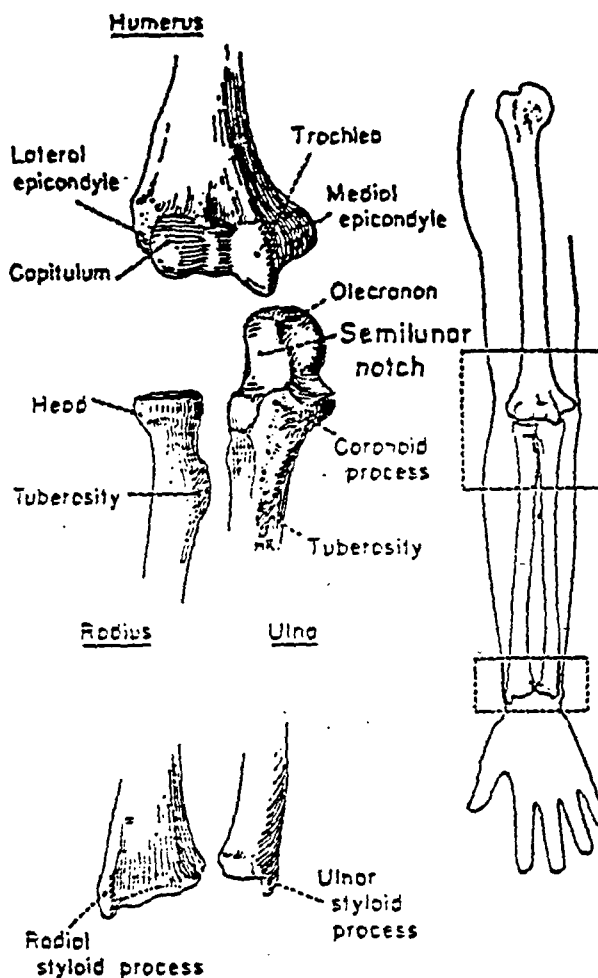


Figure 1.6 Group 1 muscles visible anteriorly (Luttgens & Wells, 1982).

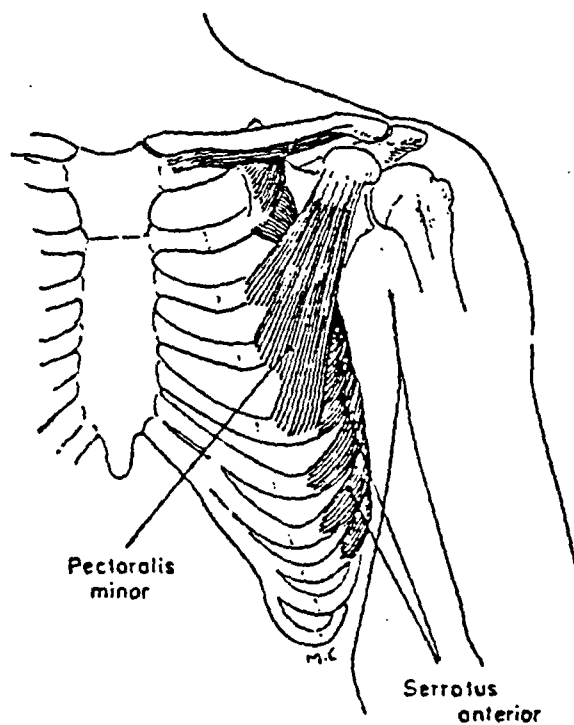


Figure 1.7 Deep Group 1 muscles visible posteriorly (Luttgens & Wells, 1982).

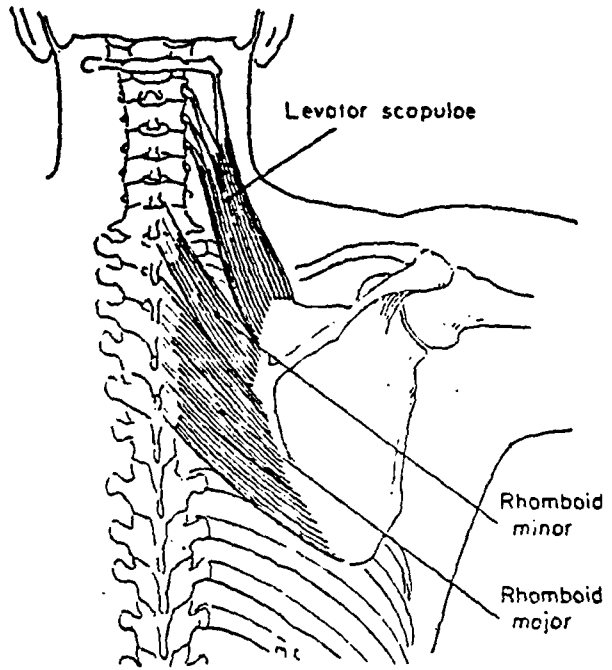
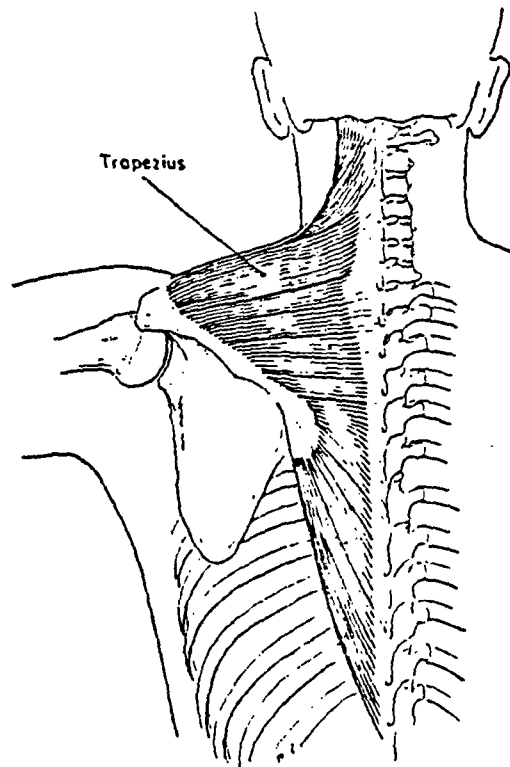


Figure 1.8 Superficial Group 1 muscles visible posteriorly (Luttgens & Wells, 1982).



Two of the ligaments, the conoid and trapezoid join the clavicle to the coracoid process. Together these two ligaments limit the relative motion possible between scapula and clavicle. The acromioclavicular ligament which passes superiorly over the joint serves to strengthen the superior joint capsule. Within the joint is a small fibrocartilaginous plate.

The scapulothoracic joint has no passive soft tissue stabilizing structures but the articular surfaces are lined with fascium.

The glenohumeral joint is stabilized by both passive and active soft tissue interaction. Passively, stabilization is achieved by a series of ligaments, fibrous joint capsule and fibrocartilaginous disc. The ligaments and joint capsule are normally lax, becoming taut when an extent of joint motion is encountered. The coracohumeral ligament, passing from the coracoid process to the greater and lesser tubercles, serves to strengthen the superior joint capsule. The glenohumeral ligament is physiologically divided into three bands: superior, running from the glenoid upper margin superiorly over the humeral head; middle, running from the glenoid upper margin to the anterior humeral head; inferior, running across the anterior glenoid margin to the inferior humeral head. This ligament serves to limit humeral abduction and external rotation with respect to the scapula. The fibrous joint capsule extends from the rim of the glenoid fossa to the rim of the humeral head articular surface. The fibrocartilaginous disc or glenoid labrum is attached around the rim of the glenoid fossa, deepening the articular surface.

The elbow is stabilized by two ligaments and a joint capsule.

1.2.2. Active

Muscles and tendons of the upper limb and shoulder can be conveniently divided into 4 groups.

1. thorax origins - scapula insertions.
2. thorax and clavicle origins - humeral insertions.
3. scapula origins - humeral insertions.
4. scapula and humeral origins - forearm insertions.

Tendons, although physiologically a passive tissue, are an intimate part of muscles functionally. As such, they are reviewed here as a single entity.

Group 1

Muscles with thorax origins and scapula insertions are all two joint muscles crossing both the sternoclavicular and acromioclavicular joints. They are primarily responsible for positioning of the clavicle and scapula on the thorax. A summary of their origins and

Figure 1.9 Posterior view of superficial shoulder muscles (Luttgens & Wells, 1982).

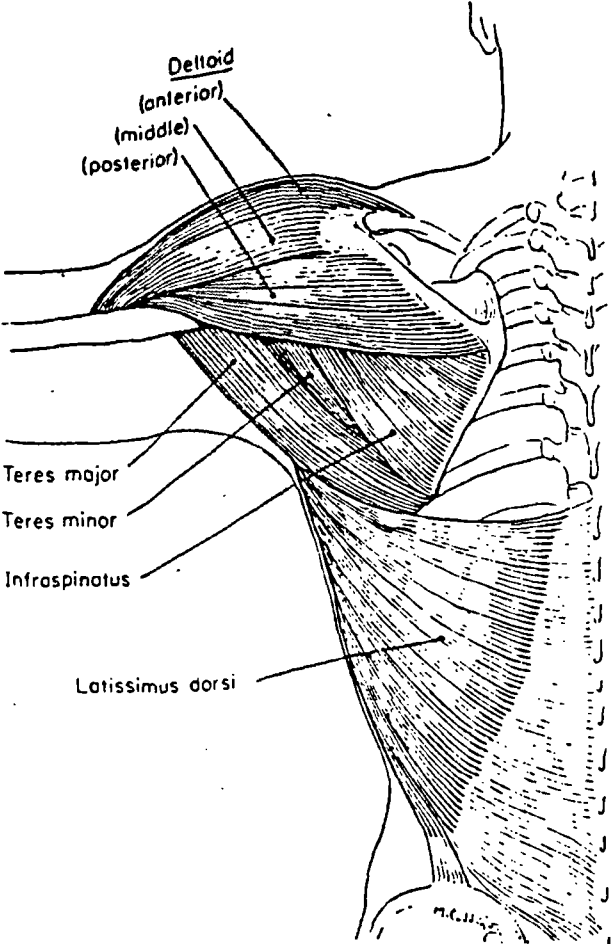
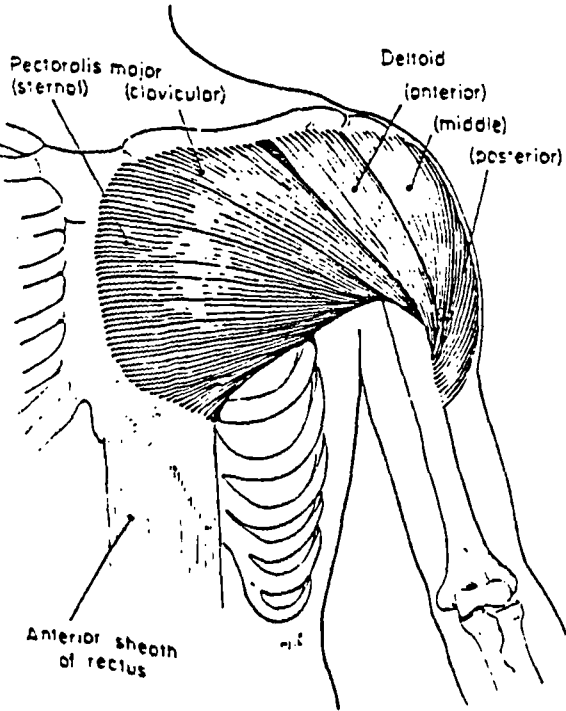


Figure 1.10 Anterior view of superficial shoulder muscles (Luttgens & Wells, 1982).



insertions is listed in table 1.1. See figures 1.6 - 1.8 for details.

Table 1.1 Group 1 muscles: thorax origins and scapular insertions

Name	Origin	Insertion
Levator scapulae	C1-C4 vertebrae	scapula medial border
Pectoralis minor	anterior thorax	coracoid process
Rhomboid major	T2-T5 vertebrae	scapula medial border
Rhomboid minor	C7-T1 vertebrae	medial end of scapular spine
Serratus anterior	ribs 1-8	medial border of costal scapula
Trapezius	C7-T12 vertebrae	lateral clavicle, acromion and scapula spine

Group 2

Muscles with thorax and clavicle origins and humeral insertions are all two and three joint muscles. All of these muscles except the sternal portion of pectoralis major cross the sternoclavicular, acromioclavicular and glenohumeral joints (figure 1.9 & 1.10). The sternal portion of pectoralis major crosses only the last two joints respectively. These muscles assist in positioning of the clavicle, scapula and humerus on the thorax. A summary of their origins and insertions is listed in table 1.2.

Table 1.2 Group 2 muscles: thorax and clavicle origins and humeral insertions

Name	Origin	Humeral Insertion
latissimus dorsi	T6-T12 vertebrae, iliac crest and lower ribs	distal to lesser tubercle
pectoralis major	clavicle and sternum	distal to greater tubercle

Group 3

Muscles with scapula origins and humeral insertions are all single joint muscles, crossing the glenohumeral joint (figure 1.11 - 1.12). Four of these muscles, including: infraspinatus, subscapularis, supraspinatus and teres minor form the rotator cuff. The rotator cuff is closely linked to overall joint stability, forming an active joint stabilizing structure. Details of the

Figure 1.11 Deep Group 3 muscles (plus triceps) visible posteriorly (Luttgens & Wells, 1982).

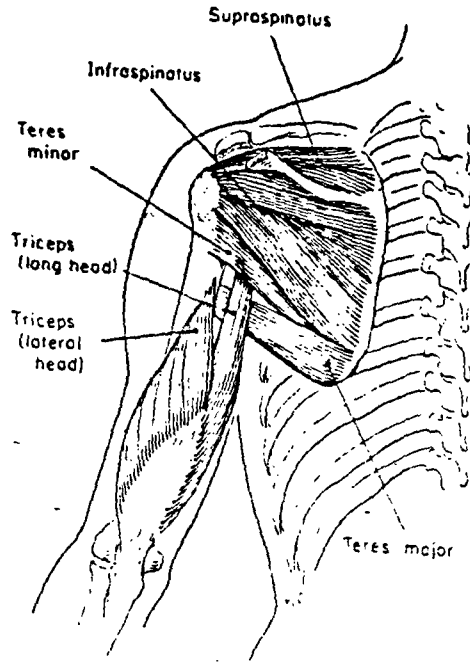
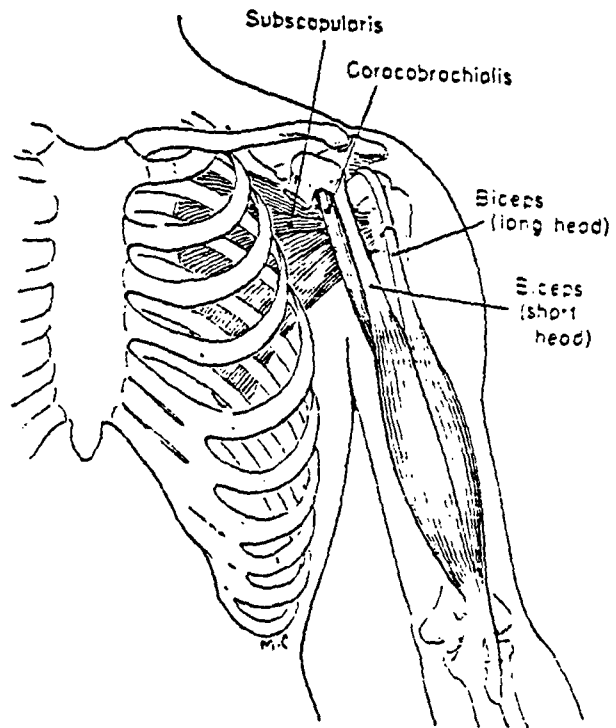


Figure 1.12 Anterior view of deep muscles including subscapularis, coracobrachialis (Group 2) and biceps (Group 4) (Luttgens & Wells, 1982).



rotator cuff in addition to the remaining muscles in this group are listed in table 1.3.

Table 1.3 Group 3 muscles: scapula origins and humeral insertions

Name	Origin	Humeral Insertion
coracobrachialis	coracoid process	distal medial humerus
deltoid	clavicle, scapula spine and acromion	deltoid tuberosity
infraspinatus	infraspinatus fossa of scapula	greater tubercle
subscapularis	subscapular fossa	lesser tubercle
supraspinatus	supraspinatus fossa	greater tubercle
teres major	dorsal aspect of scapula inferior angle	medial border of the bicipital groove
teres minor	lateral scapula border	greater tubercle

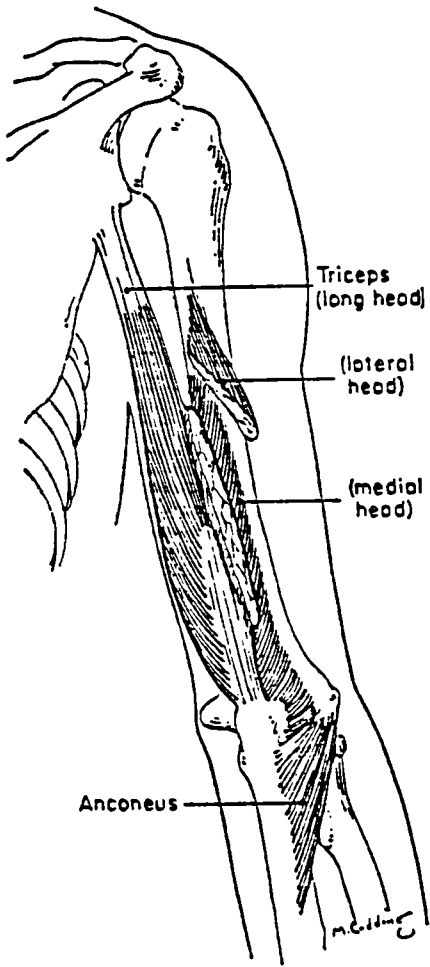
Group 4

This group contains two multi-headed muscles (figure 1.11 & 1.13). Although their prime function may be related to the elbow, they both cross the glenohumeral joint and as such are considered here. Details of these two muscles are listed in table 1.4.

Table 1.4 Group 4 muscles: scapula and humeral origins and forearm insertions

Name	Origin	Insertion
biceps brachii -long head	superior to glenoid fossa of scapula	proximal radius
-short head	coracoid process of scapula	
triceps brachii -long head	infraglenoid tubercle of scapula	olecranon process of ulna
-medial head	posterior humerus inferior to radial groove	
-lateral head	posterior humerus superior to radial groove	

Figure 1.13 Posterior view of upper arm showing the three heads of triceps (Group 4) (Luttgens & Wells, 1982).



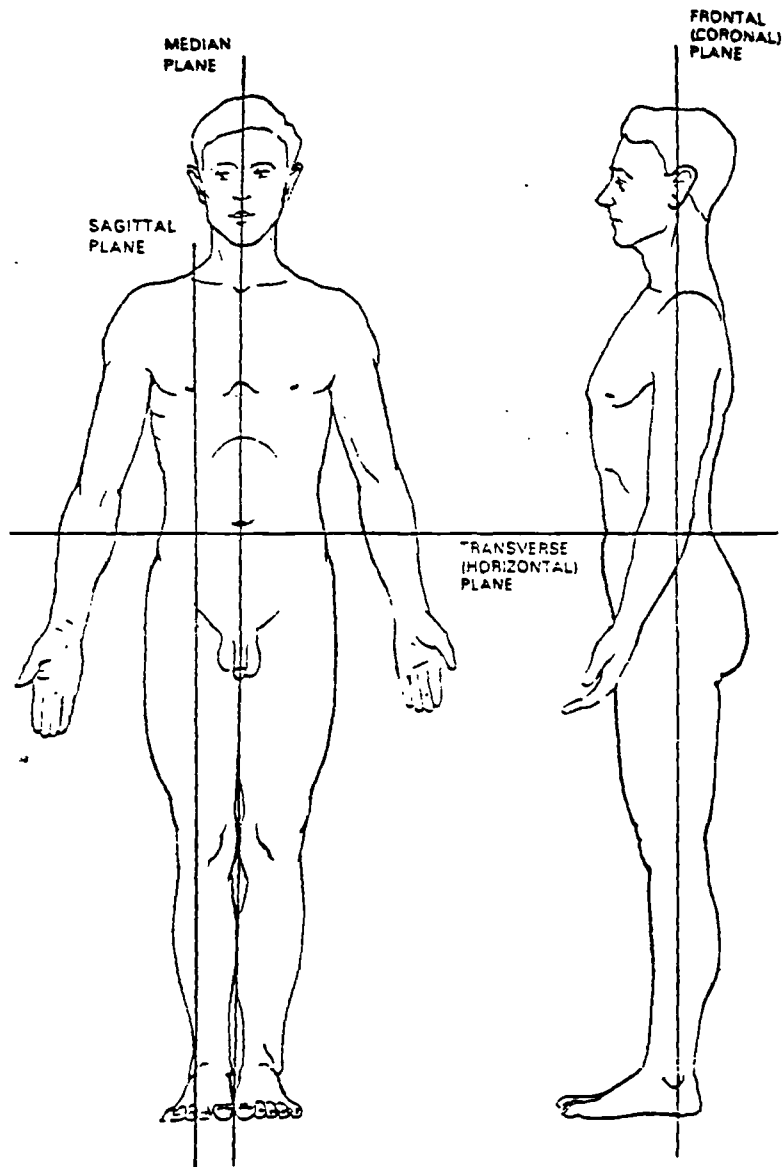


Figure 2.1 Anatomical position and planes of the human body (Zuckerman, 1988).

CHAPTER 2. FUNCTIONAL CONSIDERATIONS OF UPPER LIMB AND SHOULDER

Upper limb and shoulder function is closely linked to the anatomical configuration of the region. As a result, the study of function, in contrast to the study of lifeless static body tissues in anatomy, focuses on the functional cooperation of these living tissues. Without knowledge of this cooperation, a clear understanding of the mechanics of the region would not be possible.

This chapter is organized to review shoulder and upper limb function. The chapter begins with a review of standard terms and techniques used when describing the body and in particular the function of the shoulder and upper limb. To finish, there is a review of characteristic anatomical function for the upper limb and shoulder.

2.1. DESCRIPTION OF MOTION

The human body exists in a three-dimensional environment. Within this environment the body may assume an infinite number of postures or positions. Historically, in order to simplify the discussion of the body and its function, certain body positions and planes of reference have become standardised. This project has adopted this standard format.

A standardised base position for the body is known as the *anatomical position*. It is from this position that all movements of the body or its parts are related. In this position the subject is assumed to be standing, feet together, arms to the side with head, eyes and palms of the hands facing forwards (figure 2.1) (Zuckerman, 1988).

Three orthogonal reference planes are commonly defined for the body. These planes are used for describing the interrelationship of anatomical structures, dominant plane of motion and point of view for observation of activities (figure 2.1). The *sagittal plane* is any vertical plane cutting anterior to posterior through the body. The *frontal plane* is a vertical plane at right angles to the sagittal plane. The *transverse plane* is a horizontal plane through the body at right angles to the sagittal and frontal planes. A fourth plane named the median plane is sometimes referred to but is essentially a sagittal plane passing through the body mid-line.

The general description of upper limb and shoulder motion is linked to the orthogonal reference planes of the body. Abduction-adduction refer to the swing of the arm up and down in the frontal plane. Flexion-extension refer to the swing of the arm forward and back in the sagittal plane. This nomenclature is applicable to both the glenohumeral and elbow joints and refers to movements away from the anatomical position. Internal-external rotation

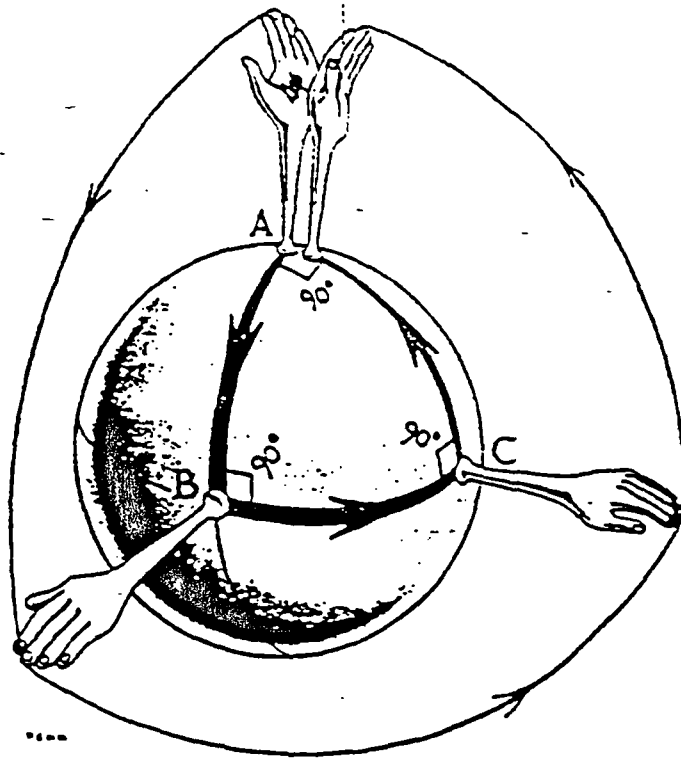


Figure 2.2 A rotation of 90 degrees is imparted to the upper limb when it makes the two cardinal displacements, AB and BC at 90 degrees to each other. Returning to the starting position, A, the rotation is evident (Sarraffian, 1983).

refers to arm rotation about its long axis. This corresponds to transverse plane rotation with the body in the anatomical position.

There are several problems associated with this system of describing joint motion in the upper limb and shoulder. Describing the motion of any structure is difficult, if that structure does not typically move in one of the planes of the body. The scapula, for example requires separate terminology to describe its movement. Combinations of individual joint motions also present problems. This usually manifests itself as a path dependency with respect to the order of joint motion description. An example of this is the axial rotation introduced into the arm when it follows two angular displacements that are at right angles to each other (see figure 2.2).

Motion of the clavicle is limited by the sternoclavicular joint and surrounding passive soft tissues. Clavicular orientation is completely described by three pairs of terms: protraction-retraction describes rotation in the transverse plane; elevation-depression describes rotation of the bone out of this plane; rotation describes orientation about its long axis. Of these descriptors, rotation is the least obvious, yet it is surprisingly large for certain arm movements. Inman et al (1944) measured rotation of the clavicle to exceed 40 degrees during large arm elevations.

The scapula unlike the clavicle is not joined directly to the thorax. Its orientation and position are determined by a combination of clavicle and humeral orientation, the shape of the posterior thorax surface and its surrounding soft tissues. As a result, scapula orientation and position are more difficult than clavicle orientation to visualize. Scapula position is directly related to clavicle orientation. For example, elevation of the clavicle results in a corresponding elevation of the scapula as is experienced when a subject shrugs their shoulders. In conjunction with this dependence, scapula orientation is affected by humeral position, soft tissues and posterior thorax surface. Scapula orientation can be described by three pairs of terms (Pronk, 1988): protraction-retraction is scapula rotation about the long axis of the body, and is closely linked to clavicular protraction-retraction; medio-lateral rotation is scapula rotation about an axis perpendicular to the dorsal scapular surface; forward-backward tipping is scapula rotation about an axis passing approximately along the scapular spine.

2.2. JOINT STABILITY

Healthy joint function presumes that stability and proper alignment of that joint is maintained. This is normally achieved through interaction of hard and soft tissues associated with a joint. Soft tissue can function to limit joint motion. In addition to this, active soft

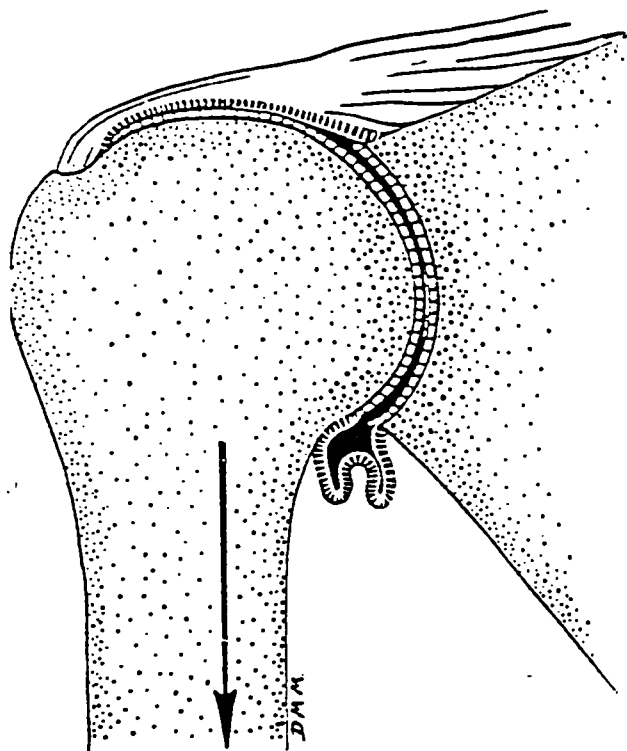


Figure 2.3 The superior part of the capsule of the glenohumeral joint and the supraspinatus tighten when the humeral head is pulled downward on the slope of the glenoid fossa (Basmajian and Bazant, 1959).

tissue function can augment joint compressive loads, thereby increasing overall joint stability. Greater joint mobility puts an increased demand on the hard and soft tissues and their ability to maintain joint stability and alignment. The shoulder being the most mobile joint of the body (Kapandji, 1970) is particularly susceptible to the problem of instability. Many authors have investigated glenohumeral instability. This instability is most commonly manifested by a humeral head excursion out of the glenoid fossa in one of three directions: anteriorly, inferiorly and least commonly posteriorly (Saha, 1971).

Basmajian & Bazant (1959) investigated the relationship between inferior instability due to arm loading and shoulder muscular activity. This study consisted of two phases: the measurement of muscular activity in 22 shoulders when the hand was loaded vertically by a hanging weight and by mechanical testing of dissected shoulders in the same anatomical position. The authors found that joint stability in this position resulted from tightening of the superior joint capsule and coracohumeral ligament, glenoid fossa orientation and activation of the supraspinatus and to a lesser extent posterior deltoid.

Active soft tissue stabilization has been investigated for abducted arm positions. With abduction, passive soft tissue is not well placed to provide the required joint stability. As a result, active soft tissues must assist in joint stability. Pande et al (1989) investigated muscle activity in four subjects suffering from posterior joint instability. Results indicated that joint instability could be induced voluntarily by the generation of muscular imbalance at the joint. Unfortunately, of the rotator cuff muscles, only infraspinatus was included in their study. Since the rotator cuff muscles appear most appropriately positioned to provide the greatest stabilizing effect, the results of their study must be approached with caution. Broström et al (1989) studied muscle activity including the full rotator cuff for four subjects with pathological joint instability. They found rotator cuff and in particular subscapularis muscle activation was closely linked to maintenance of a stable joint structure.

The contribution of hard tissue shape to joint stability has long been a focus of study. With respect to the glenohumeral joint, humeral retrotorsion and glenoid fossa orientation have been of particular interest.

Saha (1971) measured humeral retrotorsion as approximately 30 degrees in healthy subjects. He found glenoid fossa anterior-posterior tilt to be biased posteriorly in approximately 73 % of those studied with an average angle of 7.4 degrees. Anterior tilt in the remaining subjects was found to be between 2 and 10 degrees. Interestingly, Saha measured glenoid fossa tilt in 21 subjects suffering from recurrent anterior instability; 80 % were found to have anterior bias in their glenoid fossa orientation.

Cyprien et al (1983) studied joint shape of 50 normal subjects and 14 subjects suffering

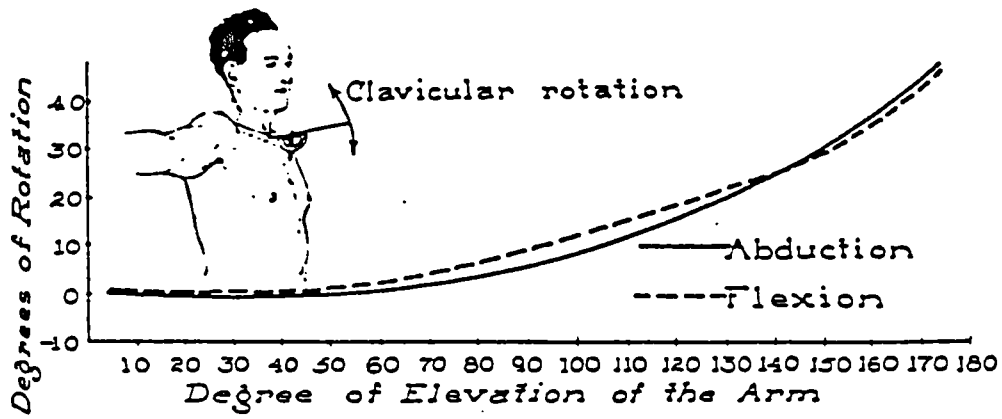


Figure 2.4 Clavicle long axis rotation with humeral elevation (Inman et al 1944).

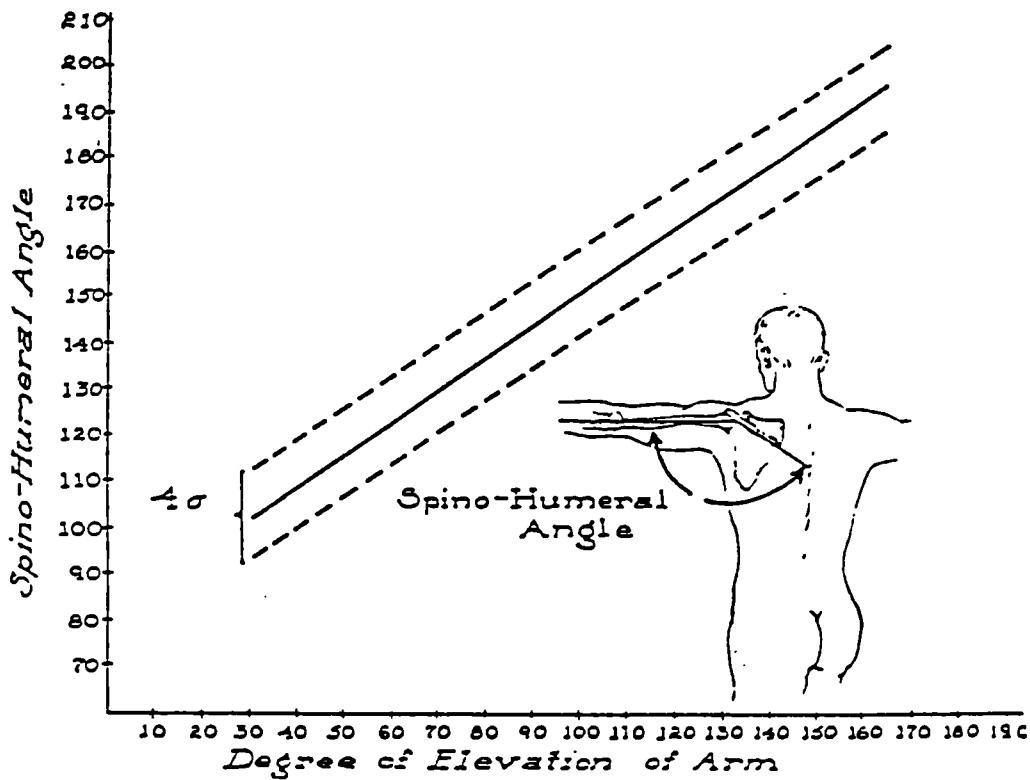


Figure 2.5 Spino-humeral angle changes during humeral abduction as measured by Inman et al (1944) using a two-dimensional x-ray technique. Between 30 and 170 degrees of humeral elevation, for every 15 degrees of elevation, 10 takes place at the glenohumeral joint and 5 between the scapula and thorax.

from recurrent anterior joint instability (15 shoulders, 6 right and 9). Results of this study failed to show any significant differences in humeral retrotorsion and glenoid fossa orientation between healthy and unstable shoulders.

Randelli and Gambrioli (1986) used computed tomography to study 50 normal subjects and 40 subjects with recurrent anterior joint instability. Humeral retrotorsion was found to be between 25 and 30 degrees in both normal and unstable shoulders. Glenoid Fossa orientation was measured at three vertical positions across the fossa. No anterior tilt was found in any of the subjects and all showed varying degrees of posterior tilt. Reduced and increased posterior tilt was only encountered in subjects suffering from traumatic shoulder erosion or fracture.

Kronberg (1990) accurately measured humeral head retrotorsion and found a relationship between decreased retrotorsion and anterior joint instability.

Brewer et al (1986) studied 10 subjects with posterior joint instability. Subject glenoid fossa orientation ranged from 15 to 22 degrees of posterior tilt. Five of the ten underwent surgical procedures to reduce posterior fossa tilt. Postoperative follow-up at one and two years showed no improvement in the untreated shoulders, and all five of the treated shoulders were stable.

In summary, stabilization of the glenohumeral joint results from the functional cooperation between hard, passive soft tissues and active soft tissues of the region. This unique relationship allows the joint to possess the largest range of motion of any joint in the body while still maintaining stability under an infinite variety of loading situations.

2.3. ABDUCTION

Historically the study of glenohumeral joint function has been simplified and standardized by limiting joint function to only two-dimensions. This has commonly involved studying arm movements in the frontal and sagittal body planes and less commonly, in the scapular and transverse planes. As a term of reference, abduction is used to describe arm elevation in both the frontal and scapular planes.

The scapular plane is defined as a plane parallel to the dorsal scapula surface. During normal movement of the shoulder, orientation of this plane can change significantly. As a result, the definition of a single stationary scapular plane for studying arm movement would appear ambiguous.

Humeral abduction is accompanied by shoulder girdle motion. Inman et al (1944) measured the relative movement of this structure for frontal plane abduction using two-dimensional radiographic and photographic techniques. Clavicle elevation was found to

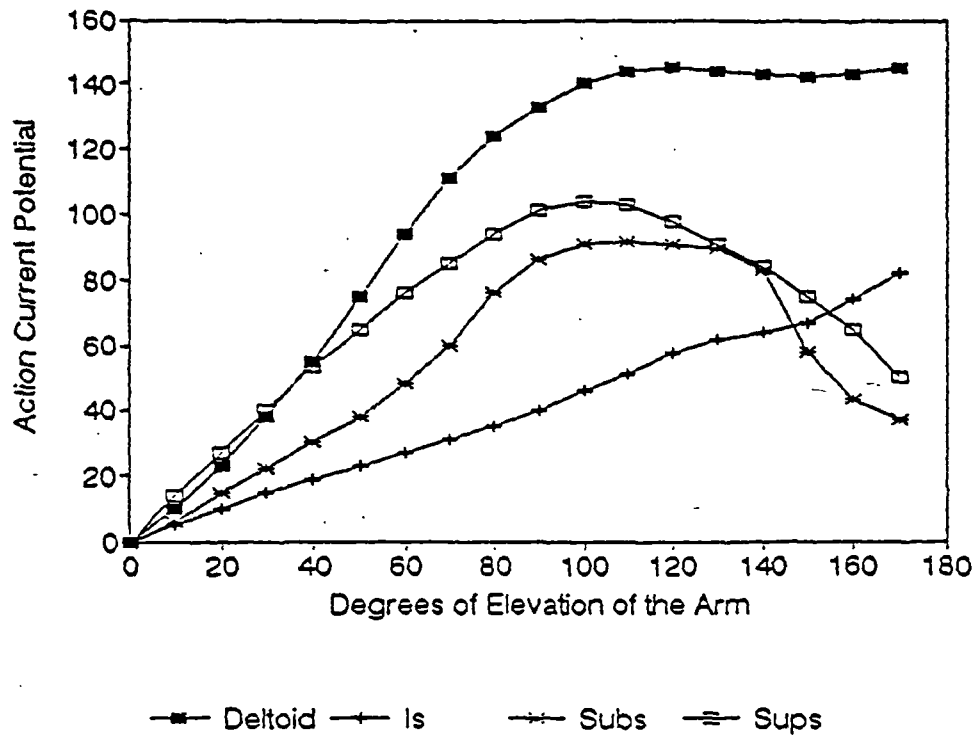


Figure 2.6 EMG levels for deltoid, infraspinatus (Is), subscapularis (Subs) and supraspinatus (Sups) during abduction, measured by Inman et al (1944).

occur for approximately the first 90 degrees of humeral elevation, where every 10 degrees of humeral elevation was accompanied by 4 degrees in the clavicle. Clavicle rotation also measured and found to reach nearly 40 degrees for full humeral abduction (figure 2.4). Scapular motion was split into two phases. The first phase extended to approximately 30 degrees of humeral abduction. Within this phase, the relationship between scapula and humeral orientation was highly subject specific. Beyond this first phase, the relationship between humeral elevation and scapula lateral rotation followed a 2 to 1 ratio (figure 2.5). The relationship between scapula lateral rotation and humeral abduction in the scapular plane was also calculated by Freedman and Munro (1966) and Poppen and Walker (1976). These studies found relative movement to be in the ratios of 1.65 and 1.25 to 1 respectively. Pronk (1988) measured the three-dimensional orientation of the scapula and clavicle retraction and elevation during frontal plane humeral abduction. His results were in close agreement with those of Inman et al (1944). Unfortunately, the results of this study are given as relative motion and not absolute orientation angles for the scapula. As a result, true three-dimensional orientation for the scapula and clavicle cannot be reconstructed.

Generally the shoulder girdle acts like a mobile foundation for the humerus. In this way, the large degree of mobility required in the shoulder is subdivided between several joints, each of which have only a fraction of the mobility of the whole. As a result of this characteristic, overall stability and strength of the structure is improved.

Many authors have investigated active soft tissue function during humeral abduction. Most of these studies have used a technique involving the measurement of muscle electrical activity for investigating muscle physical activity or force generation. This technique is known as electromyography (EMG).

Generally, EMG activity is a qualitative sign of muscle activity and therefore muscle force production. The relationship of EMG activity to muscle force is dependent on several factors including muscle length, size, fibre type, mode of function (concentric, tonic or eccentric) and electrode details. Generally, relative EMG levels are loosely indicative of relative muscle force production in muscles of the same cross sectional area. To allow comparison of inter and intra-subject EMG levels, the measured EMG levels are often normalized against levels obtained for the particular muscle under maximum voluntary contraction conditions. For further information on the subject of EMG, the reader is invited to refer to Basmajian (1974).

Of the active soft tissue that surrounds the glenohumeral joint, only deltoid and supraspinatus are well placed to be humeral abductors. Inman et al (1944) measured EMG levels for these muscles during abduction, and found both to be very active (figure 2.6).

Deltoid EMG rose to a maximum at approximately 90 degrees of abduction and remained high throughout further abduction. Supraspinatus EMG levels peaked at approximately 90 degrees and decreased with further abduction. Unfortunately, EMG levels for this study were not normalized, so comparison of these results to those of other studies can only be made on a qualitative basis. Ringelberg (1985) measured deltoid EMG levels for 0 to 90 degrees of humeral abduction. He found that middle deltoid was more active than the anterior and posterior parts of deltoid throughout the range of abduction. Saha (1973) found supraspinatus activity for abduction to be in agreement with that measured by Inman et al (1944). Järvholm (1989) in contrast to the results of Inman et al (1944) and Saha (1973), found supraspinatus activation for abduction did not decrease after 90 degrees of abduction.

In addition to deltoid and supraspinatus, the remaining rotator cuff muscles are also active during abduction. These muscles appear to assist in maintenance of joint stability and also fine control of joint position. Inman et al (1944) and Saha (1973) both measured EMG levels for each of the remaining rotator cuff muscles and found them all active throughout abduction (figure 2.6). Because of the difficulties in instrumenting these muscles, little additional information is available on their function.

2.4. FLEXION

A commonly analyzed arm activity is humeral flexion (sagittal plane elevation). As in abduction, flexion involves anatomical cooperation of the hard and soft tissues.

Humeral flexion is accompanied by shoulder girdle motion. Inman et al (1944) found clavicle elevation and rotation during humeral flexion to be the same as that measured during abduction. The relationship between scapula lateral rotation and humeral elevation was also found to be similar although not exactly the same as that measured for abduction. The first phase of motion where scapula position was highly subject specific, extended up to approximately 60 degrees of flexion. After 60 degrees, the same 2 to 1 ratio for humeral elevation to scapula lateral rotation was found. Pronk (1988) found shoulder girdle motion to be in agreement with the two-dimensional study by Inman et al (1944). In addition he found that the clavicle and scapula both tend to protract during flexion. This would have the effect of orienting the scapula in or near the plane of humeral elevation. The result is the maintenance of a common functional relationship between the scapula and humerus during humeral elevation irrespective of the plane of elevation.

Active soft tissue function during flexion is similar to that already discussed for abduction. This is not unexpected as the mechanics of elevation remain virtually unchanged between the two planes of motion.

As in abduction, deltoid and supraspinatus are well placed to be flexors. Inman et al (1944) found that deltoid and supraspinatus as the prime humeral elevators were both active throughout flexion. Deltoid was slightly less active than was measured for abduction. Saha (1973) found supraspinatus activity to be similar to what he measured for abduction.

In addition to supraspinatus and deltoid, other muscles are active during flexion. As in abduction, the rotator cuff muscles are all active during flexion. Inman et al (1944) and Saha (1973) both found infraspinatus to be more active and subscapularis to be less active during flexion than in abduction. Pectoralis major was included in the study of Inman et al (1944) and its clavicular portion was also found to be active during flexion.

2.5. OTHER MOVEMENTS

Apart from abduction and flexion, little quantitative information has been collected with respect to shoulder function. As a result, although overall function of the shoulder girdle and upper arm are understood for other activities, detailed information on active joint stabilizing and finer movement control are not well documented. To simplify the analysis of all the remaining possible arm actions, they are normally grouped with respect to their major action. These groupings include: humeral adduction, extension, internal and external rotation and transverse plane flexion (forward swing) and extension (backward swing).

Adduction or sideward depression of the arm may occur from any frontal plane arm position. Shoulder girdle position for such an activity remains essentially unchanged from that used to elevate the arm. Active soft tissues that are positioned to function as adductors would include: latissimus dorsi, teres major, sternal portion of pectoralis major and possibly the lower posterior portion of deltoid (Luttgens & Wells, 1982).

Extension or forward depression of the arm may occur from any position of the arm in the sagittal plane. As with adduction, shoulder girdle position remains essentially unchanged from that used for arm flexion. Active soft tissues that are positioned to function as extenders would include: sternal portion of pectoralis major, teres major, latissimus dorsi, posterior deltoid and the long head of triceps (Luttgens & Wells, 1982).

Internal and external rotation may occur in any arm position. Typically these actions are the result of glenohumeral joint rotation alone with the shoulder girdle playing little or no part. Active soft tissues strongly associated with internal rotation are: subscapularis, teres major, latissimus dorsi, anterior deltoid and pectoralis major. Structures strongly associated with external rotation include: infraspinatus, teres minor and at times posterior deltoid (Luttgens & Wells, 1982).

Transverse plane flexion and extension of the arm may occur from any elevated arm

position. With this activity, shoulder girdle movement would also occur. As was noted by Pronk (1988), when comparing shoulder girdle position for pure flexion and abduction, the scapula is oriented near the plane of elevation. For horizontal motion in a transverse plane, accompanying protraction and retraction of the clavicle and scapula would therefore be expected. Active soft tissues associated with transverse plane flexion are: pectoralis major, anterior deltoid, coracobrachialis and the short head of biceps. Associated with transverse plane extension are: posterior deltoid, infraspinatus, teres minor and the long head of triceps (Luttgens & Wells, 1982).

CHAPTER 3. BIOMECHANICAL JOINT MODELLING AND RELATED TOPICS

Quantitative evaluation of the forces in and transmitted between hard and soft tissues of the body has long been a topic of research for both clinicians and bioengineers. Through the study of these forces it is hoped to gain a better understanding of the mechanisms of pathological joint disease, injury, normal joint function and criteria for design of joint replacements.

Research of this type finds its roots in classical mechanical analysis techniques. In classical mechanics, analysis of a structure can include the prediction and measurement of internal and external structural loads and stresses. Additional kinematic information including position, velocity and acceleration of the structure and its parts can also be measured or predicted. Techniques that have been developed over centuries are now used in these types of analysis. Using similar techniques, it is possible to explore human body function. With such an approach the human body is viewed as a mechanism with rigid supporting structures complete with bearing interfaces allowing movement and passive and active soft tissues providing joint stability and force generation.

3.1. JOINT MODELLING OVERVIEW

Application of classical mechanics analysis techniques to predict loads and movement of the human body during various activities can be traced to the early part of this century. Historically, lower limb function, and in particular walking, has been one of the most commonly studied activities (Seireg and Arvikar, 1973). Research into upper limb function, although not as common as lower limb research, has paralleled the developments made in the lower limb.

Joint modelling, to the upper or lower limb share essentially similar problems. Joint loading is a function of not only external body loading and kinematics but also forces in the muscles and soft tissues surrounding the joint. These forces are difficult to measure in-vivo and as such are normally calculated indirectly from the external loading and kinematic information. Techniques utilized to measure loading and kinematics vary as do the techniques for calculating internal tissue loading around a joint.

One of the earliest studies to accurately calculate three-dimensional joint loads was the investigation of Paul (1967) into forces transmitted through the hip during walking. In his study, the three-dimensional kinematics of the lower limb segments were determined using photographic records of the activity. Combining these data with foot to floor contact forces

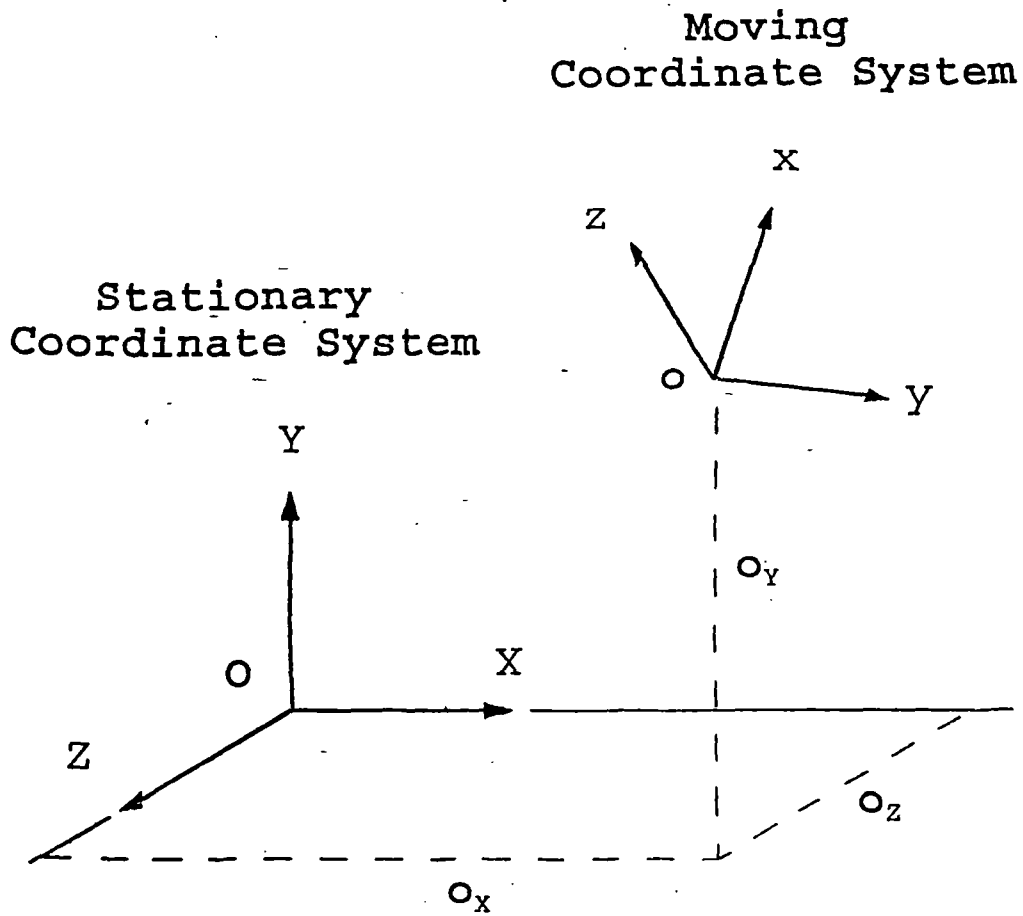


Figure 3.1 The position of a moving coordinate system with respect to a stationary coordinate system is defined by a vector, which is equivalent to the vector sum of O_x , O_y and O_z .

measured using an instrumented force plate, allowed the moments transmitted across each joint to be calculated. Using a simplified anatomical structure, the equivalent muscular forces required to balance these moments could be calculated. Combining muscle, foot to floor, gravity and inertial forces allowed the total force transmitted across the hip joint to be calculated.

3.2. BODY SEGMENT KINEMATICS

To completely describe the kinematics of a body segment requires information regarding both segment position and segment orientation in space. In three-dimensional space a body segment has six degrees of freedom. That is to say that six pieces of information are required to completely describe its physical location within its environment. Of these six pieces of information, three relate to segment position and three to its orientation in space. In a two-dimensional analysis, a segment will have three degrees of freedom, where two describe segment position and one its orientation.

Description of segment kinematics requires that the segment position and orientation be compared to a stationary or global reference. Absolute segment kinematics normally takes the form of comparing a cartesian coordinate system defined within the segment to an inertially defined coordinate system based outside the segment. Joint kinematics can be obtained similarly, by comparing position and orientation of the distal segment with respect to a coordinate system in the proximal segment. In such a system, the proximal and distal segment coordinate systems are termed the stationary and moving coordinate systems respectively.

The three-dimensional kinematic relationship between two coordinate systems is completely described by a vector relating the position of the moving coordinate system origin with respect to the stationary coordinate system and the direction cosines relating the orientation between the two coordinate systems. In such an analysis, the stationary coordinate system can be defined as X,Y,Z with unit vectors I,J,K , origin O , and the moving coordinate system as x,y,z with unit vectors i,j,k and origin, o . The vector relating the position of o , with respect to the stationary coordinate system would be in terms of X,Y,Z (see figure 3.1). Orientation of the moving coordinate system can now be given with respect to the stationary coordinate system as:

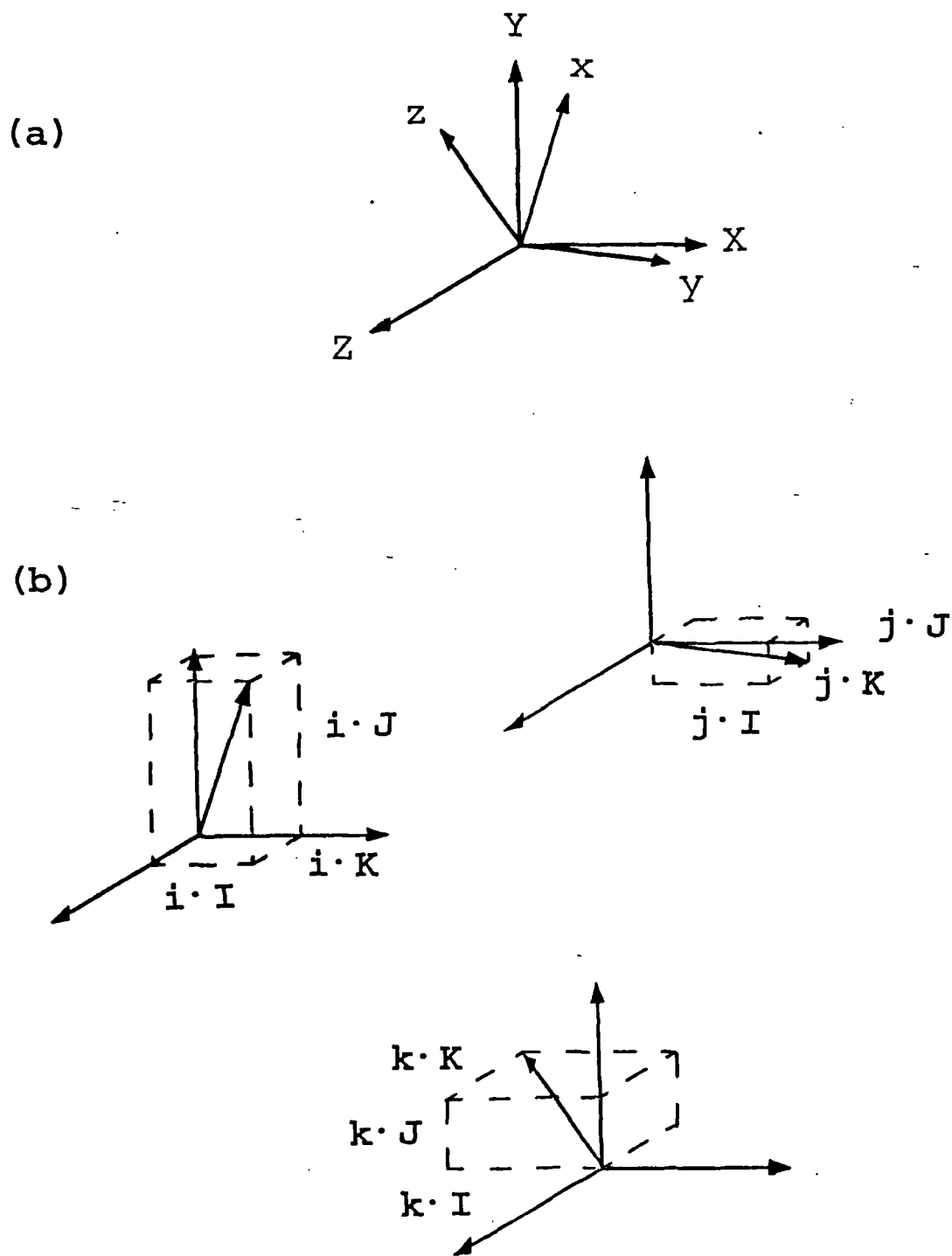


Figure 3.2 Orientation of a moving coordinate system with respect to the stationary coordinate system (a) is defined by the nine direction cosine terms of matrix $[B_{\text{moving-stationary}}]$ (b).

$$\begin{bmatrix} i \\ j \\ k \end{bmatrix} = \begin{bmatrix} i \cdot I & i \cdot J & i \cdot K \\ j \cdot I & j \cdot J & j \cdot K \\ k \cdot I & k \cdot J & k \cdot K \end{bmatrix} \begin{bmatrix} I \\ J \\ K \end{bmatrix} = [B_{\text{moving-stationary}}] * \begin{bmatrix} I \\ J \\ K \end{bmatrix} \quad (3.1a)$$

where,

$$[B_{\text{moving-stationary}}] = \begin{bmatrix} b_{1,1} & b_{1,2} & b_{1,3} \\ b_{2,1} & b_{2,2} & b_{2,3} \\ b_{3,1} & b_{3,2} & b_{3,3} \end{bmatrix} \quad (3.1b)$$

where the direction cosines are elements in matrix [B] and represent the projection of the moving coordinate system unit vectors on the stationary coordinate system unit vectors (Small et al, 1992) (see figure 3.2). Although matrix [B] has nine elements, only three of these are independent as the sums of squares for both rows and columns equal 1. These three independent elements along with the three terms of the position vector comprise the six pieces of information needed to completely describe the physical location of the segment.

All analytical methods used in three-dimensional kinematic analysis make use of the position vector and direction cosine matrix. The various techniques vary only in the method of manipulation and interpretation of the information contained within the vector and matrix (Small et al, 1992).

Generally there are two analytical techniques commonly used for kinematic analysis. In the first, segment orientation is described by a series of three ordered rotations. The rotations are calculated from the direction cosine matrix. This general technique includes Euler angle and floating axis techniques. In the second analytical technique, the relative position and orientation of two coordinate systems is stated as the rotation about and translation along some imaginary axis in space. This axis is often termed the equivalent or helical screw axis. The position and orientation of the axis plus the translation along and rotation about the axis are all calculated from the segment position vector and direction cosine matrix. Both of these analytical techniques work equally well at describing joint and segment kinematics. The choice of which is used is often based on individual experience and taste rather than on any objective criteria (Andrews, 1984).

Joint anatomy can impose kinematic restrictions on body segment movement. Ball and

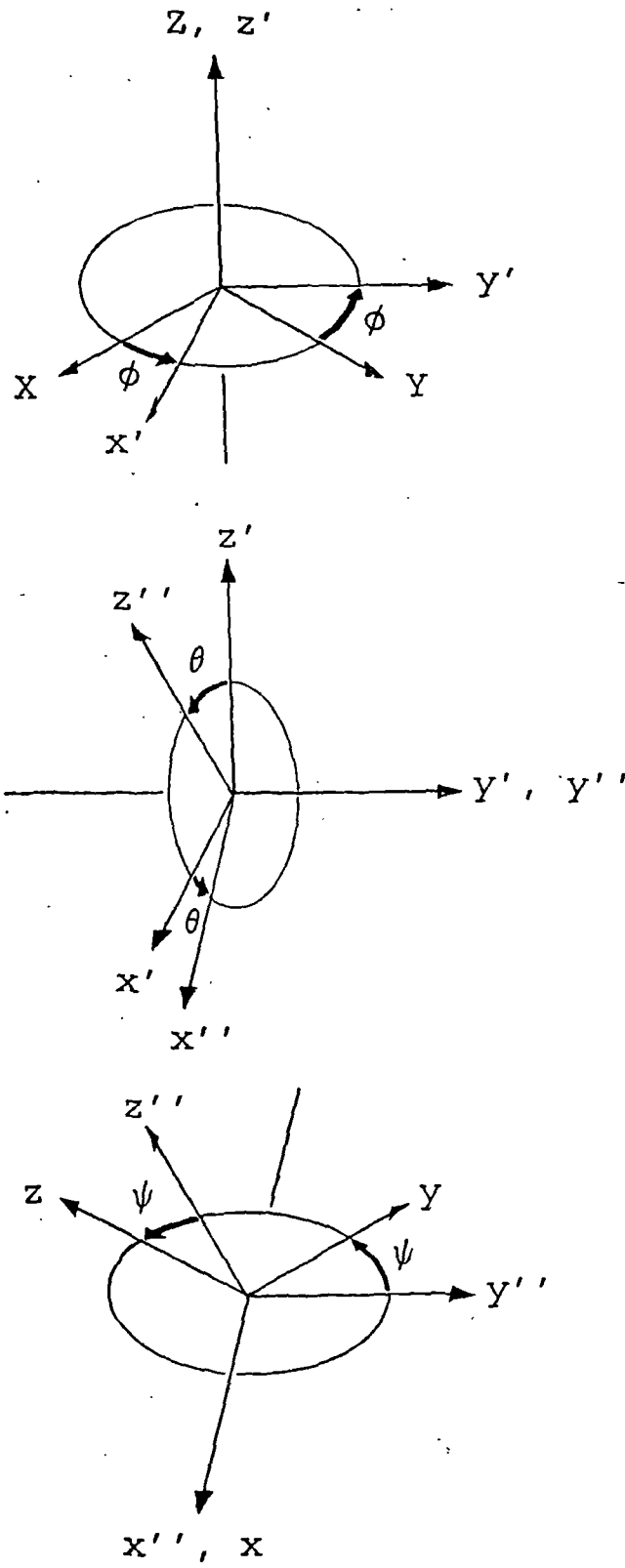


Figure 3.3 Euler angles. Three ordered rotations are required to align the stationary coordinate system, X, Y, Z and the moving coordinate system, x, y, z . The axes of rotation are Z, y' and x'' . The rotation angles, ϕ, θ and ψ are shown in their positive sense and conform to the right hand rule.

socket type joints, including the hip and glenohumeral joints, allow essentially only rotational freedom about three orthogonal axes. This gives the joint only three degrees of freedom. Analysis of segment kinematics across these joints is therefore simplified since inter-segment positioning is defined by joint geometry. Joints such as the knee and elbow, allow essentially only rotational freedom about one axis. These give the joint only one degree of freedom. This limits inter-segment kinematics to being approximately planar with positioning defined by joint geometry.

Two-dimensional kinematic analysis is much simpler than three-dimensional analysis. The kinematic relationship between two coordinate systems is completely described by a vector relating the position of the moving coordinate system origin to the stationary coordinate system and a 2x2 direction cosine matrix. Analysis of the direction cosine matrix consists of determining its corresponding two-dimensional Euler rotation angle. In normal practice, this angle is often measured directly from experimental records, completely eliminating the direction cosine stage of the analysis.

If position and orientation of a segment are determined as a function of time, the linear and angular velocity and acceleration of that segment can be determined. These parameters are not commonly measured during a normal biomechanical kinematic analysis. Instead, if these parameters are required they are determined using an "inverse kinematics" approach (Chao and An, 1990). In such an approach, the position and orientation information of a segment is numerically differentiated once to give velocity and a second time to determine acceleration. This process is complicated by the sensitivity of the differentiation process to the small errors in the position and orientation data (Pezzack et al 1977). Although filtering of the original data can improve the overall success of the differentiation process, the results remain sensitive to filter and kinematic characteristics (Ladin et al, 1989).

3.2.1. Euler Angle and Floating Axis Techniques

Both of these analysis techniques utilize the direction cosine matrix to generate a series of ordered rotations that describe the orientation of one coordinate system with respect to another. They differ in the way the axes of rotation are determined. The end result of both is a series of rotations that correspond to clinical joint angles, if the axes of rotation are properly defined.

Many different axes of rotation are possible with the Euler Angle analysis technique. The most commonly used format involves rotations about three different axes, and is referred to as a three axis or gyroscopic system. In this format, the series of three ordered rotations correspond to joint flexion-extension, ϕ , abduction-adduction, θ , and internal-external

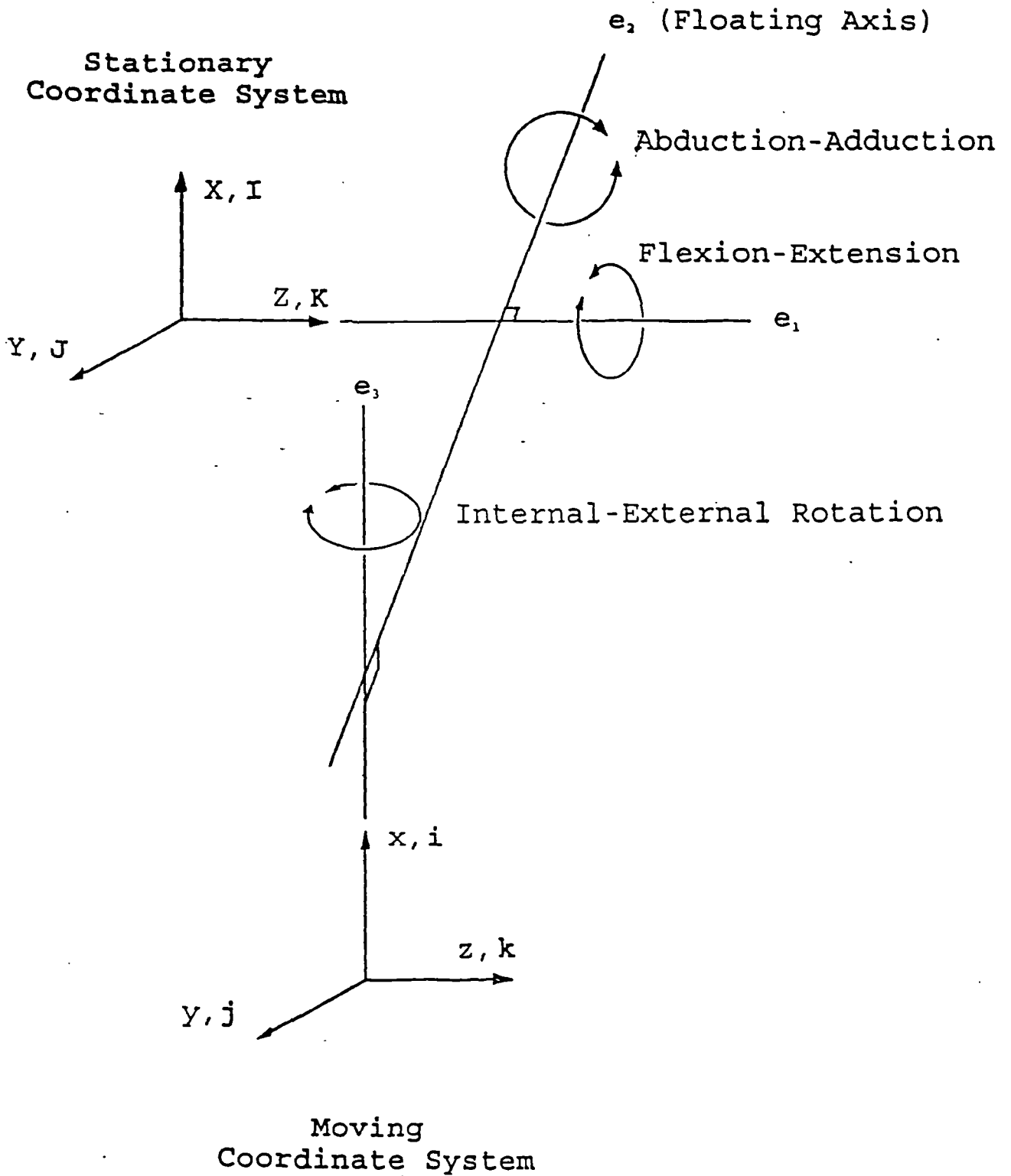


Figure 3.4 Floating axis system. Three rotations are required to align the stationary coordinate system, X, Y, Z and the moving coordinate system, x, y, z . The axes of rotation are e_1 , e_2 and e_3 . e_1 and e_2 are fixed to the stationary and moving coordinate systems respectively and e_3 is defined as perpendicular to both e_1 and e_2 .

external rotation, ψ , about the Z, y' , and x'' axes (Chao, 1980) (see figure 3.3). The direction cosine matrix is equal to the product of three ordered Euler rotation matrices:

$$\begin{bmatrix} \mathbf{i} \\ \mathbf{j} \\ \mathbf{k} \end{bmatrix} = \begin{bmatrix} 1 & 0 & 0 \\ 0 & \cos\psi & \sin\psi \\ 0 & -\sin\psi & \cos\psi \end{bmatrix} * \begin{bmatrix} \cos\theta & 0 & -\sin\theta \\ 0 & 1 & 0 \\ \sin\theta & 0 & \cos\theta \end{bmatrix} \quad (3.2)$$

$$* \begin{bmatrix} \cos\phi & \sin\phi & 0 \\ -\sin\phi & \cos\phi & 0 \\ 0 & 0 & 1 \end{bmatrix} * \begin{bmatrix} \mathbf{I} \\ \mathbf{J} \\ \mathbf{K} \end{bmatrix}$$

Comparing the product of these three rotations with the original direction cosine matrix (equation 3.1) allows calculation of the three Euler rotation angles (Small et al, 1992):

Abduction-Adduction,

$$\theta = \sin^{-1} (-\mathbf{i} \cdot \mathbf{K}) \quad -\pi/2 \leq \theta \leq \pi/2 \quad (3.3)$$

Flexion-Extension,

$$\phi = \sin^{-1} (\mathbf{i} \cdot \mathbf{J} / \cos\theta) \quad -\pi/2 \leq \phi \leq \pi/2 \quad (3.4)$$

Internal-External Rotation,

$$\psi = \sin^{-1} (\mathbf{j} \cdot \mathbf{K} / \cos\theta) \quad -\pi/2 \leq \psi \leq \pi/2 \quad (3.5)$$

There are several disadvantages when utilizing this system of defining three-dimensional segment and joint kinematics. Rotation angles in this technique are order dependent. Because of this and as a result of a lack of a standardized set of rotation axes, comparison of kinematic results between studies is often cumbersome. Visualization of this analysis technique is difficult especially when segment orientation is well removed from the anatomical position. Finally, the range of motion over which the Euler angle calculations are defined ($-\pi/2$ to $\pi/2$) can impose difficulties on the implementation of the technique for

highly mobile joints.

The floating axis technique, developed by Grood and Suntay (1983), utilizes three nonorthogonal unit vectors, e_1 , e_2 and e_3 , as rotation axes (see figure 3.4). Two of these, e_1 and e_3 , are body fixed axes imbedded in the two coordinate systems or segments whose relative motion is to be analyzed. The third axis, e_2 , is termed the floating axis and is defined as normal to the plane of e_1 and e_3 . Orientation of these axes can be determined from the direction cosine matrix using:

$$e_1 = \{ 0, 0, 1 \} \quad (3.6a)$$

$$e_3 = \{ b_{1,1}, b_{1,2}, b_{1,3} \} \quad (3.6b)$$

$$e_2 = e_3 \times e_1 \quad (3.6c)$$

Joint flexion-extension takes place around the e_1 axis, abduction-adduction around e_2 , the floating axis, and internal-external rotation around the e_3 axis.

The three rotation angles which describe the relative orientation of the two coordinate systems or segments can be calculated using:

Flexion-Extension,

$$\alpha = \sin^{-1} (-e_2 \cdot I) \quad -\pi/2 \leq \alpha \leq \pi/2 \quad (3.7)$$

Abduction-Adduction,

$$\beta = \sin^{-1} (K \cdot i) \quad -\pi/2 \leq \beta \leq \pi/2 \quad (3.8)$$

Internal-External Rotation,

$$\gamma = \sin^{-1} (-e_2 \cdot k) \quad -\pi/2 \leq \gamma \leq \pi/2 \quad (3.9)$$

where the definition of the stationary coordinate system is denoted by X,Y,Z (unit vectors I,J,K), the moving coordinate system x,y,z (unit vectors i,j,k) and the rotation axes are the same as those used for the Euler angle analysis technique discussed previously.

The floating axis technique has the advantage of rotation angles which are order independent. This occurs because the rotation axes are explicitly defined by the format of the analysis technique. This independence eliminates confusion often associated with the interpretation of Euler angle technique kinematic results.

3.2.2. Equivalent or Helical Screw Axis Technique

This analysis technique although novel, is not commonly employed in the analysis of shoulder or upper limb kinematics. As a result, calculation details for the various kinematic

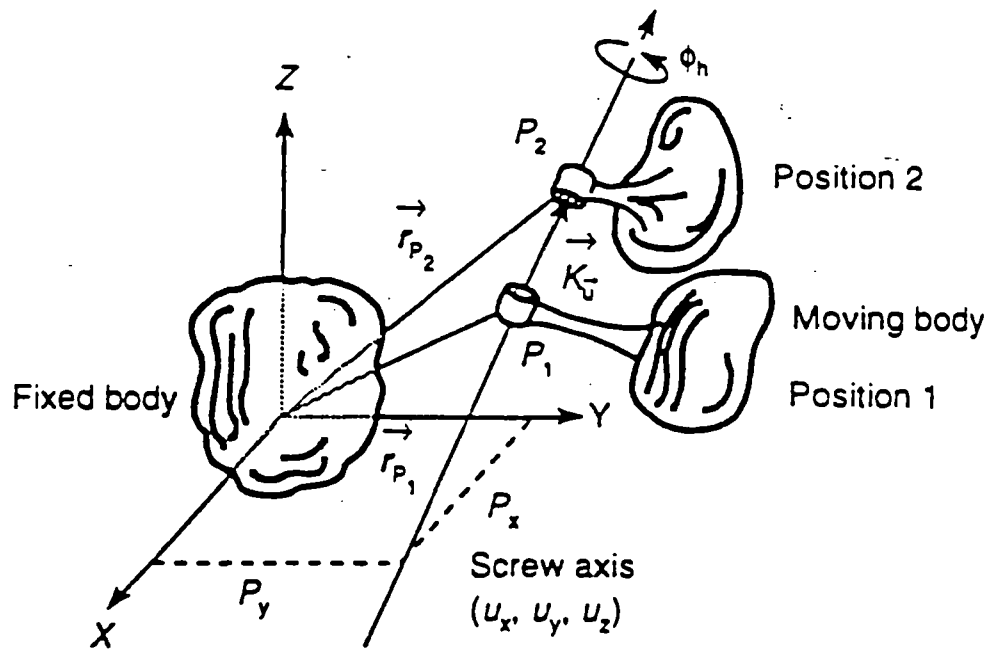


Figure 3.5 Equivalent or helical screw axis. Relative motion between two coordinate systems can be measured in terms of a rotation, ϕ_n about and a translation, K_n along an imaginary axis in space. The axis is defined by the coordinates, P_x, P_y of its intersection with a plane and the direction cosines of the axis, U_x, U_y and U_z (Small et al 1992). One of the direction cosines is redundant as the sum of their squares is unity. This reduces the number of system parameters to 6, as would be expected for a system with six degrees of freedom.

parameters used in the technique are not covered in this work. The reader is invited to refer to Small et al (1992), for further information on calculation details.

The technique utilizes the concept that the orientation between two coordinate systems may be described as a rotation about and a translation along an imaginary axis in space. This is the equivalent or helical screw axis. Complete parameterization of the relative position and orientation of a coordinate system includes: the coordinates of the screw axis intersection with a known plane, screw axis orientation and translation along and rotation about the screw axis of the moving coordinate system (see figure 3.5).

There are several disadvantages with the equivalent or helical screw axis technique. For three-dimensional motion, correlation of the analysis parameters to clinical joint motion parameters is difficult. Even for planar kinematics, agreement with the clinically relevant Euler and floating axis techniques is found only when the axis of rotation corresponds to an axis in the stationary coordinate system (Small et al, 1992). This discrepancy between clinical and helical screw axis technique kinematic descriptions tends to complicate the final interpretation of kinematic results.

3.2.3. Measurement

Data required for kinematic analysis can be measured using a variety of techniques. Photographic, X-ray, cinephotographic, goniometer, ultrasonic, magnetic and video experimental recording methods have all been used.

Historically, two-dimensional analysis techniques have been and are still widely used. Studies by Inman et al, (1944), Freedman et al, (1966) and Poppen and Walker (1976) and others have all studied two-dimensional joint kinematics using x-ray based measurement techniques. Cinephotographic and photographic techniques have also been employed in two-dimensional joint kinematic studies. Conditioning of data from these studies can involve corrections for parallax error, scaling and in the case of photographic and cinephotographic systems, lens distortion. Goniometers, both manual and electronic, have also been used.

With the integrated application of powerful computers, difficulties associated with the implementation of a three-dimensional kinematic analysis have been greatly reduced.

Many three-dimensional studies although utilizing computer based numerical analysis techniques still required extensive manual interpretation of experimental records. The study by Paul (1967) is an example of a study where biplanar cinephotographic experimental records were hand processed frame by frame to determine three-dimensional body segment kinematic data although the marker system was insufficient to determine more than three linear and two angular parameters. Three-dimensional x-ray based experimental techniques

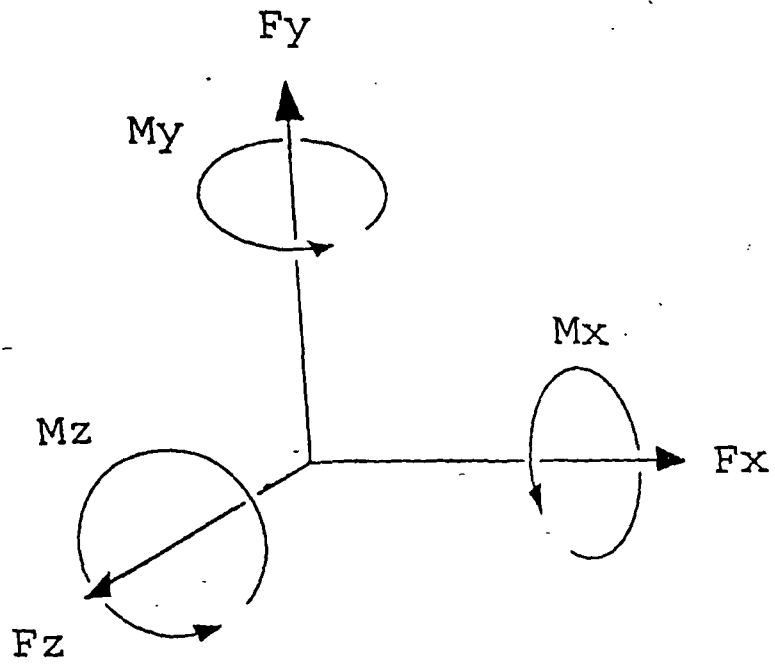


Figure 3.6 Standard convention for positive direction of forces and moments as they are applied to a point on an object. The direction of positive moment sense conforms to the right hand rule.

utilized by Wevers et al (1982), Högfors et al (1991), Runciman et al (1993) and others, all require similar manual record interpretation, although on a greatly reduced scale compared to earlier cinephotographic techniques.

In many three-dimensional kinematic measurement techniques the time consuming process of manual experimental record interpretation has been eliminated. Goniometer based systems of this type have been used by Chao (1980), Pronk (1988) and Barker (1991) among others. Video, ultrasonic and magnetic based systems with automated three-dimensional reconstruction are also all currently widely used.

3.3. EXTERNAL BODY SEGMENT AND JOINT LOADING

External segment and joint loading is the result of interaction between the segment and its environment. External loads can result from the force of gravity acting on a segment, contact between the segment and its environment or the inertia of the segment during motion. Combining the effect of these loads, allows the total external segment loading to be determined. External joint loading is a function of both this external loading and the kinematics of the adjacent segments. When calculating external joint loading the cumulative effects of the external segment loads are considered with respect to the joint rotation centre. In this way, they can be discussed in terms of their overall effect on that joint.

Loading of a segment or joint is usually given in terms of forces and moments acting on the segment or forces on a joint. For a complete description of these, both magnitude and direction information is required. To accommodate this, they are usually stated in terms of their magnitude in each of the directions of a standard three-dimensional cartesian coordinate system (F_x , F_y , F_z and M_x , M_y , M_z). Definition of this coordinate system can be laboratory or segment based. A standard format has been established for the description of the positive actions of the forces and moments when acting on a segment (see figure 3.6).

Many of the parameters required for determining external segment and joint loading are not easily measured experimentally. To overcome this problem, anthropometric studies have been conducted, where body segment parameters have been determined for a sample population.

Anthropometric studies have been conducted by several authors. Despite recent advancements in techniques such as magnetic resonance imaging (MRI) and computer aided tomography (CAT), the parameters are still obtained using indirect measurement techniques. Drillis and Contini (1966) measured body segment parameters for 20 male subjects between the age of 20 and 40. They determined: segment masses as a percentage of total body weight (see table 3.1); segment lengths as a percentage of total body height (see figure 3.7);

Table 3.1 Average Segment mass in percentage of total body mass (Drillis and Contini, 1966)

Segment	Mass (% total body mass)
Head, Neck and Trunk	55.4
Extremities	44.6
Upper Extremities	11.3
Upper Arms	6.2
Forearms	3.6
Hands	1.5
Lower Extremities	33.3
Thighs	20.9
Shanks	9.2
Feet	3.2

Table 3.2 Average location of segment centre of mass from proximal joint, in percentage of overall segment length (Drillis and Contini, 1966)

Segment	Distance (% of segment length)
Entire Arm	43.1
Upper Arm	46.1
Forearm and Hand	42.0
Forearm	42.5
Hand	43.3
Entire Leg	41.5
Thigh	42.7
Shank and Foot	46.7
Shank	40.4
Foot (from heel)	44.3

and location of centre of mass in each body segment as a ratio of the overall segment length (see table 3.2). More recently, Veeger et al (1991) carried out a similar anthropometric study focusing on the upper limb and shoulder girdle. Using the information from these types of studies, it is possible to calculate most parameters required for analysis of segment external loading.

3.3.1. Contact Loading

Interaction of the body and its environment usually involves loads being imparted to the body through some form of contact, whether that contact is with a solid object or an air or water environment. Contact loads applied to a segment are normally stated in terms of their magnitude and direction with respect to their point of application. A common biomechanical example is the foot to floor contact forces developed during the stance phase of gait. For the upper limb, contact forces usually occur at the hand. Drag force, resulting from the motion of a segment through a fluid medium, is a special form of contact force. Except in swimming or high velocity athletic performance biomechanical analysis, it is usually ignored because of its relatively small effect.

Many techniques are available for determining the magnitude and direction of contact loads. Normally, they are measured experimentally using instrumented force transducers. Most of these transducers measure the elastic strain imparted to a section of the object in contact with the body, thereby obtaining a measure of the contact load. A common example of this is the standard gait analysis force plate. For upper limb analysis, instrumented hand transducers can be used.

3.3.2. Gravitational Loading

A force due to gravity is experienced by any object that possesses mass and exists in our environment. The effect of gravitational force on a body segment is a function of segment mass, acceleration due to gravity and location of the centre of segment mass. Using body segment parameter information from an anthropometric study such as by Drillis and Contini (1966), external segment loading due to gravity can be easily calculated. The direction of this force is vertically down and its point of application is through the segment centre of mass.

3.3.3. Inertial Loading

Any accelerating body segment is subjected to some form of inertial loading, which is a function of segment mass, segment mass distribution and segment kinematics. The

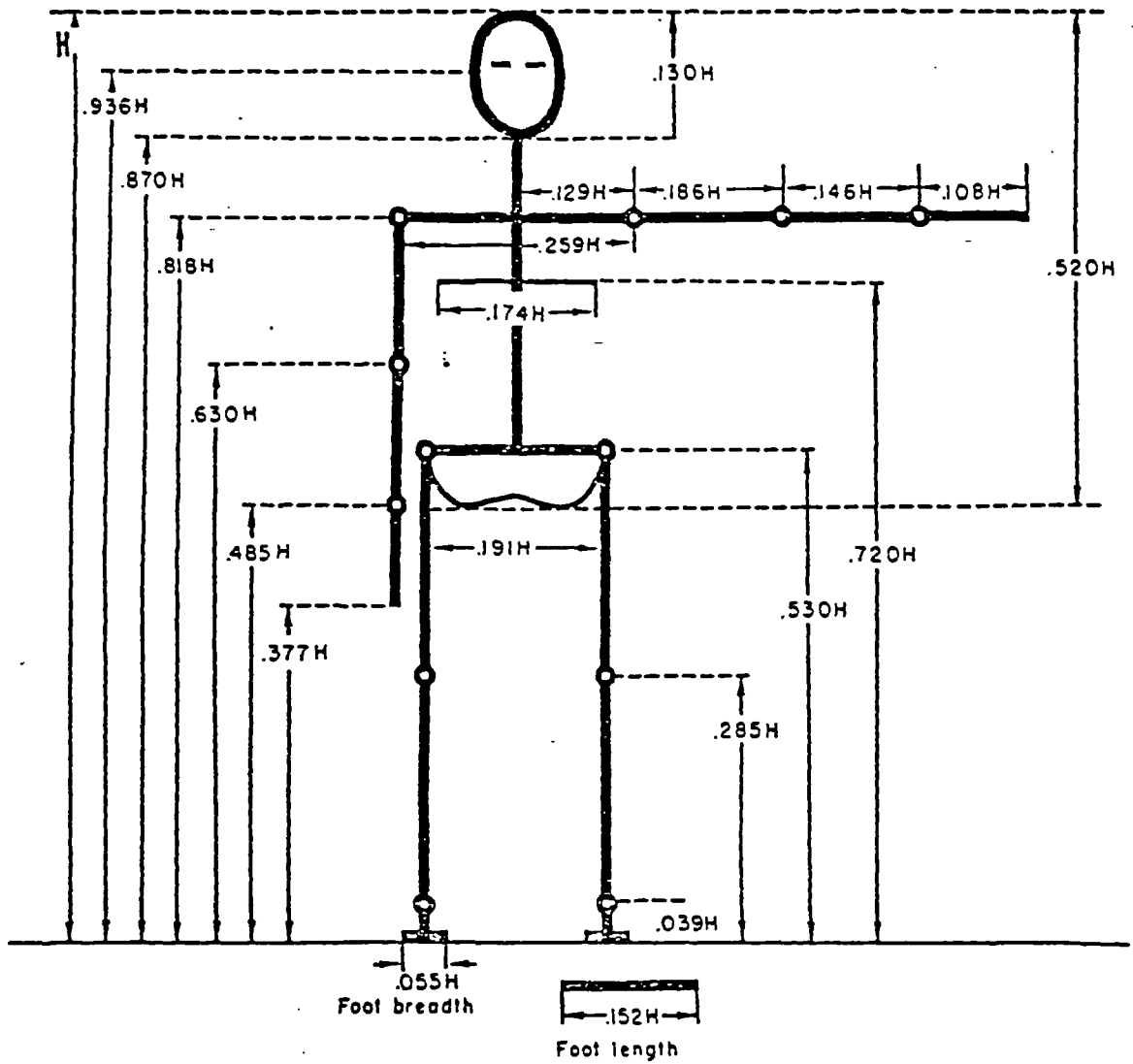


Figure 3.7 Segment length as a ratio of overall body height (Drillis and Contini, 1966).

magnitude of inertial forces about the principal axis of inertia can be calculated for a segment using:

$$F_i = M_s * a \quad (3.10)$$

Where F_i is the inertial force, M_s is segment mass and a is the linear acceleration of the segment centre of mass. This force acts through the segment centre of mass and its direction is opposite to that of the acceleration. Inertial moments are calculated in a similar fashion, using:

$$T_i = I_s * \alpha \quad (3.11)$$

where,

$$I_s = M_s * K^2 \quad (3.12)$$

where T_i is the moment imparted to the segment, I_s the segment principal axis mass moment of inertia, K the segment radius of gyration and α the angular acceleration of segment orientation. The direction of this moment is opposite to that of the angular acceleration.

Since both inertial moments and forces are a function of segment acceleration, their calculation is complicated by the difficulties associated with determining this acceleration. In addition, for many real life activities, segment accelerations and therefore inertial loads are typically small. As a result, inertial forces and moments are often omitted during biomechanical analysis studies.

3.4. INTERNAL JOINT LOADS

In classical mechanical analysis, an object is said to be in equilibrium if the net force and moment acting on that object are equal to zero. For a body segment, external segment loads are balanced by internal muscle, ligament and joint contact loads to maintain a state of equilibrium.

The structures in and around a joint are responsible for generating these internal loads. In normal joint function, the joint tissues are capable of generating the forces and moments required from them. Unfortunately, overloading can result in muscle, ligament and joint damage.

Calculating the loading in individual joint tissues can be broken into three phases. First is to calculate the net joint moment required to balance external segment loads. Second, the soft tissue loading required to produce this net joint moment can be calculated. Finally, summing both the external segment forces and soft tissue forces, yields the joint forces.

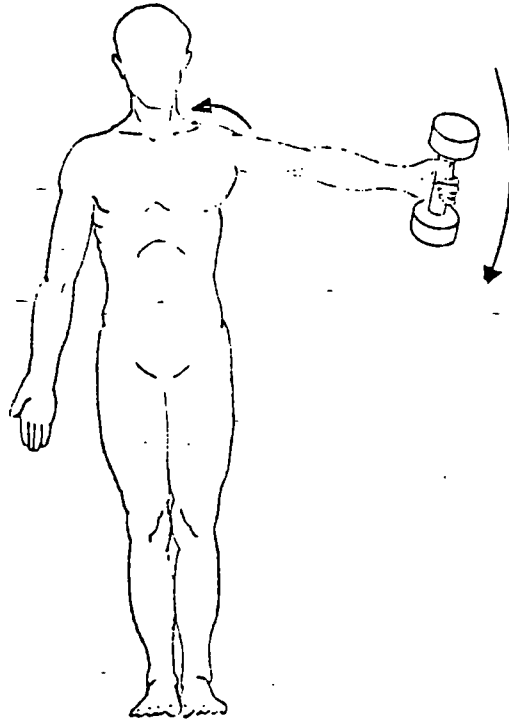


Figure 3.8 The net external segment moment due to contact, gravitational and inertial loading is equal and opposite in direction to the net joint moment, generated by the shoulder structures.

3.4.1. Net Joint Moment

Tissues in and around a joint are responsible for generating joint moments. In a biomechanical study, these moments are equal in magnitude and opposite in direction to the net moments acting on a joint resulting from external loading on the distal segment (see figure 3.8).

The magnitude and direction of the joint moment that must be generated by the joint tissues can be calculated using the equation:

$$\sum (\text{moments at a joint}) = 0 \quad (3.13)$$

where,

$$\begin{aligned} \sum (\text{moments at a joint}) = & \sum (\text{moments due to external segment loading}) \\ & + \sum (\text{joint moments}) \end{aligned}$$

In a three-dimensional environment, equation 3.13 can be applied in each of the three planes defined by a standard cartesian coordinate system. This allows the net moments generated by the joint tissues in each of these three planes to be calculated. These three independent moments completely describe the moment balance at the joint. More generally, a complete description of the moment balance at a joint can be obtained by applying equation 3.13 to any three non-parallel axes passing through the joint centre.

3.4.2. Joint Moment Generation

Many tissues within the structure of a joint contribute to moment generation. Passive soft tissue, muscle and joint hard tissue geometry may all contribute. The moment produced by any of these is a function of both the force transmitted through them and their relationship to the joint.

Muscles are primarily responsible for generating joint moments around axes of joint rotation. For the elbow, this limits muscular moment generation to basically the flexion-extension axis. For the glenohumeral joint, with its three-degrees of rotational freedom, muscles usually produce joint moments about all three of the orthogonal axes. Knowing the net joint moment that must be produced by a set of muscles, and line of actions of all of the muscles, leaves only the individual muscle forces and or components of joint contact force as unknowns within the mechanical system.

Passive soft tissue and joint hard tissue geometry normally generate joint moments around axes where there is no rotational freedom. An exception to this is at the limit of joint motion where they can generate moments to limit further motion. For normal function

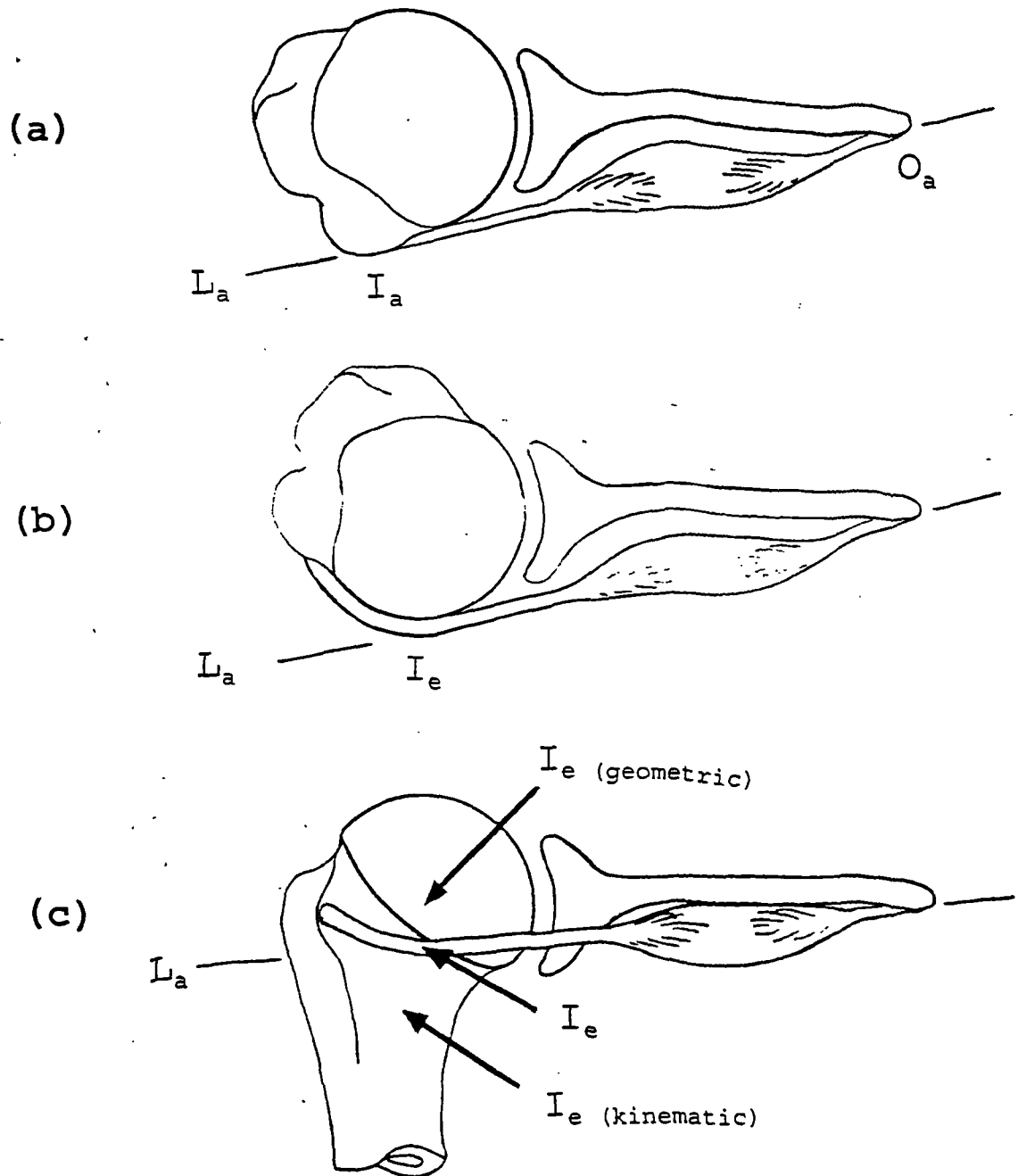


Figure 3.9 Glenohumeral joint superior view. When the anatomical line of muscle action, L_a , is straight between the anatomical origin, O , and insertion, I , no wrapping occurs, (a). For simple wrapping, definition of an effective insertion, I_e , using either a kinematic or geometric shape constraint technique allows the muscle line of action to be defined, (b). For complex wrapping, kinematic or geometric defined effective insertions, I_e (kinematic), I_e (geometric), may both be incorrectly positioned, (c).

of the glenohumeral joint, neither are involved in moment generation.

3.4.2.1. Muscle Lines of Action

The relationship between a muscle and a joint it crosses is described by the muscle's line of action. This line represents the position and direction of the muscle generated force passing across the joint. Muscle origin and insertion position, joint orientation, centre of force within the muscle and wrapping of the muscle around other anatomical structures all influence the line of action.

At a primitive level, the force a muscle exerts across a joint can be assumed to be in a straight line between its origin and insertion (see figure 3.7a). Studies including those by Högfors et al (1987) and Johnson (1990) have been conducted to determine shoulder muscle origin and insertion positions with respect to the bones on which they attach. Utilizing these data and joint kinematic data, the simplified muscle line of action across a joint can be calculated. Unfortunately, many muscles of the upper limb and shoulder do not form straight lines between their origin and insertion. Instead, their line of action is affected by the muscle passing over and around other hard and soft tissues. As a result, using the simplified straight line technique for shoulder modelling is unacceptable.

An improvement to the simplified straight line technique can be obtained if the effects of muscle wrapping are accounted for. Various techniques have been employed to achieve this, although many are poorly described in the literature. Without proper documentation the verification and replication of the wrapping correction procedures used in these studies is often difficult.

In static studies, where only a few body positions are being studied, destructive cadaveric measurements can be made of the actual muscle lines of action. Studies by: Inman et al (1944), de Luca and Forrest (1973), Poppen and Walker (1978) and Bassett et al (1990) are all examples of shoulder research utilizing this type of approach.

A second technique for muscle wrapping correction involves redefining origin or insertion positions to their effective positions. Utilizing this approach, the origin and/or insertion are moved to positions where a straight line exists between. Ideally, the new position would fall on the true anatomical line of action for the muscle. Implementation of this technique takes essentially two forms. In a basic format it can involve the assumption that a line of action remains fixed at a certain position whenever a joint angle exceeds a certain value. This format while being successfully applied by Seireg and Arvikar (1973) and Nicol (1977) to knee and elbow joints respectively is over simplified for application to a generalized glenohumeral joint study (see figure 3.9). Shoulder studies have employed a

technique where the hard tissues are modelled as solid objects and the muscles are constrained to pass over and around them. The parameters required to implement this type of algorithm are generally poorly documented in the literature. For example, the constraint placed on a muscle line of action by hard tissue was modelled as, "a simple geometric one" in the study of Högfors et al (1987). A similar but more elaborate technique was used by Van der Helm et al (1992). In this finite element study, the bony contours of the various shoulder hard tissues were modelled as simple geometric shapes (cylinder, sphere, ellipsoid and line). The muscle lines of action were then taken to be the shortest (geodesic) path between the origin and insertion positions, while wrapping around the geometric shapes. While this algorithm does allow the calculation of a theoretical muscle line of action, this line is generated irrespective of the true line position (see figure 3.9).

The techniques described for determining a muscle line of action have all assumed that the centre of force in a muscle lies in a direct line between the origin and insertion (effective or real) positions. Anatomically this may not be the case. Instead, the centre of force may be through the centroid of the muscle belly when it is viewed in cross section. Theoretically this would tend to distort the line of action for a muscle. Realistically, to investigate muscle force generation in such detail would also require muscle fibre pennation angles to be considered, further complicating the process. In reality while some research has been conducted into determining the line of centroids through certain muscles, successful application of the technique to general glenohumeral modelling has been limited.

3.4.2.2. Muscle Force

The tensile force generated within a muscle is a function of neurological, anatomical and physiological factors. Although some studies have attempted to link muscle force to these factors, results have been limited. In normal biomechanical studies, the individual muscle forces are obtained by equating their combined effect to the required internal joint moment.

In a simple three degree of freedom joint, the three components of required internal joint moment would ideally allow the solution of three individual muscle forces. Unfortunately, the glenohumeral joint is crossed by eleven muscles. The resulting system is classified as an indeterminate system where there are more unknown muscle forces than equations to solve them.

Many approaches have been developed for resolving this indeterminate system. One of the commonly used techniques has been to reduce the number of unknown muscle forces through either grouping by their functional characteristics or elimination based on EMG

observation (An et al, 1984). Shoulder studies by Inman et al (1944), de Luca and Forrest (1973) and Poppen and Walker (1978) all grouped shoulder muscles by function. Using this approach, these studies modelled major muscle and joint loading during humeral abduction. Unfortunately, much of the detailed information on functional interrelationships between the hard and soft tissues is lost as a result of the simplification.

Other techniques for resolving the indeterminate problem have included basing relative muscle forces on predetermined ratios and also as a function of muscle cross sectional area (An et al, 1984). Neither have been commonly employed in shoulder modelling.

Alternatively, optimization of muscle forces using some predetermined criteria has been used to determine a unique solution to the indeterminate system. This technique does not require the simplification of the physical system and the objective criteria can reflect arbitrary physiological or pathological factors. Many recent biomechanical studies have utilized this type of optimization approach (Seireg and Arvikar, 1973, Crowninshield, 1978, Crowninshield and Brand, 1981, An et al, 1984, Bean and Chaffin, 1988 and Karlson, 1992).

All optimization techniques arrive at a solution by determining the combination of muscle forces that optimize some predetermined criterion (the objective function) while staying within the constraints placed on the system. Two examples of the typical constraints used in such an analysis would be for all muscle forces to be tensile only and the combined muscle effect must equal the required internal joint moment while simultaneously, an objective function such as minimization of total muscle forces or total muscle stress is optimized.

Optimization formulation can be either linear or nonlinear. If the criteria and constraints developed for the optimization are linear in terms of the system variables, solution using a Simplex (or similar) algorithm is simple and robust (Bean and Chaffin, 1988). Nonlinear optimization formulation requires a nonlinear optimisation algorithm to achieve a solution. These are typically complex and convergence to a solution is not always possible (An et al, 1984).

Controversy has surrounded the use of optimization techniques for resolving the indeterminate system. Some early biomechanical studies optimized total muscle or total joint force (Seireg and Arvikar, 1973 and Yeo, 1976) using the rationale that the body would physiologically optimize overall system effort (An et al 1984). It was found that using either objective function, resulted in the muscle with greatest moment generating potential (largest moment arm) always being chosen to generate the required joint moment. Comparison to EMG and results from palpation study showed that this predicted muscle activation was not

physiologically correct (Yeo, 1976 and Barbenel, 1983). Crowninshield (1978) utilized an objective function minimizing total muscle stress. This formulation therefore made the predicted muscle activation a function of muscle cross-sectional area. In a further study by Crowninshield and Brand (1981), optimization criterion was muscle endurance where endurance was related to muscle stress. Results of both studies showed that reasonably physiologically correct muscle activation could be predicted with the proper choice and implementation of an optimization technique.

More recently, a new approach was developed by An et al (1984) for the formulation of the objective equation. In this technique the overall maximum muscle stress is minimized. Mathematically this would be written as:

$$\begin{aligned} &\text{Minimize,} && \sigma && (3.14) \\ &\text{for} && \sigma \geq F_i/PCSA_i, && i = 1 \text{ to } n \end{aligned}$$

where n is the number of muscles included in the optimization, $PCSA_i$ and F_i are the physiological cross-sectional area and force of the i^{th} muscle. In their study, the predicted muscle activation was compared to those predicted by an EMG study. They found the results of the new technique to be in close agreement with the EMG results. In general, the technique favoured equal muscle stress distribution throughout the synergistic muscles. In the one degree of freedom model they used, this corresponded to the muscle forces being directly related to their cross-sectional areas. In a three degree of freedom model, such as is required for the shoulder, muscle function is more complex so this simple relationship between cross sectional area and force would not be expected.

An improvement to the minimization of overall maximum muscle stress was proposed by Bean and Chaffin (1988). They recognised that although the original technique would resolve the indeterminate system, the solution was not necessarily unique. This meant that for a certain minimum overall maximum muscle stress, different combinations of muscle activation could still be possible. In addition, the advantages of maintaining a relationship between predicted muscle force and joint loading had been recognised. A new technique, sympathetic to both of these ends was devised. A second optimization was implemented on the system using the optimized muscle stress of the first as a muscle stress limit. The second optimization minimized the sum of the muscle forces. Being linear the technique was easily implemented, and maintained the advantages of predicting synergistic muscle activation and the physiological relationship between muscle activation and joint loading.

Using either the optimization or simplification approach to resolving the indeterminate system, yields individual muscle forces required for particular segment kinematics and external loading. Due to the small moment arms that muscles typically utilize, their forces can become very large in comparison to the external loading of the segment.

3.4.3. Joint Contact Forces

The forces transmitted across the articular surfaces of a joint are the result of both external segment loading and internal soft tissue forces. In a normal functioning joint, these forces can reach many times body weight for even simple activities.

Calculating joint contact force magnitude and direction involves considering the combined effect of both external segment and internal tissue forces. For equilibrium, the overall net force on the segment must be zero. Since both external segment and internal soft tissue forces are known, joint force can be calculated using the equation:

$$\Sigma(\text{all forces on segment}) = 0 \quad (3.15)$$

where,

$$\begin{aligned} \Sigma(\text{all forces on segment}) = & \Sigma(\text{external segment forces}) \\ & + \Sigma(\text{soft tissue forces}) \\ & + (\text{joint contact force}) \\ & + (\text{friction forces}) \end{aligned}$$

The friction forces in this equation are usually small in comparison to the other parameters for normal joints, and as such are not considered in this analysis. In a three-dimensional analysis, equation 3.14 can be applied in each of the three cartesian coordinate directions, yielding three independent joint force components. These three orthogonal components can be combined to determine the magnitude and direction of the resultant total force transmitted across the joint articular surfaces.

3.5. SHOULDER MODELS

Modelling the function of the human shoulder has been ongoing for at least the past fifty years. To understand the technical aspects and limitations of current shoulder models, a brief review of the shoulder models and their results appearing in the literature is desirable.

Early shoulder models typically utilized two-dimensional analysis techniques to analyse glenohumeral function during humeral flexion and abduction.

One of the first thorough shoulder studies was undertaken by Inman et al (1944).

Shoulder kinematics and muscle and joint loading were investigated using two-dimensional roentgenographs, an EMG study and a detailed anatomical study. The analysis technique did not include any three-dimensional information regarding scapula or humeral positioning, and only a simplified line of action for deltoid muscle force. No other muscles were considered to function as humeral elevators. Muscle EMG data was not normalized, and therefore could not be evaluated quantitatively. Instead these data were used to investigate qualitatively, the muscle activity during flexion and abduction. They estimated that maximum glenohumeral joint compression was achieved at 90 degrees of elevation reaching a maximum of 10.2 times the extremity weight. This corresponds to approximately 0.90 times body weight if their estimate of extremity weight equalling 0.09 times total body weight is used.

de Luca and Forrest (1973) developed a model for investigating shoulder function during pure abduction. Joint kinematics were determined by two-dimensional roentgenographs. Muscle lines of action were determined from these two-dimensional roentgenographs and goniometer measurements based on surface palpation. The only muscles included in this model were deltoid (3 parts) and supraspinatus (1 part). Forces of both muscles were modelled as straight lines passing through their origins and insertions. Only the components of the lines of action acting in the frontal plane were considered, thereby considering only the elevation component of each muscle's action. Relative muscle force estimated from normalized EMG data was used to solve the indeterminate problem. Although the model was complete, no overall results were given for joint and muscle loading.

Poppen and Walker (1978) investigated shoulder function at six discrete positions of humeral abduction in the scapular plane. They used two-dimensional roentgenographs of three cadaveric specimens to determine muscle lines of action and joint kinematics. The muscles were highlighted in the roentgenographic images by implanting radiopaque wires along their centre-lines. This allowed their lines of action in the scapular plane to be accurately measured. Since no three-dimensional information was included, their components out of the scapular plane were not considered. To solve the indeterminate problem, muscle force was considered to be proportional to cross-sectional area times integrated EMG signal for each muscle. This integrated EMG signal consisted of a value between 0 and 4 representing its relative magnitude, as measured experimentally. No further details of the EMG study or value allocation were given. This study estimated that maximum glenohumeral joint compressive force reaches 0.89 times body weight at 90 degrees of abduction while the maximum superior shearing force on the glenoid reaches 0.42 times body weight at approximately 60 degrees of abduction. No estimate of the

glenohumeral joint antero-posterior shearing force was given as the analysis was limited to only the scapular plane.

All three of these early shoulder models suffered from the simplifications which they utilized in their analysis techniques. They all used two-dimensional roentgenographic techniques to measure joint kinematics and in the case of the last two, muscle lines of action as well. Kinematically, the shoulder is a truly three-dimensional joint. Therefore, restricting an analysis of its function to elevation in the scapular, frontal or sagittal planes limits the applicability of the results of the study. Muscles of the shoulder that are active during elevation also contribute to humeral antero-posterior swing and internal-external rotation. None of these studies considered either of these other muscle actions. In general, although these studies do give an insight into shoulder function under very restricted circumstances, they do not afford an understanding of real-life glenohumeral joint function.

The move to three-dimensional shoulder models was a significant step in the development of modelling shoulder function. With such models, it should be possible to analyse shoulder function for real-life activities unimpeded by earlier limitations. Unfortunately, there are many difficulties associated with three-dimensional shoulder modelling. The first of these is accurate determination of segment kinematics. Both scapula and clavicle orientation and position are difficult to determine accurately, due to their subcutaneous location on the rib cage. Without this kinematic information, no three-dimensional model is possible. Upper limb loading is also difficult to determine accurately. This is a result of the large variety of complex loading situations which the upper limb and hand can routinely encounter. Finally, muscle lines of action change dramatically over the wide range of shoulder kinematics, complicating the process of determining muscle function.

An early attempt at three-dimensional shoulder modelling was made by Dvir and Berme (1978). Based on literature and their own results, they produced a spatial linkage system that mimicked normal shoulder kinematics during elevation. Although this is a three-dimensional model, it only describes kinematics during elevation, thus limiting its applicability for studying real-life shoulder function.

The development of a three-dimensional shoulder model has been partially outlined through the articles by Pronk (1989), Veeger et al (1991), Van der Helm and Veebaas (1991) and Van der Helm et al (1992). This model is based on a finite element analysis technique with many of the required geometric and inertially required parameters being obtained from cadaveric studies. Using the finite element approach has allowed the use of standard engineering analyses packages to be applied to the study, simplifying model implementation and development. Overall kinematics are determined by a combination of experimentally

measured and model-predicted values. The model predicts scapula and clavicle kinematics by assuming rib cage shape to be elliptical and scapula medio-lateral rotation to be closely related to humeral elevation. As a result, by measuring acromioclavicular joint position and trunk and humeral orientations all the relevant kinematics can be defined. Muscle wrapping is corrected for by using the shortest line over the physical constraint, where the constraints are modelled as simple geometric forms. No information is given with respect to the method used to resolve indeterminacy or measuring hand loads.

While applications and verification of this model are not documented in the literature its possible drawbacks can be predicted. Firstly, by not measuring actual subject kinematics or geometry, any related inter-individual differences between test subjects will be lost. In addition to this, while muscle wrapping is considered, the technique employed makes no allowance for the physical restrictions imposed on the soft tissues by anything other than hard tissues. The result is a model that while yielding limited insight into normal joint function, makes few allowances for inter-individual differences between test subjects.

Karlsson (1992) outlined the details and simple application of a three-dimensional shoulder model. Kinematics for this model are based on the three-dimensional shoulder rhythm developed by Högfors et al (1991). This rhythm utilises a series of polynomials to link clavicle and scapula kinematics to the humerus. Geometric parameters used are outlined in Högfors et al (1987). This included muscle origin and insertion positions and simplified hard tissue shapes for wrapping corrections. Wrapping correction details were not given but stated simply as the muscles passing over the simplified geometric forms. Indeterminacy is resolved by using an optimization approach, minimizing the sum of the square of muscle stresses.

Documented applications of this model include shoulder loading for simple humeral elevation and also an ergonomically related study of shoulder loading during hand drill use. For the simple elevation, differences were encountered between earlier EMG muscle activation and predicted muscle activation. Predicted joint compressive forces reached a maximum of approximately 0.8 times body weight which roughly agree with those of Inman et al (1944) and Poppen and Walker (1978). In the hand drill study, both humeral kinematics and hand loading were assumed to be constant, contrived values. Although no verification was included, joint loading was predicted to be up to approximately 1.3 times body weight.

The application and accuracy of this model is limited by several factors. Determining scapula and clavicle kinematics using a rhythm that is the average of a series of normal shoulders, eliminates any inter-subject details that might be important to individual shoulder function. Similarly, using contrived humeral kinematics and hand loading will again tend

to eliminate any inter-subject details that would be associated with a real-life activity. Wrapping, while not detailed, is a major source of error in a model of this type, and as such is an important aspect of the model.

3.6. TOWARDS A NEW SHOULDER MODEL

Clearly, current shoulder models fall short of providing detailed information on individual shoulder function for real-life activities. The need therefore still exists for a model suitable for studying detailed three-dimensional shoulder function. Such a model should allow the analysis of a variety of real-life activities, producing verifiable, detailed results of shoulder function for an individual subject.

The shoulder model detailed in this thesis has been developed to answer this need. The model encompasses kinematics and loading of the entire upper limb and shoulder, but focuses only on the glenohumeral joint and surrounding tissue function and loading. It is fully three-dimensional, allowing analysis of a wide variety of real-life activities. Detailed information is included in the model to tailor modelling parameters for each subject. In addition, both kinematics and loading information are measured experimentally in real time for each subject. As a result, inter-subject real-life functional differences are not lost through the modelling process.

Verification is an important aspect of any model development and the model detailed in this work is no exception. Through a combination of studies into model sensitivity to input uncertainties and comparison to literature and an EMG study, a measure of model performance is achieved.

The remainder of this work documents the development, details, implementation and verification of this shoulder model.

CHAPTER 4. IN PREPARATION FOR A NEW SHOULDER MODEL

A large amount of accurate data is required to model shoulder function properly. Therefore, an essential part of understanding the function and limitations of such a model is an understanding of the sources and manipulations of the data used by the model. This chapter focuses on this data, and in particular how it was obtained and what calculations were required to convert it into a useable format.

The information presented in this chapter can be divided as to whether it is activity related or not. The first two sections consist of data which are not activity related, such as anthropometric and anatomical data. The last two sections focus on data that is activity related, for instance hand loading and segment kinematics during an activity of interest.

4.1. ANATOMICAL DATA

Anatomical data utilized by this shoulder model consist of origins, insertions and physiological cross-sectional areas for all the muscles of the shoulder plus joint centre locations and geometry of the related hard tissues. For this study, all of these data have been obtained from either cadaveric or dry bone studies.

To describe locations of the anatomical points of interest, each hard tissue link associated with the shoulder has an origin and cartesian coordinate system defined for it. The location of the anatomical points of interest are then simply described as their three-dimensional location within that coordinate system.

To obtain a representative set of anatomical data corresponding to a normal subject, an averaged set of data can be compiled. This is accomplished by averaging the normalized dimensions of the points of interest. The normalized values are simply the original dimensions divided by some standard dimension for the specimen. For example, a set of humeral coordinates from a specimen could be normalized by dividing them by overall humeral length.

Two sources have been used for the anatomical data used in this study. The first was the cadaveric study of the shoulder by Johnson (1990). This study was complete for the shoulder girdle but omitted the required data related to the humerus and forearm. As a result, a dry bone study of the scapula, humerus and forearm was conducted.

The cadaveric study by Johnson (1990) involved detailed measurements being made on 3 specimens (six shoulders). The anatomical coordinate data were obtained through a combination of dissection and biplanar roentgenographic measurements. Using this approach, points of interest were marked during dissection using radiopaque marker pins.

Biplanar radiographs were then made of the specimen. Using the radiographic images, three-dimensional coordinates of the points were then reconstructed. The entire procedure was repeated several times, each allowing a deeper layer of musculature to be studied. Muscle physiological cross-sectional areas were calculated by dividing muscle volume by fibre length.

A dry bone study of the scapula, humerus, radius and ulna was conducted for this thesis. Measurements were made of the three-dimensional coordinates of muscle origins and insertions, joint centre locations and also several geometric parameters.

Three complete sets of bones were measured, consisting of two right and one left arm. A flat sheet with X and Y coordinate axes marked on it was used as a base for mounting the bone to be measured. Each bone was mounted using a set of polymer posts and flexible adhesive. Adjustments were made in alignment to locate the bone origin, X and Y axes above and parallel to those of the flat sheet. Points of interest were identified using McMinn and Hutchings (1988) and an earlier cadaveric investigation as reference. Measurements were made using a combination of inside, outside and straight callipers. Measurements for each bone were normalized by dividing them by their associated bone scaling dimension. These normalized measurements were then averaged with the other two specimens to produce the average scaled anatomical data. Appendix A contains a complete listing of the results of this study.

Using the averaged scaled anatomical data from either the cadaveric study or dry bone study, the actual anatomical details of a test subject were predicted. This involved measuring the test subject for the required scaling dimensions. Since all of the bony landmarks used for the scaling dimensions were surface palpable, the dimensions could be measured using calipers and rulers. The averaged scaled data were then multiplied by the subject scaling dimensions to obtain an estimate of the actual anatomical subject details.

Details of the scaling length, origin and coordinate systems used for each of the hard tissues of the shoulder are defined in the following sections.

4.1.1. Trunk

Origin: Centre line of the manubriosternal joint.

X_t : Vertically down (anatomical position).

Y_t : Horizontally to the right, as viewed from behind.

Z_t : Backwards (dorsally).

Vertical scaling dimension: Distance between T1 to T12 spinous processes.

Anterio-posterior scaling dimension: Distance from origin to T4 spinous process.

The original work by Johnson (1990) used a left handed trunk coordinate system. This was not desirable so the Z axis was reversed to the direction shown above. All affected anatomical data were also updated.

The vertical scaling dimensions quoted in the original study did not correspond numerically to the definition given. To correct for this, the anatomical data were returned to the original format using the quoted scaling dimensions, and then normalized again using the definition stated above. This new scaling dimension was obtained from the data for each specimen as coordinates for both the T1 and T12 spinous processes were given in the study.

Johnson's study only used a vertical trunk scaling dimension. This was found to not give a good representation of the test subjects, so the antero-posterior scaling dimension was added. This distance used was contained within the original study results, allowing straightforward implementation of the change.

4.1.2. Clavicle

Origin: Centre of the sternoclavicular joint.

X_c : Through the acromioclavicular joint.

Y_c : Normal to the planar surface, of the superior dorsal end.

Z_c : Cross product of X_c and Y_c axes (pointing posteriorly).

Scaling dimension: Overall clavicle length.

A discrepancy was found in the work by Johnson (1990), relating to the clavicle. The normalized coordinates appear to have been incorrectly transcribed since the Y_c dimensions were much larger than those in the X_c direction. Normalized coordinates were then inspected for each axis of the clavicle coordinate system. It was observed that through reordering the axes, the anatomical coordinate data would accurately describe muscle origin positions as observed on dry bone samples and in the literature. With this confirmation, the normalized anatomical coordinates were reassigned to their apparent proper axes. This caused study results for the X, Y and Z axes to be reassigned to the Z_c , X_c and Y_c axes respectively.

4.1.3. Scapula

Origin: Centre of the acromioclavicular joint.

X_s : Through the inferior angle.

Y_s : Pointing medially, in the plane defined by the X_s axis and the point of intersection between the medial border and scapular spine.

Z_s : Cross product of X_s and Y_s axes (pointing anteriorly).

Scaling dimension: Distance between the acromioclavicular joint and inferior angle.

Additional scapular measurements included glenoid fossa orientation. To describe this orientation, a glenoid fossa coordinate system was first defined.

Origin: Geometric centre of the fossa.

X_{gf} : Parallel to the intersection line between the X_s - Y_s plane and the glenoid fossa rim, pointing inferiorly.

Y_{gf} : perpendicular to X_{gf} directed into the fossa.

Z_{gf} : Cross product of X_{gf} and Y_{gf} (pointing anteriorly).

Using this coordinate system, fossa orientation was described using two angles. The first describes fossa tilt around the Z_s axis, and is the angle formed between the X_s and X_{gf} axes. The second describes anterior fossa tilt around the X_{gf} axis. This is the angle formed between the Y_{gf} axis and the line joining the fossa centre to the point of intersection between the medial border and scapular spine.

4.1.4. Humerus

Origin: Centre of humeral head.

X_h : Parallel to proximal aspect of shaft centre line.

Y_h : Parallel to rotation axis of elbow, pointing laterally.

Z_h : Cross product of X_h and Y_h axes (pointing posteriorly).

Scaling dimension: Distance between humeral head top and the elbow epicondyles.

Additional humeral measurements included: head diameter, shaft diameter, head to shaft offset distance, retrotorsion angle and elbow carrying angle, in the X_h - Y_h plane.

4.1.5. Ulna

Origin: Intersection of ulnar shaft centre line and elbow joint centre.

X_u : Parallel to shaft centre line, pointing distally.

Z_u : Cross product of X_u and elbow rotation axis (pointing posteriorly).

Y_u : Cross product of Z_u and X_u axes (pointing laterally).

Scaling dimension: Overall ulna length.

Additional ulnar measurements included: elbow centre to ulnar head distance and approximate average distance between ulnar and radial centre lines .

4.1.6 Radius

Origin: Intersection of radial shaft centre line and elbow joint centre.

X_r : Parallel to shaft centre line, pointing distally.

Y_r : Parallel to the hand flexion-extension axis, pointing laterally.

Z_r : Cross product of X_r and Y_r axes (pointing posteriorly).

Scaling dimension: overall ulna length.

4.2. BODY SEGMENT PARAMETERS

Body segment parameters are used by this shoulder model for calculating the external body segment loading due to gravity. The segment parameter information required for this calculation was obtained from the anthropometric study by Drillis and Contini (1966). Combining this information with test subject anthropometric data, allowed gravitational effects to be determined for that subject. For this shoulder model, the upper arm was treated as one segment and the forearm and hand as a second segment.

The magnitude of gravitational force, F_g , on each arm segment of a test subject was calculated using the ratio of segment mass to total body mass determined by Drillis and Contini (see table 3.1). Where the subject body mass was in kilograms and the resulting gravitational force in newtons:

$$F_g(\text{upper arm}) = ((\text{subject body mass}) * 0.062) * 9.81 \quad (4.1a)$$

$$F_g(\text{lower arm}) = (\text{subject body mass}) * (0.036 + 0.015) * 9.81 \quad (4.1b)$$

Before the location of centre of mass in a segment was defined, overall segment length, L , was estimated, using the ratio of segment length to body height determined by Drillis and Contini (see figure 3.7). Both subject height and the resulting segment length were in metres. The equations used to estimate segment length are:

$$L(\text{upper arm}) = (\text{subject height}) * 0.186 \quad (4.2a)$$

$$L(\text{lower arm}) = (\text{subject height}) * (0.146 + 0.108) \quad (4.2b)$$

The distance of the centre of mass to the proximal joint, L_{cm} , was then calculated for each of the two segments. This involved using the ratio of distance from the proximal joint to the centre of mass position over the entire segment length as determined by Contini and Drillis (see table 3.2). The equations used were of the form:

$$L_{cm}(\text{upper arm}) = L(\text{upper arm}) * (46.1/100) \quad (4.3a)$$

$$L_{cm}(\text{lower arm}) = L(\text{lower arm}) * (42.0/100) \quad (4.3b)$$

Combining the gravitational force magnitude, centre of mass position and the knowledge that the gravitational force direction is vertically down, completely describes the effect of gravity on these two segments.

4.3. DETERMINING BODY AND SEGMENT KINEMATICS

Kinematic information for the trunk, clavicle, scapula, humerus and forearm are all required by this shoulder model. For real-life activities, the kinematics of these structures are normally three-dimensional and dynamic in nature.

Measuring detailed kinematics in real time, for activities as varied as those which occur during use of the upper limb is a challenge to the researcher. The method utilized for this study involved placing reflective markers on the subject. Then as the subject performed the activity being studied, a Vicon motion analysis system concurrently measured marker position within the laboratory as a function of time. Combining this with information regarding marker placement and subject geometry allowed the real time subject kinematics to be calculated.

This section covers the techniques used to measure and calculate the required kinematic information. The first subsection, reviews the basic techniques associated with measuring the three-dimensional location of a point within the laboratory. The remaining subsections cover the details of calculating from these point coordinates, the segment and joint kinematics required for the model.

4.3.1. Measurement Basics

The six camera Vicon motion analysis system used for this study measures the three-dimensional coordinates of discrete points within a predetermined laboratory space. To accomplish this it uses a series of cameras, each viewing the measurement space from a different angle. Each camera emits pulsed infrared light, and monitors the reflection of this light from anything in its field of view. When a spherical reflective marker is placed in the

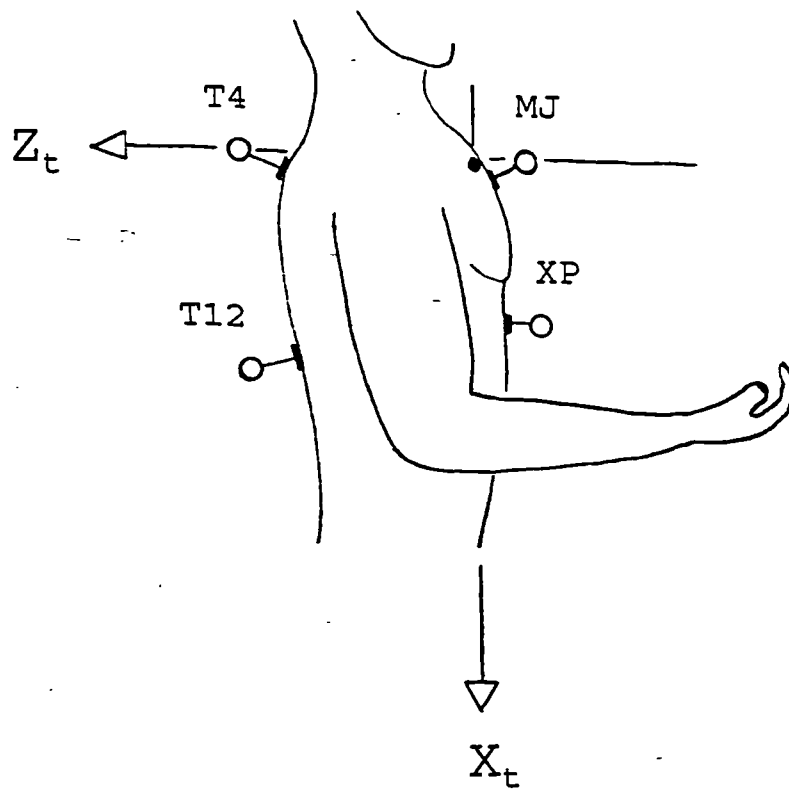


Figure 4.1 Sagittal plane view of the thorax, showing the four spherical reflective markers used for determining trunk kinematics with the motion analysis system. Clockwise from the upper left marker, they are: marker T4, over the T4 spinous process; MJ, over the manubriosternal joint; XP, over the xiphoid process and T12 over the T12 spinous process.

measurement space, each camera receives infrared light reflected back from the marker. The position of the resulting two-dimensional circular image is measured within the field of view of the camera. If this information is combined from two or more cameras, and the camera positions with respect to the measurement space are known, the three-dimensional coordinates of the marker centre can be calculated.

Camera position is determined automatically during a system calibration procedure. This involves placing a set of reflective markers in the measurement space whose three-dimensional coordinates are all known. The motion analysis system then uses the camera images of these calibration markers to calculate the three-dimensional positions of all the cameras. After calibration, the calibration markers can be removed from the measurement space since cameras are statically positioned.

The motion analysis system operates at a predetermined operating frequency. This results in dynamic marker movement being represented as a series of static marker positions. Each of these sets of static marker positions is referred to as a frame of data. The frequency used for this study was 50 Hz.

Marker continuity between frames is maintained through software, so that as long as a marker is clearly viewed by two or more cameras, it is identified as a discrete point. These points must then be manually identified as to their anatomical reference, before the system can generate the required three-dimensional coordinates of the subject markers.

Subject kinematics can be determined from discrete point coordinates in many ways. In general, a line can be defined if the coordinates of two discrete points on that line are known. Expanding on this simple technique allows systems of orthogonal lines or coordinate systems to be developed. If the positions of the discrete points are known with respect to segment anatomy, the coordinate system position for this segment can then be determined. The relative positioning of these segments can then be used to determine joint and segment kinematics. All of the techniques utilized in this study are based on this procedure.

4.3.2. Trunk

Trunk kinematics were determined using three of the four reflective markers placed on the trunk (see figure 4.1). The first, marker MJ, was positioned over the manubriosternal joint, so that with the subject in the anatomical position, it was horizontally level with and directly anterior to the anatomical trunk coordinate system origin. The second marker, T4, was placed horizontally opposite marker MJ, which was nominally over the T4 spinous process. The third marker, XP, was placed over the xiphoid process. The unused fourth marker was placed over the T12 spinous process.

The distance between the manubriosternal joint and marker MJ was required. It was assumed that the marker to skin distance would be equivalent to this. This value was determined by manually measuring the marker centre to skin distance.

A trunk marker coordinate system was then defined as follows:

X_{tm} : Through markers MJ and T4 pointing posteriorly.

Z_{tm} : Perpendicular to the plane defined by X_{tm} and marker XP, pointing to the right.

Y_{tm} : Cross product of Z_{tm} and X_{tm} axes (pointing inferiorly).

with corresponding unit direction vectors: I_{tm} , J_{tm} and K_{tm} . From these unit vectors, a direction cosine matrix, $[B_{tm-lab}]$, relating the trunk marker coordinate system to the laboratory coordinate system was developed.

The origin of this coordinate system was defined to be the same as that of the anatomical trunk coordinate system (the manubriosternal joint). The coordinates of this joint were calculated using the coordinates of marker MJ, direction vector I_{tm} and skin to marker MJ distance. The origin coordinates with respect to the lab were then calculated as:

$$\{X, Y, Z\}_{Or-lab} = \{X, Y, Z\}_{MJ-lab} + (\text{skin to MJ distance}) * (I_{tm-lab}) \quad (4.4)$$

The orientation of the trunk marker coordinate system was calculated for each subject while in the anatomical position, statically facing in the laboratory X axis direction, $+X_{lab}$. In this static position, the anatomical trunk coordinate system was assumed to be parallel and perpendicular to the laboratory coordinate system. The relationship between these two coordinate systems was described by a direction cosine matrix, $[B_{t-lab,static}]$, of the form:

$$[B_{t-lab,static}] = \begin{bmatrix} 0 & -1 & 0 \\ 0 & 0 & 1 \\ -1 & 0 & 0 \end{bmatrix} \quad (4.5)$$

The direction cosine matrix, $[B_{tm-lab,static}]$, relating the trunk marker coordinate system to the laboratory coordinate system was also calculated for this static subject position.

This allowed the direction cosine matrix, $[B_{t-tm}]$, relating the anatomical trunk coordinate system and the trunk marker coordinate system to be calculated as:

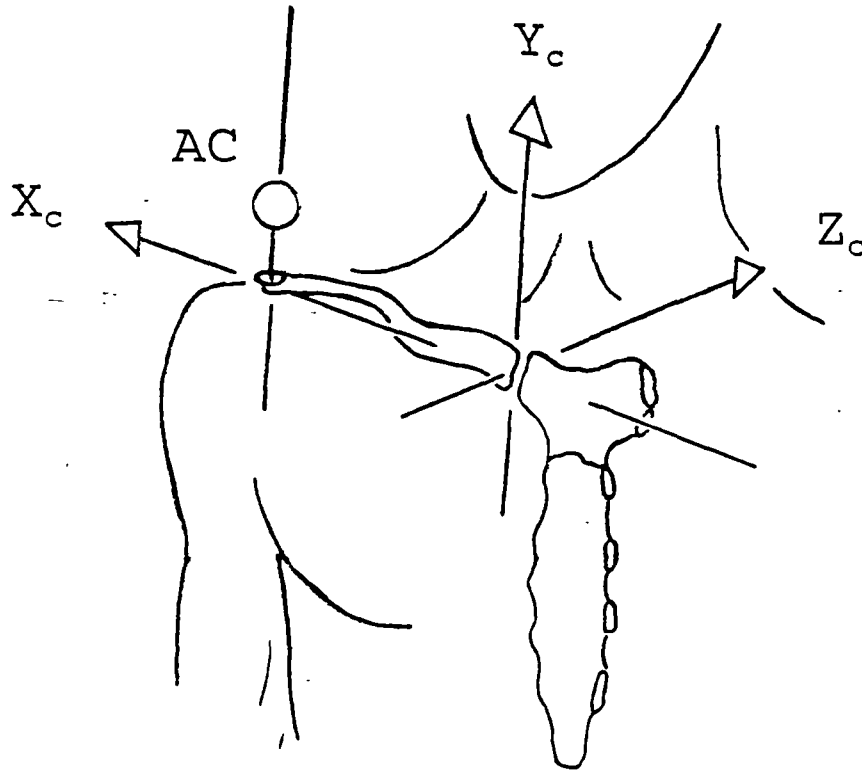


Figure 4.2 Anterior view of the thorax showing the spherical reflective marker used for determining clavicle kinematics with the motion analysis system. Marker AC is placed over the acromioclavicular joint.

$$[B_{t-tm}] = [B_{t-lab,static}] * [B_{tm-lab,static}]^{-1} \quad (4.6)$$

The direction cosine matrix, $[B_{t-lab}]$, describing the relative orientation of the anatomical trunk coordinate system with respect to the laboratory coordinate system could now be calculated for any subject activity using:

$$[B_{t-lab}] = [B_{t-tm}] * [B_{tm-lab}] \quad (4.7)$$

The combination of the three-dimensional origin location and the direction cosine matrix, $[B_{t-lab}]$, completely describes the orientation and position of the anatomical trunk coordinate system for the activity.

4.3.3. Clavicle

Clavicle kinematics were determined using one reflective marker and trunk kinematic information. The marker was placed directly over the acromioclavicular joint (see figure 4.2) and named marker AC. There is little soft tissue overlying the acromioclavicular joint and as a result, artificial motion artifacts due to soft tissue movement are minimized.

The distance between marker centre and acromioclavicular joint centre was required. This value was estimated as being equal the sum of the marker to skin distance, measured manually, and skin to joint centre distance, estimated as 0.01 m from an earlier cadaveric investigation.

Using trunk kinematic information and anatomical data, the clavicle origin (sternoclavicular joint) coordinates with respect to the lab were calculated using:

$$\{X,Y,Z\}_{Oc-lab} = \{X,Y,Z\}_{Oc-lab} + [B_{t-lab}]^{-1} * \{X,Y,Z\}_{Oc-t} \quad (4.8)$$

where the trunk origin with respect to the lab and the clavicle origin with respect to the trunk are $\{X,Y,Z\}_{Oc-lab}$ and $\{X,Y,Z\}_{Oc-t}$ respectively.

Orientation of the anatomical clavicle coordinate system was then determined. The procedure used for this calculation was iterative. The reason for an iterative solution being used was that the direction between the acromioclavicular joint and marker AC was unknown. Without this direction vector, the coordinates of the joint could not be calculated from the known marker coordinates and joint to marker distance.

It was observed that the direction vector was approximately parallel to the Y_c axis for all arm positions. Unfortunately, the orientation of this axis was as yet undefined. To start

the solution process, the direction vector between the acromioclavicular joint and marker AC was assumed to be parallel to the X_t axis. While this is approximately correct for the body in the anatomical position, with increased arm elevation it becomes less accurate.

A position for the acromioclavicular joint was determined using this direction vector, marker AC coordinates and the marker to joint distance. Combining with this, the sternoclavicular joint position and the assumption that there was no X_c axis clavicle rotation, allowed the orientation of the clavicle coordinate system to be defined as follows:

X_c : Through sternoclavicular and acromioclavicular joints pointing laterally.

Z_c : Cross product of X_t and X_c axes (pointing posteriorly).

Y_c : Cross product of Z_c and X_c axes (pointing superiorly).

with unit direction vectors I_c , J_c and K_c respectively and orientation with respect to the laboratory described by direction cosine matrix, $[B_{c-lab}]$.

This newly defined clavicle coordinate system could then be used to improve the original estimate for the marker to joint direction vector, thereby allowing a new joint position to be calculated. If this new joint position was less than 0.002 m from the previously defined position, the iteration process terminated and the new joint position was assumed to be sufficiently correct. If a larger distance was found, the process was repeated.

With clavicle kinematics defined, clinical elevation and protraction angles were calculated using the definition of Pronk (1988). The direction cosine matrix relating the clavicle to the trunk, $[B_{c-t}]$, was required for this calculation. This matrix was calculated using the direction cosine matrices relating the clavicle and trunk to the laboratory coordinate system, $[B_{c-lab}]$ and $[B_{t-lab}]$ respectively.

$$[B_{c-t}] = [B_{c-lab}] * [B_{t-lab}]^{-1} \quad (4.9)$$

The two clinical orientation angles were then determined from this matrix. Recognising the directional differences between the trunk and clavicle coordinate systems when the body is in the anatomical position, and using the matrix $[B_{c-t}]$, the angles were calculated using:

$$\begin{aligned} \text{Clavicle elevation} &= \sin^{-1} (-I_c \cdot I_t) \\ &= \sin^{-1} (-b_{1,1}) \end{aligned} \quad (4.10)$$

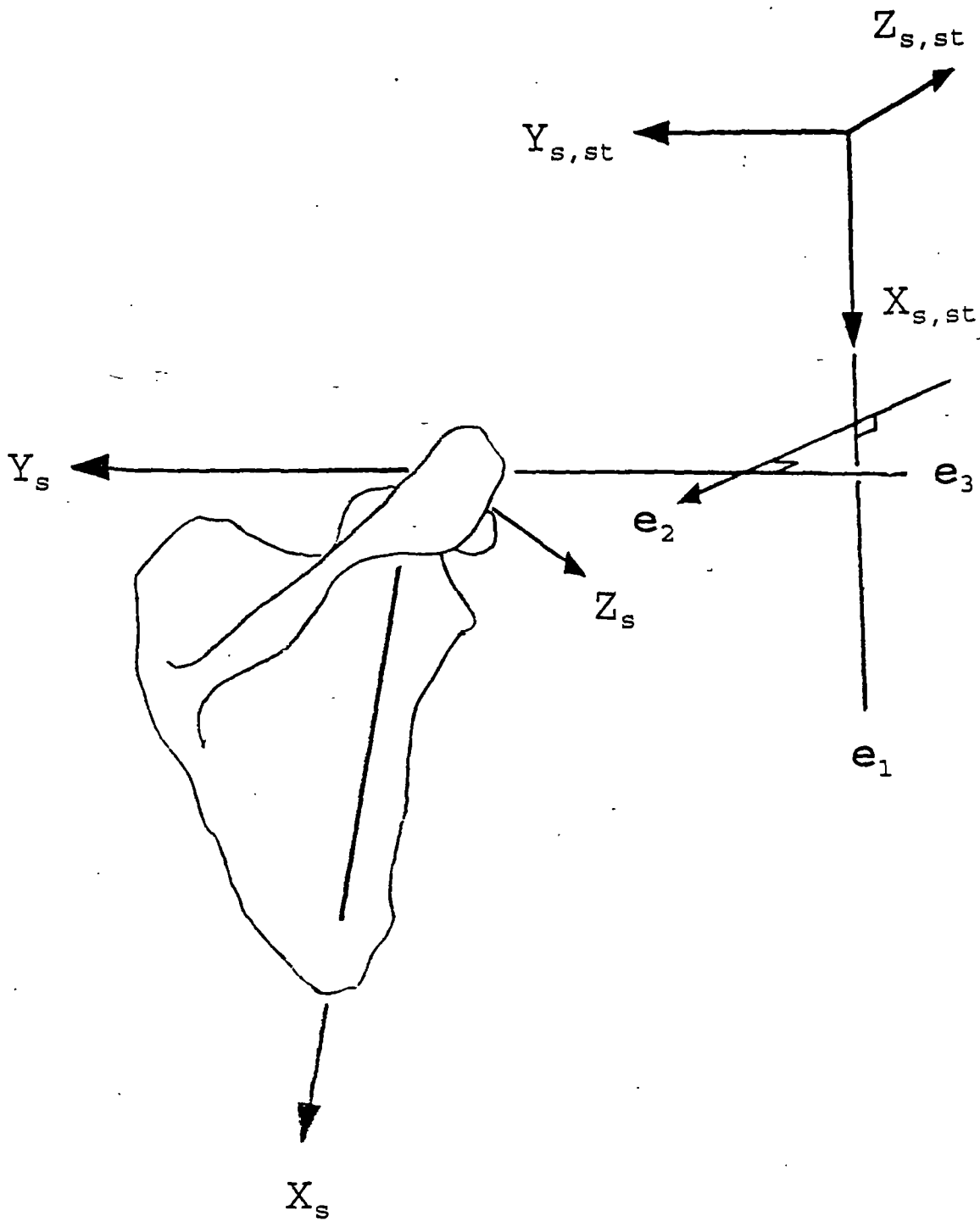


Figure 4.3 Posterior view of scapula, showing the definitions of the rotation axes and angles used for measuring scapula kinematics.

$$\begin{aligned} \text{Clavicle protraction} &= \sin^{-1} (-I_c \bullet K_c) \\ &= \sin^{-1} (-b_{1,3}) \end{aligned} \quad (4.11)$$

4.3.4. Scapula

Dynamic scapular kinematics are difficult to measure. In contrast, static scapula position and orientation can be accurately measured experimentally. To overcome the difficulties associated with dynamic scapula measurement, a technique was developed to allow an estimate of dynamic scapula kinematics to be made using statically measured position and orientation data.

This technique was based on the assumption that dynamic scapula kinematics are closely linked to arm kinematics. As such, static kinematics could be measured along with arm kinematics for a series of static positions covering the range of the dynamic activity. The dynamic scapula kinematics could then be estimated from the measured static scapula kinematics and dynamic arm kinematics.

Static scapula kinematics were measured using two reflective markers and the acromioclavicular joint position. The markers were placed directly over the inferior angle and the intersection of the medial border and the scapular spine, and named IA and MS respectively. These bony landmarks were successfully used by Pronk (1988, 1989 and 1991) for a kinematic verification study. The bony landmarks were located experimentally using palpation for each static position of the subject.

The distances between the two scapula markers and their respective bony landmarks were required. These values were calculated as the sum of marker centre to skin distance and overlying skin thickness. The marker centre to skin distance was known because the markers were secured directly to the skin using double sided tape. Therefore this distance was equal to half the marker diameter, 0.0125 m. Skin thickness was estimated as half the thickness of a fold of skin in the marker region, as measured manually.

Scapula origin (acromioclavicular joint) with respect to the laboratory was calculated using an approach analogous to that used for the clavicle origin in equation 4.8. For the scapula the equation used was:

$$\{X, Y, Z\}_{Os-lab} = \{X, Y, Z\}_{Oc-lab} + [B_{c-lab}]^{-1} * \{X, Y, Z\}_{Os-c} \quad (4.12)$$

Orientation of the scapula coordinate system was determined using an iterative technique. This was used because the direction between the two scapula markers and their bony

landmarks were unknown. Without this directional information, the locations of the bony landmarks could not be calculated.

It was observed however, that the markers could be placed over the bony landmarks in a direction perpendicular to the dorsal scapula surface. Unfortunately, the orientation of this surface was not yet defined. To overcome this difficulty, the direction between the markers and the bony landmarks was assumed to be parallel to the Z_t axis, allowing the bony landmark locations to be calculated. While this assumption is approximately correct for the anatomical body position, movement away from this position makes it less accurate.

Using the marker coordinates, this direction vector and the marker to bony landmark distance, the scapula coordinate system orientation was calculated as follows:

X_s : Through scapula origin and inferior angle, pointing inferiorly.

Z_s : Cross product of X_s and the vector from scapula origin to the intersection of the medial border and scapula spine (pointing anteriorly).

Y_s : Cross product of Z_s and X_s axes (pointing medially).

with unit vectors I_s , J_s and K_s respectively and orientation with respect to the laboratory defined by direction cosine matrix, $[B_{s-lab}]$.

This coordinate system was then used to improve the estimate of the marker centre to bony landmark direction vector. This direction vector was defined as being normal to the dorsal scapula surface (Y_s - X_s plane). Using this new direction vector, an improved estimate for the actual scapula coordinate system orientation was made. If the new bony landmark positions were less than 0.002 m from the previously defined positions, then the iteration process terminated, and the new coordinate system orientation was assumed to be sufficiently accurate. If a larger distance was found, then the process was repeated.

The three clinical scapula orientation angles were calculated using the direction cosine matrix, $[B_{s-lab}]$ and an adaptation of the floating axis technique of Grood and Suntay (1983). The definition of the resulting angles is the same as defined by Pronk (1988) (see figure 4.3).

The stationary coordinate system required for this technique was defined as being parallel and perpendicular to the trunk coordinate system. Its orientation was described by the direction cosine matrix $[B_{s-st-t}]$, where:

$$[B_{s,st-l}] = \begin{bmatrix} 1 & 0 & 0 \\ 0 & -1 & 0 \\ 0 & 0 & -1 \end{bmatrix} \quad (4.13)$$

Using this matrix and the matrices relating the scapula and trunk to the laboratory coordinate system, $[B_{s-lab}]$ and $[B_{t-lab}]$ respectively, allowed the direction cosine matrix describing scapula orientation with respect to the stationary coordinate system to be calculated as:

$$[B_{s-s,st}] = [B_{s-lab}] * [B_{t-lab}]^{-1} * [B_{s,st-l}]^{-1} \quad (4.14)$$

Using this matrix, the three rotation axes required for the floating axis technique were then defined as:

$$e_1 = \{ 1, 0, 0 \} \quad (4.14a)$$

$$e_3 = \{ b_{2,1}, b_{2,2}, b_{2,3} \} \quad (4.14b)$$

$$e_2 = e_3 \times e_1 \quad (4.14c)$$

The calculation of the three rotation scapula rotation angles: protraction-retraction, medio-lateral rotation and forward-backward tipping was then the same as that used in the normal floating axis technique, as shown in equations 3.7, 3.8 and 3.9 respectively.

Using the static scapula kinematics, dynamic kinematics were then estimated. This process required static scapula kinematics to be measured across the range of subject motion encountered in the dynamic activity. Typically, four static measurements were made for each activity. Using linear regression, the relationship between the static scapula orientation angles and a representative arm kinematic variable (humeral abduction, humeral flexion or elbow flexion) was calculated. The dynamic scapula orientation was then estimated using this relationship and the dynamically measured arm kinematics.

4.3.5. Humerus and Forearm

Kinematics of the segments of the upper limb are detailed here as a group. This is a result of the close interrelationship between the segments with respect to determining their individual kinematics.

Anatomical kinematics of the humerus are difficult to measure experimentally. If the

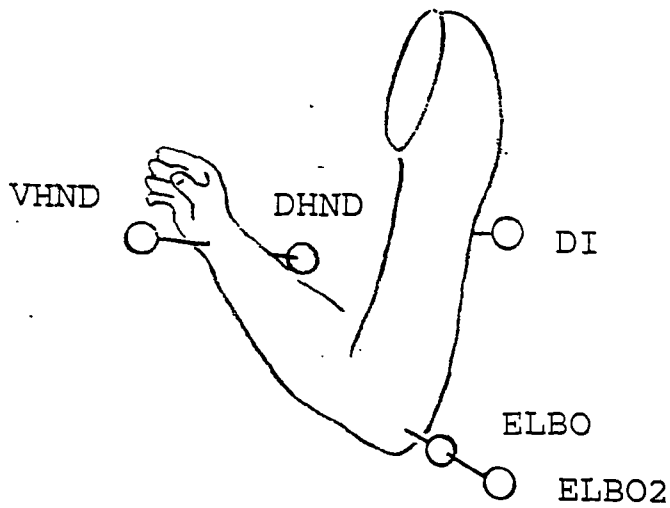


Figure 4.4 Posterior view of a disarticulated arm, showing the five spherical reflective markers used for determining humeral kinematics with the motion analysis system. Moving proximally from the shoulder they are: marker Di, located over the deltoid insertion; ELBO and ELBO2, located at the back of the elbow, ELBO is closer to the skin; DHND and VHND, located on the dorsal and ventral wrist.

elbow is assumed to be a simple hinge, then forearm motion can be assumed planar for elbow flexion-extension, allowing humeral kinematics to be measured. This assumption has been used in shoulder studies by Cyprien et al (1983), Engin and Peindl (1987), Bassett et al (1990) and Johnson (1990). Unfortunately, the carrying angles of the elbow skew the axis of elbow rotation with respect to both the upper and lower arms. The result is humeral internal-external rotation accompanying forearm flexion-extension, if forearm movement is restricted to being planar.

A new technique was developed for this study, to allow humeral kinematics to be determined experimentally. The procedure involved measuring upper arm kinematics using the planar forearm motion assumption. The result is accurate upper arm orientation but not actual anatomical orientation due to the effect of the elbow carrying angles. To calculate the corresponding humeral orientation, the geometric constraints for the elbow rotation axis are imposed on the upper arm kinematics along with the relative positions of the elbow and hand centres. Using an iterative solution, the anatomical humeral orientation and elbow flexion angles were then calculated.

The first stage of this technique was to measure upper arm kinematics experimentally, utilizing the assumption that forearm flexion-extension motion was planar. Five reflective markers were used (see figure 4.4), they included: marker DI placed directly over the humeral centre line at the deltoid insertion; markers ELBO and ELBO2 placed in line, posterior to the elbow centre with the body in the anatomical position; markers DHND and VHND (dorsal and ventral hand markers) placed equidistant to and directly opposite the forearm centre line, on the distal forearm.

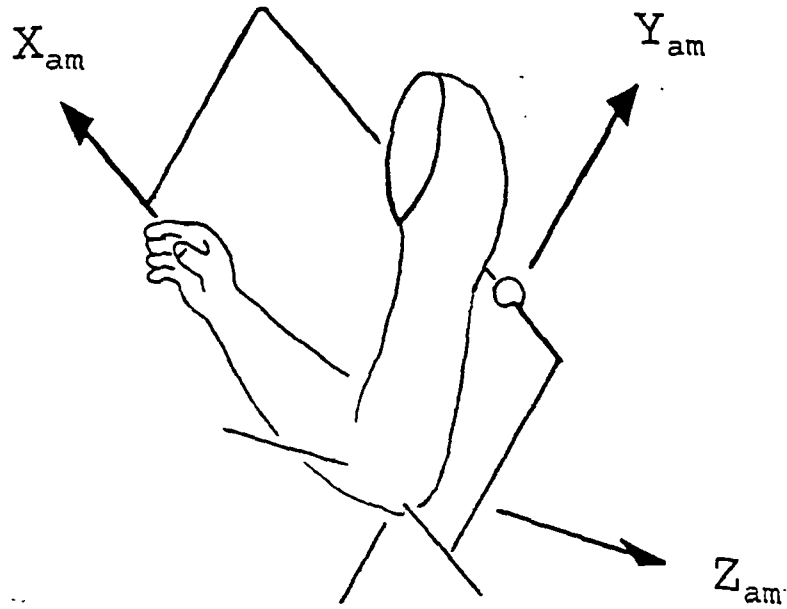
Bony landmark to marker centre distances were required for markers DI and ELBO. The distance between marker DI and the humeral centre line was measured manually, using palpation. The distance between marker ELBO and the elbow centre was also measured manually, using the medial and lateral epicondyles as an indicator to the elbow centre location.

Upper arm and lower arm kinematics were now calculated. This began with the calculation of the elbow centre which corresponds to the anatomic ulna coordinate system origin, using markers ELBO and ELBO2:

$$\{X,Y,Z\}_{\text{Ou-lab}} = \{X,Y,Z\}_{\text{ELBO-lab}} + (\text{ELBO to elbow distance}) * (\{X,Y,Z\}_{\text{ELBO-lab}} - \{X,Y,Z\}_{\text{ELBO2-lab}}) / A_1 \quad (4.15)$$

where,

$$A_1 = [(X_{\text{ELBO-lab}} - X_{\text{ELBO2-lab}})^2 + (Y_{\text{ELBO-lab}} - Y_{\text{ELBO2-lab}})^2 + (Z_{\text{ELBO-lab}} - Z_{\text{ELBO2-lab}})^2]^{1/2}$$



DI to humeral centre line distance

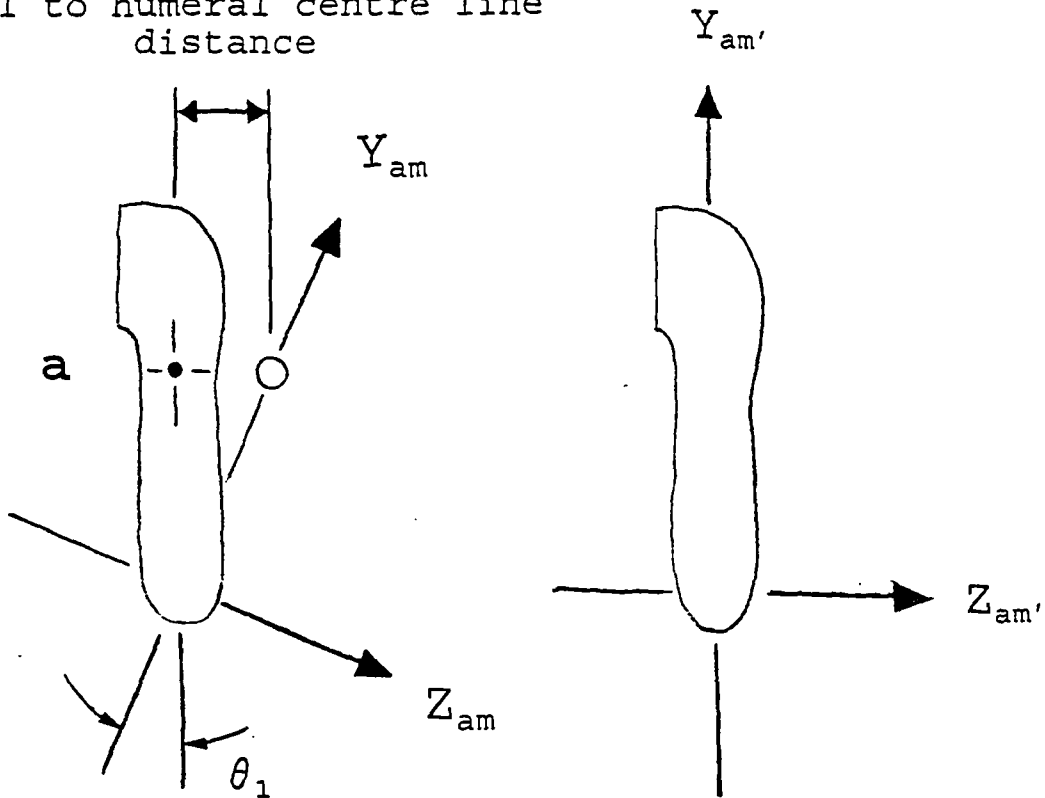


Figure 4.5 (top) Posterior view of a disarticulated arm, showing the arm marker coordinate system.

Figure 4.6 (bottom) Two posterior arm views. On the left, the relationship of the arm marker coordinate system to the arm anatomy, including the humeral shaft centre line at the deltoid insertion, a. The upper arm coordinate system is shown on the right.

Using the elbow centre and position of markers DI, DHND and VHND, an arm marker coordinate system was established (see figure 4.5). For this procedure, the elbow must not be straight. For most arm function, this is normally the case. The coordinate system was defined as:

Origin: Elbow centre.

X_{am} : Through the mid-point between markers DHND and VHND.

Z_{am} : Cross product of X_{am} and a vector through the origin and DI (pointing laterally).

Y_{am} : Cross product of Z_{am} and X_{am} (pointing proximally).

with unit vectors I_{am} , J_{am} and K_{am} respectively and orientation with respect to the laboratory defined by direction cosine, $[B_{am-lab}]$.

Upper arm orientation can be determined from the arm marker coordinate system orientation if the relationship between the two coordinate systems is known. The relationship turns out to be a simple rotation about the forearm centre line (see figure 4.6). To calculate the magnitude of this rotation, the position of marker DI with respect to the arm marker coordinate system must first be known. This value was calculated using:

$$\{X,Y,Z\}_{DI-am} = [B_{am-lab}] * (\{X,Y,Z\}_{DI-lab} - \{X,Y,Z\}_{Ou-lab}) \quad (4.16)$$

The rotation angle magnitude between the two coordinate systems was then calculated using:

$$\theta_1 = \sin^{-1} ((DI \text{ to humeral centre line distance}) / (Y_{DI-am})) \quad (4.17)$$

The arm marker coordinate system can now be rotated about its X_{am} axis by an angle equal to θ_1 . This rotation makes its $X_{am} - Y_{am}$ axes coplanar with the plane defined by the upper arm and forearm. This new arm marker coordinate system orientation was calculated using:

$$[B_{am'-lab}] = \begin{bmatrix} 1 & 0 & 0 \\ 0 & \cos\theta_1 & -\sin\theta_1 \\ 0 & \sin\theta_1 & \cos\theta_1 \end{bmatrix} * [B_{am-lab}] \quad (4.18)$$

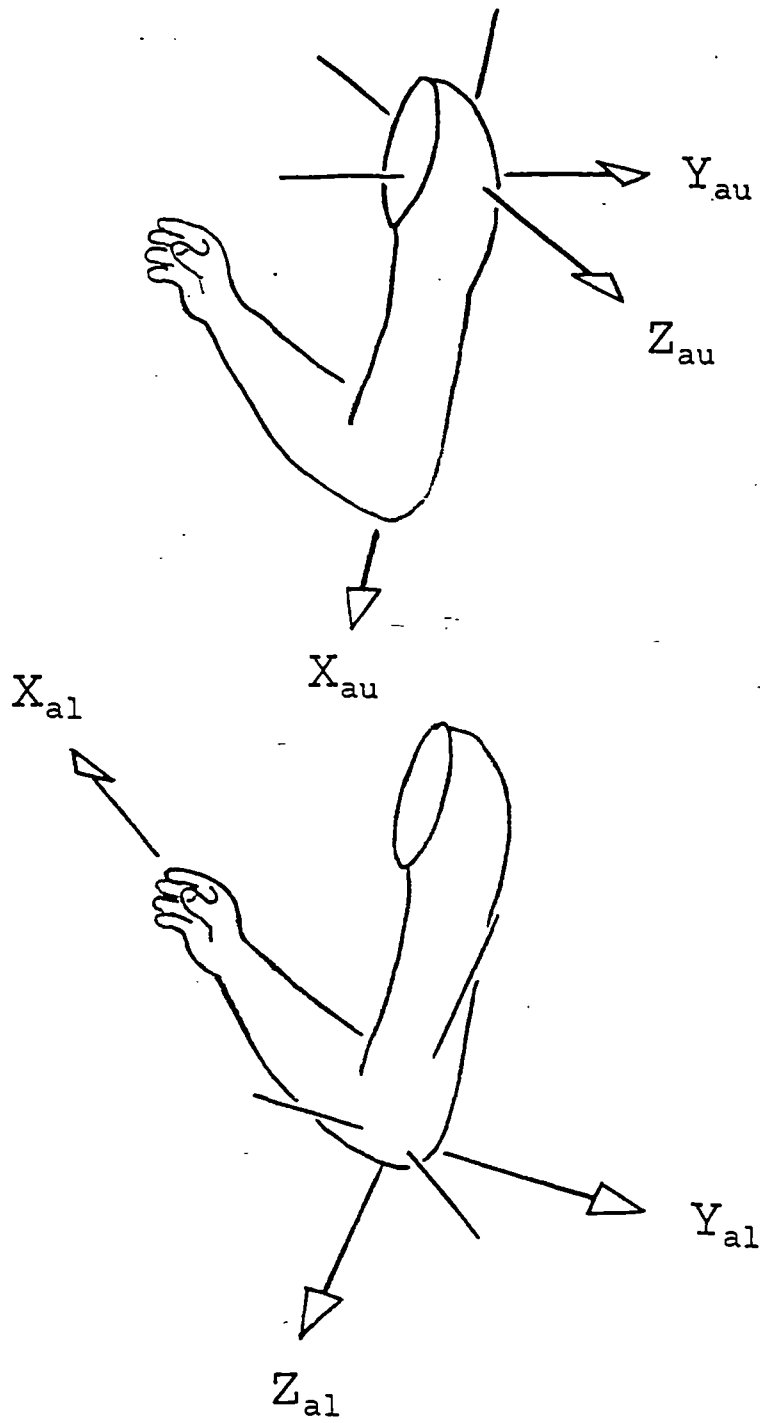


Figure 4.7 (top) Posterior view of a disarticulated arm showing the upper arm coordinate system.

Figure 4.8 (bottom) Posterior view of a disarticulated arm showing the lower arm coordinate system.

The position of a point, **a**, on the upper arm centre line as it passes beneath marker DI can be determined. Using an equation similar to 4.16, marker DI position can be calculated in terms of the new arm marker coordinate system. Using this data, the position of **a** in terms of the new arm coordinate system is now:

$$X_{\mathbf{a-am}'} = X_{\text{DI-am}'} \quad (4.19\text{a})$$

$$Y_{\mathbf{a-am}'} = Y_{\text{DI-am}'} \quad (4.19\text{b})$$

$$Z_{\mathbf{a-am}'} = 0 \quad (4.19\text{c})$$

The position of point **a**, in terms of the laboratory coordinate system is then:

$$\{X, Y, Z\}_{\mathbf{a-lab}} = \{X, Y, Z\}_{\text{Ou-lab}} + [B_{\mathbf{am}'-lab}]^{-1} * \{X, Y, Z\}_{\mathbf{a-am}'}$$

The upper arm coordinate system orientation (see figure 4.7) can now be defined as:

$X_{\mathbf{au}}$: Through point **a** and elbow centre pointing distally.

$Y_{\mathbf{au}}$: Cross product of $X_{\mathbf{au}}$ and vector through the elbow centre and the mid-point between markers DHND and VHND.

$Z_{\mathbf{au}}$: Cross product of $X_{\mathbf{au}}$ and $Y_{\mathbf{au}}$ (pointing posteriorly).

with unit vectors $I_{\mathbf{au}}$, $J_{\mathbf{au}}$ and $K_{\mathbf{au}}$ respectively and orientation with respect to the laboratory defined by direction cosine matrix, $[B_{\mathbf{au-lab}}]$. Similarly, the lower arm coordinate system orientation (see figure 4.8) can be defined as:

$X_{\mathbf{al}}$: Through elbow centre and the mid-point between markers DHND and VHND, pointing distally.

$Z_{\mathbf{al}}$: Parallel to a vector joining markers DHND and VHND, pointing dorsally.

$Y_{\mathbf{al}}$: Cross product of $Z_{\mathbf{al}}$ and $X_{\mathbf{al}}$ (pointing laterally).

with unit vectors $I_{\mathbf{al}}$, $J_{\mathbf{al}}$ and $K_{\mathbf{al}}$ respectively and orientation with respect to the laboratory defined by direction cosine matrix, $[B_{\mathbf{al-lab}}]$.

The hand centre position can be calculated using the lower arm coordinate system orientation, elbow centre coordinates, $\{X, Y, Z\}_{\text{Ou-lab}}$ and the hand centre to elbow distance as measured for each subject. Recognising the hand is in the lower arm X axis direction, $X_{\mathbf{al}}$, from the elbow, its position can be calculated as:

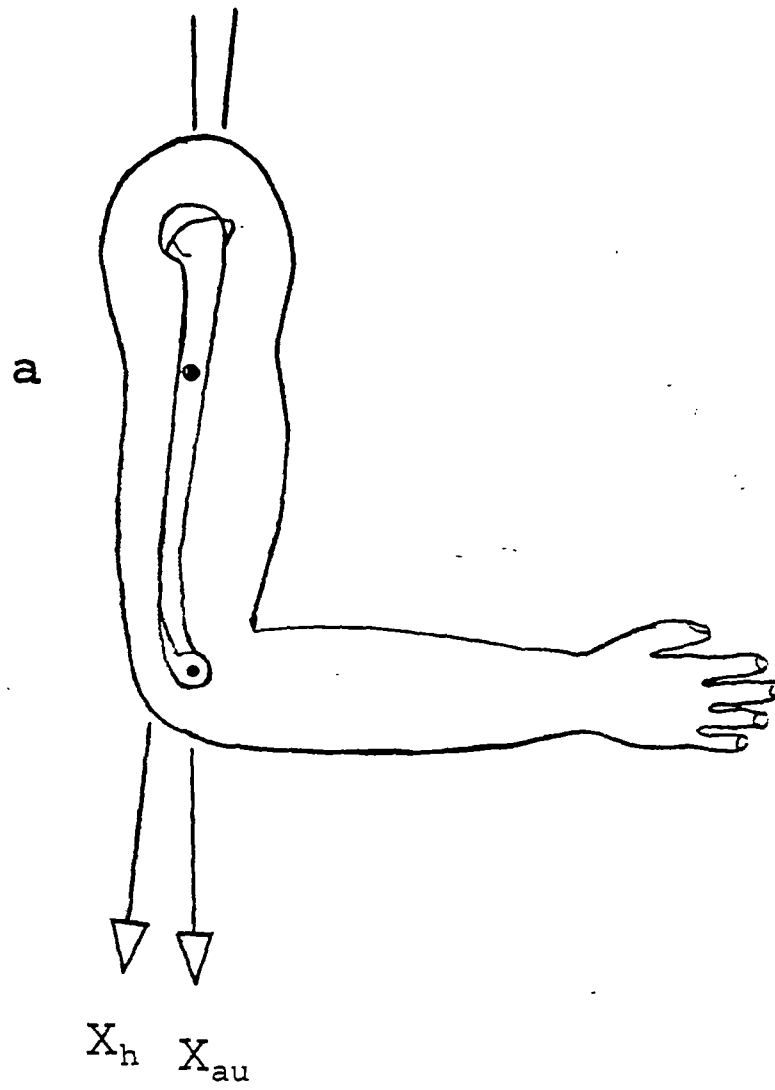


Figure 4.9 Sagittal view of an upper arm and humerus, showing the difference between the definitions of the upper arm X axis, X_{au} , and the humeral X axis, X_h , resulting from elbow forward set.

(4,20)

$$\{X, Y, Z\}_{\text{hand centre-lab}} = \{X, Y, Z\}_{\text{Ou-lab}} + [B_{\text{al-lab}}]^{-1} * \{(\text{hand centre to elbow distance}), 0, 0\}$$

Upper and lower arm kinematics can be determined from their respective direction cosine matrices recognising that in the anatomical position, the coordinate systems for the trunk, upper and lower arms are all parallel.

The trunk coordinate system was used as the stationary coordinate system for determining shoulder orientation angles. Using a floating axis technique adopted from the work of Grood and Suntay (1983), the rotation axes were defined as follows:

$$e_1 = \{ b_{2,1}, b_{2,2}, b_{2,3} \} \quad , \text{from } B_{\text{r-lab}} \quad (4.21a)$$

$$e_3 = \{ b_{1,1}, b_{1,2}, b_{1,3} \} \quad , \text{from } B_{\text{au-lab}} \quad (4.21b)$$

$$e_2 = e_3 \times e_1 \quad , \text{the floating axis} \quad (4.21c)$$

Due to the high degree of arm mobility, this technique does not allow a unique solution for upper arm orientation angles if the humerus is elevated above 90 degrees. To overcome this problem, the floating axis direction is reversed if humeral elevation is above 90 degrees. The upper arm flexion and abduction angles are then calculated using equations 3.7 and 3.8. As a result of the change in floating axis, the quoted upper arm flexion will always be in the range of ± 90 degrees.

The calculation for upper arm rotation is also effected by the floating axis direction change. Upper arm rotation was determined by imposing flexion and abduction rotation sequences on the stationary coordinate system orientation. The resulting coordinate system was then compared to the upper arm coordinate system to determine the rotation angle (about the X_{au} axis) existing between them. This became the value of upper arm rotation.

The upper arm coordinate system was used as the stationary coordinate system for determining forearm orientation angles with respect to the upper limb. Again using a floating axis technique adopted from the work of Grood and Suntay (1983), the rotation axes were defined as:

$$e_1 = \{ b_{2,1}, b_{2,2}, b_{2,3} \} \quad , \text{from } [B_{\text{au-lab}}] \quad (4.22a)$$

$$e_3 = \{ b_{1,1}, b_{1,2}, b_{1,3} \} \quad , \text{from } [B_{\text{al-lab}}] \quad (4.22b)$$

$$e_2 = e_3 \times e_1 \quad (4.22c)$$

The lower arm orientation angles were then calculated using equations similar to equations

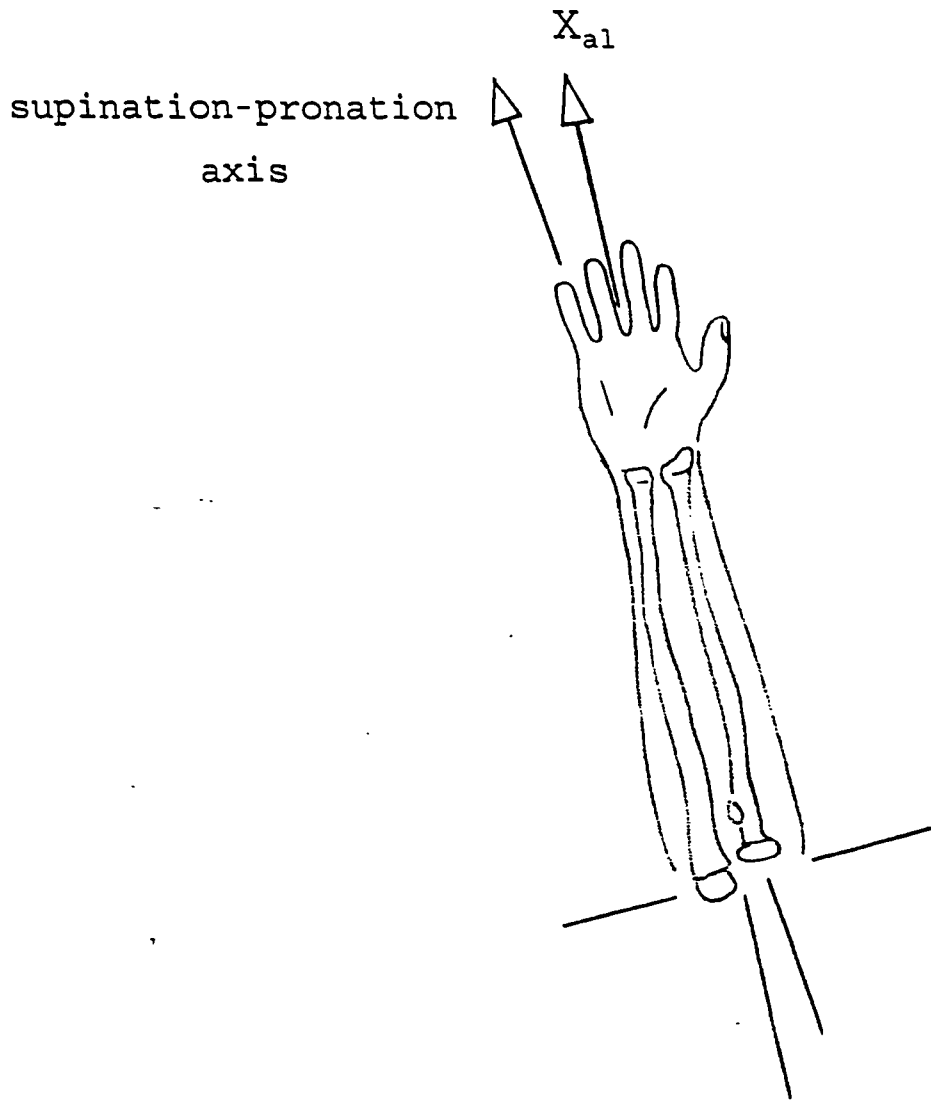


Figure 4.10 Ventral view of forearm, showing the supination-pronation axis definition.

3.7, 3.8 and 3.9. Slight alterations were required in these equations to account for the normal range of motion of the lower arm in both flexion and pronation.

Using upper and lower arm kinematics, the anatomical kinematics of the humerus, ulna and radius can be determined.

To begin the process of solving for these kinematics, the difference between the humeral coordinate system and the upper limb coordinate system had to be accounted for. In particular, the X_{au} axis passes along the long axis of the humerus and between the epicondyles, where the humeral X axis, X_h , was parallel to the shaft (see figure 4.9). The difference between them results from the forward offset of the elbow with respect to the shaft. This difference was corrected by calculating the angle between the two axes and imposing this rotation on the upper arm orientation as measured previously. The angle between axes was assumed to be in the $X_{au} - Z_{au}$ plane.

The humeral X axis, X_h , and the new position of the upper arm X axis X_{au}' should now be parallel. As a result, humeral flexion and abduction can be calculated using the same equations as were used in determining upper arm flexion and abduction but substituting the new upper arm coordinate system orientation for the experimentally measured original.

An iterative procedure was used to solve for the two remaining unknown kinematic variables, humeral internal-external rotation and ulnar flexion. This involved imposing the known anatomical kinematics along with the anatomical bone geometry and the known elbow and hand positions. By systematically incrementing the values for the unknown kinematic variables, the predicted locations of the hand could be compared to the known hand position. The increment used for the two unknown variables was 0.5 degrees, resulting in hand position changes between iterations of approximately 0.005 m. When the residual difference between the two was minimized, the predicted humeral internal-external rotation and ulnar flexion were assumed to be sufficiently accurate.

Several assumptions were required for this iterative procedure. The first was that humeral head offset was ignored, which resulted from the upper arm and humeral X axes being parallel to the humeral shaft centre line. Since the upper arm coordinate system did not consider head offset, then it did not need to be included in this procedure. Humeral and ulnar carrying angles were assumed to be in the $X_h - Y_h$ and $X_u - Y_u$ planes respectively. The rotation axis for forearm pronation-supination was assumed to pass through the ulnar and radial heads (see figure 4.10). The magnitude of forearm pronation-supination was assumed to be equal to that calculated for the lower arm previously.

The result of the iterative procedure was that humeral, ulnar and radial kinematics were completely defined. The definitions of these angles for upper arm elevations over 90 degrees

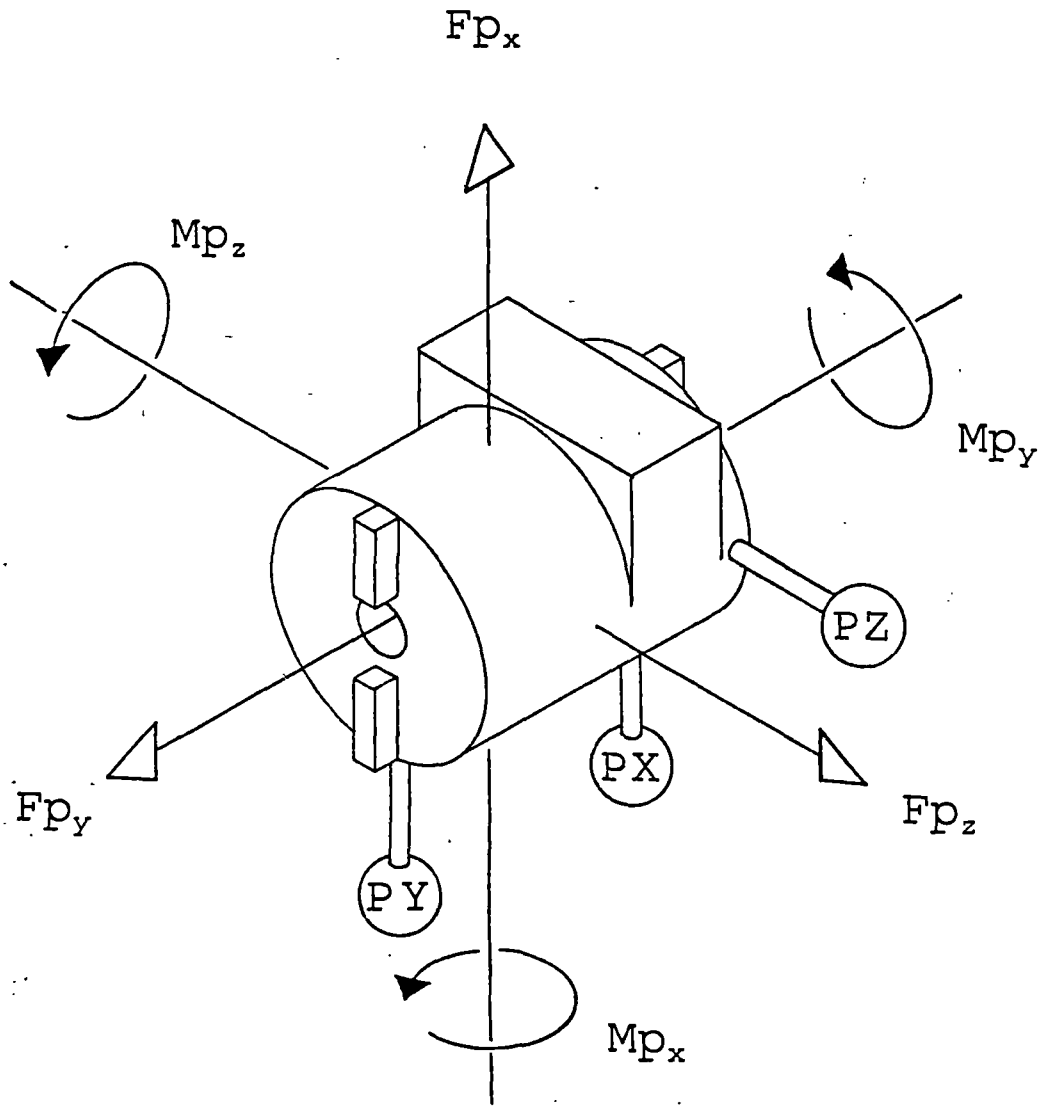


Figure 4.11 Instrumented hand transducer with positive loading conventions shown. These are positive as applied by the transducer to the hand. The three reflective spherical markers, P_X , P_Y and P_Z , are shown in place.

do not agree with normal clinical definitions but they are unique and they do describe limb kinematics accurately.

Origin of the humerus was calculated using scapula position and orientation with respect to the laboratory and the humeral origin with respect to the scapula, $\{X,Y,Z\}_{Oh-s}$. The humeral coordinate system origin position with respect to the laboratory was calculated as:

$$\{X,Y,Z\}_{Oh-lab} = \{X,Y,Z\}_{Os-lab} + [B_{s-lab}]^{-1} * \{X,Y,Z\}_{Oh-s} \quad (4.23)$$

For comparison to two-dimensional studies in the literature, humeral elevation for pure flexion and abduction activities must be known. Unfortunately the floating axis definition change for humeral elevations greater than 90 degrees causes the resulting kinematic variables to be difficult to interpret directly. To address this, humeral elevation was calculated in both the frontal and sagittal planes.

For humeral elevation during abduction, the angle formed between the humeral shaft centre line, X_h , and vertical when projected on the frontal plane was calculated using:

$$\text{Humeral frontal plane elevation} = \cos^{-1} (b_{1,1} / A_2) \quad (4.24)$$

where,
$$A_2 = (b_{1,1}^2 + b_{1,2}^2)^{1/2}$$

and the direction cosine matrix variables, $b_{1,1}$ and $b_{1,2}$ were taken from matrix, $[B_{h-1}]$.

Humeral elevation during flexion was calculated similarly except as viewed in the sagittal plane:

$$\text{Humeral sagittal plane elevation} = \cos^{-1} (b_{1,1} / A_3) \quad (4.25)$$

where,
$$A_3 = (b_{1,1}^2 + b_{1,3}^2)^{1/2}$$

4.4. HAND LOADING

Forces and moments applied to the hand are required for this shoulder model. For real-life activities, these loads are normally three-dimensional and dynamic.

Two techniques were used in this study to measure hand loading. The first involved using a piezoelectric Kistler floor mounted force plate. In the second, loading was measured using a specially designed and constructed strain gauged hand transducer. Both of these devices measured the loads being applied to the hand.

This section details the techniques used to measure and calculate activity hand loads. Included in this is a review of the development and calibration of the instrumented hand transducer.

4.4.1. The Force Plate

The force plate used in this study facilitated the measurement of the forces and moments applied to the hand by the floor. The instrument itself was a Kistler force plate No. 9811b, mounted flush with the floor surface.

The force plate itself consists of a rigid upper plate supported on four posts. Any loading on the upper plate is therefore transmitted through the four supporting posts. The posts are instrumented with piezoelectric material to measure forces in each of the three cartesian coordinate directions. This material generates an electric charge proportional to the change in force transmitted through it. The electrical charges are all conditioned using charge amplifiers and the resulting signals combined to yield eight signal channels. Combining the magnitudes of these signals with calibration information allows the forces and moments applied through the plate to be accurately calculated. Force plate performance was determined by Fleming, et al (1993) and they found that it measured forces within $\pm 0.5\%$ (standard deviation $< 0.5\%$) of the applied force and moments to within $\pm 5\%$ (standard deviation $< 2\%$) of the applied moments. Appendix B gives a listing of the equations and calibration values used for the force plate.

The forces and moments calculated using the force plate, are in terms of a force plate based origin. Hand loads in turn were determined from these force plate loads. For equilibrium between the hand and force plate, the measured forces must be equal to the forces exerted by the plate on the hand. Moments about the X_{lab} and Z_{lab} axes cannot be transmitted between the hand and forceplate. Moments about the Y_{lab} axis applied to the hand can be calculated if the hand is assumed to be at the centre of pressure position on the plate. The coordinates, X_{cp} and Z_{cp} of the centre of pressure with respect to the plate origin can be calculated using the relationships:

$$\sum M_{cp_x} = 0 = M_{fp_x} - (F_{fp_y} * Z_{cp}) + (F_{fp_z} * ay) \quad (4.26a)$$

and,
$$\sum M_{cp_z} = 0 = M_{fp_z} - (F_{fp_y} * X_{cp}) + (F_{fp_x} * ay) \quad (4.26b)$$

The coordinates are then:

$$X_{cp} = (M_{fp_z} + (F_{fp_x} * ay)) / F_{fp_y} \quad (4.27a)$$

$$Z_{cp} = (-M_{fp_x} + (F_{fp_z} * ay)) / F_{fp_y} \quad (4.27b)$$

where F_{fp_x} , F_{fp_y} , F_{fp_z} and M_{fp_x} , M_{fp_y} , M_{fp_z} are the forces and moments measured with the force plate and a_y is the distance of the force plate origin below the floor surface. The moment about the Y_{lab} axis through the centre of pressure is then:

$$M_{cp_y} = M_{fp_y} - (F_{fp_x} * Z_{cp}) + (F_{fp_z} * X_{cp}) \quad (4.28)$$

The forces moments applied on the hand by the plate can then be defined as:

$$\begin{aligned} F_{h_x} &= F_{fp_x} & M_{h_x} &= 0 \\ F_{h_y} &= F_{fp_y} & M_{h_y} &= M_{cp_y} \\ F_{h_z} &= F_{fp_z} & M_{h_z} &= 0 \end{aligned}$$

Using the centre of pressure as the means for calculating M_{h_y} is not the most desirable method. Alternatively, the measured forces and moments could have been applied directly to the joint centres, if their spacial relationship was defined. Unfortunately, programming this type of conversion was complicated by model software architecture. As a consequence, this less accurate method of converting force plate loads into hand loads was used.

4.4.2. The Hand Transducer

The second instrument used in this study for measuring hand loads was the portable, instrumented hand transducer. This instrument was designed to measure the components of forces and moments needed to completely describe hand loading, while not being restrictive in its positioning within the lab. As a result, hand loading was measured for many activities where previously it could not have been.

4.4.2.1 Development and Design

A modular approach was used in the design of this instrument. A variety of mounting systems and hand interfaces were produced for use with the instrumented transducer section.

In general the instrumented transducer section was fashioned after the short pylon transducer currently in use within the department for measurement of prosthesis loading during amputee gait (Berme et al, 1976). The new transducer, while similar in concept to the pylon transducer, was considerably heavier, with a load rating of approximately 3 times the older unit (up to 300 Nm in bending).

Both the pylon and the new hand transducer use elastic strain deformation during loading

to produce an electric output from which the loading particulars can be calculated. The area of the transducer where strain is measured is tubular. To measure strain, the transducer uses a series of foil electrical resistance type strain gauges, bonded to the surface of the transducer. In total 16 strain gauges are used, arranged in two rows around the transducer circumference, forming 6 channels. These channels are sensitive to the corresponding 3 forces and 3 moments transmitted through the transducer. A coordinate system was defined within the transducer, origin at its physical centre and coordinate axes X_p , Y_p and Z_p (see Figure 4.11). Full wheatstone bridges were utilized for each channel. A complete description of gauge placement is outlined in a paper describing the original pylon transducer by Berme et al (1976).

The new transducer was constructed from HE 30TB aluminium alloy, with a proof strength of 120 MPa. In the pylon transducer, insensitivity to axial loading had been a problem which resulted from the pylon design. To make the design stiff enough in bending, it had to be made too stiff to axial loading. Its sensitivity to axial loading was reduced as a result. For this design, to achieve the best compromise between bending and axial loading stiffness, the relationship between wall thickness and transducer diameter as a function of bending and axial load strength was investigated. Using the equations describing stress in a tube loaded axially and in bending, respectively:

$$M = \sigma * I/c \quad (4.29a)$$

where, $I = (\pi/64) * (d_o^4 - d_i^4) \quad (4.29b)$

and, $F = \sigma * (\pi/4) * (d_o^2 - d_i^2) \quad (4.30)$

where M and F are the bending moment and axial load in the tube, σ is maximum stress, I is the area moment of inertia, c is the maximum radius and d_o and d_i are the outer and internal tube diameters (Shigley and Mitchell, 1983). Substituting 4.29b into 4.29a,

$$M = ((\pi * \sigma) / 32d_o) * (d_o^4 - d_i^4) \quad (4.31a)$$

rearranging 4.30,

$$d_i^2 = d_o^2 - ((4*F) / (\pi*\sigma)) \quad (4.31b)$$

and combining equations 4.31a and 4.31b,

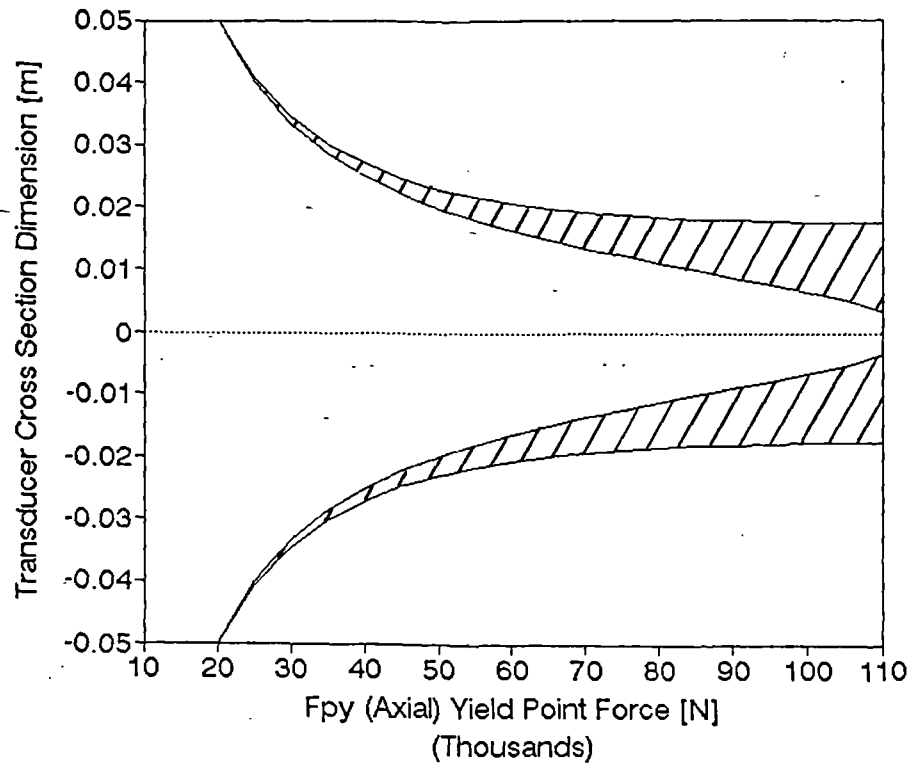


Figure 4.12 Yield point axial forces corresponding to a range of transducer cross section dimensions. This graph corresponds to a yield point bending load of 500 Nm and a material proof stress of 120 MPa. For example, for an inner and outer tube radii of 0.004 m and 0.016 m, the corresponding axial transducer yield point load would be 1.1×10^5 N and its yield point bending moment would be 500 Nm.

$$M = ((\pi * \sigma) / 32d_o) * (d_o^4 - [d_o^2 - ((4*F) / (\pi*\sigma))]^2) \quad (4.31c)$$

this equation then yields a binomial relationship between axial force, bending moment and the outer tube diameter.

$$0 = d_o^2 - (4*M/F)d_o - (2*F/(\pi*\sigma)) \quad (4.32)$$

Using this equation and fixing the yield point bending moment at 500 Nm, yield point axial force was varied (note, this calculation assumes that the axial and bending loads are applied independently, and not simultaneously). This produced an accompanying change in the required internal and external tube diameters. Figure 4.12 shows the results of this investigation. Outer and inner tube diameters of 0.042 m and 0.030 m were chosen, yielding an axial load limit of approximately 80000 N. This combination will produce a reasonable compromise between axial stiffness and overly large tube diameter.

All bolting requirements were designed for a factor of safety of 2. This included both the flange to transducer bolts (16 in total) and the centre mounting bolts.

Electrical signal conditioning from the transducer was achieved using a standard 6 channel resistance strain gauge amplifier and an auxiliary $\times 10$ signal amplifier and two pole 50 Hz low pass filter. Using this equipment, output from the transducer contained little noise, ($< \pm 0.010$ volts) and provided a good signal for the loading conditions experienced during use. The bridge excitation voltages applied to the transducer and the total amplifier gain used are detailed in Table 4.1.

Amplifier drift was small but data collected from the transducer were normalized against five frames of no load transducer output for each collection. To obtain the no load output, each data collection began with the subject not in contact with the hand transducer. This eliminated the need to ensure fully balanced bridge circuits during experimental sessions.

Experimental transducer data was collected via a 12 bit analogue to digital signal converter with an input voltage range of ± 10 v. The conversion between the resulting recorded computer units and the transducer voltage output was 0.0048828 [V/computer unit]. Transducer calibration data was collected using a digital voltage meter, eliminating this data conversion.

4.4.2.2 Hand Loads

With the instrumented hand transducer being portable, a method had to be developed to calculate hand loading from the forces and moments measured in the transducer. This would

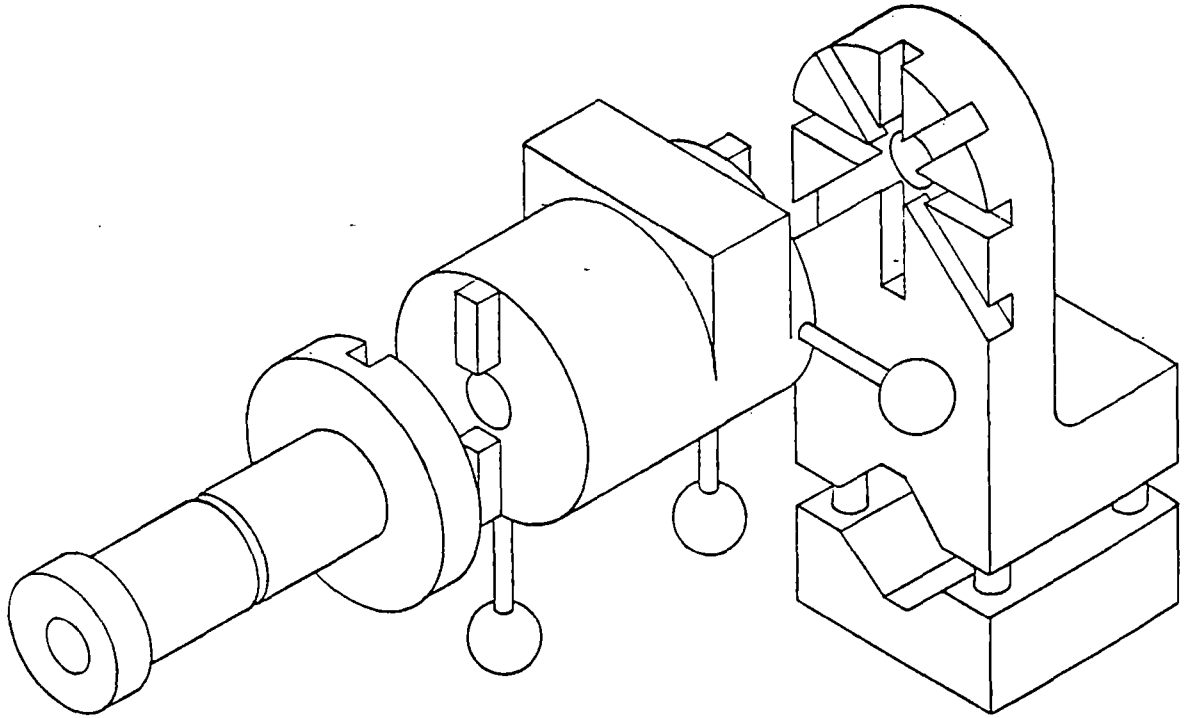


Figure 4.13 Instrumented hand transducer shown with a hand grip (left) and mounting (right) used for some experimental set ups. The three spherical reflective markers used for determining transducer location in the laboratory are shown in place.

require detailed information on both the position and orientation of the transducer within the laboratory. For flexibility, a technique that would not require predetermined transducer placement within the laboratory was desirable. The technique chosen involved the use of spherical reflective markers attached to the transducer, allowing its position and orientation to be measured directly, using the Vicon motion analysis system.

Three reflective markers were attached to the transducer. Specially machined support posts were used for each marker, ensuring their accurate placement with respect to the transducer. The markers, named PX, PY and PZ, were positioned on the transducer as shown in figure 4.13. A coordinate system for the markers was then defined as:

Origin: Centre of marker PX.

Y_{pm} : Through marker PY.

Z_{pm} : Cross product of Y_{pm} and a vector through PZ.

X_{pm} : Cross product of Y_{pm} and Z_{pm} .

with unit direction vectors I_{pm} , J_{pm} and K_{pm} respectively and a direction cosine matrix, $[B_{pm-lab}]$, relating the coordinate system orientation with respect to the laboratory. The transducer coordinate system orientation could then be determined by recognising that a rotation, θ_2 (approximately 45 degrees) around the Y_{pm} axis would make them parallel. The orientation of the transducer coordinate system with respect to the laboratory could then be described by:

$$[B_{p-lab}] = \begin{bmatrix} \cos\theta_2 & 0 & -\sin\theta_2 \\ 0 & 1 & 0 \\ \sin\theta_2 & 0 & \cos\theta_2 \end{bmatrix} * [B_{pm-lab}] \quad (4.33)$$

An accurate value for the magnitude of θ_2 was determined during the final stages of the calibration process.

The transducer origin position could also be determined using a translation equal to the distance between marker PX and the transducer centre in the transducer coordinate system, although this was not required for this study.

Forces and moments $\{F_{p_x}, F_{p_y}, F_{p_z}, M_{p_x}, M_{p_y}, M_{p_z}\}$, measured with the transducer could then be converted to being with respect to the laboratory coordinate system using:

Table 4.1 Total amplifier gain and bridge excitation voltages used for the instrumented hand transducer during experimental and calibration sessions.

Channel	Load	Total Amplifier Gain	Bridge Voltage [v]
1	Fp _x	10000	5
2	Fp _y	10000	10
3	Fp _z	10000	5
4	Mp _x	2000	5
5	Mp _y	2000	5
6	Mp _z	2000	5

$$\{F_x, F_y, F_z\}_{p'-lab} = [B_{p'-lab}]^{-1} * \{F_{p_x}, F_{p_y}, F_{p_z}\} \quad (4.34a)$$

and, $\{M_x, M_y, M_z\}_{p'-lab} = [B_{p'-lab}]^{-1} * \{M_{p_x}, M_{p_y}, M_{p_z}\} \quad (4.34a)$

Hand loads were calculated using the assumption that all loads are applied through the hand grip centre to the hand. This is analogous to the assumption used in calculating force plate hand loads, and suffers from similar uncertainties. Using this assumption, hand loading can be determined from the transducer loads, knowing the displacement between the hand grip and transducer centres, D_1 . The hand loads $\{F_h, F_y, F_z, M_h, M_y, M_z\}$ in with respect to the laboratory coordinate system would then be:

$$\begin{aligned} F_{h_x} &= F_{x_{p'-lab}} & M_{h_x} &= M_{x_{p'-lab}} - (F_{z_{p'-lab}} * D_1) \\ F_{h_y} &= F_{y_{p'-lab}} & M_{h_y} &= M_{y_{p'-lab}} \\ F_{h_z} &= F_{z_{p'-lab}} & M_{h_z} &= M_{z_{p'-lab}} + (F_{x_{p'-lab}} * D_1) \end{aligned}$$

4.4.2.3 Calibration

The instrumented hand transducer had to be calibrated before it could be used experimentally. The procedure for calibration was effectively split into two separate parts. The first was the transducer calibration, where the relationship between loading and output signals were determined. The second part included a system calibration of the transducer within the motion analysis laboratory. This calibration allowed the rotational offset between the transducer spherical markers and the transducer coordinate system to be accurately measured in addition to the overall accuracy of the transducer for measuring hand loading to be determined.

Two approaches can be used for transducer calibration, linear and the non-linear. The linear approach, is used in this work. A complete review of both techniques is presented by Magnissalis (1992). Magnissalis draws the conclusion that while a non-linear approach may be marginally more accurate, the added complications and expense are not justifiable for a transducer of this type.

A linear calibration approach assumes that each output signal can be expressed as a linear combination of the applied load components. The signal for each output channel of the transducer would then be the linear combination of the combined effects of the loading. Mathematically this would take the form:

$$\begin{aligned} SF_x &= m_{1,1}F_{p_x} + m_{1,2}F_{p_y} + m_{1,3}F_{p_z} + m_{1,4}M_{p_x} + m_{1,5}M_{p_y} + m_{1,6}M_{p_z} & (4.35) \\ SF_y &= m_{2,1}F_{p_x} + m_{2,2}F_{p_y} + m_{2,3}F_{p_z} + m_{2,4}M_{p_x} + m_{2,5}M_{p_y} + m_{2,6}M_{p_z} \end{aligned}$$

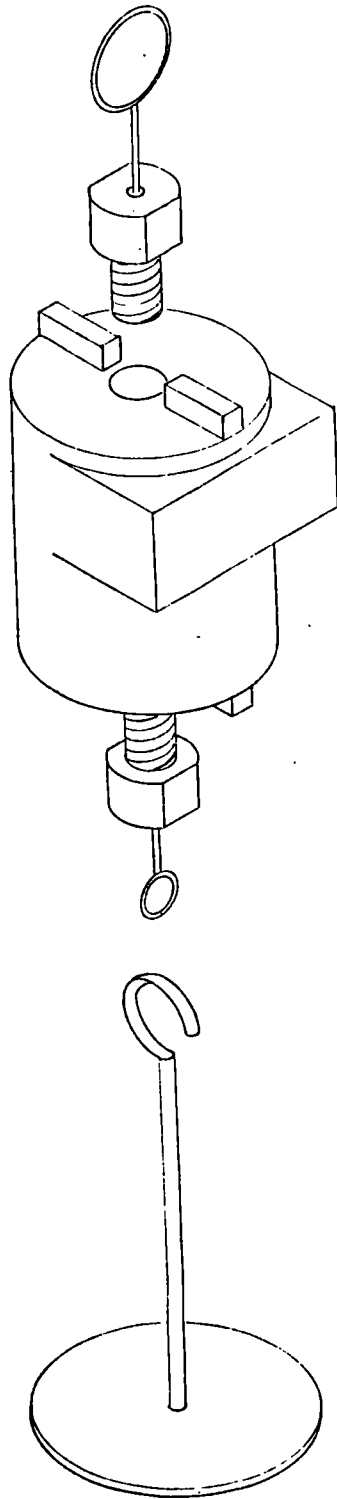


Figure 4.14 Exploded view of equipment used for F_{p_y} (axial) transducer channel calibration.

$$\begin{aligned}
SFz &= m_{3,1}Fp_x + m_{3,2}Fp_y + m_{3,3}Fp_z + m_{3,4}Mp_x + m_{3,5}Mp_y + m_{3,6}Mp_z \\
SMx &= m_{4,1}Fp_x + m_{4,2}Fp_y + m_{4,3}Fp_z + m_{4,4}Mp_x + m_{4,5}Mp_y + m_{4,6}Mp_z \\
SMy &= m_{5,1}Fp_x + m_{5,2}Fp_y + m_{5,3}Fp_z + m_{5,4}Mp_x + m_{5,5}Mp_y + m_{5,6}Mp_z \\
SMz &= m_{6,1}Fp_x + m_{6,2}Fp_y + m_{6,3}Fp_z + m_{6,4}Mp_x + m_{6,5}Mp_y + m_{6,6}Mp_z
\end{aligned}$$

where the six output signals are SFx ... SMz and $m_{1,1} \dots m_{6,6}$ are the linear coefficients to be determined during the calibration procedure. Equation 4.35 can be written more simply:

$$[S] = [M] * [L] \quad (4.36)$$

In normal use, pylon loading is calculated from the output signal. Therefore, to determine the loading from this output signal, equation 4.36 would need to be rearranged to:-

$$[L] = [C] * [S] \quad (4.37)$$

where [C] is simply the inverse of matrix [M] ($[C] = [M]^{-1}$). Matrix [C] is called the calibration matrix. Units used for the parameters of [L], [S] and [C] were N or Nm, volt, and N/volt or Nm/volt respectively.

Determining the calibration matrix involves first calculating the components of matrix [M]. This is done by loading each of the channels of the transducer and measuring corresponding output signal voltages. Many different loading formats have been used for previous calibrations of the pylon transducer and they were reviewed by Magnissalis (1992). Because of size differences, none of the equipment used for previous pylon calibrations was suitable for this transducer. As a result, a new loading format for transducer calibration has been adopted.

Ideally, load would be applied to each transducer channel independently. The resulting six output signals for each load could then be analyzed using linear regression to determine the corresponding 6 components of a column of matrix [M]. Unfortunately, some two channel loading does occur during this calibration, which complicates the procedure. In general, if two channels are loaded simultaneously, for example shear and torsion, loading for one of these channels will increase while the other remains constant. The resulting transducer output signals would then be expected to contain a constant offset due to constant shear loading and a variable component due to the changing torsional loading. Calculating the slopes of the lines then allows the column of matrix [M] to be determined for the channel with varying load. Similarly, an offset magnitude indicates transducer output as a

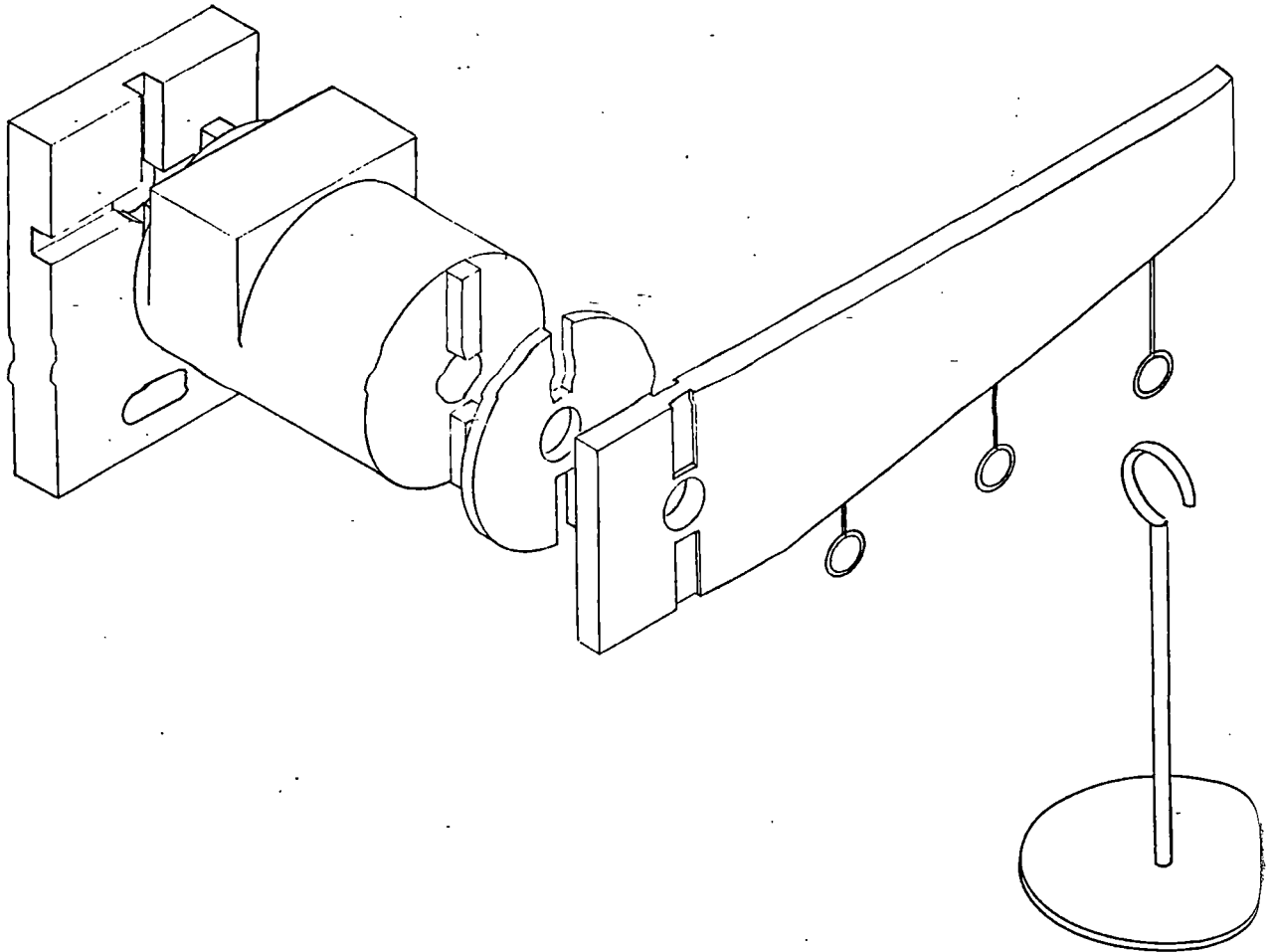


Figure 4.15 Exploded view of equipment used for M_p , (torsional) transducer channel calibration, including from left to right: mounting base; transducer; 3 mm spacer; loading bar with three loading cables placed horizontally at 0.10 m, 0.20 m and 0.30 m radii from the Y_p axis; and weight pan. F_{p_x} and M_{p_z} channels were also loaded using this configuration, but this did not interfere with calibration.

result of the constant loading.

Details of the four calibration procedures are outlined below, with specific measurements and calculations listed in Appendix C:

Axial Loading, F_{p_y} :

The transducer was set up as shown in figure 4.14, and freely suspended from a solid object. Seven masses up to 60 kg in total were added to the weight pan. The corresponding six channels of pylon output were recorded and plotted against weight being supported by the transducer. Using linear regression, the relationships between F_{p_y} load and electrical output were determined. Regression correlation to the F_{p_y} data was better than 0.999. The slope of the regressed lines formed the second column of matrix [M].

Torsional Loading, M_{p_y} :

The transducer was set up as shown in figure 4.15. The entire assembly was attached to a vertical surface, and the torsion bar was levelled using a machinist's level. A bolt through the base plate slot was used to prevent the assembly from shifting off level during use. This ensured that all subsequent calibration loading was made relative to this orientation bench mark.

A 20 kg mass was then used to apply M_{p_y} (torsion) to the transducer, and consequently F_{p_x} (shear) and M_{p_z} (bending) as well. The mass was placed in turn on the three positions of the bar and the transducer output recorded. The bar was then reversed and the procedure repeated.

The corresponding transducer outputs for the six loading situations were plotted against the theoretical torsion being applied to the transducer. Using linear regression, the relationships between M_{p_y} load and the resulting transducer output were determined from the line slopes ($r > 0.999$ for M_{p_y} data). An offset in the data occurred as a result of the unavoidable shear and bending loading but this had no effect on the plotted line slopes. The process was repeated using a 40 kg mass ($r > 0.999$ for M_{p_y} data) and the resulting relationships averaged with those determined using the 20 kg mass. The averaged relationships formed the fifth column of matrix [M].

Z_p Axis Bending and X_p Shear Loading, M_{p_z} and F_{p_x} :

The transducer was set up as shown in figure 4.16. The base plate remained in place from the torsional tests ensuring proper transducer orientation.

A 25 kg mass was added to the weight pan producing M_{p_z} and F_{p_x} loading in the transducer. The hanger was moved to the three positions along the tube subsequently increasing M_{p_z} loading while F_{p_x} remained constant. Transducer signal output was recorded for each loading situation. The assembly was then inverted so that the X_p was now pointing vertically down. This had the effect of reversing the direction of loading on the transducer. The loading and recording process was then repeated.

The recorded transducer signal output was plotted against the theoretical M_{p_z} loading for

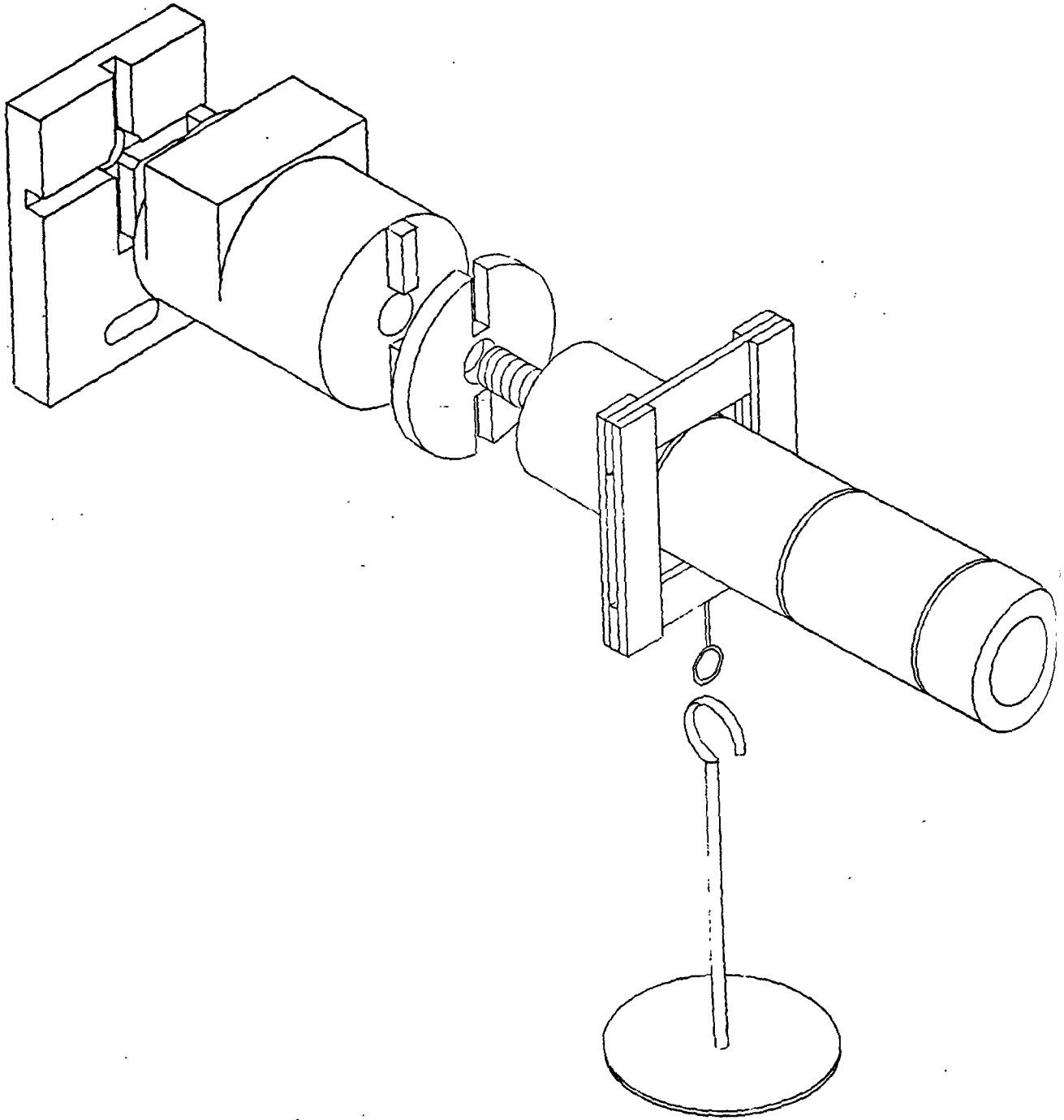


Figure 4.16 Exploded view of equipment used for F_{p_z} (shear) and M_{p_z} (bending) transducer channel calibrations, including from left to right: mounting base; transducer; 5 mm spacer; loading bar with three loading grooves placed at 0.10 m, 0.20 m and 0.30 m positions along its length; round edge hanger; and weight pan. This equipment was also used F_{p_x} (shear) and M_{p_x} (bending) transducer channel calibrations but the transducer was rotated clockwise 90 degrees to start that calibration procedure.

the X_p axis up and the X_p axis down transducer positions. Using linear regression, the relationships between transducer output and Mp_z loading were obtained from the line slopes ($r > 0.999$ for Mp_z data). These values were then averaged for the two transducer positions.

Fp_x (shear) loading remained a constant magnitude before and after inversion but at inversion went from being positive to negative. This resulted in offsets in transducer output, which reversed their directions when the assembly was inverted. These offsets are the transducer's response to the applied Fp_x (shear) loading. To determine the magnitude of the offsets, extrapolation was used on the recorded data to determine the transducer output when there was no Mp_z loading. The relationships between transducer output and Fp_x were then determined from these offsets using linear regression ($r > 0.999$ for Fp_x data).

The entire process was then repeated with a 50 kg mass and the relationships averaged. The averaged relationships for Mp_z and Fp_x loading then became the sixth and first columns of matrix [M].

X_p Axis Bending and Z_p Shear Loading, Mp_x and Fp_z :

The transducer was set up as shown in figure 4.16, except the assembly was rotated so that the X_p axis was pointing in the Z_p axis direction shown in the figure.

The procedure used was then similar to that used previously for Z_p axis bending and X_p shear loading. The resulting relationships calculated for Mp_x and Fp_z then became the fourth and third columns of matrix [M] respectively.

After all the columns of matrix [M] were determined, the matrix was inverted and checked for accuracy. The resulting calibration matrix [C] was:

$$[C] = \begin{bmatrix} -229.6 & 1.0 & -7.5 & -14.7 & 0.2 & 8.7 \\ 0.2 & 389.3 & -3.5 & -0.1 & -27.7 & -0.9 \\ -8.3 & -3.5 & 226.1 & 7.8 & -4.3 & 9.5 \\ 0.1 & 0.0 & -0.2 & -20.5 & 0.2 & -0.3 \\ 0.1 & 0.1 & 0.0 & -0.1 & -32.8 & 0.0 \\ 0.0 & 0.0 & -0.1 & -0.2 & -0.2 & 20.5 \end{bmatrix}$$

where the parameters of this matrix are in units of N/volt or Nm/volt.

This essentially completed the calibration of the transducer proper, but several other parameters were still required along with a system test.

The rotational offset between the transducer coordinate system and the transducer marker coordinate system while designed to be 45 degrees, had to be accurately measured. This was accomplished by setting the transducer up in the motion analysis lab, and levelling it as had been done for the calibration procedure. Ten frames of data were collected and the true rotational offset calculated using the measured positions of the three reflective markers.

Details of the collected data and calculating this angle are listed in Appendix D. The rotational offset was calculated to be:

$$\theta_2 = 47.2 \text{ degrees}$$

A system test was conducted using the transducer as it would be for an experimental data session. This was to obtain an estimate of overall measurement accuracy by comparison of applied loads to measured loading.

All six channels of the transducer were loaded using a combination of masses and loading situations. Loading and data collection details are listed in Appendix D. Maximum forces and moments applied to the transducer were 200 N and 70 Nm respectively. The corresponding accuracy of the measurements was on average approximately $\pm 1 \%$ with a standard deviation of $\pm 1 \%$.

CHAPTER 5. THE SHOULDER MODEL

Joint modelling involves the use of available information to predict joint loading and function which could not be determined directly. For this study, many different techniques and procedures have been used to predict detailed function from the anthropometric, subject geometric, kinematic and external loading information. A detailed knowledge of these is essential to an understanding of the model and the predicted shoulder function. These procedures and techniques are the focus of this chapter.

The chapter is subdivided into several sections. The first focuses on determining effective origin and insertion positions for muscles wrapped around hard tissues, resulting in curved lines of action. The second covers calculation of joint moments generated by both external and internal loading. Calculation of joint forces is outlined in the third section. The final section covers optimization of muscle forces.

5.1. MUSCLE WRAPPING

The line of action for each muscle is assumed to be a straight line between its effective origin and insertion positions. In a simple situation the effective positions may be coincident with the anatomical positions. The line of action is then a straight line between anatomical origin and insertion. In a more complex situation, where the muscle may curve around hard tissue, the effective origin and insertion positions are no longer coincident with the anatomical origin and insertion. To determine the line of action for such a situation requires the "effective" anatomical positions to be determined.

Several techniques have been documented in the literature for determining a muscle's line of action when it is wrapped around hard tissue. Details of each of these techniques were discussed in chapter 3. In general, they all have drawbacks that prevented them from being applied in this study. As a result, an alternative technique was required to calculate the effective origin and insertion positions for the shoulder musculature.

5.1.1. Development of a New Technique

A technique has been developed to allow effective origin and insertion positions to be determined. In general the procedure simplifies the complex three-dimensional anatomical environment into two-dimensions. The two-dimensional planar environment is termed the dominant muscle plane. For presentation in this work, the technique is discussed initially as it applies to humeral head wrapping. Application of the techniques for humeral shaft wrapping and combinations of the two are discussed later.

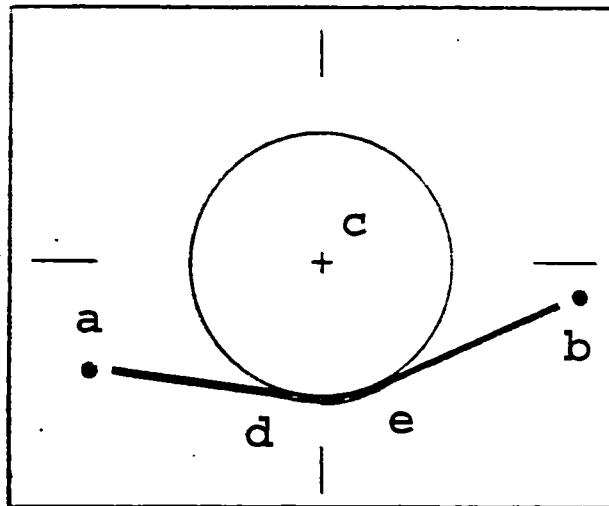
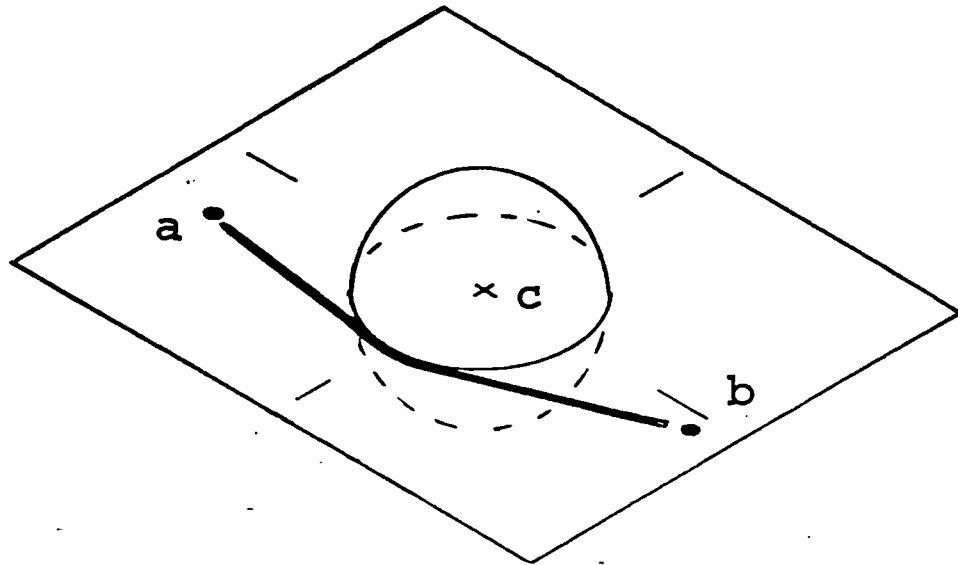


Figure 5.1, (top) Intersection of a string between two points, **a** and **b**, and a sphere. The string will lie in the plane defined by the points **a** and **b** and the sphere centre **c**. The intersection between sphere and plane will always be a circle. This plane is analogous to the dominant muscle plane.

Figure 5.2, (bottom) Details of the intersection between the string and the sphere as viewed in the two-dimensional plane. Effective origin or insertion positions would be analogous to points **d** and **e**.

5.1.1.1 The Dominant Muscle Plane

The main simplifying assumption used in this technique is that the three-dimensional anatomical environment can be accurately modelled using a two-dimensional approach. This allows the three-dimensional effective origin and insertion positions to be determined in a two-dimensional environment and transformed back into the three-dimensional one.

To visualize the concept a simple example can be used. A sphere is placed between two discrete points in a three-dimensional environment. A string is passed over the sphere and through the two points. When the string is pulled taut, it will lie in the plane defined by the two points and the sphere centre (see figure 5.1). If the three points are collinear, then the string will still lie in the plane but the plane will not be uniquely defined. This plane whether unique or not is analogous to the dominant muscle plane in a simplified form.

Assuming that the plane is uniquely defined, the contact points between string and sphere can be easily calculated if the two-dimensional dominant muscle plane is used. Figure 5.2 shows the details of the three-dimensional environment as they are viewed in the two-dimensional plane. The intersection of the sphere and this plane will form a circle with radius equal to that of the sphere. Points, **d** and **e**, are the contact points (effective origin or insertion positions) between the string and sphere, between which the string is curved and on either side of which a straight line can be drawn to the points **a** and **b** respectively. If the three-dimensional relative orientations of points **a**, **b** and **c** are known, then the orientation of the dominant muscle plane and the relative positions of the three points on that plane can be calculated. If the diameter of the sphere is known the two-dimensional coordinates of points **d** and **e** can be determined using simple geometry. These two-dimensional coordinates can then be translated back into the original three-dimensional environment, yielding the coordinates of the three-dimensional coordinates of the contact points between the string and sphere.

5.1.1.2 Anatomical Assumptions

The basics of the dominant muscle plane technique can be applied to solve effective origin and insertion positions for a muscle wrapped around a spherical anatomical feature. For this study, the humeral head was assumed to be a sphere. The main hurdle in the application of the technique is determining the orientation of the plane, after which if the anatomical geometry is known, the theoretical path of the muscle can be readily calculated.

Muscles do not follow the shortest line between their origin and insertion. They are constrained by both hard and soft tissues within the body. As a consequence, the plane that a muscle lies in as it passes over a spherical anatomical feature is altered from the theoretical

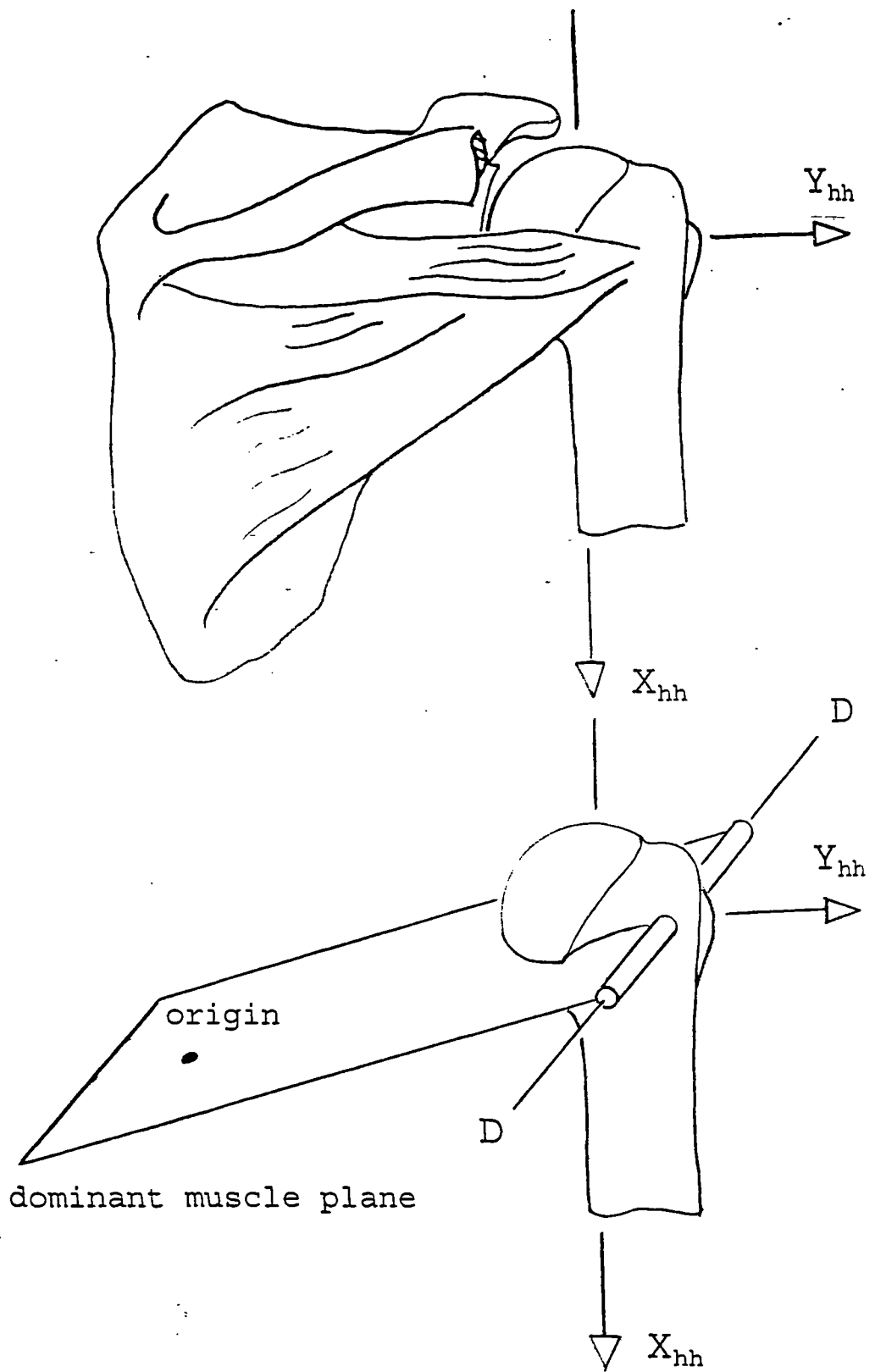


Figure 5.3 Posterior view of scapula (distal acromium removed) and humerus showing the three fascicles of infraspinatus as they are positioned anatomically, (a, top). Using fascicle origin position and a line, D-D, parallel to Z_{hh} and through the anatomical insertion a dominant muscle plane can be defined for the middle fascicle of infraspinatus, (b, bottom). Continued on next page.

shortest line plane defined in the example above. Also, if the muscle origin, insertion and spherical centre are collinear a unique plane is still required. The simple approach used in the example above requires modification if it is to be used in a universal approach to muscle wrapping correction.

Examining the anatomical orientation of infraspinatus, its corresponding dominant muscle planes can be determined. Figure 5.3a shows the infraspinatus as it occurs anatomically. Using the middle fascicle as an example, its dominant muscle plane can be determined if a line, D-D, is drawn through the anatomical insertion. This plane would now contain the muscle origin and the line, D-D. Figure 5.3b shows the plane as it would occur for the middle fascicle. If the line D-D is fixed with respect to the humerus, middle infraspinatus will remain approximately in the plane for any humeral position normally encountered. The same technique can be applied to the superior and inferior fascicles. Therefore the dominant muscle plane for infraspinatus can be determined for any humeral position. A similar approach can be used for determining the dominant muscle planes for all of the muscles passing over the humeral head. Only the definition of the line D-D varies between the muscles.

Since the dominant muscle plane does not pass through the sphere centre, the radius of the intersection circle (between plane and sphere) is not equal to the sphere radius. Circle radius must be calculated and is related to the perpendicular distance between the plane and sphere centre.

Details of the dominant muscle plane developed for this anatomical situation are now the same as for the simplified example. The effective insertion for a muscle wrapping around the humeral head would be equivalent to one of the contact points, d or e from the simple example. The correct one to use for the effective insertion position would be dependant on anatomical details. The remaining details of implementation of this technique are similar to the simple example.

5.1.2. Implementation of the New Technique

The dominant muscle plane technique allows the effective insertion positions to be determined for all of the muscles wrapping around either or both the humeral head and shaft. An outline of the implementation for head, shaft and combined muscle wrapping is given below. Calculation and implementation details are listed in appendix E.

5.1.2.1 Humeral Head Wrapping

Infraspinatus, subscapularis, supraspinatus and the proximal portion of biceps long head

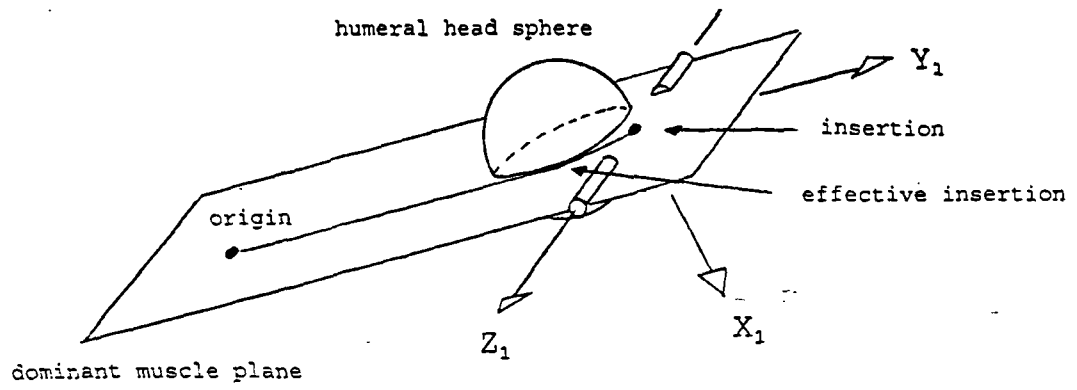


Figure 5.3c (Continued) With the humeral head modelled as a sphere, the dominant muscle plane contains all of the details of the curved path of middle infraspinatus as it wraps around the humeral head.

are all muscles that can only wrap around the spherical humeral head. The differences in the technique as it is applied to each of these muscles is mainly in the direction of the line on which the dominant muscle plane is based. To obtain the required lines, a humeral head coordinate system was defined as follows:

Origin: Humeral head centre.

X_{hh} : parallel to the proximal humeral shaft.

Z_{hh} : Cross product of a vector through the articular surface centre and the X_{hh} (pointing posteriorly).

Y_{hh} : Cross product of Z_{hh} and X_{hh} axes (pointing laterally).

This is similar to the humeral coordinate system but rotated about the X_h axis by an angle equal to humeral retrotorsion angle, θ_{ht} (25 degrees).

The lines required to define the dominant muscle planes can now be based on the humeral head coordinate system. For infraspinatus and subscapularis, the line used to define the dominant muscle plane will be parallel to the Z_{hh} axis and passing through their respective insertions. Supraspinatus and biceps long head will both use planes defined using the X_{hh} axis and their insertions. This section of biceps long head is assumed to insert into the intertubercular groove location for this procedure.

Implementing the procedure for calculating effective insertion positions requires several checks to be made. First, all origin and insertion positions must be outside the spherical humeral head. If not, they are moved to positions outside the sphere surface using a translation of the point in a radial direction away from the humeral head centre. A second check is made to determine if the individual muscles are wrapped. This is accomplished by determining the dominant muscle plane and examining for intersection between a line joining the anatomical origin and insertion and the circular intersection of the humeral head. When line and circle intersect, wrapping is indicated and the correction procedure implemented.

For biceps long head, infraspinatus, subscapularis, and supraspinatus the effective insertion was determined using this technique. The geometric form of the scapula virtually eliminates any wrapping of these muscles on the scapula. Therefore, by combining the anatomical muscle origin and effective insertion (if not required then the anatomical insertion) the line of action for the muscle would then be a straight line passing through these two points.

The anatomic details of the wrapping for biceps are slightly different than the other three muscles. Where the other three muscles insert into the humeral head, the long head of

head to shaft
offset distance

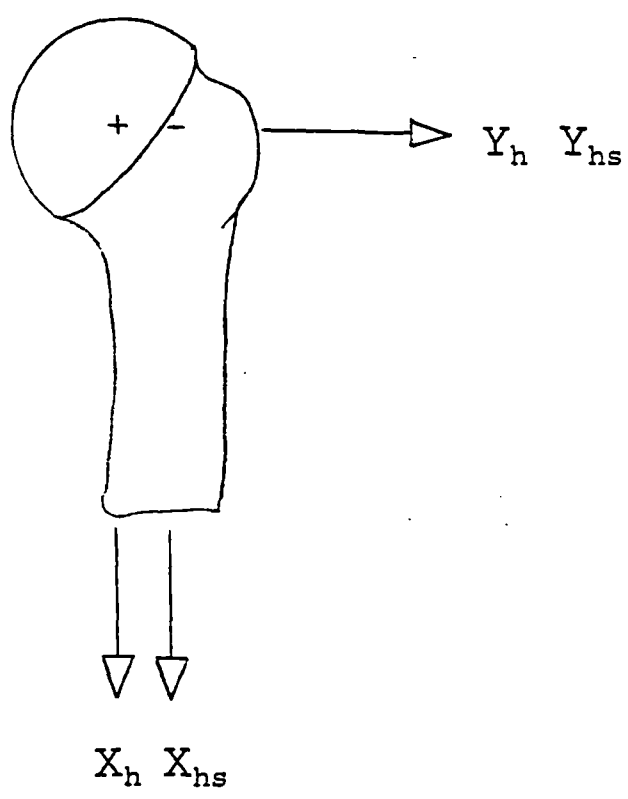
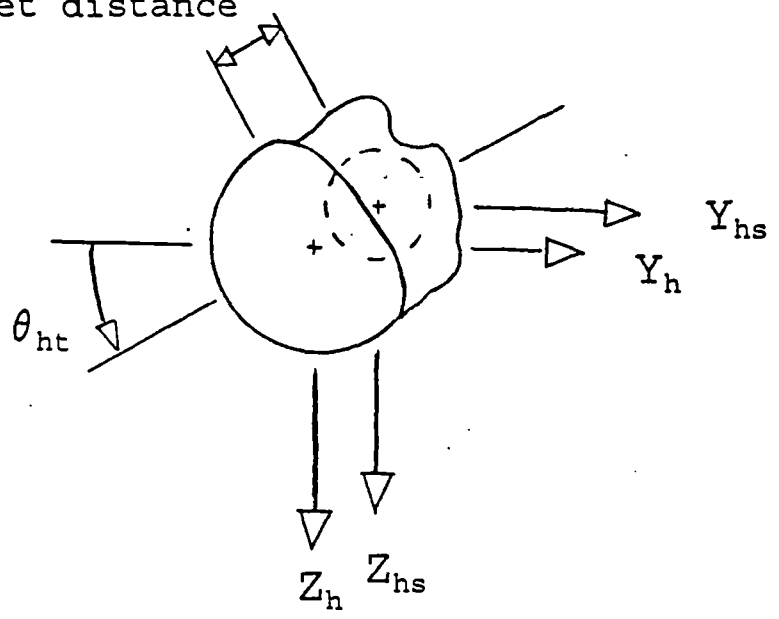


Figure 5.4 A humeral shaft coordinate system X_{hs} , Y_{hs} and Z_{hs} , is defined using the humeral coordinate system X_h , Y_h and Z_h , head to shaft offset distance and humeral retrotorsion angle, θ_{ht} .

biceps passes through the intertubercular groove and inserts on the radius. To simplify the analysis, biceps was split into two theoretical parts, the first was proximal to and inserted in the groove and the second was distal to and with origin in the groove. Each section of the muscle is then considered separately for modelling purposes. To accurately model the anatomical function of the muscle, the tension in each section was constrained to be equal.

5.1.2.2 Humeral Shaft Wrapping

A group of muscles including deltoid, latissimus dorsi, pectoralis major, teres major and teres minor are all muscles that can wrap around the humeral shaft. Most of these muscles can also wrap around the humeral head. This combined wrapping complicates the procedure of determining the effective insertion positions for these muscles. The technique used to correct for humeral shaft wrapping, if required, is the same for all of these muscles. The following section details this technique and particulars of the application of it to each muscle are covered in the next subsection.

The dominant muscle plane technique can be used to determine the effective origin or insertion positions for muscles wrapped around the humeral shaft. The difference in the application of the technique from humeral head wrapping is that a spherical anatomical feature is not being considered, but rather the humeral shaft is modelled as a cylinder. Reducing the three-dimensional anatomical details onto a two-dimensional plane requires viewing the cylinder end on. From this perspective (see figure 5.4) the circular cross section of the cylinder can be seen in addition to the muscle origin and muscle insertion positions. This two-dimensional image is essentially the same as occurred in the dominant muscle plane in the simple example. To save confusion, this plane while not containing the muscle, is still termed the dominant muscle plane, since determining the effective muscle origin within the plane is the same for either humeral shaft or head wrapping.

Determining the dominant muscle plane for humeral shaft wrapping required defining a humeral shaft coordinate system. This coordinate system was parallel to the humeral coordinate system but with its origin at the proximal end of the humeral shaft, level with the humeral head centre (at the intersection of the shaft centre line and the $Y_h - Z_h$ plane). Both origin and insertion positions for the muscles being checked for wrapping were converted to be with respect to this coordinate system before any calculations proceeded.

Using the dominant muscle plane and the techniques outlined in the simple example, the two-dimensional position of the effective origin or insertion of a wrapped muscle can be determined. Converting this two-dimensional position into the anatomical three-dimensional

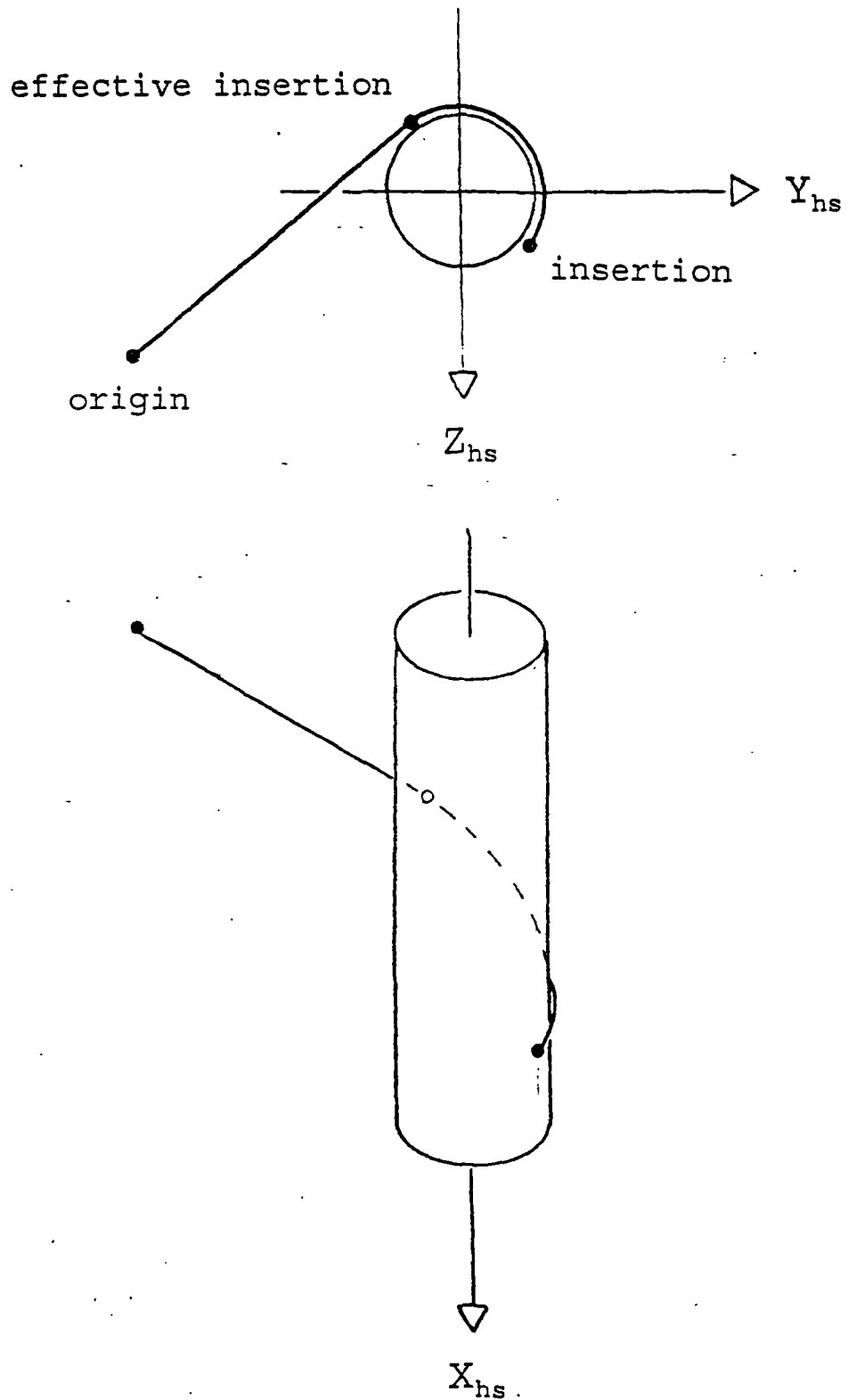


Figure 5.5 Two simplified views of *teres major* as it wraps around the humeral shaft. The humeral shaft is modelled as a cylinder for wrapping correction. An effective insertion can be defined where wrapping ends and between it and the anatomical origin the muscle lies in a straight line.

position requires a technique different to that used for humeral head wrapping. The only piece of information missing for the three-dimensional description is the distance of the effective origin or insertion along the cylindrical humeral shaft. This distance can be determined in several ways. The technique chosen assumes that the X_{hs} progression of the muscle remains constant along the entire muscle length. The ratio of wrapped to straight length for the muscle in the dominant muscle plane was calculated. This ratio is the same as the ratio of the wrapped to straight length of muscle in three-dimensions. Combining this with the origin and insertion positions allowed the three-dimensional coordinates of the effective insertion to be calculated.

Checks were required before the dominant muscle plane technique could be applied to humeral shaft wrapping. If a muscle insertion position was calculated as being inside the cylinder, then it was moved outside the cylinder surface. This correction was made in a radial direction away from the cylinder centre line. The possibility also exists in this technique for the muscle origin to appear inside the circle on the dominant muscle plane. This might occur at extremes of humeral elevation. No corrections were made for this situation, but an error flag was produced and processing on this frame of data aborted. To date, this situation has not occurred and as such cannot be considered to be a problem. The final check was made to determine if the muscles were wrapped. If a line joining muscle origin and insertion intersected with the intersection circle on the dominant muscle plane then wrapping was indicated and the correction procedure was implemented.

5.1.2.3 Humeral Head and Shaft Wrapping

Many of the shoulder muscles can wrap around both the humeral head and shaft and determining the effective origin or insertion positions for such a situation is complex. To avoid the associated difficulties, all of the muscles in question were checked to see if they wrapped around the humeral head first. If head wrapping was indicated then it was corrected and no shaft wrapping was considered. Shaft wrapping was then checked for those muscles not wrapped around the head. This simplification is based on the assumption that the sphere representing the humeral head actually projects over the proximal end of the cylinder representing the humeral shaft. As such, any muscle wrapped over the sphere will not be significantly wrapped on the cylinder. The resulting muscle lines of action while being representative are not exactly the same as would occur anatomically. Deltoid, latissimus dorsi, pectoralis major, teres major, teres minor are all muscles included in the group that can wrap around both the humeral head and shaft. Latissimus dorsi, teres major, teres minor, anterior deltoid and posterior deltoid were all checked for humeral head

wrapping using a dominant muscle plane through their anatomical insertion and parallel to the Z_{hh} axis. Middle deltoid was similarly checked but made use of the X_{hh} axis instead. As deltoid passes over the humeral head, it also passes over the distal ends of the rotator cuff muscles. This effectively increases the diameter of the spherical anatomical formation. To account for this, the diameter of the sphere representing the humeral head was increased. Latissimus dorsi and teres major always pass inferior to the humeral head. This relationship had to be checked and the effective insertion constrained to this location for large humeral elevations. Head wrapping, if indicated for any of the muscles, was corrected. Any fascicles not wrapped around the head were checked and corrected if necessary for shaft wrapping. This procedure produced anatomically representative effective insertions for all of the muscles considered for all of the arm positions encountered in this study.

5.2. JOINT MOMENTS AND FORCES

In classical mechanics, the net force and moment applied to an object must be zero for that object to be in equilibrium. Using this relationship, equations can be developed that completely describe the forces and moments being applied to a body segment.

In this section the mathematical equations describing this equilibrium condition are derived. Beginning with the general condition for moment equilibrium, the section progresses on to the equations describing both external and internal joint moments. Equations describing joint contact forces are then developed.

Two of the muscles that contribute to shoulder equilibrium also contribute to the elbow moment balance. These muscles can contribute to the generation of moments at both joints simultaneously. In an attempt to model this characteristic, elbow in addition to shoulder moment balance is included in this study.

5.2.1. Moment Equilibrium

For equilibrium, the sum of all moments imparted to a body segment must equal zero when they are taken about a reference point. For analysis, moments are usually summed about a convenient point such as the proximal joint centre on the segment. The moments imparted to the segment can originate from external segment loads and internal structural loads. Applying this to the shoulder and elbow, the equations describing moment equilibrium would then be:

$$\begin{aligned}
 0 &= \sum M(\text{glenohumeral joint}) & (5.1) \\
 &= \sum M(\text{external loading distal to joint}) + \sum M(\text{internal structure loads})
 \end{aligned}$$

Table 5.1 Muscles crossing the glenohumeral and elbow joints.

No.	Muscle	Fascicle	Glenohumeral	Elbow
1	Biceps	Long head	✓	✓
2	"	Short head	✓	✓
3	Coracobrachialis		✓	
4	Deltoid	Anterior	✓	
5	"	Middle-anterior	✓	
6	"	Middle	✓	
7	"	Middle-posterior	✓	
8	"	Posterior	✓	
9	Infraspinatus	Superior	✓	
10	"	Middle	✓	
11	"	Inferior	✓	
12	Latissimus dorsi	Superior	✓	
13	"	Middle	✓	
14	"	Lateral	✓	
15	Pectoralis major	Clavicular	✓	
16	"	Middle	✓	
17	"	Inferior	✓	
18	Subscapularis	Superior	✓	
19	"	Middle	✓	
20	"	Inferior	✓	
21	Supraspinatus		✓	
22	Teres major		✓	
23	Teres minor		✓	
24	Triceps	Long head	✓	✓
25	"	Medial head		✓
26	"	Lateral head		✓

and,

$$\begin{aligned} 0 &= \sum M(\text{elbow joint}) & (5.2) \\ &= \sum M(\text{external loading distal to joint}) + \sum M(\text{internal structure loads}) \end{aligned}$$

If these two equations are applied to the axes of rotation for each of the two joints, moments generated by internal structure loads will be produced by muscle action across the joints. To maintain the relationship between axes of rotation and moment equilibrium, the coordinate system of the segment is used for moment analysis. Equation 5.1 can be rewritten for the three axes of glenohumeral joint rotation, X_h , Y_h and Z_h .

$$\begin{aligned} 0 &= \sum M_h(\text{glenohumeral joint}) & (5.3a) \\ &= \sum M_h(\text{external loading distal to joint}) + \sum M_h(\text{muscle activity}) \end{aligned}$$

$$\begin{aligned} 0 &= \sum M_y(\text{glenohumeral joint}) & (5.3b) \\ &= \sum M_y(\text{external loading distal to joint}) + \sum M_y(\text{muscle activity}) \end{aligned}$$

$$\begin{aligned} 0 &= \sum M_z(\text{glenohumeral joint}) & (5.3c) \\ &= \sum M_z(\text{external loading distal to joint}) + \sum M_z(\text{muscle activity}) \end{aligned}$$

Similarly, the moment equilibrium equation for the elbow rotation axis, Y_e would be:

$$\begin{aligned} 0 &= \sum M_y(\text{elbow joint}) & (5.4) \\ &= \sum M_y(\text{external loading distal to joint}) + \sum M_y(\text{muscle activity}) \end{aligned}$$

All of the external loading on the arm has been calculated and as such the moments resulting from this loading can be written explicitly for equations 5.3 and 5.4. Moments due to muscle activity can not be calculated directly because of indeterminacy. As a result, moments generated about the joint due to muscle activity are written as a function of the unknown muscle forces. Muscles acting across the glenohumeral and elbow joints are listed in table 5.1.

5.2.1.1 Moments Due to External Loading

Using kinematic, hand loading and body segment parameter information the equations for joint moments resulting from external loading can be written.

Beginning with moments generated at the glenohumeral joint, figure 5.6 shows all of the

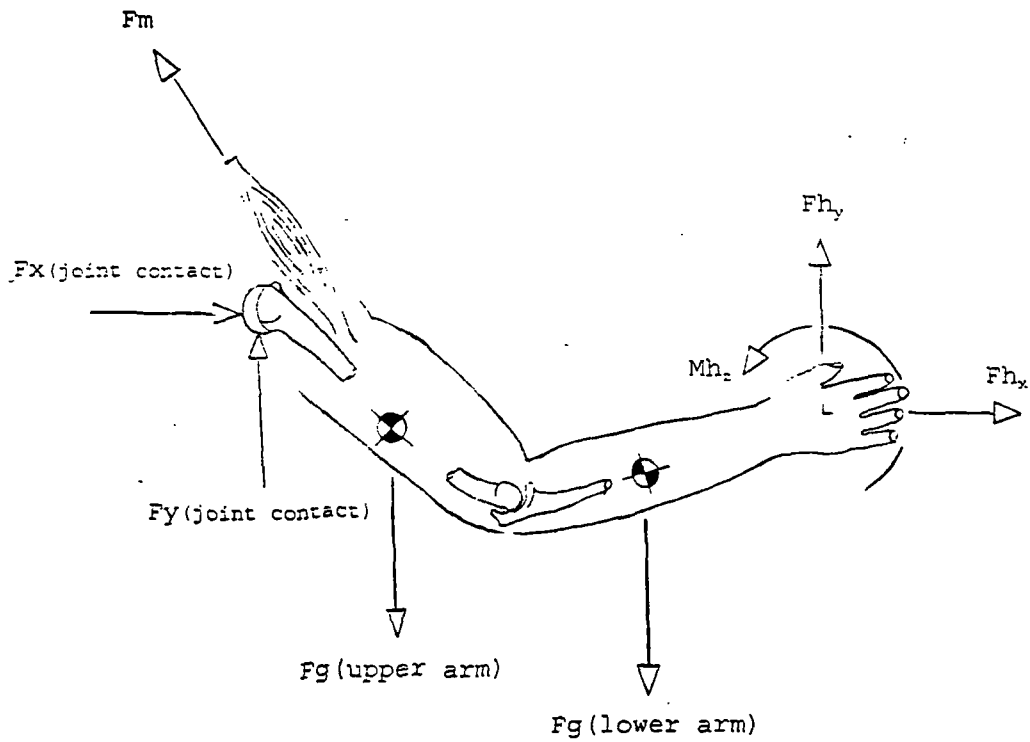


Figure 5.6 Sagittal, $X_h - Z_h$ plane, free body diagram of the arm showing the applied forces and moments that must be considered for glenohumeral force and moment analysis in this plane. For this analysis all of these values must be in terms of the humeral coordinate system. The loads include: hand forces and moments, M_h and F_h ; gravitational forces $F_g(\text{upper arm})$ and $F_g(\text{lower arm})$; force applied to the arm by muscle activity, F_m ; and the joint contact forces, $F_x(\text{joint contact})$ and $F_y(\text{joint contact})$.

external loads which could contribute to moments about the Y_h axis, My_h (external and distal to joint). Gravitational forces on the arm can be rewritten as force vectors in terms of the humeral coordinate system. Knowing gravity acts in the $-Y_{lab}$ direction, the gravitational force on the upper and lower arms would then be:

$$Fg(\text{upper arm})_h = [B_{h-lab}] * \{0, -1 * Fg(\text{upper arm}), 0\} \quad (5.5)$$

$$Fg(\text{lower arm})_h = [B_{h-lab}] * \{0, -1 * Fg(\text{lower arm}), 0\} \quad (5.6)$$

Similarly, hand forces and moments measured using the instrumented hand transducer or force plate can be rewritten as vectors in terms of the humeral coordinate system.

$$[Fh_h] = [B_{h-lab}] * \{Fh_x, Fh_y, Fh_z\}_{lab} \quad (5.7a)$$

$$[Mh_h] = [B_{h-lab}] * \{Mh_x, Mh_y, Mh_z\}_{lab} \quad (5.7b)$$

The gravitational force vectors act through the upper and lower arm centres of mass. These centres of mass were assumed to be on the X_h and X_u axes for the upper and lower arm respectively. From body segment parameter information, the distance between the upper and lower arm centres of mass and the shoulder and elbow, $Lcm(\text{upper arm})$ and $Lcm(\text{lower arm})$ respectively, are known. These distances can be rewritten as vectors in terms of the humeral coordinate system.

$$Lcm(\text{upper arm})_h = \{Lcm(\text{upper arm}), 0, 0\} \quad (5.8)$$

$$(5.9)$$

$$Lcm(\text{lower arm})_h = [B_{h-lab}] * ([B_{u-lab}]^{-1} * \{Lcm(\text{lower arm}), 0, 0\} + \{X, Y, Z\}_{Ou-lab} - \{X, Y, Z\}_{Oh-lab})$$

The hand centre is the point of application for the hand forces and must be known in terms of the humeral coordinate system. Hand centre position can be written as a vector in terms of the humeral coordinate system:

$$(5.10)$$

$$L(\text{hand centre})_h = [B_{h-lab}] * (\{X, Y, Z\}_{hand\ centre-lab} - \{X, Y, Z\}_{Oh-lab})$$

The equations for describing moments due to external loading around the glenohumeral joint centre can now be written. Each equation follows the format, where the joint moments generated by hand moments are derived first followed by hand forces,

gravitational force on the lower arm and gravitational force on the upper arm.

$$\Sigma Mx_h(\text{external loading distal to joint}) \quad (5.11)$$

$$\begin{aligned} &= Mh_{x-h} \\ &+ (L(\text{hand centre})_{y-h} * Fh_{z-h} - L(\text{hand centre})_{z-h} * Fh_{y-h}) \\ &+ (Lcm(\text{lower arm})_{y-h} * Fg(\text{lower arm})_{z-h} - Lcm(\text{lower arm})_{z-h} * Fg(\text{lower arm})_{y-h}) \\ &+ (Lcm(\text{upper arm})_{y-h} * Fg(\text{upper arm})_{z-h} - Lcm(\text{upper arm})_{z-h} * Fg(\text{upper arm})_{y-h}) \end{aligned}$$

$$\Sigma My_h(\text{external loading distal to joint}) \quad (5.12)$$

$$\begin{aligned} &= Mh_{y-h} \\ &+ (L(\text{hand centre})_{z-h} * Fh_{x-h} - L(\text{hand centre})_{x-h} * Fh_{z-h}) \\ &+ (Lcm(\text{lower arm})_{z-h} * Fg(\text{lower arm})_{x-h} - Lcm(\text{lower arm})_{x-h} * Fg(\text{lower arm})_{z-h}) \\ &+ (Lcm(\text{upper arm})_{z-h} * Fg(\text{upper arm})_{x-h} - Lcm(\text{upper arm})_{x-h} * Fg(\text{upper arm})_{z-h}) \end{aligned}$$

$$\Sigma Mz_h(\text{external loading distal to joint}) \quad (5.13)$$

$$\begin{aligned} &= Mh_{z-h} \\ &+ (L(\text{hand centre})_{x-h} * Fh_{y-h} - L(\text{hand centre})_{y-h} * Fh_{x-h}) \\ &+ (Lcm(\text{lower arm})_{x-h} * Fg(\text{lower arm})_{y-h} - Lcm(\text{lower arm})_{y-h} * Fg(\text{lower arm})_{x-h}) \\ &+ (Lcm(\text{upper arm})_{x-h} * Fg(\text{upper arm})_{y-h} - Lcm(\text{upper arm})_{y-h} * Fg(\text{upper arm})_{x-h}) \end{aligned}$$

The equation describing moments around the elbow rotation axis due to external loading can now be derived. All of the external forces and moments must be written as vectors in terms of the ulnar coordinate system. Using an approach similar to that used in equations 5.6, 5.7a and 5.7b:

$$Fg(\text{lower arm})_h = [B_{u-lab}] * \{0, -1 * Fg(\text{lower arm}), 0\} \quad (5.14)$$

$$Fh_h = [B_{u-lab}] * \{Fh_x, Fh_y, Fh_z\}_{lab} \quad (5.14a)$$

$$Mh_h = [B_{u-lab}] * \{Mh_x, Mh_y, Mh_z\}_{lab} \quad (5.14b)$$

The location of the application of the forces can be given with respect to the ulnar coordinate system origin. Using an approach similar to that used in equations 5.8 and 5.10:

$$Lcm(\text{lower arm})_u = \{Lcm(\text{lower arm}), 0, 0\} \quad (5.15)$$

$$(5.16)$$

$$L(\text{hand centre})_u = [B_{u-lab}] * (\{X, Y, Z\}_{hand\ centre-lab} - \{X, Y, Z\}_{Ou-lab})$$

The equation for describing the moment due to external loading around the Y_u axis can now be written. Using an approach similar to that used for equation 5.12, the equation will be:

$$\begin{aligned} \Sigma My_u(\text{external loading distal to elbow joint}) & \quad (5.17) \\ & = Mh_{y-u} \\ & + (L(\text{hand centre})_{z-u} * Fh_{x-u} - L(\text{hand centre})_{x-u} * Fh_{z-u}) \\ & + (Lcm(\text{lower arm})_{z-u} * Fg(\text{lower arm})_{x-u} - Lcm(\text{lower arm})_{x-u} * Fg(\text{lower arm})_{z-u}) \end{aligned}$$

5.2.1.2 Moments Due to Muscle Action

Using kinematics in conjunction with the anatomical and effective muscle origin and insertion data the equations for joint moments resulting from muscle activity can be written.

Before any moment equations can be derived, the lines of action for each muscle included in the analysis must be calculated. The line of action is calculated as a unit direction vector pointing from the muscle insertion (effective or anatomic) to the muscle origin. To calculate the lines of action, all origin and insertion data were converted to be with respect to the humerus and ulna for the glenohumeral and elbow moment analyses respectively. This conversion began with a conversion of all data to be with respect to the trunk coordinate system (see equations E4a - E4e in appendix E for details on data conversion to the trunk coordinate system). This was followed by the conversion to the humeral and ulnar coordinate systems. For any point A, the conversions would be:

$$\{X, Y, Z\}_{A-h} = [B_{h-lab}] * [B_{t-lab}]^{-1} * (\{X, Y, Z\}_{A-t} - \{X, Y, Z\}_{Oh-t}) \quad (5.18)$$

and,

$$\{X, Y, Z\}_{A-u} = [B_{u-lab}] * [B_{t-lab}]^{-1} * (\{X, Y, Z\}_{A-t} - \{X, Y, Z\}_{Ou-t}) \quad (5.19)$$

For a muscle, origin a , and effective or anatomic insertion b , the unit vector describing the line of action, L_a , with respect to the humerus or ulna would then be:

$$\{I, J, K\}_{L_a-h} = \{(X_{a-h} - X_{b-h})/A_1, (Y_{a-h} - Y_{b-h})/A_1, (Z_{a-h} - Z_{b-h})/A_1\} \quad (5.20)$$

and,

$$\{I, J, K\}_{L_a-u} = \{(X_{a-u} - X_{b-u})/A_2, (Y_{a-u} - Y_{b-u})/A_2, (Z_{a-u} - Z_{b-u})/A_2\} \quad (5.21)$$

where,

$$A_1 = ((X_{a-h} - X_{b-h})^2 + (Y_{a-h} - Y_{b-h})^2 + (Z_{a-h} - Z_{b-h})^2)^{1/2}$$

$$A_2 = ((X_{a-u} - X_{b-u})^2 + (Y_{a-u} - Y_{b-u})^2 + (Z_{a-u} - Z_{b-u})^2)^{1/2}$$

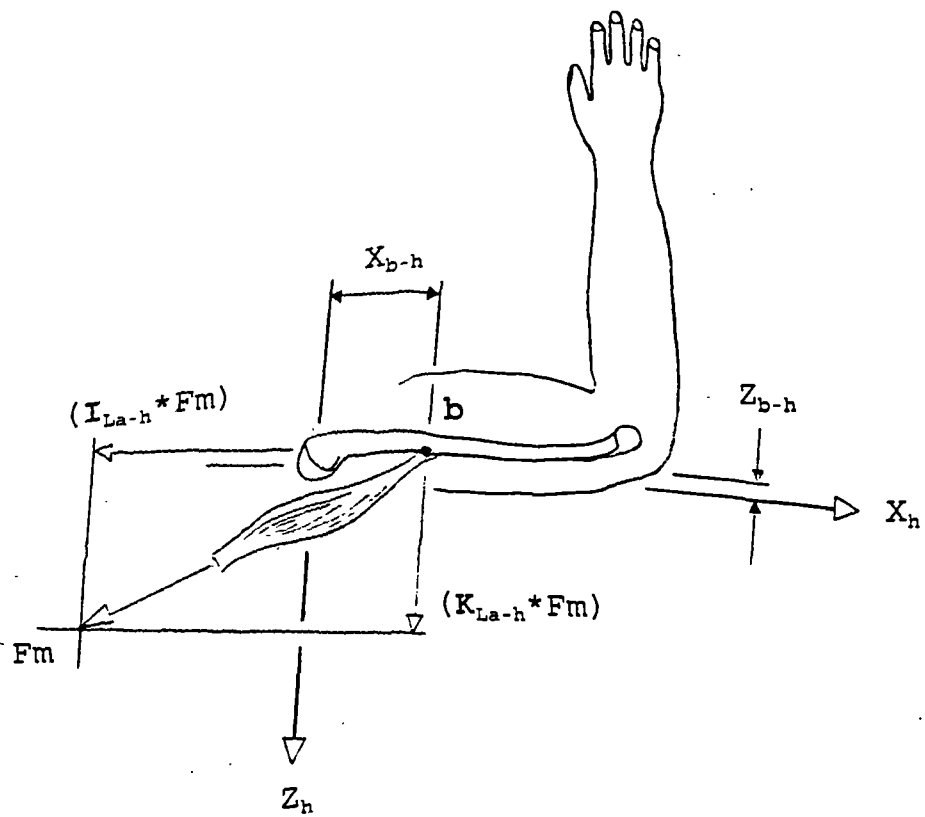


Figure 5.7 A muscle crossing the glenohumeral joint with insertion b , will produce a joint moment My_h (muscle activity) when it is active. Muscle force, F_m , will act in the direction of the line of muscle action, La .

Determining lines of action for biceps requires special attention. Biceps is split into two functional sections. The proximal biceps section originates on the scapula and inserts into the intertubercular groove. This allows the effective insertion for proximal biceps to be determined using the format used for the other muscles passing over the humeral head. The distal section originates in the intertubercular groove and inserts on the radial tuberosity. Force in each section is constrained to be equal.

Beginning with moments produced around the glenohumeral joint, figure 5.7 shows a single muscle which would contribute to moments about the Y_h axis. Moments generated by muscle action are cumulative, so that the approach used for this single muscle can be applied to all of the muscles crossing the joint to yield the total moment generated by muscle action about the Y_h axis, $\sum My_h(\text{muscle activity})$. The moment around the Y_h axis produced by a single muscle inserted at b into the humerus can be calculated as a function of muscle force, F_m .

$$My_h(\text{muscle activity}) = Z_{b-h} * (I_{La-h} * F_m) - X_{b-h} * (K_{La-h} * F_m)$$

or,

(5.22a)

$$My_h(\text{muscle activity}) = (Z_{b-h} * I_{La-h} - X_{b-h} * K_{La-h}) * F_m$$

Similarly, the equations representing moments generated by the muscle around the X_h and Z_h axes can be written:

$$Mx_h(\text{muscle activity}) = (Y_{b-h} * K_{La-h} - Z_{b-h} * J_{La-h}) * F_m \quad (5.22b)$$

$$Mz_h(\text{muscle activity}) = (X_{b-h} * J_{La-h} - Y_{b-h} * I_{La-h}) * F_m \quad (5.22c)$$

Equations 5.22a - 5.22c can be rewritten in a matrix format, where the parameters of matrix $[D]$ are the values within the round brackets from the equations 5.22a - 5.22c. In matrix notation, the equations would then be:

$$\begin{bmatrix} Mx_h \\ My_h \\ Mz_h \end{bmatrix}_{(\text{muscle activity})} = [D] * F_m \quad (5.23)$$

where $[D]$ is a 3 x 1 matrix representing the perpendicular moment arm length the muscle is acting on. Expanding matrix $[D]$ to include all of the muscles crossing the glenohumeral joint would result in a 3 x 24 matrix corresponding to the 24 muscle elements crossing the joint. With this expansion, equation 5.23 would become:

$$[\Sigma M_x(\text{muscle activity})] = \begin{bmatrix} d_{1,1} & \dots & d_{1,24} \\ d_{2,1} & \dots & d_{2,24} \\ d_{3,1} & \dots & d_{3,24} \end{bmatrix} * \begin{bmatrix} Fm_1 \\ \vdots \\ Fm_{24} \end{bmatrix} \quad (5.24)$$

where the calculated moments are the moments generated by muscle action about the glenohumeral joint, $\Sigma Mx_n(\text{muscle activity})$, $\Sigma My_n(\text{muscle activity})$ and $\Sigma Mz_n(\text{muscle activity})$.

Using a similar approach, the moment generated by muscle action about the elbow joint can be calculated. The moment produced around the ulna Y axis, Y_u , by a muscle inserted at b into the ulna would be:

$$My_u(\text{muscle activity}) = (Z_{b-u} * I_{b-u} + X_{b-u} * K_{b-u}) * Fm \quad (5.25)$$

This equation can be written in a matrix format, where the parameters of matrix [E] are the values within the round brackets from equation 5.25. In matrix notation, the equation would then be:

$$My_u(\text{muscle activity}) = [E] * Fm \quad (5.26)$$

where [E] is a 1 x 1 matrix representing the perpendicular moment arm length that the muscle is acting on. Expanding matrix [E] to include all of the muscles crossing the elbow joint would result in a 1 x 5 matrix corresponding to the 5 muscle elements crossing the joint (see table 5.1).

$$\Sigma My_u(\text{muscle activity}) = [e_{1,1} \dots e_{1,5}] * \begin{bmatrix} Fm_1 \\ Fm_2 \\ Fm_{24} \\ Fm_{25} \\ Fm_{26} \end{bmatrix} \quad (5.27)$$

Triceps wraps around the elbow joint when elbow flexion exceeds approximately 90 degrees. An effective insertion was therefore required for triceps when elbow flexion exceeded approximately 90 degrees. After 90 degrees of flexion, the effective insertion remains fixed at approximately the position of the anatomical insertion at 90 degrees of flexion.

Using this characteristic, wrapping was corrected for by using a simple geometric constraint on the perpendicular moment arm lengths $e_{1,4}$, $e_{1,5}$ and $e_{1,6}$. Since no advanced wrapping correction was used for this, it was not documented earlier in this chapter. Using the anatomical insertion position, the largest moment arm that the muscle can act on in the $X_u - Z_u$ plane is if the muscle was pulling perpendicularly to a line joining ulna origin and muscle insertion. This situation occurs at approximately 45 degrees of elbow flexion. The length of the largest moment arm in the $X_u - Z_u$ plane would be:

$$l_{\max} = (X_{b-u}^2 + Z_{b-u}^2)^{1/2}$$

At 90 degrees of flexion, the moment arm for triceps is reduced to approximately 70 percent of this. If the calculated values for $e_{1,4}$, $e_{1,5}$ and $e_{1,6}$ are less than 70 percent of l_{\max} , then wrapping is indicated and can be corrected for by setting $e_{1,4}$, $e_{1,5}$ and or $e_{1,6}$ to 70 percent of l_{\max} .

In calculating the glenohumeral joint moments generated by muscle action, all of the muscles crossing the joint were considered. For the elbow, only a few of the total number of muscles have been considered. While this study was not focusing on the elbow joint, by including it in our analysis, it was hoped to gain an insight into the two joint function of biceps and triceps. To avoid the complications of modelling the remaining muscles, their functions were included in the function of biceps and triceps. For this study, biceps was assumed to produce half of the required elbow flexion moment. To simulate the action of the other flexors, the parameters of matrix [E] relating to biceps, $e_{1,1}$ and $e_{1,2}$ were doubled. This had the effect of doubling the moment generating potential for biceps with respect to its calculated value. Triceps is the main elbow extensor, and as such it is considered to produce all of the elbow extensor joint moment.

The repercussions of this departure from anatomy will be minimized by the anatomical muscle configuration. If optimization of biceps muscle force produces an excess of elbow flexion moment, then the medial and lateral heads of triceps can act as antagonists. These fascicles cross the elbow and insert on the humerus, therefore their action does not affect the modelled shoulder function. If optimization of biceps muscle force produces an insufficient amount of moment at the shoulder, its action will be supplemented by coracobrachialis. Because coracobrachialis shares a common origin with biceps short head and a similar line of action to its humeral insertion, the supplementary action will not affect modelled shoulder function.

The two fascicles of biceps and the first of triceps cross both the elbow and

glenohumeral joints, if matrices [D] and [E] are combined then a single matrix relationship can be developed to describe moments produced by the muscles around both the glenohumeral and elbow joints. This change would involve combining matrices [D] and [E] to form a single 4 x 26 matrix, [F]. This matrix would then relate muscle force in the 26 fascicles to the four moment equations. To combine matrices [D] and [E] they first must be converted to a 26 column format. Matrix [D] from equation 5.24 can be converted to a 3 x 26 format by adding zeros in columns 25 and 26.

$$[\Sigma M_h(\text{muscle activity})] = \begin{bmatrix} d_{1,1} & \dots & d_{1,24} & 0 & 0 \\ d_{2,1} & \dots & d_{2,24} & 0 & 0 \\ d_{3,1} & \dots & d_{3,24} & 0 & 0 \end{bmatrix} * \begin{bmatrix} Fm_1 \\ \vdots \\ Fm_{26} \end{bmatrix} \quad (5.28a)$$

rewriting,

$$[\Sigma M_h(\text{muscle activity})] = [D'] * \begin{bmatrix} Fm_1 \\ \vdots \\ Fm_{26} \end{bmatrix} \quad (5.28b)$$

Matrix [E] from equation 5.27 can be converted to a 1 x 26 format by splitting the matrix between columns 2 and 3 and adding zeros to make up columns 3 to 23.

$$\Sigma My_e(\text{muscle activity}) = [e_{1,1} \ e_{1,2} \ 0 \ \dots \ 0 \ e_{1,3} \ e_{1,4} \ e_{1,5}] * \begin{bmatrix} Fm_1 \\ \vdots \\ Fm_{26} \end{bmatrix} \quad (5.29a)$$

rewriting,

$$\Sigma My_e(\text{muscle activity}) = [E'] * \begin{bmatrix} Fm_1 \\ \vdots \\ Fm_{26} \end{bmatrix} \quad (5.29b)$$

Combining matrices [D'] and [E'] from equations 5.28b and 5.29b, produces a matrix [F] which can be used to calculate all of the elbow and glenohumeral joint moments generated by all of the muscles being considered in this study. The first three rows of [F] are formed from [D'] and the fourth from [E'].

$$\begin{bmatrix} \sum Mx_h(\text{muscle activity}) \\ \sum My_h(\text{muscle activity}) \\ \sum Mz_h(\text{muscle activity}) \\ \sum My_u(\text{muscle activity}) \end{bmatrix} = \begin{bmatrix} f_{1,1} & \dots & f_{1,26} \\ f_{2,1} & \dots & f_{2,26} \\ f_{3,1} & \dots & f_{3,26} \\ f_{4,1} & \dots & f_{4,26} \end{bmatrix} * \begin{bmatrix} Fm_1 \\ \vdots \\ Fm_{26} \end{bmatrix} \quad (5.30)$$

5.2.2. Force Equilibrium

For equilibrium, the sum of all forces imparted to a body segment must equal zero. The forces on a segment can originate from external segment forces and internal joint loading consisting of both muscle forces and joint contact forces. Applying this to the shoulder, the equations describing force equilibrium would then be:

$$\begin{aligned} 0 &= \sum F(\text{glenohumeral joint}) \\ &= \sum F(\text{external and distal to joint}) + \sum F(\text{muscle activity}) + \sum F(\text{joint contact}) \end{aligned} \quad (5.31)$$

For determining joint stability, it is desirable to know the joint contact forces in terms of the glenoid fossa coordinate system. To determine forces with respect to this coordinate system, orientation of the glenoid fossa coordinate system must be calculated. This can be calculated using scapula coordinate system orientation and the two glenoid fossa orientation angles (see section 4.1.3 for the definition of these angles). Two sequential rotations are required to move from the scapula to the glenoid fossa coordinate system orientation. The rotations take place about the Z_s and X_{gr} axes respectively and are represented in matrix form as:

$$\begin{aligned} [B_{gf-lab}] &= \begin{bmatrix} 1 & 0 & 0 \\ 0 & \cos\theta_1 & \sin\theta_1 \\ 0 & -\sin\theta_1 & \cos\theta_1 \end{bmatrix} \\ &* \begin{bmatrix} \cos\theta_2 & \sin\theta_2 & 0 \\ -\sin\theta_2 & \cos\theta_2 & 0 \\ 0 & 0 & 1 \end{bmatrix} * [B_{s-lab}] \end{aligned} \quad (5.32)$$

where, $\theta_1 = -1$ *(angle between X_s and X_{gr} axes in the X_s - Y_s plane)
 $\theta_2 = -1$ *(angle between Z_s and Z_{gr} axes in the X_s - Y_s plane)

Applying equation 3.31 to the three axes of the glenoid fossa coordinate system, X_{gr} , Y_{gr} and Z_{gr} .

$$\begin{aligned}
0 &= \sum Fx_{gr}(\text{glenohumeral joint}) & (5.33a) \\
&= \sum Fx_{gr}(\text{external and distal to joint}) + \sum Fx_{gr}(\text{muscle activity}) + \sum Fx_{gr}(\text{joint contact})
\end{aligned}$$

$$\begin{aligned}
0 &= \sum Fy_{gr}(\text{glenohumeral joint}) & (5.33b) \\
&= \sum Fy_{gr}(\text{external and distal to joint}) + \sum Fy_{gr}(\text{muscle activity}) + \sum Fy_{gr}(\text{joint contact})
\end{aligned}$$

$$\begin{aligned}
0 &= \sum Fz_{gr}(\text{glenohumeral joint}) & (5.33c) \\
&= \sum Fz_{gr}(\text{external and distal to joint}) + \sum Fz_{gr}(\text{muscle activity}) + \sum Fz_{gr}(\text{joint contact})
\end{aligned}$$

External forces on the arm have been calculated and can be written explicitly. Forces due to muscle action cannot be calculated directly because of indeterminacy. Recognising that joint contact forces are a function of both external forces and muscle action and using the equality condition of equation 5.31, joint contact forces can be determined as a function of the known external loads and unknown muscle forces.

5.2.2.1 Forces Due to External Loading

External forces applied to the arm consist of the force of gravity on the upper arm, $Fg(\text{upper arm})$, lower arm, $Fg(\text{lower arm})$ and hand forces, Fh . These forces were calculated with respect to the humeral coordinate system in equations 5.5, 5.6 and 5.7a of section 5.2.1.1. Summing these forces gives the total external forces applied to the arm. These forces can then be converted to be with respect to the glenoid fossa coordinate system.

$$\begin{aligned}
&\sum Fx_{gr}(\text{external and distal to joint}) & (5.34a) \\
&= [B_{gf-lab}] * [B_{h-lab}]^{-1} * (Fg(\text{upper arm})_x + Fg(\text{lower arm})_x + Fh_x)
\end{aligned}$$

$$\begin{aligned}
&\sum Fy_{gr}(\text{external and distal to joint}) & (5.34b) \\
&= [B_{gf-lab}] * [B_{h-lab}]^{-1} * (Fg(\text{upper arm})_y + Fg(\text{lower arm})_y + Fh_y)
\end{aligned}$$

$$\begin{aligned}
&\sum Fz_{gr}(\text{external and distal to joint}) & (5.34c) \\
&= [B_{gf-lab}] * [B_{h-lab}]^{-1} * (Fg(\text{upper arm})_z + Fg(\text{lower arm})_z + Fh_z)
\end{aligned}$$

5.2.2.2 Forces Due to Muscle Action

All of the muscles that cross the glenohumeral joint can apply force to the arm. The overall force produced by muscular action is the cumulative total of individual muscle

forces. Quantifying the force contributed by each muscle utilizes the same procedure, so calculations are shown here for only a single muscle.

The muscle force is not known, therefore the force imparted by a muscle to the arm cannot be written explicitly. Using a format similar to that used in the quantification of moments generated about the glenohumeral joint by muscle action, forces imparted to the arm by the muscles can be written in terms of the individual muscle forces.

Calculating the force imparted to the arm by each muscle requires its line of action at effective or anatomical insertion to be known. The unit direction vectors describing these lines of action were calculated previously for determining the contribution of each muscle to moment generation around the glenohumeral and elbow joints (section 5.2.1.1). To calculate the force imparted by a muscle to the humerus with respect to the glenoid fossa coordinate system, the unit direction vector describing the muscle's line of action must first be converted to be with respect to the glenoid fossa coordinate system.

$$\{I, J, K\}_{La-gf} = [B_{gf-lab}] * [B_{h-lab}]^{-1} * \{I, J, K\}_{La-h} \quad (5.35)$$

Using equation 5.20, and unit direction vectors $\{I, J, K\}_{La-gf}$ for the line of action of any muscle crossing the glenohumeral joint, the force imparted by that muscle to the humerus can be determined with respect to the glenoid fossa coordinate system.

$$F_{x_{gf}(\text{muscle action})} = I_{La-gf} * F_m \quad (5.36a)$$

$$F_{y_{gf}(\text{muscle action})} = J_{La-gf} * F_m \quad (5.36b)$$

$$F_{z_{gf}(\text{muscle action})} = K_{La-gf} * F_m \quad (5.36c)$$

these equations can be rewritten in matrix form as:

$$[F_{gf(\text{muscle action})}] = [G] * F_m \quad (5.37)$$

where [G] is a 3 x 1 matrix consisting of the unit direction vector in terms of the glenoid fossa coordinate system for the muscle being analysed.

Expanding on equation 5.37, the cumulative total force resulting from the muscle action of all muscles crossing the glenohumeral joint would be:

$$[\Sigma F_g(\text{muscle action})] = \begin{bmatrix} g_{1,1} & \dots & g_{1,24} \\ g_{2,1} & \dots & g_{2,24} \\ g_{3,1} & \dots & g_{3,24} \end{bmatrix} * \begin{bmatrix} Fm_1 \\ \vdots \\ Fm_{24} \end{bmatrix} \quad (5.38)$$

noting that the medial and lateral heads of triceps (muscle numbers 25 and 26) do not cross the glenohumeral joint.

Converting matrix [G] from equation 5.38 into a 3 x 26 matrix would allow the muscle force matrix consisting of muscle forces Fm_1 to Fm_{26} to be used. This conversion requires that two columns of zeros forming columns 25 and 26 be added to matrix [G]. The total muscle force applied to the arm by muscles crossing the glenohumeral joint would then be:

$$[\Sigma F_g(\text{muscle action})] = \begin{bmatrix} g_{1,1} & \dots & g_{1,24} & 0 & 0 \\ g_{2,1} & \dots & g_{2,24} & 0 & 0 \\ g_{3,1} & \dots & g_{3,24} & 0 & 0 \end{bmatrix} * \begin{bmatrix} Fm_1 \\ \vdots \\ Fm_{26} \end{bmatrix} \quad (5.39a)$$

rewriting,

$$[\Sigma F_g(\text{muscle action})] = \begin{bmatrix} h_{1,1} & \dots & h_{1,26} \\ h_{2,1} & \dots & h_{2,26} \\ h_{3,1} & \dots & h_{3,26} \end{bmatrix} * \begin{bmatrix} Fm_1 \\ \vdots \\ Fm_{26} \end{bmatrix} \quad (5.39b)$$

5.2.2.3 Joint Contact Forces

Glenohumeral joint contact forces can be calculated from muscle force and external loading on the arm. The total resultant contact force at the glenohumeral joint will pass through the humeral head centre. This is a characteristic feature of any ball and socket type joint with an extremely low coefficient of friction. Since the resultant contact force passes through the humeral head centre, it will not generate a moment about the humeral coordinate system origin. It was for this reason that the humeral coordinate system origin was used as the reference point for humeral moment analysis.

Glenohumeral joint contact forces can be determined as a function of external forces applied to the arm and the muscle forces $Fm_1 - Fm_{26}$. Reordering the equilibrium equations 5.33a - 5.33c, joint contact force can be written in terms of the external and muscle forces,

$$\begin{aligned} \Sigma F_{x_g}(\text{joint contact}) & & (5.40a) \\ & = -1 * (\Sigma F_{x_g}(\text{external and distal to joint}) + \Sigma F_{x_g}(\text{muscle action})) \end{aligned}$$

$$\begin{aligned} \Sigma F_{y_g}(\text{joint contact}) & & (5.40b) \\ & = -1 * (\Sigma F_{y_g}(\text{external and distal to joint}) + \Sigma F_{y_g}(\text{muscle action})) \end{aligned}$$

$$\begin{aligned} \Sigma F_{z_g}(\text{joint contact}) & & (5.40c) \\ & = -1 * (\Sigma F_{z_g}(\text{external and distal to joint}) + \Sigma F_{z_g}(\text{muscle action})) \end{aligned}$$

where the external forces on the humerus were determined explicitly in equations 5.34a - 5.34c and muscle force on the humerus was determined as a function of the 26 individual muscle forces in equation 5.39b.

5.3. OPTIMIZATION

In classical mechanics, a set of four moment equilibrium equations as were derived in section 5.2, would allow four independent muscle forces to be calculated. In this study, there are 26 unknown independent muscle forces. To solve for all of these forces requires a technique other than is found in classical mechanics. The method used in this study is called a double linear optimization.

Linear optimization allows the optimum solution of a set of independent variables subject to a series of linear constraint equations. During the solution process, variables are optimized against an objective function while being constrained by the linear constraint equations. The Simplex algorithm as detailed by Press et al (1989) was used to perform the linear optimization procedures in this study. For further details on the theory and coding of the Simplex algorithm or linear optimization, see Press et al (1989).

The double linear optimization approach used in this study required repeating the optimization of the muscle forces against two objective functions sequentially. In the first optimization, the overall maximum muscle stress was minimized subject to the required constraint equations. Details of the constraint equations will be discussed later. Mathematically, the first objective function would be:

$$\text{Minimize } \sigma \quad (5.41)$$

$$\text{where, } \sigma \geq (F_{m_i}/PCSA_i), \quad i = 1 \text{ to } 26$$

in which $PCSA_i$ represents the physiological cross-sectional area of the i^{th} muscle and σ is

redundant optimization variable, OV_{27} was introduced. The second objective equation was then written as:

$$\text{Minimize, } 1 * Fm_1 + 1 * Fm_2 + \dots + 1 * Fm_{26} + 0 * OV_{27} \quad (5.45)$$

Where the stress within each muscle is constrained to be less than the maximum muscle stress, σ , as determined in the first optimization. This constraint can be written for each muscle using the form:

$$\text{Muscle 1, } (PCSA_1 * \sigma) \geq 1 * Fm_1 + 0 * Fm_2 + \dots + 0 * Fm_{26} + 0 * OV_{27} \quad (5.46a)$$

$$\text{Muscle 2, } (PCSA_2 * \sigma) \geq 0 * Fm_1 + 1 * Fm_2 + \dots + 0 * Fm_{26} + 0 * OV_{27} \quad (5.46b)$$

⋮

$$\text{Muscle 26, } (PCSA_{26} * \sigma) \geq 0 * Fm_1 + 0 * Fm_2 + \dots + 1 * Fm_{26} + 0 * OV_{27} \quad (5.46c)$$

Two sets of optimization constraint equations were used in this study. The first set consisted of the four moment equilibrium equations, 5.3a, 5.3b, 5.3c and 5.4 derived in section 5.2. The constraint equations were written remembering that the relationship derived for moments due to external loading (equations 5.11, 5.12, 5.13 and 5.17) were explicit and for moments due to muscle action (equation 5.30) were a function of individual muscle force.

$$\begin{aligned} -1 * \sum M_h(\text{external loading distal to joint}) \\ = f_{1,1} * Fm_1 + f_{1,2} * Fm_2 + \dots + f_{1,26} * Fm_{26} + 0 * (OV_{27} \text{ or } \sigma) \end{aligned} \quad (5.47a)$$

$$\begin{aligned} -1 * \sum My_h(\text{external loading distal to joint}) \\ = f_{2,1} * Fm_1 + f_{2,2} * Fm_2 + \dots + f_{2,26} * Fm_{26} + 0 * (OV_{27} \text{ or } \sigma) \end{aligned} \quad (5.47b)$$

$$\begin{aligned} -1 * \sum Mz_h(\text{external loading distal to joint}) \\ = f_{3,1} * Fm_1 + f_{3,2} * Fm_2 + \dots + f_{3,26} * Fm_{26} + 0 * (OV_{27} \text{ or } \sigma) \end{aligned} \quad (5.47c)$$

$$\begin{aligned} -1 * \sum My_u(\text{external loading distal to joint}) \\ = f_{4,1} * Fm_1 + f_{4,2} * Fm_2 + \dots + f_{4,26} * Fm_{26} + 0 * (OV_{27} \text{ or } \sigma) \end{aligned} \quad (5.47d)$$

Optimizing with this set of constraint equations produced a set of muscle forces that balanced joint moments without considering joint stability.

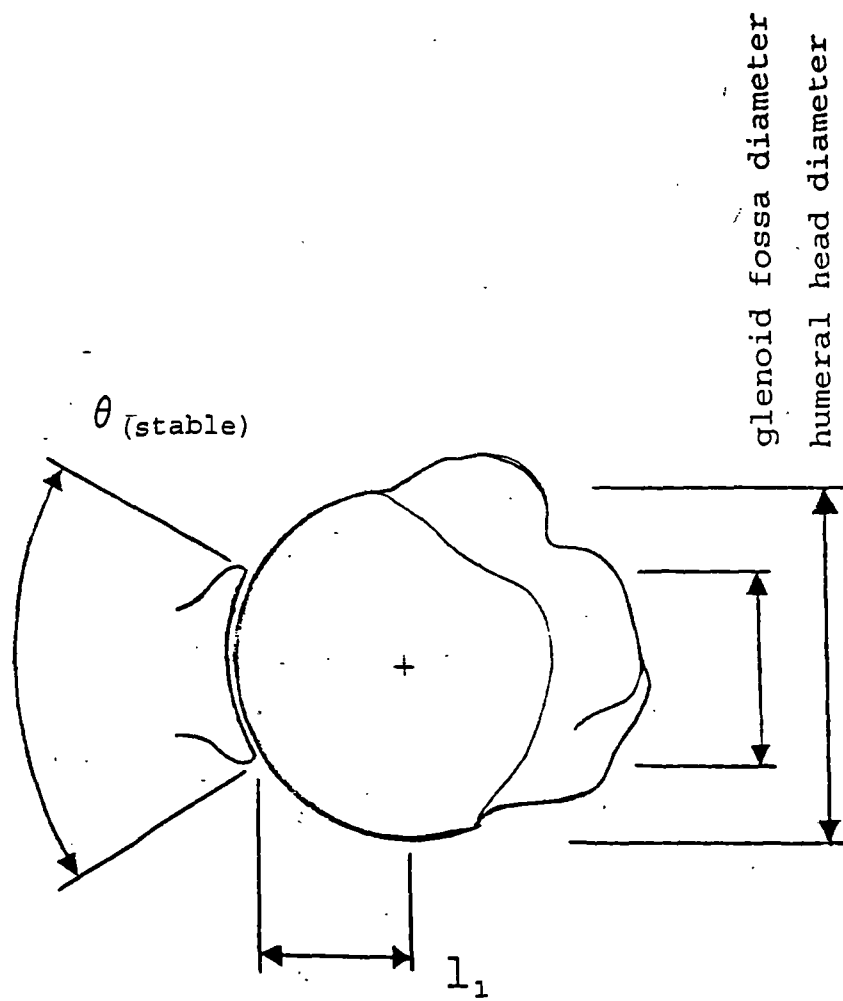


Figure 5.8 A simplified view of the glenoid fossa and humeral head showing the region of stability and instability for the total resultant contact force. Values for $\theta_{(stable)}$ and l_1 are calculated using equations 5.48 and 5.50 respectively.

The second set of constraint equations used in this study imposed the requirement of joint stability on the chosen muscle forces in addition to the joint moment balance constraints. Anatomically, shoulder muscle action does provide some glenohumeral joint stability in addition to the production of the joint moments required for equilibrium, therefore imposing these constraints on the optimized muscle forces would appear to be more physiologically correct.

For the glenohumeral joint, stability is maintained as long as the resultant joint contact force passes through the glenoid fossa. If the resultant force passes through the glenoid fossa centre, then the joint will be stable. Shear forces at the joint tend to move the resultant contact force away from the glenoid fossa centre and as such tend to destabilize the joint. When shear forces become large enough to move the resultant joint contact force beyond the glenoid fossa rim, then the joint will be unstable. Physiologically this situation can be averted by increased activity in subscapularis, infraspinatus and supraspinatus. These muscles tend to increase joint compression while not increasing joint shear forces, thereby moving the resultant joint contact force back towards the glenoid fossa centre.

Constraining the optimized muscle forces to provide a stable glenohumeral joint required determining a relationship between joint contact forces and joint geometry. With respect to geometry, the joint will remain stable as long as the total resultant joint contact force passes through the glenoid fossa. Figure 5.8 shows the stable region for this force for a two-dimensional view of the joint. The angle describing the stable region for the force, $\theta_{(stable)}$, can be calculated from joint geometry.

(5.48)

$$\theta_{(stable)} = 2 * \sin^{-1}(\text{glenoid fossa diameter}/\text{humeral head diameter})$$

where the anatomical dimensions were measured during the anatomical study and are listed in appendix A. In the two-dimensional view of figure 5.8, the resultant joint contact force is the total of a compressive and a shearing contact force. The relative magnitude of these two components determine whether stability is maintained. Using the principle of similar triangles, stability will be maintained for:

(5.49)

$$((0.5 * \text{glenoid fossa diameter})/l_1) \geq (\text{shear force}/\text{compressive force})$$

where,

$$l_1 = 0.5 * (\text{humeral head diameter}) * \cos(\theta_{(stable)}/2) \quad (5.50)$$

The two-dimensional situation of figure 5.8 can be expanded to the anatomical three-dimensional configuration required for this study. The Y_{gf} axis direction joint contact force, $F_{y_{gf}}(\text{joint contact})$, will be normal to the glenoid fossa and as such will be the joint compressive force. Joint contact forces in the X_{gf} and Z_{gf} axis directions, $F_{x_{gf}}(\text{joint contact})$ and $F_{z_{gf}}(\text{joint contact})$, will act parallel to the glenoid fossa and will therefore both be joint shear forces. In a normal biomechanical analysis, the total shear force could be calculated using the sum of squares of the two shear force components. Using this approach and assuming the glenoid fossa is circular and all of the forces are acting in a positive direction, equation 5.49 can be rewritten to represent the three-dimensional anatomical situation.

(5.51)

$$((0.5 * \text{glenoid fossa diameter})/l_1) \geq ((F_{x_{gf}}(\text{joint contact})^2 + F_{z_{gf}}(\text{joint contact})^2)^{1/2} / F_{y_{gf}}(\text{joint contact}))$$

A non-linear joint stability constraint equation written in terms of the individual joint forces could now be created from the relationship in equation 5.51. Unfortunately, the linear optimization technique being used in this study requires all constraint equations to be linear.

A linear relationship between the three joint contact forces and joint geometry was required. If shear forces, $F_{x_{gf}}(\text{joint contact})$ and $F_{z_{gf}}(\text{joint contact})$ are considered separately, then equation 5.51 can be reduced to two linear relationships.

(5.52a)

$$((0.5 * \text{glenoid fossa diameter})/l_1) \geq (F_{x_{gf}}(\text{joint contact})/F_{y_{gf}}(\text{joint contact}))$$

(5.52b)

$$((0.5 * \text{glenoid fossa diameter})/l_1) \geq (F_{z_{gf}}(\text{joint contact})/F_{y_{gf}}(\text{joint contact}))$$

These relationships, if considered separately do not ensure a stable joint. This is because the total shear force can still be large enough not to satisfy the basic criteria for stability as outlined in equation 5.49. If however the left sides of equations 5.52a and 5.52 b are reduced by a factor equal to 0.707, then the resulting joint contact forces will always satisfy equation 5.49 and therefore ensure joint stability. Rewriting equations 5.52a and 5.52b:

$$C \geq (F_{x_{gf}}(\text{joint contact})/F_{y_{gf}}(\text{joint contact})) \quad (5.53a)$$

$$C \geq (F_{z_{gf}}(\text{joint contact})/F_{y_{gf}}(\text{joint contact})) \quad (5.53b)$$

where,

$$C = 0.707 * ((0.5 * \text{glenoid fossa diameter})/l_1)$$

and C can be referred to as the stability factor.

The constraint equations ensuring that muscle forces produce a stable joint can be derived using the relationships developed in equations 5.53a and 5.53b. Rewriting the first equation in a different format assuming that the joint will always be in compression and recognising that the shear forces, $F_{x_{gf}(\text{joint contact})}$ and $F_{y_{gf}(\text{joint contact})}$, can act in either a positive or negative direction:

$$-C * F_{y_{gf}(\text{joint contact})} \leq (F_{x_{gf}(\text{joint contact})} \leq C * F_{y_{gf}(\text{joint contact})}) \quad (5.54)$$

Remembering that joint contact forces were determined as a function of external arm forces and the muscle forces, equation 5.54a can be rewritten as:

$$\begin{aligned} -C * (\sum F_{y_{gf}(\text{external and distal to joint})} + \sum F_{y_{gf}(\text{muscle action})}) & \quad (5.55a) \\ \leq (F_{x_{gf}(\text{external and distal to joint})} + \sum F_{x_{gf}(\text{muscle action})}) & \\ \leq C * (\sum F_{y_{gf}(\text{external and distal to joint})} + \sum F_{y_{gf}(\text{muscle action})}) & \end{aligned}$$

Splitting this equation, and reorganising yields:

$$A_1 \leq \sum F_{x_{gf}(\text{muscle action})} + (C * \sum F_{y_{gf}(\text{muscle action})}) \quad (5.56a)$$

and,

$$A_2 \leq -\sum F_{x_{gf}(\text{muscle action})} + (C * \sum F_{y_{gf}(\text{muscle action})}) \quad (5.56b)$$

where

$$A_1 = -F_{x_{gf}(\text{external and distal to joint})} - (C * \sum F_{y_{gf}(\text{external and distal to joint})})$$

$$A_2 = F_{x_{gf}(\text{external and distal to joint})} - (C * \sum F_{y_{gf}(\text{external and distal to joint})})$$

The left hand sides of both 5.56a and 5.56b have been determined explicitly and the right hand sides have been determined as a function of the 26 unknown muscle forces, F_{m_1} - $F_{m_{26}}$. Incorporating this information equations 5.56a and 5.56b can be rewritten in the standard optimization format.

$$(5.57a)$$

$$A_1 \leq (h_{1,1} + C * h_{2,1}) * F_{m_1} + (h_{1,2} + C * h_{2,2}) * F_{m_2} + \dots + (h_{1,26} + C * h_{2,26}) * F_{m_{26}} + 0 * (OV_{27} \text{ or } \sigma)$$

$$(5.57b)$$

$$A_2 \leq (-h_{1,1} + C * h_{2,1}) * F_{m_1} + (-h_{1,2} + C * h_{2,2}) * F_{m_2} + \dots + (-h_{1,26} + C * h_{2,26}) * F_{m_{26}} + 0 * (OV_{27} \text{ or } \sigma)$$

The constraint equations corresponding to the relationship developed in equation 5.53b can be derived similarly. Their final form is:

(5.57c)

$$A_3 \leq (h_{3,1} + C \cdot h_{2,1}) \cdot Fm_1 + (h_{3,2} + C \cdot h_{2,2}) \cdot Fm_2 + \dots + (h_{3,26} + C \cdot h_{2,26}) \cdot Fm_{26} + 0 \cdot (OV_{27} \text{ or } \sigma)$$

(5.57d)

$$A_4 \leq (-h_{3,1} + C \cdot h_{2,1}) \cdot Fm_1 + (-h_{3,2} + C \cdot h_{2,2}) \cdot Fm_2 + \dots + (-h_{3,26} + C \cdot h_{2,26}) \cdot Fm_{26} + 0 \cdot (OV_{27} \text{ or } \sigma)$$

where,

$$A_3 = -Fz_{gf}(\text{external and distal to joint}) - (C \cdot \sum Fy_{gf}(\text{external and distal to joint}))$$

$$A_4 = Fz_{gf}(\text{external and distal to joint}) - (C \cdot \sum Fy_{gf}(\text{external and distal to joint}))$$

Several details pertaining to optimization implementation are worthy of note. The Simplex algorithm is susceptible to large variations in the magnitude and significant figures of the input parameters. To avoid difficulties encountered during the initial stages of this study, the optimization parameters were limited to two significant figures and the units of the parameters arranged to eliminate large magnitude differences in the input parameters. As a result, units for force during optimization were 100's of N, centimeters for moment arm parameters and 1000's of mm² for physiological cross-sectional area. For example, for middle deltoid with a physiological cross sectional area of 217 mm², the muscle area parameter used for optimization was 0.22. The stability factor, C, was divided by 2 to allow a "factor of safety" of 2 for joint stability.

6. VERIFICATION STUDIES

In an ideal world, validation of a model such as has been developed in this thesis would include a comparison of predicted to measured tissue loading for a variety of activities. If agreement was found between the two, then the model would be assumed valid. Unfortunately, direct measurement of shoulder tissue loading is not normally possible, thereby complicating the validation process.

Two techniques are used in this thesis for model validation. The first is through a comparison of model results to the results of simplified two-dimensional studies in the literature. The second is through a qualitative comparison of electromyographic (EMG) muscle activation data for the shoulder muscles to predicted shoulder muscle force.

This chapter is divided into three main sections. The first section discusses details of a preliminary study where a single subject performed pure abduction. The second section details an investigation into model stability and data uncertainty magnification. The final section documents and discusses EMG and model results obtained for a group of subjects performing a set of five activities. Appendix F contains experimental data relating to this chapter.

6.1. PRELIMINARY STUDY

During the shoulder model development a set of data was required for testing model operation. The activity chosen for analysis was pure abduction. This was to allow a comparison of model results to those documented in the literature. A single subject performed the activity, allowing the required kinematic and geometric data to be collected. The results from this study, while not conclusive, did indicate that the model was operating correctly and that predicted muscle activation correlated with that in the literature.

The techniques used in this study, while simple in comparison to later studies, do include all of the procedures necessary to investigate shoulder function using the model documented in this thesis.

6.1.1. Experimental Procedure

A single male subject, age 25, mass 65 kg and height 1.75 m was used for this study. The subject had no history of shoulder problems or previous athletic training.

The activity chosen for analysis was pure abduction in the frontal plane. The activity was performed as a series of four static positions that spanned the range of shoulder abduction. External humeral rotation was kept to a minimum, thereby limiting the range of

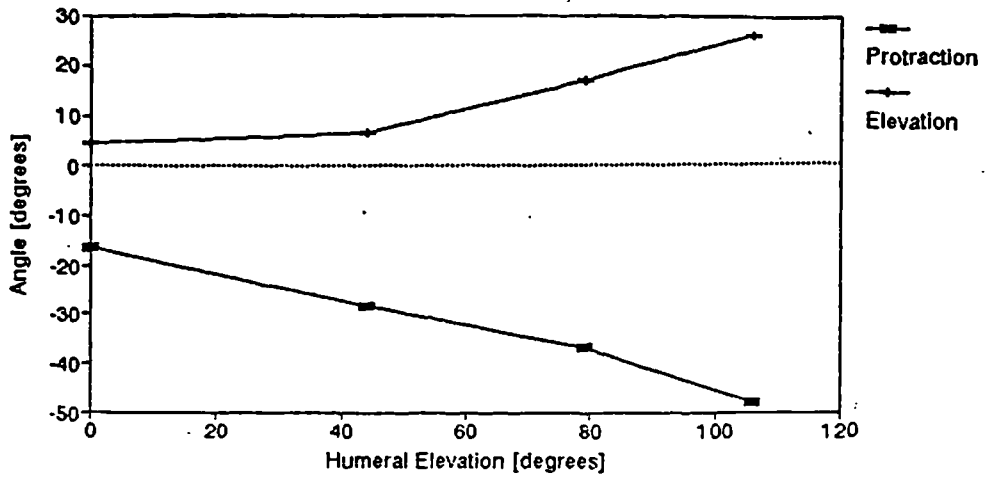


Figure 6.1 Clavicle angular orientation during frontal plane humeral abduction.

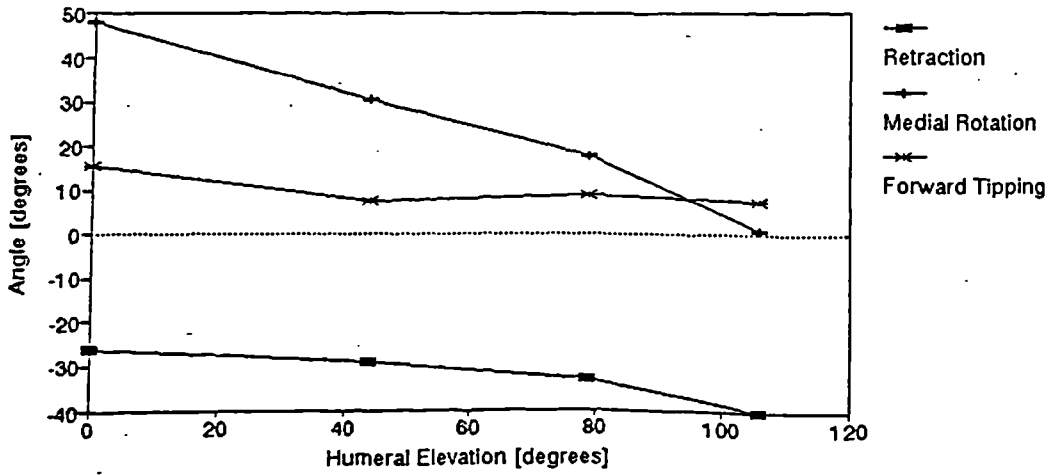


Figure 6.2 Scapula angular orientation during frontal plane humeral abduction.

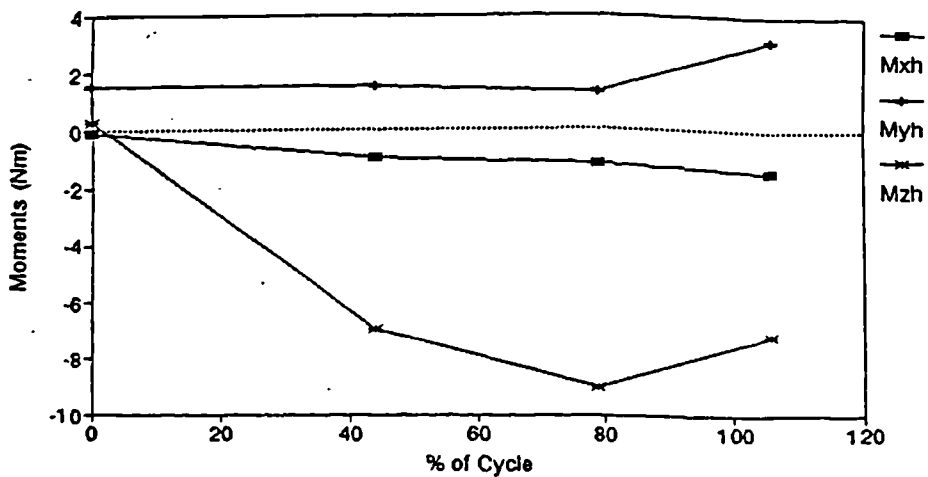


Figure 6.3 Moments at the glenohumeral joint due to external loading of the arm during frontal plane humeral abduction.

abduction to approximately 120 degrees of humeral elevation. The subject was seated with a slightly bent elbow posture throughout data collection.

Kinematics were measured using the 6 camera Vicon motion analysis system. The subject was placed in the anatomical position facing the $+X_{lab}$ direction for the first data collection. This allowed the matrix relating the trunk marker coordinate system to the trunk coordinate system to be calculated. For each subsequent data collection, the subject was positioned with an increasingly abducted arm position. The scapula was palpated to find the location for markers IA and MS. These markers were then affixed to the subject's skin using double sided tape. All of the other subject markers were affixed to the skin using this same tape, but were elevated from the skin by using marker supports.

All of the required subject measurements were taken before kinematic data collection. Mass was measured using a set of clinical scales (sliding weight type, ± 0.1 kg). All of the other measurements were measured manually using a tape measure (± 0.002 m) in conjunction with a pair of specially fabricated large callipers and palpation where required.

Data collected with the motion analysis system were analysed using the Vicon analysis software. Marker positions measured by the system were identified and stored as three-dimensional coordinates to a file within the mainframe VAX environment. Files were analysed using a Zenith 286 personal computer in a Microsoft DOS version 3.5 environment. The shoulder biomechanical model was programmed and run in Turbo Pascal, Borland version 5.1. All data generated by the model were imported into a spreadsheet package for plotting and statistical analysis.

Data analysis was conducted in two stages. In the first stage, subject kinematics were determined from the three-dimensional marker data collected using the motion analysis system. If hand loading was being measured it would also have been processed in this first stage. Scapula kinematics for were measured directly in this static study. If a dynamic abduction analysis was being conducted, a linear regression analysis would be applied to the static scapula orientation as a function of arm elevation in the frontal plane. The relationship obtained would then have been applied to the dynamic data to predict scapula orientation for each frame of dynamic data. Muscle and joint forces were then calculated using a numerical procedure (with and without the constraint of glenohumeral joint stability).

6.1.2 Results

Data was collected for four static positions spanning the range of pure arm abduction in the frontal plane. Figure 6.1 and 6.2 show the clavicle and scapula kinematics as determined from the three-dimensional reflective marker coordinates. In both figures the

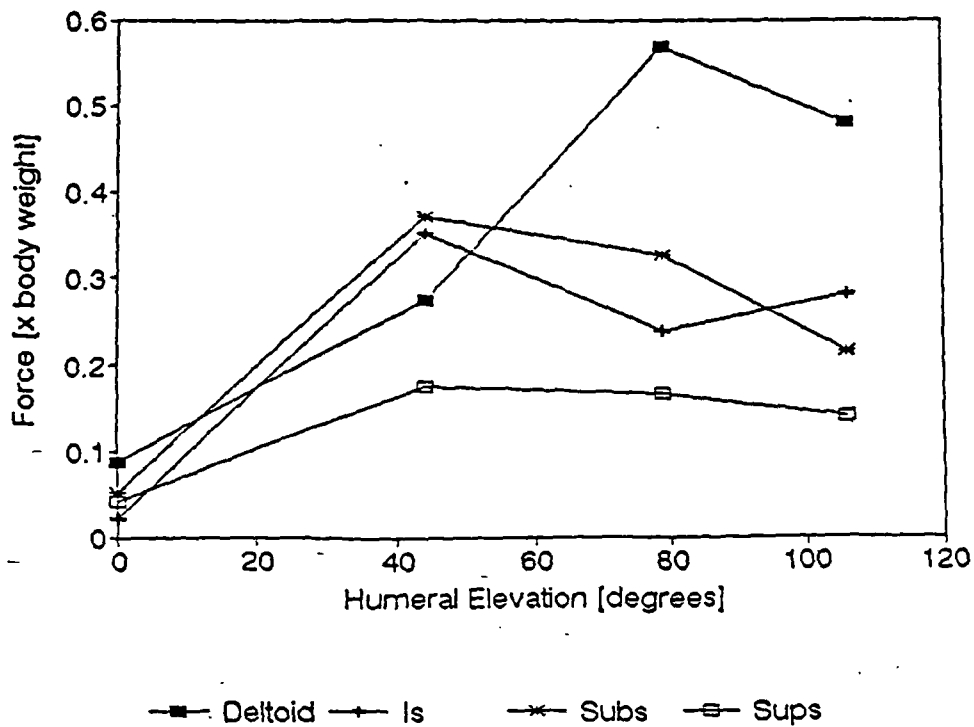


Figure 6.4 Muscle forces predicted for frontal plane abduction.

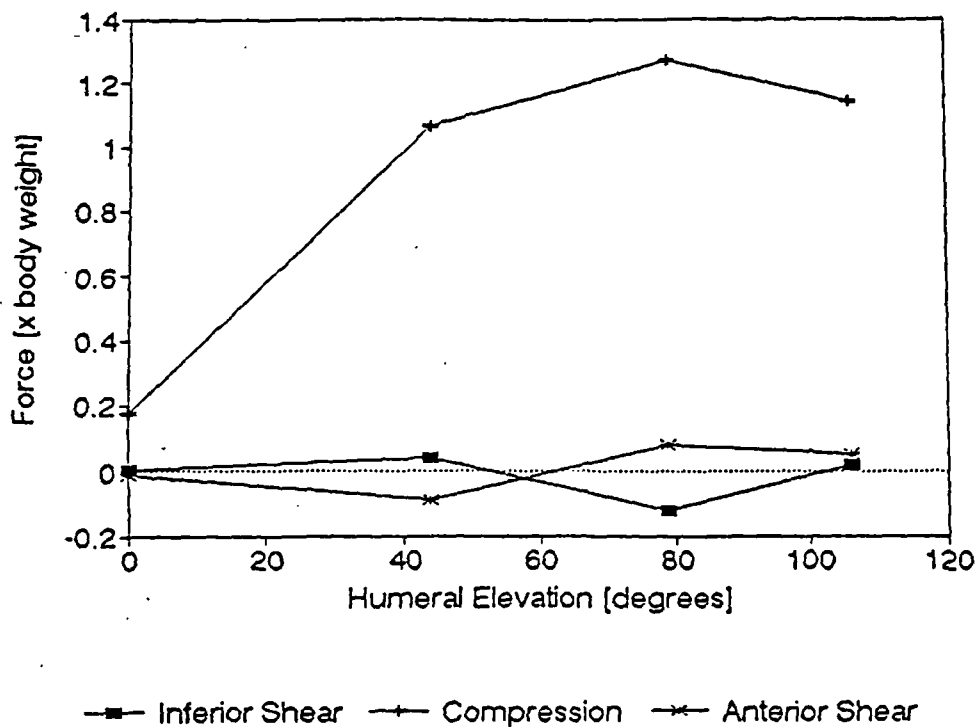


Figure 6.5 Glenohumeral joint contact forces predicted for frontal plane abduction. Forces are in terms of the glenoid fossa coordinate system and are in terms forces applied by the humeral head to the glenoid fossa.

angular orientations of the structures are plotted against humeral elevation in the frontal plane.

Shoulder moments calculated from kinematic, anthropometric and subject geometric data are plotted against humeral elevation in figure 6.3. Humeral elevation in the frontal plane with no internal or external arm rotation corresponds to glenohumeral joint rotation about the Z_h axis. Physiologically, this moment would reach a maximum magnitude at approximately 90 degrees. The calculated moment reached a maximum of -9 Nm at the third arm position corresponding to 79 degrees elevation.

Calculated muscle forces predicted for the activity are plotted against humeral elevation in figure 6.4. Muscle forces-predicted for both sets of optimization constraints are identical. This implies that the joint was stable by definition for the first set of optimized muscle forces. With the predicted compressive force approximately 10 times larger than either shear force, the constraint equations for stability would be satisfied (see figure 6.5). Forces are given as a fraction of body weight. Although 26 muscle elements are included in the model, the group shown in this figure was chosen to correspond to the muscles included the EMG study by Inman et al (1944). The plotted muscle forces are the cumulative total for the fascicles that anatomically comprise each muscle. Biceps and coracobrachialis were the only other two muscles predicted to be active during the activity. Biceps long head was calculated to be transmitting load for the first two arm positions and coracobrachialis and biceps short head the final two arm positions.

Glenohumeral joint contact forces during abduction are plotted against humeral elevation in figure 6.5. Forces are given as a function of body weight and are in terms of forces applied to the glenoid fossa. The joint compressive force reached a maximum of approximately 1.2 times body weight. Joint shear forces were all small in comparison to the compressive force reaching a maximum of approximately 0.1 times body weight superiorly and 0.1 times body weight both anteriorly and posteriorly. It is of note that the anterior-posterior shearing force acts posteriorly up to approximately 60 degrees of elevation and thereafter it shifts to an anterior direction.

6.1.3 Discussion

Verification of the measured clavicle and scapula orientation is possible through comparison to shoulder girdle orientation measurements made by Pronk (1989). Figure 6.6 shows the results of the study by Pronk, where changes in clavicle and scapula orientation were measured for 18 subjects performing humeral abduction in the frontal plane. Measured values for clavicle elevation and protraction and scapula lateral rotation and

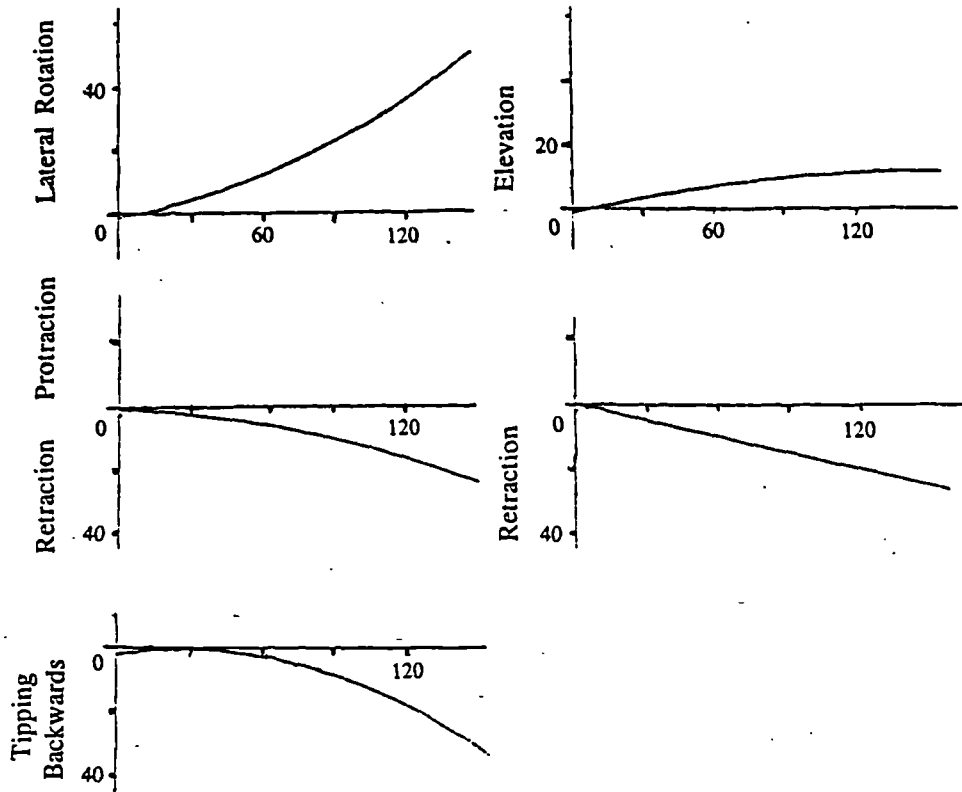


Figure 6.6 Motions of scapula (left) and clavicle (right) during humeral abduction in the frontal plane (Pronk, 1988).

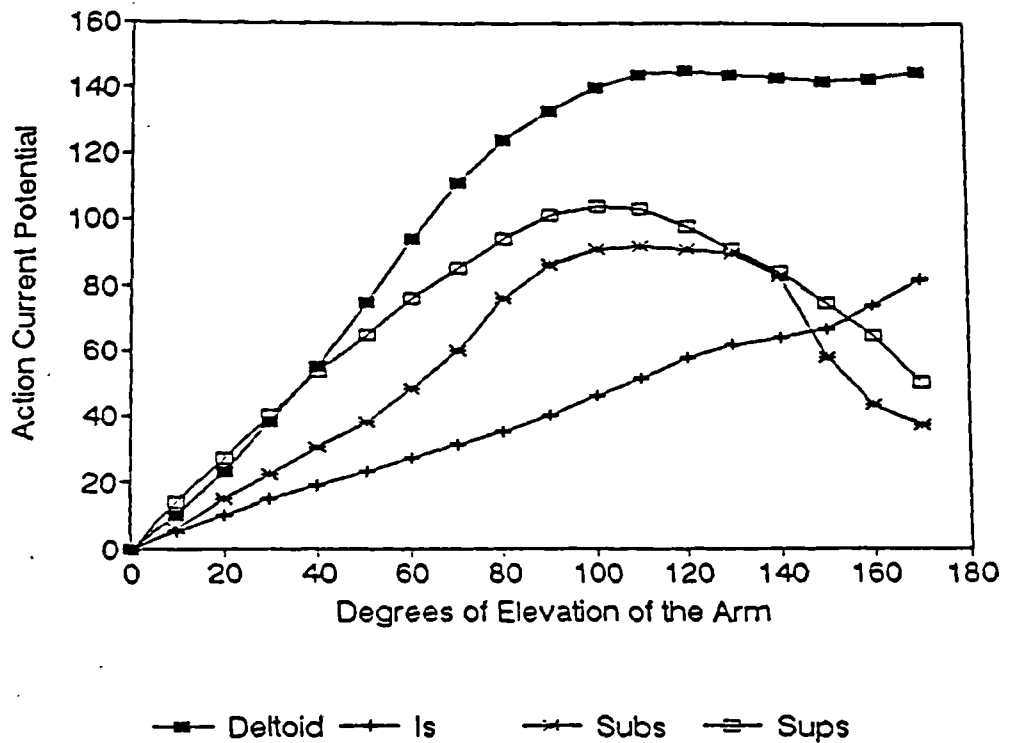


Figure 6.7 EMG muscle activation for Deltoid, infraspinatus (Is), subscapularis (Subs) and supraspinatus (Sups) during humeral abduction in the frontal plane (Inman et al, 1944).

tipping, shown in figure 6.1 and figure 6.2, are all in agreement with the values found by Pronk. The change in measured scapula protraction during abduction was found to be opposite to that determined by Pronk. In general this difference between the results of these two studies is small and most likely due to the use of only a single subject in this study.

Moments about the shoulder due to external loading distal to the joint would be expected to decrease for humeral elevation above 90 degrees. This is a result of the perpendicular moment arm length for the gravitational force with respect to the glenohumeral joint decreasing above this level of humeral elevation. Referring to figure 6.3, the moment about the Z_h axis does decrease, however the moment about the Y_h axis increases. This increase in conjunction with the decrease in the Z_h moment is consistent with increased external humeral rotation for the fully elevated arm position. Similar increases in external rotation accompanying humeral abduction above 90 degrees have been documented by both Inman et al (1944) and Saha (1983). Moments about the X_h axis remain essentially constant throughout the range of abduction. This is due to the force of gravity acting on the forearm with the elbow slightly flexed.

Figure 6.7 shows the EMG muscle activation measured for abduction by Inman et al (1944). The EMG study by Inman et al did not include a normalization process to correct for magnitude variations resulting from electrode or subject differences. As a consequence, the EMG data can only be used qualitatively for comparison to the individual muscle activation predicted in this study. Comparing figure 6.7 to the results predicted in this study (figure 6.4) several similarities can be seen. First and foremost, all of the muscles indicated to be active by the EMG study were predicted to be active in this study. Upon examining the shape of the lines representing EMG magnitude and predicted muscle force for each muscle, the overall shapes are generally consistent. This would indicate a correlation between the muscle activation predicted in this study and the EMG muscle activation measured by Inman et al.

Glenohumeral joint contact forces during abduction have been estimated in many two-dimensional studies. A complete review of these studies was covered in section 3.5. Joint compressive forces of approximately 0.9 times body weight were predicted in studies by both Inman et al (1944) and Poppen and Walker (1978). In contrast, a maximum joint compressive force of 1.2 times body weight was predicted in this study. The discrepancy may be explained by the difference between two-dimensional and three-dimensional analysis techniques.

In the two-dimensional studies, muscle functions were simplified by eliminating their out of plane actions. Muscle forces calculated to provide joint equilibrium within the analysis

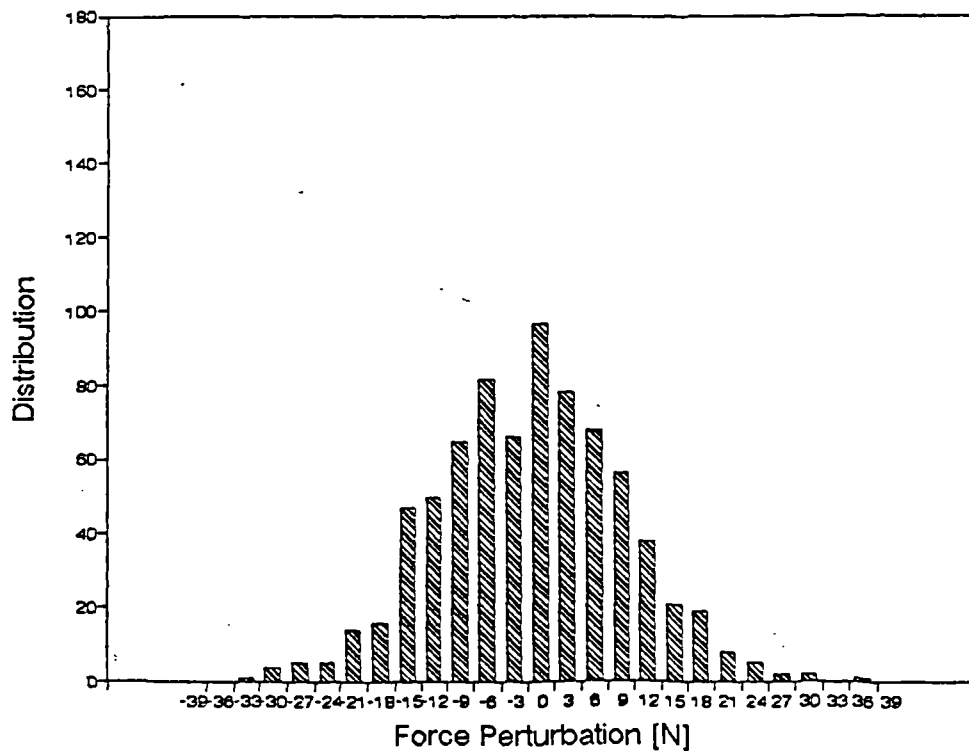
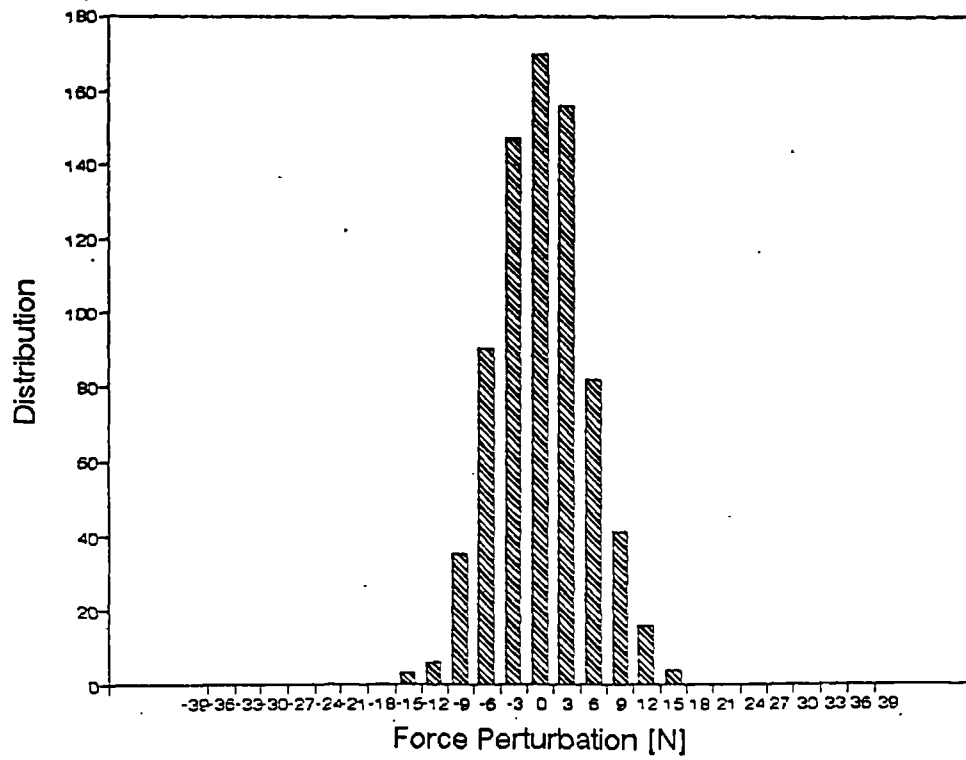


Figure 6.8 Distribution of hand force data perturbed using the algorithm outlined in section 6.2.1. for desired perturbation uncertainties of 5 [N] (a, top) and 10 [N] (b, bottom). Each distribution was taken over 50 iterations of five frames of hand forces (F_{h_x} , F_{h_y} and F_{h_z}).

plane will therefore not necessarily provide joint equilibrium out of the plane. In order to provide this equilibrium, muscle forces and hence joint contact forces may be higher. This could explain the joint compressive forces being higher in this three-dimensional study as opposed to the results of the two-dimensional studies.

A joint compressive force of 0.8 times body weight was predicted by the three-dimensional study by Karlsson (1992). Muscle activation predicted by Karlsson was not in agreement with EMG muscle activation measured for abduction. As a result, the joint contact force calculated using this muscle activation cannot be assumed to be representative of physiological joint loading.

6.2. MODEL SENSITIVITY TO INPUT DATA

All of the data used by the model have certain corresponding uncertainties. As a result, shoulder function predicted using the model will also contain a certain level of uncertainty due to the input data. In order to quantify this uncertainty a series of five tests was performed. In each test, an input data set collected for an activity was perturbed using a Monte Carlo based algorithm. The model response to input data uncertainties was then obtained by comparing the perturbed input data with corresponding model output.

Five separate tests were included in this analysis. These five covered the range of input data used in the shoulder model and included: marker coordinates, hand loading, subject geometry dimensions and anatomical muscle origin and insertion coordinates. In each of the first four tests, an individual input data set was perturbed. In the fifth test all input data were perturbed using estimates of the uncertainties that might be normally expected.

This section details the sensitivity tests conducted on the shoulder model. The first sub-section contains details of the perturbation algorithm used in all of the subsequent tests. The following five sub-sections detail the input data sensitivity tests. The final sub-section discusses and summarizes the results of the sensitivity study.

6.2.1 Data Perturbation

In the data collection environment used for this project, accurate quantification of all the input data uncertainties is difficult. To quantify model sensitivity, it was desirable to have a set of input data containing a certain known level of uncertainty. The algorithm detailed here was used to superimpose a certain level of uncertainty onto the model input data.

If a set of collected data is assumed to be accurate, then by perturbing the data, uncertainties can be introduced into the data set. Using this approach, input data with a known uncertainty was produced from experimentally collected data. The algorithm used

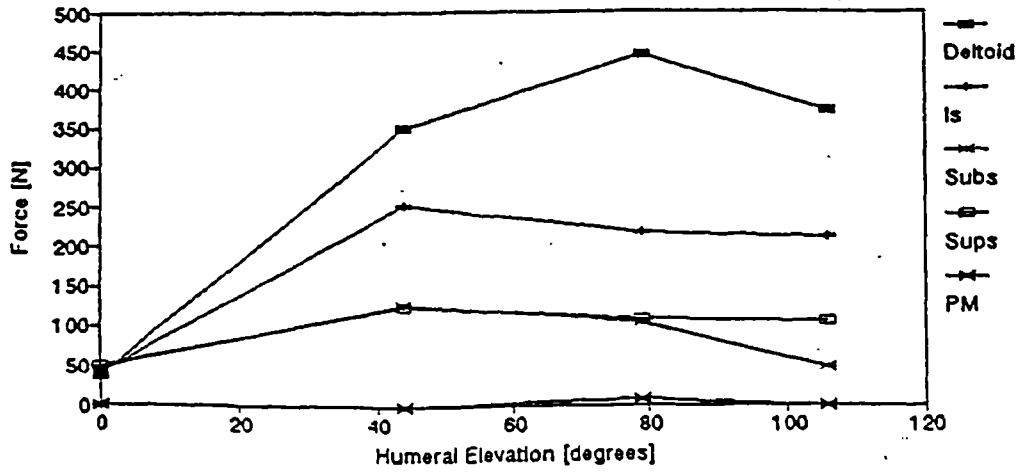


Figure 6.9a Average force for Deltoid, infraspinatus (Is), subscapularis (Subs), supraspinatus (Sups) and pectoralis major (PM) during abduction with elbow flexion of 90 degrees and a hand load of 1 kg.

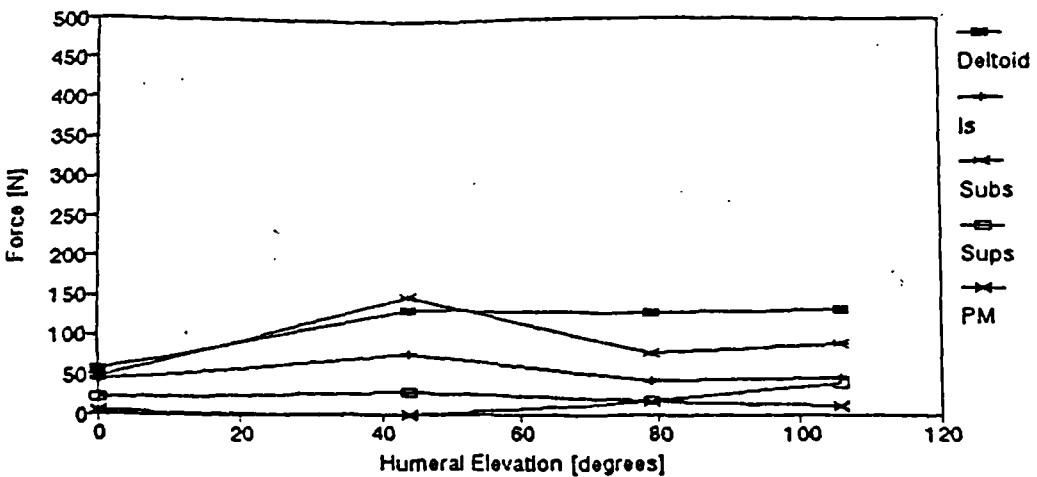
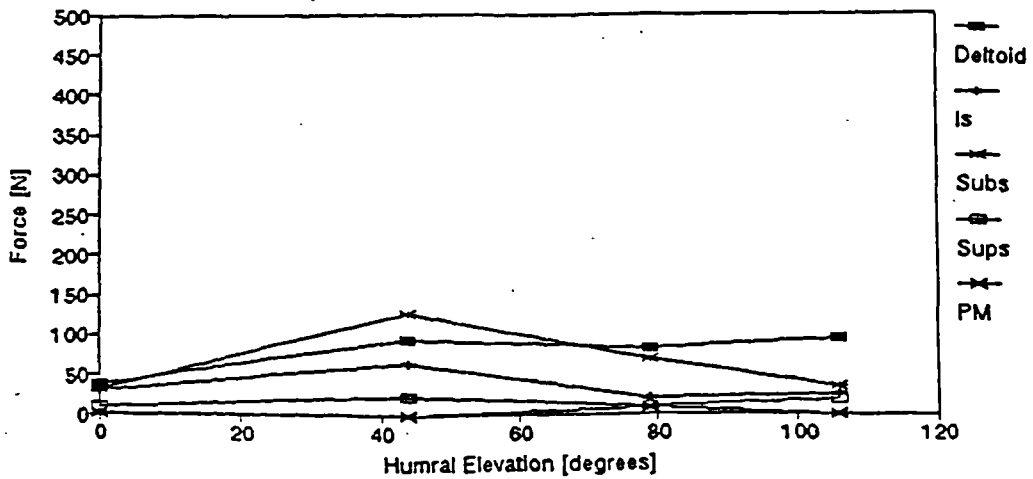


Figure 6.9b & c Muscle force standard deviations resulting from ± 5 mm (b, middle) and ± 10 mm (c, bottom) reflective marker coordinate data uncertainty for humeral abduction with 90 degrees elbow flexion and a 1 kg hand load.

to perturb the collected data was based on a Monte Carlo technique. The algorithm utilizes the square distribution of a series of random numbers to produce a normally distributed set of data perturbations (Bryant, 1980, Runciman, 1989). For this study, the algorithm took the form:

$$x' = x + ((P-6)*S)$$

where,

$$P = r_1 + r_2 + \dots + r_{12}$$

where x is the data variable to be perturbed, r_1 through r_{12} are random numbers between 0 and 1, S is the desired uncertainty standard deviation and x' is the perturbed data variable.

For each of the five tests conducted using this perturbation algorithm, a different set of input data was perturbed. To give a reasonable representation of the model response to the perturbed data, a large number of perturbed data sets were produced from each input data set. In this way the perturbed data uncertainty could be compared directly to the resulting model output uncertainty.

To demonstrate the data perturbations generated by the algorithm, the distributions of two sets of data perturbations are shown in figure 6.8. The perturbations shown in each graph are the perturbations applied to the original input data. The distributions were accumulated for 3 input hand forces measured for 5 frames of data, with 50 sets of perturbed data being produced from each frame. As a result, a total of 750 (3x5x50) perturbations were used for calculating the distributions in each graph. The graphs in figure 6.8a and 6.8b correspond to desired perturbation uncertainties of 5 and 10 [N] respectively. Actual standard deviations for the perturbations are 5.04 [N] and 10.47 [N] respectively. This represents less than a 5 % error in the resulting uncertainty produced by the algorithm when compared to the desired uncertainty. Perturbation averages for the two figures are -1.24 and -2.63 [N] respectively. This indicates a shift in the perturbed data with respect to the original data.

Perturbations produced by the algorithm are independent of the data to which they are applied. As such the perturbation algorithm would be assumed to generate a set of data perturbations statistically similar to those shown in figure 6.8 for all five of the tests for which it was used.

6.2.2 Reflective Marker Uncertainty

The three-dimensional coordinates of the reflective markers are measured using the Vicon motion analysis system. This information is used to determine segment kinematics.

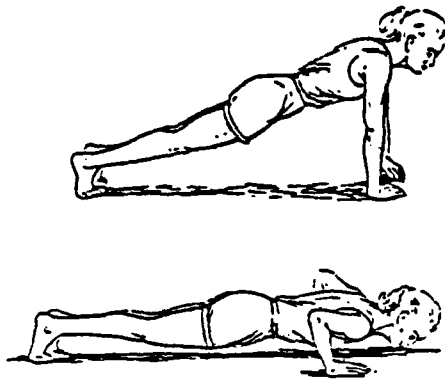


Figure 6.10 Two views showing the range of motion for a standard athletic push-up (Wells, 1976).

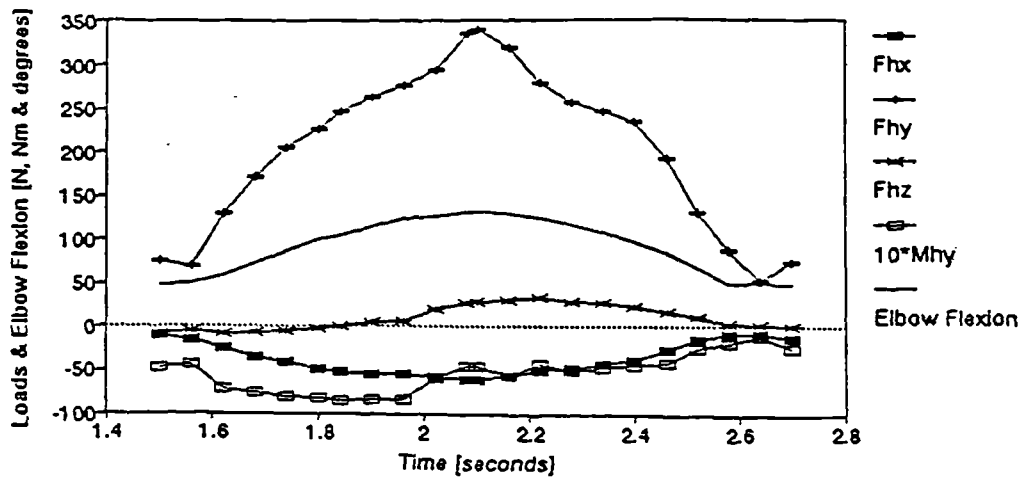


Figure 6.11a Hand loading and elbow flexion during an athletic push-up with the subject facing in the $+X_{lab}$ direction.

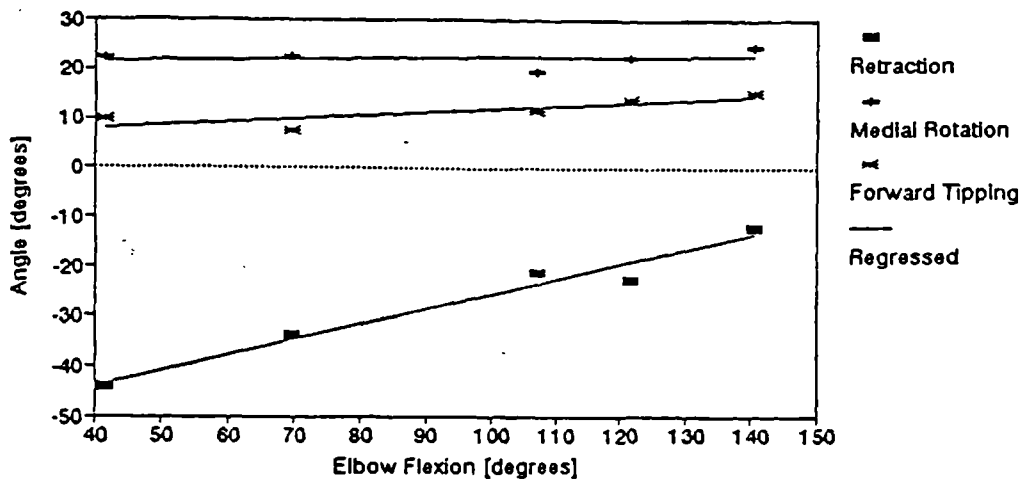


Figure 6.11b Measured static and estimated (using linear regression) dynamic scapula orientation for a push-up plotted against elbow flexion.

Any uncertainty in measuring marker coordinates or in the relative marker to segment positioning will introduce uncertainty in calculating kinematics. To understand the model response to uncertainties in this data, muscle forces were calculated using perturbed reflective marker coordinate data.

The experimental data set chosen for the basis of the analysis was the frontal plane abduction data presented in section 6.1. To increase the complexity of the arm loading, the elbow flexion angle was increased to 90 degrees and a hand load of 1 kg was added.

All four frames of the abduction sequence were included in the analysis. Perturbation standard deviations of 5 mm and 10 mm were used for the test. 50 sets of perturbed data were analysed for each of these standard deviations.

The average muscle forces estimated for the experimental data are plotted in figure 6.9a. These results along with the other results of the sensitivity analysis are in units of Newtons and not normalized with respect to subject weight. Also, only the joint moment balance constraint has been used for optimizing muscle forces in the sensitivity analysis.

The standard deviations of the calculated muscle forces for both 5 mm and 10 mm input data uncertainty are shown in figures 6.9b and 6.9c respectively. As can be seen in both figures, the muscle force standard deviations are dependent on not only limb position but also on the muscle being considered. On average, doubling the input data uncertainty increased the predicted muscle force uncertainty by approximately 65 %.

The uncertainty of calculating muscle forces resulting from the uncertainty associated with the reflective markers cannot be easily quantified because of the variation in sensitivity with limb position and the muscle being examined. The manufacturer's stated performance for the motion analysis system is that it will measure marker coordinates inside the measurement volume to within ± 1 mm. In addition to this, there is the uncertainty associated with skin artifacts which also contribute to the marker coordinate uncertainty. Considering both of these, and realizing that the total uncertainty is the square root of the sum of the individual uncertainties squared, (Holman, 1978) marker coordinates could be expected to be measured within an uncertainty of better than ± 5 mm. This would produce an uncertainty in predicted muscle forces of better than the magnitude obtained in this test for ± 5 mm marker data perturbation.

6.2.3 Hand Load Uncertainty

Three-dimensional hand forces and moments were measured using the Kistler force plate and the instrumented hand transducer. Any uncertainty in measuring these hand loads will introduce uncertainty in calculating muscle forces for the activity being considered. To

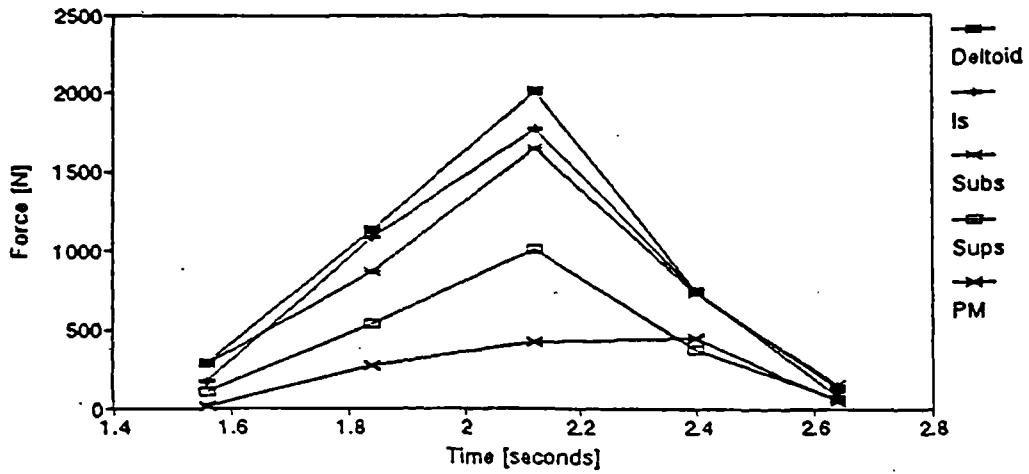


Figure 6.12a Average force calculated for Deltoid, infraspinatus (Is), subscapularis (Subs), supraspinatus (Sups) and pectoralis major (PM) during five frames of an athletic push-up.

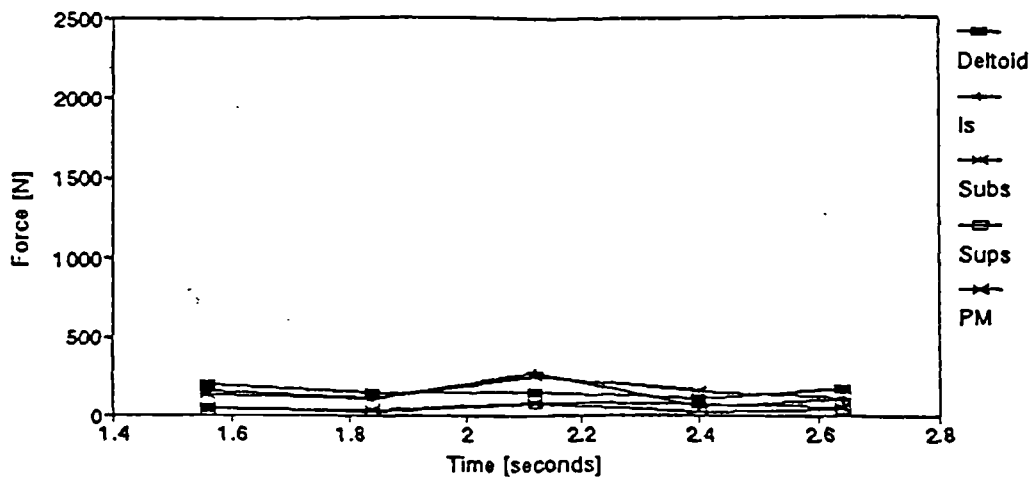
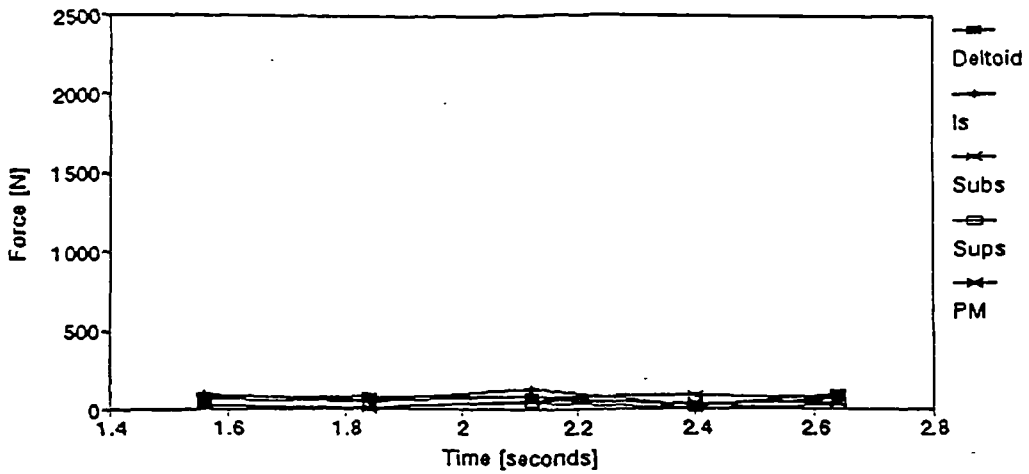


Figure 6.12b & c Muscle force standard deviations resulting from ± 5 N (b, middle) and ± 10 N (c, bottom) hand force data uncertainty for an athletic push-up.

understand the model response to uncertainties in this data, muscle forces were calculated using perturbed hand force and moment data. For clarity, the test was split, with sensitivity to hand force uncertainty investigated first followed by sensitivity to hand moment uncertainty.

The experimental data chosen for the basis of the analysis was an athletic push-up sequence (see figure 6.10). This activity was chosen over the simpler abduction activity discussed previously because it better represents an activity where measured hand load data uncertainty would be a concern. As a result of the experimental details of this activity not being discussed previously, they are presented here followed by the sensitivity tests to which they were used.

An athletic male subject (age 26, height 1.80 m and mass 70 kg) performed the activity. This subject had no previous history of shoulder disorders. A series of 4 continuous push-ups was performed with the subject's right hand flat on the Kistler force plate and the subject facing in the $+X_{lab}$ direction. Kinematics and body geometry information were measured using the techniques outlined in section 6.1 for abduction. A series of five static positions was used to estimate scapula position. To reduce subject fatigue during the static collections, the static push-up sequence was done in an upright position against a chest level bar. The remaining details of the static collections were the same as used in section 6.1 for abduction. Hand forces and M_h moment for one of the four push-up cycles are shown in figure 6.11a. The measured hand moment, M_h , is plotted at 10 times its measured value for presentation clarity. Elbow flexion angle is also included as it is representative of body kinematics during the activity. Data was collected at 50 Hz, but two of every three records have been removed for presentation purposes.

Scapula orientation was estimated using the series of 5 statically measured orientations. Figure 6.11b shows these discrete scapula orientation angles plotted against elbow flexion. Using linear regression the relationships between scapula orientation angles and elbow flexion were obtained and are plotted as continuous lines in the figure. The maximum regression error is less than 3 degrees for these relationships.

For the sensitivity test, a series of five frames of data was chosen from the dynamic push-up results. Using the estimated scapula orientation data and experimentally measured kinematic and hand loading data gave a complete set of experimental data for analysis using the shoulder model.

For the investigation into model sensitivity to hand load uncertainties, hand force data was perturbed using standard deviations of 5 N and 10 N. Fifty sets of perturbed data were analysed for each of these standard deviations and each of the five frames of data. The

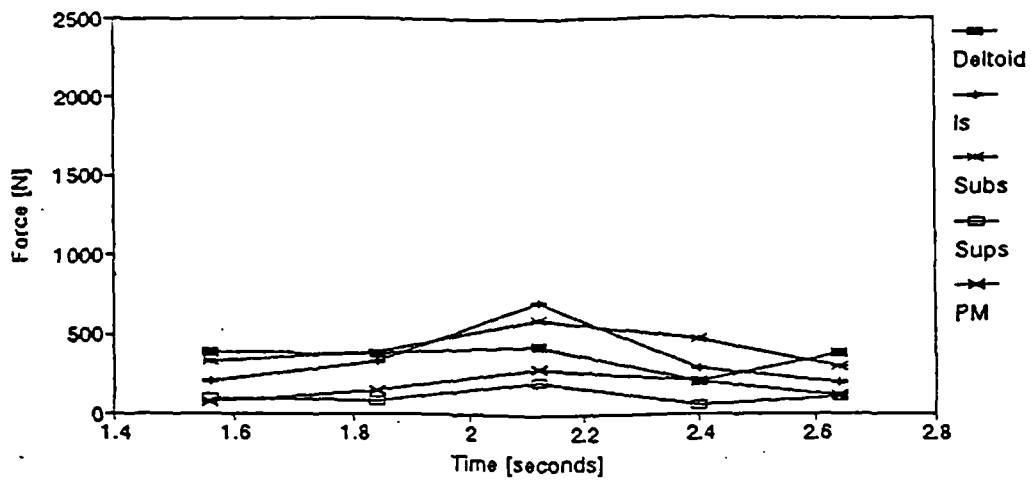
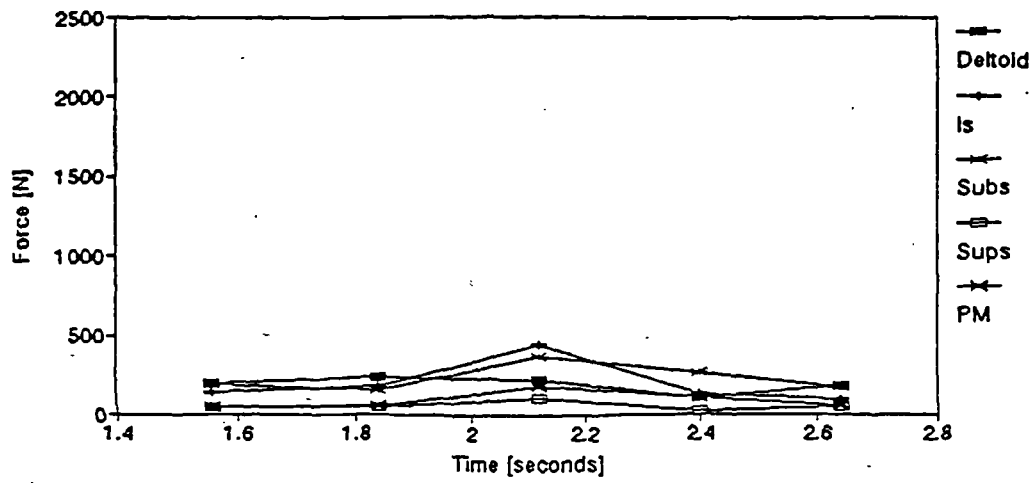


Figure 6.13 Muscle force standard deviations resulting from ± 5 Nm (a, middle) and ± 10 Nm (b, bottom) hand moment data uncertainty for an athletic push-up.

process was then repeated with hand moment data being perturbed with standard deviations of 5 Nm and 10 Nm.

The average muscle forces estimated for the experimental data are plotted in figure 6.12a. The standard deviations of the calculated muscle forces for both 5 N and 10 N input data uncertainty are shown in figures 6.12b and 6.12c respectively. The standard deviation of the muscle forces calculated for hand moment data with standard deviations 5 Nm and 10 Nm are plotted in figure 6.13a and 6.13b. Average muscle force uncertainty approximately doubled for both the doubling of the input data hand force uncertainty from ± 5 N to ± 10 N and the doubling of the input hand moment uncertainty from ± 5 Nm to ± 10 Nm. This is as would be expected because of the linear relationship between external segment loading and muscle force required to provide joint equilibrium.

The uncertainty of calculated muscle forces resulting from the hand load measurement uncertainty cannot be stated specifically. The contribution of hand forces to the shoulder moment due to external loading is a function of both the force and location of the hand with respect to the shoulder. Uncertainty in the muscle forces required to balance the shoulder moment due to external loading are therefore a function of the force uncertainty and also body kinematics. In contrast, there is a direct relationship between moments applied to the hand and the corresponding shoulder moment that must be balanced by shoulder muscular action to maintain joint equilibrium.

A calibration study by Fleming et al (1993) found hand forces could be measured to within ± 1 % and moments to within ± 3 % with the Kistler force plate used in this project. The instrumented hand transducer performance was found to be approximately ± 1 % for the loads applied during calibration. As a result, hand force uncertainty measured using the force plate, for the maximum vertical force push-up, F_h , would be approximately ± 4 N and $< \pm 1$ Nm for the measured hand moment. This would indicate that predicted muscle force uncertainty resulting from measured hand load uncertainties would be approximately equal to those obtained for the ± 5 N hand force uncertainty analysis.

6.2.4 Subject Geometry

Subject geometry was measured manually for each subject. This information is essential to the proper modelling of an individual's shoulder function. Any geometry measurement uncertainty will introduce uncertainty in calculating muscle forces for the activity being studied. To understand the model response to geometry data uncertainties, muscle forces were calculated using perturbed geometry data. All of the geometric data (except subject height and mass) were included in the two parts of this test. In the first part all subject

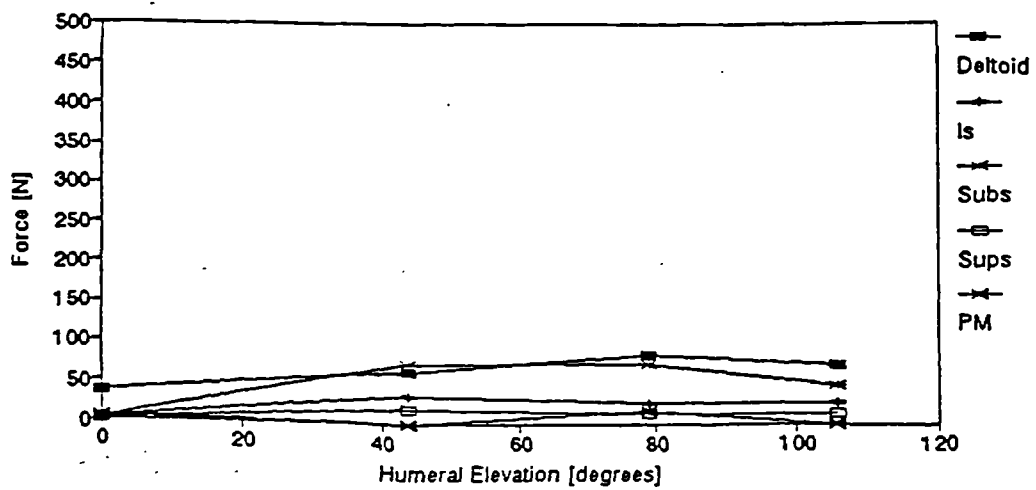
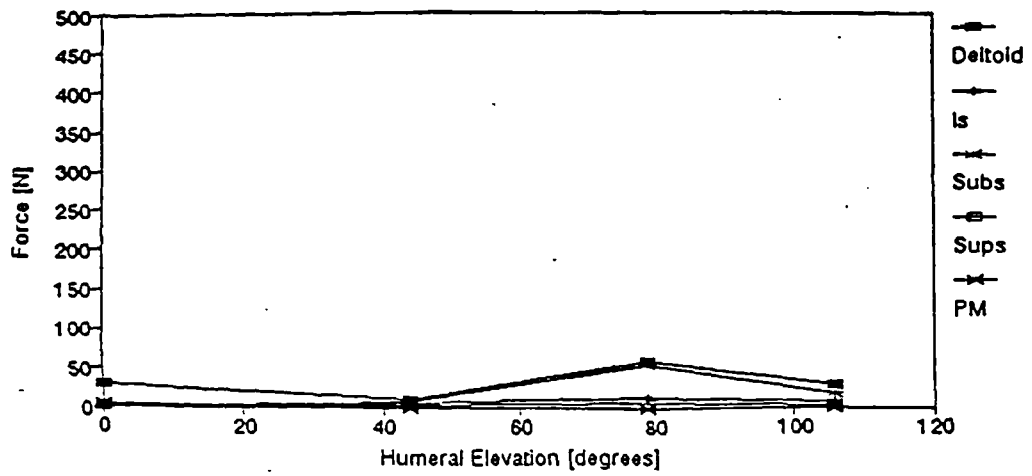


Figure 6.14 Muscle force standard deviations resulting from ± 5 mm (a, top) and ± 10 mm (b, bottom) subject scaling dimension uncertainty for humeral abduction with a 90 degree flexed elbow and a 1 kg hand load.

scaling dimensions were perturbed. In the second part the reflective marker to bony landmark distances were perturbed. By considering the results of the two parts of this test, insight into model sensitivity to geometric scaling dimensions should be achieved.

The experimental data set chosen for the basis of the analysis was the frontal plane abduction data as used for the test of model response to marker coordinate uncertainty, section 6.2.2.

All four frames of the abduction sequence were included in the analysis. Perturbation standard deviations of 5 mm and 10 mm were used for both parts of the test. 50 sets of perturbed data were analysed for each of these standard deviations.

The average muscle forces estimated for the experimental data were equivalent to the earlier results plotted in figure 6.9a. The standard deviations of the calculated muscle forces for both ± 5 mm and ± 10 mm anatomical scaling dimension data uncertainty are shown in figure 6.14. The standard deviations of the calculated muscle forces for both the ± 5 mm and ± 10 mm reflective marker to bony landmark dimension uncertainty are shown in figure 6.15. As can be seen in both figures, the muscle force standard deviations are again dependent on not only limb position but also on the muscle being considered. The model appears more sensitive to uncertainty in the anatomical scaling dimensions with larger increase in calculated muscle uncertainty than was calculated for the marker to bony landmark dimension uncertainty. Doubling the anatomical scaling data uncertainty produced approximately a 170 % increase in calculated muscle uncertainty. In contrast, doubling the reflective marker to bony landmark distance uncertainty only produced an 80 % increase in the calculated muscle uncertainty.

6.2.5 Anatomical Muscle Origin and Insertion Uncertainty

Anatomical muscle origin and insertion data were obtained from the study by Johnson (1990) and the dry bone study documented previously in this thesis. To understand model response to uncertainties in this data, muscle forces were calculated using perturbed anatomical muscle origin and insertion data.

The experimental data set chosen for the basis of the analysis was the frontal plane abduction data as used previously in this model sensitivity study.

Perturbing anatomical muscle origin and insertion data requires the consideration of the anatomical bone scaling factors. To provide a realistic uncertainty, the data must be in an unscaled form before the perturbation is applied. If the data were perturbed while in a normalized state then the resulting coordinate data uncertainty would also be a function of the scaling length. This would impose different data uncertainty levels on each of the

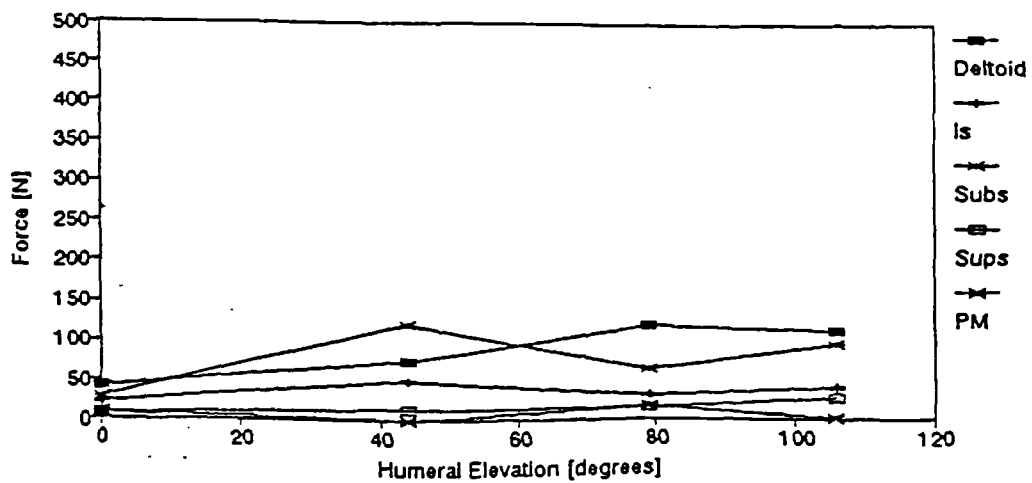
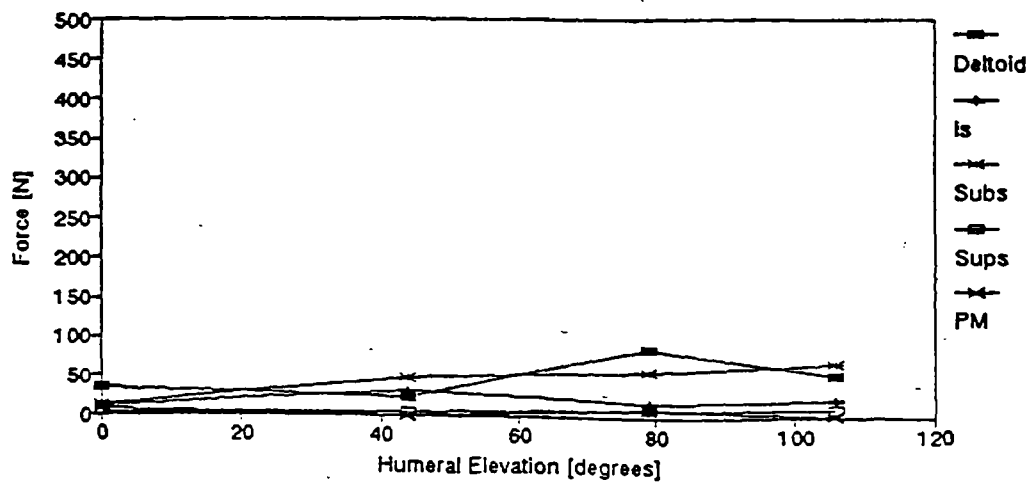


Figure 6.15 Muscle force standard deviations resulting from ± 5 mm (a, top) and ± 10 mm (b, bottom) reflective marker to bony landmark dimension uncertainty for humeral abduction with a 90 degree flexed elbow and a 1 kg hand load.

shoulder segments.

All four frames of the abduction sequence were included in the analysis. Perturbation standard deviations of 2.5 mm and 5 mm were used in the test. 50 sets of perturbed data were analysed for each of these standard deviations.

The average muscle forces estimated for the experimental data are equivalent to the earlier results plotted in figure 6.9a. The standard deviations of the calculated muscle forces for both ± 2.5 mm and ± 5 mm anatomical muscle origin and insertion data uncertainty are shown in figure 6.16. The model does not appear particularly sensitive to uncertainty in this anatomical data with only a 50 % (approximate) increase in the calculated muscle force uncertainty with a doubling of the input data uncertainty.

6.2.6 Combined Input Data Uncertainty

In the previous tests of this sensitivity study, model response to perturbed input data has been investigated for individual input data types. These contrived examples of input data uncertainty, while providing useful information on model characteristics, do not indicate how the model would perform with actual experimental data. In actual experimental data, each input data type has a certain level of uncertainty associated with it. To complete this study, it is desirable to investigate model response to input data that are all perturbed by realistic known uncertainties. The results of this investigation should then indicate model response to actual experimental data.

Procedures for perturbing all of the input data are available from the previous stages of this sensitivity study. For choosing the appropriate data uncertainties, consideration was given to the actual experimental uncertainty that might be associated with that particular data type. Accurate quantification of these uncertainties is difficult if not impossible when inter-subject and intra-subject variations must be considered along with activity and experimental variations used during data collection.

The values for input data uncertainty standard deviations used in this test have been chosen to be approximately representative of experimental data uncertainties. If a discrepancy were found between actual experimental data uncertainty and the values used for this test, an approximation of the actual model performance could still be obtained through the use of the results of this test and the increase in muscle uncertainty accompanying increased input data uncertainty as documented in each of the previous tests.

Four frames of the previously used abduction sequence were included in the analysis. Input data uncertainty standard deviations used in this analysis included: 2.0 mm for reflective marker coordinate data, 5.0 mm for subject geometry dimensions, 2 N for hand

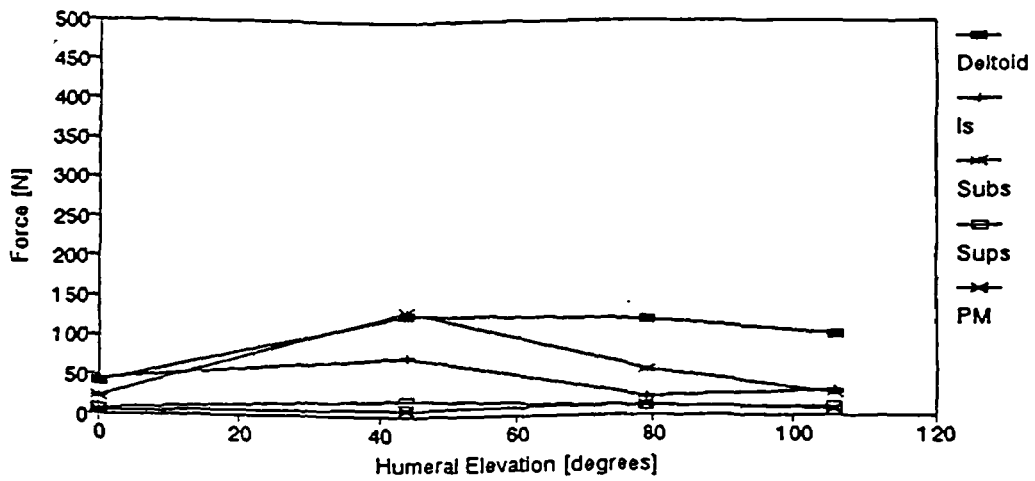
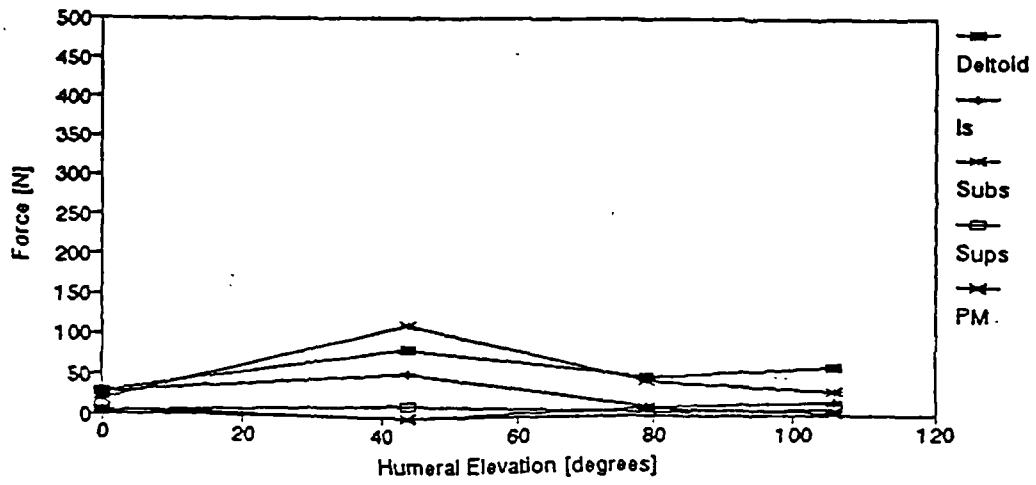


Figure 6.16 Muscle force standard deviations resulting from ± 2.5 mm (a, top) and ± 5 mm (b, bottom) muscle origin and insertion anatomical data uncertainty for humeral abduction with a 90 degree flexed elbow and a 1 kg hand load.

forces, 1 Nm for hand moments and 2.5 mm for anatomical muscle origin and insertion data. 50 sets of perturbed data were produced for each frame of data for analysis.

The average muscle forces estimated for the experimental data were equivalent to the earlier results plotted in figure 6.9a. The standard deviations of the calculated muscle forces for the combined input data uncertainties are shown in figure 6.17. The resulting muscle force uncertainty (for those muscles that were active for this activity) was approximately ± 50 N. The corresponding average muscle force was approximately 250 N.

Average glenohumeral joint contact forces for this activity are plotted in figure 6.18a. The standard deviation of the contact forces resulting from the input data uncertainties are plotted in figure 6.18b. Comparing the average and standard deviation values for the joint contact forces illustrates the lack of model sensitivity to input data uncertainties. For the activity and input data uncertainties considered in this example, calculated joint contact force uncertainties are better than approximately ± 20 % of the maximum joint compressive force.

6.3 MODEL AND EMG ACTIVITY ANALYSIS

Historically shoulder function analysis has been limited to two-dimensional low load activities. While providing useful information on the shoulder function under these limited circumstances, these studies give little insight into function during real life three-dimensional activities. To redress this situation, a series of activities has been included for analysis in this study that represent maximum shoulder loading an individual might encounter in real life activities.

The activities chosen for analysis fall into two groups. The first represents an extension of documented two-dimensional studies. The activities included in this group are pure flexion and pure frontal plane abduction both with a 2 kg hand load. Results achieved from these activities should correlate with the results documented by the earlier studies while still providing useful new information. Activities to be studied in the second group are standard athletic activities within the capability of most young fit individuals. Included in this group for analysis are the standard athletic push-up (see figure 6.10), chin-up with supinated hand grip, and vertical press-up which resembles rising out of an arm chair using upper limb propulsion only.

All of the activities chosen for analysis have the advantage that they are common activities that can be readily repeated by most individuals. This eliminates ambiguity associated with the results, simplifying interpretation and application.

Shoulder function for each of the activities, while specific to that activity, is similar to that encountered commonly in real life for other activities. For example, shoulder function

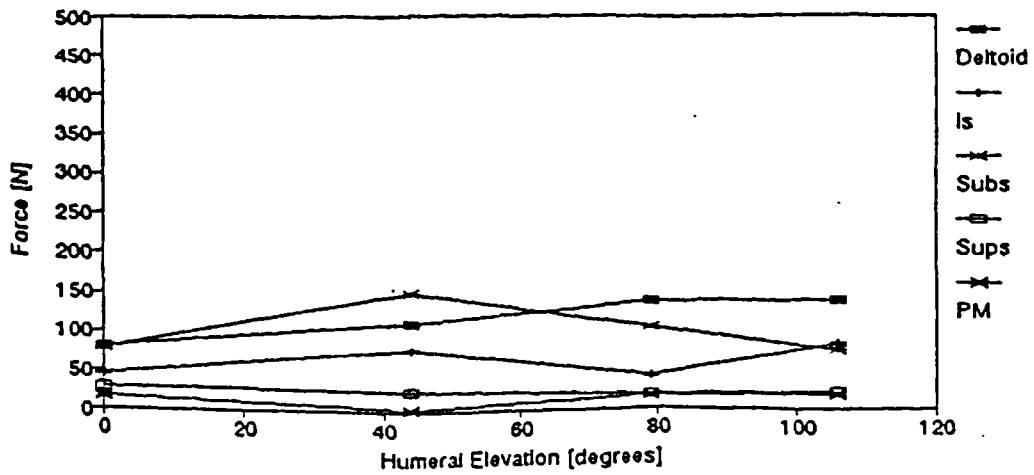


Figure 6.17 Muscle force standard deviations resulting from input data uncertainties of ± 2 mm for marker coordinates, ± 5 mm for subject geometry dimensions, ± 2 N for hand forces, ± 1 Nm for hand moments and ± 2.5 mm for anatomical muscle origin and insertion data during abduction with 90 degrees elbow flexion and a 1 kg hand load.

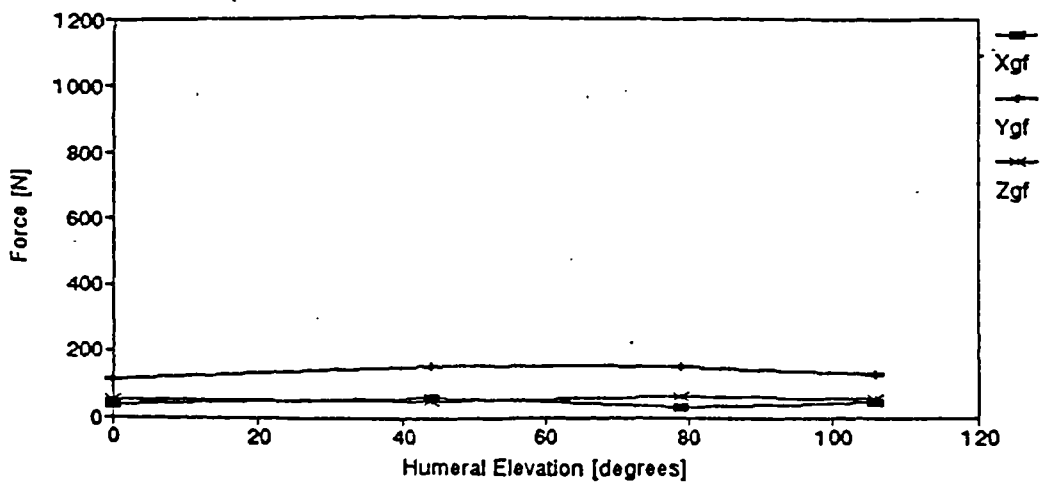
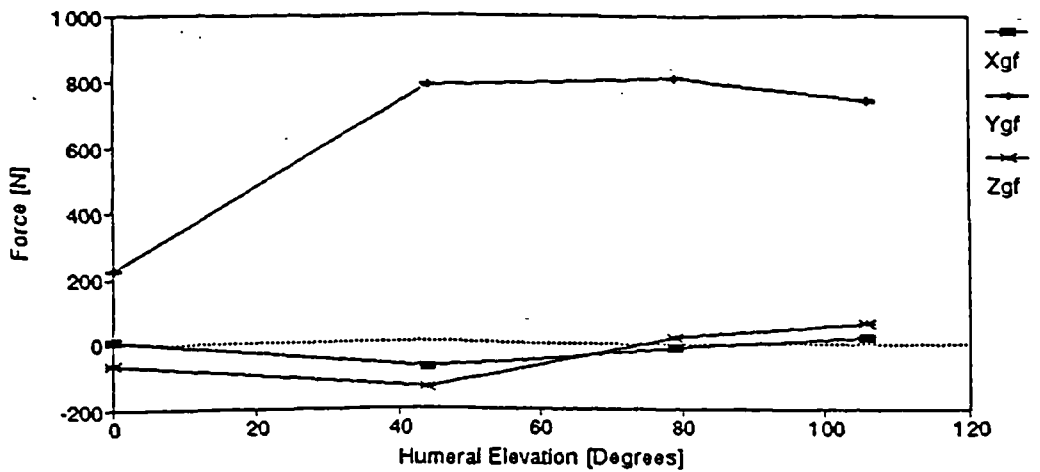


Figure 6.18 Glenohumeral joint contact forces for abduction with elbow flexion of 90 degrees and a hand load of 1 kg (a, middle). Joint contact force standard deviations for perturbed input data (b, bottom).

in a push-up is similar to that used during a forward fall or to push open a heavy door. Using this approach, the results obtained for the two groups of activities can be applied to a diverse range of other real life activities that otherwise might be uneconomical to investigate individually.

Direct verification of the model results for these five activities is not feasible. While documented EMG and biomechanical study results were used in the earlier corroboration of the abduction results, no similar data is available for these five activities. To ensure that model results are representative of physiological joint function, a verification of the model under the more demanding circumstances of the five activities was required.

To facilitate this verification, an EMG study of muscle activation for the five activities was conducted. Facilities for this study were not available at the University of Strathclyde. Instead, the study was conducted at the Karolinska Institute, in Stockholm, Sweden, where facilities and expertise for conducting such an EMG study were available.

In order to eliminate any functional differences between subjects used for the EMG and modelling analyses, the same five subjects were used for both. The subjects were 5 young healthy male volunteers aged between 24 and 32 (mean 27 years) and body mass from 64 to 80 kg (mean 68 kg). All of the subjects were relatively fit with no previous strenuous athletic training. None of the subjects had undergone surgery in the shoulder region or had any previous history of shoulder pain or dysfunction.

6.3.1 EMG Study Materials and Methods

A verification study of the shoulder model was conducted, to allow a comparison of predicted muscle activation to EMG muscle activation for the five activities. For completeness EMG muscle activity over a cross section of the shoulder musculature was monitored. To facilitate comparison of predicted and measured results, hand force and joint angles were measured during the activities.

Each of the five activities were performed for a series of five slow to moderate paced cycles without stopping. After a short rest period the activity was repeated. Overall activity order for each subject was chosen at random thereby reducing any data artifacts this might have created. Each activity began with the subject in the anatomical position (except press-up where the subject was seated) with arms straight and no load being transmitted into the hand transducer. For abduction and flexion, the subject was handed the hand load after data collection began.

For both abduction and flexion, the subjects were standing throughout data collection. Abduction and flexion were performed in the frontal and sagittal planes respectively. The

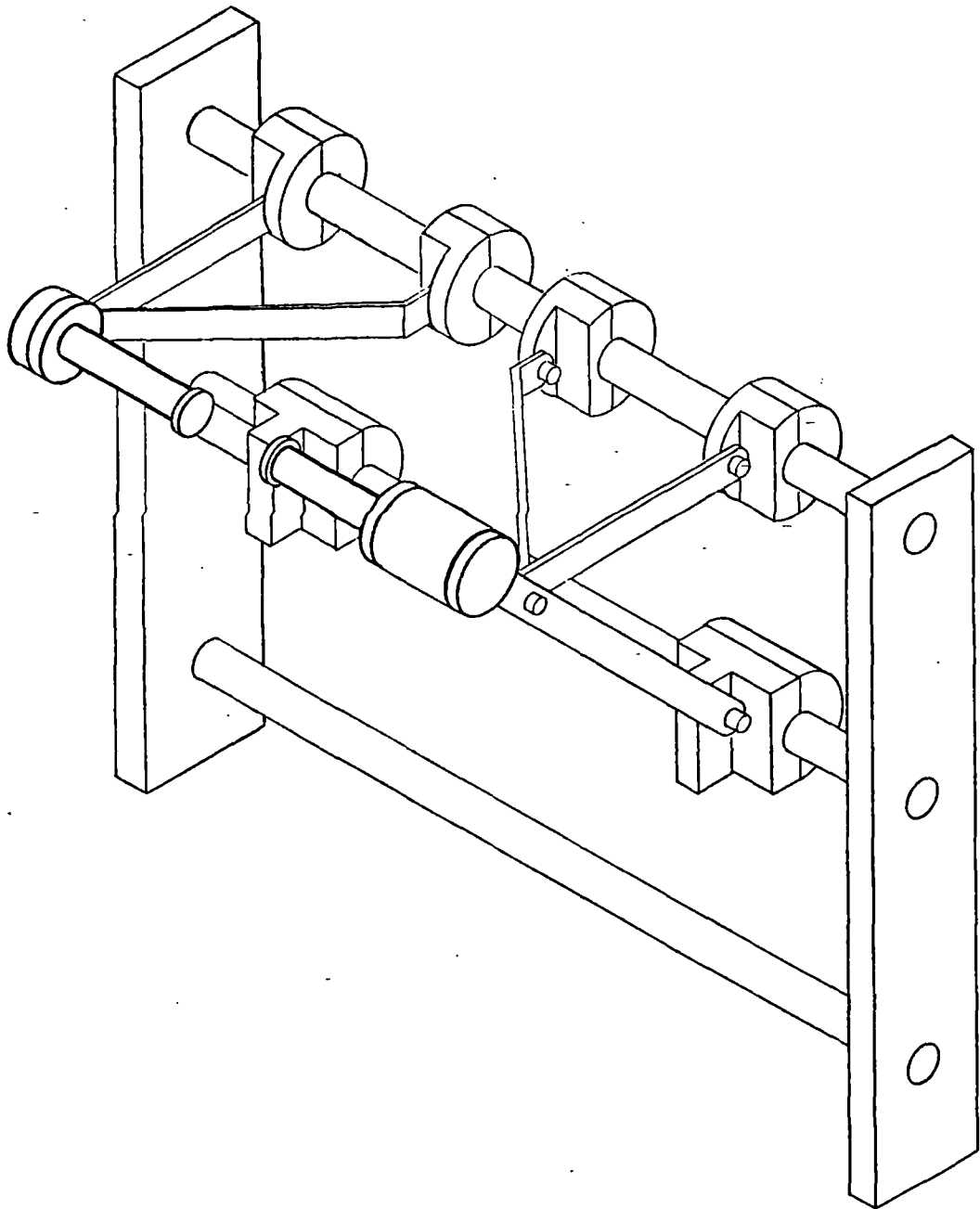


Figure 6.19 Mounting frame used to support the chin-up hand grips with an existing wall bar system. The right hand grip includes the instrumented hand transducer.

subjects were instructed to limit arm rotation and perform the activity with a slightly flexed elbow. The range of shoulder motion of interest for abduction was 0 to 140 degrees and for flexion 0 to 90 degrees.

Chin-ups were performed using supinated hands and a pair of hand grips approximately 2 metres above the floor. One of these hand grips was mounted on the instrumented hand transducer to allow hand forces to be measured during the activity. The dummy hand grip and the transducer were mounted on a supporting structure that was secured on an existing wall bar system (see figure 6.19). The hand grips were specially designed for this study to ensure electrical isolation of the subject from the instrumented hand transducer.

Transducer calibration was required to allow transducer outputs (measured in computer units) to be converted to hand forces in Newtons. For this calibration a 15 kg mass was suspended from the instrumented hand grip thereby loading only the F_{p_x} and F_{p_z} force channels. If transducer cross effects are ignored then the diagonal of the transducer calibration matrix [C] (determined in the original calibration procedure) gives the independent channel calibration parameters $c_{1,1} \dots c_{6,6}$ in units of N/volt or Nm/volt (from section 4.4.2.3). Using these, together with the applied force in Newtons and the measured forces in computer units, the overall calibration factor for each transducer force channel was calculated. For the two channels that were loaded factors A_1 and A_2 were defined as:

$$A_1 = F_{p_x}(\text{computer units}) * c_{1,1}, \quad [\text{computer units N/volt}]$$

$$A_2 = F_{p_z}(\text{computer units}) * c_{3,3}, \quad [\text{computer units N/volt}]$$

Using these and the applied load, a conversion factor, A_3 , was calculated that relates the signal output voltage of the transducer to the measured computer units.

(6.1)

$$A_3 = \text{applied load} / (A_1^2 + A_2^2)^{1/2}, \quad [\text{volts/computer unit}]$$

This factor was then applied with the calibration parameters, $c_{1,1}$, $c_{2,2}$ and $c_{3,3}$, to convert forces applied to the transducer from the measured computer units to Newtons.

Orientation of the transducer as used for the chin-up activity was required to convert measured forces into the standard hand force convention used in the remainder of this thesis. The transducer mounting frame placed its $X_p - Z_p$ plane parallel to the $X_{lab} - Y_{lab}$ plane. To complete the definition of transducer orientation, only the rotation angle between the X_p axis and vertical ($+Y_{lab}$) was required. This was determined using the data obtained by hanging the 15 kg mass from the hand grip. Using the measured F_{p_x} and F_{p_z} channel forces (in units

of Newtons) and realizing that the applied force was equivalent to a $+Fh_y$ force, the rotation angle, θ_1 , was then calculated using:

$$\theta_1 = -1 * \tan^{-1} (Fp_z / Fp_x) \quad (6.2)$$

where θ_1 is the rotation angle between the X_p and Y_{lab} axes around the Y_p axis (using the right hand rule for positive direction convention). Hand forces were then calculated from the measured forces using:

$$[Fp'] = \begin{bmatrix} \cos\theta_1 & 0 & -\sin\theta_1 \\ 0 & 1 & 0 \\ \sin\theta_1 & 0 & \cos\theta_1 \end{bmatrix} * [Fp] \quad (6.3)$$

and, $Fh_x = -1 * Fp'_z$, $Fh_y = Fp'_x$ and $Fh_z = -1 * Fp'_y$

Push-ups were performed on a pair of hand platforms 0.2 metres high. To allow measurement of the hand forces during this activity, the right hand platform was constructed from the instrumented hand transducer fitted with two electrically isolated end plates. A standard flat hand format was used for this activity with each subject finding his own hand placement. Transducer orientation for this activity was parallel to the standard laboratory convention used throughout this thesis ($+X_p$ pointing forward, $+Y_p$ up and $+Z_p$ to the right). As such, forces measured by the transducer were in terms of the standard hand force convention used throughout this thesis.

The press-ups were performed on a set of parallel bars. The instrumented hand transducer and a similar dummy hand grip were mounted on the two bars. This set up allowed hand forces for the activity to be measured. The subject started from a seated position between the bars and with a lifting action similar to rising from a chair, pushed themselves up to a straight arm position. This activity was performed with straight legs and the subject's feet were permitted to remain on the floor. Bar spacing and starting position height were not restricted with each subject finding his own combinations. Transducer orientation was set so that the $+Z_p$ axis was pointing up. With this orientation hand forces were calculated from the measured forces using:

$$Fh_x = Fp_y, \quad Fh_y = Fp_z \quad \text{and} \quad Fh_z = Fp_x$$

Table 6.1 Muscles included in the EMG study.

Muscle	Abbreviation
Deltoid anterior	Da
Deltoid middle	Dm
Deltoid posterior	Dp
Infraspinatus	Is
Latissimus Dorsi	LD
Subscapularis	Subs
Supraspinatus	Sups
Triceps	TB

For EMG recording of shoulder muscle activity, pairs of electrodes were placed in or over the region of the muscle belly of interest. The muscles included in this study are outlined in Table 6.1. Two types of electrode pairs were used, fine wire intramuscular electrodes to monitor the rotator cuff muscles and disposable stick on surface electrodes for the remainder of the muscles of interest. The fine wire electrodes made from polyurethane insulated 0.025mm copper wire and inserted using a large bore hypodermic needle remained implanted in the subject throughout the experimental session. Details of the preparation and insertion technique used for subscapularis were developed by Németh (1990) and were similar to those used for infraspinatus and supraspinatus. Electrode to data collection system connection was via a spring connector (Basmajian 1974). Surface electrode preparation consisted of drying the skin with an alcohol scrub. Surface electrodes type Blue Sensor N-00-S were then applied over the mid muscle belly region in the direction of the muscle fibres using an inter-electrode spacing of approximately 20mm.

A second type of stick on disposable electrode was used for subject grounding. This electrode, type Blue Sensor VL-00-S, was applied to dry skin over the bony region of the subject's wrist. By applying the electrode in this area, unwanted EMG activity adjacent to the ground electrode was reduced.

Body position was monitored during the activities using a pair of Penny & Giles flexible electrogoniometers and a video recorder. To reduce parallax errors on the video record, the camera position was chosen where possible, to be approximately perpendicular to the dominant plane of motion for each activity.

For flexion and abduction a goniometer was placed across the shoulder. Due to skin movement artifacts, goniometer measurements of motion were proportionally less than actual shoulder motion. This discrepancy was corrected by measuring with a protractor the range of shoulder motion directly from the video record. Using this motion range the goniometer data was scaled accordingly to correct for skin artifacts. For the remaining three activities a goniometer was placed across the subject's elbow. Elbow motion, being closely linked to overall body position for each of the three activities and easily measured, afforded a good indicator of body position.

A battery powered amplifier and stabilized power supply was constructed to activate and amplify the goniometer full Wheatstone bridge circuitry. This amplifier and power supply provided a bridge voltage of 1 volt to the goniometer and amplified the resulting output signal with a gain of 1000.

A calibration of the goniometers was conducted to establish the relationship between their angular displacement and measured computer units. Each goniometer was fastened in

tum to a plastic swinging arm protractor (± 0.5 degree) using double sided tape. The goniometers were connected as normal to the data collection system. Each goniometer was subject to a series of angles based on the protractor. Computer units measured during this process were then compared with the corresponding applied angular displacement to calculate the required relationship for converting measured angular displacement from computer units to degrees.

No hand moments were measured for the three athletic activities. Only the three transducer channels measuring force applied to the hand were monitored.

EMG and goniometer data was transmitted from the subject to the data collection system via a 16 channel telemetry system, type Noraxon oy Telemetry 16, made by Glonner. Hand force data was input to the telemetry system receiver directly. Using an IBM 386 computer, fitted with a 12 bit analogue to digital (A-D) converter and data collection software MYOSOFT 2000, raw EMG, goniometer and hand force data were collected simultaneously using a 1000 Hz sampling rate. Data was displayed before and during collection, allowing on-line monitoring of electrode, goniometer and force transducer functions.

EMG signal conditioning was implemented using a specially developed software package. Data treatment consisted of analogue to digital converter offset correction, full wave rectification, time averaging using a 0.2 second envelope, baseline EMG signal magnitude removal and magnitude normalization.

Baseline EMG levels were measured for each subject. For this collection the subject was asked to remain still and relaxed. The EMG magnitudes for each muscle measured during this period then became the baseline of EMG magnitudes to which all recorded EMG signals were compared for that subject.

EMG activity for each test was normalized against the maximum average EMG activity over a 2 second period as measured during a maximum voluntary contraction. The maximum voluntary contraction was collected from each muscle of interest individually. The subject was asked to exert an isometric force against an assistant in a direction to maximize the use of the muscle of interest. During the collection, the assistant forced the subject into an eccentric muscle contraction mode, thereby increasing EMG to its maximum. The EMG signals from this procedure were processed using the same procedure as for the normal EMG signals, except the calculated magnitudes became the normalizing factors for all other data collections. This normalization process was required in order to allow inter and intra-subject comparison (Arborelius, 1986a, Arborelius, 1986b).

Goniometer and hand force data were also conditioned using the EMG signal conditioning software package. Data treatment consisted of analogue to digital converter

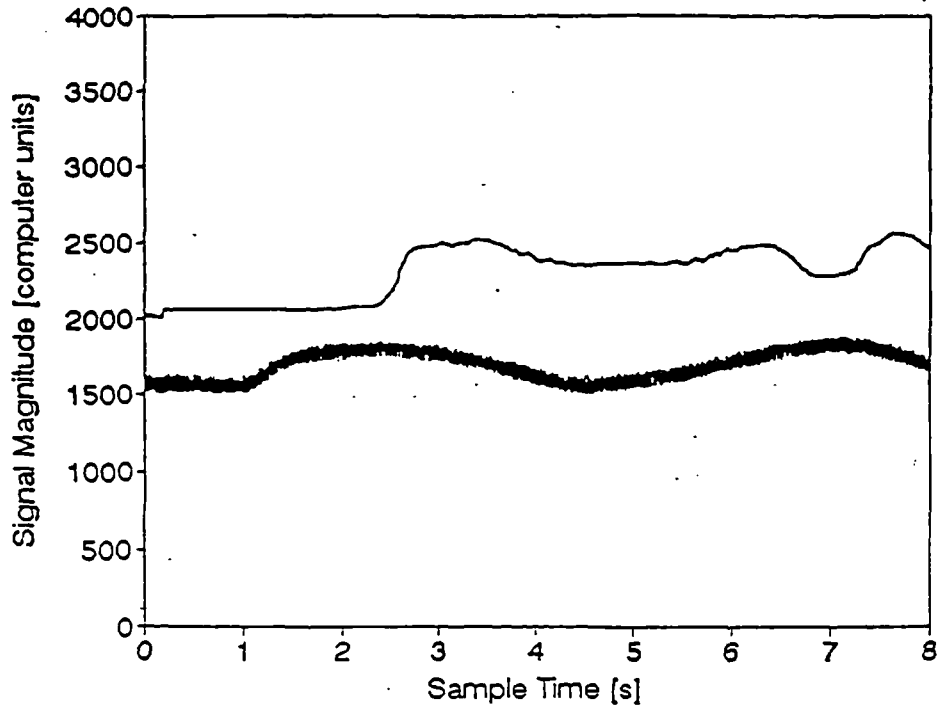


Figure 6.20 Sample of raw hand force signal, F_{p_z} (top line in graph) and raw goniometer signal (bottom line in graph) for a press-up.

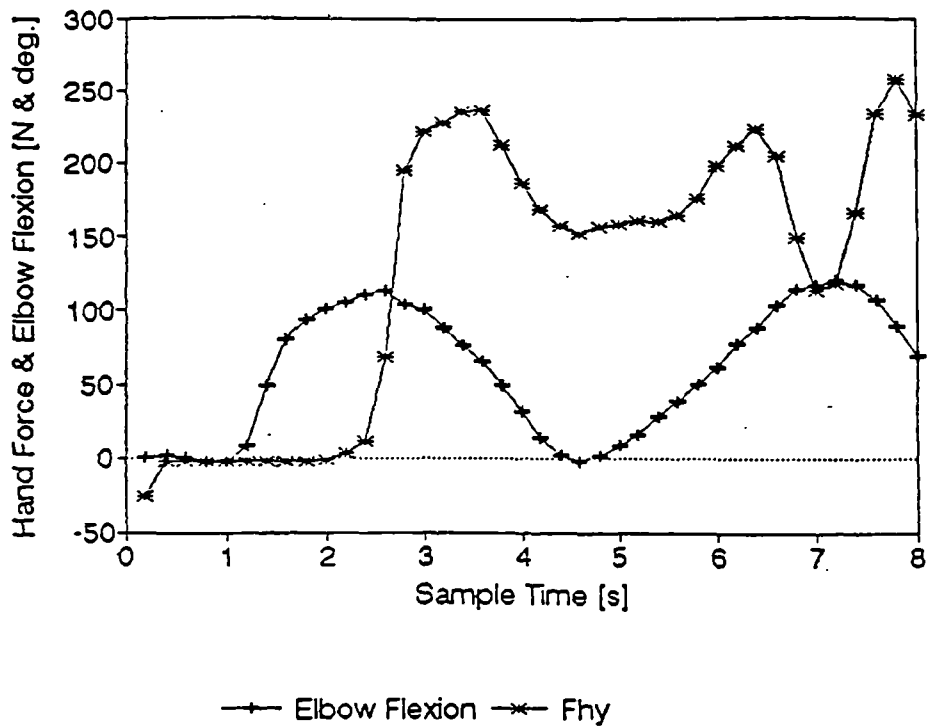


Figure 6.21 Hand force, F_h , and elbow flexion calculated from the data samples shown in figure 6.20.

offset correction, amplifier drift correction, time averaging using a 0.2 second envelope and scaling to convert the data into standard scientific units.

EMG, goniometer and hand force data was combined and normalized, using the software package developed for this project. The procedure divided each activity cycle into 20 equal time intervals. If these intervals fell between data samples then a straight line interpolation was used to determine the appropriate data value for the interval. Averaging interval values across the cycles being included produced data normalized for a single cycle of the activity. For a typical activity, approximately 40 repetitive cycles were combined, each subject contributing 8 repetitive cycles (4 from each of their 2 collections). The resulting data represents typical muscle activation, hand force and joint angles over the course of a single cycle for each of the five activities being studied.

6.3.2 Sample EMG Study Results

Calibration of the instrumented transducer orientation while mounted on the supports used for chin-up analysis yielded a rotational offset, θ_1 , between the $+X_p$ axis and the $+Y_{lab}$ axis of - 52 [degrees]. Using the same measured data, the conversion factor A_1 between measured forces in computer units and newtons was calculated to be 0.00233 [volts/computer unit].

Flexible electro goniometer calibration yielded an average conversion factor 0.455 [degrees/computer unit].

A sample of hand force data in the Z_p direction measured using the instrumented hand transducer and elbow flexion measured using a flexible electro goniometer during a press-up is shown in figure 6.20. The sample begins with no load being applied to the transducer and no subject elbow flexion. The offsets in the force and angle data are due to analogue to digital converter shift and strain gauge bridge imbalance. Figure 6.21 shows the same sample of data with the offsets removed, signals averaged using the 0.2 second time envelope and the relevant calibration factors applied. This is the form to which all of this type of data was converted before normalization.

A sample of supraspinatus raw EMG data for a press-up is shown in figure 6.22. This muscle used an intramuscular fine wire electrode for EMG measurement. EMG signals measured using surface electrodes were typically smaller in magnitude than those measured using fine wire electrodes. Some A-D converter saturation is evident in this sample of supraspinatus EMG signal as it reaches the extremes of the converter range (0 and 4096 computer units). Signal distribution was plotted (figure 6.23) to investigate the amount of signal information lost through this saturation. As can be seen in figure 6.23, the majority

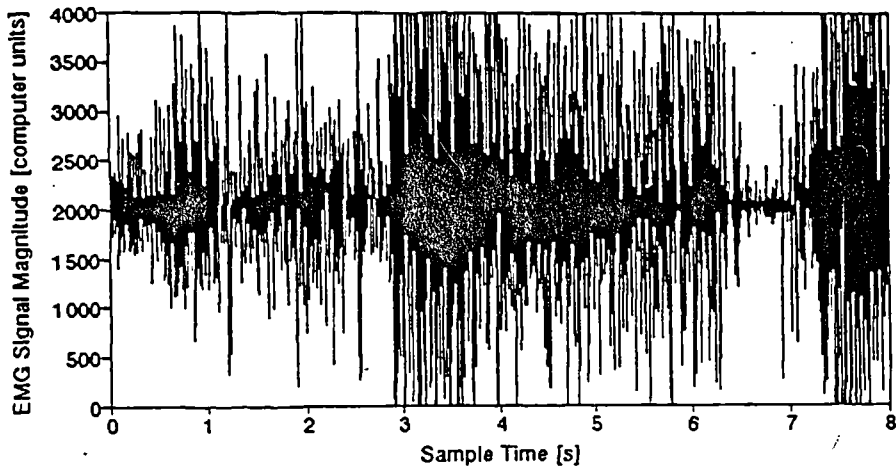


Figure 6.22 Sample of raw EMG signal as obtained from the A-D converter in the data collection system for supraspinatus during a press-up activity.

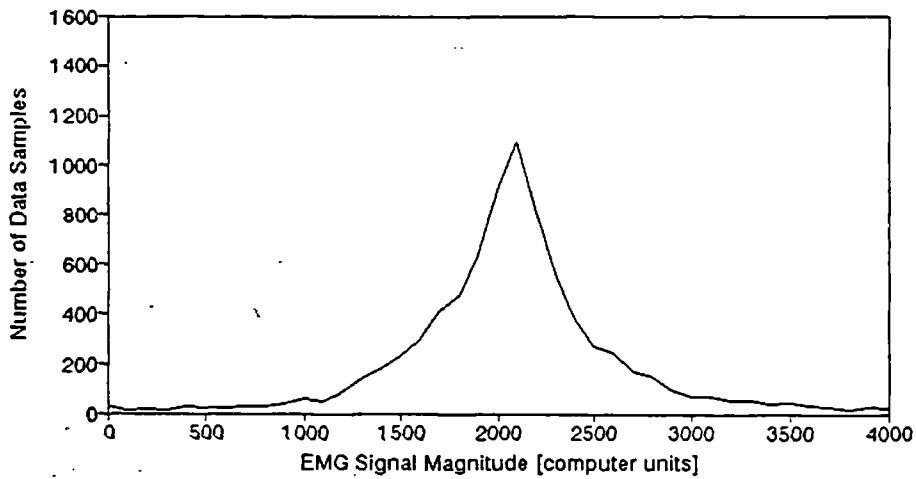


Figure 6.23 Distribution of raw EMG signal sample shown in figure 6.22.

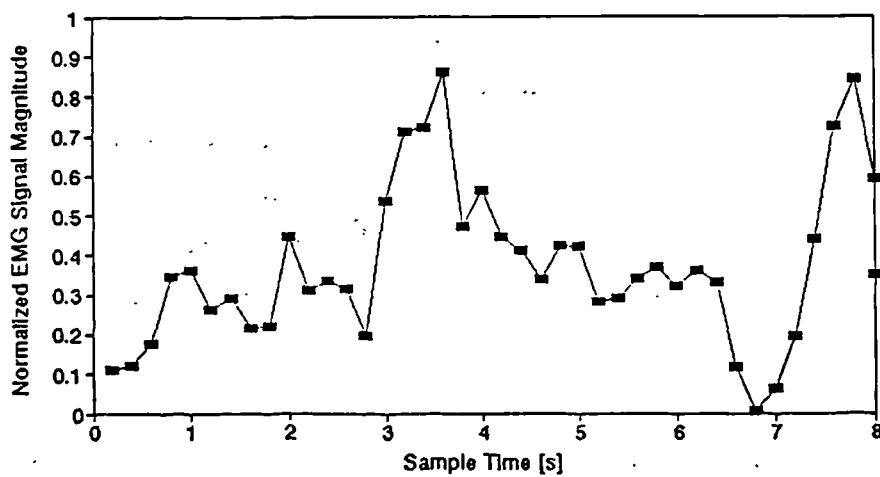


Figure 6.24 Processed EMG signal data for sample shown in figure 6.22, supraspinatus during a press-up.

of information contained in the signal is centred at the A-D converter centre point. As a result, the signal information lost due to A-D converter saturation was assumed insignificant. Figure 6.24 shows the same supraspinatus data sample after rectification, A-D converter offset correction and averaging using a 0.2 second time envelope, baseline EMG signal removal and normalization against the maximum voluntary contraction EMG magnitude.

Normalized hand loading and EMG magnitude results for the five activities are presented along with the activity analysis results in the following sections. A discussion of these results and conclusions that can be made from them are also included with the activity analysis discussion and conclusions.

6.3.3 Activity Analysis Materials and Methods

All experimental data required for modelling shoulder function for the activities being studied were collected during a series of sessions in the motion analysis laboratory at the University of Strathclyde Bioengineering Unit. Using the collected data and the model presented in this thesis, shoulder function was predicted for the five activities being studied.

Results of this and the EMG study were to be compared in order to verify shoulder function predicted by the model. To ensure that any differences encountered in this comparison were not due to differences in the experimental procedures or actual function differences, the experimental details were constrained to be as close to those in the EMG study as was possible.

All five of the activities included in the EMG study were performed by the same five subjects for this study. Each activity was performed in two sets of 5 cycles separated by a rest period. Eight seconds of data were collected for each set. Activity order was random. Subjects were instructed to perform the activities at a slow to moderate pace. Subject positioning was constrained to be facing the $+X_{lab}$ direction for each of the activities. For the activities where hand loads were measured, no subject contact with the load sensing device occurred until after data collection had begun. All other data collection details not discussed below were the same as used in abduction data collection discussed in section 6.1.

Abduction and flexion activities were performed using a 2 kg hand load. Subjects were asked to use a slightly bent arm and limit arm rotation during the activity. Four static sets of data were collected for arm position ranging from 0 to 120 degrees elevation for both activities. Scapula markers were placed using palpation for each of these collections. Relationships relating scapula orientation to humeral elevation were then calculated using linear regression.

Chin-ups were again performed using a supinated hand grip and a pair of hand grips

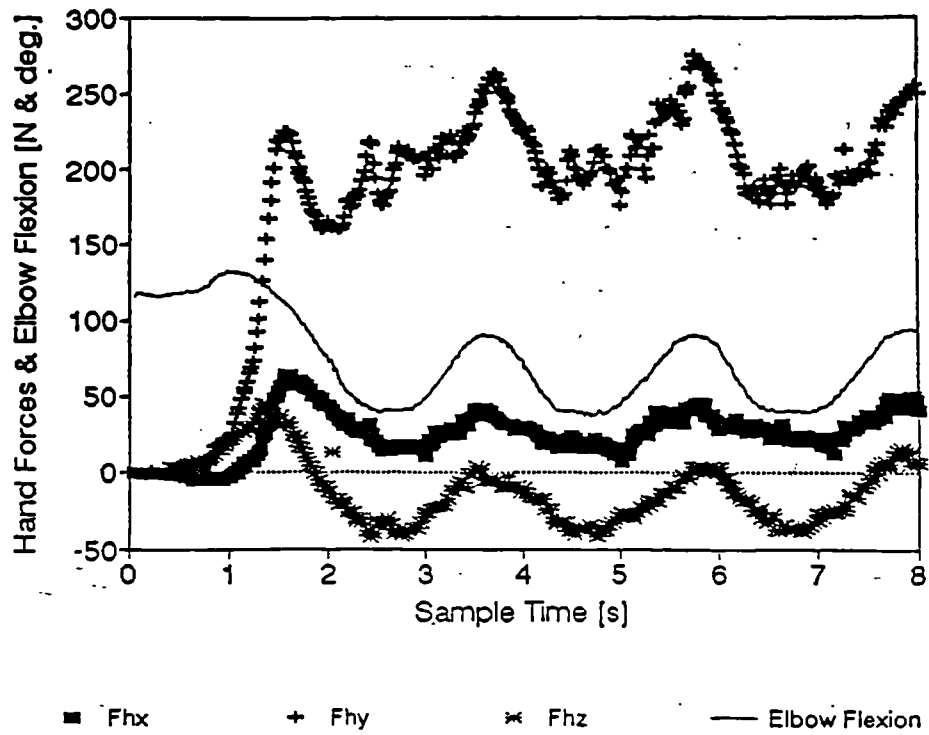


Figure 6.25a Sample of raw hand forces and elbow flexion angle data measured for a press-up. Note, for approximately the first 0.5 seconds there is no hand loading.

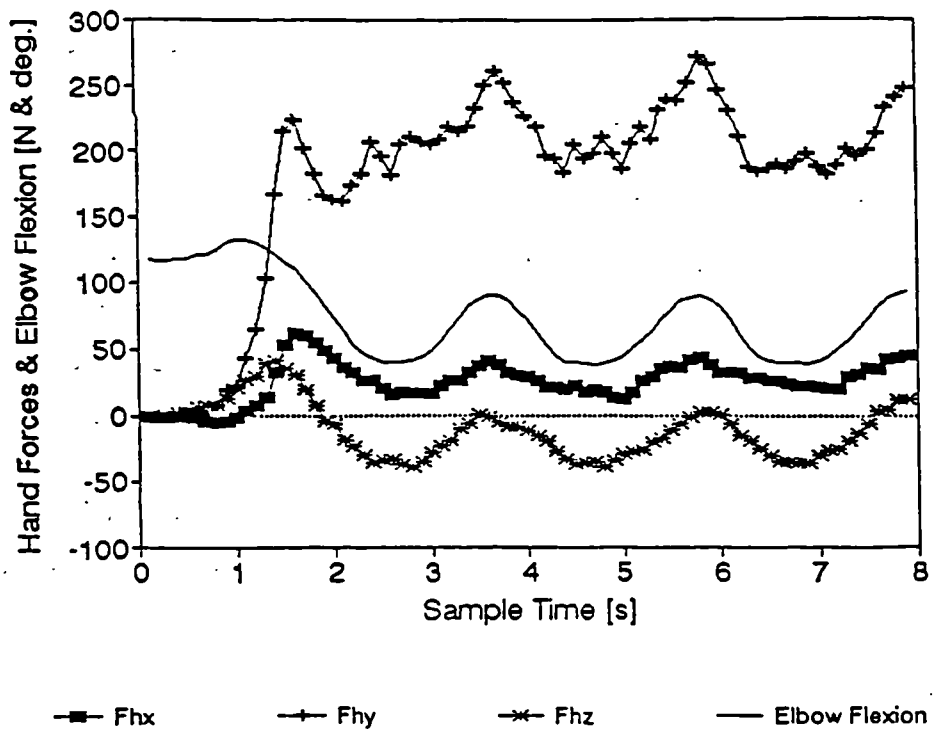


Figure 6.25b Sample of averaged hand forces and elbow flexion angle data for a press-up. This data was calculated using the raw data seen in figure 6.25a.

approximately 2 metres above the floor. Both of the grips were mounted on a gymnastic high bar. The instrumented hand grip was connected to the amplifier equipment discussed earlier in this thesis (section 4.4.2.). Four sets of static data were collected across the range motion in the activity. A small set of wooden steps and wooden blocks were used to position the subject at the height used for each collection. Scapula markers were placed while the subject supported their weight with their hands. They also supported their weight with their hands during static data collection. Relationships relating scapula orientation to elbow flexion were then calculated using linear regression.

Push-ups were performed with the subject's right hand flat on a 200 mm block on the Kistler force plate. The upper surface of the block to the force plate origin distance, a_y , required for centre of pressure calculations (equations 4.26 & 4.27) was then 0.257 m. A series of four static positions were used to estimate scapula position. To reduce subject fatigue during the static collections, the static push-up sequence was done in an upright position against a chest level bar. Scapular markers were placed for each data collection using palpation. Relationships relating scapula orientation and elbow flexion were then calculated using linear regression.

Press-ups were performed on a pair of specially fabricated parallel bars. The hand grips were mounted on these bars and adjusted for width to suit the subject. Typically the hand grips were placed closer together than they were for the EMG study as in that study, equipment limitations constrained corresponding width adjustment. A set of wooden blocks was used to support the subject. Using these blocks, four sets of static data were collected across the range of body position in this activity. Scapula orientation relationships were then determined as for the push-up and chin-up activities.

Data analysis was the same for each of the five activities. Where hand loading was measured the forces and moments were taken as their change with respect to the no load signal levels recorded at the start of each collection. Hand loading for flexion and abduction was assumed to be a constant $-Y_{lab}$ direction force, with no inertial component. In the absence of inertia, the constant hand forces utilized for flexion and abduction would accurately simulate segment loading for a static or quasi-static activity format.

Using the hand loading, reflective marker coordinate data and subject geometric data shoulder function was modelled for the five activities. Predicted muscle forces, joint contact forces, hand loading, joint moments due to external loading and shoulder kinematics were averaged using a 0.1 second time envelope. Viewing each set of activity data, 2 cycles from each collection were chosen to include in normalization. Cycle data was rejected if a significant portion of data was missing or a portion of the cycle was not representative of

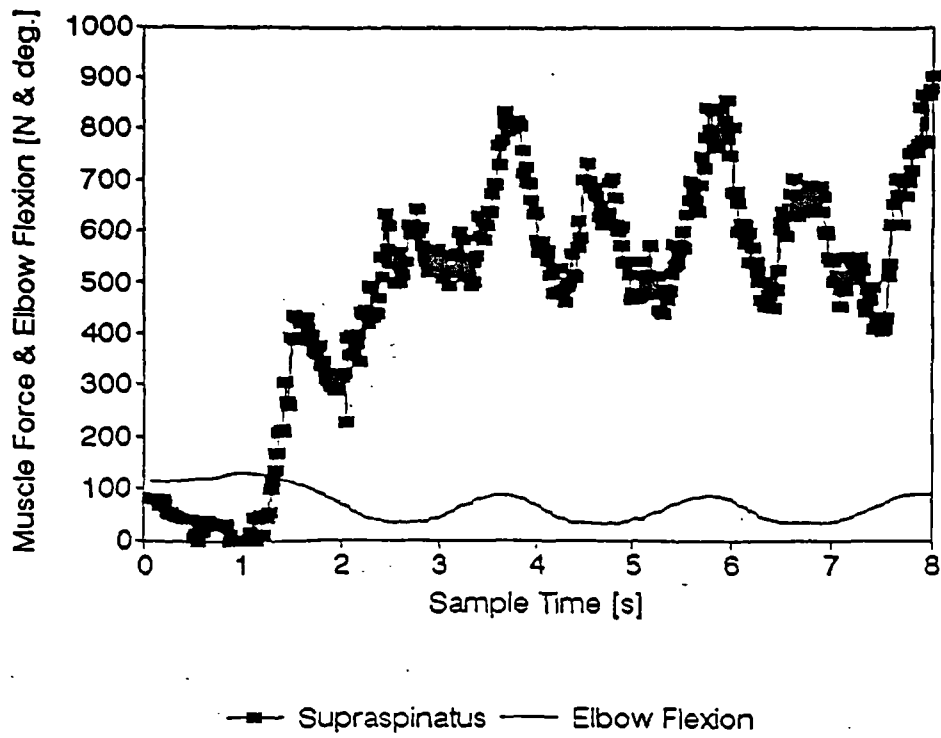


Figure 6.26a Sample of predicted supraspinatus force and measured elbow flexion angle for a press-up.

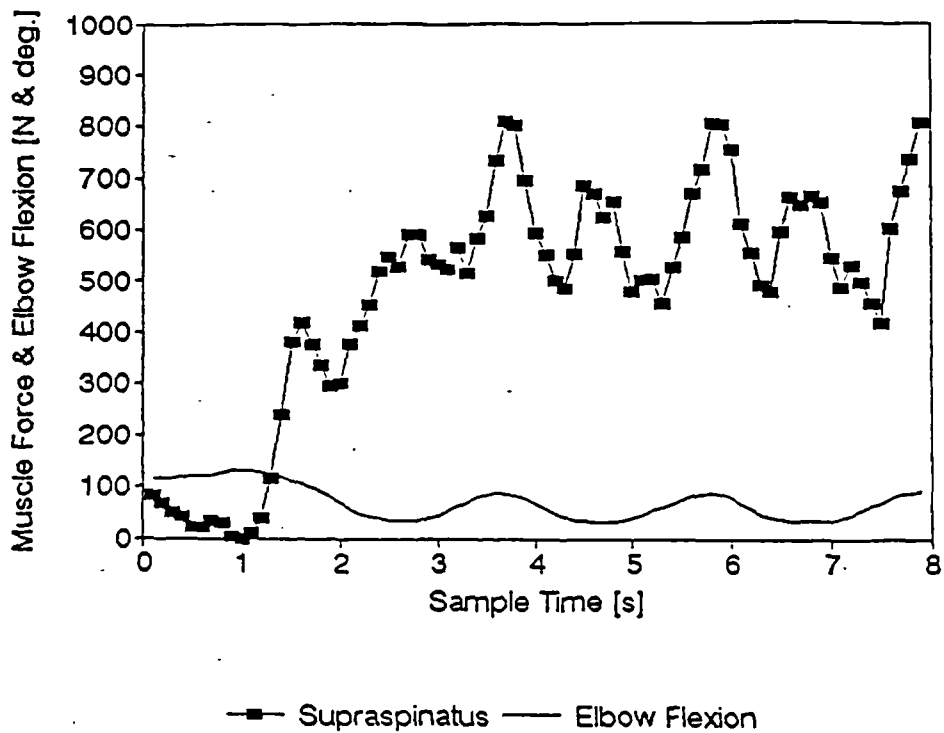


Figure 6.26b Sample of average predicted supraspinatus force and elbow flexion angle for a press-up. This data was calculated using the raw data in figure 6.26a.

the activity. The data normalization procedure was the same as was used for the EMG analysis. The resulting normalized data represents the average predicted muscle activation, hand loading, joint contact forces, joint moments and shoulder kinematics of the five activities studied.

6.3.4 Sample Activity Analysis Study Results

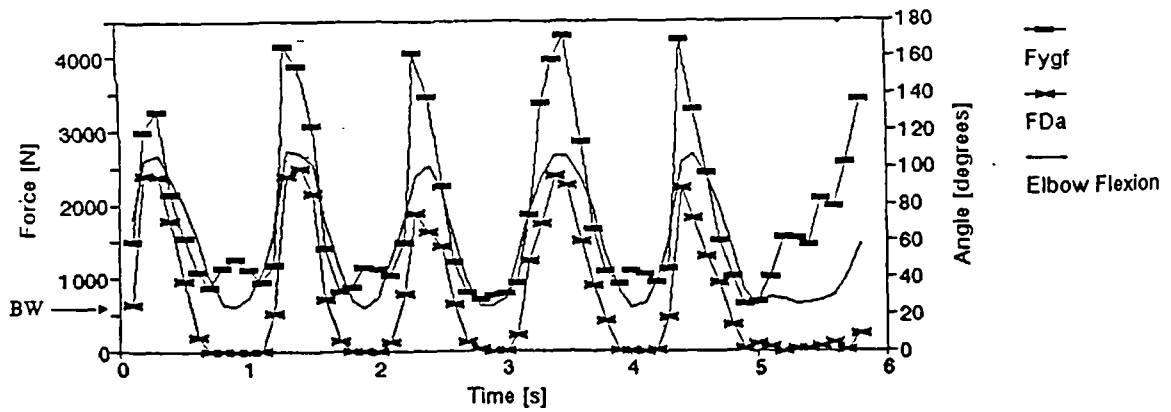
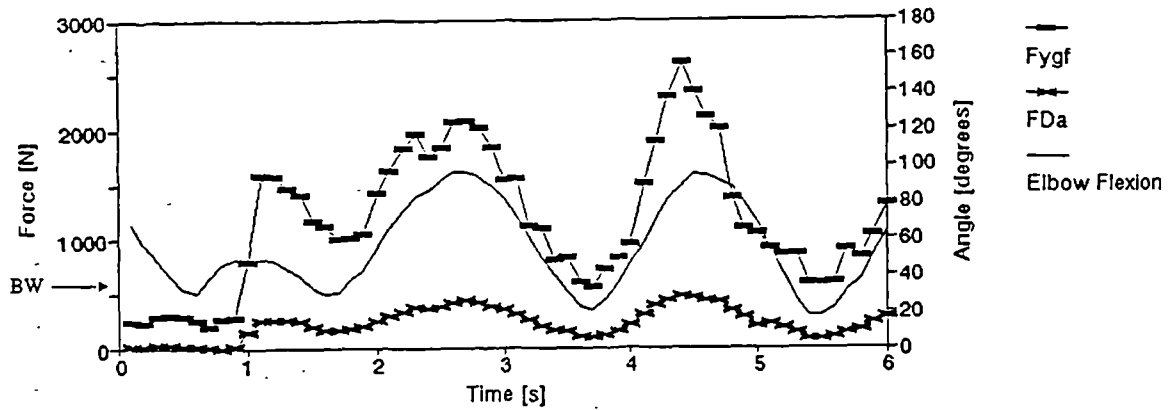
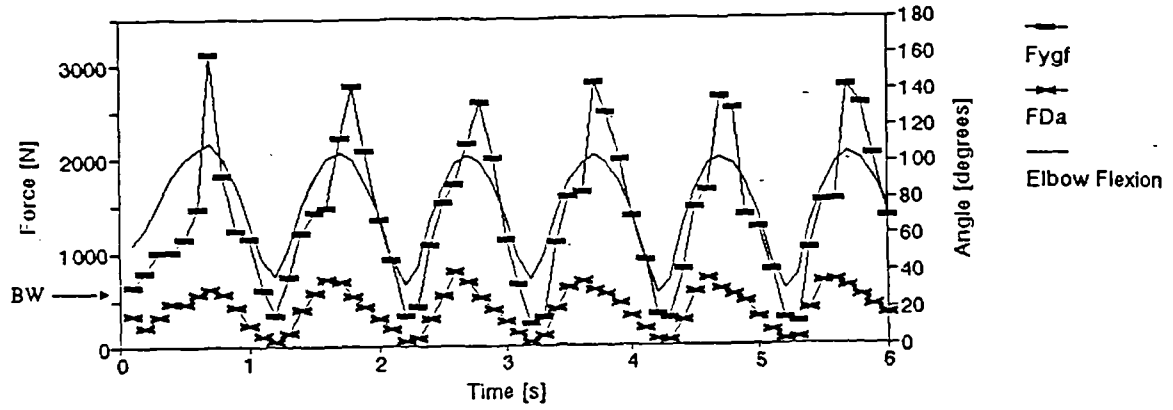
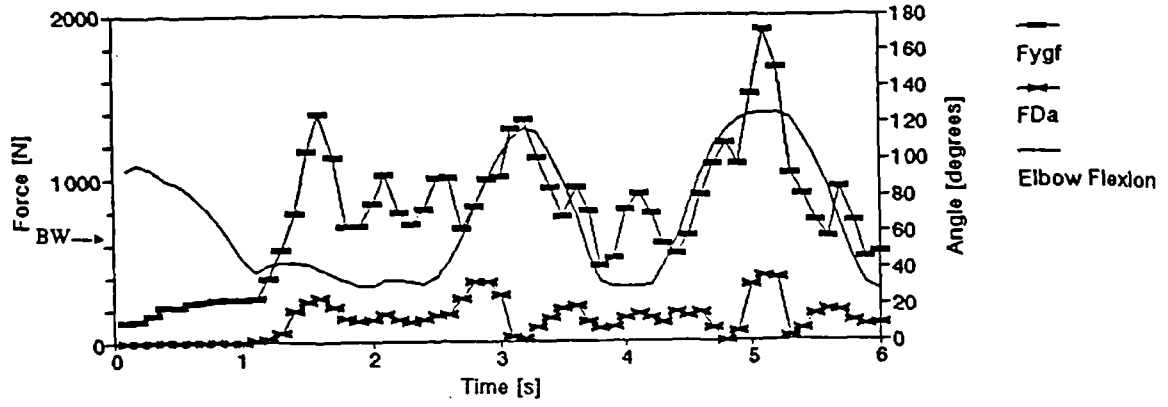
Figure 6.25a shows a sample of raw hand force data and elbow flexion angle for three cycles of a press-up. For approximately the first 0.5 seconds, there is no load transmitted through the transducer. The transducer signal magnitudes measured during this period are used to correct the transducer signals for amplifier drift and A-D converter offset. Figure 6.25b shows the same hand force and elbow flexion angle data sample after averaging.

Figure 6.26a contains a sample of predicted supraspinatus force and elbow flexion angle for the same three press-up cycles shown in figure 6.25. These data were obtained using only the moment balance constraint equations for optimization and are representative of the type of muscle prediction data produced by the shoulder model. In some collections, missing marker data from the motion analysis system caused intermittent breaks in the data available for analysis. In general this was not a significant problem. Figure 6.26b shows the same sample of predicted supraspinatus force after averaging.

Measured elbow flexion, optimized muscle force and joint contact force as predicted for each of the five subjects performing one of their two series of push-ups are shown in figure 6.27. Variations in cycle frequency and body weight complicate the comparison of data in this form. Normalizing the push-up data for each subject and averaging, condenses the cyclic information into a form more suited for interpretation (figure 6.28). Variation between individual subject joint forces and the five subject average is as high as $\pm 50\%$ for this activity.

6.3.5. Results and Discussion

Results from both EMG and motion analysis studies are presented in this section. Muscle activation, joint moments, and joint contact forces are presented for each activity. The majority of the results that are presented were obtained without implementation of the joint stability constraint. Results achieved with the stability constraint are presented only when they are significantly different from those achieved without stability. Model verification is detailed through the comparison of predicted model results to measured EMG muscle activation. Before the EMG results can be used for this verification, results of a comparison between hand forces measured during the two studies must be presented.



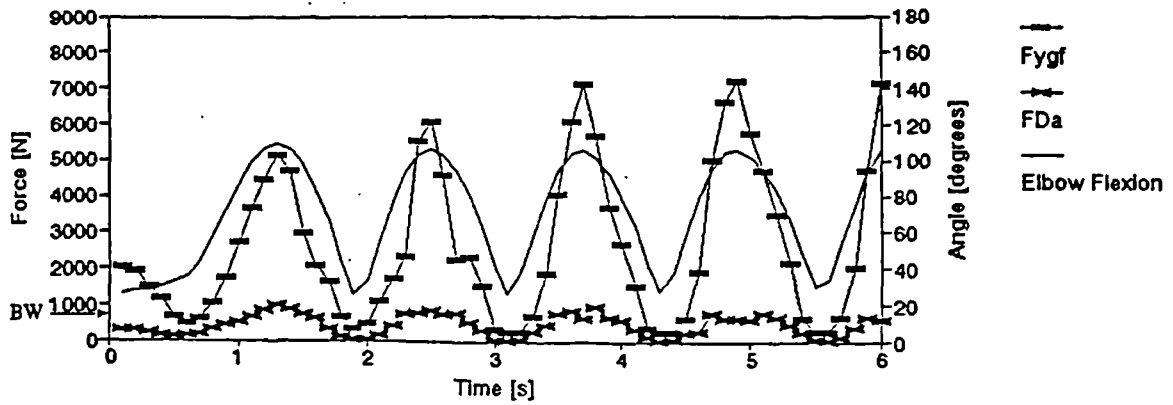


Figure 6.27 (above and opposite) Samples of predicted glenohumeral joint compressive forces, $F_{y_{gf}}$, anterior deltoid forces, F_{Da} , and elbow flexion for a series of push-ups by each subject. Subject body weight, BW , is indicated on each graph. Proceeding down from the top of the opposite page, samples are for SUB08, SUB09, SUB11, SUB12 and SUB13. Note, only 6 of 8 seconds of one series is shown for each subject. Normalized results for each activity were calculated using two cycles from each of the two 8 second series collected for each subject.

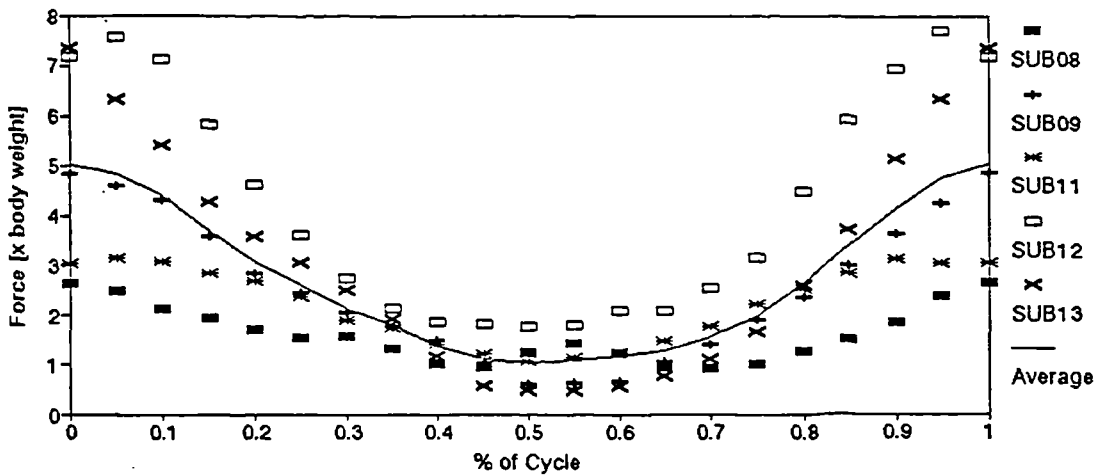


Figure 6.28 Normalized glenohumeral joint compressive forces, $F_{y_{gf}}$, for a push-up. Averages for each subject and the overall average are shown in terms of one cycle of the activity. The cycle is defined to begin at the start of the power phase of the activity.

6.3.5.1 Hand Forces

Figure 6.29 and 6.30 contain the averaged and normalized hand forces measured for the push-up, press-up and chin-up activities during the EMG and motion analysis experimental sessions respectively. These forces represent the average muscle forces that were measured for each activity plotted over a single cycle of the activity. Each cycle was defined to start with the power phase of the activity cycle.

The highest magnitude normalized hand force was measured for the chin-up activity and reached 0.7 times body weight in the $+Y_{lab}$ direction. This is in comparison to 0.5 and approximately 0.4 times body weight peak normalized hand force magnitudes in the same direction for the push-up and press-up activities respectively.

Fluctuations in the $+Y_{lab}$ direction forces measured during the motion analysis study were as high as 0.3 times body weight.

In general, forces measured for each activity show good agreement between the two experimental sessions. Examining the force profiles, representing the change in hand force with each activity cycle, shows the same shape being produced for each activity, irrespective of whether it was from the EMG or motion analysis study. This is particularly evident for the vertical hand force, F_{h_y} .

For every activity, the peak vertical hand forces, F_{h_y} , measured during the motion analysis session are larger than their corresponding EMG study magnitudes. This difference varies between activities and during the progression of the activities, but reaches a maximum of up to approximately 0.1 times body weight.

The F_{h_z} force measured for the press-up was consistently negative for the EMG study but varied from positive to negative and back to positive for the motion analysis study. This difference appears to have occurred through a positive constant magnitude shift of the force during the motion analysis study.

Hand forces measured during an activity are characteristic of both the subject, activity and experimental environment. As such, a comparison of hand forces measured during the EMG and motion analysis studies should give a good indication of the comparative experimental conditions of each study. For validation purposes it is essential that shoulder function and therefore hand forces remained consistent between the two experimental sessions. Without this equivalence, consistent shoulder function between the two studies could not be guaranteed.

The dynamic aspect of each of these activities is evident by the large fluctuations in the measured hand loads. For the chin-up $+Y_{lab}$ direction hand force varies from 0.7 to 0.35 times body weight. This represents more than a 0.1 times body weight fluctuation away

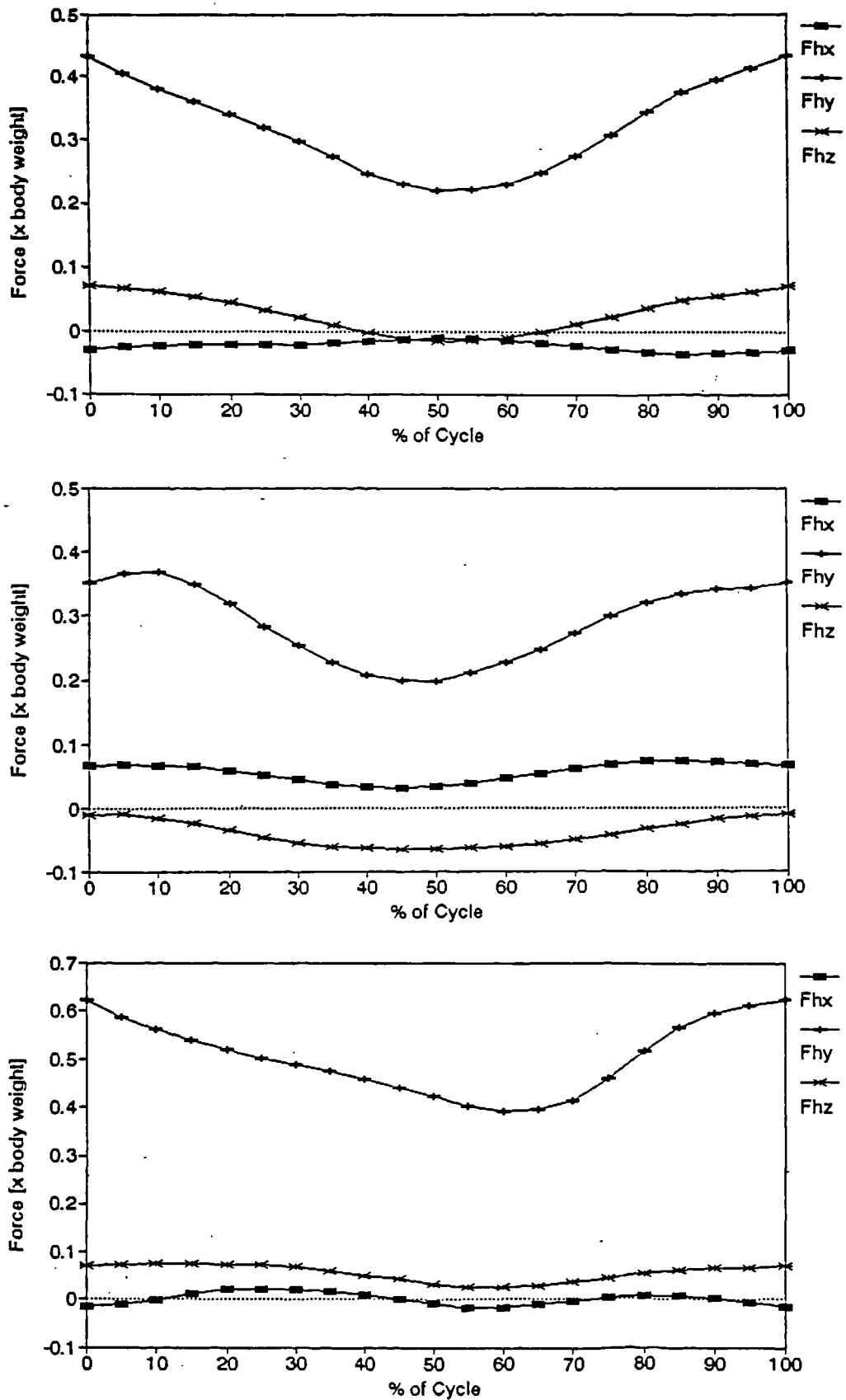


Figure 6.29 Average hand forces measured for the push-up (top), press-up (middle) and chin-up (bottom) during the EMG study.

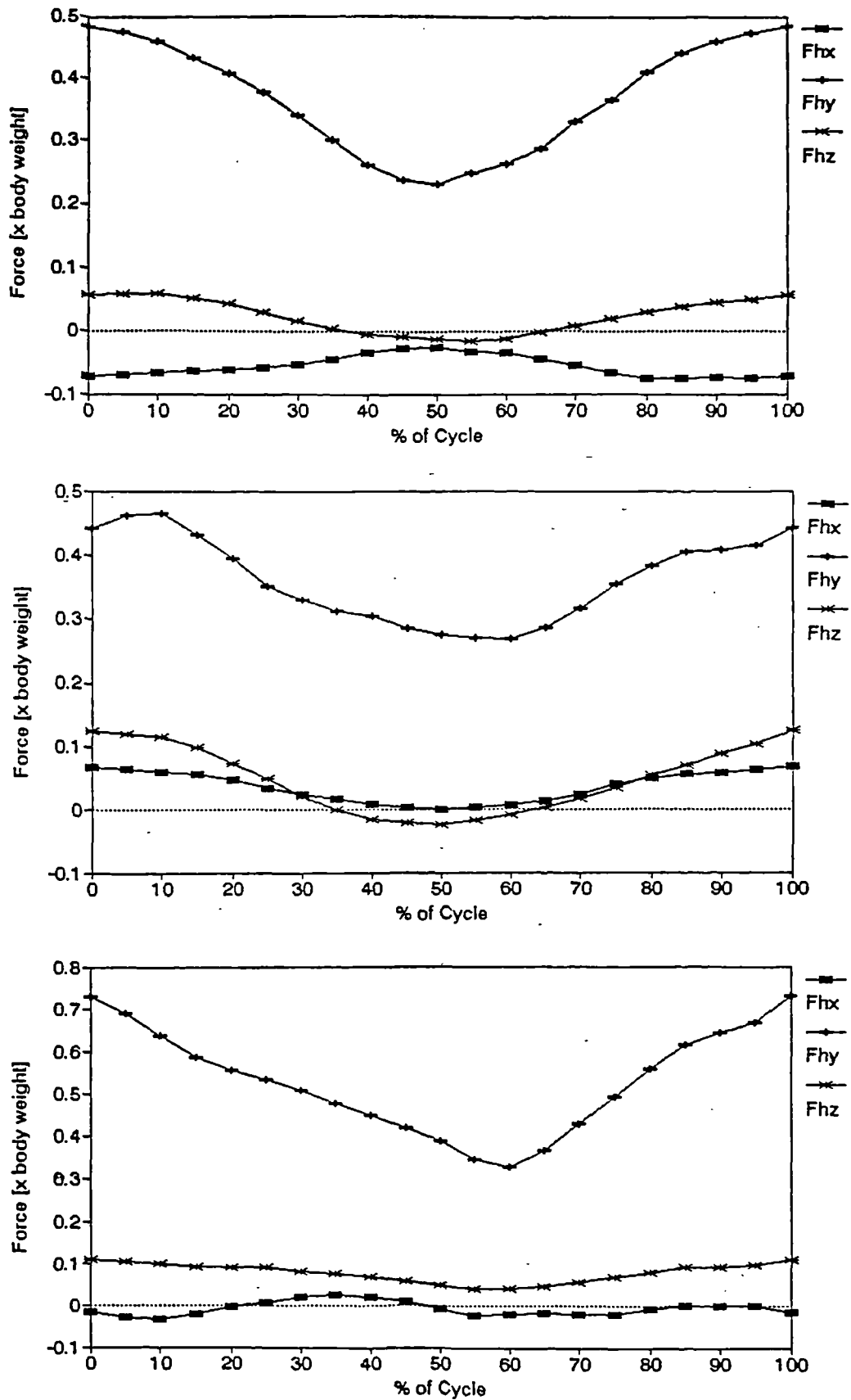


Figure 6.30 Hand forces for the push-up (top), press-up (middle) and chin-up (bottom) measured during the motion analysis study.

from the force required to suspended a subject evenly by their hands.

Two different averaging time envelopes were used in the data analysis of the studies. A 0.2 second envelope was used for EMG study data and a 0.1 second envelope was used for motion analysis study data. The effect of this would be to smooth the EMG data more than the motion analysis data. This would in part explain the magnitude difference between the F_{h_y} force values of the two studies. The increased smoothing of the EMG analysis would tend to reduce force fluctuations thereby reducing peak force magnitudes and increasing minimum force magnitudes.

Measured press-up F_{h_z} hand forces showed differences between the two studies consistent with a variation in hand grip separation distance. For the EMG study, the hand grip separation distance was larger than the grip separation distance used in the motion analysis study. As a result, during the EMG study, subjects had to push vertically down as well as out on the grips. This would tend to decrease the vertical hand force, F_{h_y} , and impose a negative shift on the F_{h_z} force. The measured hand forces show this relationship.

Cycle end point discontinuities are evident in some of the hand forces plotted in figures 6.29 and 6.30. These are most evident for the vertical, F_{h_y} , hand forces as a result of their large fluctuations during the activity cycle. These discontinuities are a characteristic of the normalization process and the type of activities included in this study. For normalization each subject activity cycle was identified by its start and end points. This accurately located the cycle beginning and end for normalization. Referring back to figure 6.25, discontinuities are evident in the vertical, F_{h_y} , hand force both at the cycle end (approximately 3.5 and 5.8 seconds) and mid points. With normalization, these end point discontinuities would be maintained while the mid point discontinuities through the natural variation in their timing would be attenuated.

The purpose of measuring EMG study hand forces was to establish whether shoulder function could be assumed consistent with that in the motion analysis study. The forces measured for the activities in either study appear to be in good overall agreement, apart from small differences in measured press-up hand forces that appear to be the result of the hand grip spacing variation. Based on this, it is assumed that shoulder function remained consistent through the activities in both the EMG and motion analysis studies. Under this condition, verification of predicted muscle activation should be possible by a qualitative comparison with the measured EMG muscle activation.

6.3.5.2 Abduction

Figures 6.31 and 6.32 show the measured EMG and predicted muscle activation

respectively for a 2 kg hand load. The model results were determined without the constraint of joint stability. Figure 6.31 also includes the average frontal plane humeral elevation angle in degrees for the EMG study. Measured EMG muscle activation magnitude is plotted as a fraction of the maximum voluntary contraction EMG level. Predicted muscle activation magnitude is plotted in terms of muscle stress. Stress levels were calculated by dividing the predicted muscle forces by subject weight and then by muscle cross-sectional area in cm^2 .

Increased EMG muscle activation over the baseline EMG levels were measured in all of the shoulder muscles included in this study. Of these muscles, triceps and latissimus dorsi were the least activated. Deltoid was activated to approximately 0.7 times the maximum voluntary contraction EMG level evenly across its anterior, middle and posterior sections. Supraspinatus, infraspinatus and subscapularis were all similarly activated but to a slightly lower level. Of these three muscles, supraspinatus was the most activated and subscapularis the least activated during the early and late phases of the cycle. Maximum EMG levels in deltoid, infraspinatus, subscapularis and supraspinatus occurred at approximately 25 % through the cycle. This corresponds to 90 degrees of abduction during the arm elevating phase.

The measured EMG muscle activation reflects the phasic nature of this activity. Relative muscle activation was highest in all of the muscles during the first 50 % of the overall cycle. This corresponds to the arm elevation phase of the activity. During the second phase of the activity when the arm is being lowered, muscle activation was reduced.

Muscle activation was also predicted in all eight of the muscles included in the EMG study. In addition, pectoralis major activation has also been plotted. Activation of pectoralis major was limited to its clavicular section only. Triceps and latissimus dorsi were again the least activated. Activation in the three sections of deltoid was not as consistent as measured in the EMG study, with no anterior deltoid activation at the cycle start. Supraspinatus, infraspinatus and subscapularis were again relatively evenly activated with supraspinatus being the most and subscapularis the least activated during the early and late cycle phases. On average, deltoid was again more highly activated than infraspinatus, subscapularis and supraspinatus. All predicted muscle activations were approximately symmetrical about the cycle mid point.

Figure 6.33a contains the average glenohumeral joint moments and humeral frontal plane elevation angle calculated for the motion analysis study. Shoulder moments are stated in terms of the humeral coordinate system. Units of Nm have been retained for the joint moments.

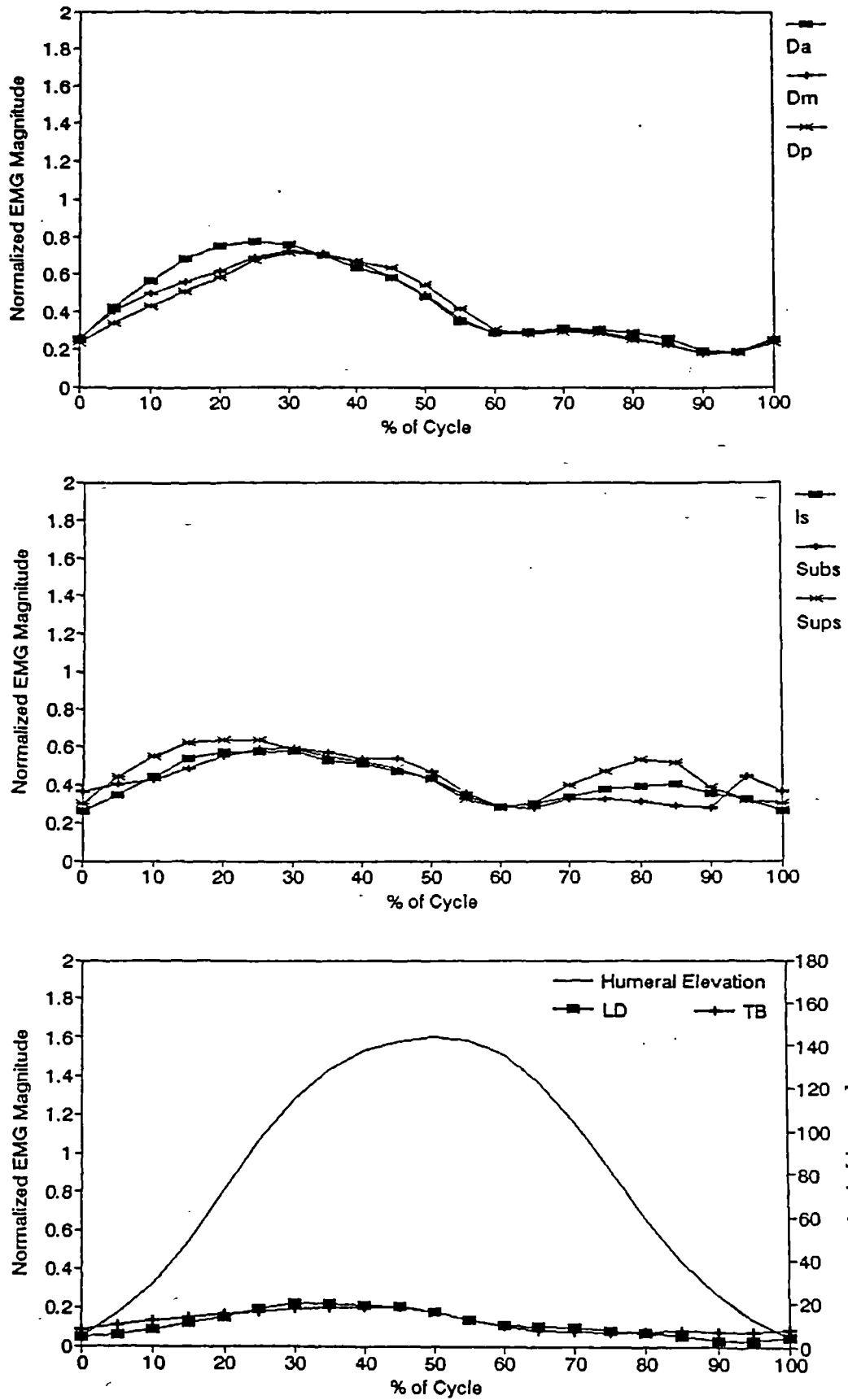


Figure 6.31 Measured EMG muscle activation for anterior, middle and posterior deltoid (Da, Dm, Dp), infraspinatus (Is), subscapularis (Subs), supraspinatus (Sups), latissimus dorsi (LD) and triceps (TB) during abduction with a 2 kg hand load.

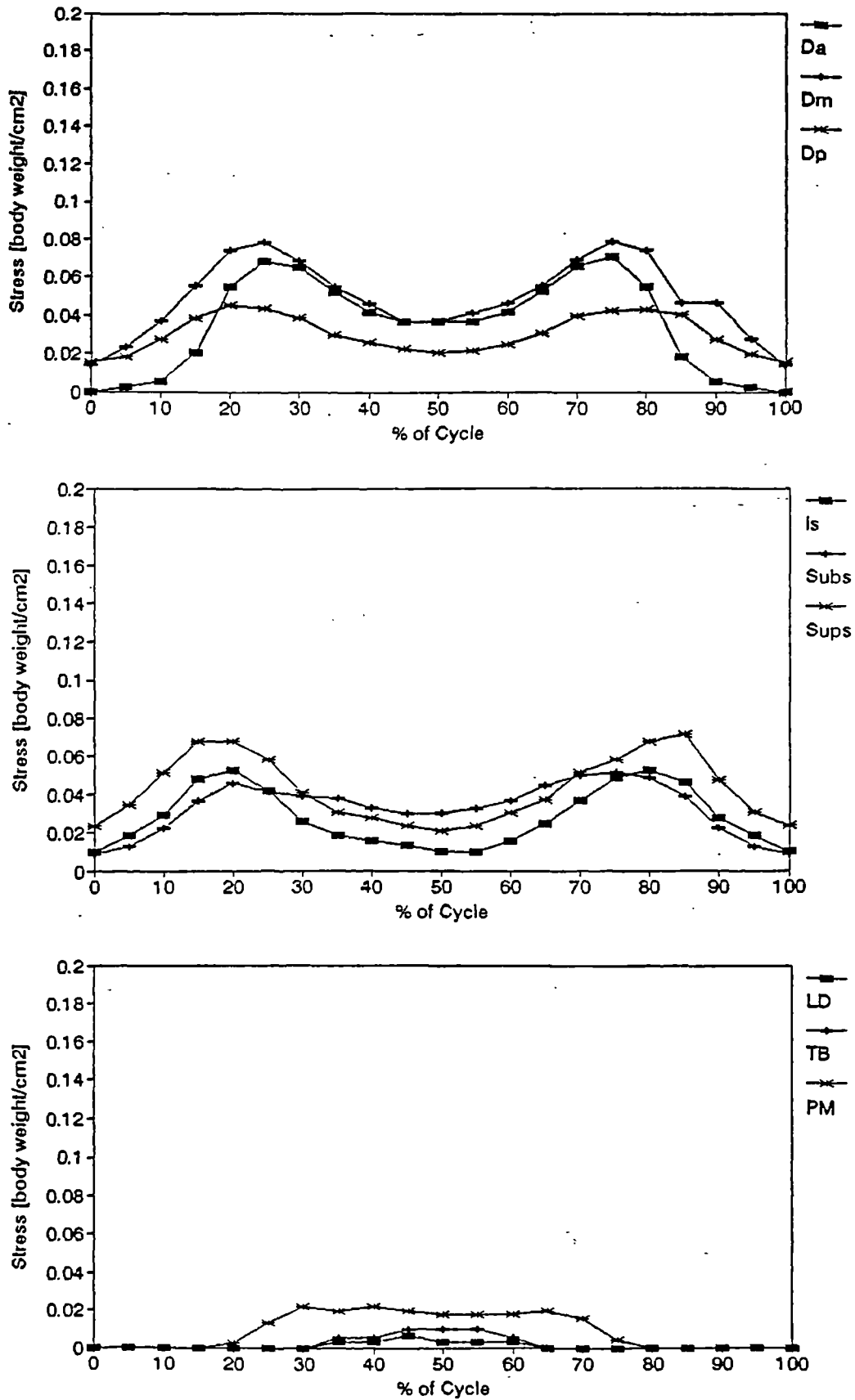


Figure 6.32 Average predicted muscle activation for anterior, middle and posterior deltoid (Da, Dm, Dp), infraspinatus (Is), subscapularis (Subs), supraspinatus (Sups), latissimus dorsi (LD), pectoralis major (PM) and triceps brachia (TB) during abduction with a 2 kg hand load.

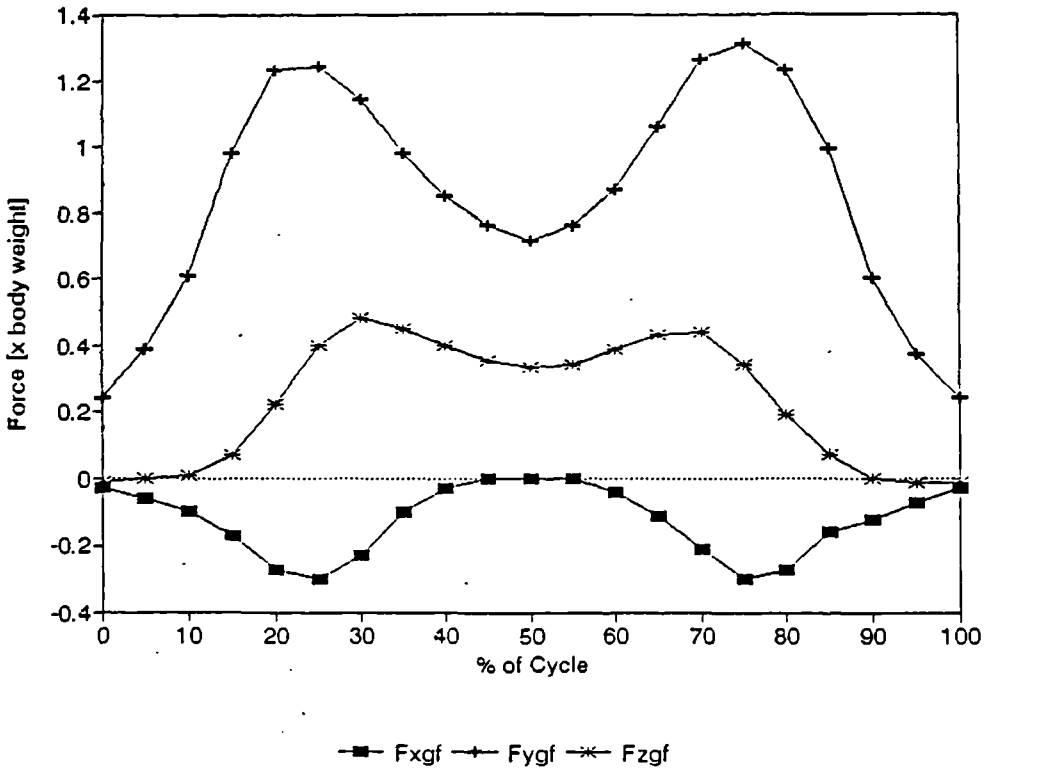
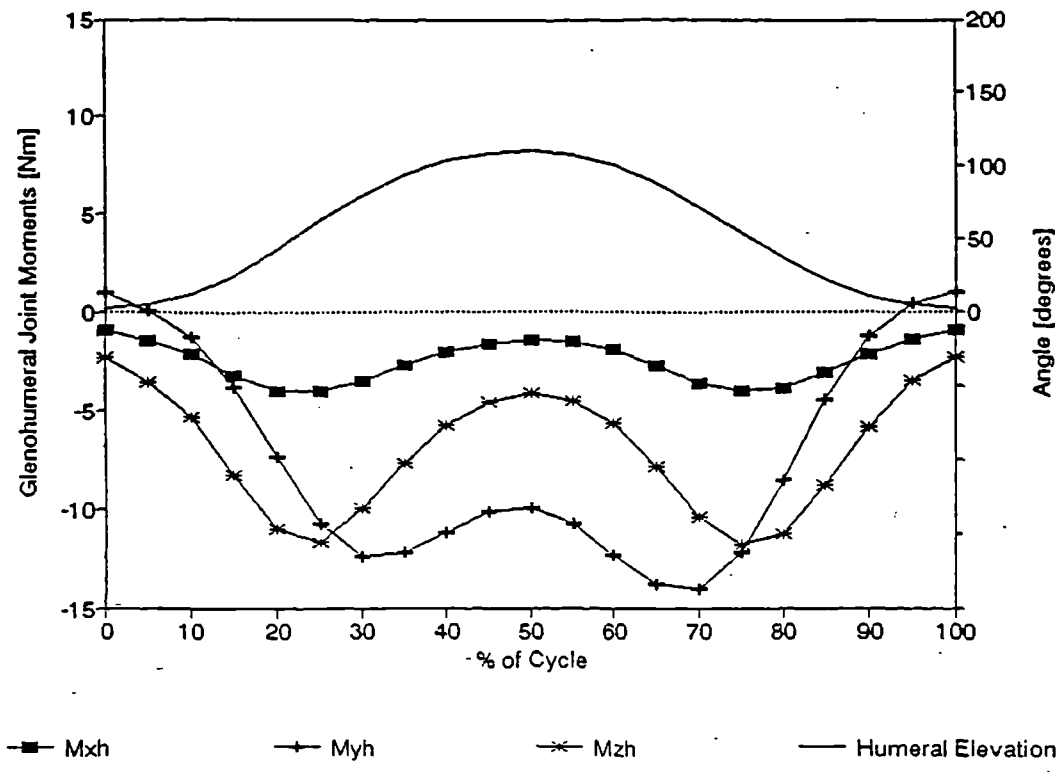


Figure 6.33 Average glenohumeral joint moment due to external loading, and elbow flexion angle during abduction with a 2 kg hand load (a, top). Average glenohumeral joint contact forces for abduction with a 2 kg hand load (b, bottom).

Glenohumeral joint moments My_h and Mz_h both reached approximately -12 Nm. This corresponds to a total resultant joint moment magnitude of approximately 16 Nm.

The calculated joint elevation angle was not as large as was measured during the EMG study, reaching only 120 degrees as opposed to 140 degrees.

Figure 6.33b contains the predicted glenohumeral joint contact forces normalized with respect to body weight. The joint compressive force, Fy_{gf} , reached a maximum of over 1.2 times body weight (a range of 0.9 - 1.8 times body weight was observed over the five subjects). The anterior shearing force (+ Fz_{gf} direction) was relatively small below approximately 90 degrees of humeral elevation. Above 90 degrees of humeral elevation, this shearing force increased rapidly to a maximum of approximately 0.5 times body weight. The superior shearing force reached a maximum of 0.3 times body weight (- Fx_{gf} direction).

When the joint stability constraint was included in muscle optimization, middle deltoid and subscapularis became more highly activated, increasing the joint compressive force. These relative increases in middle deltoid and subscapularis activation were not apparent in the measured EMG muscle activation. With the stability constraint, joint compression reached up to 1.5 times body weight, while the shear forces remained essentially unchanged.

Deltoid and supraspinatus are muscles ideally situated to act as prime effectors during abduction. It is not surprising that their activation levels were found to be high in both measured EMG and predicted muscle activation. Measured and predicted muscle activation levels for these two muscles are consistent with those measured by Inman et al (1944), (figure 6.7) and Saha (1973). The consistently high supraspinatus activity for humeral elevations above 90 degrees reported by Järholm (1989), in contrast to findings by Inman et al (1944) and Saha (1973) were also not observed in either the measured EMG or predicted muscle activations of this study. Biasing of EMG activity to middle deltoid, reported by Ringelberg (1985) is not present in the measured EMG activation and only marginally so in the predicted activation of this study.

High levels of infraspinatus and subscapularis activation are found in both the EMG and predicted results. Similar activation levels have been reported for these muscles by Inman et al (1944) and Saha (1973). Because the stability constraint was not included, predicted muscle activation can be assumed to be related only to joint moment balance. Since similar activation for these two muscles was also measured, it can be assumed that physiologically these muscles must also act to provide joint moment equilibrium.

The effect of inertial forces on measured EMG muscle activation is evident from the change in relative magnitudes between the first and second half of the activity cycle. During the first half of the activity, inertial forces and gravitational forces are cumulative, thereby

increasing the glenohumeral joint moment that must be balanced by shoulder musculature. During the second phase inertial forces reverse their direction and thereby tend to reduce the joint moment that must be balanced by muscle activity. Measured EMG muscle activation reflects this characteristic, in general the musculature is more highly activated during the first phase and less so in the second. The corresponding predicted muscle activations do not show this variation between the phases because inertial forces were not considered in the model.

Some humeral external rotation accompanied abduction during the motion analysis study. For abduction with no humeral rotation, the M_{y_h} glenohumeral joint moment magnitude would remain relatively small. Examining figure 6.33a, at maximum humeral elevation (50 % through the cycle), the M_{y_h} joint moment is actually larger in magnitude than the M_{z_h} joint moment, indicating the arm was externally rotated more than 45 degrees. While this rotation was not a problem in this study, it does indicate the importance of accurate kinematic measurements, without which, this significant characteristic of humeral elevation could have been overlooked.

An approximation for the joint compressive force corresponding to abduction without a hand load can be calculated based on the results of this experiment. In the preliminary study of abduction, the maximum glenohumeral joint moment was approximately 9 Nm at 80 degrees of humeral elevation. This value corresponded to abduction without a hand load. The ratio of this moment to the value of total moment measured for 80 degrees in this study (14 Nm) would be approximately 0.6. Applying this ratio to the calculated joint moments would yield a compressive joint force of approximately 0.7 - 0.8 times body weight. This correlates with the findings of previous two-dimensional shoulder models by Inman et al (1944) and Poppen and Walker (1978) and the three-dimensional model by Karlsson (1992).

The rapid increase of anterior shear force with arm elevations above 90 degrees of humeral elevation may be significant with respect to anterior glenohumeral joint instability.

Muscle activation predicted for abduction appears to be generally consistent with the muscle activation measured during the EMG study. However, because of inertial forces not being considered, predicted shoulder function was generally symmetrical for the elevation and lowering phases of the activity. In contrast, measured muscle activation, while showing this symmetry also showed the effects of inertial forces present in the physiological system. As a function of the activity frequency, inertial forces on the body could be reduced to zero if activity analysis was for static body positions. Similarly, the effects could be assumed insignificant if the activity was performed at a slow frequency.

Based on the correlation between predicted and measured muscle activation, in addition

to the agreement between predicted joint compressive loads to those of previous studies, the predictions of physiological joint function by the shoulder model for static or quasi static abduction can be assumed realistic.

6.3.5.3 Flexion

Physiologically, arm elevation in either the sagittal or frontal planes is similar. As a consequence, the review and discussion of the results achieved for flexion highlight the differences from the abduction results as opposed to restating points that have already been discussed.

Figures 6.34 and 6.35 show the measured EMG and predicted muscle activation for flexion with a 2 kg hand load respectively. The model results were determined without the constraint of joint stability. Figure 6.34 also includes the average sagittal plane humeral elevation angle in degrees for the EMG study.

Increased EMG muscle activation over the baseline EMG levels were again measured in all of the shoulder muscles included in this study. Of these muscles, triceps and latissimus dorsi were the least activated. For deltoid, the anterior and posterior sections were more and less activated, respectively, than the middle section. Anterior deltoid reached a maximum of approximately 0.65 times its maximum contraction EMG level. Supraspinatus, infraspinatus and subscapularis were all similarly activated to approximately 0.5 times their maximum voluntary contraction level. Of these three muscles, subscapularis is the most activated early in the cycle and least activated for the majority of the remaining 60 % of the cycle. Maximum EMG levels in most of the muscles corresponded to 60 degrees of humeral elevation during the arm elevating phase.

Muscle activation was also predicted in all of the muscles included in the EMG study except latissimus dorsi. Activation of pectoralis major was again limited to its clavicular section only. For the majority of the flexion cycle, anterior deltoid activation was greater and posterior deltoid less than middle deltoid activation. Supraspinatus, infraspinatus and subscapularis were again relatively evenly activated with supraspinatus being the most and subscapularis the least activated for the majority of the cycle.

Figure 6.36a contains the average shoulder moments and humeral frontal plane elevation angle calculated for the motion analysis study. The glenohumeral joint moment M_{y_0} reached approximately -17 Nm.

The calculated humeral elevation angles determined for the two studies were both approximately equal to 90 degrees.

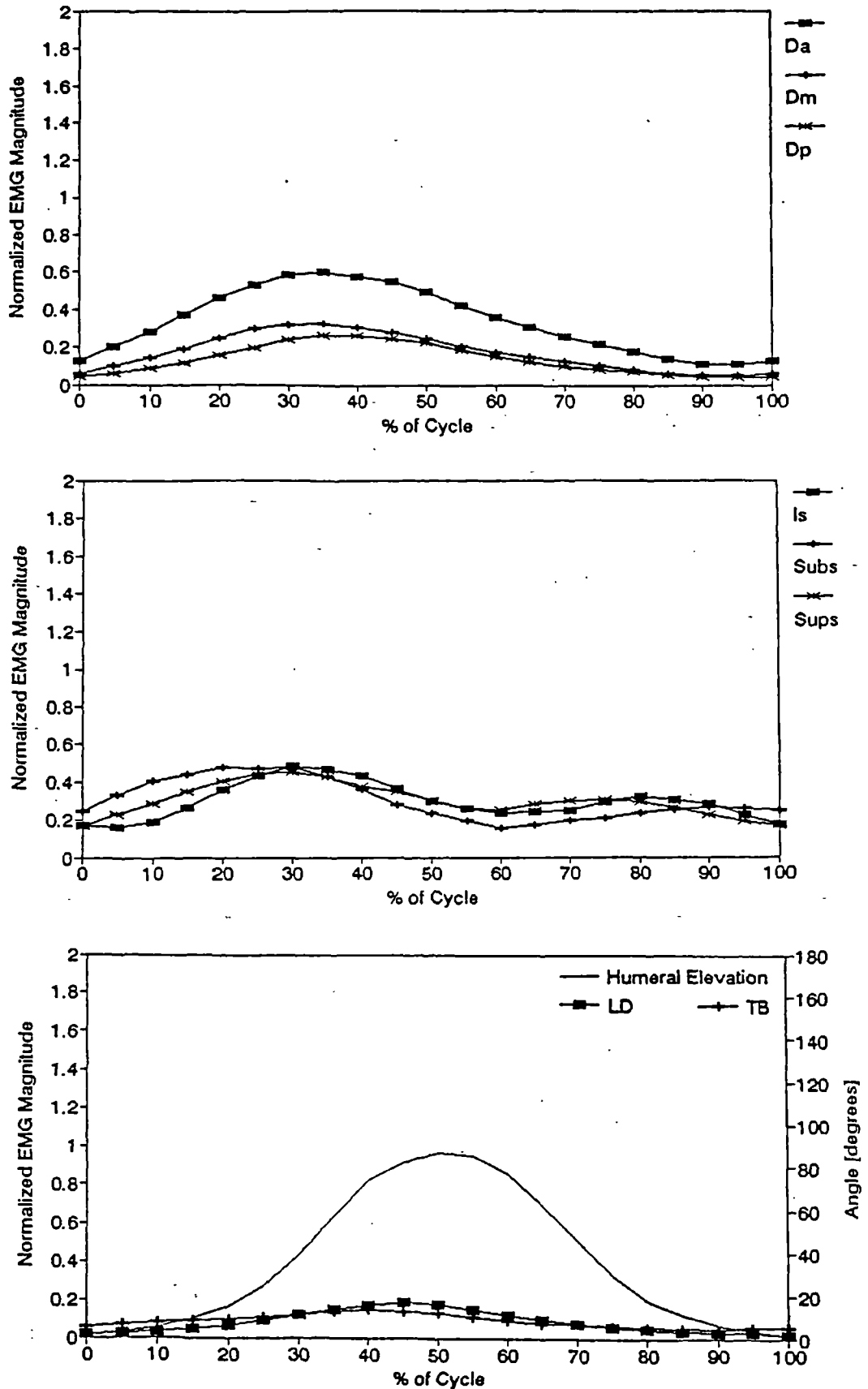


Figure 6.34 Measured EMG muscle activation for anterior, middle and posterior deltoid (Da, Dm, Dp), infraspinatus (Is), subscapularis (Subs), supraspinatus (Sups), latissimus dorsi (LD) and triceps (TB) for flexion with a 2 kg hand load.

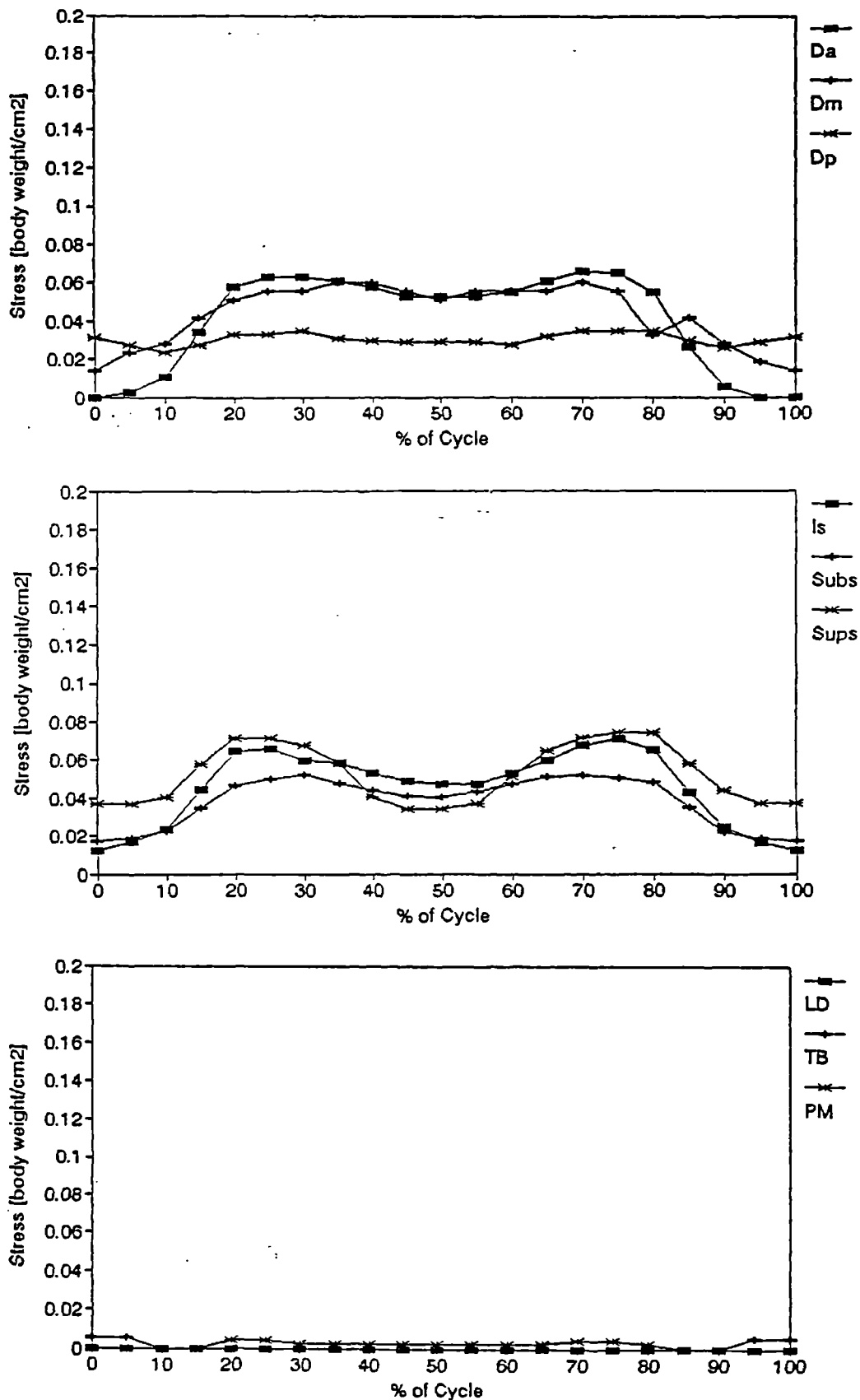


Figure 6.35 Average predicted muscle activation for anterior, middle and posterior deltoid (Da, Dm, Dp), infraspinatus (Is), subscapularis (Subs), supraspinatus (Sups), latissimus dorsi (LD), pectoralis major (PM) and triceps brachia (TB) during flexion with a 2 kg hand load.

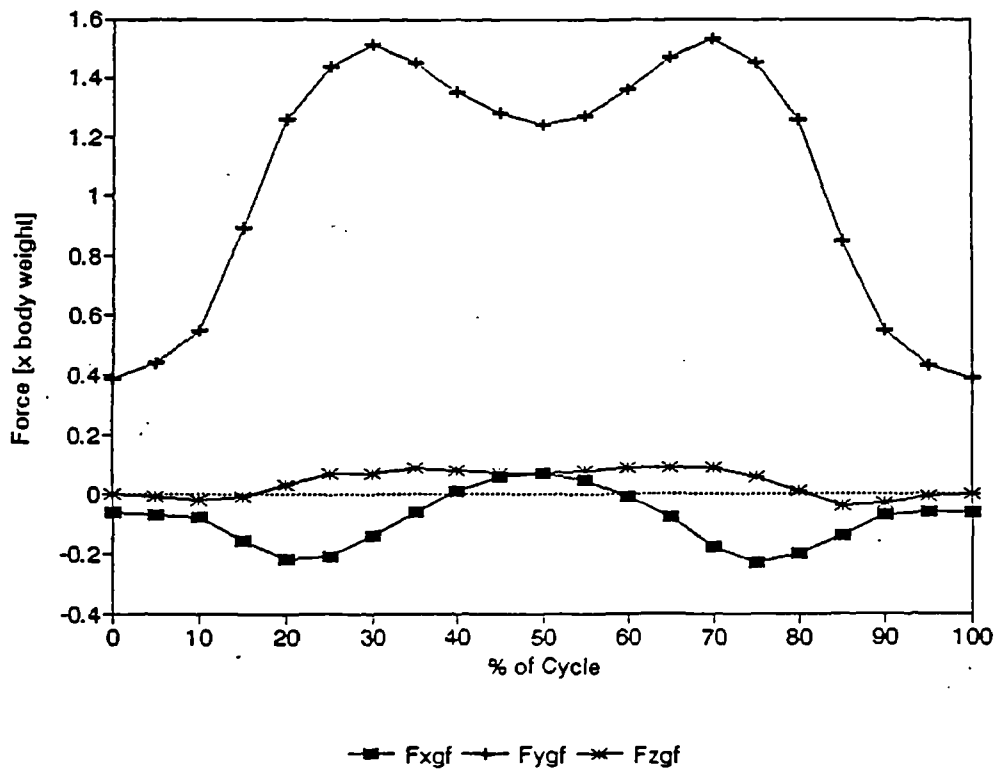
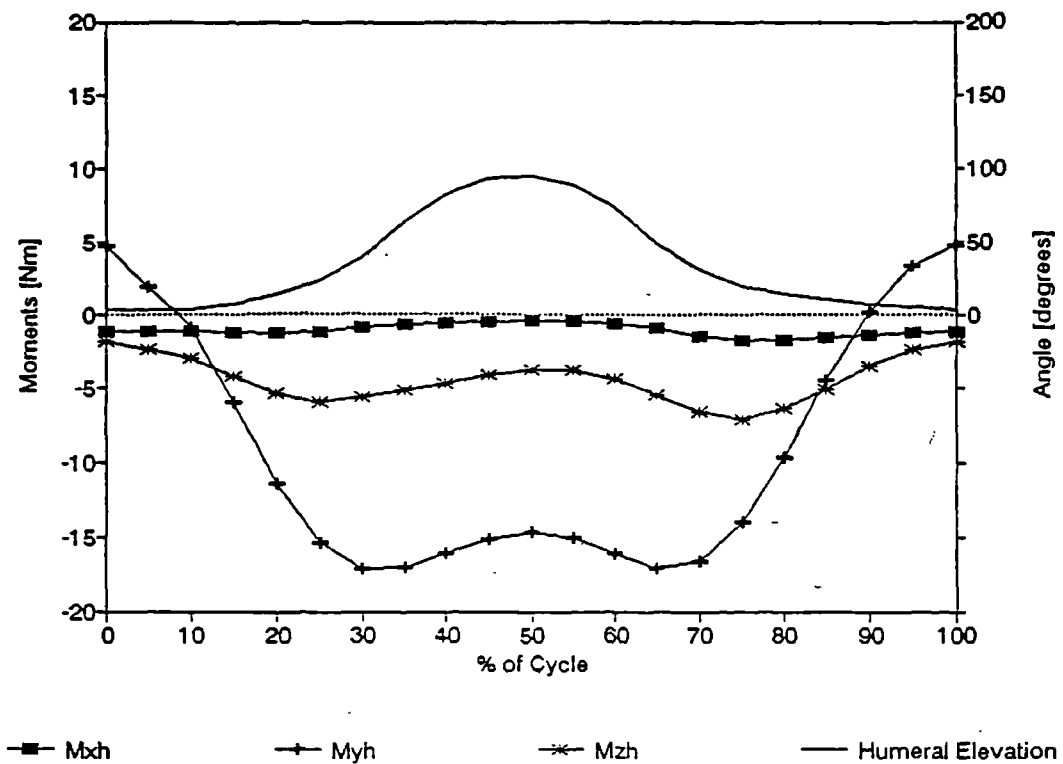


Figure 6.36 Average glenohumeral joint moment due to external loading, and elbow flexion angle during flexion with a 2 kg hand load (a, top). Average glenohumeral joint contact forces for flexion with a 2 kg hand load (b, bottom).

Figure 6.36b contains the predicted glenohumeral joint contact forces normalized with respect to body weight. The joint compressive force, $F_{y_{gb}}$, reached a maximum of over 1.4 times body weight (a range of 1.4 - 2.0 times body weight was observed for the five subjects) with the anterior, $F_{z_{gf}}$ and superior, $-F_{x_{gf}}$ shear forces in comparison, reaching only approximately 0.1 and 0.2 times body weight respectively.

As a result of the relatively small shear forces, imposing the constraint of joint stability on muscle force optimization produced no significant changes in muscle activation.

Anterior deltoid and supraspinatus are well situated to act as prime effectors during this activity. It is not surprising that their activation levels were found to be high in both EMG and predicted muscle activation. The predicted and measured muscle activation are consistent with those measured by Inman et al (1944). In their study, no distinction was made between the parts of deltoid. Pectoralis major activation was determined however and being closely related physiologically to anterior deltoid, gives an indication of possible anterior deltoid activation. They found the clavicular head of pectoralis major to be active during flexion where it was not during abduction. This correlates with the increased anterior deltoid and pectoralis major (clavicular head) activation observed in this study for flexion over abduction.

The role of infraspinatus and subscapularis in this activity, similar to that found for abduction is less clear. With generally similar activation levels both measured and predicted, the function of these muscles during this activity must be related to joint moment balance. Increased subscapularis and decreased infraspinatus EMG activation measured early in the cycle was not found in the predicted activation. Activation levels during flexion reported by Inman et al (1944) and Saha (1973) also do not show this relationship. In fact both of these studies reported results similar to those predicted in this study. The predicted subscapularis activation over the majority of the remaining cycle is similar to that measured in the EMG study. With respect to the cause of this discrepancy, two facts must be considered. Subscapularis, being well placed to increase joint compressive forces while not increasing joint shearing forces, may be more active early in the cycle as a means to improve overall joint stability. In contrast the absence of inertial forces in the model may also play a role in this observed discrepancy. Whatever the cause, the effect appears to be restricted to the early phase of the flexion activity cycle.

Very little humeral rotation accompanied flexion during the motion analysis study. This is evidenced by the M_{y_h} joint moment, which is significantly larger than either of the other two joint moments. More interesting is the fact that the maximum M_h joint moment occurs at approximately 60 degrees of humeral elevation. At this humeral elevation angle, with a

slightly flexed forearm, the hand would be level with the shoulder. The perpendicular moment arm of the hand load with respect to the shoulder and therefore the moment generating potential of the hand load would be greatest at this position.

Muscle activation predicted for flexion appears to be generally consistent to that measured during the EMG study and that reported in previous studies by Inman et al (1944) and Saha (1973). Because of the absence of inertial force consideration in predicting shoulder function, the results are constrained by the same limitations as the abduction results.

6.3.5.4 Push-up

The push-up activity is the first of the 3 athletic activities to be presented. Each of these activities is a complex three-dimensional high joint load activity, far beyond the scope of previous two-dimensional shoulder models.

Figures 6.37 and 6.38 show the measured EMG and predicted muscle activation for a flat hand push-up cycle. Model results were determined without the constraint of joint stability. Figure 6.37 also includes the average elbow flexion angle in degrees for the EMG study. Increased EMG muscle activation over the baseline EMG levels were measured in all of the shoulder muscles included in this study. Of these muscles, middle deltoid, posterior deltoid and latissimus dorsi were the least activated. Anterior deltoid and triceps were highly activated both early and late in the cycle but reached their maxima at 50 % of the activity cycle. Supraspinatus, infraspinatus and subscapularis, were all highly activated with subscapularis consistently the least activated of the three. Maximum infraspinatus and supraspinatus activation occurred during the second phase of the cycle.

Muscle activation was also predicted in all eight of the muscles which were included in the EMG study. All three fascicles of pectoralis major showed activation. Latissimus dorsi was again the least activated of the muscles. Anterior deltoid and triceps were again both highly active early and late in the cycle. Middle and posterior deltoid showed little activation. Considering supraspinatus, infraspinatus and subscapularis, subscapularis was again the least and supraspinatus the most activated. While this may be similar to EMG results, the shape of the curves representing muscle activation during the cycle show few similarities to the measured EMG results.

Figure 6.39a contains the average shoulder moments and elbow flexion angle for the motion analysis study. The majority of the total shoulder moment was about the Y_h axis. The moment about this axis, My_h , reached a maximum magnitude of approximately 70 Nm in the negative moment direction. Moments about the other humeral coordinate system axes were significantly less, reaching magnitudes of less than 10 Nm each.

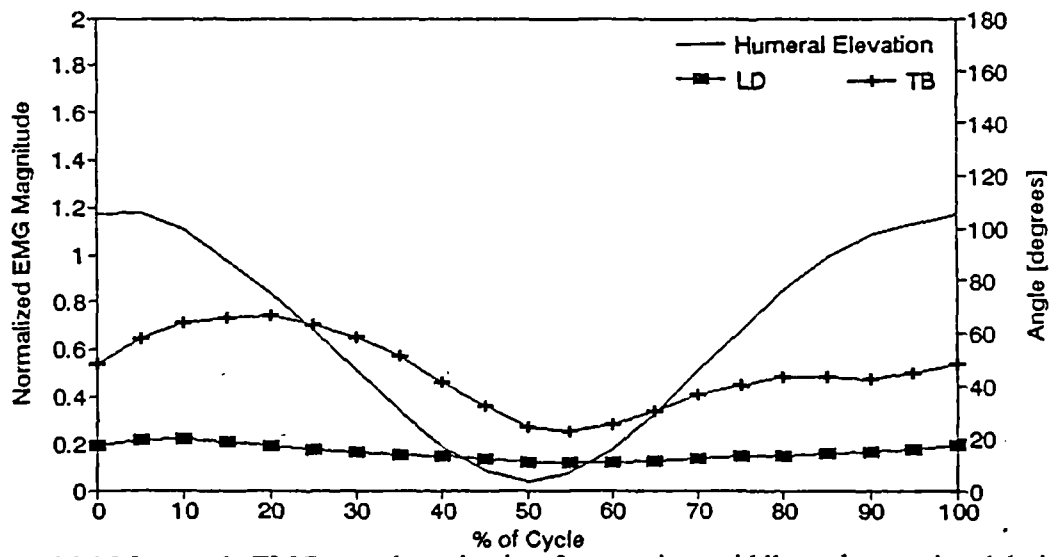
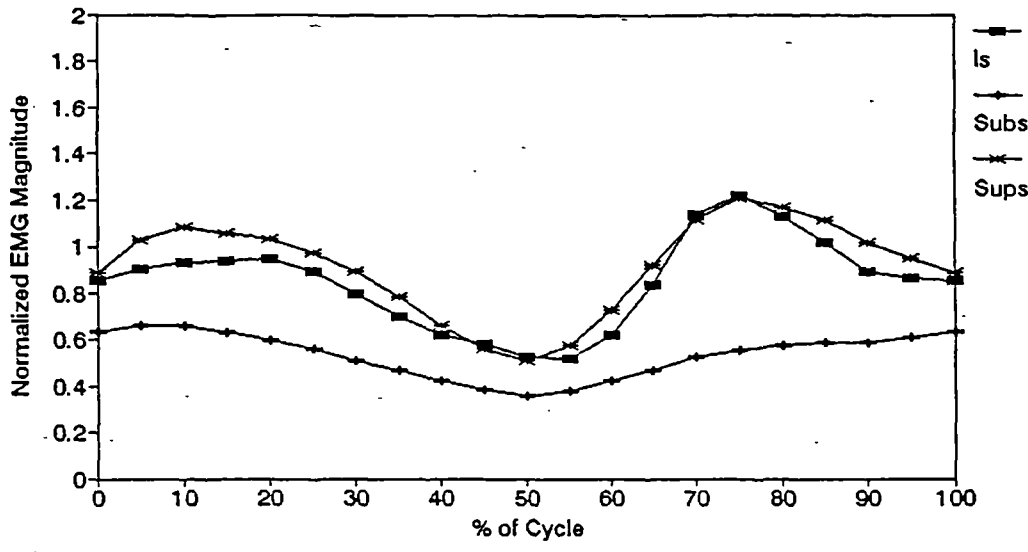
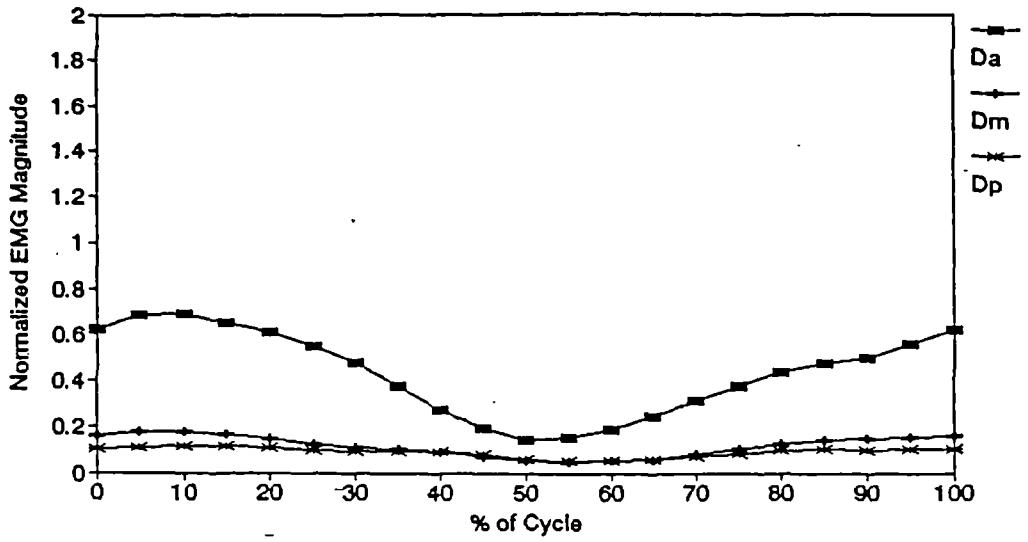


Figure 6.37 Measured EMG muscle activation for anterior, middle and posterior deltoid (Da, Dm, Dp), infraspinatus (Is), subscapularis (Subs), supraspinatus (Sups), latissimus dorsi (LD) and triceps (TB) for a push-up.

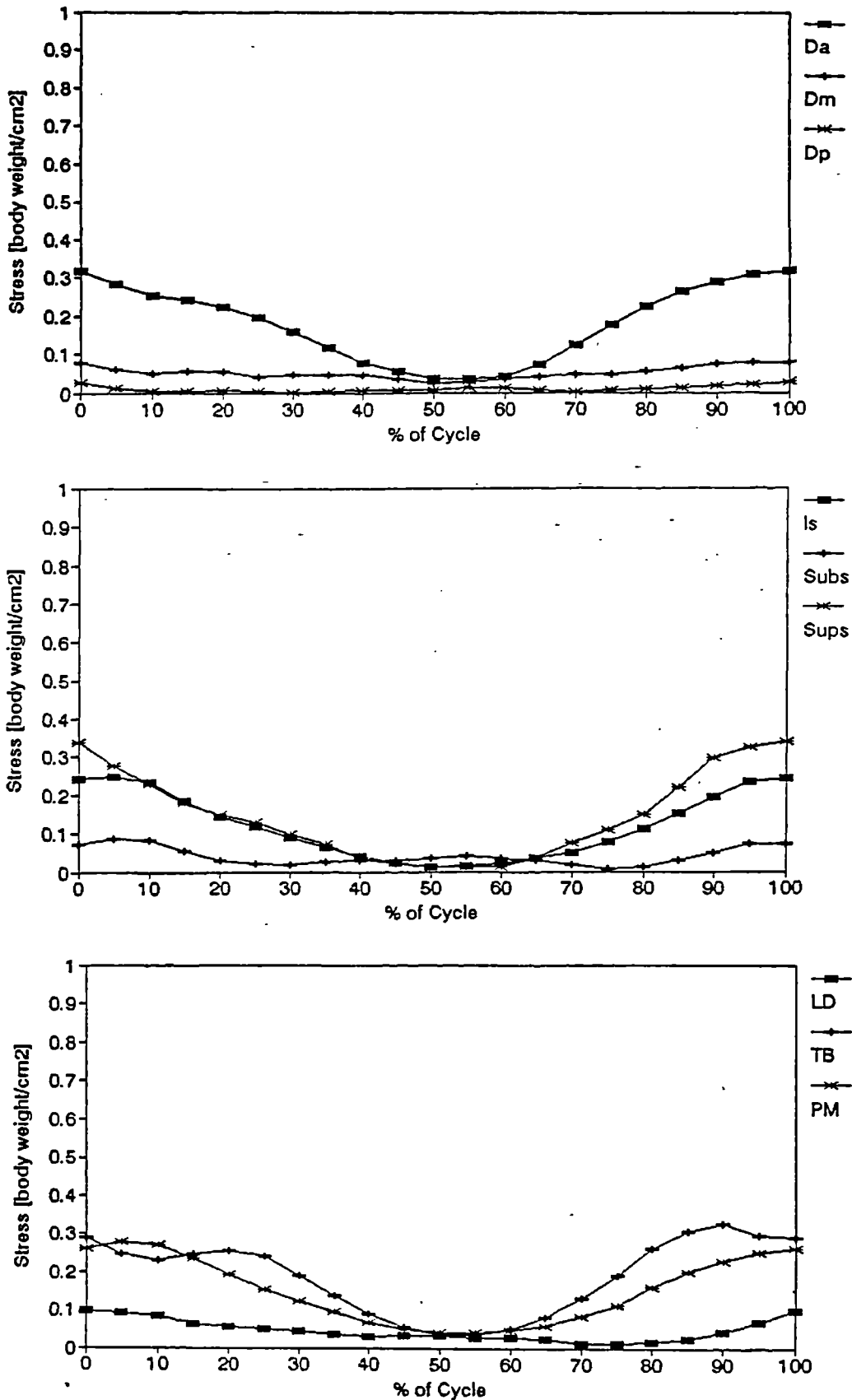


Figure 6.38 Average predicted muscle activation for anterior, middle and posterior deltoid (Da, Dm, Dp), infraspinatus (Is), subscapularis (Subs), supraspinatus (Sups), latissimus dorsi (LD), pectoralis major (PM) and triceps brachia (TB) during a push-up.

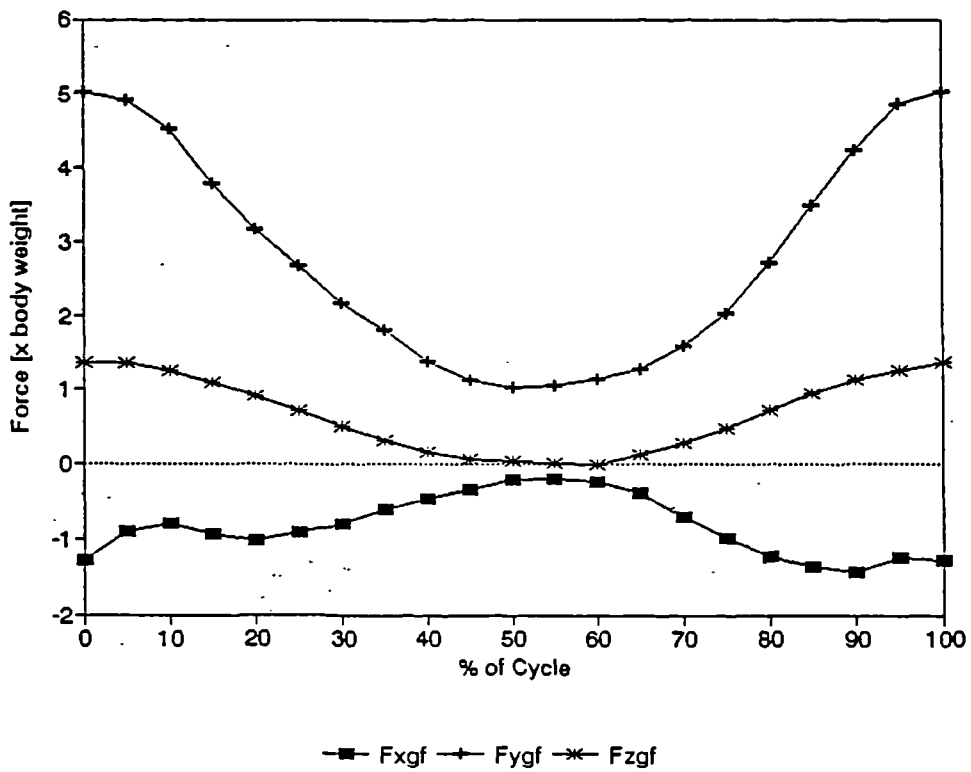
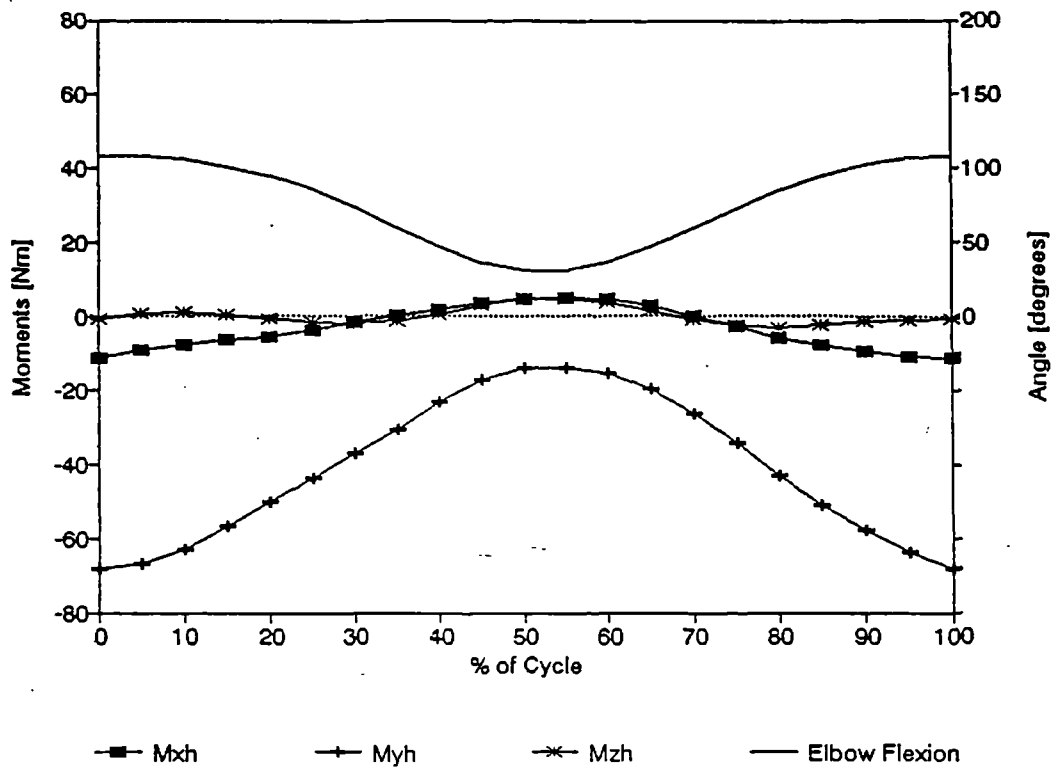


Figure 6.39 Average glenohumeral joint moment due to external loading and elbow flexion angle during a push-up (a, top). Average glenohumeral joint contact forces during a push-up (b, bottom).

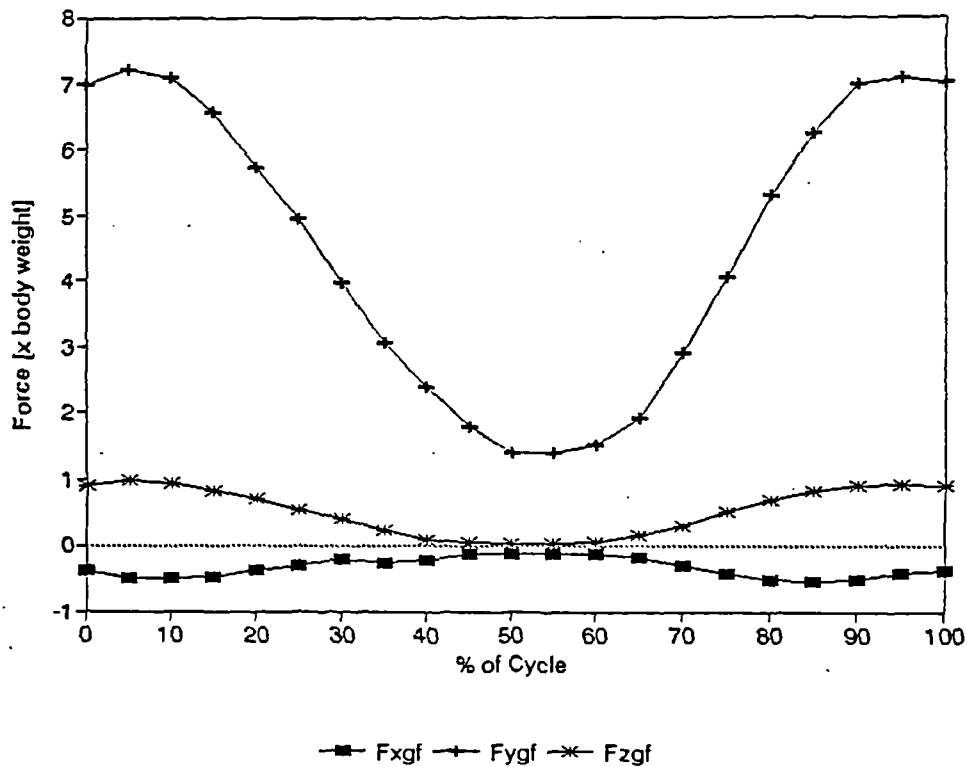
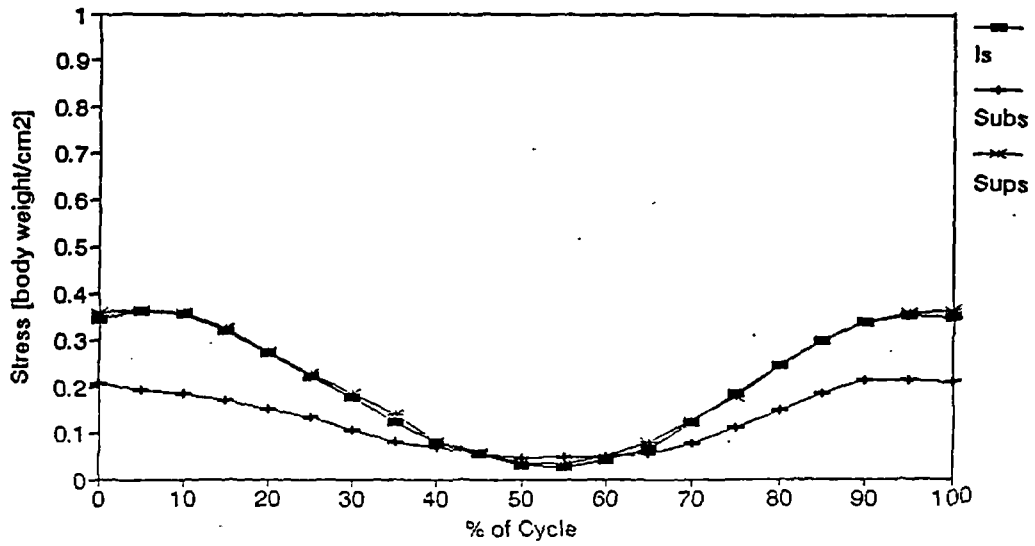


Figure 6.40 Muscle activation predicted using the joint stability constraint for infraspinatus (Is), subscapularis (subs) and supraspinatus (Sups) during a push-up (a, top). The corresponding average glenohumeral joint contact forces (b, bottom).

Figure 6.39b contains the predicted glenohumeral joint contact forces normalized with respect to body weight. Maximum joint compressive force, $F_{y_{gb}}$ was calculated at over 5 times body weight (a range of 3.0 - 7.5 times body weight was observed for the five subjects). Shear forces in the superior, $-F_{x_{gf}}$ and anterior, $F_{z_{gf}}$ directions attained maximum magnitudes over 1 times body weight each.

Figure 6.40a shows predicted infraspinatus, subscapularis and supraspinatus activation when the joint stability constraint was included in the muscle optimization. Similar to the measured EMG muscle activation, all three muscles are calculated to be highly active, with subscapularis consistently the least of the three. The curves representing muscle activation during the cycle appear similar to those of the EMG results. Apart from these three muscles, anterior deltoid was the only other muscle significantly affected by the inclusion of a joint stability constraint. With stability, its activation level was reduced by approximately 50 % from the results achieved without stability.

The compressive joint force increased to over 7 times body weight with the inclusion of the joint stability constraint (figure 6.40b). In addition to this, the shear force acting in the superior direction was reduced by approximately 50 %. This increase in compressive joint force and decrease in joint shearing force would both tend to increase the stability of the glenohumeral joint. Orientation of this maximum predicted joint contact force with respect to the scapula and humerus is shown in figure 6.41a and figure 6.41b. The force on the scapula is approximately parallel to the scapular plane formed by the acromioclavicular joint, inferior angle and medial spine root. With respect to the humerus, the force is directed along a line approximately parallel to the anatomical neck of the humerus. As a result, in both bones, the force is applied in a direction of high physiological strength.

Muscle activation predicted both with and without stability for deltoid, triceps and latissimus dorsi appear consistent with the results of the EMG study and the qualitative muscle activations stated by Luttgens & Wells (1982) for transverse plane flexion.. In contrast infraspinatus, subscapularis and supraspinatus activation predicted without the joint stability constraint do not appear consistent with the EMG results. When joint stability was imposed, the resulting predicted activation for these muscles was more consistent with the EMG results. The role of these three muscles as active stabilizers (section 2.2) is not well understood, however, the difference between the predicted muscle activations (with and without stability) indicate that for this activity, they all play a role in maintaining joint stability, as their EMG activation indicates more activity than is required to balance joint moments.

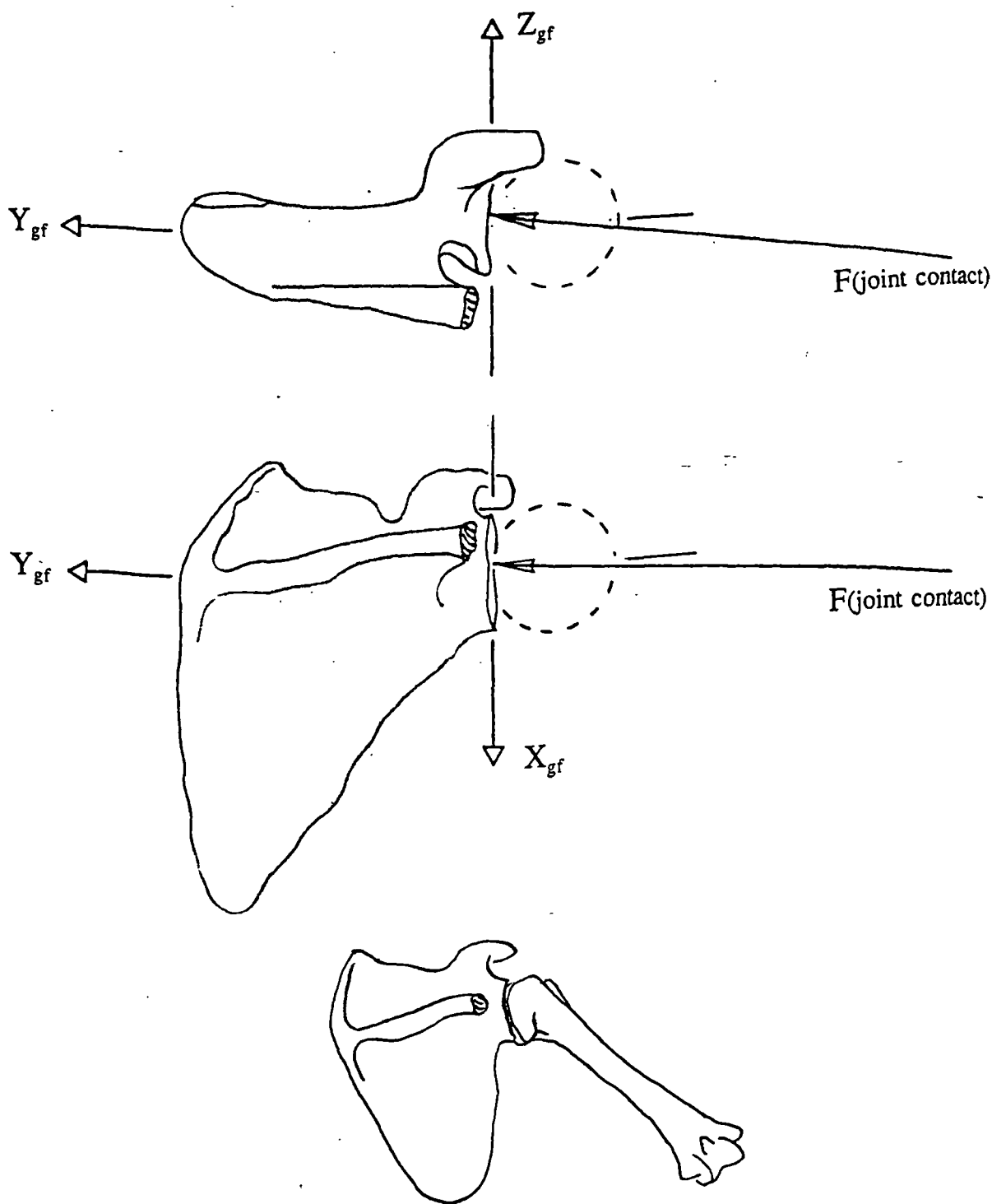


Figure 6.41a Superior and posterior orthogonal projections of the scapula showing the maximum joint contact force direction, $F(\text{joint contact})$, calculated while using the joint stability constraint for the push-up activity (top and middle respectively). The corresponding total joint contact force magnitude is 7 times body weight. The distal acromion has been removed for clarity and the humeral head sphere is shown schematically as a dotted line. The corresponding relative positioning of the scapula and humerus during this point of the push-up cycle is shown (bottom).

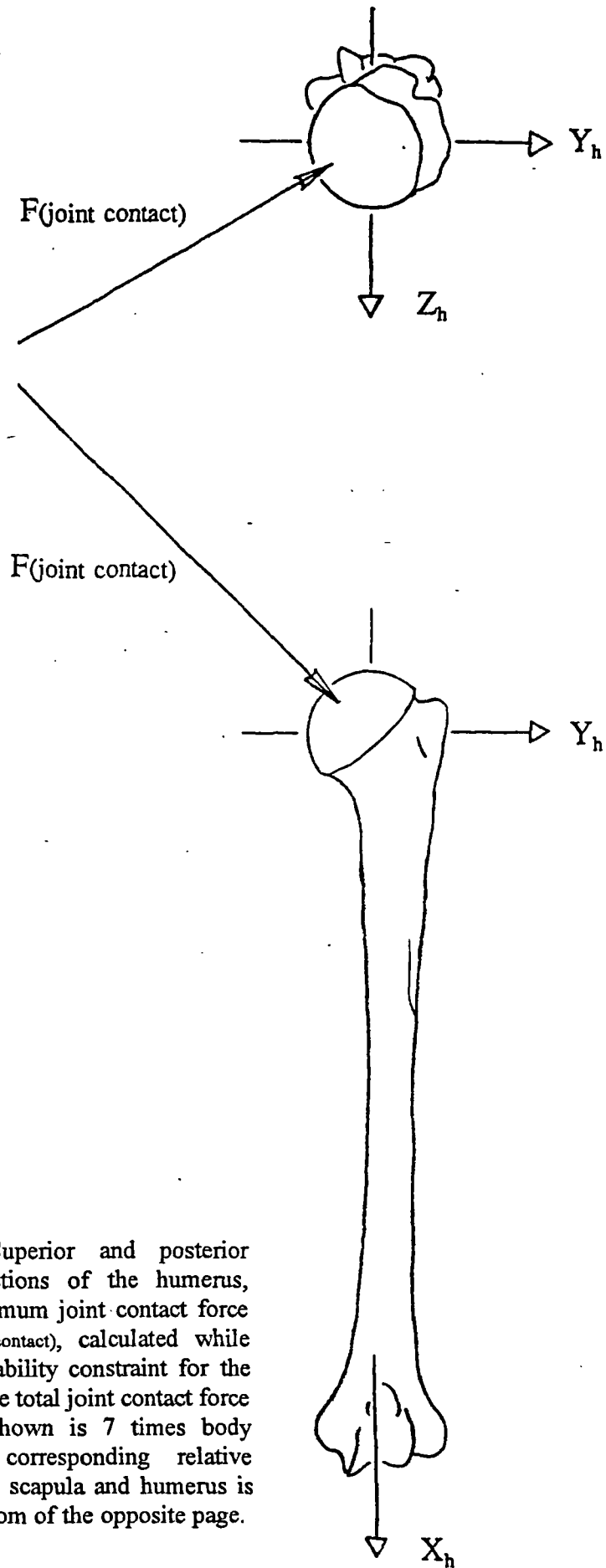


Figure 6.41b Superior and posterior orthogonal projections of the humerus, showing the maximum joint contact force direction, $F(\text{joint contact})$, calculated while using the joint stability constraint for the push-up cycle. The total joint contact force for the instant shown is 7 times body weight. The corresponding relative positioning of the scapula and humerus is shown on the bottom of the opposite page.

Overall, the results achieved with the shoulder model appear to be in good agreement with muscle activation measured during the EMG study. For muscles acting as prime motion generators such as triceps, latissimus dorsi and deltoid, the predicted activation appears consistent with the measured muscle activation. For infraspinatus, subscapularis and supraspinatus, the activation predicted with the constraint of stability appear more consistent than those achieved without the constraint of stability. The role of these three muscles in improving joint stability while not well understood is clearly indicated in the results obtained for this activity.

6.3.5.5 Press-up

Figures 6.42 and 6.43 show the measured EMG and predicted muscle activation for a vertical press-up cycle. Model results were determined without the constraint of joint stability. Figure 6.43 also includes the average elbow flexion angle in degrees for the EMG study. Increased EMG muscle activation over the baseline EMG levels were again measured in all of the shoulder muscles included in this study. Of these muscles, the three sections of deltoid were the least active. Triceps and latissimus dorsi were both highly activated both early and late in the cycle but reached their maxima in the first phase of the activity cycle. Supraspinatus, infraspinatus and subscapularis, were all highly activated with infraspinatus the least active of the three. Subscapularis was more active than infraspinatus both early and late in the press-up cycle.

Muscle activation was also predicted in all eight of the muscles included in the EMG study. Middle deltoid was the only deltoid section to be predicted as being highly active. In contrast, subscapularis was predicted to have only a minimal activity level. Both of these activity levels are not consistent with the measured EMG magnitudes for these muscles. The remaining predicted muscle activations appear to be consistent with muscle activation measured in the EMG study.

Figure 6.44a contains the average shoulder moments and elbow flexion angle for the motion analysis study. The majority of the total shoulder moment was again about the Y_h axis. The moment about this axis, M_{y_h} , reached a maximum magnitude of over 60 Nm in the negative moment direction. Moments about the other humeral coordinate system axes were significantly less, reaching magnitudes of less than 20 Nm each.

There is a difference of approximately 35 degrees between the minimum elbow flexion angles in the EMG and motion analysis studies. This was expected as the subjects were asked to avoid fully extended elbow postures during the motion analysis study.

Figure 6.44b contains the predicted glenohumeral joint contact forces normalized with

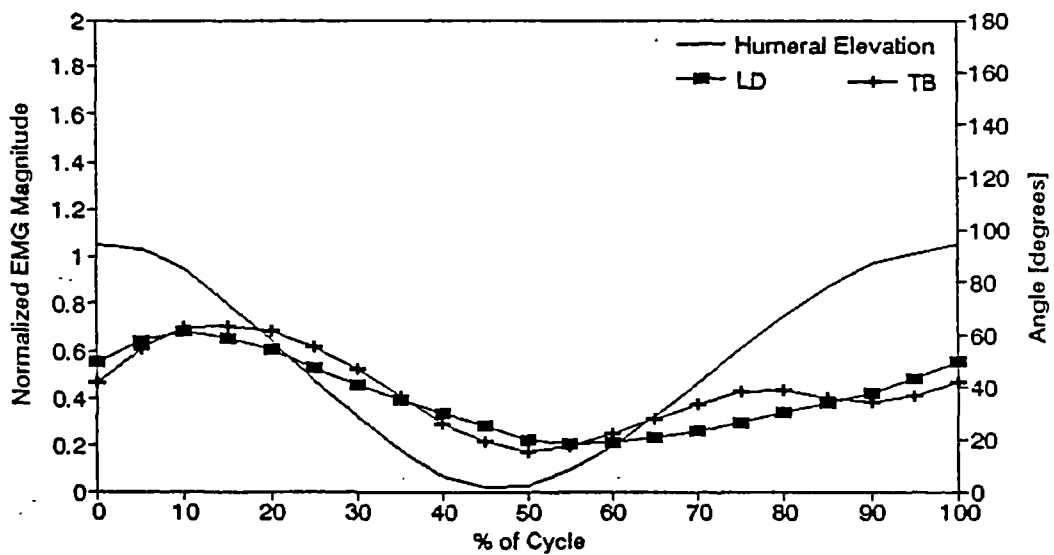
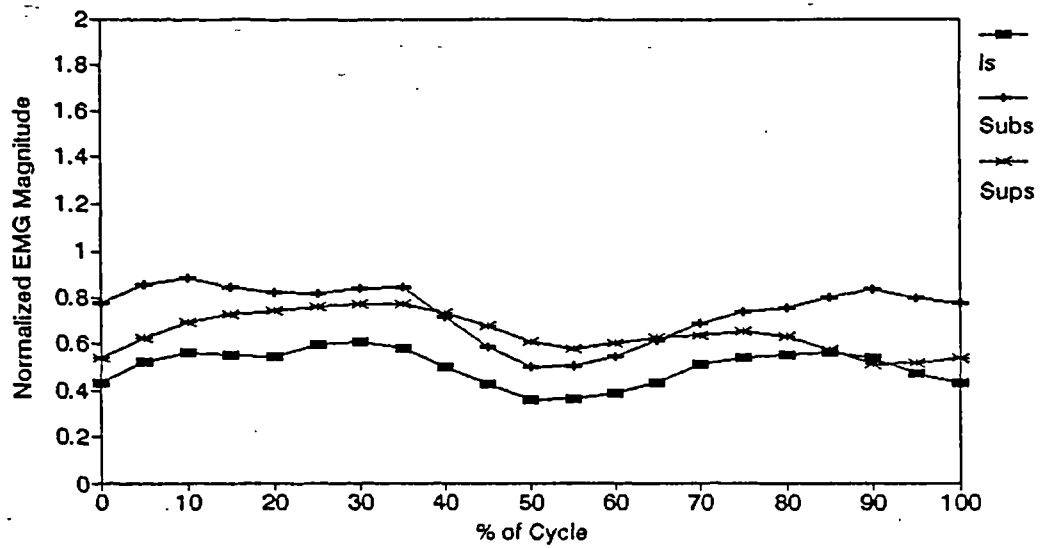
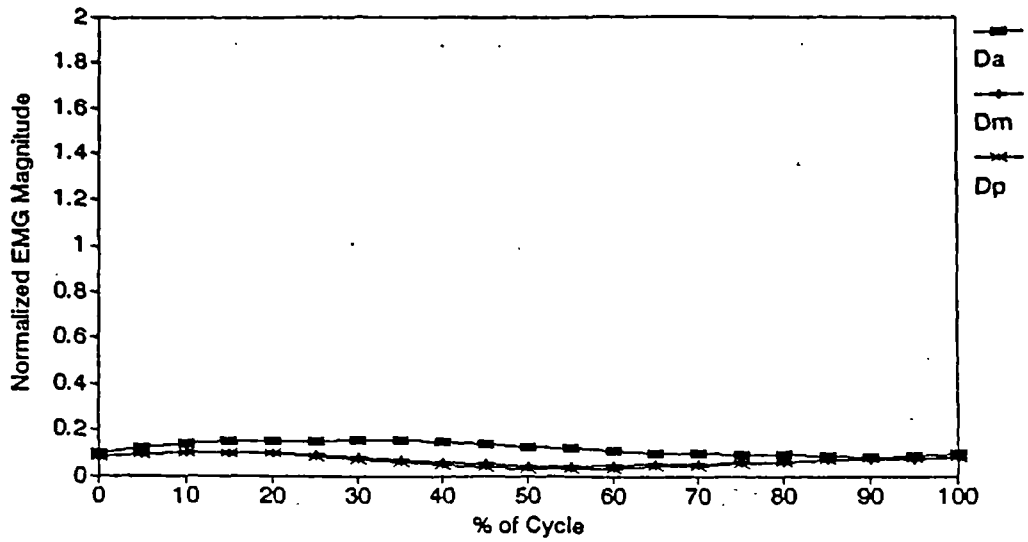


Figure 6.42 Measured EMG muscle activation for anterior, middle and posterior deltoid (Da, Dm, Dp), infraspinatus (Is), subscapularis (Subs), supraspinatus (Sups), latissimus dorsi (LD) and triceps (TB) for a press-up.

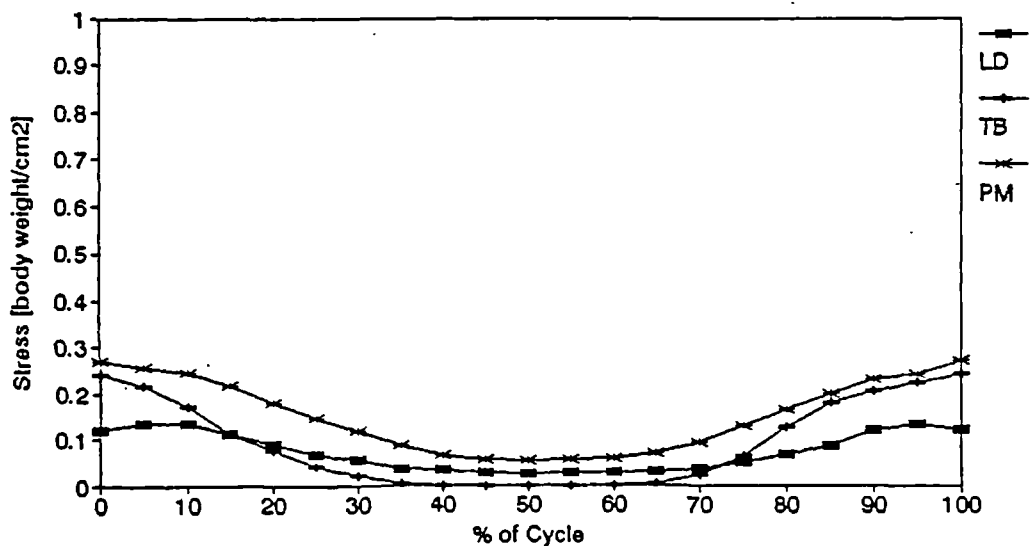
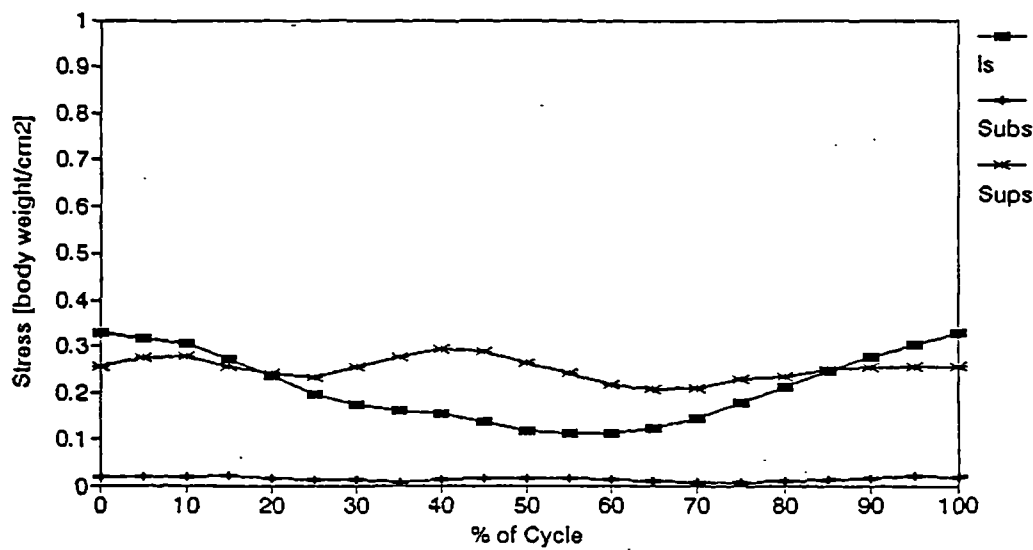
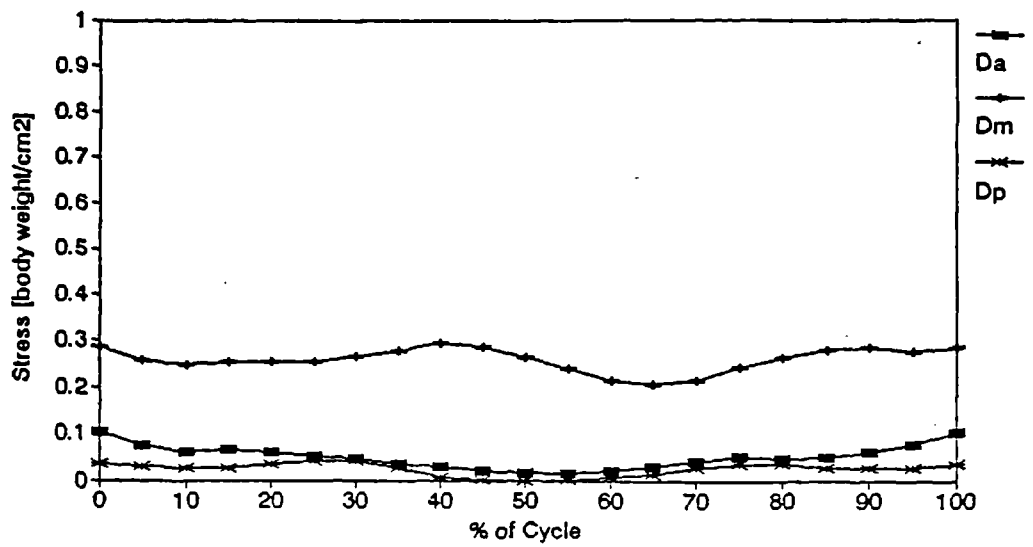


Figure 6.43 Average predicted muscle activation for anterior, middle and posterior deltoid (Da, Dm, Dp), infraspinatus (Is), subscapularis (Subs), supraspinatus (Sups), latissimus dorsi (LD), pectoralis major (PM) and triceps brachia (TB) during a press-up.

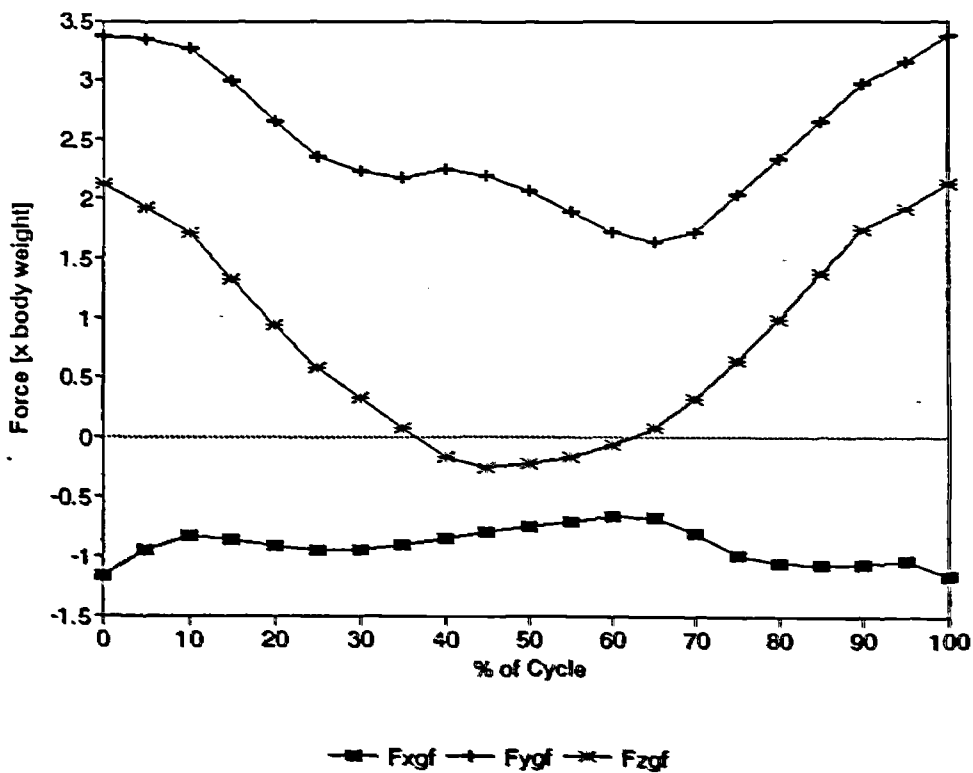
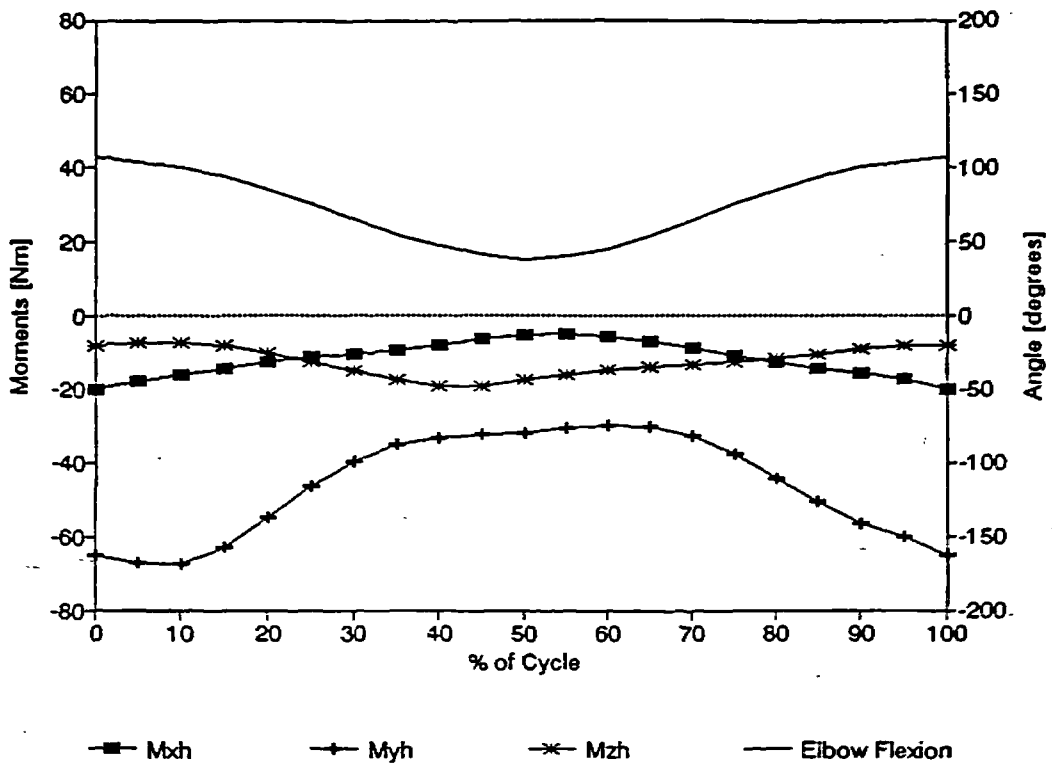


Figure 6.44 Average glenohumeral joint moment due to external loading, and elbow flexion angle during a press-up (a, top). Average glenohumeral joint contact forces during a press-up (b, bottom).

respect to body weight. Maximum joint compressive force, $F_{y_{gf}}$, was calculated at over 3 times body weight (a range of 2.3 - 5.4 times body weight was observed for the five subjects). Shear forces in the superior, $-F_{x_{gf}}$ and anterior, $F_{z_{gf}}$ directions attained maximum magnitudes over 1 and 2 times body weight respectively.

Muscle activation predicted when using the constraint of joint stability altered some of the relative muscle activation levels but these still do not appear consistent with activation measured during the EMG study. Changes appear to be limited to early and late in the cycle where middle deltoid activation was reduced and infraspinatus and supraspinatus activity was increased. The joint compressive force was subsequently increased to over 4 times body weight with a corresponding reduction in shear force magnitudes to less than 1 times body weight in the superior-inferior and anterior-posterior directions.

Muscle activation predicted without stability for anterior and posterior deltoid, infraspinatus, supraspinatus, latissimus dorsi and triceps appear consistent with the results of the EMG study. In contrast, middle deltoid and subscapularis activation predicted both with and without the joint stability constraint do not appear consistent with the EMG results.

The source of this discrepancy is not fully understood but may be attributable to a combination of the hand grip spacing variation between the two studies and the lack of correction for pectoralis major wrapping around the thorax. With decreased hand grip spacing, more humeral internal rotation would be required in the motion analysis study. This may have altered the roles of pectoralis major and deltoid as prime motion generators between the two studies. With respect to pectoralis major wrapping around the thorax, the wrapping is minimal for abducted and flexed arm positions. With the arm extended as was the case in this activity, the muscle is extensively wrapped around the thorax. By not correcting the line of action for this, the muscle tends to adduct the arm in addition to flexing it from the extended position. For moment balance, another muscle would be required to counteract this non-physiological adduction moment. Middle deltoid would be well placed to provide this moment, resulting in its activity that was not consistent with the EMG study.

Overall, results achieved with the shoulder model while reasonably representative, do show inconsistencies when compared to the muscle activation measured during the EMG study. Whether as a result of experimental differences between the studies or the lack of correction for the wrapping of pectoralis major on the thorax the shoulder function predicted for this activity cannot be assumed to be physiologically correct. These differences however, do show the significant changes that can occur in shoulder function for subtle differences in either activity or anatomical details.

6.3.5.6 Chin-up

Figures 6.45 and 6.46 show the measured EMG and predicted muscle activation for a chin-up cycle. Model results were determined without the constraint of joint stability. Figure 6.46 also includes the average elbow flexion angle in degrees for the EMG study. Increased EMG muscle activation over the baseline EMG levels were again measured in all of the shoulder muscles included in this study. Middle and posterior deltoid activation reached their maxima at 40 % through the cycle. Posterior deltoid was more activated than middle deltoid and anterior deltoid activation was consistently low throughout the entire activity. Subscapularis, infraspinatus and supraspinatus were all highly active throughout the activity, with subscapularis the most active and supraspinatus the least active of the three. Latissimus dorsi activation reached a maximum at 45 % through the cycle.

Predicted muscle activation for the chin-up shows some similarities and some differences to the measured EMG muscle activation. All three sections of deltoid were predicted to be active, with the posterior more active than middle deltoid and both of these more active than anterior deltoid. Middle deltoid was most active during the middle 60 % of the activity. Predicted subscapularis activity was higher than supraspinatus activity and there was no predicted infraspinatus activity. Triceps was predicted to be consistently active throughout the activity. Latissimus dorsi activity, in contrast to measured EMG muscle activity, peaked at the cycle end points.

Figure 6.47a contains the average shoulder moments and elbow flexion angle for the motion analysis study. The majority of the total shoulder moment was again about the Y_h axis. The moment about this axis, My_h , reached a maximum of over 100 Nm. Moments about the other humeral coordinate system axes were less, reaching magnitudes of less than 30 Nm each. Examining the elbow flexion angle, it reaches a minimum value at approximately 60 % of the way through the chin-up cycle. This first 60 % of the cycle corresponds to the period of body elevation during the activity. The extended duration of this part of the cycle is an indicator of the extreme shoulder loads developed during this activity.

Figure 6.47b contains the predicted glenohumeral joint contact forces normalized with respect to body weight. Maximum joint compressive force, Fy_{gb} was calculated at over 4 times body weight (with a range of 3.1 to 4.9 times body weight between subjects). Shear forces in the superior, $-Fx_{gf}$ and posterior, $-Fz_{gf}$ directions attained maximum magnitudes under 1 body weight each. The maximum shear forces were predicted for the cycle mid point, which corresponds to the period of the minimum joint compressive force of just over 2 times body weight.

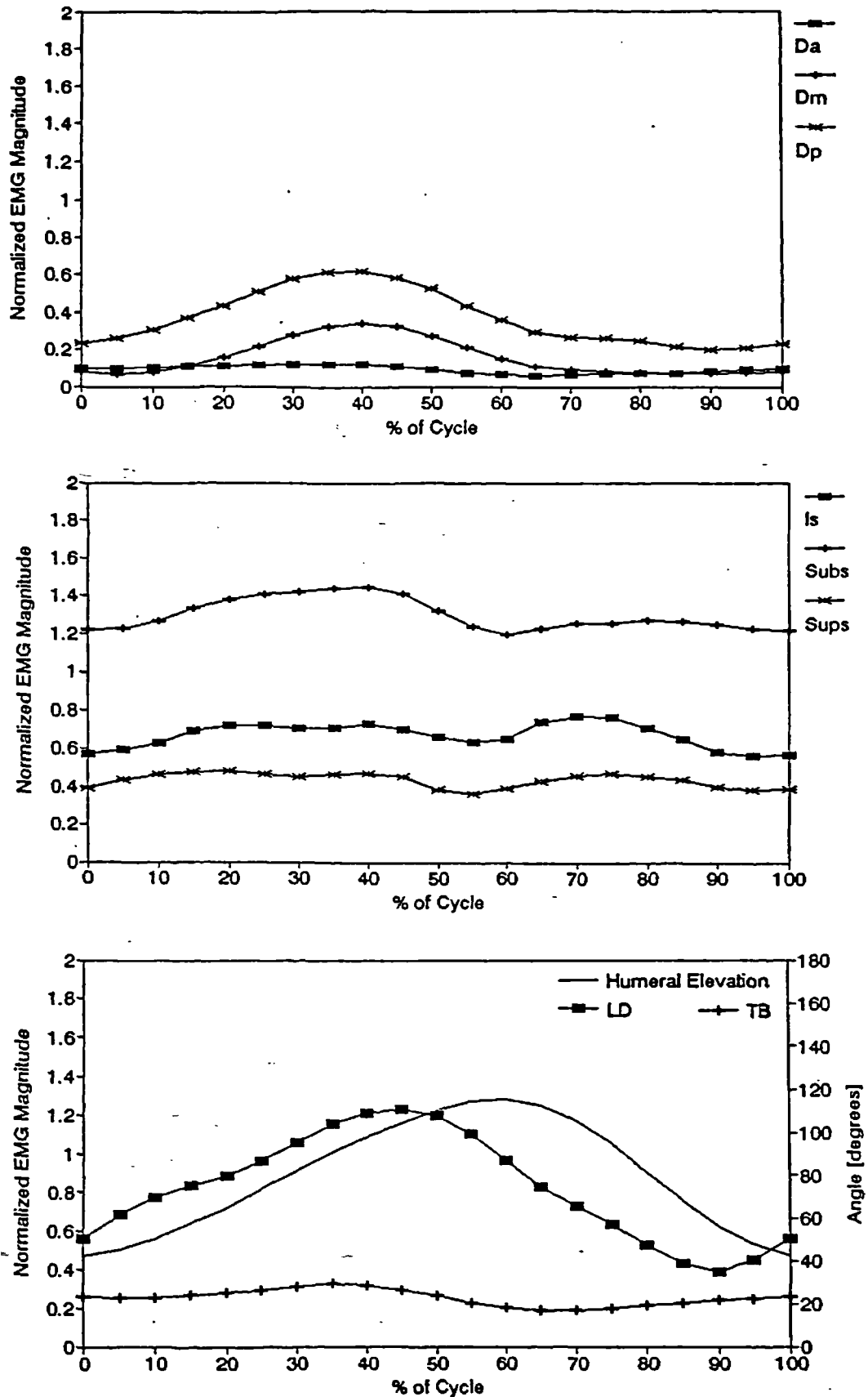


Figure 6.45 Measured EMG muscle activation for anterior, middle and posterior deltoid (Da, Dm, Dp), infraspinatus (Is), subscapularis (Subs), supraspinatus (Sup), latissimus dorsi (LD) and triceps (TB) for a chin-up.

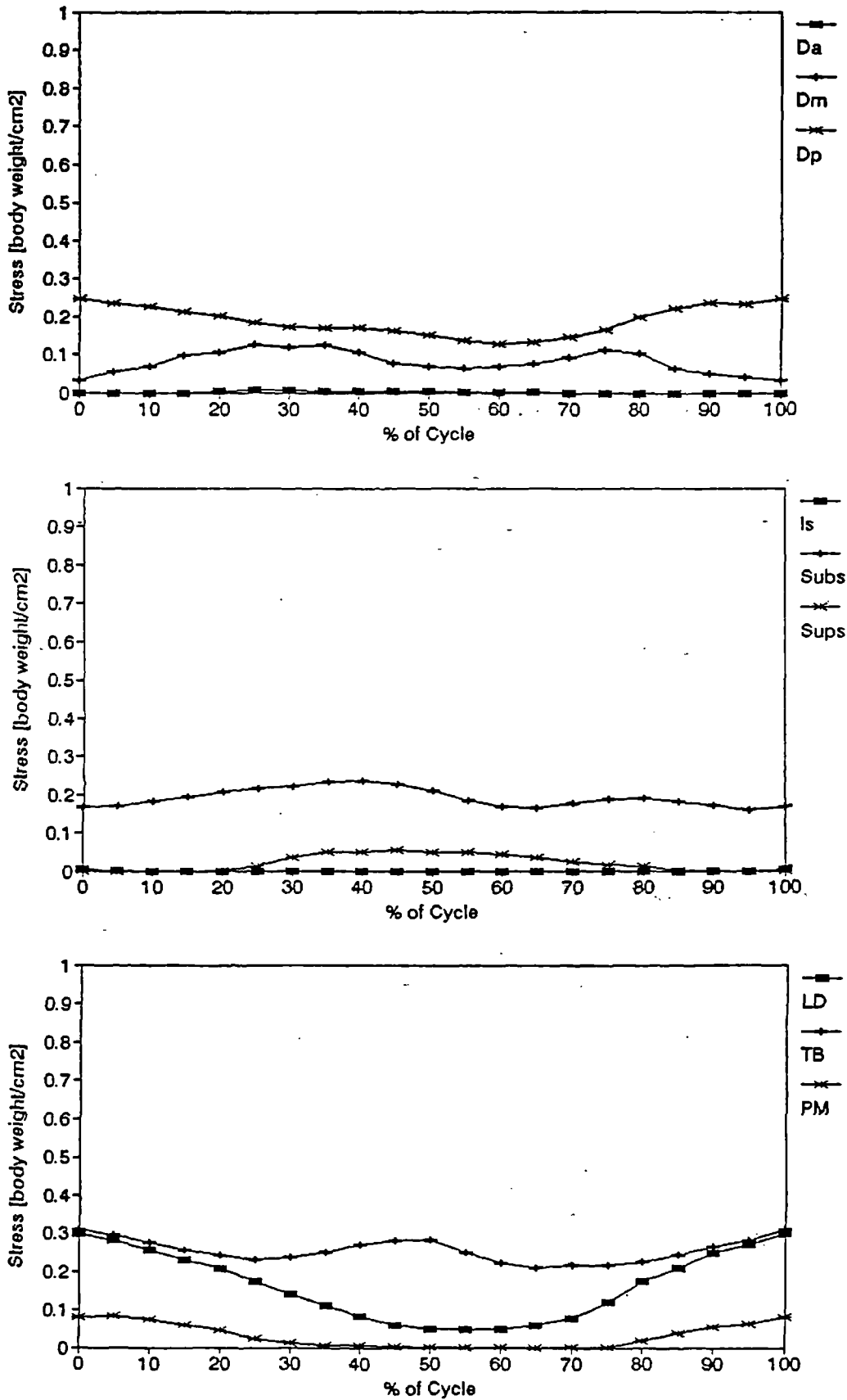


Figure 6.46 Average predicted muscle activation for anterior, middle and posterior deltoid (Da, Dm, Dp), infraspinatus (Is), subscapularis (Subs), supraspinatus (Sups), latissimus dorsi (LD), pectoralis major (PM) and triceps brachia (TB) during a chin-up.

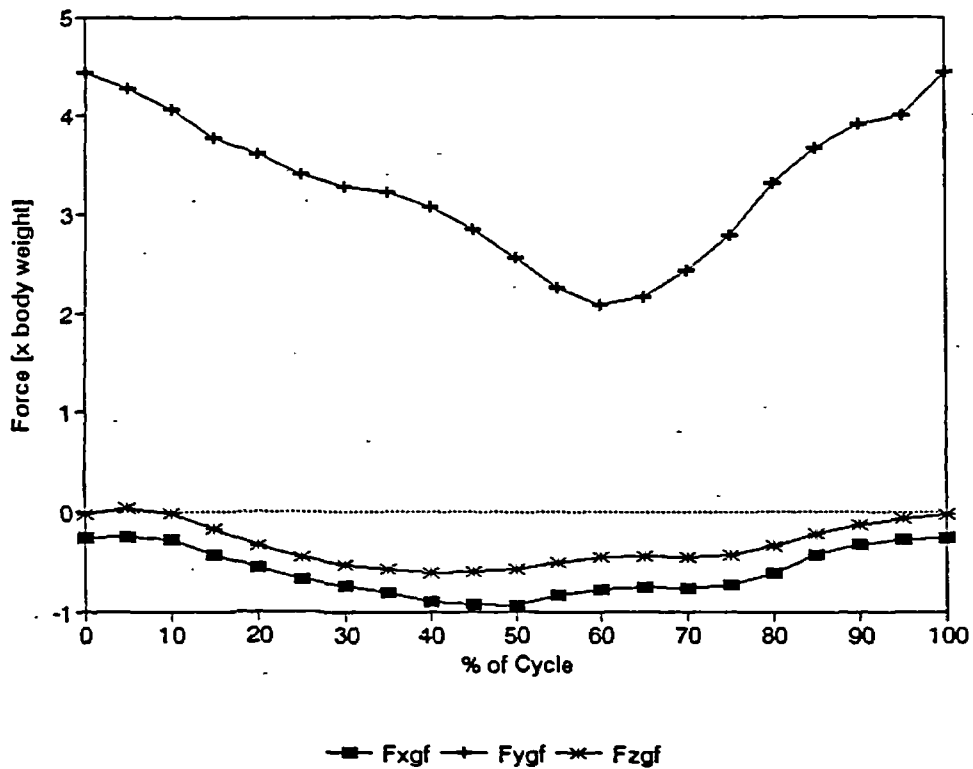
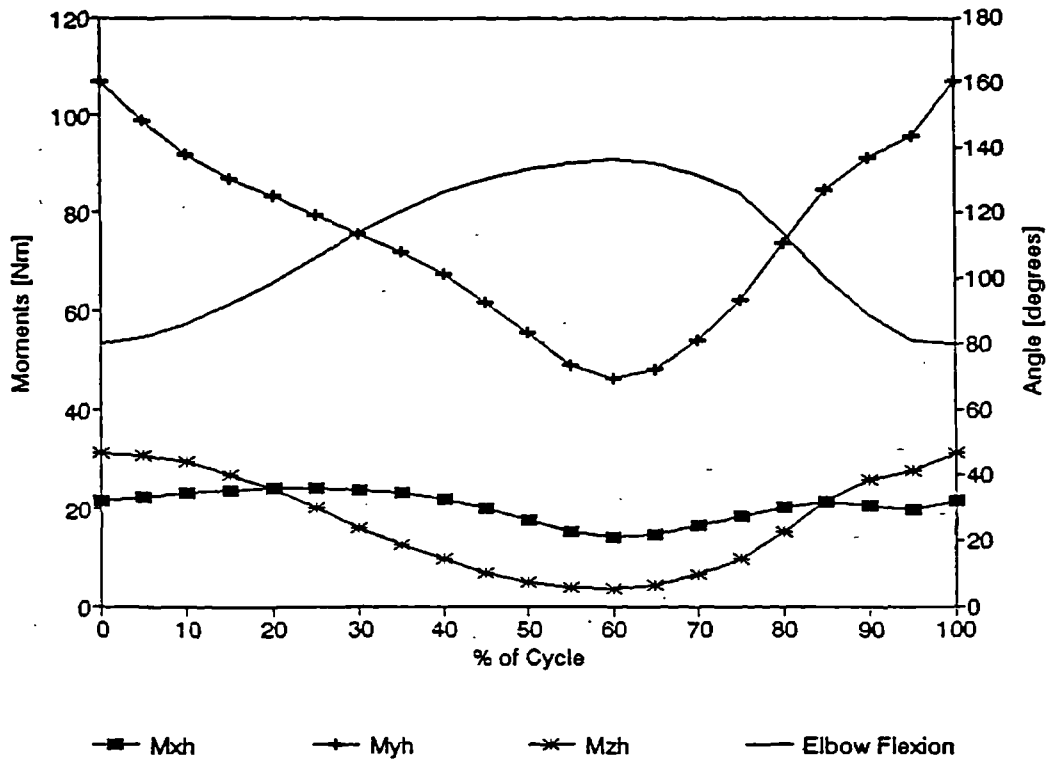


Figure 6.47 Average glenohumeral joint moment due to external loading, and elbow flexion angle during a chin-up (a, top). Average glenohumeral joint contact forces during a chin-up (b, bottom).

Muscle activation predicted when using the constraint of joint stability had little effect in predicted muscle activation except for in the region of 50 % through the cycle. With this constraint, predicted muscle activation for subscapularis, supraspinatus and infraspinatus all increased. The resulting predicted muscle activation appears more consistent with the muscle activation measured during the EMG study. The overall effect on the joint contact forces was to maintain joint compression at roughly over 4 times body weight throughout the activity.

Muscle activation predicted with stability for anterior, middle and posterior deltoid, and triceps all appear consistent with the results of the EMG study. In contrast infraspinatus, subscapularis and supraspinatus were predicted to be less active than a comparison to the EMG study results might indicate.

Triceps activity, predicted without joint stability, originally became very large at the cycle mid point. At the cycle mid point the elbow is fully flexed and the body is decelerating towards the hand grips. Triceps is well placed to provide the elbow moment required to generate this deceleration. In the predicted results, the triceps activity reflected this. Examining the measured triceps EMG activation, no evidence of an increase in activity at this point during the cycle was evident. Upon further examination, it was discovered that the elbow moment was produced by impingement of the forearm on the biceps muscle belly as opposed to triceps activity. Looking at the predicted triceps force for each subject, it was found that only a few frames of data for three of the five subjects contained the high hand loading generated by this impingement. These frames were removed, and data normalization repeated.

Of all the muscles included in this study, predicted latissimus dorsi activation for this activity is the most inconsistent with respect to the measured EMG muscle activation. During the cycle where measured activation increased, predicted activation was decreasing and where measured activation decreased, predicted activation increased. There are possibly many reasons for this discrepancy. First and foremost, latissimus dorsi function affects not only the humerus but also all of the other hard tissues of the shoulder. During a chin-up, latissimus dorsi is well placed to control elevation of the clavicle and scapula and as this function would be required in a chin-up, it would be expected to be active to provide this control. In this model this aspect of latissimus dorsi function is not considered and as such its predicted activation does not include this aspect of its function.

Overall, results achieved with the shoulder model for the chin-up activity were consistent with measured EMG muscle activation if model limitations were taken into account. Shoulder function involves muscle action across all of the shoulder joints. With this model, by only considering the glenohumeral joint, muscle function across the others is lost. For

some activities, the ramifications of this simplification are negligible, but for an activity as demanding as a chin-up, they can become significant. The inconsistency of predicted latissimus dorsi activity is only one such example resulting from this simplification.

7.0 SUMMARY

The shoulder is one of the most complex and mobile joints of the human body. Functionally, it plays a key role in many upper limb activities required during daily living. As an integral part of the upper limb and its function, few would argue the importance of this joint or the consequences of its dysfunction on quality of life. It is then surprising to realize the relatively small number of studies that have researched detailed shoulder function.

Early shoulder research was generally limited to studying function during flexion and abduction. This was a consequence of the difficulties inherent in the complex three-dimensional nature of the joint. By limiting activities to simple two-dimensional ones, the joint could be studied two-dimensionally, simplifying analysis and interpretation. While functional information from these activities did provide some limited insight into joint function, clearly for a joint as mobile and inherently unstable as the shoulder, they provided little information into the true functional limits of the joint.

The deficiencies of early shoulder research have been recognised by more recent investigators. This has led to the use of three-dimensional models for investigating shoulder function. To date, these studies have required contrived subject geometry, loading and segment kinematics to attempt to predict joint function. By the use of this "generic" data, information regarding detailed joint function is lost, in much the same way as it was lost by the earlier two-dimensional studies. In addition to this, verification of these studies has been poorly documented, thereby casting doubt over the physiological accuracy of their results. As a consequence, their results have added little additional information to the knowledge of the detailed shoulder function occurring in real life activities.

The shoulder model in this thesis has been developed on the premise that to accurately model shoulder function, accurate details for individual shoulder function must be considered. This has resulted in an emphasis being placed on the collection of accurate real time three-dimensional kinematic and loading information for each subject and activity. In addition to this, anatomical geometry that was not available from the subjects was based on anthropometric data and programmed to allow later changes to be made if an individual's data became available.

Muscle wrapping, as an important aspect of shoulder function was the focus of a considerable amount of attention with respect to development and implementation. Previous shoulder models while considering wrapping, only briefly documented the techniques used for its implementation.

Active soft tissue stabilization of the glenohumeral joint is not well understood. In

previous two and three-dimensional biomechanical studies of the shoulder this aspect of muscle function has often been omitted. The algorithm developed for this thesis to provide active soft tissue stabilization was based solely on mechanical joint restraint, ie. development of forces in appropriate structures to transmit shear forces and moments. As such it cannot be considered wholly representative of the physiological stabilizing process. Recognising this, it was included only as a means of investigating this poorly understood aspect of shoulder function. It would appear from the results of this project, that the effect of joint stability on muscle function cannot be fully predicted using such an algorithm, but modelling muscle function without considering joint stability, as was done in previous studies, would be more incorrect.

In lower limb biomechanics, gait is a commonly studied activity that represents a common, repeatable activity, providing locomotion for most individuals. For the upper limb, no such standard activity exists for biomechanical analysis. In previous shoulder research, pure flexion and abduction have been studied but these two activities are not representative of any common real life activity. Thus the need still exists for an activity or a series of activities to be defined that can be considered as representing standard loading in the upper limb.

The three athletic activities included in this project were chosen to provide insight into shoulder function during maximal loading. Each of them is commonly understood, and involves shoulder function similar to that used in many more common real life activities. While it is not assumed that these activities will become standardized for all upper limb analysis, they are commonly understood, repeatable, easily implemented activities that involve complex upper limb and shoulder function.

Measured EMG muscle activation has been used as the principal method for verifying the accuracy of model predictions in this thesis. While the use of EMG was not as desirable as would be the use of direct functional measurements, difficulties in obtaining direct measurements precluded them from use in this study.

7.1. CONCLUSIONS

Five activities were included in this project for analysis with the shoulder biomechanical model. The first two of these represent an extension to earlier two-dimensional shoulder biomechanics studies. The final three activities were chosen to allow an investigation of shoulder function during maximum shoulder loading which might be encountered in a real life three-dimensional complex activity.

The model was tested for input data uncertainty amplification using a series of five tests.

In each of these, model input data was perturbed to a known uncertainty standard deviation. Corresponding model output uncertainties were analysed and compared to the input uncertainty. No model instability was observed in any of these tests. In the final test, all input data was perturbed using estimates of experimental uncertainty magnitude. The resulting model output had an associated uncertainty of approximately $\pm 20\%$ of the maximum joint compressive force predicted during the test.

Verification of predicted results was through comparison with previous two-dimensional shoulder biomechanics studies and by comparison of predicted muscle activation to measured EMG muscle activity. With respect to comparison to previous studies, predicted muscle activation and joint forces appear to be consistent with muscle activation and joint loads calculated in these studies. In the preliminary study conducted in this thesis, the maximum glenohumeral joint compressive force was calculated to be 1.2 times body weight during abduction. This was for a single subject only. Muscles predicted to be active during abduction included all parts of deltoid, infraspinatus, supraspinatus and subscapularis.

An EMG study of eight shoulder muscles was conducted. Data was collected, normalized and averaged for 5 subjects performing 2 sets of 4 repetitions of the 5 activities. Results of this study are representative of muscle function across the shoulder musculature during the five activities. Hand loads and a representative kinematic parameter were also measured during this study. These were then used to confirm the similarity of shoulder function during the motion analysis study to that in the EMG study.

Model results for the five activities were averaged and normalized for 5 subjects performing 2 sets of 2 repetitions of each activity cycle. Predicted muscle activation for the five activities was consistent with the muscle activation measured during the EMG study for the flexion, abduction and the athletic push-up. Discrepancies in some of the predicted results for the press-up and chin-up appear to be related to limitations of the model. The maximum glenohumeral joint compressive forces for abduction and flexion with a 2 kg hand load were calculated to be to be just over 1.2 and 1.4 times body weight respectively. This would correspond to maximum joint compressive force of approximately 0.8 - 0.9 times body weight with no hand load. The highest joint compressive force was calculated for the athletic push-up, where it reached a maximum of 5 times body weight when joint stability was not a constraint of optimization. When joint stability was required, the compressive force increased to a maximum of 7 times body weight. Physiologically, the maximum average load would be expected to be between these two values. Variation in the maximum joint forces observed between individuals was as high as $\pm 50\%$ the average calculated values for each activity.

A comparison can be made of maximum articular surface stress resulting from the forces predicted this study and stress in the articular surfaces of the hip. The study by Paul (1967) predicted a maximum hip force of 8 times body weight for a fast walking individual. Since the force is transmitted through the femoral head (0.040 m diameter), the resulting articular surface stress is approximately 6500 [x body weight / m²]. In comparison, using the maximum joint compressive force of 7 times body weight as calculated in this study for a push-up using the stability constraint and a glenoid fossa diameter of 0.026 m, results in an articular surface stress of approximately 13000 [x body weight / m²]. This would indicate that the maximum predicted hip stress is approximately half that predicted for the glenoid fossa. Considering the relative physical strength required in a push-up exceeds that of fast walking, the ratio of these stresses does not appear inconsistent.

Model limitations highlighted by the activity analysis and verification procedure included uncharacteristic muscle activation during extremes of humeral extension and also during depression of the shoulder girdle. Apart from these limited circumstances, the good correlation of predicted results to measured EMG muscle activation indicates that physiological joint function is predicted by the model.

7.2. FUTURE WORK

There are several areas of the glenohumeral joint biomechanical model and glenohumeral joint biomechanics that can be highlighted as possible targets for further work.

Model limitations encountered in the press-up and chin-up activity need to be addressed. A major improvement to the shoulder model would be the inclusion of a wrapping correction for muscles passing over the thorax. Function of the muscles across other joints must also be reconsidered. In the early project stages, other joints including the acromioclavicular, sternoclavicular and scapulothoracic joints were included. Problems in implementation and poor early results saw them eliminated from the model in favour of the glenohumeral and simplified elbow joints.

Shoulder kinematics and the role of bone geometry in shoulder function are not well understood. With the model and the experimental protocols developed for this project, their relationship to joint stability, muscle activity and overall joint function could be investigated.

Further work could also be conducted in the application of the shoulder model to the investigation of shoulder function for a variety of other activities.

REFERENCES

- An KN, Kwak BM, Chao EY and Morrey BF (1984) Determination of muscle and joint forces: a new technique to solve the indeterminate problem. **J. Biomechanical Eng.** **106**, 364-367.
- Andrews JG (1984) On the specification of joint configurations and motions. (letter to the editor) **J. biomechanics** **17**, 155-158.
- Arborelius UP, Ekholm J, Nemeth G, Svensson O and Nisell R (1986) Shoulder joint load and muscular activity during lifting. **Scand. J. Rehab. Med.** **18**, 71-82.
- Arborelius UP, Ekholm J, Nisell R, Nemeth G and Svensson O (1986) Shoulder load during machine milking; An electromyographic and biomechanical study. **Ergonomics** **29**, 1591-1607.
- Barbenel JC (1983) The application of optimization methods for the calculation of joint and muscle forces. **Eng. in Med.** **12**, 29-33.
- Barker TM (1991) PhD Thesis, University of Strathclyde, Glasgow, Scotland.
- Basmajian JV and Bazant FJ (1959) Factors preventing downward dislocation of the adducted shoulder joint. **J. Bone and Jt. Surg.**, **41-A**, 1182-1186.
- Basmajian JV (1974) **Muscles alive their functions revealed through electromyography.** Williams & Wilkins, Baltimore.
- Bassett RW, Browne AO, Morrey BF and An KN (1990) Glenohumeral muscle force and moment mechanics in a position of shoulder instability. **J. Biomechanics** **23**, 405-415.
- Bean JC and Chaffin DB (1988) Biomechanical model calculation of muscle contraction forces: a double linear programming method. **J. Biomechanics** **21**, 59-66.
- Berne N, Lawes P, Solomonidis S and Paul JP (1976) A shorter pylon transducer for measurement of prosthetic forces and moments during amputee gait. **Eng. in Med.** **4**, 6-8.
- Brewer BJ, Wubben RC and Guillermo F (1986) Excessive retroversion of the glenoid cavity. **J. Bone and Jt. Surg.**, **68-A**, 724-730.
- Broström L, Kronberg M and Németh G (1989) Muscle activity during shoulder dislocation. **Acta Orthop. Scand.** **60**, 639-641.
- Bryant JT (1980) PhD Thesis, Department of Mechanical Engineering, Queen's University, Kingston.
- Chao EYS (1980) Justification of triaxial goniometer for the measurement of joint rotations. **J. Biomechanics** **13**, 989-1006.
- Chao EYS and An KN (1990) Human joint and muscle force estimation, in **Biomechanics of human movement: applications in rehabilitation, sports and ergonomics.** ed Berne N and Cappozzo A. Bertec Corporation, Worthington Ohio, U.S.A.

- Crowninshield RD (1978) Use of optimization techniques to predict muscle forces. **J. Biomechanical Eng.** 100, 88-92.
- Crowninshield RD and Brand RA (1981) A physiological based criterion of muscle force prediction in locomotion. **J. Biomechanics** 14, 793-801.
- Cyprien JM, Vasey HM, Burdet A, Bonvin JC, Kritsikis N and Vuagnat P (1983) Humeral retrotorsion and glenohumeral relationship in the normal shoulder and in recurrent anterior dislocation. **Clin. Orthop. Rel. Res.** 175, 8-17.
- de Luca CJ and Forrest WJ (1973) Force analysis of individual muscles acting simultaneously on the shoulder joint during isometric abduction. **J. Biomechanics** 6, 385-393.
- Drillis R and Contini R (1966) Body segment mass properties. **Technical report No. 1166.03.** New York University.
- Dvir Z and Berme N (1978) The shoulder complex in elevation of the arm: a mechanism approach. **J. Biomechanics** 11, 219-225.
- Engin AE and Peindl R (1987) On the biomechanics of human shoulder complex - I. Kinematics for determination of the shoulder complex sinus. **J. Biomechanics** 20, 103-117.
- Fleming HE, Hall MG, Paul JP, Millbank SFD and Dolan MJ (1993) **Calibration of Force Platforms.** Project A-2002, CAMARC-II Draft Technical Report, Bioengineering Unit, University of Strathclyde, Glasgow.
- Freedman L and Munro RR (1966) Abduction of the arm in the scapular plane: scapular and glenohumeral movements. **J. Bone and Jt.Surg.** 48-A, 1503-1510.
- Grood ES and Suntay WJ (1983) A joint coordinate system for the clinical description of three-dimensional motions: application to the knee. **J. Biomechanical Eng.** 105, 136-144.
- Högfors C, Sigholm G and Herberts P (1987) Biomechanical model of the human shoulder-I. Elements. **J. Biomechanics** 20, 157-166.
- Högfors C, Peterson B, Sigholm G and Herberts P (1991) Biomechanical model of the human shoulder joint-II. The shoulder rhythm. **J. Biomechanics** 24, 699-709.
- Holman JP (1978) **Experimental methods for engineers.** McGraw-Hill, Inc., Toronto.
- Inman VT, Saunders M and Abbott LC (1944) Observations on the function of the shoulder joint. **J. Bone and Jt. Surg.** 26, 1-30.
- Järvholm U, Palmerud G, Herberts P, Högfors C and Kadefors R (1989) Intramuscular pressure and EMG in the supraspinatus muscle at shoulder abduction. **Clin. Orthop. Rel. Res.** 245, 102-109.
- Johnson GR (1990) **A study of the muscles of the shoulder complex with particular emphasis on the mechanism of the shoulder girdle.** Department of Mechanical Materials and Manufacturing Engineering, University of Newcastle upon Tyne.

- Kapandji IA (1970) **The Physiology of Joints, Vol.1 Upper Limb**. Churchill Livingstone, New York.
- Karlsson D (1992) **Force Distributions in the Human Shoulder**, Ph.D. Thesis, Chalmers University of Technology, Göteborg, Sweden.
- Kronberg M (1990) Shoulder joint stability. **Acta Orthop. Scand.**61,93.
- Ladin Z, Flowers WC and Messner W (1989) A quantitative comparison of a position measurement system and accelerometry. **J. Biomechanics** 4, 295-308.
- Luttgens K and Wells KF (1982) **Kinesiology, scientific basis of human motion**. Saunders College Publishing, Philadelphia.
- Magnissalis EA (1992) **Studies of Prosthetic loading by means of pylon transducers**. PhD Thesis, University of Strathclyde, Glasgow, Scotland.
- McMinn RMH and Hutchings RT (1988) **A colour atlas of human anatomy**. Second edition, Wolfe Medical Publications Ltd., London.
- Németh G, Kronberg M, Brostrom L (1990) Electromyogram (EMG) recordings from the subscapularis muscle: Description of a Technique. **J. Orthop. Rel. Res.** 8, 151-153.
- Nicol AC (1977) PhD Thesis, University of Strathclyde, Glasgow.
- Pande P, Hawkins R and Peat M (1989) Electromyography in voluntary posterior instability of the shoulder. **Am. J. Sports Med.** 17, 644-648.
- Paul JP (1967) PhD Thesis, University of Strathclyde, Glasgow.
- Pezzack JC, Norman RW and Winter DA (1977) An assessment of derivative determining techniques used for motion analysis. technical note. **J. of Biomechanics** 10, 377-382.
- Poppen NK and Walker PS (1976) Normal and abnormal motion of the shoulder. **J. Bone and Jt. Surg.** 58-A, 195-201.
- Poppen NK and Walker PS (1978) Forces at the glenohumeral joint in abduction. **Clin. Orthop. Rel. Res.** 135, 165-170.
- Pronk GM (1988) Three-dimensional determination of the position of the shoulder girdle during humerus elevation. **International Series on Biomechanics, Biomechanics XI-B**, Free University Press, Amsterdam, 1988.
- Pronk GM (1989) A kinematic model of the shoulder girdle: a resume. **J. Biomed. Eng.** 13, 119-123.
- Pronk GM (1991) **The shoulder girdle, analysed and modelled kinematically**. Phd Thesis, Delft University of Technology, Delft.
- Randelli M and Gambrioli PL (1986) Glenohumeral osteometry by computed tomography in normal and unstable shoulders. **Clin. Orthop.** 208, 151-156.

- Ringelberg JA (1985) EMG and force production of some human shoulder muscles during isometric abduction. **J. Biomechanics** 18, 939-947.
- Runciman RJ (1989) **Development of a stereo radiogrammetric measurement system for estimating the alignment and geometry of the metacarpophalangeal joints.** MSc Thesis, Department of Mechanical Engineering, Queen's University, Kingston.
- Runciman RJ, Bryant JT, Small CF, Fujita N and Cooke TDV (1993) Stereoradiogrammetric technique for estimating alignment of the joints in the hand and wrist. **J. Biomed. Eng.** 15, 99-105.
- Saha AK (1971) Dynamic stability of the glenohumeral joint. **Acta Orthop. Scand.** 42, 491-505.
- Saha AK (1973) Mechanics of elevation of glenohumeral joint. **Acta Orthop. Scand.** 44, 668-678.
- Saha AK (1983) Mechanism of Shoulder Movements and a Plea for the Recognition of "Zero Position" of Glenohumeral Joint. (Reprinted from Indian J. Surg. 12(2):153, 1950) **Clin. Orthop. Rel. Res.** 173, 3-10.
- Sarrafian SK (1983) Gross and functional anatomy of the shoulder. **Clin. Orthop. Rel. Res.** 173, 11-19.
- Seireg A and Arvikar RJ (1973) A mathematical model for evaluation of forces in lower extremities of the musculo-skeletal system. **J. Biomechanics** 6, 313-326.
- Shigley JE and Mitchell LD (1983) **Mechanical Engineering Design.** McGraw-Hill Book Company, Toronto.
- Shipman P, Walker A and Bichell D (1985) **The Human Skeleton.** Harvard University Press, Cambridge.
- Small CF, Bryant JT and Pichora DR (1992) Rationalization of kinematic descriptors for three-dimensional hand and finger motion. **J. Biomed. Eng.** 14, 133-141. Saunders, Philadelphia.
- Van der Helm FCT and Veebaas R (1991) Modelling the mechanical effect of muscles with large attachment sites: application to the shoulder mechanism. **J. Biomechanics** 24, 1151-1163.
- Van der Helm FCT, Veeger HEJ, Pronk GM, Van der Woude LH and Rozendal RH (1992) Geometry parameters for musculoskeletal modelling of the shoulder system. **J. Biomechanics** 25, 129-144.
- Veeger HEJ, Van der Helm FCT, Van der Woude LHV, Pronk GM and Rozendal RH (1991) Inertia and muscle contraction parameters for musculoskeletal modelling of the shoulder mechanism. **J. Biomechanics** 24, 615-629.
- Wells KF (1976) **Kinesiology: scientific basis of human motion.** W.B. Saunders Company, Philadelphia.

Wevers HW, Siu D and Cooke TDV (1982) A quantitative method of assessing malalignment and joint space loss in the human knee. **J. Biomechanics** 4, 319-324.

Yeo BP (1976) Investigations concerning the principle of minimum total muscular force. **J. Biomechanics** 9, 413-416.

Zuckerman Lord (1988) **A New System of Anatomy**. Oxford University Press, Oxford.

APPENDIX A

This appendix contains anatomical data that were measured during a dry bone study of the scapula and upper limb. Details of the measurement techniques and other particulars of the study can be found in section: 4.1. Anatomical Data. All dimensions given are in mm, except the scaled values.

DRY BONE SCAPULA, HUMERAL, ULNAR & RADIAL MEASUREMENTS

**** HUMERAL ****

Date: February 10, 1993 Data collected: 1-3: Feb. 9, 93

Humeral coordinate system origin at head centre, X-axis parallel to shaft, Y-axis parallel to elbow rotation axis and Z-axis posteriorly.

Scaling dimension (Top to condyles)	** Number 1 **			** Number 2 **			** Number 3 **			** Average Scaled **		
	Xs	Ys	Zs	Xs	Ys	Zs	Xs	Ys	Zs	Xs	Ys	Zs
	275			295			300					
Coracobrachialis	120	0	-7	125	-5	-10	125	0	-10	0.426	-0.006	-0.031
Deltoid	110	10	-10	115	15	-9	105	15	-10	0.380	0.046	-0.033
Infraspin	-3	20	8	-5	24	8	-8	20	13	-0.018	0.074	0.033
Latissimus Dorsi	43	8	-13	68	5	-15	65	0	-11	0.201	0.015	-0.045
Pectoralis Major	75	10	-12	70	12	-17	90	15	-13	0.270	0.042	-0.048
Subscapularis	-5	0	-22	-5	3	-25	0	10	-25	-0.012	0.015	-0.083
Supraspinatus	-15	20	-7	-15	20	-8	-15	23	0	-0.052	0.072	-0.018
Teres Major	43	8	-13	68	5	-15	65	0	-11	0.201	0.015	-0.045
Teres Minor	7	12	12	10	18	14	0	12	20	0.020	0.048	0.053
Triceps Lateral	100	10	0	115	5	5	115	12	0	0.379	0.031	0.006
Triceps Medial	100	0	1	120	-5	4	115	-4	0	0.385	-0.010	0.006
Intertuber. groove	-8	10	-15	-10	13	-19	-5	20	-12	-0.027	0.049	-0.053
Head diameter	42			46			43			44		
Shaft diameter	17			22			21			20		
Elbow Centre Y, is head/shaft offset	257	8	-10	270	11	-13	278	11	-18	0.925	0.034	-0.047
Torsion angle	32			28			15			25		
Carring angle	2			5			5			4		

**** ULNAR ****

Ulnar coordinate system origin at elbow centre, X-axis parallel to shaft, Y-axis parallel to elbow rotation axis and Z-axis posteriorly.

Scaling dimension (overall length)	245			260			260			255		
Triceps	-17	0	5	-15	0	15	-15	0	15	-0.062	0.000	0.045
Elbow Cent. to head	225			245			245			0.934		
Ulnar-Radial Centre line distance	20			20			20			0.078		

**** RADIAL ****

Radial coordinate system origin at elbow centre, X-axis parallel to shaft, Y-axis lateral for supinated hand. Ulnar scaling dimension used for radius.

Biceps	42	-5	-10	40	-5	-8	45	0	-10	0.166	-0.013	-0.037
Elbow-Hand Centre	270			310			310			1.162		

**** SCAPULA ****

Date: Feb. 10, 1993 Data collected: 1&2: Feb. 14, 92; 3: Feb. 9, 93

Coordinate system origin at acromio-clavicular joint centre, X-axis through inferior angle, Y-axis in plane defined by med. spine root and Z-axis anteriorly.

		** Number 1 **			** Number 2 **			** Number 3 **			** Average Scaled **		
		Xs	Ys	Zs	Xs	Ys	Zs	Xs	Ys	Zs	Xs	Ys	Zs
Scaling dimension (AC - Inf Ang)		165			185			170					
Biceps	Short Hd	16	0	35	27	-10	37	9	-12	30	0.099	-0.042	0.196
	Long Hd	20	0	10	30	-2	10	20	-4	9	0.134	-0.011	0.056
Coracobrachialis		16	0	35	27	-10	37	9	-12	30	0.099	-0.042	0.196
Deltoid	Medial	-5	-10	-4	-5	-18	-3	-10	-13	-4	-0.039	-0.078	-0.021
	Post. 1	15	-18	-26	20	-10	-29	15	-8	-33	0.096	-0.070	-0.169
	Post. 2	50	33	-21	70	40	-15	52	30	-23	0.329	0.198	-0.115
Infraspin	Superior	95	50	-6	100	50	0	80	50	-5	0.529	0.289	-0.022
	-	100	25	-8	120	35	-3	125	40	-5	0.663	0.192	-0.031
	Inferior	140	15	-5	145	10	-3	152	17	-6	0.842	0.082	-0.027
Levator Scapulae		50	70	4	80	65	10	55	65	4	0.353	0.386	0.034
Pect Minor		18	12	28	30	0	37	20	12	24	0.130	0.048	0.170
Rhomb Maj	Superior	100	60	-3	110	62	0	98	58	-5	0.592	0.347	-0.016
	-	110	55	-4	125	50	3	112	45	-5	0.667	0.289	-0.012
	-	123	45	-4	140	40	1	135	36	-5	0.765	0.234	-0.016
	-	135	35	-4	155	35	1	155	22	-5	0.856	0.177	-0.016
	Inferior	153	15	-3	170	20	1	165	10	-5	0.939	0.086	-0.014
Rhomboid Minor		90	68	-2	100	65	0	85	65	-4	0.529	0.382	-0.012
Serr Ant	Superior	40	60	17	65	65	20	58	68	7	0.312	0.372	0.084
	-	65	73	6	82	70	10	77	66	2	0.430	0.403	0.034
	-	90	68	1	100	65	3	63	60	0	0.486	0.372	0.007
	-	110	55	-1	125	50	4	105	52	-2	0.653	0.303	0.001
	-	123	45	-1	140	40	4	125	40	-2	0.746	0.241	0.001
	-	135	35	-1	155	35	4	143	30	-2	0.832	0.193	0.001
	-	153	15	0	170	20	4	158	18	-2	0.925	0.102	0.003
	-	155	0	3	175	0	3	170	4	2	0.962	0.008	0.015
	Inferior	140	-10	5	155	-12	7	160	-10	2	0.876	-0.061	0.027
Subscap	Superior	85	60	-7	85	55	4	75	50	-5	0.472	0.318	-0.017
	-	95	50	-1	100	50	5	112	36	-6	0.592	0.262	-0.005
	Inferior	140	15	0	145	10	2	138	12	-8	0.815	0.072	-0.012
Supraspinatus		68	55	0	75	50	7	62	47	-3	0.394	0.293	0.007
Teres Major		140	-10	0	155	-12	-3	140	-15	-5	0.837	-0.071	-0.015
Teres Minor		110	-5	-1	125	-10	-7	115	-12	-9	0.673	-0.052	-0.032
Trapezius	Lateral	0	0	-7	5	5	-7	-5	-2	2	-0.001	0.005	-0.023
	-	12	3	-14	15	6	-13	0	2	-12	0.051	0.021	-0.075
	-	28	12	-19	30	15	-17	13	8	-19	0.136	0.067	-0.106
	-	40	20	-20	45	25	-14	25	16	-21	0.211	0.117	-0.107
	-	45	30	-20	60	32	-14	38	24	-22	0.274	0.165	-0.109
	-	55	40	-17	75	40	-12	47	33	-21	0.338	0.218	-0.097
	-	67	45	-11	80	46	-10	57	40	-20	0.391	0.252	-0.079
	Medial	80	55	-7	92	50	-5	65	46	-18	0.455	0.291	-0.058
Triceps		58	-14	3	64	-20	0	50	-20	-7	0.331	-0.104	-0.008
Glenoid Fossa Details:													
Centre		37	-5	10	44	-10	8	35	-14	4	0.223	-0.056	0.042
Diameter		25			26			26			26		
Xs-Xgf Angle (super.)		42			40			38			40		
Zs-Zgf angle (anter.)		10			5			5			7		

APPENDIX B

This appendix contains the equations and calibration factors used to calculate forces and moments with respect to the force plate origin, from the eight force plate data channels. Details of the application of this information can be found in section 4.4.

The correlation of the eight force data channels to the physical loading within the four posts of the force plate is detailed below.

Force plate output was in terms of computer units. A 12 channel analogue to digital signal converter was used, giving output in the range of 1-4096 units. The offset of 2048 computer units was removed from each channel before any data calculation began.

Calibration factors were applied to each of the eight force plate data channels. These factors converted the output from computer units to units of force in newtons. The calibration factors were:

Channel No.	Source	Calibration Factor [N/unit]
1	$F_{z_{1+2}}$	0.31252
2	$F_{z_{3+4}}$	0.31252
3	$F_{x_{1+4}}$	-0.31381
4	$F_{x_{2+3}}$	-0.31381
5	F_{y_1}	0.63356
6	F_{y_2}	0.63356
7	F_{y_3}	0.63356
8	F_{y_4}	0.63356

Forces and moments with respect to the force plate origin are calculated from the loading of the force plate posts. Equations for calculating forces and moments in terms of an origin within the force plate were then:

$$F_{fp_x} = F_{x_{1+4}} + F_{x_{2+3}}$$

$$F_{fp_y} = F_{y_1} + F_{y_2} + F_{y_3} + F_{y_4}$$

$$F_{fp_z} = F_{z_{1+2}} + F_{z_{3+4}}$$

$$M_{fp_x} = a(-F_{y_1} + F_{y_2} + F_{y_3} - F_{y_4})$$

$$M_{fp_y} = b(-F_{z_{1+2}} + F_{z_{3+4}}) + a(+F_{x_{1+4}} - F_{x_{2+3}})$$

$$M_{fp_z} = b(F_{y_1} + F_{y_2} - F_{y_3} - F_{y_4})$$

where $a = 0.12$ m, $b = 0.2$ m

APPENDIX C

This appendix contains details of hand transducer calibration and listings of the data recorded for the calibration process. Also included are the calibration matrix, [C] and [M] matrices determined from the calibration.

TRANSDUCER CALIBRATION

F_p (Axial) Loading:

The transducer was set up with the weight pan in place when the first set of readings were recorded. Therefore the net transducer loading is equal to the weight of the applied masses but opposite in sign due to transducer coordinate system definition.

$$F_p = - (\text{applied mass}) * 9.81 \quad (\text{C.1})$$

No load data was recorded again after the loading cycle.

Channels 5,6 and 7 showed linear trends that included the no load collections, so it can be assumed that the trends are due to amplifier drift, and can be removed from the data. This was done by calculating the net drift for each channel over the 8 data collections and dividing the net by 8 to find the estimated drift between collections. The total estimated drift for each collections was then removed from the recorded data.

Plotting the data, the resulting line slopes for each channel represent the relationship between loading and transducer output. Linear regression was used to find the slopes.

Date: Nov. 4, 1992
File: PYCAL21.WK1

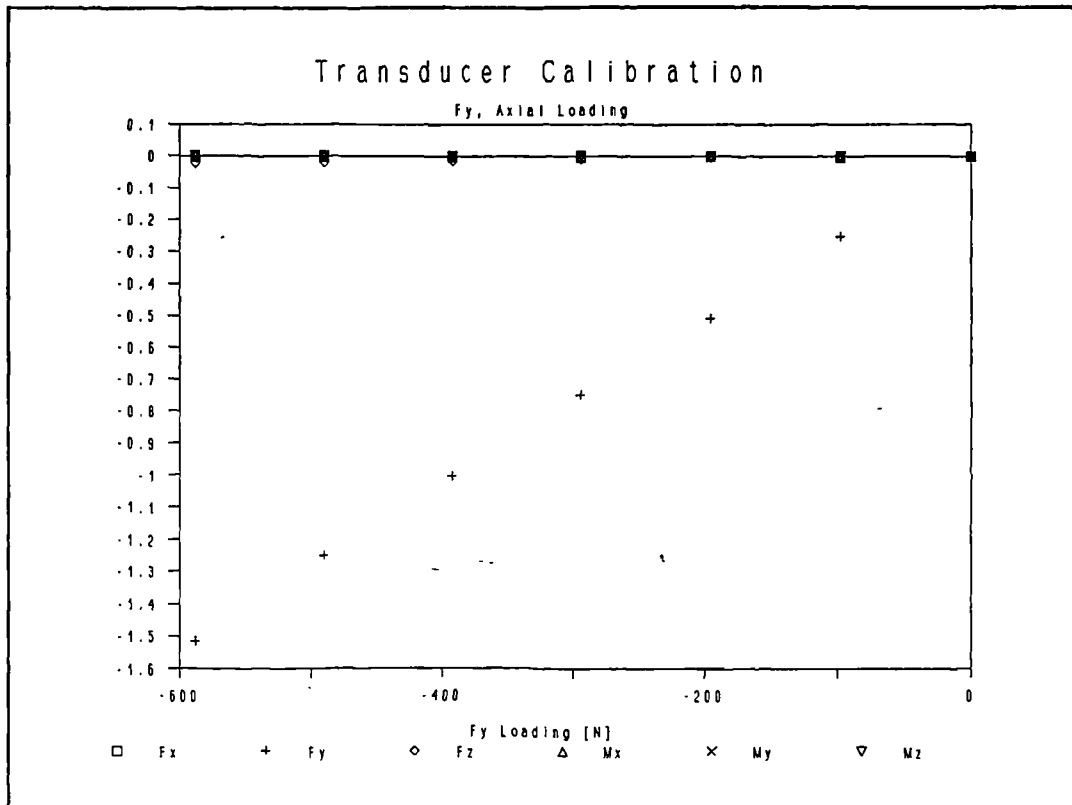
Amplifier Gain: Ch.1-3 10000, Ch. 4-6 2000
Bridge Voltage: Ch.2 10 V, Ch.1 & 3-6 5 V

***** Raw Data *****

Trial	Load [kg]	F _p [N]	Channel Output [V]					
			1	2	3	4	5	6
1	0	0	0.010	0.008	-0.001	0.005	0.044	0.050
2	10	-98	0.005	-0.242	-0.003	0.006	0.044	0.050
3	20	-196	0.007	-0.498	-0.007	0.006	0.043	0.051
4	30	-294	0.006	-0.741	-0.013	0.006	0.043	0.052
5	40	-392	0.007	-0.992	-0.018	0.007	0.042	0.052
6	50	-490	0.005	-1.240	-0.023	0.008	0.039	0.053
7	60	-588	0.004	-1.508	-0.026	0.008	0.039	0.053
8	0	0	0.009	-0.009	-0.003	0.009	0.041	0.053
Amp Drift, [V/Collection]:			-0.0001	0.0001	-0.0003	0.0006	-0.0004	0.0004

***** Zeroed and With Amp Drift Removed *****

Trial	Load [kg]	F _p [N]	Channel Output [V]					
			1	2	3	4	5	6
1	0	0	0.000	0.000	0.000	0.000	0.000	0.000
2	10	-98	-0.005	-0.250	-0.002	0.000	0.000	0.000
3	20	-196	-0.003	-0.506	-0.005	0.000	0.000	0.000
4	30	-294	-0.004	-0.749	-0.011	-0.001	0.000	0.001
5	40	-392	-0.003	-1.001	-0.016	0.000	0.000	0.000
6	50	-490	-0.004	-1.249	-0.021	0.000	-0.003	0.001
7	60	-588	-0.005	-1.517	-0.023	0.000	-0.002	0.000
8	0	0	0.000	0.000	0.000	0.000	0.000	0.000



***** Data Regression *****

<pre> -- Channel 1 -- Regression Output: Constant -0.001786 Std Err of Y Est 0.001540 R Squared 0.397503 No. of Observations 7 Degrees of Freedom 5 X Coefficient(s) 0.000005 Std Err of Coef. 0.000002 </pre>	<pre> -- Channel 2 -- Regression Output: Constant 0.001357 Std Err of Y Est 0.006226 R Squared 0.999890 No. of Observations 7 Degrees of Freedom 5 X Coefficient(s) 0.002566 Std Err of Coef. 0.000012 </pre>
<pre> -- Channel 3 -- Regression Output: Constant 0.001500 Std Err of Y Est 0.001183 R Squared 0.986119 No. of Observations 7 Degrees of Freedom 5 X Coefficient(s) 0.000043 Std Err of Coef. 0.000002 </pre>	<pre> -- Channel 4 -- Regression Output: Constant 0.000071 Std Err of Y Est 0.000377 R Squared 0.166666 No. of Observations 7 Degrees of Freedom 5 X Coefficient(s) 0.000000 Std Err of Coef. 0.000000 </pre>
<pre> -- Channel 5 -- Regression Output: Amp Drift, [V/Collection]: Constant -0.00014 Std Err of Y Est 0.000878 R Squared 0.644737 No. of Observations 7 Degrees of Freedom 5 X Coefficient(s) 0.000005 Std Err of Coef. 0.000001 </pre>	<pre> -- Channel 6 -- Regression Output: Constant 0.000786 Std Err of Y Est 0.000338 R Squared 0.5 No. of Observations 7 Degrees of Freedom 5 X Coefficient(s) -0.000000 Std Err of Coef. 0.000000 </pre>

***** Regression Tabulation *****

Note: The above regression results yield the second column of matrix, [M]. This column would be: [units in V/N]

```

m1,2 = 0.0000054
m2,2 = 0.0025663
m3,2 = 0.0000430
m4,2 = 0.0000007
m5,2 = 0.0000051
m6,2 = -0.0000015

```


Mp_y (torsional) Loading:

The transducer was set up with the loading bar horizontal and pointing in the + Z_p axis direction. The no load readings were recorded without the weight pan in place. Therefore calculating applied loads must include the weight pan mass. Transducer loading is calculated as:

$$M_{p_y} = (\text{applied mass} + \text{weight pan mass}) * 9.81 * Z_p \text{ radius} \quad (C.2)$$

where the weight pan mass is 0.702 kg.

20 and 40 kg masses were used for calibration and their respective results were averaged to obtain the final calibration matrix [M] values. After the two loads were applied to the calibration assembly the loading bar was reversed and the loading cycle repeated.

Amplifier drift was again calculated and corrected for using the same technique as was used in the axial load calibration procedure.

Date: Nov. 3, 1992
File: PYCAL22.WK1

Amplifier Gain: Ch.1-3 10000, Ch. 4-6 2000
Bridge Voltage: Ch.2 10 V, Ch.1 & 3-6 5 V

***** Raw Data *****

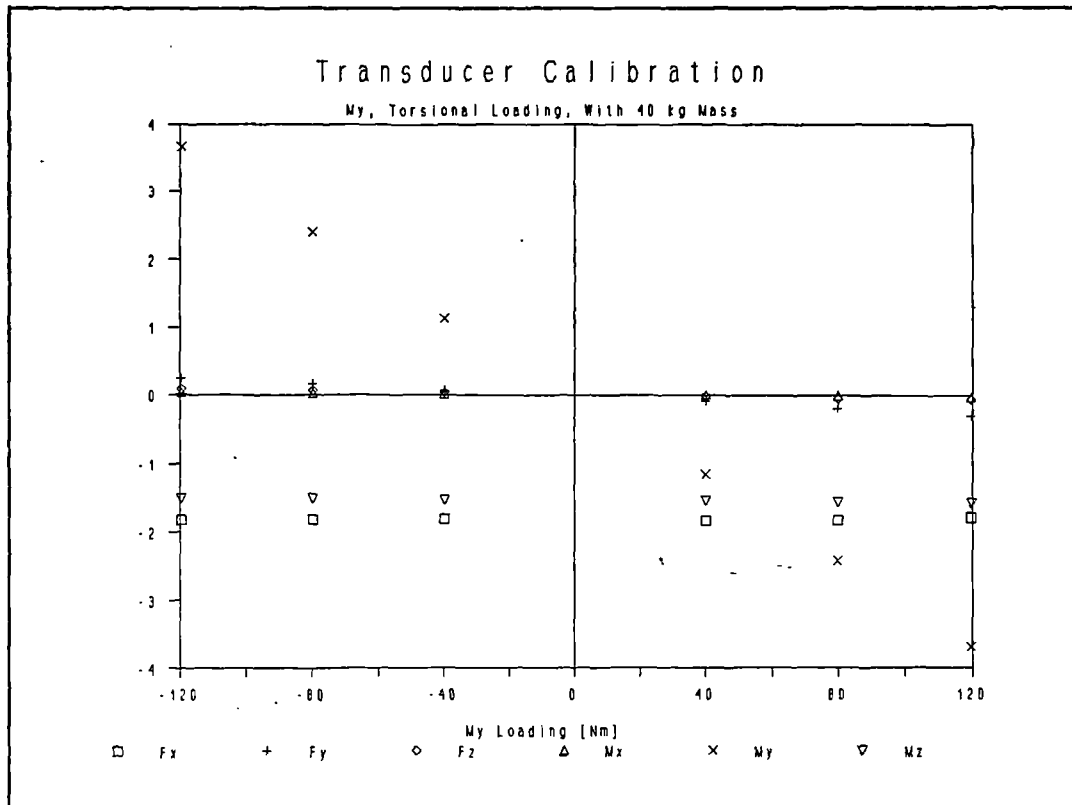
Load [kg]	Radius Z _p dir [m]	Mp _y [Nm]	Channel Output [V]					
			1	2	3	4	5	6
0	no pan	-	-0.012	0.045	-0.069	0	0	0.002
1	20	0.1	-0.938	-0.002	-0.073	0.006	-0.584	-0.779
2	20	0.2	-0.932	-0.043	-0.086	0.000	-1.233	-0.788
3	20	0.3	-0.926	-0.087	-0.101	-0.005	-1.885	-0.795
4	40	0.1	-1.823	-0.038	-0.085	0.006	-1.153	-1.535
5	40	0.2	-1.810	-0.147	-0.117	-0.005	-2.420	-1.554
6	40	0.3	-1.764	-0.251	-0.136	-0.025	-3.690	-1.564
7	no pan	-	0.020	0.048	-0.073	-0.002	0.004	0.002
Amp Drift, [V/Collection]:			0.0046	0.0004	-0.0006	-0.0003	0.0006	0.0000

0	no pan	-	-0.1	0.046	-0.053	0.001	0.075	-0.007
1	20	-0.3	-1.018	0.164	-0.015	0.023	1.949	-0.774
2	20	-0.2	-1.020	0.128	-0.028	0.015	1.304	-0.777
3	20	-0.1	-1.021	0.080	-0.039	0.012	0.656	-0.783
4	40	-0.3	-1.928	0.269	0.029	0.043	3.740	-1.517
5	40	-0.2	-1.917	0.186	0.006	0.031	2.470	-1.521
6	40	-0.1	-1.912	0.09	-0.015	0.025	1.218	-1.535
7	no pan	-	-0.104	0.019	-0.057	0.001	0.079	-0.01
Amp Drift, [V/Collection]:			-0.0006	-0.0039	-0.0006	0.0000	0.0006	-0.0004

***** Reordered, Zeroed & With Amp Drift Removed *****

Load [kg]	Radius [m]	Mp _y [Nm]	Channel Output [V]					
			1	2	3	4	5	6
40	-0.3	-119.7	-1.826	0.238	0.084	0.042	3.663	-1.508
40	-0.2	-79.8	-1.814	0.159	0.062	0.030	2.392	-1.512
40	-0.1	-39.9	-1.809	0.067	0.041	0.024	1.140	-1.525
40	0.1	39.9	-1.829	-0.085	-0.014	0.007	-1.155	-1.537
40	0.2	79.8	-1.821	-0.194	-0.045	-0.004	-2.423	-1.556
40	0.3	119.7	-1.779	-0.299	-0.064	-0.023	-3.693	-1.566
20	-0.3	-60.9	-0.917	0.122	0.039	0.022	1.873	-0.767
20	-0.2	-40.6	-0.919	0.090	0.026	0.014	1.228	-0.769
20	-0.1	-20.3	-0.919	0.046	0.016	0.011	0.579	-0.775
20	0.1	20.3	-0.931	-0.047	-0.003	0.006	-0.585	-0.781
20	0.2	40.6	-0.929	-0.089	-0.016	0.001	-1.234	-0.790
20	0.3	60.9	-0.928	-0.133	-0.030	-0.004	-1.887	-0.797

Note: Because the transducer output is zeroed against the data obtained when no load or weight pan were suspended from the transducer, the total My load is calculated as, Mp_y = (applied mass + mass of weight pan) * 9.8 * Z_p radius.



***** 40 kg Data Regression *****

```

-- Channel 1 --
Regression Output:
Constant                -1.813000
Std Err of Y Est        0.017642
R Squared               0.239287
No. of Observation      6
Degrees of Freedom      4
X Coefficient(s) 0.000093
Std Err of Coef. 0.000083

```

```

-- Channel 2 --
Regression Output:
Constant                -0.01876
Std Err of Y Est        0.014055
R Squared               0.996385
No. of Observations    6
Degrees of Freedom      4
X Coefficient(s) -0.00221
Std Err of Coef. 0.000066

```

```

-- Channel 3 --
Regression Output:
Constant                0.010857
Std Err of Y Est        0.004039
R Squared               0.996416
No. of Observations    6
Degrees of Freedom      4
X Coefficient(s) -0.00063
Std Err of Coef. 0.000019

```

```

-- Channel 4 --
Regression Output:
Constant                0.012714
Std Err of Y Est        0.004442
R Squared               0.972553
No. of Observations    6
Degrees of Freedom      4
X Coefficient(s) -0.00025
Std Err of Coef. 0.000021

```

```

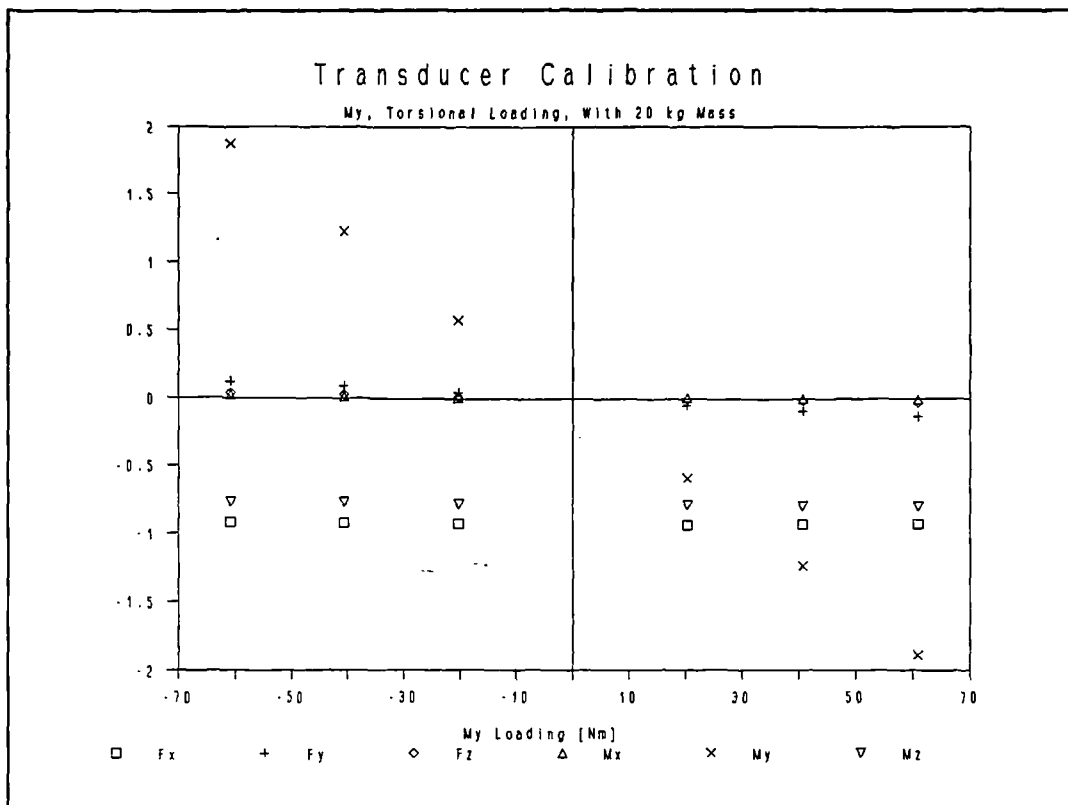
-- Channel 5 --
Regression Output:
Constant                -0.012857
Std Err of Y Est        0.055636
R Squared               0.999700
No. of Observations    6
Degrees of Freedom      4
X Coefficient(s) -0.03043
Std Err of Coef. 0.000263

```

```

-- Channel 6 --
Regression Output:
Constant                -1.53409
Std Err of Y Est        0.004477
R Squared               0.970752
No. of Observations    6
Degrees of Freedom      4
X Coefficient(s) -0.00024
Std Err of Coef. 0.000021

```



***** 20 kg Data Regression *****

```
-- Channel 1 --
Regression Output:
Constant          -0.923833
Std Err of Y Est   0.002943
R Squared         0.802124
No. of Observations 6
Degrees of Freedom 4
X Coefficient(s)  -0.00011
Std Err of Coef.  0.000027
```

```
-- Channel 2 --
Regression Output:
Constant          -0.00207
Std Err of Y Est  0.004664
R Squared         0.998353
No. of Observations 6
Degrees of Freedom 4
X Coefficient(s)  -0.00213
Std Err of Coef. 0.000043
```

```
-- Channel 3 --
Regression Output:
Constant          0.005143
Std Err of Y Est  0.001875
R Squared         0.995913
No. of Observations 6
Degrees of Freedom 4
X Coefficient(s)  -0.00054
Std Err of Coef. 0.000017
```

```
-- Channel 4 --
Regression Output:
Constant          0.008285
Std Err of Y Est  0.001866
R Squared         0.968752
No. of Observations 6
Degrees of Freedom 4
X Coefficient(s)  -0.00019
Std Err of Coef. 0.000017
```

```
-- Channel 5 --
Regression Output:
Constant          -0.004143
Std Err of Y Est  0.031157
R Squared         0.999640
No. of Observations 6
Degrees of Freedom 4
X Coefficient(s)  -0.03057
Std Err of Coef. 0.000290
```

```
-- Channel 6 --
Regression Output:
Constant          -0.77973
Std Err of Y Est  0.002390
R Squared         0.968066
No. of Observations 6
Degrees of Freedom 4
X Coefficient(s)  -0.00024
Std Err of Coef. 0.000022
```

***** Regression Tabulation *****

Note: The above regression results yield the fifth column of matrix [M]. The values corresponding to the fifth column are the average of the 20 & 40 kg X coefficients calculated for each channel. [units in V/Nm]

```
m1,5 = -0.0000083
m2,5 = -0.0021756
m3,5 = -0.0005917
m4,5 = -0.0002221
m5,5 = -0.0305055
m6,5 = -0.0002448
```

Mp_p (bending) and Fp_x (shear) Loading:

The transducer was set up with the loading tube attached and the X_p axis pointing up. The no load readings were recorded without the hanger or weight pan in place. Therefore the Mp_p, bending moment applied by the transducer will be:

$$Mp_p = (\text{applied mass} + \text{weight pan mass} + \text{hanger mass}) * 9.81 \quad (C.3)$$

$$* (Y_p \text{ radius} + \text{spacer thickness} + \text{transducer origin to end distance})$$

where Mp_p will be negative for this assembly orientation and loading configuration. The Fp_x, shear loading will be:

$$Fp_x = (\text{applied mass} + \text{weight pan mass} + \text{hanger mass}) * 9.81 \quad (C.4)$$

and Fp_x loading will be positive for this assembly orientation.

25 and 50 kg masses were used for calibration and their respective results were averaged to obtain the final calibration matrix [M] values. After the two loads were applied to the calibration assembly the assembly was inverted and the loading cycle repeated.

Amplifier drift was again calculated and corrected for using the same technique as was used in the axial load calibration procedure.

Date: Nov 4, 1992 Amplifier Gain: Ch.1-3 10000, Ch.4-6 2000
File: PYCAL23.WK1 Bridge Voltage: Ch.2 10 V, Ch.1 & 3-6 5 V

***** Raw Data *****

Load [kg]	Radius Y _p dir [m]	Mp _p [Nm]	Fp _x [N]	Channel Output [V]					
				1	2	3	4	5	6
----- X _p -axis Pointing Up -----									
0	---	No Pan or Hanger	---	0.000	-0.003	-0.010	0.002	0.000	0.008
1	50	0.3		-2.540	-0.042	0.261	0.113	-0.038	-9.100
2	50	0.2		-2.440	-0.028	0.172	0.095	-0.019	-6.670
3	50	0.1		-2.350	-0.018	0.079	0.058	-0.009	-4.220
4	25	0.3		-1.301	-0.012	0.125	0.070	-0.003	-4.630
5	25	0.2		-1.252	-0.009	0.078	0.050	0.006	-3.400
6	25	0.1		-1.207	-0.012	0.034	0.032	0.008	-2.140
0	---	No Pan or Hanger	---	-0.006	-0.012	-0.013	0.003	0.014	0.008
Amp. Drift, [Volts/Collection]:				-0.0009	-0.0013	-0.0004	0.0001	0.0020	0.0000

----- X_p-axis Pointing Down -----

0	---	No Pan or Hanger	---	0.000	0.005	-0.045	-0.004	0.022	0.002
1	50	0.1		2.330	0.012	-0.129	-0.060	0.006	4.220
2	50	0.2		2.430	0.010	-0.218	-0.098	-0.015	6.670
3	50	0.3		2.520	-0.007	-0.336	-0.138	-0.027	9.100
4	25	0.1		1.160	-0.009	-0.082	-0.030	0.025	2.170
5	25	0.2		1.202	-0.008	-0.130	-0.052	0.017	3.420
6	25	0.3		1.252	0.002	-0.179	-0.070	0.011	4.650
0	---	No Pan or Hanger	---	-0.035	0.002	-0.019	-0.006	0.022	0.027
Amp. Drift, [V/Collection]:				-0.0050	-0.0004	0.0037	-0.0003	0.0000	0.0036

***** Reordered, Zeroed & With Amp Drift Removed *****

Load [kg]	Radius [m]	Mp _p [Nm]	Fp _x [N]	Channel Output [V]					
				1	2	3	4	5	6
X _p up									
50	0.3	-186.3	499	-2.539	-0.038	0.271	0.111	-0.040	-9.108
50	0.2	-136.4	499	-2.438	-0.022	0.183	0.093	-0.023	-6.678
50	0.1	-86.5	499	-2.347	-0.011	0.090	0.056	-0.015	-4.228
X _p dn									
50	0.1	86.5	-499	2.335	0.007	-0.088	-0.056	-0.016	4.214
50	0.2	136.4	-499	2.440	0.006	-0.180	-0.093	-0.037	6.661
50	0.3	186.3	-499	2.535	-0.011	-0.302	-0.133	-0.049	9.087
X _p up									
25	0.3	-94.9	254	-1.298	-0.004	0.137	0.067	-0.011	-4.638
25	0.2	-69.5	254	-1.248	0.000	0.090	0.047	-0.004	-3.408
25	0.1	-44.0	254	-1.202	-0.001	0.047	0.029	-0.004	-2.148
X _p dn									
25	0.1	44.0	-254	1.180	-0.012	-0.052	-0.025	0.003	2.154
25	0.2	69.5	-254	1.227	-0.011	-0.104	-0.047	-0.005	3.400
25	0.3	94.9	-254	1.282	0.000	-0.156	-0.064	-0.011	4.627

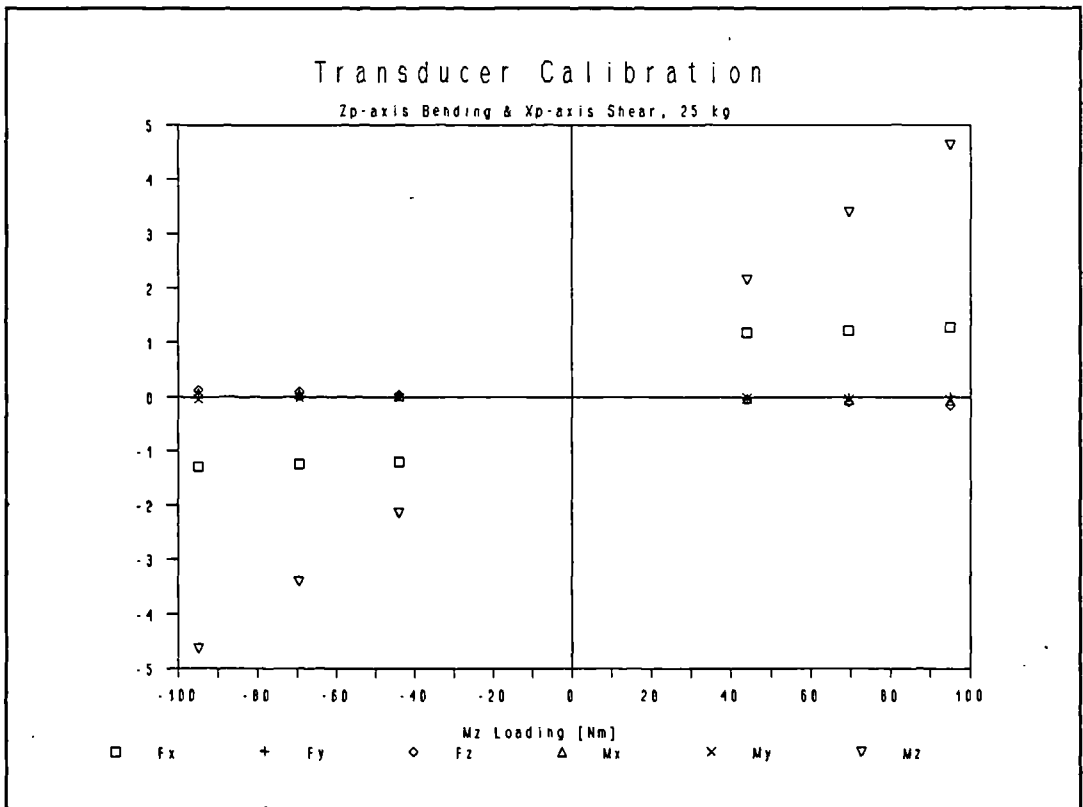
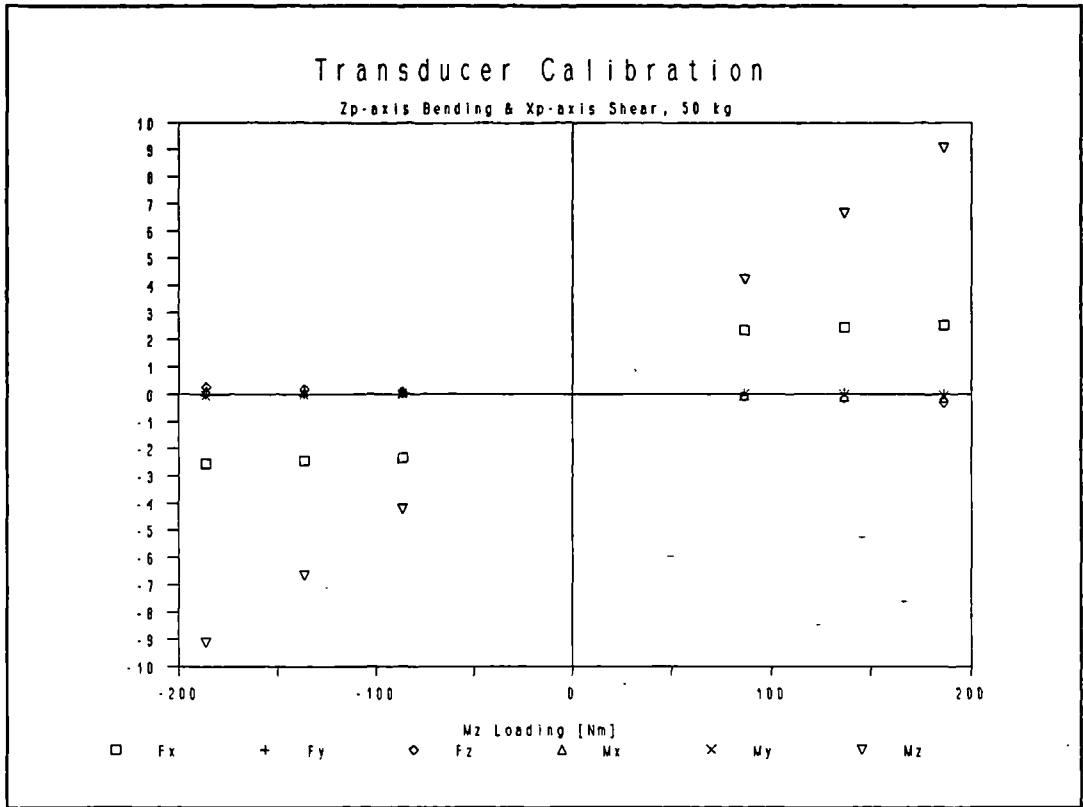
Note: Because the transducer output is zeroed against the data obtained for no loading, for both the X_p up & down pylon positions, total loads are calculated as:

$$Fp_x = (+-) (\text{applied mass} + \text{wt pan mass} + \text{hanger mass}) * 9.81, \quad \{+ve \text{ for } X_p\text{-axis up}\}$$

$$Mp_p = (+-) ((\text{applied mass} + \text{wt pan mass} + \text{hanger mass}) * (\text{radius} + \text{trans. centre to end} + \text{flange thickness} + \text{key spacer}) * 9.81$$

$$\quad \{-ve \text{ for } X_p\text{-axis up}\}$$

trans. centre to end = 53.15 mm key spacer thickness = 5.0 mm
flange thickness = 15.10 mm wt pan mass = 0.702 kg
hanger mass = 0.242 kg



***** 50 kg, X, "up" Data Regression *****

-- Channel 1 --
 Regression Output:
 Constant -2.17968940
 Std Err of Y Est 0.004082482
 R Squared 0.999093900
 No. of Observations 3
 Degrees of Freedom 1
 X Coefficient(s) 0.001920
 Std Err of Coef. 0.000057

-- Channel 2 --
 Regression Output:
 Constant 0.012541
 Std Err of Y Est 0.001632
 R Squared 0.992502
 No. of Observations 3
 Degrees of Freedom 1
 X Coefficient(s) 0.000266
 Std Err of Coef. 0.000023

-- Channel 3 --
 Regression Output:
 Constant -0.06596261
 Std Err of Y Est 0.001632993
 R Squared 0.999837487
 No. of Observations 3
 Degrees of Freedom 1
 X Coefficient(s) -0.00181
 Std Err of Coef. 0.000023

-- Channel 4 --
 Regression Output:
 Constant 0.010846
 Std Err of Y Est 0.007756
 R Squared 0.962121
 No. of Observations 3
 Degrees of Freedom 1
 X Coefficient(s) -0.00055
 Std Err of Coef. 0.000109

-- Channel 5 --
 Regression Output:
 Constant 0.00815625
 Std Err of Y Est 0.003674234
 R Squared 0.958588957
 No. of Observations 3
 Degrees of Freedom 1
 X Coefficient(s) 0.000250
 Std Err of Coef. 0.000052

-- Channel 6 --
 Regression Output:
 Constant -0.00403
 Std Err of Y Est 0.008164
 R Squared 0.999994
 No. of Observations 3
 Degrees of Freedom 1
 X Coefficient(s) 0.048873
 Std Err of Coef. 0.000115

***** 50 kg, X, "down" Data Regression *****

-- Channel 1 --
 Regression Output:
 Constant 2.163416666
 Std Err of Y Est 0.004082482
 R Squared 0.999167360
 No. of Observations 3
 Degrees of Freedom 1
 X Coefficient(s) 0.002002
 Std Err of Coef. 0.000057

-- Channel 2 --
 Regression Output:
 Constant 0.025644
 Std Err of Y Est 0.006123
 R Squared 0.814431
 No. of Observations 3
 Degrees of Freedom 1
 X Coefficient(s) -0.00018
 Std Err of Coef. 0.000086

-- Channel 3 --
 Regression Output:
 Constant 0.102867797
 Std Err of Y Est 0.011839200
 R Squared 0.993940041
 No. of Observations 3
 Degrees of Freedom 1
 X Coefficient(s) -0.00214
 Std Err of Coef. 0.000167

-- Channel 4 --
 Regression Output:
 Constant 0.011691
 Std Err of Y Est 0.000816
 R Squared 0.999777
 No. of Observations 3
 Degrees of Freedom 1
 X Coefficient(s) -0.00077
 Std Err of Coef. 0.000011

-- Channel 5 --
 Regression Output:
 Constant 0.01108625
 Std Err of Y Est 0.003674234
 R Squared 0.975806451
 No. of Observations 3
 Degrees of Freedom 1
 X Coefficient(s) -0.00033
 Std Err of Coef. 0.000052

-- Channel 6 --
 Regression Output:
 Constant -0.00335
 Std Err of Y Est 0.008164
 R Squared 0.999994
 No. of Observations 3
 Degrees of Freedom 1
 X Coefficient(s) 0.048801
 Std Err of Coef. 0.000115

***** 25 kg, X₁ "up" Data Regression *****

-- Channel 1 --		-- Channel 2 --	
Regression Output:		Regression Output:	
Constant	-1.11827797	Constant	0.001941
Std Err of Y Est	0.001632993	Std Err of Y Est	0.002449
R Squared	0.999418174	R Squared	0.355263
No. of Observations	3	No. of Observations	3
Degrees of Freedom	1	Degrees of Freedom	1
X Coefficient(s)	0.001882	X Coefficient(s)	0.000050
Std Err of Coef.	0.000045	Std Err of Coef.	0.000068

-- Channel 3 --		-- Channel 4 --	
Regression Output:		Regression Output:	
Constant	-0.03201482	Constant	-0.00435
Std Err of Y Est	0.001224744	Std Err of Y Est	0.000816
R Squared	0.999630938	R Squared	0.999091
No. of Observations	3	No. of Observations	3
Degrees of Freedom	1	Degrees of Freedom	1
X Coefficient(s)	-0.00177	X Coefficient(s)	-0.00075
Std Err of Coef.	0.000034	Std Err of Coef.	0.000022

-- Channel 5 --		-- Channel 6 --	
Regression Output:		Regression Output:	
Constant	0.003230416	Constant	0.003962
Std Err of Y Est	0.002857738	Std Err of Y Est	0.012247
R Squared	0.75	R Squared	0.999951
No. of Observations	3	No. of Observations	3
Degrees of Freedom	1	Degrees of Freedom	1
X Coefficient(s)	0.000137	X Coefficient(s)	0.048967
Std Err of Coef.	0.000079	Std Err of Coef.	0.000340

***** 25 kg, X₁ "down" Data Regression *****

-- Channel 1 --		-- Channel 2 --	
Regression Output:		Regression Output:	
Constant	1.090309166	Constant	-0.02405
Std Err of Y Est	0.003265986	Std Err of Y Est	0.003674
R Squared	0.997953702	R Squared	0.838894
No. of Observations	3	No. of Observations	3
Degrees of Freedom	1	Degrees of Freedom	1
X Coefficient(s)	0.002005	X Coefficient(s)	0.000233
Std Err of Coef.	0.000090	Std Err of Coef.	0.000102

-- Channel 3 --		-- Channel 4 --	
Regression Output:		Regression Output:	
Constant	0.038770773	Constant	0.008631
Std Err of Y Est	0.000408248	Std Err of Y Est	0.001632
R Squared	0.999969434	R Squared	0.996581
No. of Observations	3	No. of Observations	3
Degrees of Freedom	1	Degrees of Freedom	1
X Coefficient(s)	-0.00205	X Coefficient(s)	-0.00077
Std Err of Coef.	0.000011	Std Err of Coef.	0.000045

-- Channel 5 --		-- Channel 6 --	
Regression Output:		Regression Output:	
Constant	0.014794166	Constant	0.014935
Std Err of Y Est	0.000816496	Std Err of Y Est	0.008164
R Squared	0.993243243	R Squared	0.999978
No. of Observations	3	No. of Observations	3
Degrees of Freedom	1	Degrees of Freedom	1
X Coefficient(s)	-0.00027	X Coefficient(s)	0.048630
Std Err of Coef.	0.000022	Std Err of Coef.	0.000227

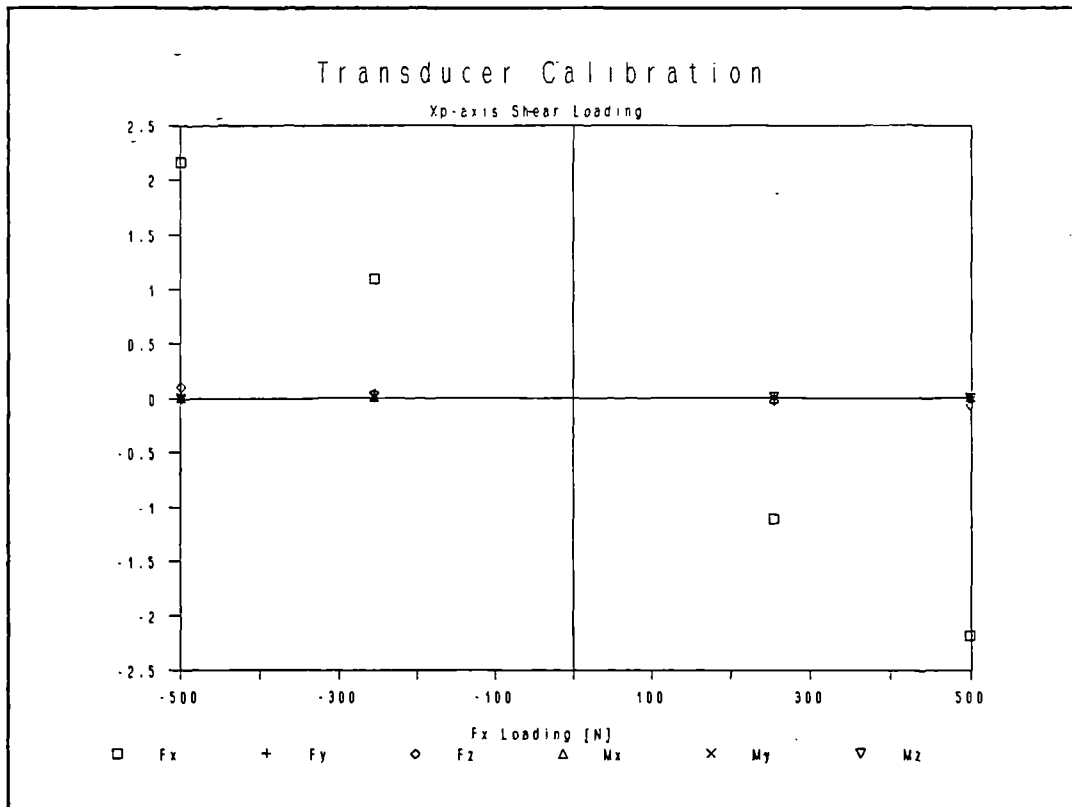
***** Regression Tabulation *****

Note: The above regression results yield matrix, [M], first & sixth columns. Beginning with the sixth column, or Mp, calibration values, the coefficients are equal to the average of the 25 & 50 kg X coefficients achieved for each channel. This is in fact the slope of the lines corresponding to pylon output as Mp loading increases and Fp_x loading remains constant. [Units are V/Nm]

m_{1,6} = 0.0019528
 m_{2,6} = 0.0000920
 m_{3,6} = -0.0019470
 m_{4,6} = -0.0007144
 m_{5,6} = -0.0000544
 m_{6,6} = 0.0488181

To calculate the first column of matrix [M], or F_{p_x} calibration values, the regression "constant", (Y intercept) for each of the four shear loading situations (X_p up & down and 25 & 50 kg loading) must be examined. By plotting these four values for each all six channels and regressing each set, the slope of these lines will correspond to the desired first column values.

Condition	F_{p_x} [N]	----- Extrapolated Channel Output [V] -----					
		1	2	3	4	5	6
Xt up 50 Kg	499	-2.17969	0.01254	-0.06596	0.01085	0.00816	-0.00403
25 Kg	254	-1.11828	0.00194	-0.03201	-0.00436	0.00323	0.00396
Xt dn 25 Kg	-254	1.09031	-0.02406	0.03877	0.00863	0.01479	0.01494
50 Kg	-499	2.16342	0.02564	0.10287	0.01169	0.01109	-0.00335



***** Fp, Shear Loading Data Regression *****

```
-- Channel 1 --
Regression Output:
Constant          -0.01106038
Std Err of Y Est  0.004242926
R Squared         0.999996966
No. of Observations 4
Degrees of Freedom 2
X Coefficient(s)  -0.00435
Std Err of Coef.  0.000005
```

```
-- Channel 2 --
Regression Output:
Constant          0.004017
Std Err of Y Est  0.025815
R Squared         0.000005
No. of Observations 4
Degrees of Freedom 2
X Coefficient(s)  0.000000
Std Err of Coef.  0.000032
```

```
-- Channel 3 --
Regression Output:
Constant          0.010915282
Std Err of Y Est  0.012617747
R Squared         0.981252494
No. of Observations 4
Degrees of Freedom 2
X Coefficient(s)  -0.00016
Std Err of Coef.  0.000015
```

```
-- Channel 4 --
Regression Output:
Constant          0.006703
Std Err of Y Est  0.008543
R Squared         0.131324
No. of Observations 4
Degrees of Freedom 2
X Coefficient(s)  -0.00000
Std Err of Coef.  0.000010
```

```
-- Channel 5 --
Regression Output:
Constant          0.009316770
Std Err of Y Est  0.004508784
R Squared         0.431539233
No. of Observations 4
Degrees of Freedom 2
X Coefficient(s)  -0.00000
Std Err of Coef.  0.000005
```

```
-- Channel 6 --
Regression Output:
Constant          0.002878
Std Err of Y Est  0.010428
R Squared         0.066927
No. of Observations 4
Degrees of Freedom 2
X Coefficient(s)  -0.00000
Std Err of Coef.  0.000013
```

***** Regression Tabulation *****

Note: The above regression results yield matrix [M] first column. These values are the regression "X coefficients" for each channel. These values correspond to the slope of the response of the transducer output to a pure X_p direction shear force. [Units are V/N]

```
m1,1 = -0.0043509
m2,1 = 0.0000001
m3,1 = -0.0001630
m4,1 = -0.0000059
m5,1 = -0.0000070
m6,1 = -0.0000050
```

M_p (bending) and F_p (shear) Loading:

The transducer was set up with the loading tube attached and the Z_p axis pointing down. The no load readings were recorded without the hanger or weight pan in place. Therefore the M_p, bending moment applied by the transducer will be:

$$M_{p_x} = (\text{applied mass} + \text{weight pan mass} + \text{hanger mass}) * 9.81 \quad (C.3)$$

$$* (Y_p \text{ radius} + \text{spacer thickness} + \text{transducer origin to end distance})$$

where M_p will be negative for this assembly orientation and loading configuration. The F_p, shear loading will be:

$$F_{p_z} = (\text{applied mass} + \text{weight pan mass} + \text{hanger mass}) * 9.81 \quad (C.4)$$

and F_p loading will be negative for this assembly orientation.

25 and 50 kg masses were used for calibration and their respective results were averaged to obtain the final calibration matrix [M] values. After the two loads were applied to the calibration assembly the assembly was inverted and the loading cycle repeated.

Amplifier drift was again calculated and corrected for using the same technique as was used in the axial load calibration procedure.

Date: Nov 4, 1992 Amplifier Gain: Ch.1-3 10000, Ch.4-6 2000
File: PYCAL24.WK1 Bridge Voltage: Ch.2 10 V, Ch.1 & 3-6 5 V

```

***** Raw Data *****
Load Radius      Mp_x      Fp_z      Channel Output [V]
[kg] Yp dir      [Nm]      [N]        1          2          3          4          5          6
[m]

----- Z_p-axis Pointing Down -----
0 --- No Pan or Hanger ---          -0.040  -0.017  -0.007  0.012  0.013  0.002
1  50   0.3          -0.538  -0.013  -2.560  9.090  0.037  0.092
2  50   0.2          -0.375  -0.020  -2.460  6.680  0.027  0.068
3  50   0.1          -0.223  -0.035  -2.370  4.250  0.017  0.042
4  25   0.3          -0.277  -0.018  -1.309  4.660  0.014  0.052
5  25   0.2          -0.210  -0.030  -1.264  3.420  0.012  0.040
6  25   0.1          -0.127  -0.037  -1.224  2.180  0.015  0.024
0 --- No Pan or Hanger ---          -0.040  -0.017  -0.007  0.012  0.013  0.002
Amp. Drift, [V/Collection]:          0.0000  0.0000  0.0000  0.0000  0.0000  0.0000

----- Z_p-axis Pointing Up -----
0 --- No Pan or Hanger ---          -0.017  -0.008  -0.001  0.000  0.014  -0.001
1  50   0.1           0.198  0.012  2.350  -4.230  0.043  -0.035
2  50   0.2           0.360  0.013  2.440  -6.680  0.060  -0.060
3  50   0.3           0.507  0.025  2.520  -9.120  0.091  -0.080
4  25   0.1           0.106  -0.014  1.200  -2.170  0.028  -0.020
5  25   0.2           0.186  -0.008  1.253  -3.420  0.037  -0.032
6  25   0.3           0.264  0.000  1.300  -4.660  0.047  -0.045
0 --- No Pan or Hanger ---          -0.004  -0.037  0.001  -0.019  0.025  0.000
Amp. Drift, [V/Collection]:          0.0019 -0.0041  0.0003 -0.0027  0.0016  0.0001

***** Reordered, Zeroed & With Amp Drift Removed *****
Load Radius      Mp_x      Fp_z      Channel Output [V]
[kg] Yp dir      [Nm]      [N]        1          2          3          4          5          6
[m]

Z_p down
50  0.3   -186.3   -499  -0.498  0.004  -2.553  9.078  0.024  0.090
50  0.2   -136.4   -499  -0.335  -0.003  -2.453  6.668  0.014  0.066
50  0.1    -86.5   -499  -0.183  -0.018  -2.363  4.238  0.004  0.040

Z_p up
50  0.1    86.5    499  0.213  0.024  2.351  -4.227  0.027  -0.034
50  0.2   136.4    499  0.373  0.029  2.440  -6.675  0.043  -0.059
50  0.3   186.3    499  0.518  0.045  2.520  -9.112  0.072  -0.079

Z_p down
25  0.3   -94.9   -254  -0.237  -0.001  -1.302  4.648  0.001  0.050
25  0.2   -69.5   -254  -0.170  -0.013  -1.257  3.408  -0.001  0.038
25  0.1   -44.0   -254  -0.087  -0.020  -1.217  2.168  0.002  0.022

Z_p up
25  0.1    44.0    254  0.116  0.011  1.200  -2.159  0.008  -0.020
25  0.2    69.5    254  0.194  0.021  1.253  -3.406  0.015  -0.032
25  0.3    94.9    254  0.270  0.033  1.299  -4.644  0.024  -0.045

```

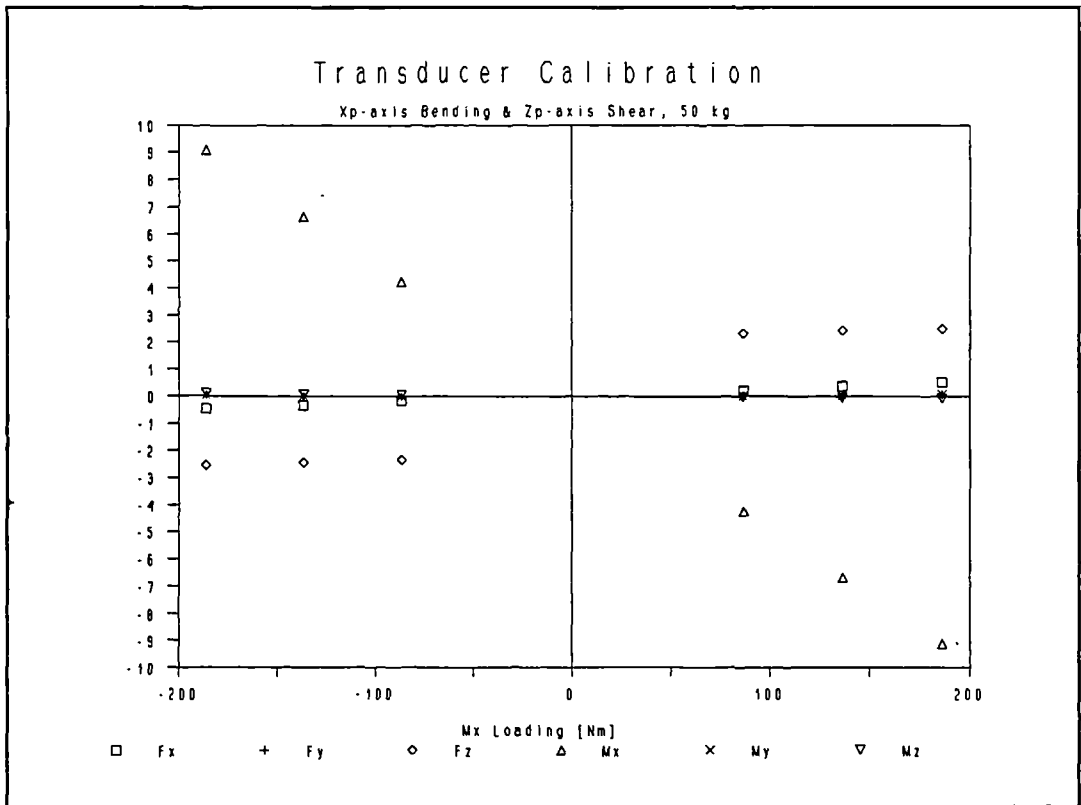
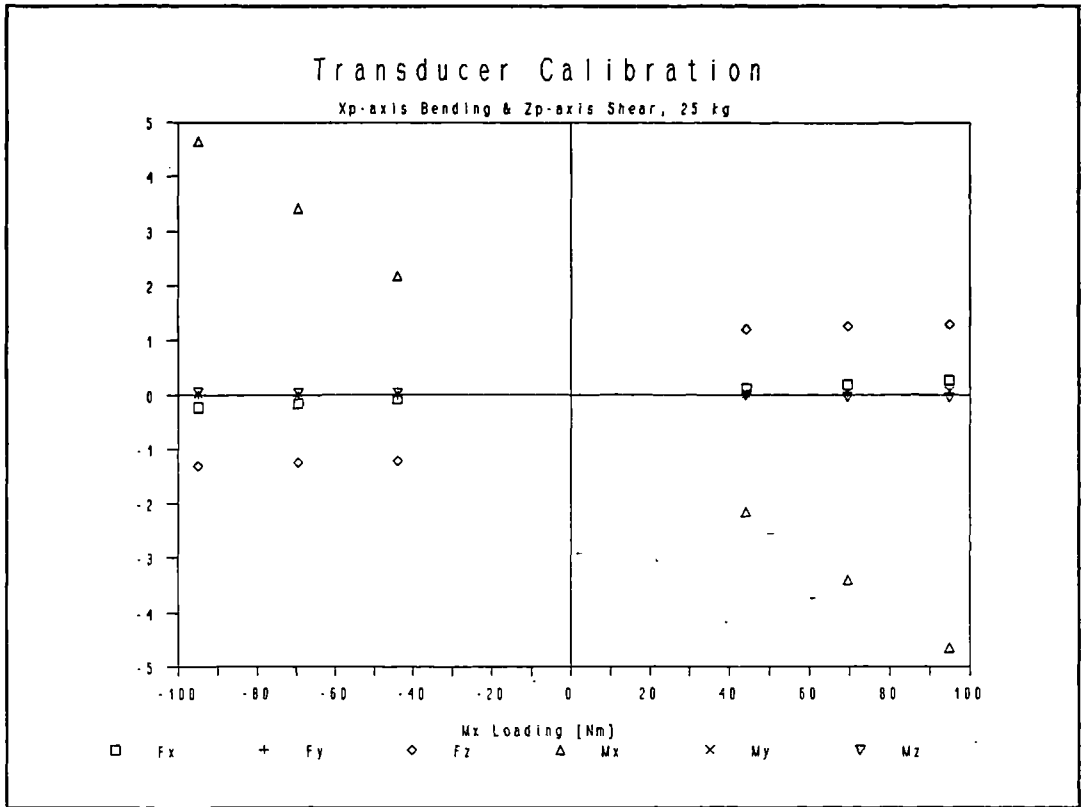
Note: Because the transducer output is zeroed against the data obtained for no loading, for both the Z_p up & down pylon positions, total loads are calculated as:

$$F_{p_z} = (+-) (\text{applied mass} + \text{wt pan mass}) * 9.81, \quad \{+ve \text{ for } Z_p\text{-axis up}\}$$

$$M_{p_x} = (+-) ((\text{applied mass} + \text{wt pan mass}) * (\text{radius} + \text{trans. centre to end} + \text{flange thickness} + \text{key spacer}) * 9.81$$

$$\{-ve \text{ for } Z_p\text{-axis down}\}$$

trans. centre to end = 53.15 mm key spacer thickness = 5.0 mm
flange thickness = 15.10 mm wt pan mass = 0.702 kg



***** 50 kg, Z, "Down" Data Regression *****

-- Channel 1 --
 Regression Output:
 Constant 0.091702083
 Std Err of Y Est 0.004490731
 R Squared 0.999593681
 No. of Observations 3
 Degrees of Freedom 1
 X Coefficient(s) 0.003154
 Std Err of Coef. 0.000063

-- Channel 2 --
 Regression Output:
 Constant -0.03572
 Std Err of Y Est 0.003265
 R Squared 0.957783
 No. of Observations 3
 Degrees of Freedom 1
 X Coefficient(s) -0.00022
 Std Err of Coef. 0.000046

-- Channel 3 --
 Regression Output:
 Constant -2.19674883
 Std Err of Y Est 0.004082482
 R Squared 0.999077490
 No. of Observations 3
 Degrees of Freedom 1
 X Coefficient(s) 0.001902
 Std Err of Coef. 0.000057

-- Channel 4 --
 Regression Output:
 Constant 0.048683
 Std Err of Y Est 0.008164
 R Squared 0.999994
 No. of Observations 3
 Degrees of Freedom 1
 X Coefficient(s) -0.04847
 Std Err of Coef. 0.000115

-- Channel 5 --
 Regression Output:
 Constant -0.013325
 Std Err of Y Est 0
 R Squared 1
 No. of Observations 3
 Degrees of Freedom 1
 X Coefficient(s) -0.00020
 Std Err of Coef. 0

-- Channel 6 --
 Regression Output:
 Constant -0.00297
 Std Err of Y Est 0.000816
 R Squared 0.999466
 No. of Observations 3
 Degrees of Freedom 1
 X Coefficient(s) -0.00050
 Std Err of Coef. 0.000011

***** 50 kg, Z, "up" Data Regression *****

-- Channel 1 --
 Regression Output:
 Constant -0.04881089
 Std Err of Y Est 0.006123724
 R Squared 0.999195920
 No. of Observations 3
 Degrees of Freedom 1
 X Coefficient(s) 0.003057
 Std Err of Coef. 0.000086

-- Channel 2 --
 Regression Output:
 Constant 0.003870
 Std Err of Y Est 0.004490
 R Squared 0.918256
 No. of Observations 3
 Degrees of Freedom 1
 X Coefficient(s) 0.000213
 Std Err of Coef. 0.000063

-- Channel 3 --
 Regression Output:
 Constant 2.205613452
 Std Err of Y Est 0.004082482
 R Squared 0.998840151
 No. of Observations 3
 Degrees of Freedom 1
 X Coefficient(s) 0.001696
 Std Err of Coef. 0.000057

-- Channel 4 --
 Regression Output:
 Constant 0.002307
 Std Err of Y Est 0.004082
 R Squared 0.999998
 No. of Observations 3
 Degrees of Freedom 1
 X Coefficient(s) -0.04891
 Std Err of Coef. 0.000057

-- Channel 5 --
 Regression Output:
 Constant -0.01376226
 Std Err of Y Est 0.005715476
 R Squared 0.968551894
 No. of Observations 3
 Degrees of Freedom 1
 X Coefficient(s) 0.000449
 Std Err of Coef. 0.000080

-- Channel 6 --
 Regression Output:
 Constant 0.004252
 Std Err of Y Est 0.002041
 R Squared 0.995952
 No. of Observations 3
 Degrees of Freedom 1
 X Coefficient(s) -0.00045
 Std Err of Coef. 0.000028

***** 25 kg, Z, "down" Data Regression *****

-- Channel 1 --
 Regression Output:
 Constant 0.040270833
 Std Err of Y Est 0.006531972
 R Squared 0.996221736
 No. of Observations 3
 Degrees of Freedom 1
 X Coefficient(s) 0.002949
 Std Err of Coef. 0.000181

-- Channel 2 --
 Regression Output:
 Constant -0.03729
 Std Err of Y Est 0.002041
 R Squared 0.977436
 No. of Observations 3
 Degrees of Freedom 1
 X Coefficient(s) -0.00037
 Std Err of Coef. 0.000056

-- Channel 3 --
 Regression Output:
 Constant -1.14253541
 Std Err of Y Est 0.002041241
 R Squared 0.998847926
 No. of Observations 3
 Degrees of Freedom 1
 X Coefficient(s) 0.001671
 Std Err of Coef. 0.000056

-- Channel 4 --
 Regression Output:
 Constant 0.0197
 Std Err of Y Est 0.000000
 R Squared 1
 No. of Observations 3
 Degrees of Freedom 1
 X Coefficient(s) -0.04877
 Std Err of Coef. 0.000000

-- Channel 5 --
 Regression Output:
 Constant 0.002032916
 Std Err of Y Est 0.002041241
 R Squared 0.107142857
 No. of Observations 3
 Degrees of Freedom 1
 X Coefficient(s) 0.000019
 Std Err of Coef. 0.000056

-- Channel 6 --
 Regression Output:
 Constant -0.00158
 Std Err of Y Est 0.001632
 R Squared 0.993243
 No. of Observations 3
 Degrees of Freedom 1
 X Coefficient(s) -0.00055
 Std Err of Coef. 0.000045

***** 25 kg, Z, "up" Data Regression *****

-- Channel 1 --
 Regression Output:
 Constant -0.01774523
 Std Err of Y Est 0.000816496
 R Squared 0.999943990
 No. of Observations 3
 Degrees of Freedom 1
 X Coefficient(s) 0.003034
 Std Err of Coef. 0.000022

-- Channel 2 --
 Regression Output:
 Constant -0.00906
 Std Err of Y Est 0.000816
 R Squared 0.997322
 No. of Observations 3
 Degrees of Freedom 1
 X Coefficient(s) 0.000438
 Std Err of Coef. 0.000022

-- Channel 3 --
 Regression Output:
 Constant 1.114727142
 Std Err of Y Est 0.002449489
 R Squared 0.998787638
 No. of Observations 3
 Degrees of Freedom 1
 X Coefficient(s) 0.001955
 Std Err of Coef. 0.000068

-- Channel 4 --
 Regression Output:
 Constant -0.00854
 Std Err of Y Est 0.004082
 R Squared 0.999994
 No. of Observations 3
 Degrees of Freedom 1
 X Coefficient(s) -0.04886
 Std Err of Coef. 0.000113

-- Channel 5 --
 Regression Output:
 Constant -0.00618863
 Std Err of Y Est 0.000408248
 R Squared 0.998676105
 No. of Observations 3
 Degrees of Freedom 1
 X Coefficient(s) 0.000311
 Std Err of Coef. 0.000011

-- Channel 6 --
 Regression Output:
 Constant 0.002498
 Std Err of Y Est 0.000408
 R Squared 0.999478
 No. of Observations 3
 Degrees of Freedom 1
 X Coefficient(s) -0.00049
 Std Err of Coef. 0.000011

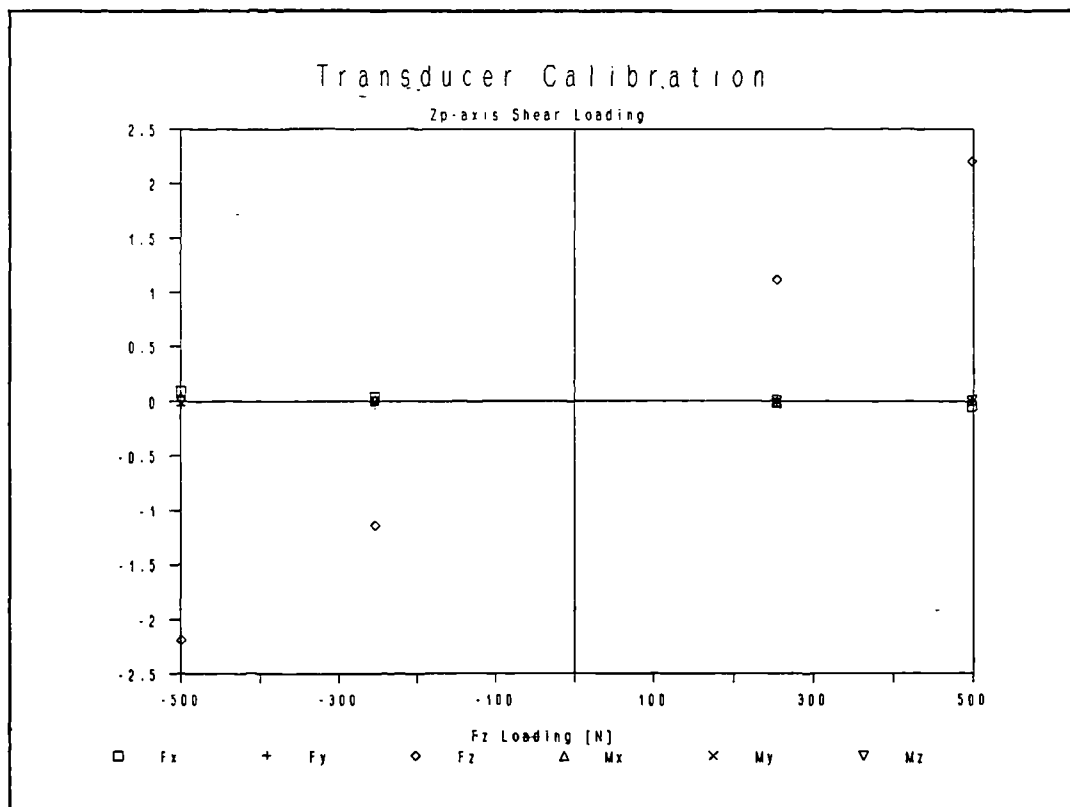
***** Regression Tabulation *****

Note: The above regression results yield matrix, [M], third and fourth columns. Beginning with the fourth column, or Mp, calibration values, the coefficients are equal to the average of the 25 & 50 kg X coefficients achieved for each channel. This is in fact the slope of the lines corresponding to pylon output as Mp, loading increases and Fp, loading remains constant. [Units are V/Nm]

m_{1,4} = 0.0030490
 m_{2,4} = 0.0000144
 m_{3,4} = 0.0018066
 m_{4,4} = -0.0487557
 m_{5,4} = 0.0001451
 m_{6,4} = -0.0005005

To calculate the third column, or F_p , calibration values, the regression "constant", (Y intercept) for each of the four shear loading situations (Z_p up & down and 25 & 50 kg loading) must be examined. By plotting these four values for each all six channels and regressing each set, the slope of these lines will correspond to the desired first column calibration values.

Condition	F_p [N]	----- Channel Output [V] -----					
		1	2	3	4	5	6
Zp dn 50 Kg	-499	0.09170	-0.03572	-2.19675	0.04868	-0.01333	-0.00298
25 Kg	-254	0.04027	-0.03729	-1.14254	0.01970	0.00203	-0.00159
Zp up 25 Kg	254	-0.01775	-0.00907	1.11473	-0.00855	-0.00619	0.00250
50 Kg	499	-0.04881	0.00387	2.20561	0.00231	-0.01376	0.00425



***** FP, Shear Loading Data Regression *****

```

-- Channel 1 --
Regression Output:
Constant          0.016354196
Std Err of Y Est  0.009384660
R Squared         0.984891483
No. of Observations 4
Degrees of Freedom 2
X Coefficient(s)  -0.00013
Std Err of Coef.  0.000011
    
```

```

-- Channel 2 --
Regression Output:
Constant          -0.01955
Std Err of Y Est  0.006263
R Squared         0.936452
No. of Observations 4
Degrees of Freedom 2
X Coefficient(s)  0.000042
Std Err of Coef.  0.000007
    
```

```

-- Channel 3 --
Regression Output:
Constant          -0.00473516
Std Err of Y Est  0.014880459
R Squared         0.999963814
No. of Observations 4
Degrees of Freedom 2
X Coefficient(s)  0.004417
Std Err of Coef.  0.000018
    
```

```

-- Channel 4 --
Regression Output:
Constant          0.015535
Std Err of Y Est  0.014236
R Squared         0.783357
No. of Observations 4
Degrees of Freedom 2
X Coefficient(s)  -0.00004
Std Err of Coef.  0.000017
    
```

```

-- Channel 5 --
Regression Output:
Constant          -0.00781074
Std Err of Y Est  0.008856422
R Squared         0.051307644
No. of Observations 4
Degrees of Freedom 2
X Coefficient(s)  -0.00000
Std Err of Coef.  0.000011
    
```

```

-- Channel 6 --
Regression Output:
Constant          0.000546
Std Err of Y Est  0.000221
R Squared         0.997149
No. of Observations 4
Degrees of Freedom 2
X Coefficient(s)  0.000007
Std Err of Coef.  0.000000
    
```

***** Regression Tabulation *****

Note: The above regression results yield matrix [M] third column. These values are the regression "X coefficients" for each channel. These values correspond to the slope of the response of the pylon output to a pure Zp direction shear force. [Units are V/N]

```

m1,3 = -0.0001353
m2,3 = 0.0000429
m3,3 = 0.0044178
m4,3 = -0.0000483
m5,3 = -0.0000037
m6,3 = 0.0000074
    
```

Correlation of Matrix [M] and Matrix [C] Calculation:

The column data for matrix [M] determined during this calibration procedure, can be correlated here along with the calculated calibration matrix, [C].

The amplifier details for the calibration procedure was:

Amplifier Gain: Ch 1-3 10000, Ch 4-6 2000
 Bridge Voltage: Ch.2 10 V, Ch.1 & 3-6 5 V

The resulting correlated data for matrix [M] was:

	-435.1	0.5	-13.5	304.9	-0.8	195.3	
	0.0	256.6	4.3	1.4	-217.6	9.2	
SIGNAL [V] =	-16.3	4.3	441.8	180.7	-59.2	-194.7	x LOAD
	-0.6	0.1	-4.8	-4875.6	-22.2	-71.4	[x10 ⁻⁵ N]
	-0.7	0.5	-0.4	14.5	-3050.6	-5.4	
	-0.5	-0.2	0.7	-50.1	-24.5	4881.8	

If each output channel is divided by its corresponding bridge voltage, and total amplifier gain, matrix [M] corresponding to unity bridge voltage and gain would be:

	-8.702	0.011	-0.271	6.098	-0.017	3.906	
	0.000	2.566	0.043	0.014	-2.176	0.092	
SIGNAL [V] =	-0.326	0.086	8.836	3.613	-1.183	-3.894	x LOAD
	-0.059	0.007	-0.483	-487.557	-2.221	-7.144	[x10 ⁻⁵ N]
	-0.070	0.051	-0.037	1.451	-305.055	-0.544	
	-0.050	-0.015	0.074	-5.005	-2.448	488.181	

Inverting the original version of matrix [M], the calibration matrix [C] for the transducer is [Units of N/V]:

	-229.6	1.0	-7.5	-14.7	0.2	8.7
	0.2	389.3	-3.5	-0.1	-27.7	-0.9
	-8.3	-3.5	226.1	7.8	-4.3	9.5
	0.1	0.0	-0.2	-20.5	0.2	-0.3
	0.1	0.1	0.0	-0.1	-32.8	0.0
	0.0	0.0	-0.1	-0.2	-0.2	20.5

Where this matrix is valid for the amplifier settings used for the calibration process, which were:

Amplifier Gain: Ch 1-3 10000, Ch 4-6 2000
 Bridge Voltage: Ch.2 10 V, Ch.1 & 3-6 5 V

APPENDIX D

This appendix contains details of the instrumented hand transducer system calibration, included is: the calculation details for accurately determining the rotational offset, θ_2 between the transducer and transducer marker coordinate system; and the system test used to determine overall accuracy of hand loads measured with the transducer.

Transducer to Marker Coordinate System Offset:

The transducer was oriented in the laboratory with: the Z_p axis horizontal and X_p axis vertical and pointing up, using the same procedure as was used for transducer calibration; and the Y_p axis pointing in the Z_{lab} axis direction. This effectively made the $X_p - Z_p$ plane parallel to the $X_{lab} - Y_{lab}$ plane. The angle now formed between the marker X axis, X_{pm} and vertical is equal the rotational offset angle between the transducer coordinate system and the transducer marker coordinate system.

Ten frames of data were collected using the Vicon motion analysis system. The rotational offset angle was then calculated using, [all units if not otherwise stated are in mm]:

$$\theta_2 = \tan^{-1} ((X_{PZ-lab} - X_{PX-lab}) / (Y_{PZ-lab} - Y_{PX-lab}))$$

For frame No 1,

$$\begin{aligned} \theta_2 &= \tan^{-1} ((1369.1 - 1286.1) / (956.2 - 879.8)) \\ &= \tan^{-1} (83.0 / 76.4) \\ &= 47.4 \text{ degrees} \end{aligned}$$

The data collected and the calculated rotational offsets are:

File: PYCAL27.WK1 Date: Nov. 6, 92

Frame No.	Marker	Coordinate X_{lab}	Coordinate Y_{lab}	Coordinate Z_{lab}	Marker to Transducer Rotational Offset, θ_2
1	PX	1286.085	879.819	361.719	47.4
	PY	1287.245	878.891	477.265	
	PZ	1369.148	956.153	362.415	
2	PX	1286.781	880.051	361.719	47.2
	PY	1286.781	878.891	477.265	
	PZ	1369.148	956.385	362.647	
3	PX	1287.013	879.819	361.719	47.0
	PY	1287.013	879.123	477.265	
	PZ	1368.916	956.385	362.647	
4	PX	1287.013	880.051	361.951	47.0
	PY	1287.013	878.659	477.033	
	PZ	1369.148	956.617	362.415	
5	PX	1286.085	879.819	361.719	47.4
	PY	1287.245	878.891	477.265	
	PZ	1369.38	956.385	362.647	
6	PX	1286.781	880.051	361.719	47.1
	PY	1286.781	878.659	476.801	
	PZ	1368.916	956.385	362.647	
7	PX	1286.549	879.819	361.719	47.4
	PY	1286.781	878.891	477.497	
	PZ	1369.612	956.385	362.415	
8	PX	1286.781	880.051	361.719	47.2
	PY	1286.781	878.891	476.801	
	PZ	1369.148	956.385	362.415	
9	PX	1286.317	879.819	361.719	47.4
	PY	1287.245	879.123	477.265	
	PZ	1369.612	956.385	362.647	
10	PX	1287.013	880.051	361.719	47.0
	PY	1286.781	878.891	477.265	
	PZ	1369.148	956.617	362.647	

Average Offset: 47.2

Instrumented Hand Transducer System Test:

The transducer assembly was set up in the motion analysis lab as it would be during an experimental session. Four different loading formats were used, loading six transducer channels, similar as was done for the original calibration. The overall results give an indication of the accuracy of hand load measurements made using the transducer experimentally. The measured loads are the average of 10 frames of data collected at 50 Hz.

File: PYCAL28.WK1
Date: Nov. 11, 92
Using Files: SCAP1000 - 12.ANA

Forces and Moments Measured With the Pylon and converted to be W.R.T. the Lab Coordinate System by using Vicon Markers Attached to the Transducer. All amplifier details were the same as was used for transducer calibration, see Appendix C for details.

F_p, (axial) Loading: Transducer was set up with the assembly used in the F_p, (axial) loading transducer calibration, with the Y_p axis pointing vertically down. 10 kg and 20 kg masses were applied. The resulting measured loads should only be 98.1 and 196.2 N in the F_{y_{lab}} direction:

----- Measured Loads, w.r.t. the Lab. Coordinate System -----												
	Fx [N]		Fy [N]		Fz [N]		Mx [Nm]		My [Nm]		Mz [Nm]	
	AVG	STD	AVG	STD	AVG	STD	AVG	STD	AVG	STD	AVG	STD
No Load	-14.8	1.0	64.4	1.2	-8.4	0.3	-1.0	0.0	0.4	0.1	3.0	0.1
+98.1 N Fy	-14.7	1.9	160.1	0.9	-9.6	0.4	-1.1	0.1	0.4	0.1	3.2	0.1
+196.2 N Fy	-15.2	1.0	255.7	0.9	-13.5	0.6	-1.6	0.1	0.4	0.1	3.0	0.0
Net Change:												
+98.1 N Fy	0.1	2.1	95.8	1.4	-1.2	0.5	-0.1	0.1	0.0	0.2	0.1	0.1
+196.2 N Fy	-0.4	1.4	191.3	1.5	-5.1	0.7	-0.6	0.1	0.0	0.2	-0.1	0.1
AVG Error:	-0.2		-3.6		-3.1		-0.4		0.0		0.0	

M_p, (torsional) Loading: Transducer was set up with the assembly used in the M_p, (torsional) loading transducer calibration (bar in the -Z_p direction), with the Y_p axis pointing vertically up and the X_p axis pointing in the Z_{lab} axis direction. A 20 kg mass was applied at the three torsion bar positions. The resulting measured loads should be 203 N in the F_{y_{lab}} direction, increasing M_{z_{lab}} and M_{x_{lab}} while loaded were not calculated:

----- Measured Loads, w.r.t. the Lab. Coordinate System -----												
	Fx [N]		Fy [N]		Fz [N]		Mx [Nm]		My [Nm]		Mz [Nm]	
	AVG	STD	AVG	STD	AVG	STD	AVG	STD	AVG	STD	AVG	STD
No Load	-22.4	0.5	19.3	0.3	1.7	0.6	2.4	0.1	3.8	0.1	1.2	0.1
-20.3 Nm Mz	-19.3	0.9	222.9	0.6	1.9	1.0	14.2	0.1	3.6	0.1	-17.5	0.1
-40.5 Nm Mz	-23.2	0.9	221.4	0.7	2.2	0.9	13.9	0.2	4.7	0.1	-38.4	0.0
-60.8 Nm Mz	-23.6	0.7	221.4	0.6	-1.2	1.1	13.7	0.2	4.8	0.1	-59.3	0.0
Net Change:												
-20.3 Nm Mz	3.1	1.1	203.7	0.7	0.2	1.1	11.8	0.1	-0.2	0.1	-18.6	0.1
-40.5 Nm Mz	-0.8	1.1	202.1	0.8	0.6	1.1	11.4	0.2	0.8	0.1	-39.5	0.1
-60.8 Nm Mz	-1.2	0.9	202.1	0.7	-2.8	1.2	11.3	0.2	1.0	0.2	-60.4	0.1
Avg Error:	0.4		0.3		-0.7		-		0.5		1.0	

M_{p_x} (bending) and F_{p_x} (shear) Loading: Transducer was set up with the hand grip used in the experimental sessions, with the X_p axis pointing vertically up and the Y_p axis pointing in the Z_{lab} axis direction. 10 and 20 kg masses were applied at the hand grip centre using a weight pan suspended from the grip centre position (marked by a groove in the hand grip). The resulting measured net loads should be 98.1 and 196.2 N in the $F_{Y_{lab}}$ direction and the bending load measured in the transducer, M_{p_x} , should translate into no $M_{X_{lab}}$ being calculated because actually there are no moments being applied by the hand grip on the weight pan.

----- Measured Loads, w.r.t. the Lab. Coordinate System -----												
	Fx [N]		Fy [N]		Fz [N]		Mx [Nm]		My [Nm]		Mz [Nm]	
	AVG	STD	AVG	STD	AVG	STD	AVG	STD	AVG	STD	AVG	STD
No Load	-16.3	0.4	21.9	0.3	-14.7	0.8	2.1	0.0	2.8	0.1	1.8	0.1
+98.1 N Fy	-18.7	0.9	117.7	0.7	-14.7	1.1	1.9	0.1	3.1	0.1	1.9	0.1
+196.2 N Fy	-19.6	2.1	215.0	1.1	-14.1	1.1	2.0	0.2	3.1	0.1	2.0	0.1
Net Change:												
+98.1 N Fy	-2.4	1.0	95.9	0.8	-0.1	1.3	-0.2	0.1	0.3	0.1	0.1	0.1
+196.2 N Fy	-3.3	2.2	193.2	1.1	0.6	1.3	-0.1	0.2	0.3	0.1	0.2	0.1
Avg Error:	-2.9		-2.6		0.3		-0.2		0.3		0.1	

M_{p_x} (bending) and F_{p_x} (shear) Loading: Transducer was set up with the hand grip used in the experimental sessions, with the Z_p axis pointing vertically up and the Y_p axis pointing in the Z_{lab} axis direction. 10 and 20 kg masses were applied at the hand grip centre using a weight pan suspended from the grip centre position (marked by a groove in the hand grip). The resulting measured net loads should be 98.1 and 196.2 N in the $F_{Y_{lab}}$ direction and the bending load measured in the transducer, M_{p_x} , should translate into no $M_{X_{lab}}$ being calculated because actually there are no moments being applied by the hand grip on the weight pan.

----- Measured Loads, w.r.t. the Lab. Coordinate System -----												
	Fx [N]		Fy [N]		Fz [N]		Mx [Nm]		My [Nm]		Mz [Nm]	
	AVG	STD	AVG	STD	AVG	STD	AVG	STD	AVG	STD	AVG	STD
No Load	-2.4	0.3	-1.5	0.4	-15.8	0.9	-2.5	0.1	1.0	0.1	1.6	0.1
+98.1 N Fy	-1.1	0.7	94.5	0.7	-16.9	0.9	-2.5	0.1	0.7	0.1	1.9	0.0
+196.2 N Fy	-1.6	1.4	191.3	0.6	-20.1	1.1	-2.3	0.1	0.7	0.1	2.1	0.1
Net Change:												
+98.1 N Fy	1.3	0.8	96.1	0.8	-1.1	1.3	0.0	0.1	-0.2	0.1	0.3	0.1
+196.2 N Fy	0.8	1.5	192.9	0.7	-4.3	1.4	0.2	0.1	-0.3	0.1	0.5	0.1
Avg Error:	1.1		-2.7		-2.7		0.1		-0.3		0.4	

Overall Average Error and Measurement Standard Deviation:

The results of the different phases of this system test can be combined. The overall uncertainties for measuring hand loads using the instrumented transducer will be:

----- Measured Loads, w.r.t. the Lab. Coordinate System -----												
	Fx [N]		Fy [N]		Fz [N]		Mx [Nm]		My [Nm]		Mz [Nm]	
	AVG	STD	AVG	STD	AVG	STD	AVG	STD	AVG	STD	AVG	STD
	-0.4	2.2	-2.1	1.5	-1.6	1.4	-0.2	0.2	0.1	0.2	0.4	0.1

APPENDIX E

This appendix contains the mathematical details for correcting shoulder muscle wrapping around the humeral head and shaft. Humeral head wrapping is detailed first and shaft wrapping second.

E.1. Humeral Head Wrapping:

The muscles that can wrap around the humeral head include: biceps long head, deltoid, infraspinatus, latissimus dorsi, pectoralis major, subscapularis, supraspinatus, teres major and teres minor. As such they require effective insertions to be determined for them so that their lines of action across the glenohumeral joint are accurate. Biceps is assumed to insert into the intertubercular groove for this procedure. Some of these muscles can also wrap around the humeral shaft. They are checked for head wrapping first and if it is indicated then shaft wrapping is ignored.

The humeral head coordinate system must be defined before the procedure for determining the effective muscle insertion positions due to humeral head wrapping can begin. The coordinate system is similar to the humeral coordinate system except it is rotated about the X_h axis by an angle equal in magnitude to humeral retrotorsion, θ_{ht} , as measured during the anatomical dry bone study but in the negative direction (using the right hand rule). The matrix describing the humeral head coordinate system with respect to the humeral coordinate system is:

$$[B]_{hh-h} = \begin{bmatrix} 1 & 0 & 0 \\ 0 & \cos\theta_3 & \sin\theta_3 \\ 0 & -\sin\theta_3 & \cos\theta_3 \end{bmatrix} \quad (E1)$$

where,

$$\theta_3 = -1 * \theta_{ht}$$

The orientation of the humeral head coordinate system with respect to the trunk coordinate system is now:

$$[B_{hh-t}] = [B_{hh-h}] * [B_{h-lab}] * [B_{t-lab}^{-1}] \quad (E2)$$

Humeral head coordinate system origin is the same as the humeral coordinate system origin. Its position can be calculated by using the following anatomical data: origin of the clavicle with respect to the trunk, $\{X,Y,Z\}_{Oc-t}$; origin of the scapula with respect to the clavicle, $\{X,Y,Z\}_{Os-c}$; origin of the humerus with respect to the scapula, $\{X,Y,Z\}_{Oh-s}$; in conjunction with the direction cosine matrices of these structures and an equation similar to equation 4.8. The humeral origin with respect to the trunk would then be:

$$\begin{aligned} \{X,Y,Z\}_{Oh-t} &= [B_{t-lab}] * [B_{s-lab}]^{-1} * \{X,Y,Z\}_{Oh-s} \\ &\quad + [B_{t-lab}] * [B_{c-lab}]^{-1} * \{X,Y,Z\}_{Os-c} \\ &\quad + \{X,Y,Z\}_{Oc-t} \end{aligned} \quad (E3)$$

Similarly, all of the origin and insertion positions of the muscles being checked for humeral head wrapping were converted to be with respect to the trunk coordinate system. This process is similar for any point, A, being transferred to the trunk system using the

appropriate equation depending on its anatomic location:

Trunk: No changes required.

$$\text{Clavicle: } \{X, Y, Z\}_{A-t} = [B_{t-lab}] * [B_{c-lab}]^{-1} * \{X, Y, Z\}_{A-c} + \{X, Y, Z\}_{Oc-t} \quad (\text{E4a})$$

$$\text{Scapula: } \{X, Y, Z\}_{A-t} = [B_{t-lab}] * [B_{s-lab}]^{-1} * \{X, Y, Z\}_{A-s} + [B_{t-lab}] * [B_{c-lab}]^{-1} * \{X, Y, Z\}_{Os-c} + \{X, Y, Z\}_{Oc-t} \quad (\text{E4b})$$

$$\text{Humerus: } \{X, Y, Z\}_{A-t} = [B_{t-lab}] * [B_{h-lab}]^{-1} * \{X, Y, Z\}_{A-h} + [B_{t-lab}] * [B_{s-lab}]^{-1} * \{X, Y, Z\}_{Oh-s} + [B_{t-lab}] * [B_{c-lab}]^{-1} * \{X, Y, Z\}_{Os-c} + \{X, Y, Z\}_{Oc-t} \quad (\text{E4c})$$

$$\text{Ulna: } \{X, Y, Z\}_{A-t} = [B_{t-lab}] * [B_{u-lab}]^{-1} * \{X, Y, Z\}_{A-u} + [B_{t-lab}] * [B_{h-lab}]^{-1} * \{X, Y, Z\}_{Ou-h} + [B_{t-lab}] * [B_{r-lab}]^{-1} * \{X, Y, Z\}_{Oh-s} + [B_{t-lab}] * [B_{c-lab}]^{-1} * \{X, Y, Z\}_{Os-c} + \{X, Y, Z\}_{Oc-t} \quad (\text{E4d})$$

$$\text{Radius: } \{X, Y, Z\}_{A-t} = [B_{t-lab}] * [B_{r-lab}]^{-1} * \{X, Y, Z\}_{A-r} + [B_{t-lab}] * [B_{u-lab}]^{-1} * \{X, Y, Z\}_{Or-u} + [B_{t-lab}] * [B_{h-lab}]^{-1} * \{X, Y, Z\}_{Ou-h} + [B_{t-lab}] * [B_{s-lab}]^{-1} * \{X, Y, Z\}_{Oh-s} + [B_{t-lab}] * [B_{c-lab}]^{-1} * \{X, Y, Z\}_{Os-c} + \{X, Y, Z\}_{Oc-t} \quad (\text{E4e})$$

R_{sphere} is the sphere diameter used to model the humeral head. Two values were used for R_{sphere} for the group of muscles including: biceps long head, infraspinatus, subscapularis and supraspinatus a value equal to $\frac{1}{2}$ the humeral head diameter as measured during the dry bone anatomical study was used; for the remaining muscles the following relationship was used:

$$R_{\text{sphere}} = \frac{1}{2} (\text{humeral head diameter} + 0.01) \quad [\text{m}] \quad (\text{E5})$$

No humeral anatomical muscle insertions can be inside the sphere used to model the humeral head. To ensure this, all muscle insertions are checked to see if they are inside the sphere and if so they are moved radially outward to just outside the sphere. The coordinates of point A, will be inside the sphere if:

$$R_{\text{sphere}} \geq A_1$$

where,

$$A_1 = ((X_{A-t} - X_{Oh-t})^2 + (Y_{A-t} - Y_{Oh-t})^2 + (Z_{A-t} - Z_{Oh-t})^2)^{\frac{1}{2}} \quad (\text{E6})$$

Moving point A, outside the sphere requires it to be moved radially away from the humeral head centre. The new position for point A will be:

$$X_{A'-t} = ((0.001 + R_{\text{sphere}}) / A_1) * (X_{A-t} - X_{Oh-t}) + X_{Oh-t} \quad (\text{E7a})$$

$$Y_{A-t} = ((0.001+R_{\text{sphere}}/A_1)*(Y_{A-t}-Y_{\text{Oh-t}}) + Y_{\text{Oh-t}} \quad (\text{E7b})$$

$$Z_{A-t} = ((0.001+R_{\text{sphere}}/A_1)*(Z_{A-t}-Z_{\text{Oh-t}}) + Z_{\text{Oh-t}} \quad (\text{E7c})$$

The dominant muscle plane is defined for any muscle being checked for humeral head wrapping. Depending on the particular muscle, the definition of the line D-D (see figure 5.3b) can be either parallel to the X_{hh} or Z_{hh} axes. The axes used for the muscle fascicles are:

Muscle	D-D parallel to axis
Biceps, long head	X_{hh}
Deltoid, anterior (2 fascicles)	Z_{hh}
Deltoid, middle	X_{hh}
Deltoid, posterior(2 fascicles)	Z_{hh}
Infraspinatus(3 fascicles)	Z_{hh}
Latissimus dorsi	Z_{hh}
Pectoralis major	Z_{hh}
Subscapularis(3 fascicles)	Z_{hh}
Supraspinatus	X_{hh}
Teres major	Z_{hh}
Teres minor	Z_{hh}

where the direction of D-D would be defined from the matrix $[B_{hh-t}]$ as:

$$D-D = \{b_{1,1}, b_{1,2}, b_{1,3}\}$$

or,

$$D-D = \{b_{3,1}, b_{3,2}, b_{3,3}\}$$

when D-D is parallel to the X_{hh} or Z_{hh} axes respectively.

A coordinate system, X_1, Y_1, Z_1 , can now be defined where the Y_1-Z_1 plane is equivalent to the dominant muscle plane. The definition of this coordinate system would be:

Origin: Muscle insertion.

Z_1 : Parallel to line D-D (pointing in the direction of the humeral head axis on which D-D is based).

X_1 : Cross product of Z_1 and a line through the origin and muscle origin position.

Y_1 : Cross product of the Z_1 and X_1 axes.

with direction cosine matrix $[B_{1-t}]$, describing its orientation with respect to the trunk coordinate system.

Coordinates of the muscle origin, M_{origin} , and humeral head centre, HHC, can now be given in terms of this coordinate system using the origin, $\{X, Y, Z\}_{\text{O1-t}}$, of coordinate system 1 with respect to the trunk.

$$\{X, Y, Z\}_{M_{\text{origin-1}}} = [B_{1-t}] * (\{X, Y, Z\}_{M_{\text{origin-t}}} - \{X, Y, Z\}_{\text{O1-t}}) \quad (\text{E8a})$$

$$\{X, Y, Z\}_{\text{HHC-1}} = [B_{1-t}] * (\{X, Y, Z\}_{\text{HHC-t}} - \{X, Y, Z\}_{\text{O1-t}}) \quad (\text{E8b})$$

For wrapping to occur the humeral head sphere must intersect the dominant muscle

plane. This only occurs if:

$$X_{\text{HHC-1}} \leq R_{\text{sphere}}$$

The radius of the intersection circle, R_1 , between the humeral head sphere and the dominant muscle plane, defined by Y_1 - Z_1 axes will be:

$$R_1 = R_{\text{sphere}} \sin (\cos^{-1}(X_{\text{HHC-1}}/R_{\text{sphere}})) \quad (\text{E9})$$

Latissimus dorsi and teres major require a special check for humeral head wrapping. Because both of these muscles wrap under the glenohumeral joint, anatomically their dominant muscle plane cannot rise above the humeral head sphere during large humeral elevation angles. A check must be made on plane position to see if it is improperly positioned above the sphere centre using the normal plane definition. The plane is improperly positioned if:

$$X_{\text{HHC-1}} > 0$$

If the plane is improperly positioned then it must be repositioned to pass through the humeral head centre. The radius of the intersection circle formed by the sphere and the plane will now be:

$$R_1 = R_{\text{sphere}}$$

The dominant muscle plane can now be redefined as:

Origin: Muscle insertion.

Z_1 : Parallel to line D-D (pointing in the direction of the humeral head axis on which D-D is based).

X_1 : Cross product of Z_1 and a line through the humeral head centre and muscle origin.

Y_1 : Cross product of the Z_1 and X_1 axes.

The dominant muscle plane will now be properly positioned for latissimus dorsi or teres major. The remainder of their analysis would proceed as normal.

The coordinates of the muscle origin $\{Y,Z\}_{\text{Morigin-1}}$, muscle insertion $\{Y,Z\}_{\text{Minertion-1}}$, and intersection circle centre $\{Y,Z\}_{\text{HHC-1}}$ on the two-dimensional plane must now be converted to coordinate system 2, origin at the intersection circle centre and Y_2 and Z_2 axes parallel to coordinate system 1 (ie. $[B_{2-1}] = [B_{1-1}]$).

$$\{Y,Z\}_{\text{Morigin-2}} = \{Y,Z\}_{\text{Morigin-1}} - \{Y,Z\}_{\text{HHC-1}} \quad (\text{E10a})$$

$$\{Y,Z\}_{\text{Minertion-2}} = \{Y,Z\}_{\text{Minertion-1}} - \{Y,Z\}_{\text{HHC-1}} \quad (\text{E10b})$$

$$\{Y,Z\}_{\text{HHC-2}} = \{Y,Z\}_{\text{HHC-1}} - \{Y,Z\}_{\text{HHC-1}} \quad (\text{E10c})$$

The standard moment imparted to the humerus by muscle activity is also required for wrapping correction. The format for this parameter is the moment direction around the X_2 axis imparted by the muscle to the humerus. The moment direction parameters for the muscle fascicles are:

Muscle	Moment Direction Parameter
Biceps, long head	+MD
Deltoid, anterior (2 fascicles)	-MD
Deltoid, middle	+MD
Deltoid, posterior(2 fascicles)	+MD
Infraspinatus(3 fascicles)	+MD
Latissimus dorsi	-MD
Pectoralis major	-MD
Subscapularis(3 fascicles)	-MD
Supraspinatus	+MD
Teres major	-MD
Teres minor	+MD

It should be noted that none of these muscles switch their moment direction due to arm elevation when their wrapping around the humeral head is being considered.

The information is now in the form where a standard routine (outlined in sections E.1.1. and E.1.2) can be used to check for muscle wrapping and correct it if necessary. The standard routine is used to correct for both humeral head and humeral shaft wrapping. It will be covered here for continuity but only referred to during the discussion of humeral shaft wrapping.

E.1.1. Check for Muscle Wrapping:

The muscle origin, muscle insertion and intersection circle are now ready to be checked to see if there is intersection between the circle and a line between the muscle origin and insertion. This process is broken into three parts: origin-insertion line parallel to the Z_2 axis, parallel to the Y_2 axis and not parallel to either.

1. Origin-insertion line parallel to the Z_2 axis:

If $Y_{Morigin-2} = Y_{Minsertion-2}$ then the origin-insertion line is parallel to the Z_2 axis. Assuming both origin and insertion are outside the circle, intersection between the line and the circle will occur if:

$$R_1 > \text{abs}(Y_{Minsertion-2}) \quad (E11)$$

providing,

$$Z_{Morigin-2} \leq 0 \leq Z_{Minsertion-2}$$

or,

$$Z_{Morigin-2} \geq 0 \geq Z_{Minsertion-2}$$

2. Origin-insertion line parallel to the Y_2 axis:

If $Z_{Morigin-2} = Z_{Minsertion-2}$ then the origin-insertion line is parallel to the Y_2 axis. Assuming both origin and insertion are outside the circle, intersection between the line and the circle will occur if:

$$R_1 > \text{abs}(Z_{Minsertion-2}) \quad (E12)$$

providing,

$$Y_{Morigin-2} \leq 0 \leq Y_{Minsertion-2}$$

or,

$$Y_{Morigin-2} \geq 0 \geq Y_{Minsertion-2}$$

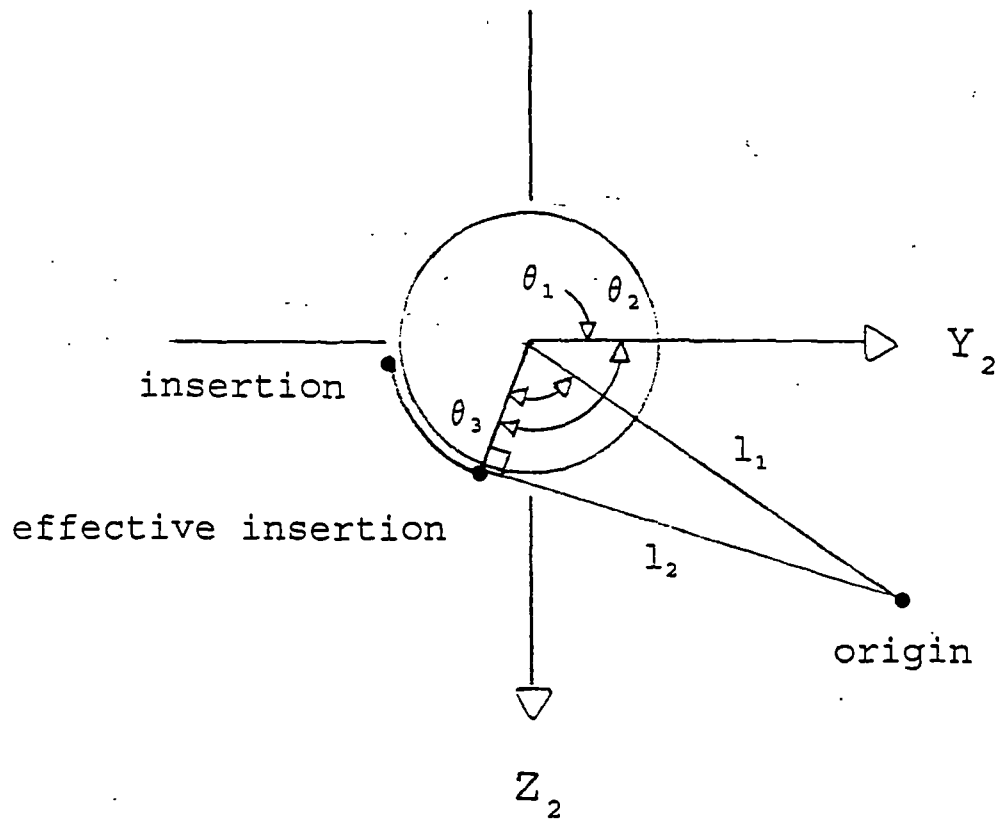


Figure E1 View of muscle origin, insertion and intersection of the humeral head or shaft on the dominant muscle plane. The angles θ_1 to θ_3 are shown with θ_1 innermost and θ_3 outermost. Using geometry, variables l_1 , l_2 , θ_1 and θ_2 can be calculated. Using this information along with the muscle direction parameter, MD, allows θ_3 and then the effective insertion position to be determined.

3. Origin-insertion line not parallel to Y_2 or Z_2 axes:

A line through the origin and insertion line can be described using the standard slope intercept equation:

$$Z = m * Y + b \quad (E13)$$

where,

$$m = (Z_{\text{Morigin-2}} - Z_{\text{Minsertion-2}}) / (Y_{\text{Morigin-2}} - Y_{\text{Minsertion-2}})$$

and b is the Z_2 axis intercept of the line. The intersection circle on the dominant muscle plane can be described using the equation of a circle:

$$R_1^2 = Z^2 + Y^2 \quad (E14)$$

Squaring equation E13 and substituting it into E14 yields the binomial equation:

$$0 = (m^2+1)Y^2 + (2mb)Y + (b^2-R_1^2) \quad (E15)$$

Solving for the roots of this equation using the binomial theorem, yields the Y_B coordinates of any possible intercepts, B , between the line and circle. If two roots, Y_{B1} and Y_{B2} are found then the line passes through the circle. Assuming that both muscle origin and insertion are outside the circle, these intercepts will be on the line between origin and insertion providing:

$$Y_{\text{Morigin-2}} \leq Y_{B1} \leq Y_{\text{Minsertion-2}}$$

or,

$$Y_{\text{Morigin-2}} \geq Y_{B1} \geq Y_{\text{Minsertion-2}}$$

E.1.2. Correcting for Muscle Wrapping:

If the line between the muscle origin and insertion passed through the circle on the dominant muscle plane, then the muscle will be wrapped around the circle. Correcting for this requires four variables (see figure E.1) to be defined:

$$l_1 = (Y_{\text{Morigin-2}}^2 + Z_{\text{Morigin-2}}^2)^{1/2} \quad (E16)$$

$$l_2 = (l_1^2 - R_1^2)^{1/2} \quad (E17)$$

$$\theta_1 = \tan^{-1}(Z_{\text{Morigin-2}}/Y_{\text{Morigin-2}}) \quad (E18)$$

$$\theta_2 = (\pi/2) - \tan^{-1}(R_1/l_2) \quad (E19)$$

The line of action for all muscles that wrap around the shaft and head of the humerus have effective insertions. No effective origins are required. The procedure for determining the effective insertions follows a technique where the angle, θ_3 , between the effective insertion and the dominant muscle plane Y_2 axis is calculated. Then using this angle, the intersection circle radius R_1 and moment direction parameter, the effective muscle insertion location can be calculated.

The procedure for determining the angle θ_3 , between the effective insertion and the Y_2 axis is subdivided into two sections, depending on the location of the muscle origin (figure E2).

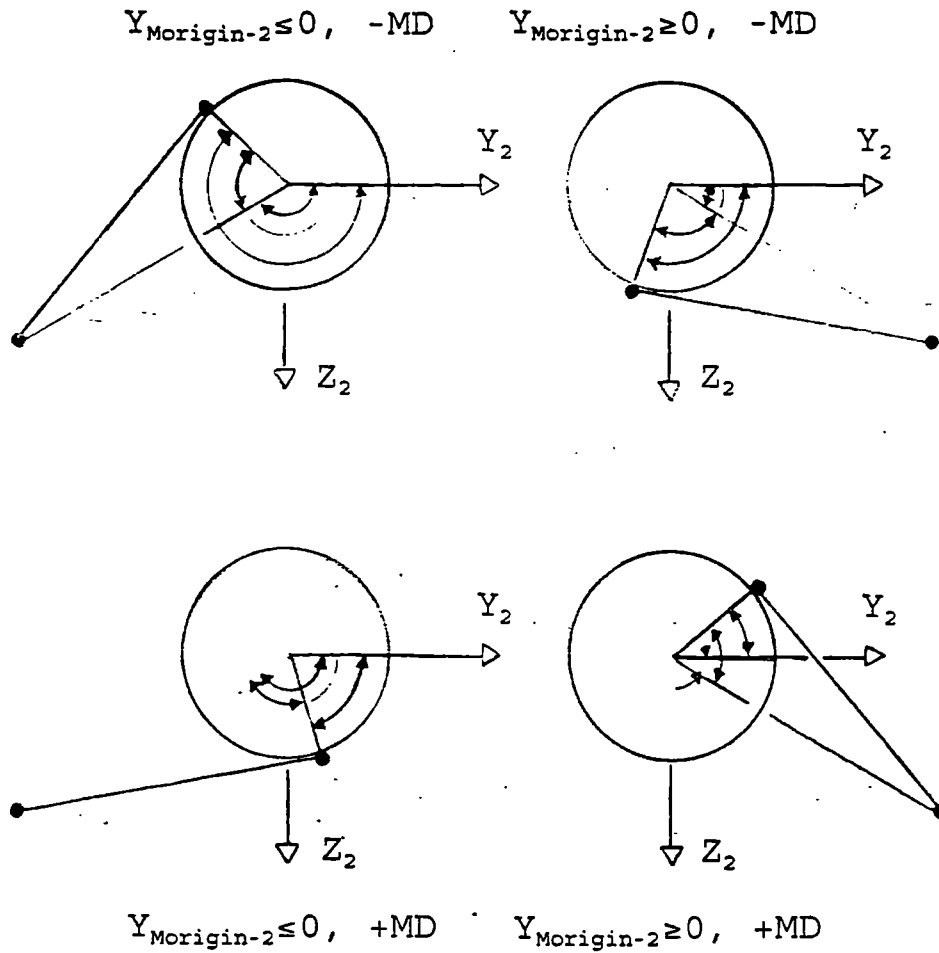


Figure E2 Four views of the dominant muscle plane similar to that shown in figure E.1. In each view, the angles θ_1 to θ_4 are shown with θ_1 , innermost and θ_4 , outermost. To improve clarity, only the angle numbers are shown. These four views correspond to the four equations (E20a - E20d) used to calculate θ , and the effective muscle insertion positions.

1. For $Y_{\text{Morigin-2}} \geq 0$:

$$\text{For -MD, } \theta_3 = \theta_1 + \theta_2 \quad (\text{E20a})$$

$$\text{For +MD, } \theta_3 = \theta_1 - \theta_2 \quad (\text{E20b})$$

2. For $Y_{\text{Morigin-2}} < 0$:

$$\text{For -MD, } \theta_3 = \pi + \theta_1 + \theta_2 \quad (\text{E20c})$$

$$\text{For +MD, } \theta_3 = \pi + \theta_1 - \theta_2 \quad (\text{E20d})$$

The effective muscle insertion positions can now be determined with respect to the $\{X,Y,Z\}_2$ coordinate system. The effective muscle insertions would be:

$$X_{\text{MEinsertion-2}} = 0 \quad (\text{E21a})$$

$$Y_{\text{MEinsertion-2}} = R_1 * \cos(\theta_3) \quad (\text{E21b})$$

$$Z_{\text{MEinsertion-2}} = R_1 * \sin(\theta_3) \quad (\text{E21c})$$

E.1.3 The Effective Insertion Coordinates:

The effective insertion coordinates can now be converted to be with respect to the anatomical humeral coordinate system so that they can be used for calculation of muscle lines of action.

The effective insertions are in terms of the dominant muscle plane coordinate system $\{X,Y,Z\}_2$. The direction cosine matrix, $[B_{2-t}]$, describing the relationship of the dominant muscle plane $\{X,Y,B\}_2$ with respect to the trunk is known. Using this matrix and the matrices describing orientation of the trunk and humeral coordinate system with respect to the lab, the anatomical coordinates can be calculated:

$$\{X,Y,Z\}_{\text{MEinsertion-h}} = [B_{h-lab}] * [B_{t-lab}]^{-1} * [B_{2-t}]^{-1} * \{X,Y,Z\}_{\text{MEinsertion-2}} \quad (\text{E22})$$

E.2. Humeral Shaft Wrapping:

The muscles that can wrap around the humeral shaft include: deltoid, latissimus dorsi, pectoralis major, teres major and teres minor. As such they require effective insertions to be determined for them so that their lines of action across the glenohumeral joint are accurate. Some of these muscles can also wrap around the humeral head. They were checked for head wrapping first and if it was indicated then shaft wrapping is ignored.

The humeral shaft coordinate system $\{X,Y,Z\}_{hs}$, must be defined before the procedure for determining the effective muscle insertion positions due to humeral shaft wrapping can begin.

The humeral shaft coordinate system is similar to the humeral coordinate system except it has a different origin. The origin of the humeral coordinate system is at the humeral head centre, the humeral shaft origin is at the intersection of the humeral shaft centre line and the $Y_h - Z_h$ plane. The origin of the humeral shaft coordinate system with respect to the humeral coordinate system can be calculated from the humeral torsion angle, θ_{ht} , and the head to shaft offset distance, $L(\text{head to shaft offset})$, measured during the anatomical dry bone study. The coordinates of the humeral coordinate system origin with respect to the humeral coordinate system will be:

$$X_{O_{hs-h}} = 0 \quad (\text{E23a})$$

$$Y_{O_{hs-h}} = L(\text{head to shaft offset}) * \cos(\theta_{ht}) \quad (\text{E23b})$$

$$Z_{O_{hs-h}} = -L(\text{head to shaft offset}) * \sin(\theta_{ht}) \quad (\text{E23c})$$

Coordinates of the humeral shaft origin can be converted to be with respect to the trunk coordinate system and origin using equation E4c. The direction cosine matrix describing the orientation of the humeral shaft coordinate system with respect to the trunk will now be:

$$[B_{hs-t}] = [B_{h-lab}] * [B_{t-lab}]^{-1} \quad (\text{E24})$$

remembering,

$$[B_{h-lab}] = [B_{hs-lab}]$$

All of the muscle origin and insertion data to be used for correcting humeral shaft wrapping must be converted to be with respect to the humeral shaft coordinate system. First it can be converted to being with respect to the trunk coordinate system using equations E4a, E4b and E4c. Any point A can then be converted to be with respect the humeral shaft coordinate system using:

$$\{X,Y,Z\}_{A-hs} = [B_{hs-t}] * (\{X,Y,Z\}_{A-t} - \{X,Y,Z\}_{O_{hs-t}}) \quad (\text{E25})$$

$R_{cylinder}$ is the cylinder diameter used to model the humeral shaft. The value used for $R_{cylinder}$ was a value equal to $\frac{1}{2}$ the humeral shaft diameter as measured during the dry bone anatomical study.

No humeral shaft muscle insertions can be inside the cylinder used to model the humeral shaft. To ensure this, all muscle insertions are checked to see if they are inside the cylinder and if so they are moved radially outward to just outside the cylinder. The coordinates of any point, A, will be inside the cylinder if:

where,

$$R_{\text{cylinder}} \geq A_2$$

$$A_2 = (Y_{A\text{-hs}}^2 + Z_{A\text{-hs}}^2)^{1/2} \quad (\text{E26})$$

Moving point A, outside the cylinder requires it to be moved radially away from the cylinder centre line. The new position for point A will be:

$$X_{A'\text{-hs}} = X_{A\text{-hs}} \quad (\text{E27a})$$

$$Y_{A'\text{-hs}} = ((0.001 + R_{\text{cylinder}}) / A_2) * Y_{A\text{-hs}} \quad (\text{E27b})$$

$$Z_{A'\text{-hs}} = ((0.001 + R_{\text{cylinder}}) / A_2) * Z_{A\text{-hs}} \quad (\text{E27c})$$

No muscle origins can be inside the cylinder (as viewed in cross section). The condition is checked using equation E26. If this situation occurs then an error message is printed and the frame of data aborted.

The standard moment imparted to the humerus by muscle activity is also required for wrapping correction. The format for this parameter is the moment direction around the X_{hs} axis imparted by the muscle to the humerus. The moment direction parameters for the muscle fascicles are:

Muscle	Moment Direction Parameter
Deltoid, anterior (2 fascicles)	-MD
Deltoid, middle	+MD
Deltoid, posterior(2 fascicles)	+MD
Latissimus dorsi	-MD
Pectoralis major	-MD
Teres major	-MD
Teres minor	+MD

All of these muscles are normally strong rotators when they become wrapped. Some can also act as weak rotators in the opposite direction to what is listed above. Only anterior deltoid (2 fascicles) appears to also wrap in the opposite direction. As a result, all muscles except anterior deltoid are considered as only single direction rotators for wrapping calculations. The change in anterior deltoid wrapping was noticed during simple verification checks used during the development of the wrapping algorithms. The problem only became apparent when the dominant muscle plane as defined for humeral head wrapping passed above the humeral head centre. To account for this situation, the moment direction parameter used for anterior deltoid was reversed when the dominant muscle plane (as defined for head wrapping) was above the humeral head centre. ie. when,

$$X_{\text{HHC-1}} > 0$$

then the moment direction parameter for anterior deltoid is changed to +MD.

The radius, R_1 , of the intersection circle between the cylinder and the dominant muscle plane will be equal to R_{cylinder} .

The dominant muscle plane coordinate system $\{X,Y,Z\}_2$, is defined as the same as the humeral shaft coordinate system, $\{X,Y,Z\}_{\text{hs}}$. The dominant muscle plane, $Y_2 - Z_2$, which is the same as $Y_{\text{hs}} - Z_{\text{hs}}$, then shows the cylinder in a cross sectional view.

The information is now in the form where a standard routine (outlined in sections

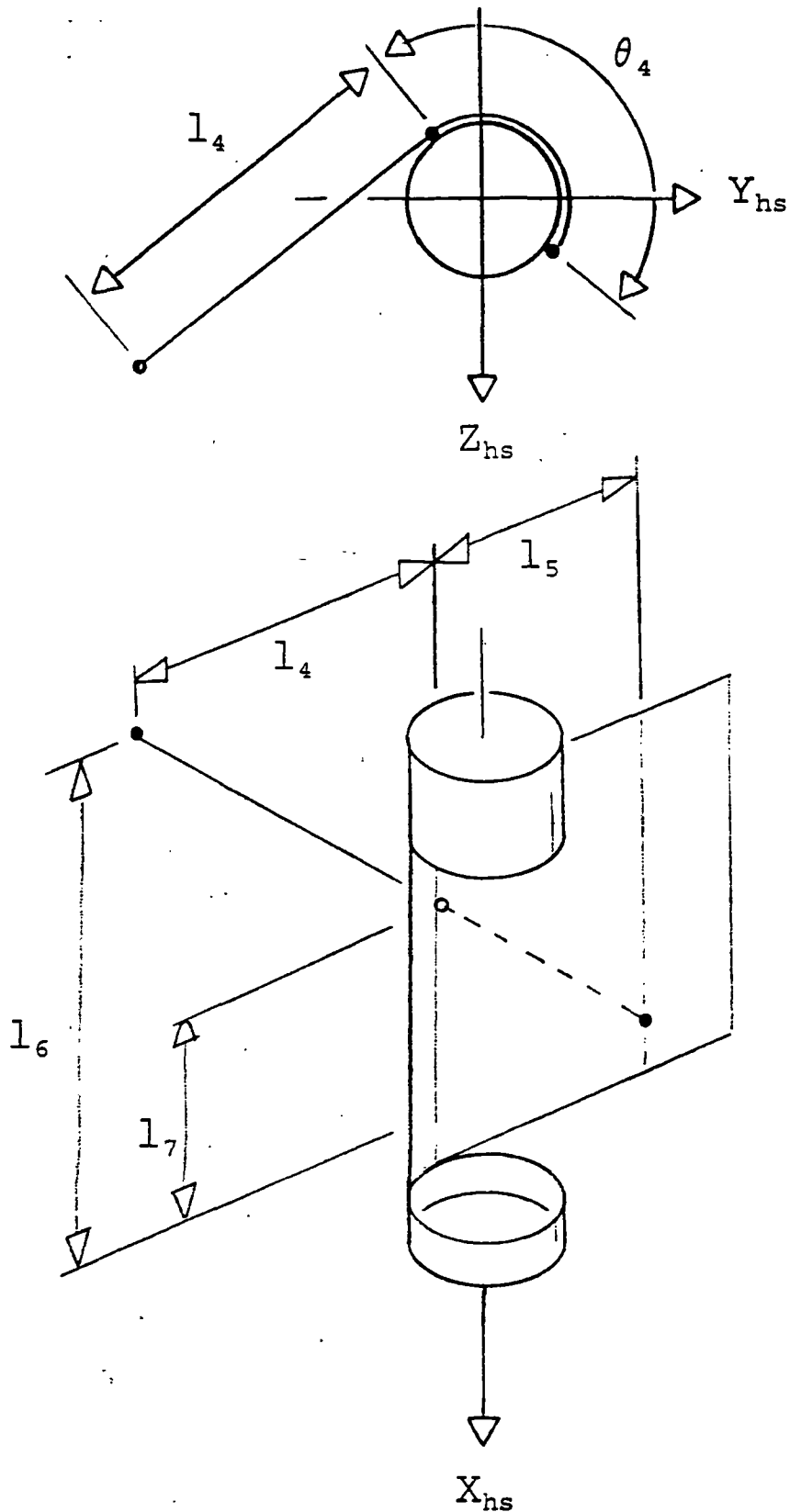


Figure E3 Two simplified views of teres major as it wraps around the humeral shaft showing all of the geometry variables required to determine the effective insertion position from the anatomical origin and insertion positions. This figure corresponds to figure 5.5. The top view shows the geometry as it would be seen in the dominant muscle plane.

E.1.1. and E.1.2) can be used to check for muscle wrapping and correct it if necessary. The coordinates of the effective insertion, $Y_{MEinsertion-hs}$ and $Z_{MEinsertion-hs}$ are returned if required.

After checking for and calculating if required the effective insertion positions on the dominant muscle plane, the effective insertion coordinates can be calculated in terms of the humeral coordinate system. Before this can be done, the X coordinate of the effective muscle insertion, $X_{MEinsertion-hs}$, in terms of the humeral shaft coordinate system is required. This calculation starts by finding the distance between muscle origin and effective insertion in the $Y_{hs} - Z_{hs}$ (dominant muscle) plane (figure E3).

$$l_4 = ((Y_{MEinsertion-hs} - Y_{Morigin-hs})^2 + (Z_{MEinsertion-hs} - Z_{Morigin-hs})^2)^{1/2} \quad (E28)$$

A vector, f_1 , through the humeral shaft origin and anatomical insertion can be defined on the $Y_{hs} - Z_{hs}$ plane. Using an iterative technique, this vector can be rotated about the X_{hs} axis until it is within a certain tolerance of a vector, f_2 , through the humeral shaft origin and effective insertion. This will allow the wrapping angle, θ_4 , to be calculated. The vectors are defined as:

$$f_1 = \{0, Y_{Minsertion-hs}, Z_{Minsertion-hs}\} \quad (E29)$$

$$f_2 = \{0, Y_{MEinsertion-hs}, Z_{MEinsertion-hs}\} \quad (E30)$$

For each step of the iterative procedure, f_1 will be rotated by a matrix [A] where:

$$[A] = \begin{bmatrix} 1 & 0 & 0 \\ 0 & \cos\theta_4 & \sin\theta_4 \\ 0 & -\sin\theta_4 & \cos\theta_4 \end{bmatrix} \quad (E31)$$

The θ_4 increment direction is determined by the muscle moment directional parameter. For +MD, θ_4 is increased in 2 degree increments from 0. For -MD; θ_4 is decreased in 2 degree increments from 0.

The residual error between the two vectors is checked for each iteration and when it reaches a minimum and it is less than the cylinder radius, the angle θ_4 can be assumed found. The residual error, A_2 , was calculated using:

$$A_2 = ((Y_{f1} - Y_{f2})^2 + (Z_{f1} - Z_{f2})^2)^{1/2} \quad (E32)$$

Using the wrapping angle, θ_4 , and the cylinder diameter, $R_{cylinder}$, the wrapped muscle length, l_5 , in the $Y_{hs} - Z_{hs}$ plane can be calculated as:

$$l_5 = (\theta_4/180) * (R_{cylinder} * \pi) \quad (E33)$$

where the equation is stated for the units of degrees used for θ_4 .

The total X_{hs} distance between the anatomical muscle origin and insertion, l_6 is required.

$$l_6 = X_{Morigin} - X_{Minsertion} \quad (E34)$$

The X_{hs} direction distance between the anatomical and effective muscle insertions, l_7 , can now be determined using similar triangles.

$$l_7/l_6 = l_5/(l_4 + l_5) \quad (\text{E35})$$

X_{hs} effective insertion position is now simply a combination of the ratio of lengths l_4 and l_5 , the distance l_6 and the anatomical insertion position.

$$X_{MEinsertion-hs} = X_{Minsertion-hs} + l_7 \quad (\text{E36})$$

This completes the calculation of the effective insertion position with respect to the humeral shaft coordinate system. The effective insertion coordinates can now be converted to be with respect to the humeral coordinate system. Using the values calculated in equations E23a - c, and remembering that the humeral and humeral shaft coordinate systems differ only in their origin positions, the effective insertion position with respect to the humeral coordinate system will be:

$$X_{MEinsertion-h} = X_{MEinsertion-hs} + 0 \quad (\text{E37a})$$

$$Y_{MEinsertion-h} = Y_{MEinsertion-hs} + Y_{Ohs-h} \quad (\text{E37b})$$

$$Z_{MEinsertion-h} = Z_{MEinsertion-hs} + Z_{Ohs-h} \quad (\text{E37c})$$

With the effective insertion coordinates in this form, they can be used in place of the anatomical insertion coordinates for use in calculating a muscle's line of action.

APPENDIX F

This appendix contains details of the data and results presented in chapter 6. All of the data is presented in spreadsheet format.

Muscle forces given in the spreadsheets all use the same format. All of the muscles were numbered during analysis (see chapter 5 for details) and the results are presented here using the same muscle order. In general muscles were listed alphabetically and their fascicles numbered using a convention of anterior to posterior, superior to inferior and or medial to lateral. See table 5.1 for the listing of muscle order.

- Contents:**
1. Preliminary study results
 2. Model sensitivity to marker coordinate data
 3. Kinematic and loading for a dynamic push-up
 4. Predicted muscle activation for a push-up
 5. Model sensitivity to hand loads for a push-up
 6. Model sensitivity to anatomical subject geometry
 7. Model sensitivity to muscle origin and insertion data
 8. Model sensitivity to all input data
 9. Karolinska transducer calibration
 10. Karolinska flexible goniometer calibration
 11. Motion analysis study abduction results
 12. Motion analysis study flexion results
 13. Motion analysis study push-up results
 14. Motion analysis study press-up results
 15. Motion analysis study chin-up results

Preliminary Study Results

MUSCLE ACTIVATION, ARM ELEVATION, GLENOID FOSSA FORCES AND JOINT MOMENTS FOR STATIC ABDUCTION WITH AND WITHOUT JOINT STABILITY SCAPULA ORIENTATION ESTIMATED FROM MEASURED STATIC SEQUENCES

Subject details: weight [N]: 591 File: THES0500.WK1 Note: humeral abduction angle is height [m]: 1.75 Date: June 9, 1993 elevation in the frontal plane Subject No. SCAPOS

Measured kinematics and hand loading [degrees, N & Nm]:

Abd An [deg]	Frame	trunk	clavicle	scapula	humerus	forearm	Fhx	Fhy	Fhz	Mhx	Mhy	Mhz											
0	1	0	0	-16	5	0	-28	48	15	-12	0	5	20	0	-7	0	0	0	0	0	0	0	
44	2	-10	4	-28	7	0	-29	30	6	43	-10	20	0	8	0	0	0	0	0	0	0	0	0
79	3	-8	5	-37	17	0	-33	18	9	82	68	-53	20	0	-10	0	0	0	0	0	0	0	0
106	4	-10	12	4	-48	26	0	-40	1	8	-60	117	54	30	0	-15	0	0	0	0	0	0	0

Muscle forces without stability constraint [N]:

Abd An [deg]	Inter:	Biceps			Coraco			Deltoid			Intra Spinalus	Latisimus Dorsi	Pectoralis Major			Sub Scapularis	Supr Spin	Teres Maj	Triceps	Intensity [0.1*N/mm2]				
		SH	LH	Brac	SH	LH	Brac	SH	LH	Brac			Min	Maj	Min						LH	Maj	Min	
0	1	0	17	0	0	0	0	0	0	0	0	0	0	0	0	7	24	25	0	0	7	13	17	0.83
44	2	0	53	0	6	0	76	80	0	56	73	80	0	0	0	43	76	101	104	0	0	69	69	3.47
79	3	47	0	33	62	0	72	75	127	52	69	19	0	0	0	26	72	95	98	0	0	65	65	3.26
106	4	21	0	27	52	0	60	63	107	44	58	63	0	0	0	46	80	82	0	35	0	55	55	2.74

Muscle forces with stability constraint [N]:

Abd An [deg]	Inter:	Biceps			Coraco			Deltoid			Intra Spinalus	Latisimus Dorsi	Pectoralis Major			Sub Scapularis	Supr Spin	Teres Maj	Triceps	Intensity [0.1*N/mm2]				
		SH	LH	Brac	SH	LH	Brac	SH	LH	Brac			Min	Maj	Min						LH	Maj	Min	
0	1	0	17	0	0	0	0	19	32	13	0	0	0	0	0	7	24	25	0	0	7	17	14	0.83
44	2	0	53	0	6	0	76	80	0	56	73	80	0	0	0	43	76	101	104	0	0	69	69	3.47
79	3	47	0	33	62	0	72	75	127	52	69	19	0	0	0	26	72	95	98	0	0	65	65	3.26
106	4	21	0	27	52	0	60	63	107	44	58	63	0	0	0	46	80	82	0	35	0	55	55	2.74

PCSA, [mm2]: 200 200 100 166 195 217 229 388 157 209 233 100 100 100 150 158 197 273 216 263 296 415 207 200 200 200

Glenoid Fossa Forces [N]

Abd An [deg]	Inter:	Fzgf			Fygf			Fxgf			Joint Moments [Nm]			Joint Orientation Angles [deg]			Humeral elevation [deg]			
		Abd	Inter	Mau	Myu	Mzh	Myh	Mzh	Abd	Inter	Mau	Myu	Mzh	flex	abd	rot	el	flex	Sag	Frontal
0	1	4	103	-7	0	1	0.0	-0.1	-0.1	1.5	0.3	0	1	-17	0	-21	17	1	-17	0
44	2	26	631	-51	44	2	0.0	0.1	-0.9	1.6	-7.0	44	2	1	44	-33	18	2	1	44
79	3	-73	751	47	79	3	-0.1	0.3	-1.2	1.3	-9.1	79	3	52	72	-70	17	3	52	79
106	4	14	677	31	106	4	-0.1	1.1	-1.4	3.2	-7.2	106	4	-52	113	29	27	4	126	106

Model Stability Results, Test 1: Sensitivity to marker coordinates

MUSCLE ACTIVATION FOR PURE ARM ABDUCTION WITH A 1 kg HAND WEIGHT AND FLEXED ELBOW (90 degrees) WITH PERTURBED MARKER COORDINATES

Subject details: Weight [N]: 591
 Height [m]: 1.75
 Subject No. SCAI05

File: ERRDAT22.WK1
 Date: October 8, 1992
 Using data From SCAI05000 - 03.A3D,
 RPROG1.PAS & ERRDAT22.OP2

AVERAGE MUSCLE FORCE [N]:		Coraco		Deltoid		Infra		Latisissimus		Pectoralis		Sub		Supr		Triceps		Intensity						
Abduct.	Input	Biceps	LH	SH	LH	SH	LH	SH	Major	Minor	Major	Minor	Scapularis	Spinalis	Major	Minor	Major	Minor	Intensity					
0	0	21	34	0	0	0	37	0	0	27	14	0	0	0	46	0	0	51	0	0	0	0	0	1.89
44	0	0	63	0	81	81	84	88	0	88	90	98	0	0	0	12	119	128	0	0	0	85	85	4.27
79	0	0	61	37	70	81	84	143	59	77	84	0	0	0	0	0	104	110	0	0	0	73	73	3.86
106	0	28	0	35	67	9	78	81	137	56	74	81	0	0	0	0	49	106	0	0	0	71	71	3.52
0	5	21	33	0	0	4	33	10	0	21	12	0	0	1	32	6	0	49	0	0	0	0	0	1.86
44	5	0	87	4	72	77	84	108	0	74	97	87	0	0	19	31	90	139	0	0	0	92	92	4.63
79	5	23	39	24	69	65	82	88	82	80	79	88	0	0	0	8	73	112	0	4	0	75	75	3.74
106	5	21	3	30	59	20	77	81	110	56	74	81	0	0	0	0	46	104	0	10	1	70	69	3.50
0	10	19	36	0	0	7	33	25	0	22	17	1	0	3	33	10	1	49	0	0	0	3	2	1.82
44	10	0	88	10	60	64	87	102	0	77	101	82	0	0	30	29	75	144	0	0	0	86	95	4.79
79	10	17	44	16	65	61	85	89	85	82	81	84	0	0	10	70	116	0	7	1	77	73	3.86	
106	10	19	8	27	52	31	81	84	108	56	77	83	1	0	2	11	58	97	0	17	3	73	69	3.87

STANDARD DEVIATION OF MUSCLE FORCE [N]:		Coraco		Deltoid		Infra		Latisissimus		Pectoralis		Sub		Supr		Triceps		Intensity						
Abduct.	Input	Biceps	LH	SH	LH	SH	LH	SH	Major	Minor	Major	Minor	Scapularis	Spinalis	Major	Minor	Major	Minor	Intensity					
0	5	6	6	0	0	10	12	15	0	12	19	0	0	4	1	0	0	10	0	0	0	0	0	0.29
44	5	1	12	12	27	18	32	10	0	12	16	36	0	0	0	0	0	23	0	0	0	16	16	0.77
79	5	29	30	17	12	13	8	8	4	6	7	8	0	0	0	0	21	48	10	0	12	0	7	0.34
106	5	11	8	12	16	27	9	10	33	7	9	10	0	0	0	0	35	10	0	21	5	8	13	0.42
0	10	10	9	3	0	13	19	23	0	16	22	5	0	5	24	17	4	22	0	0	0	12	9	0.47
44	10	2	15	18	35	32	37	29	0	15	20	42	0	0	55	38	54	28	0	0	0	19	19	0.93
79	10	25	34	18	21	25	13	14	56	9	12	21	0	0	3	22	53	18	0	17	4	12	18	0.59
106	10	19	15	17	27	30	15	16	45	16	14	15	4	0	11	26	51	41	0	27	13	14	22	0.69

% Increase: 19 30 35 49 47 39 82 37 53 35 57 61 171 184 122 51 56 21 76 36 231 81 93
 avg % Incr: 64

Kinematics and Loading for a Dynamic Push-up

Kinematics and Hand Loading for SCAP0412, A Dynamic Push-up Sequence

File: SCAP0401.WK1

Date: April 22, 92

Note: units of kinematics in degrees and loads in N & Nm.

Time [s]	Frame	TRUNK	CLAVICAL	SCAPULA	UPPER ARM	LOWER ARM	Fx	Fy	Fz	Mx	My	Mz	10*My										
1.5	75	68	-3	1	-13	13	0	-41	22	8	39	29	-28	48	0	-121	-11	75	-8	0	-5	0	-47
1.56	76	68	-3	2	-12	13	0	-41	22	9	40	30	-33	50	0	-117	-16	68	-6	0	-5	0	-45
1.62	81	68	-3	1	-18	14	0	-38	22	9	37	32	-31	59	0	-118	-25	129	-9	0	-7	0	-71
1.68	84	70	-4	1	-19	16	0	-34	22	10	31	36	-28	71	0	-117	-36	170	-7	0	-8	0	-77
1.74	87	74	-3	1	-25	18	0	-30	22	11	22	37	-21	86	0	-120	-42	203	-6	0	-8	0	-80
1.8	90	78	-3	1	-28	18	0	-28	22	12	14	42	-15	98	0	-119	-49	225	-3	0	-8	0	-82
1.84	92	80	-3	2	-28	18	0	-24	22	12	4	48	-9	113	0	-119	-52	248	-1	0	-8	0	-85
1.9	95	82	-7	4	-31	21	0	-21	23	13	4	48	-9	113	0	-120	-56	262	4	0	-8	0	-83
1.96	98	86	-7	3	-35	20	0	-19	23	13	-5	48	-1	122	0	-120	-55	276	6	0	-8	0	-80
2.02	101	89	-7	3	-32	20	0	-17	23	14	-11	48	5	126	0	-119	-59	294	20	0	-6	0	-60
2.08	104	90	-6	2	-34	18	0	-17	23	14	-15	49	9	129	0	-119	-61	305	28	0	-5	0	-46
2.1	105	90	-5	2	-32	18	0	-16	23	14	-17	47	10	130	0	-119	-61	310	28	0	-5	0	-46
2.16	106	89	-6	2	-32	18	0	-17	23	14	-13	49	7	127	0	-119	-57	319	29	0	-6	0	-56
2.22	111	88	-6	2	-32	20	0	-18	23	14	-7	51	1	124	0	-117	-51	279	32	0	-4	0	-44
2.28	114	84	-6	4	-29	20	0	-21	23	13	3	53	-10	116	0	-114	-47	257	28	0	-5	0	-51
2.34	117	81	-5	3	-27	18	0	-23	22	13	12	51	-18	108	0	-112	-44	245	27	0	-5	0	-48
2.4	120	77	-5	3	-23	16	0	-26	22	12	23	49	-27	97	0	-110	-38	234	22	0	-5	0	-45
2.46	123	72	-4	3	-20	15	0	-30	22	11	28	43	-32	84	0	-111	-27	191	17	0	-4	0	-41
2.52	126	69	-3	2	-18	13	0	-35	22	10	33	37	-32	60	0	-113	-15	129	11	0	-3	0	-25
2.58	129	66	-3	1	-16	12	0	-41	22	9	38	31	-30	50	0	-118	-8	87	3	0	-2	0	-20
2.64	132	64	-2	1	-14	9	0	-41	22	8	32	24	-16	48	0	-130	-9	52	2	0	-1	0	-12
2.7	135	64	-1	1	-12	8	0	-42	22	8	36	24	-21	47	0	-127	-13	74	-8	0	-3	0	-26

Measured Static Push-up Sequence Kinematics (from files: SCAP0406 - 10.EU1) [degrees]

Frame	TRUNK	CLAVICAL	UPPER ARM	LOWER ARM	HAND LOADS																		
1	18	-3	2	-22	19	0	-44	22	10	77	36	-41	42	0	-128	0	0	0	0	0	0	0	0
1	22	-3	-0	-20	24	0	-34	23	8	68	48	-34	70	0	-129	0	0	0	0	0	0	0	0
1	25	-3	-3	-30	23	0	-21	20	12	48	68	-19	107	0	-119	0	0	0	0	0	0	0	0
1	23	-3	-2	-31	22	0	-23	23	14	19	78	7	122	0	-121	0	0	0	0	0	0	0	0
1	25	-2	-3	-33	22	0	-12	25	15	-49	67	81	141	0	-122	0	0	0	0	0	0	0	0

Regression of Scapula Orientation Vs Elbow Flexion:

..... Xs Ys Zs	
Regression Output:	Constant	Regression Output:	Constant	Regression Output:	Constant
Std Err of Y Est	2.811	Std Err of Y Est	2.017	Std Err of Y Est	1.878
R Squared	0.962	R Squared	0.07	R Squared	0.738
No. of Observations	5	No. of Observations	5	No. of Observations	5
Degrees of Freedom	3	Degrees of Freedom	3	Degrees of Freedom	3
X Coefficient()	0.305	X Coefficient()	0.012	X Coefficient()	0.068
Std Err of Coe	0.035	Std Err of Coe	0.025	Std Err of Coe	0.023

Model Stability Results, Test 2: Sensitivity to hand loads

MUSCLE ACTIVATION FOR A DYNAMIC PUSH-UP SEQUENCE WITH PERTURBED HAND FORCES AND USING SCAPULA ORIENTATION ESTIMATED FROM MEASURED STATIC SEQUENCES

Subject details: Weight [N]: 686 File: EFRDAT32.WK1
 Height [m]: 1.80 Date: October 6, 1992
 Subject No.: SCAP04 Using data from SCAP04020.A3D, EFRIPROG3.PAS & EFRDAT32.OP2

AVERAGE MUSCLE FORCE [N]:

Time:	Input	Biceps	SH	LH	Brac	Coraco	Deltoid	Infra	Latissimus	Pectoralis	Sub	Supr	Teres	Triceps	Intensity												
[s]	SI	Dev	SH	LH	Brac	Coraco	Deltoid	--Spinatus--	----Dorsi----	----Major----	--Scapularis--	Spin	Maj	Min	Intensity												
1.56	0	71	71	38	68	68	78	82	0	57	75	40	0	0	96	78	103	107	0	0	0	16	361	361	18.05		
1.84	0	0	0	181	343	343	397	52	0	289	378	415	0	0	271	0	0	487	385	0	542	0	0	500	675	675	33.75
2.12	0	0	0	338	641	641	743	0	0	540	709	528	0	0	911	743	0	1013	0	0	0	0	54	248	248	12.39	
2.40	0	0	0	124	235	235	273	0	0	188	260	285	0	0	186	198	59	335	273	120	372	0	0	43	20	2.14	
2.64	0	43	43	21	41	41	47	0	0	34	45	0	0	0	32	19	0	50	47	56	64	0	0	43	20	2.14	
1.56	5	57	73	25	65	69	81	80	0	54	65	48	0	0	23	2	0	96	77	100	110	0	0	60	155	3.68	
1.84	5	0	5	183	347	347	402	78	0	293	384	408	0	0	274	1	0	494	356	0	549	0	0	29	366	366	18.29
2.12	5	0	0	333	632	632	732	0	0	533	699	545	0	0	423	0	5	899	724	0	999	0	0	550	668	668	33.29
2.40	5	2	0	125	238	238	275	1	0	200	263	268	0	0	189	200	53	338	270	87	376	0	0	44	250	250	12.52
2.64	5	52	54	25	52	51	61	26	0	42	52	7	1	1	35	12	5	75	61	30	83	1	0	46	20	2.77	
1.56	10	46	89	19	74	81	102	92	3	68	79	75	2	1	23	5	2	109	74	105	141	3	0	1	66	60	4.70
1.84	10	0	18	186	354	354	410	88	0	298	391	390	0	0	279	8	0	503	331	0	559	0	0	36	373	373	18.63
2.12	10	0	0	324	616	616	714	0	0	519	670	492	0	0	426	0	22	873	633	0	973	0	0	500	649	649	32.44
2.40	10	6	0	128	243	243	282	21	0	205	269	292	0	0	192	198	40	346	248	81	384	0	0	69	256	256	12.81
2.64	10	51	71	25	54	62	81	59	5	56	69	26	1	1	32	7	5	87	66	22	110	2	0	1	45	45	3.68

STANDARD DEVIATION OF MUSCLE FORCE [N]:

Time:	Input	Biceps	SH	LH	Brac	Coraco	Deltoid	Infra	Latissimus	Pectoralis	Sub	Supr	Teres	Triceps	Intensity													
[s]	SI	Dev	SH	LH	Brac	Coraco	Deltoid	--Spinatus--	----Dorsi----	----Major----	--Scapularis--	Spin	Maj	Min	Intensity													
1.56	5	29	17	16	20	17	18	27	0	22	35	44	0	0	20	8	0	25	20	21	25	0	0	16	23	0.83		
1.84	5	0	8	5	10	10	12	53	0	8	11	38	0	0	8	5	0	14	36	0	16	0	0	34	10	10	0.52	
2.12	5	0	0	14	27	27	31	0	0	23	30	78	0	0	43	0	12	39	41	0	43	0	0	90	29	29	1.43	
2.40	5	4	0	4	8	8	10	4	0	7	9	10	0	0	7	7	32	12	15	66	13	0	0	40	9	9	0.44	
2.64	5	23	21	12	12	18	22	21	34	0	20	29	17	3	3	0	16	11	26	21	27	28	3	0	1	22	20	0.95
1.56	10	44	40	22	38	43	39	59	21	39	57	67	8	5	6	29	14	7	49	39	46	52	13	0	4	36	37	1.73
1.84	10	0	24	10	19	19	22	86	0	16	21	61	0	0	15	21	0	27	79	0	30	0	0	61	20	20	1.01	
2.12	10	0	0	28	49	49	57	0	0	41	48	188	0	0	45	0	40	65	182	0	77	0	0	153	51	51	2.57	
2.40	10	15	0	8	16	16	18	57	0	13	17	30	0	0	12	24	38	22	53	86	25	0	0	58	17	17	0.83	
2.64	10	42	33	21	37	35	32	47	19	28	41	36	5	4	1	30	14	13	47	40	27	44	11	0	5	36	31	1.47

% increase: 84 111 68 88 93 83 113 . 72 61 113 310 184 . 40 99 81 84 196 42 82 711 . 69 87 72
 avg % increase: 113

MUSCLE ACTIVATION FOR A DYNAMIC PUSH-UP SEQUENCE WITH PERTURBED HAND MOMENTS AND USING SCAPULA ORIENTATION ESTIMATED FROM MEASURED STATIC SEQUENCES

Subject details: Weight [N]: 686
 Height [m]: 1.80
 Subject No: SCAP04
 File: ERRDAT33.WK1
 Date: October 8, 1992
 Using data From SCAP0420.A3D, ERRPROG3.PAS & ERRDAT33.OP2

AVERAGE MUSCLE FORCE [N]:

Time:	Input	Biceps	SH	LH	Brac	Coraco	Deltoid	Infra	Latisimus	Pectoralis	Sub	Supr	Triceps	Intensity														
[s]	SI Dev	SH	LH	UH	Brac	Coraco	Deltoid	---Spiratus---	----Dorsi----	----Major----	-Scapularis--	Spin	Maj	Min	Intensity													
[s]	SI Dev	SH	LH	UH	Brac	Coraco	Deltoid	---Spiratus---	----Dorsi----	----Major----	-Scapularis--	Spin	Maj	Min	Intensity													
1.56	0	71	71	36	68	78	82	0	57	75	40	0	0	86	78	103	107	0	0	0	71	67	3.57					
1.84	0	0	181	343	397	52	0	289	379	415	0	0	271	0	487	385	0	542	0	0	16	361	361	18.05				
2.12	0	0	338	641	841	743	0	540	709	528	0	0	421	0	911	743	0	1013	0	0	590	675	675	33.75				
2.40	0	0	124	235	235	273	0	198	260	285	0	0	186	198	59	335	273	120	372	0	0	54	248	248	12.39			
2.64	0	43	43	21	41	47	0	0	34	45	0	0	0	32	19	0	58	47	56	64	0	0	43	20	2.14			
1.56	5	64	80	19	74	71	108	79	5	55	61	49	6	0	24	9	1	118	84	98	147	3	5	0	68	48	4.90	
1.84	5	0	50	198	372	431	122	0	313	411	338	0	0	294	19	0	527	382	2	588	0	0	46	392	392	19.58		
2.12	5	0	2	334	635	635	736	0	526	653	506	0	0	387	0	42	861	603	0	1003	0	0	445	669	669	33.43		
2.40	5	17	9	131	249	249	289	6	205	269	284	0	0	197	184	55	348	245	133	394	0	0	53	262	262	13.12		
2.64	5	62	74	19	53	48	86	35	7	28	31	18	7	12	0	35	11	5	92	67	73	117	7	6	2	48	4.01	
1.56	10	88	142	27	88	78	156	108	46	57	61	57	9	0	35	11	0	142	98	118	213	32	18	7	93	67	7.64	
1.84	10	0	55	198	377	388	450	181	0	322	407	313	0	0	276	46	1	536	309	44	613	0	0	111	409	409	20.44	
2.12	10	0	11	303	661	662	761	10	0	489	557	331	0	0	308	0	88	825	482	17	1047	0	0	408	698	698	34.89	
2.40	10	37	25	140	273	284	293	11	0	199	254	272	0	0	216	169	78	305	189	151	432	0	30	60	288	288	14.39	
2.64	10	81	105	26	77	77	124	72	46	54	66	47	15	19	1	43	28	11	120	90	103	168	20	39	6	62	45	6.46

STANDARD DEVIATION OF MUSCLE FORCE (in Newtons):

Time:	Input	Biceps	SH	LH	Brac	Coraco	Deltoid	Infra	Latisimus	Pectoralis	Sub	Supr	Triceps	Intensity														
[s]	SI Dev	SH	LH	UH	Brac	Coraco	Deltoid	---Spiratus---	----Dorsi----	----Major----	-Scapularis--	Spin	Maj	Min	Intensity													
[s]	SI Dev	SH	LH	UH	Brac	Coraco	Deltoid	---Spiratus---	----Dorsi----	----Major----	-Scapularis--	Spin	Maj	Min	Intensity													
1.56	5	48	44	21	40	43	38	54	28	36	53	53	20	0	28	17	4	57	52	76	52	11	17	3	39	42	1.72	
1.84	5	0	52	16	31	31	36	143	0	26	34	121	0	0	24	37	0	46	98	15	49	0	0	92	32	32	1.62	
2.12	5	0	9	37	71	71	82	0	0	58	140	247	0	0	113	0	68	134	234	2	112	0	0	236	74	74	3.72	
2.40	5	28	25	10	20	20	23	50	0	31	44	57	0	0	15	34	56	35	84	142	31	0	0	77	21	21	1.03	
2.64	5	46	40	19	38	38	38	44	25	30	38	38	16	24	2	29	19	13	54	50	69	46	23	21	8	40	38	1.69
1.56	10	79	71	36	72	68	69	66	65	57	76	78	26	0	52	24	0	108	85	131	97	76	50	30	81	64	2.87	
1.84	10	0	78	37	71	52	61	199	0	40	87	197	0	0	68	76	8	88	174	120	83	0	0	156	55	55	2.75	
2.12	10	0	26	105	128	133	141	35	0	163	254	293	0	0	170	0	122	226	305	68	211	0	0	348	141	141	7.03	
2.40	10	63	54	27	35	52	78	45	0	77	105	110	0	0	28	80	99	144	150	177	55	0	81	107	37	37	1.85	
2.64	10	62	73	32	59	68	76	82	89	59	75	71	26	35	6	46	47	24	105	87	113	105	43	65	22	64	55	2.81
% Increase		66	78	129	85	85	86	53	282	119	96	46	57	48	214	73	113	80	109	57	98	90	251	413	59	84	70	
avg % Increase:		113																										

Model Stability Results, Test 3: Sensitivity to subject geometry

MUSCLE ACTIVATION FOR PURE ARM ABDUCTION WITH A 1 kg HAND WEIGHT AND FLEXED ELBOW WITH PERTURBED SUBJECT GEOMETRY DATA - PART 1: ANATOMICAL SCALING DATA

Subject details: Weight [N] 591
 Height [m] 1.75
 Subject No. SCAP05

File: ERRDAT42.WK1
 Date: October 13, 1992
 Using data from SCAP0500 - 03.A31, ERRPT005.PAS & ERRDAT42.DP2

AVERAGE MUSCLE FORCE [N]:

Abduct. [deg.]	Input SI Dev	Biceps		Coraco	Deltoid	Intra ---Spinatus---	Latissimus ----Dorsl----	Pectoralis ---Major-----	Sub -Scapularis--	Supr Spin	Teres Maj	Triceps -LH- --MH & LH--	Intensity [P.O.1 N/mm2]													
		LH	SH																							
0	0	21	34	0	0	27	14	0	0	46	0	0	0	0	0	2										
44	0	0	83	0	81	84	86	0	0	0	0	12	119	120	0	0	85	85	4							
79	0	0	61	37	70	81	84	143	59	77	84	0	0	104	110	0	0	73	73	4						
108	0	0	28	0	35	67	8	78	81	137	56	74	81	0	0	0	49	106	0	0	0	71	71	4		
0	5	20	35	0	0	6	38	16	0	28	1	0	0	4	47	1	0	52	0	0	0	0	0	0	2	
44	5	0	85	0	83	87	86	101	0	70	92	101	0	0	0	41	127	131	0	0	0	0	0	87	87	4
79	5	87	0	40	76	71	86	92	110	84	84	82	0	0	0	56	112	120	0	0	0	0	0	80	80	4
108	5	33	0	40	75	1	87	81	98	83	83	81	0	0	0	5	111	119	0	0	0	0	0	79	79	4
0	10	19	35	0	0	11	39	20	0	28	1	0	0	5	47	1	0	53	0	0	0	0	0	0	0	2
44	10	0	85	0	83	82	89	102	0	71	93	102	0	0	5	47	116	133	0	0	0	0	0	89	89	4
79	10	65	0	39	74	83	88	89	101	82	82	80	0	0	0	33	96	117	0	0	0	0	0	78	78	4
108	10	31	0	38	73	9	85	88	97	82	81	88	0	0	0	8	98	115	0	0	0	0	0	77	77	4

STANDARD DEVIATION OF MUSCLE FORCE [N]:

Abduct. [deg.]	Input SI Dev	Biceps		Coraco	Deltoid	Intra ---Spinatus---	Latissimus ----Dorsl----	Pectoralis ---Major-----	Sub -Scapularis--	Supr Spin	Teres Maj	Triceps -LH- --MH & LH--	Intensity														
		LH	SH																								
0	5	1	1	0	0	12	1	17	0	1	1	0	0	6	1	2	0	2	0	0	0	0	0	0	0	0	
44	5	0	1	0	2	6	2	2	0	2	2	2	0	0	0	4	3	3	0	0	0	0	2	2	0	0	
79	5	4	0	2	4	12	5	5	35	3	5	5	0	0	0	0	35	20	7	0	0	0	4	4	0	0	
108	5	2	0	2	3	9	3	3	11	2	3	3	0	0	0	0	8	10	4	0	0	0	3	3	0	0	
0	10	2	2	0	0	16	2	18	0	1	2	0	0	6	2	2	0	3	0	0	0	0	0	0	0	0	
44	10	1	7	0	6	22	23	14	0	9	12	14	0	0	0	25	18	32	18	0	0	0	12	12	1	1	
79	10	7	0	4	6	19	10	10	40	7	9	10	0	0	0	37	38	13	0	0	0	0	8	9	0	0	
108	10	7	0	4	6	21	9	10	25	7	9	10	0	0	0	18	31	13	0	0	0	0	9	9	0	0	
% Increase:	136	268	134	146	104	279	85	42	192	203	205	205	205	205	205	205	205	205	205	205	205	205	205	205	205	205	192
avg % Increase:	173																										192

MUSCLE ACTIVATION FOR PURE ARM ABDUCTION WITH A 1 kg HAND WEIGHT AND FLEXED ELBOW
WITH PERTURBED SUBJECT GEOMETRY DATA, PART 2: MARKER TO ANATOMY DISTANCES

Subject details: Weight [N]: 591
Height [m]: 1.75
Subject No. SCAP05

File: ERRDAT44.WK1
Date: October 14, 1992
Using data from SCAP0500-03.A3D, ERRPRG08.PAS & ERRDAT44.O1?2

AVERAGE MUSCLE FORCE [N]:		Deltoid		Infra		Latisimus		Pectoralis		Sub		Supr		Teres		Triceps		Intensity								
Abduct	Input	Coreco	Brac	SH	LH	SH	LH	SH	LH	SH	LH	SH	LH	SH	LH	SH	LH	[0.1° N/mm2]								
0	0	21	34	0	0	0	27	14	0	0	0	0	0	0	0	0	0	0	1.69							
44	0	0	83	0	81	84	98	0	68	90	88	0	0	0	0	12	119	128	0	0	0	85	85	4.27		
79	0	0	61	37	70	81	84	143	59	77	84	0	0	0	8	0	0	104	110	0	0	0	73	73	3.66	
108	0	26	0	35	67	8	78	81	137	56	74	81	0	0	0	0	0	49	106	0	0	0	71	71	3.52	
0	5	20	35	0	0	9	38	29	0	27	4	0	0	0	0	8	48	7	0	52	0	0	0	0	1.73	
44	5	0	85	0	84	72	88	103	0	71	94	93	0	0	0	1	44	125	134	0	0	0	89	89	4.46	
79	5	85	1	40	76	58	88	82	93	84	84	92	0	0	4	0	0	33	111	120	0	0	0	80	80	4.00
108	5	34	0	41	77	1	90	94	93	85	85	94	0	0	0	2	19	107	122	0	0	0	81	81	4.07	
0	10	20	35	0	0	10	37	27	0	25	8	0	0	0	0	7	40	8	0	52	0	0	0	0	1.73	
44	10	0	86	0	75	74	95	105	0	73	95	86	0	0	0	17	39	104	136	0	0	0	91	90	4.55	
79	10	44	22	34	73	56	87	91	85	84	83	90	0	0	8	0	0	23	104	119	0	0	0	79	79	3.97
108	10	31	1	38	71	17	87	89	103	83	83	81	1	0	0	5	18	94	114	0	0	0	79	78	3.95	

STANDARD DEVIATION OF MUSCLE FORCE [N]:		Deltoid		Infra		Latisimus		Pectoralis		Sub		Supr		Teres		Triceps		Intensity								
Abduct	Input	Coreco	Brac	SH	LH	SH	LH	SH	LH	SH	LH	SH	LH	SH	LH	SH	LH	[0.1° N/mm2]								
0	5	3	3	0	0	15	3	16	0	3	9	0	0	0	0	7	4	9	0	4	0	0	0	0	0.13	
44	5	1	3	0	5	11	4	5	0	3	4	24	0	0	0	5	28	15	6	0	0	0	4	4	0.20	
79	5	11	9	3	8	24	7	7	44	5	7	7	0	0	10	0	0	37	21	9	0	0	6	6	0.31	
108	5	6	0	4	7	9	8	8	21	6	8	8	0	0	2	0	0	17	28	23	11	0	0	7	7	0.36
0	10	6	5	0	0	15	7	19	0	10	12	0	0	0	8	15	14	0	8	0	8	0	0	0	0	0.27
44	10	1	8	0	25	20	10	0	7	9	34	0	0	0	0	37	41	44	13	0	0	0	9	10	0.45	
79	10	33	31	14	15	27	11	11	52	8	10	12	0	0	16	0	0	33	30	15	0	0	0	10	10	0.49
108	10	14	6	13	17	26	15	17	36	11	14	16	6	0	3	0	0	22	33	40	26	0	0	14	16	0.68
%increase:	182	238	289	218	50	142	59	35	111	85	57	-48	6	174	19	84	106	84	101							
avg %increase:	77																									

Model Stability Results, Test 4: Sensitivity to origin-insertion data

MUSCLE ACTIVATION FOR PURE ARM ABDUCTION WITH A 1 kg HAND WEIGHT AND FLEXED ELBOW WITH PERTURBED MUSCLE ORIGIN/INSERTION DATA

Subject details: Weight [N]: 581
 Height [m]: 1.75
 Subject No.: SCAPOS05
 File: ERRDAT52.WK1
 Date: December 28, 1992
 Using data from SCAPOS0500 - 03.A3D, MAINERR03.PAS, ERRPHK07.PAS & ERRDAT52.OP2

AVERAGE MUSCLE FORCE [N]:		Coreaco		Deltoid		Intra		Latissimus		Pectoralis		Sub		Supr		Teres		Triceps		Intensity		
Abduct.	Input	SH	LH	SH	LH	SH	LH	SH	LH	SH	LH	SH	LH	Spin	Maj	Min	Maj	Min	-LH-	--MH & LH--	(0.1° N/mm2)	
0	0	0	0	0	0	0	0	0	0	0	0	0	0	0	0	0	0	0	0	0	0	1.68
44	0	0	83	0	81	84	96	0	68	80	88	0	0	0	0	0	0	0	0	0	0	85
79	0	0	61	37	70	70	81	84	143	59	77	84	0	0	0	0	0	0	0	0	0	73
106	0	28	0	35	67	9	78	81	137	58	74	81	0	0	0	0	0	0	0	0	0	71
0	2.5	21	34	0	0	3	38	19	0	25	13	1	0	6	0	0	3	42	6	0	0	2
44	2.5	2	85	11	74	65	89	101	0	70	92	85	0	0	0	0	0	9	46	73	132	0
79	2.5	35	26	24	71	65	82	88	132	59	78	86	0	0	5	0	0	7	90	112	0	0
106	2.5	24	0	31	63	13	78	81	130	56	74	81	0	0	1	0	0	0	49	106	0	2
0	5.0	23	34	0	0	5	28	21	0	20	18	7	0	8	0	0	4	41	8	0	52	0
44	5.0	6	82	24	62	53	60	97	0	71	81	73	0	0	3	0	0	25	36	40	133	0
79	5.0	34	31	28	68	48	82	86	107	61	80	87	0	0	6	0	0	4	74	114	0	1
106	5.0	23	0	31	55	32	75	79	109	55	72	73	0	0	3	0	0	0	21	103	0	27

STANDARD DEVIATION OF MUSCLE FORCE [N]:		Coreaco		Deltoid		Intra		Latissimus		Pectoralis		Sub		Supr		Teres		Triceps		Intensity			
Abduct.	Input	SH	LH	SH	LH	SH	LH	SH	LH	SH	LH	SH	LH	Spin	Maj	Min	Maj	Min	-LH-	--MH & LH--	(0.1° N/mm2)		
0	0	0	0	0	0	0	0	0	0	0	0	0	0	0	0	0	0	0	0	0	0	0	
44	2.5	2	7	18	23	27	23	11	0	8	10	36	0	0	0	0	0	22	38	54	15	0	
79	2.5	29	18	4	12	5	5	22	3	4	5	0	0	10	0	0	0	18	26	6	0	4	
106	2.5	7	0	11	9	22	6	6	17	4	5	6	0	3	0	0	0	0	30	8	0	5	
0	5.0	6	5	2	0	11	15	17	0	12	17	15	0	6	0	0	0	6	12	0	8	0	
44	5.0	15	14	22	35	36	34	23	0	11	19	45	0	0	9	0	0	38	40	56	20	0	
79	5.0	35	33	17	15	29	14	9	53	6	9	10	0	13	0	0	0	17	41	12	0	10	
106	5.0	9	2	11	17	29	8	8	40	6	8	19	0	8	0	0	0	0	29	11	0	32	
%increase:		56	39	16	85	52	68	47	138	50	50	80	2	128				5	77	3	15	55	283
avg %increase:																						75	26

Model Stability Results, Test 5: Sensitivity to input data

MUSCLE ACTIVATION FOR PURE ARM ABDUCTION WITH A 1 kg HAND WEIGHT AND FLEXED ELBOW WITH ALL INPUT DATA PERTURBED

Subject details: Weight [N]: 591
 Height [m]: 1.75
 Subject No.: SCAP04

File: ERRDAT61.WK1
 Date: Dec 18, 1992
 Using data from SCAP0500 - 03.A3D

AVERAGE MUSCLE FORCE [N]:		Coreco		Deltoid		Infra		Latissimus		Pectoralis		Sub		Supr		Teres		Triceps		Intensily				
Abduct.	Input	Biceps	Coreco	Coreco	Brac	SH	LH	SH	LH	SH	LH	SH	LH	SH	LH	SH	LH	SH	LH	SH	LH			
0	-	21	34	0	0	37	0	0	27	14	0	0	0	0	46	0	0	51	0	0	0	1.69		
44	-	0	63	0	81	84	98	0	68	90	98	0	0	0	12	119	126	0	0	0	85	65	4.27	
79	-	0	61	37	70	81	84	143	59	77	84	0	0	0	0	104	110	0	0	0	73	73	3.86	
106	-	28	0	35	67	9	78	81	137	59	74	81	0	0	0	49	106	0	0	0	71	71	3.52	
0	-	17	44	0	0	10	37	34	0	23	18	0	0	1	9	42	24	8	63	0	0	4	3	2.21
44	-	4	90	10	74	68	97	109	0	76	88	88	0	0	4	63	69	143	0	0	0	95	92	4.76
79	-	54	14	36	74	52	89	83	75	65	85	87	0	0	4	18	90	122	0	3	0	81	81	4.06
106	-	36	0	41	73	17	83	88	75	68	76	72	0	0	4	52	127	0	16	0	85	85	4.24	

STANDARD DEVIATION OF MUSCLE FORCE [N]:

AVERAGE GLENOID FOSSA FORCE [N]:		Coreco		Deltoid		Infra		Latissimus		Pectoralis		Sub		Supr		Teres		Triceps		Intensily								
Abduct.	Input	Biceps	Coreco	Coreco	Brac	SH	LH	SH	LH	SH	LH	SH	LH	SH	LH	SH	LH	SH	LH	SH	LH							
0	-	13	16	0	0	19	27	31	3	19	24	2	2	12	3	0	4	12	33	27	18	29	0	0	11	9	0.81	
44	-	7	17	18	28	37	30	20	0	14	23	45	0	0	3	0	0	3	0	50	46	58	76	0	0	16	22	0.87
79	-	30	28	12	15	31	13	14	64	10	13	20	0	0	17	0	0	22	36	44	18	0	12	0	12	12	0.60	
106	-	19	0	11	24	26	16	18	54	12	31	40	0	0	16	0	0	22	36	44	18	0	31	2	15	15	0.74	

PERTURBATION DETAILS:
 -- Data Type -- Superimposed Uncertainty std

File: ERRDAT62.WK1
 Date: Dec 19, 1992

GLENOID FOSSA FORCES FOR ALL INPUT DATA PERTURBED:

GLENOID FOSSA FORCE STD [N]:

Abduct.	(Deg.)	Xgf	Ygf	Zgf	Xgf	Ygf	Zgf
0	-	9	225	-84	38	115	58
44	-	-77	782	-134	65	159	51
79	-	-13	813	18	34	153	65
106	-	18	740	60	50	129	80

Marker coordinates
 Subject scaling dimensions
 Marker to bony landmark dimensions
 Hand forces
 Hand moments
 Muscle origin-insertion coordinates

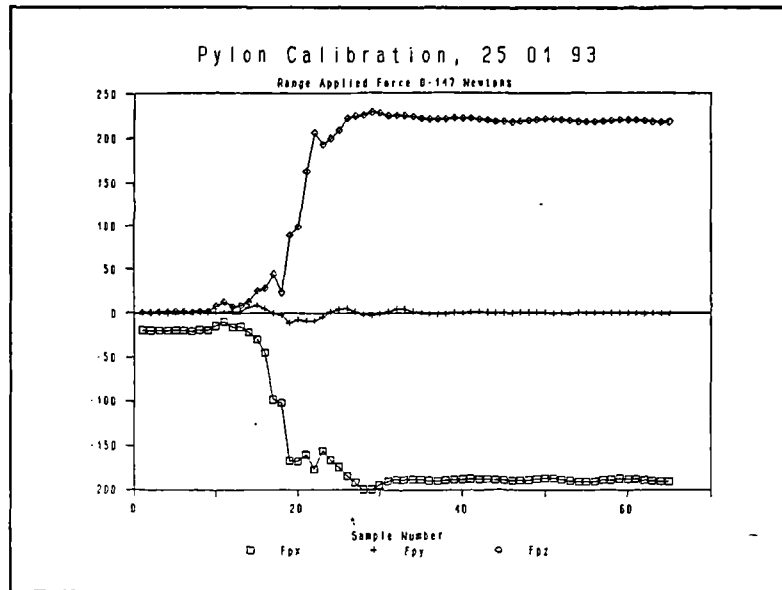
2.0 mm
 5.0 mm
 5.0 mm
 2.0 N
 1.0 Nm
 2.5 mm

Karolinska Transducer Calibration

File: CALIB02.WK1

Date: Jan 25 93

Notes: Original sampling rate was 1000 Hz. Data was averaged [100 samples at a time] and corrected for offset using the program EMGCONV.PAS to produce the RAW DATA, see graph CALIB02A.PIC for raw data details.



RESULTS: *** Computer Units ***

	Avg.Raw	Net	Calibration	Force
Vertical			Values	
Load [N]	0	147	0	147 [N/Volts] [N Units/Volt]

Xp	-19.50	-189.30	0.00	-169.80	-229.60	38986
Yp	-0.30	-0.43	0.00	-0.13	389.30	-51
Zp	1.72	220.70	0.00	218.98	226.10	49511

Because it is only a vertical force applied to the Pylon Fpx and Fpz can be used to solve the pylon orientation in space. See Calculation details this date in the notes.

$$\begin{aligned} \text{Theta} &= -1 * \text{ATAN}(\text{Fpz} / \text{Fpx}) \\ &= -1 * \text{ATAN}(49511/38986) \\ &= -52 \text{ degrees} \end{aligned}$$

The total vertical force measured is the resultant of the Xp and Zp Forces listed above. This resultant force in units [N Units/volt] can then be compared to the actual applied load to enable the overall analogue input volts to computer units to be calculated.

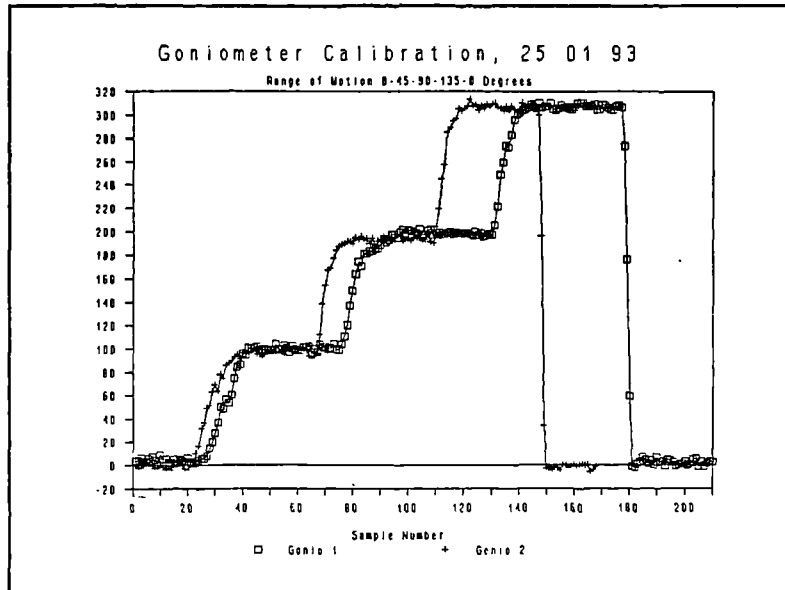
$$\begin{aligned} \text{Measured Resultant Force} &= (\text{Fpz}^2 + \text{Fpx}^2)^{0.5} \\ &= (49511^2 + 38986^2)^{0.5} \\ &= 63018 \text{ [Newton*Units/Volts]} \end{aligned}$$

$$\begin{aligned} \text{System Calibration Factor} &= \text{Applied Load/Measured Resultant Force} \\ &= 147/63018 \\ &= 0.00233 \text{ [Volts/Unit]} \end{aligned}$$

Total Channel Calibration Values: Xp: -0.536 [Newtons/computer unit]
 Yp: 0.908 [Newtons/computer unit]
 Zp: 0.527 [Newtons/computer unit]

Karolinska Flexible Goniometer Calibration

File: CALIB01.WK1
Date: Jan 25 93



Notes: Original sampling rate was 1000 Hz. Data was averaged [100 samples at a time] and corrected for offset using the program EMGCONV.PAS to produce the RAW DATA, see graph CALIB01A.PIC for raw data details.

RESULTS:

	Avg. Raw Computer Units				Net Computer Units			
Alignment [deg]	0	45	90	135	0	45	90	135
Gonio 1	4.20	100.21	199.13	307.34	0	96.01	194.93	303.14
Gonio 2	-1.15	97.10	193.54	307.24	0	98.25	194.69	308.39

Average units per degree: 2.16 2.16 2.26

Calibration factor for goniometers: 2.20 [computer unit/degree]
or, 0.455 [degrees/computer unit]

NORMALIZED MUSCLE ACTIVATION, ARM ELEVATION, GLENOID FOSSA FORCES AND JOINT MOMENTS
FOR DYNAMIC ABDUCTION WITH JOINT STABILITY
SCAPULA ORIENTATION ESTIMATED FROM MEASURED STATIC SEQUENCES
Date: June 20, 1993
File: ABDUCT03.WK1

NORMALIZED MUSCLE FORCES (% body weight):		Deltoid		Coreo		Biceps		LH		Brac		Pectoralis		Sub		Supra		Teres		Triceps		Intensity	
%	Inter:	SH	LH	Coreo	Brac	SH	LH	Coreo	Brac	SH	LH	Coreo	Brac	SH	LH	Coreo	Brac	Maj	Min	Maj	Min	Intensity	Intensity
0	0.00	0.02	0.07	0.00	0.01	0.00	0.04	0.08	0.02	0.04	0.03	0.00	0.00	0.00	0.00	0.00	0.00	0.08	0.01	0.01	0.00	0.01	1.94
5	0.05	0.02	0.05	0.00	0.01	0.00	0.01	0.05	0.09	0.01	0.05	0.00	0.00	0.00	0.00	0.00	0.00	0.10	0.01	0.01	0.00	0.03	2.78
10	0.10	0.02	0.10	0.01	0.00	0.01	0.08	0.13	0.01	0.07	0.08	0.03	0.00	0.00	0.00	0.00	0.00	0.14	0.02	0.01	0.00	0.05	3.93
15	0.15	0.02	0.14	0.01	0.01	0.01	0.05	0.11	0.18	0.10	0.13	0.07	0.00	0.00	0.00	0.00	0.00	0.19	0.02	0.03	0.00	0.09	6.36
20	0.20	0.04	0.14	0.01	0.01	0.05	0.13	0.15	0.20	0.02	0.09	0.12	0.11	0.00	0.00	0.00	0.14	0.21	0.19	0.21	0.00	0.08	7.96
25	0.25	0.07	0.12	0.01	0.08	0.11	0.17	0.16	0.04	0.06	0.08	0.09	0.00	0.00	0.00	0.00	0.21	0.22	0.21	0.20	0.00	0.08	7.30
30	0.30	0.06	0.09	0.00	0.03	0.07	0.16	0.14	0.03	0.05	0.06	0.08	0.00	0.00	0.00	0.00	0.22	0.21	0.26	0.13	0.00	0.08	7.35
35	0.35	0.06	0.07	0.00	0.01	0.08	0.15	0.11	0.02	0.05	0.04	0.03	0.00	0.00	0.00	0.00	0.20	0.28	0.11	0.00	0.06	0.05	7.12
40	0.40	0.08	0.06	0.00	0.00	0.04	0.14	0.10	0.01	0.04	0.03	0.02	0.01	0.00	0.00	0.00	0.19	0.28	0.09	0.00	0.04	0.06	7.07
45	0.45	0.05	0.05	0.00	0.01	0.03	0.13	0.08	0.02	0.05	0.02	0.01	0.02	0.00	0.00	0.00	0.18	0.15	0.27	0.12	0.00	0.04	7.97
50	0.50	0.05	0.04	0.00	0.01	0.03	0.13	0.08	0.02	0.07	0.01	0.01	0.01	0.00	0.00	0.00	0.19	0.14	0.26	0.12	0.00	0.03	8.23
55	0.55	0.08	0.04	0.00	0.01	0.04	0.12	0.09	0.01	0.07	0.01	0.01	0.03	0.00	0.00	0.00	0.18	0.15	0.26	0.12	0.00	0.03	8.07
60	0.60	0.06	0.04	0.00	0.00	0.04	0.13	0.14	0.01	0.04	0.02	0.02	0.02	0.00	0.00	0.00	0.19	0.16	0.27	0.11	0.00	0.02	7.16
65	0.65	0.06	0.07	0.00	0.01	0.07	0.13	0.14	0.01	0.03	0.04	0.05	0.01	0.00	0.00	0.00	0.21	0.17	0.27	0.14	0.00	0.02	6.21
70	0.70	0.05	0.12	0.00	0.03	0.09	0.15	0.16	0.01	0.05	0.07	0.09	0.00	0.00	0.00	0.00	0.23	0.17	0.24	0.10	0.00	0.04	6.21
75	0.75	0.03	0.16	0.00	0.07	0.11	0.15	0.18	0.03	0.08	0.11	0.10	0.00	0.00	0.00	0.00	0.21	0.19	0.19	0.19	0.01	0.05	6.50
80	0.80	0.02	0.17	0.00	0.04	0.11	0.13	0.20	0.02	0.11	0.13	0.09	0.00	0.00	0.00	0.00	0.16	0.20	0.14	0.20	0.01	0.05	6.99
85	0.85	0.01	0.17	0.00	0.01	0.03	0.09	0.18	0.00	0.10	0.12	0.07	0.00	0.00	0.00	0.00	0.18	0.16	0.06	0.20	0.01	0.04	6.15
90	0.90	0.02	0.11	0.00	0.00	0.00	0.01	0.07	0.01	0.07	0.06	0.04	0.00	0.00	0.00	0.00	0.09	0.04	0.14	0.02	0.02	0.00	3.99
95	0.95	0.02	0.07	0.00	0.00	0.00	0.03	0.06	0.08	0.02	0.05	0.04	0.01	0.00	0.00	0.00	0.04	0.07	0.06	0.09	0.02	0.01	3.25
100	1.00	0.02	0.05	0.00	0.01	0.00	0.04	0.06	0.02	0.04	0.03	0.00	0.00	0.00	0.00	0.00	0.02	0.03	0.05	0.08	0.01	0.01	1.94

PCSA, [mm2]:		200		100		186		195		217		229		369		157		209		233		100		100		100		150		197		273		293		296		415		207		200		200		200	
%	Inter:	Fygl	Fzgl	Fygl	Fzgl	Fygl	Fzgl	Fygl	Fzgl	Fygl	Fzgl	Fygl	Fzgl	Fygl	Fzgl	Fygl	Fzgl	Fygl	Fzgl	Fygl	Fzgl	Fygl	Fzgl	Fygl	Fzgl	Fygl	Fzgl	Fygl	Fzgl	Fygl	Fzgl	Fygl	Fzgl	Fygl	Fzgl	Fygl	Fzgl	Fygl	Fzgl	Fygl	Fzgl	Fygl	Fzgl				
0	0.00	-0.02	0.32	-0.01	0	0.0	0.3	-3.5	-0.9	1.0	-2.3	0	0.00	-21	2	0	0.00	-21	2	0	0.00	-21	2	0	0.00	-21	2	0	0.00	-21	2	0	0.00	-21	2	0	0.00	-21	2	0	0.00	-21	2	0	0.00	-21	2
5	0.05	-0.04	0.45	0.00	5	0.1	0.3	-3.8	-1.5	0.0	-3.6	5	0.05	-19	5	5	0.05	-19	5	5	0.05	-19	5	5	0.05	-19	5	5	0.05	-19	5	5	0.05	-19	5	5	0.05	-19	5	5	0.05	-19	5	5	0.05	-19	5
10	0.10	-0.07	0.66	0.01	10	0.1	0.4	-4.2	-2.1	-1.3	-5.4	10	0.10	-15	12	10	0.10	-15	12	10	0.10	-15	12	10	0.10	-15	12	10	0.10	-15	12	10	0.10	-15	12	10	0.10	-15	12	10	0.10	-15	12	10	0.10	-15	12
15	0.15	-0.10	1.12	0.06	15	0.2	0.3	-4.8	-3.2	-3.9	-8.4	15	0.15	-11	25	20	0.20	-5	44	20	0.20	-5	44	20	0.20	-5	44	20	0.20	-5	44	20	0.20	-5	44	20	0.20	-5	44	20	0.20	-5	44	20	0.20	-5	44
20	0.20	-0.13	1.48	0.16	20	0.2	0.3	-4.7	-4.1	-7.4	-11.0	20	0.20	-5	44	25	0.25	5	63	25	0.25	5	63	25	0.25	5	63	25	0.25	5	63	25	0.25	5	63	25	0.25	5	63	25	0.25	5	63	25	0.25	5	63
25	0.25	-0.08	1.53	0.23	25	0.3	0.2	-4.3	-4.1	-10.5	-11.6	25	0.25	5	63	30	0.30	14	80	30	0.30	14	80	30	0.30	14	80	30	0.30	14	80	30	0.30	14	80	30	0.30	14	80	30	0.30	14	80	30	0.30	14	80
30	0.30	0.06	1.39	0.22	30	0.3	0.1	-3.6	-3.5	-12.3	-10.1	30	0.30	14	80	35	0.35	20	91	35	0.35	20	91	35	0.35	20	91	35	0.35	20	91	35	0.35	20	91	35	0.35	20	91	35	0.35	20	91	35	0.35	20	91
40	0.40	0.15	1.13	0.18	40	0.4	-0.1	-1.8	-2.2	-12.2	-6.6	40	0.40	29	97	40	0.40	29	97	40	0.40	29	97	40	0.40	29	97	40	0.40	29	97	40	0.40	29	97	40	0.40	29	97	40	0.40	29	97	40	0.40	29	97
45	0.45	0.15	1.09	0.17	45	0.5	-0.2	-0.9	-1.9	-11.8	-5.8	45	0.45	33	100	45	0.45	33	100	45	0.45	33	100	45	0.45	33	100	45	0.45	33	100	45	0.45	33	100	45	0.45	33	100	45	0.45	33	100	45	0.45	33	100
50	0.50	0.14	1.08	0.17	50	0.5	-0.2	-0.8	-1.7	-11.8	-5.3	50	0.50	36	101	50	0.50	36	101	50	0.50	36	101	50	0.50	36	101	50	0.50	36	101	50	0.50	36	101	50	0.50	36	101	50	0.50	36	101	50	0.50	36	101
55	0.55	0.13	1.10	0.18	55	0.6	-0.1	-1.2	-1.8	-12.3	-5.5	55	0.55	38	100	55	0.55	38	100	55	0.55	38	100	55	0.55	38	100	55	0.55	38	100	55	0.55	38	100	55	0.55	38	100	55	0.55	38	100	55	0.55	38	100
60	0.60	0.12	1.10	0.18	60	0.6	-0.1	-1.9	-2.0	-13.1	-6.2	60	0.60	31	96	60	0.60	31	96	60	0.60	31	96	60	0.60	31	96	60	0.60	31	96	60	0.60	31	96	60	0.60	31	96	60	0.60	31	96	60	0.60	31	96
65	0.65	0.09	1.22	0.20	65	0.7	0.0	-3.2	-2.7	-14.0	-8.1	65	0.65	22	86	65	0.65	22	86	65	0.65	22	86	65	0.65	22	86	65	0.65	22	86	65	0.65	22	86	65	0.65	22	86	65	0.65	22	86	65	0.65	22	86
70	0.70	0.03	1.41	0.23	70	0.7	0.2	-4.8	-3.6	-14.0	-10.5	70	0.70	11	71	70	0.70	11	71	70	0.70	11	71	70	0.70	11	71	70	0.70	11	71	70	0.70	11	71	70	0.70	11	71	70	0.70	11	71	70	0.70	11	71
75	0.75	-0.10	1.50	0.22	75	0.8	0.3	-5.6	-4.0	-11.8	-11.8	75	0.75	-1	53	75	0.75	-1	53	75	0.75	-1	53	75	0.75	-1	53	75	0.75	-1	53	75	0.75	-1	53	75	0.75	-1	53	75	0.75	-1	53	75	0.75	-1	53
80	0.80	-0.13	1.40	0.13	80	0.8	0.3	-5.5	-3.9	-8.4	-11.3	80	0.80	-8	36	80	0.80	-8	36	80	0.80	-8	36	80	0.80	-8	36	80	0.80	-8	36	80	0.80	-8	36	80	0.80	-8	36	80	0.80	-8	36	80	0.80	-8	36
85	0.85	-0.07	1.12	0.05	85	0.9	0.3	-4.8	-3.1	-4.5	-8.8	85	0.85	-13	22	85	0.85	-13	22	85	0.85	-13	22	85	0.85	-13	22	85	0.85	-13	22	85	0.85	-13	22	85	0.85	-13	22	85	0.85	-13	22	85	0.85	-13	22
90	0.90	-0.07	0.99	-0.01	90	0.9	0.3	-4.0	-2.1	-1.1	-5.8	90	0.90	-17	11	90	0.90	-17	11	90																											

NORMALIZED MUSCLE ACTIVATION, ARM ELEVATION, GLENOID FOSSA FORCES AND JOINT MOMENTS
FOR DYNAMIC FLEXION WITH JOINT STABILITY
SCAPULA ORIENTATION ESTIMATED FROM MEASURED STATIC SEQUENCES
Date: June 21, 1983
File: FLEX03.WK1

NORMALIZED MUSCLE FORCES (% body weight):		Deltoid		Infra		Latissimus		Pectoralis		Sub		Supra		Teres		Triceps		Intensity	
Inter: %		LH		Brac		Coraco		Brac		Maj		Min		LH		RHL		[°/N/mm2]	
0	0.00	0.01	0.07	0.00	0.00	0.03	0.09	0.09	0.08	0.01	0.00	0.00	0.12	0.00	0.01	0.00	0.04	0.04	2.68
5	0.05	0.01	0.04	0.00	0.01	0.04	0.09	0.05	0.06	0.03	0.01	0.00	0.00	0.00	0.01	0.00	0.03	0.03	2.65
10	0.10	0.02	0.06	0.00	0.01	0.03	0.06	0.03	0.06	0.03	0.00	0.00	0.00	0.00	0.00	0.00	0.04	0.03	2.67
15	0.15	0.02	0.11	0.01	0.05	0.09	0.11	0.09	0.11	0.09	0.11	0.09	0.14	0.10	0.04	0.01	0.00	0.05	3.87
20	0.20	0.03	0.14	0.02	0.06	0.13	0.11	0.13	0.14	0.14	0.14	0.14	0.19	0.14	0.05	0.04	0.00	0.07	4.67
25	0.25	0.05	0.13	0.04	0.11	0.14	0.12	0.14	0.15	0.15	0.15	0.15	0.19	0.13	0.08	0.21	0.00	0.10	4.79
30	0.30	0.09	0.09	0.06	0.11	0.13	0.12	0.15	0.15	0.15	0.15	0.15	0.18	0.13	0.10	0.21	0.00	0.11	4.58
35	0.35	0.10	0.06	0.06	0.11	0.12	0.13	0.14	0.01	0.09	0.12	0.14	0.00	0.00	0.11	0.10	0.17	0.11	4.22
40	0.40	0.09	0.04	0.06	0.11	0.11	0.13	0.13	0.02	0.07	0.11	0.13	0.00	0.00	0.14	0.09	0.12	0.10	4.00
45	0.45	0.08	0.03	0.06	0.10	0.11	0.12	0.12	0.02	0.06	0.10	0.13	0.00	0.00	0.14	0.09	0.08	0.10	3.86
50	0.50	0.07	0.03	0.06	0.09	0.10	0.12	0.12	0.02	0.06	0.09	0.13	0.00	0.00	0.14	0.09	0.09	0.10	3.86
55	0.55	0.07	0.03	0.06	0.10	0.10	0.12	0.12	0.02	0.06	0.10	0.13	0.00	0.00	0.15	0.10	0.09	0.10	3.96
60	0.60	0.08	0.04	0.06	0.10	0.11	0.12	0.13	0.01	0.08	0.11	0.13	0.00	0.00	0.16	0.11	0.09	0.10	3.97
65	0.65	0.08	0.06	0.06	0.11	0.12	0.13	0.14	0.00	0.09	0.12	0.14	0.00	0.00	0.17	0.13	0.10	0.11	4.31
70	0.70	0.08	0.12	0.05	0.12	0.13	0.15	0.15	0.00	0.11	0.14	0.16	0.00	0.00	0.18	0.14	0.08	0.12	4.72
75	0.75	0.04	0.15	0.03	0.11	0.14	0.12	0.15	0.00	0.12	0.15	0.16	0.00	0.00	0.19	0.15	0.06	0.10	4.94
80	0.80	0.02	0.15	0.01	0.08	0.13	0.08	0.15	0.12	0.12	0.15	0.12	0.00	0.00	0.20	0.15	0.04	0.08	4.86
85	0.85	0.01	0.11	0.00	0.03	0.07	0.08	0.12	0.01	0.09	0.10	0.06	0.00	0.00	0.13	0.10	0.03	0.07	3.83
90	0.90	0.01	0.08	0.00	0.00	0.02	0.06	0.10	0.03	0.07	0.05	0.02	0.00	0.00	0.06	0.05	0.06	0.04	2.98
95	0.95	0.01	0.06	0.00	0.00	0.03	0.09	0.07	0.06	0.02	0.00	0.00	0.00	0.00	0.02	0.04	0.10	0.12	2.74
100	1.00	0.01	0.05	0.00	0.00	0.00	0.03	0.09	0.00	0.00	0.00	0.00	0.00	0.00	0.01	0.04	0.11	0.12	2.68

PCSA, [mm2]: 200 200 100 186 195 217 229 308 157 209 233 100 100 100 150 158 197 273 216 293 296 415 207 200 200 200

NORMALIZED GLENOID FOSSA FORCES (% body weight):

Inter: %		Fzgl		Fygl		Fzgl		Mxh		Myh		Mzh		SAGITTAL AND FRONTAL PLANE HUMERAL ELEVATION (degrees):		
Inter: %		Fzgl		Fygl		Fzgl		Mxh		Myh		Mzh		Inter: %		
0	0.00	-0.04	0.45	0.00	0.00	0.00	0.2	-1.8	-1.1	4.7	-1.5	0	0.00	-32	3	
5	0.05	-0.05	0.48	-0.01	0.00	0.00	0.1	0.3	-3.1	-1.1	1.9	-2.4	5	0.05	-23	4
10	0.10	-0.07	0.58	-0.02	0.00	0.00	0.1	0.4	-4.3	-1.2	-1.0	-3.0	10	0.10	-15	4
15	0.15	-0.12	0.83	-0.01	0.00	0.00	0.2	0.6	-5.8	-1.2	-6.0	-4.2	15	0.15	1	8
20	0.20	-0.16	1.30	0.03	0.00	0.00	0.2	0.7	-7.1	-1.3	-11.4	-5.4	20	0.20	21	13
25	0.25	-0.17	1.47	0.07	0.00	0.00	0.3	0.7	-7.3	-1.2	-15.3	-6.0	25	0.25	41	23
30	0.30	-0.13	1.53	0.07	0.00	0.00	0.3	0.6	-6.6	-0.9	-17.1	-5.6	30	0.30	59	39
35	0.35	-0.06	1.47	0.06	0.00	0.00	0.4	0.5	-5.4	-0.7	-17.0	-5.2	35	0.35	74	63
40	0.40	0.00	1.36	0.07	0.00	0.00	0.4	0.4	-4.1	-0.6	-16.1	-4.7	40	0.40	84	82
45	0.45	0.04	1.29	0.07	0.00	0.00	0.5	0.3	-3.1	-0.5	-15.1	-4.1	45	0.45	89	93
50	0.50	0.05	1.24	0.07	0.00	0.00	0.5	0.2	-2.6	-0.5	-14.8	-3.8	50	0.50	90	95
55	0.55	0.03	1.28	0.07	0.00	0.00	0.6	0.2	-3.0	-0.5	-15.0	-3.8	55	0.55	87	89
60	0.60	-0.01	1.37	0.08	0.00	0.00	0.6	0.4	-4.1	-0.6	-16.1	-4.4	60	0.60	79	74
65	0.65	-0.06	1.48	0.08	0.00	0.00	0.7	0.5	-5.6	-0.9	-17.0	-5.4	65	0.65	68	49
70	0.70	-0.16	1.55	0.09	0.00	0.00	0.7	0.6	-6.9	-1.4	-16.5	-6.6	70	0.70	48	30
75	0.75	-0.19	1.50	0.06	0.00	0.00	0.8	0.7	-7.3	-1.8	-14.0	-7.1	75	0.75	30	20
80	0.80	-0.16	1.28	0.01	0.00	0.00	0.8	0.8	-8.7	-1.7	-9.8	-6.4	80	0.80	12	14
85	0.85	-0.10	0.88	-0.04	0.00	0.00	0.9	0.9	-5.2	-1.6	-4.4	-5.0	85	0.85	-5	11
90	0.90	-0.05	0.57	-0.03	0.00	0.00	0.9	0.4	-3.6	-1.4	0.2	-3.5	90	0.90	-18	7
95	0.95	-0.04	0.46	-0.01	0.00	0.00	1.0	0.2	-2.4	-1.2	3.3	-2.4	95	0.95	-28	5
100	1.00	-0.04	0.45	0.00	0.00	0.00	1.0	0.2	-1.8	-1.1	4.7	-1.8	100	1.00	-32	3

Motion Analysis Study Push-up Results

NORMALIZED MUSCLE ACTIVATION, ARM ELEVATION, GLENOID FOSSA FORCES AND JOINT MOMENTS
 FOR A DYNAMIC PUSH-UP WITHOUT JOINT STABILITY
 SCAPULA ORIENTATION ESTIMATED FROM MEASURED STATIC SEQUENCES
 File: PUSHUP02.WK1
 Date: June 20, 1993

NORMALIZED MUSCLE FORCES (%body weight):		Deltoid		Coraco		Biceps		LH		Brac		Latissimus		Pectoralis		Sub		Scapularis		Supra		Teres		Triceps		Intensity				
%	Inter:	SH	Biceps	UH	Brac	Coraco	Brac	UH	SH	Brac	Coraco	UH	SH	Brac	UH	SH	Brac	UH	SH	Brac	UH	SH	Brac	UH	SH	Brac	UH	SH	Brac	
0	0.00	0.00	0.00	0.00	0.00	0.00	0.00	0.00	0.00	0.00	0.00	0.00	0.00	0.00	0.00	0.00	0.00	0.00	0.00	0.00	0.00	0.00	0.00	0.00	0.00	0.00	0.00	0.00	0.00	
5	0.05	0.01	0.06	0.20	0.57	0.51	0.13	0.00	0.09	0.33	0.52	0.68	0.05	0.16	0.07	0.44	0.42	0.50	0.42	0.50	0.40	0.17	0.06	0.67	0.00	0.24	0.49	0.70	0.70	23.63
10	0.10	0.00	0.00	0.20	0.50	0.46	0.11	0.00	0.03	0.30	0.49	0.62	0.05	0.14	0.06	0.44	0.42	0.50	0.42	0.50	0.40	0.17	0.06	0.67	0.00	0.24	0.46	0.64	0.64	21.50
15	0.15	0.01	0.02	0.18	0.49	0.43	0.12	0.00	0.03	0.22	0.39	0.53	0.04	0.11	0.04	0.38	0.37	0.43	0.28	0.11	0.03	0.53	0.00	0.18	0.49	0.62	0.62	0.62	20.66	
20	0.20	0.01	0.00	0.17	0.46	0.37	0.12	0.01	0.04	0.16	0.30	0.42	0.04	0.09	0.03	0.32	0.30	0.35	0.18	0.06	0.00	0.44	0.00	0.15	0.51	0.58	0.58	0.58	19.28	
25	0.25	0.00	0.00	0.14	0.45	0.29	0.09	0.00	0.03	0.14	0.25	0.32	0.08	0.03	0.28	0.23	0.26	0.12	0.03	0.02	0.38	0.00	0.13	0.48	0.51	0.51	0.51	0.51	17.02	
30	0.30	0.00	0.00	0.10	0.36	0.24	0.10	0.00	0.02	0.10	0.19	0.25	0.04	0.07	0.02	0.22	0.18	0.21	0.09	0.02	0.04	0.29	0.00	0.12	0.38	0.41	0.41	0.41	13.68	
35	0.35	0.02	0.01	0.07	0.25	0.19	0.10	0.01	0.02	0.08	0.14	0.18	0.04	0.05	0.02	0.17	0.13	0.17	0.10	0.04	0.07	0.21	0.00	0.10	0.27	0.31	0.31	0.31	10.25	
40	0.40	0.03	0.02	0.05	0.17	0.13	0.10	0.02	0.02	0.05	0.09	0.11	0.03	0.04	0.02	0.11	0.10	0.12	0.09	0.05	0.09	0.10	0.02	0.07	0.18	0.22	0.22	0.22	7.43	
45	0.45	0.04	0.04	0.03	0.12	0.09	0.08	0.02	0.01	0.03	0.05	0.07	0.03	0.04	0.03	0.08	0.08	0.09	0.10	0.06	0.09	0.06	0.05	0.04	0.11	0.15	0.15	0.15	5.37	
50	0.50	0.04	0.05	0.02	0.08	0.06	0.06	0.05	0.03	0.01	0.01	0.03	0.03	0.04	0.03	0.06	0.06	0.08	0.10	0.08	0.10	0.04	0.06	0.04	0.07	0.10	0.10	0.10	4.05	
55	0.55	0.03	0.04	0.02	0.06	0.06	0.06	0.04	0.02	0.03	0.05	0.03	0.03	0.03	0.02	0.06	0.07	0.08	0.10	0.09	0.12	0.04	0.08	0.05	0.07	0.10	0.10	0.10	4.29	
60	0.60	0.03	0.02	0.03	0.09	0.07	0.08	0.05	0.01	0.02	0.04	0.07	0.03	0.03	0.02	0.07	0.07	0.09	0.10	0.08	0.11	0.04	0.08	0.06	0.10	0.13	0.13	0.13	5.21	
65	0.65	0.02	0.00	0.04	0.15	0.12	0.09	0.02	0.02	0.04	0.08	0.10	0.03	0.03	0.01	0.09	0.09	0.11	0.07	0.07	0.07	0.08	0.11	0.05	0.07	0.16	0.16	0.16	6.82	
70	0.70	0.01	0.00	0.00	0.08	0.25	0.22	0.10	0.00	0.02	0.05	0.12	0.15	0.02	0.02	0.00	0.14	0.13	0.14	0.05	0.04	0.05	0.22	0.01	0.06	0.26	0.26	0.26	8.31	
75	0.75	0.01	0.00	0.11	0.36	0.31	0.10	0.00	0.05	0.08	0.17	0.23	0.01	0.03	0.00	0.21	0.18	0.17	0.04	0.01	0.02	0.32	0.00	0.06	0.38	0.39	0.39	0.39	13.01	
80	0.80	0.01	0.00	0.14	0.46	0.39	0.12	0.00	0.07	0.13	0.23	0.34	0.01	0.04	0.00	0.30	0.26	0.22	0.07	0.02	0.01	0.44	0.00	0.06	0.52	0.53	0.53	0.53	17.56	
85	0.85	0.00	0.01	0.17	0.53	0.47	0.14	0.00	0.10	0.20	0.31	0.41	0.01	0.06	0.00	0.37	0.30	0.31	0.14	0.03	0.02	0.65	0.00	0.10	0.81	0.85	0.85	0.85	21.64	
90	0.90	0.01	0.03	0.19	0.58	0.52	0.16	0.00	0.15	0.28	0.41	0.47	0.02	0.09	0.01	0.41	0.31	0.42	0.22	0.12	0.03	0.87	0.00	0.13	0.65	0.75	0.75	0.75	24.93	
95	0.95	0.01	0.06	0.19	0.62	0.55	0.17	0.00	0.17	0.32	0.50	0.60	0.03	0.13	0.04	0.39	0.36	0.51	0.32	0.19	0.03	0.95	0.00	0.22	0.59	0.78	0.78	0.78	26.28	
100	1.00	0.00	0.09	0.19	0.65	0.58	0.17	0.01	0.20	0.35	0.51	0.60	0.05	0.17	0.07	0.59	0.39	0.55	0.34	0.17	0.03	1.00	0.00	0.24	0.58	0.82	0.82	0.82	27.57	

PCSA, [mm2]: 200 200 100 106 195 217 229 308 157 209 230 100 100 100 100 150 158 197 2/3 2/3 2/3 296 415 207 200 200 200

NORMALIZED GLENOID FOSSA FORCES (% body weight):		NORMALIZED JOINT MOMENTS (Nm):		HUMERAL AND FOREARM ORIENTATION ANGLES (degrees):		HAND FORCES AND MOMENTS (% body weight):																								
%	Inter:	Fxgl	Fygl	Fzgl	Mxgl	Mygl	Mzgl	Inter:	Fx	Fy	Fz	Mx	My	Mz																
0	0.00	-1.28	5.02	1.37	0	0	-6.9	16.2	-11.1	-68.0	-0.8	6	108	0.00	-0.07	0.49	0.06	0.00	0.00	0.00	0.00	0.00	0.00	0.00	0.00	0.00	0.00	0.00	0.00	
5	0.05	-0.90	4.92	1.35	5	0.1	-6.6	14.9	-9.1	-66.5	0.7	4	108	0.05	-0.07	0.48	0.06	0.00	0.00	0.00	0.00	0.00	0.00	0.00	0.00	0.00	0.00	0.00	0.00	0.00
10	0.10	-0.78	4.53	1.26	10	0.1	-6.1	15.4	-7.5	-62.7	0.9	0	106	0.10	-0.07	0.46	0.06	0.00	0.00	0.00	0.00	0.00	0.00	0.00	0.00	0.00	0.00	0.00	0.00	0.00
15	0.15	-0.93	3.78	1.10	15	0.2	-5.5	17.2	-6.4	-56.4	0.2	15	101	0.15	-0.06	0.44	0.05	0.00	0.00	0.00	0.00	0.00	0.00	0.00	0.00	0.00	0.00	0.00	0.00	0.00
20	0.20	-1.02	3.17	0.92	20	0.2	-4.8	18.6	-5.4	-48.7	-0.7	20	95	0.20	-0.06	0.41	0.04	0.00	0.00	0.00	0.00	0.00	0.00	0.00	0.00	0.00	0.00	0.00	0.00	0.00
25	0.25	-0.92	2.67	0.73	25	0.3	-3.7	17.8	-3.8	-43.4	-1.7	25	85	0.25	-0.06	0.38	0.03	0.00	0.00	0.00	0.00	0.00	0.00	0.00	0.00	0.00	0.00	0.00	0.00	0.00
30	0.30	-0.77	2.18	0.52	30	0.3	-2.4	15.1	-1.9	-36.8	-2.1	30	73	0.30	-0.05	0.34	0.02	0.00	0.00	0.00	0.00	0.00	0.00	0.00	0.00	0.00	0.00	0.00	0.00	0.00
35	0.35	-0.60	1.60	0.32	35	0.4	-1.1	10.8	0.1	-30.3	-1.3	35	59	0.35	-0.05	0.30	0.00	0.00	0.00	0.00	0.00	0.00	0.00	0.00	0.00	0.00	0.00	0.00	0.00	0.00
40	0.40	-0.46	1.39	0.16	40	0.4	0.3	8.8	2.0	-23.0	0.2	40	46	0.40	-0.04	0.26	-0.01	0.00	0.00	0.00	0.00	0.00	0.00	0.00	0.00	0.00	0.00	0.00	0.00	0.00
45	0.45	-0.32	1.13	0.06	45	0.5	1.2	3.8	3.5	-17.2	2.7	45	36	0.45	-0.03	0.24	-0.01	0.00	0.00	0.00	0.00	0.00	0.00	0.00	0.00	0.00	0.00	0.00	0.00	0.00
50	0.50	-0.20	1.02	0.05	50	0.5	1.7	1.7	4.6	-14.0	4.7	50	30	0.50	-0.03	0.23	-0.01	0.00	0.00	0.00	0.00	0.00	0.00	0.00	0.00	0.00	0.00	0.00	0.00	0.00
55	0.55	-0.16	1.07	0.03	55	0.8	1.9	1.9	4.9	-14.0	4.7	55	31	0.55	-0.03	0.25	-0.02	0.00	0.00	0.00	0.00	0.00	0.00	0.00	0.00	0.00	0.00	0.00	0.00	0.00
60	0.60	-0.22	1.15	0.01	60	0.8	1.5	3.7	4.5	-15.4	3.8	60	36	0.60	-0.04	0.28	-0.01	0.00	0.00	0.00	0.00	0.00	0.00	0.00	0.00	0.00	0.00	0.00	0.00	0.00
65	0.65	-0.38	1.26	0.12	65	0.7	0.3	6.7	2.7	-18.7	1.4	65	46	0.65	-0.04	0.29	-0.00	0.00	0.00	0.00	0.00	0.00	0.00	0.00	0.00	0.00	0.00	0.00	0.00	0.00
70	0.70	-0.70	1.58	0.29	70	0.7	-1.2	10.7	-0.1	-28.5	-1.0	70	58	0.70	-0.06	0.33	0.01	0.00	0.00	0.00	0.00	0.00	0.00	0.00	0.00	0.00	0.00	0.00	0.00	0.00
75	0.75	-0.96	2.03	0.46	75	0.8	-2.7	14.8	-2.9	-34.0	-2.5	75	72	0.75	-0.07	0.37	0.02	0.00	0.00	0.00	0.00	0.00	0.00	0.00	0.00	0.00	0.00	0.00	0.00	0.00
80	0.80	-1.21	2.70	0.73	80	0.8	-3.9	18.7	-5.7	-42.7	-3.1	80	84	0.80	-0.08	0.41	0.03	0.00	0.00	0.00	0.00	0.00	0.00	0.00	0.00	0.00	0.00	0.00	0.00	0.00
85	0.85	-1.37	3.48	0.96	85	0.9	-4.9	20.3	-7.8	-50.9	-2.4	85	94	0.85	-0.08	0.44	0.04	0.00	0.00	0.00	0.00	0.00	0.00	0.00	0.00	0.00	0.00	0.00	0.00	0.00
90	0.90	-1.43	4.25	1.14	90	0.9	-5.7	19.9	-8.6	-57.4	-1.8	90	102	0.90	-0.07	0.46	0.04	0.00	0.00	0.00	0.00	0.00	0.00	0.00	0.00	0.00	0.00	0.00	0.00	0.00
95	0.95	-1.24	4.88	1.26	95	1.0	-6.3	17.4	-10.8	-63.4	-1.0	95	107	0.95	-0.08	0.47	0.05	0.00	0.00	0.00	0.00	0.00	0.00	0.00	0.00	0.00	0.00	0.00	0.00	0.00
100	1.00	-1.28	5.02	1.37	100	1.0	-6.9	16.2	-11.1	-68.0	-0.8	100	108	1.00	-0.07	0.49	0.06													

NORMALIZED MUSCLE ACTIVATION, ARM ELEVATION, GLENOID FOSSA FORCES AND JOINT MOMENTS
FOR A DYNAMIC PUSH-UP WITH JOINT STABILITY
SCAPULA ORIENTATION ESTIMATED FROM MEASURED STATIC SEQUENCES
Date: June 20, 1993
File: PUSHUP03.WK1

NORMALIZED MUSCLE FORCES (% body weight):		Deltoid		Coraco		Biceps		LH		Brac		Intra		Latissimus		Pectoralis		Sub		Supra		Teres		Triceps		Intensity		
%	Inter:	%	Inter:	%	Inter:	%	Inter:	%	Inter:	%	Inter:	%	Inter:	%	Inter:	%	Inter:	%	Inter:	%	Inter:	%	Inter:	%	Inter:	%	Inter:	
0	0.00	0.00	0.04	0.13	0.38	0.44	0.28	0.24	0.22	0.54	0.75	0.76	0.05	0.14	0.04	0.27	0.32	0.58	0.82	0.51	0.47	1.06	0.11	0.61	0.52	0.74	0.74	24.55
5	0.05	0.00	0.04	0.14	0.35	0.48	0.28	0.35	0.15	0.80	0.75	0.81	0.08	0.14	0.03	0.28	0.45	0.59	0.62	0.46	0.40	1.08	0.16	0.54	0.53	0.74	0.74	24.51
10	0.10	0.00	0.03	0.15	0.33	0.46	0.28	0.35	0.14	0.60	0.73	0.79	0.09	0.14	0.02	0.30	0.48	0.54	0.61	0.43	0.37	1.06	0.18	0.48	0.55	0.72	0.71	23.78
15	0.15	0.00	0.02	0.16	0.31	0.39	0.27	0.27	0.20	0.52	0.69	0.70	0.08	0.13	0.02	0.29	0.41	0.46	0.56	0.40	0.35	0.96	0.20	0.45	0.52	0.66	0.66	21.84
20	0.20	0.00	0.01	0.16	0.26	0.32	0.23	0.17	0.24	0.44	0.61	0.57	0.06	0.13	0.05	0.24	0.34	0.40	0.51	0.36	0.30	0.81	0.12	0.44	0.49	0.59	0.56	19.44
25	0.25	0.00	0.01	0.13	0.22	0.28	0.20	0.10	0.27	0.35	0.52	0.48	0.05	0.12	0.05	0.19	0.26	0.34	0.46	0.30	0.27	0.67	0.08	0.45	0.43	0.51	0.50	18.76
30	0.30	0.00	0.01	0.11	0.17	0.19	0.15	0.09	0.20	0.26	0.40	0.37	0.03	0.09	0.03	0.15	0.21	0.31	0.31	0.25	0.25	0.55	0.10	0.26	0.33	0.41	0.40	13.48
35	0.35	0.01	0.02	0.09	0.16	0.18	0.11	0.09	0.14	0.19	0.26	0.29	0.04	0.06	0.03	0.12	0.16	0.22	0.25	0.18	0.19	0.41	0.12	0.28	0.24	0.31	0.31	10.31
40	0.40	0.02	0.04	0.08	0.15	0.15	0.10	0.07	0.10	0.12	0.17	0.20	0.03	0.05	0.05	0.10	0.10	0.13	0.21	0.15	0.17	0.25	0.13	0.19	0.16	0.22	0.22	7.53
45	0.45	0.03	0.05	0.03	0.10	0.09	0.07	0.06	0.07	0.08	0.12	0.12	0.03	0.04	0.04	0.08	0.08	0.10	0.16	0.13	0.15	0.17	0.12	0.12	0.10	0.15	0.15	5.54
50	0.50	0.03	0.06	0.02	0.08	0.06	0.05	0.04	0.07	0.05	0.06	0.07	0.04	0.04	0.03	0.07	0.08	0.10	0.13	0.10	0.13	0.11	0.11	0.07	0.07	0.10	0.11	4.28
55	0.55	0.03	0.06	0.02	0.08	0.05	0.06	0.04	0.05	0.04	0.06	0.06	0.03	0.03	0.03	0.07	0.08	0.07	0.14	0.11	0.14	0.11	0.12	0.07	0.07	0.11	0.11	4.37
60	0.60	0.02	0.04	0.03	0.10	0.07	0.07	0.05	0.04	0.06	0.08	0.09	0.03	0.04	0.03	0.09	0.07	0.08	0.14	0.10	0.16	0.15	0.11	0.09	0.09	0.14	0.15	4.97
65	0.65	0.01	0.01	0.05	0.11	0.12	0.09	0.06	0.05	0.11	0.13	0.16	0.02	0.05	0.02	0.11	0.10	0.13	0.14	0.11	0.10	0.24	0.07	0.15	0.13	0.20	0.20	6.53
70	0.70	0.00	0.01	0.10	0.21	0.16	0.11	0.09	0.13	0.16	0.26	0.26	0.02	0.04	0.02	0.13	0.15	0.18	0.17	0.19	0.19	0.24	0.05	0.25	0.23	0.28	0.28	8.65
75	0.75	0.00	0.01	0.14	0.27	0.23	0.19	0.10	0.21	0.20	0.40	0.47	0.03	0.06	0.03	0.21	0.20	0.23	0.20	0.25	0.21	0.30	0.05	0.36	0.35	0.41	0.41	13.57
80	0.80	0.00	0.01	0.16	0.29	0.35	0.20	0.11	0.24	0.30	0.54	0.54	0.04	0.09	0.05	0.27	0.24	0.31	0.44	0.31	0.30	0.72	0.03	0.47	0.50	0.54	0.54	17.85
85	0.85	0.00	0.02	0.17	0.32	0.42	0.30	0.15	0.28	0.47	0.63	0.68	0.04	0.11	0.05	0.30	0.30	0.39	0.56	0.43	0.44	0.80	0.04	0.53	0.56	0.64	0.64	21.30
90	0.90	0.00	0.04	0.16	0.34	0.45	0.29	0.21	0.29	0.52	0.72	0.78	0.04	0.13	0.04	0.31	0.35	0.46	0.65	0.50	0.46	1.00	0.07	0.58	0.56	0.71	0.71	23.84
95	0.95	0.00	0.05	0.14	0.33	0.46	0.29	0.24	0.26	0.50	0.75	0.79	0.05	0.12	0.05	0.29	0.30	0.53	0.67	0.52	0.46	1.05	0.08	0.53	0.74	0.74	0.74	24.57
100	1.00	0.00	0.04	0.13	0.30	0.44	0.29	0.24	0.22	0.54	0.75	0.78	0.05	0.14	0.04	0.27	0.32	0.50	0.62	0.51	0.47	1.06	0.11	0.61	0.52	0.74	0.74	24.55

NORMALIZED GLENOID FOSSA FORCES (% body weight):		NORMALIZED JOINT MOMENTS (Nm):		HUMERAL AND FOREARM ORIENTATION ANGLES (degrees):		HAND FORCES AND MOMENTS (% body weight) & (% body weight/m) wrt the lab.																								
%	Inter:	%	Inter:	%	Inter:	Inter:	Inter:																							
0	0.00	-0.40	7.00	0.91	0	0.00	-16	55	-1	103	0.00	-0.07	0.49	0.06	0.00	0.00	0.00	0.00	0.00	0.00	0.00	0.00	0.00	0.00	0.00	0.00	0.00	0.00	0.00	
5	0.05	-0.49	7.20	0.87	5	0.05	-14	61	-3	108	0.05	-0.07	0.48	0.06	0.00	0.00	0.00	0.00	0.00	0.00	0.00	0.00	0.00	0.00	0.00	0.00	0.00	0.00	0.00	
10	0.10	-0.50	7.10	0.95	10	0.10	-10	63	-7	109	0.10	-0.07	0.46	0.08	0.00	0.00	0.00	0.00	0.00	0.00	0.00	0.00	0.00	0.00	0.00	0.00	0.00	0.00	0.00	
15	0.15	-0.48	6.55	0.83	15	0.2	-5.1	19.8	-6.8	-54.7	-3.2	15	0.15	0	61	-17	102	0.15	-0.06	0.44	0.05	0.00	0.00	0.00	0.00	0.00	0.00	0.00	0.00	0.00
20	0.20	-0.40	5.73	0.71	20	0.2	-4.1	19.1	-5.3	-48.3	-3.4	20	0.20	11	59	-27	93	0.20	-0.06	0.41	0.04	0.00	0.00	0.00	0.00	0.00	0.00	0.00	0.00	0.00
25	0.25	-0.30	4.86	0.55	25	0.3	-3.0	17.4	-3.6	-41.8	-3.5	25	0.25	23	55	-39	83	0.25	-0.06	0.38	0.03	0.00	0.00	0.00	0.00	0.00	0.00	0.00	0.00	0.00
30	0.30	-0.20	3.97	0.41	30	0.3	-1.9	14.4	-1.5	-35.3	-3.0	30	0.30	33	50	-49	71	0.30	-0.05	0.34	0.02	0.00	0.00	0.00	0.00	0.00	0.00	0.00	0.00	0.00
35	0.35	-0.25	3.06	0.23	35	0.4	-0.8	10.4	0.5	-29.0	-1.5	35	0.35	39	44	-53	58	0.35	-0.05	0.30	0.00	0.00	0.00	0.00	0.00	0.00	0.00	0.00	0.00	0.00
40	0.40	-0.22	2.38	0.09	40	0.4	0.5	6.5	2.3	-22.0	0.3	40	0.40	44	39	-56	45	0.40	-0.04	0.28	-0.01	0.00	0.00	0.00	0.00	0.00	0.00	0.00	0.00	0.00
45	0.45	-0.14	1.79	0.05	45	0.5	1.3	3.6	3.7	-16.7	2.9	45	0.45	46	35	-53	36	0.45	-0.03	0.24	-0.01	0.00	0.00	0.00	0.00	0.00	0.00	0.00	0.00	0.00
50	0.50	-0.12	1.41	0.04	50	0.5	1.7	1.8	4.7	-13.8	4.8	50	0.50	48	33	-52	30	0.50	-0.03	0.23	-0.01	0.00	0.00	0.00	0.00	0.00	0.00	0.00	0.00	0.00
55	0.55	-0.13	1.39	0.04	55	0.6	1.9	2.1	4.9	-14.0	4.6	55	0.55	46	33	-52	31	0.55	-0.03	0.25	-0.02	0.00	0.00	0.00	0.00	0.00	0.00	0.00	0.00	0.00
60	0.60	-0.14	1.53	0.06	60	0.8	1.4	3.8	4.4	-15.5	3.6	60	0.60	46	35	-53	36	0.60	-0.04	0.26	-0.01	0.00	0.00	0.00	0.00	0.00	0.00	0.00	0.00	0.00
65	0.65	-0.18	1.92	0.15	65	0.7	0.4	6.7	2.6	-18.3	1.3	65	0.65	43	40	-53	46	0.65	-0.04	0.29	-0.00	0.00	0.00	0.00	0.00	0.00	0.00	0.00	0.00	0.00
70	0.70	-0.30	2.89	0.30	70	0.7	-1.2	10.6	-0.2	-26.1	-1.0	70	0.70	37	45	-50	58	0.70	-0.06	0.33	0.01	0.00	0.00	0.00	0.00	0.00	0.00	0.00	0.00	0.00
75	0.75	-0.42	4.06	0.49	75	0.8	-2.7	14.5	-2.8	-34.0	-1.9	75	0.75	29	49	-42	71	0.75	-0.07	0.37	0.02	0.00	0.00	0.00	0.00	0.00	0.00	0.00	0.00	0.00
80	0.80	-0.51	5.28	0.69	80	0.8	-4.0	18.0	-5.3	-42.6	-2.3	80	0.80	19	54	-33	84	0.80	-0.08	0.41	0.03	0.00	0.00	0.00	0.00	0.00	0.00	0.00	0.00	0.00
85	0.85	-0.54	6.25	0.82	85	0.8	-4.7	19.0	-7.0	-49.4	-2.0	85	0.85	6	56	-21	93	0.85	-0.08	0.44	0.04	0.00	0.00	0.00	0.00	0.00	0.00	0.00	0.00	0.00
90	0.90	-0.51	6.96	0.91	90	0.8	-5.1	18.4	-8.0	-53.7	-1.5	90	0.90	-6	56	-10	99	0.90	-0.07	0.46	0.04	0.00	0.00	0.00	0.00	0.00	0.00	0.00	0.00	0.00
95	0.95	-0.43	7.07	0.92	95	1.0	-5.2	17.8	-8.5	-55.2	-1.4	95	0.95	-14	56	-2	102	0.95	-0.08	0.47	0.05	0.00	0.00	0.00	0.00	0.00	0.00	0.00	0.00	0.00
100	1.00	-0.40	7.00	0.91	100	1.0	-5.4	18.0	-8.2	-56.2	-1.2	100	1.00	-16	55	-1	103	1.00	-0.07	0.49	0.06	0.00	0.00	0.00	0.00	0.00	0.00	0.00	0.00	0.00

Motion Analysis Study Press-up Results

NORMALIZED MUSCLE ACTIVATION, ARM ELEVATION, GLENOID FOSSA FORCES AND JOINT MOMENTS

FOR A DYNAMIC PRESS-UP WITHOUT JOINT STABILITY

SCAPULA ORIENTATION ESTIMATED FROM MEASURED STATIC SEQUENCES

Date: June 20, 1993

File: PRESS01.WK1

% Intensity	Biceps		Coraco		Deltoid		Infra		Latissimus		Pectoralis		Sub		Supra		Terres		Triceps		Intensity		
	SH	LH	Brac	Brac	Ant	Post	Spinatus	Dorsal	Maj	Minor	Maj	Minor	Scapularis	Spin	Min	Maj	Minor	Min	Maj	Minor			
0	0.00	0.01	0.01	0.18	0.33	0.06	0.82	0.15	0.01	0.65	0.81	0.43	0.05	0.28	0.03	0.24	0.37	0.92	0.14	0.01	0.00	0.82	27.70
5	0.05	0.00	0.04	0.18	0.24	0.04	0.56	0.13	0.01	0.63	0.78	0.41	0.02	0.30	0.06	0.20	0.36	0.80	0.14	0.01	0.00	0.81	27.25
10	0.10	0.00	0.05	0.17	0.18	0.05	0.54	0.12	0.00	0.60	0.75	0.41	0.00	0.30	0.10	0.18	0.36	0.76	0.14	0.01	0.00	0.82	26.04
15	0.15	0.01	0.07	0.17	0.18	0.07	0.55	0.13	0.00	0.53	0.85	0.39	0.00	0.25	0.09	0.17	0.31	0.67	0.15	0.01	0.00	0.75	23.08
20	0.20	0.01	0.07	0.16	0.14	0.08	0.55	0.16	0.00	0.47	0.58	0.32	0.00	0.20	0.07	0.13	0.25	0.56	0.13	0.01	0.00	0.71	20.41
25	0.25	0.02	0.09	0.14	0.11	0.09	0.55	0.18	0.00	0.40	0.48	0.24	0.00	0.17	0.03	0.10	0.19	0.49	0.11	0.00	0.00	0.69	18.00
30	0.30	0.03	0.14	0.12	0.10	0.06	0.58	0.18	0.00	0.37	0.44	0.17	0.00	0.14	0.03	0.07	0.13	0.43	0.09	0.00	0.00	0.75	17.48
35	0.35	0.02	0.23	0.10	0.08	0.06	0.60	0.12	0.00	0.38	0.41	0.11	0.00	0.10	0.01	0.04	0.07	0.37	0.07	0.00	0.00	0.82	16.10
40	0.40	0.02	0.35	0.08	0.07	0.04	0.64	0.04	0.00	0.40	0.38	0.09	0.00	0.09	0.01	0.02	0.03	0.31	0.09	0.00	0.00	0.87	15.08
45	0.45	0.02	0.43	0.06	0.05	0.02	0.62	0.01	0.00	0.38	0.28	0.07	0.00	0.08	0.00	0.01	0.01	0.29	0.12	0.00	0.00	0.85	14.48
50	0.50	0.04	0.44	0.04	0.05	0.01	0.57	0.00	0.00	0.35	0.21	0.06	0.00	0.07	0.00	0.00	0.01	0.30	0.14	0.00	0.00	0.78	13.82
55	0.55	0.04	0.38	0.05	0.05	0.01	0.52	0.01	0.00	0.32	0.21	0.06	0.00	0.07	0.01	0.01	0.01	0.30	0.14	0.00	0.00	0.71	13.10
60	0.60	0.03	0.29	0.06	0.06	0.02	0.47	0.03	0.00	0.29	0.24	0.07	0.00	0.07	0.01	0.03	0.03	0.29	0.11	0.00	0.00	0.64	12.48
65	0.65	0.02	0.17	0.07	0.07	0.04	0.45	0.06	0.00	0.29	0.30	0.10	0.00	0.08	0.01	0.03	0.05	0.31	0.08	0.00	0.00	0.61	11.82
70	0.70	0.01	0.07	0.10	0.09	0.06	0.47	0.12	0.00	0.32	0.38	0.14	0.00	0.10	0.01	0.05	0.08	0.37	0.06	0.00	0.00	0.62	11.15
75	0.75	0.01	0.02	0.12	0.13	0.07	0.53	0.17	0.00	0.38	0.44	0.20	0.00	0.12	0.03	0.08	0.16	0.45	0.07	0.00	0.00	0.60	10.48
80	0.80	0.01	0.01	0.14	0.13	0.05	0.57	0.16	0.00	0.44	0.52	0.25	0.00	0.14	0.06	0.11	0.23	0.54	0.08	0.00	0.00	0.70	9.82
85	0.85	0.01	0.01	0.15	0.16	0.03	0.61	0.13	0.00	0.51	0.59	0.30	0.01	0.17	0.08	0.13	0.30	0.63	0.09	0.00	0.00	0.74	9.15
90	0.90	0.01	0.00	0.18	0.20	0.03	0.62	0.12	0.00	0.57	0.67	0.35	0.03	0.23	0.10	0.17	0.34	0.71	0.13	0.00	0.00	0.76	8.48
95	0.95	0.01	0.01	0.18	0.25	0.04	0.60	0.12	0.01	0.60	0.74	0.40	0.04	0.27	0.08	0.19	0.34	0.75	0.15	0.01	0.00	0.76	7.82
100	1.00	0.01	0.01	0.19	0.33	0.06	0.62	0.15	0.01	0.65	0.81	0.43	0.05	0.28	0.03	0.24	0.37	0.82	0.14	0.01	0.00	0.76	7.15

NORMALIZED GLENOID FOSSA FORCES (x body weight):

% Intensity	Fzgl			Fygl			Fzgl			Mx			My			Mz			
	Inter:	Fzgl	Fygl	Fzgl	Fygl	Fzgl	Mx	Fy	Fz	Mx	Fy	Fz	Mx	Fy	Fz	Mx	Fy	Fz	
0	0.00	-1.17	3.37	2.13	0.00	0.00	2.2	19.0	-20.0	-64.9	-8.1	0.00	0.07	0.44	0.12	-0.001	0.002	-0.018	
5	0.05	-0.84	3.34	1.93	0.01	1.8	17.8	-17.8	-67.2	-7.1	5	0.05	0.06	0.46	0.12	-0.001	0.002	-0.016	
10	0.10	-0.83	3.27	1.72	0.01	1.4	16.3	-16.2	-67.5	-7.2	10	0.10	0.08	0.47	0.11	-0.001	0.002	-0.016	
15	0.15	-0.86	2.99	1.33	0.02	1.1	14.0	-14.2	-62.8	-8.3	15	0.15	0.06	0.43	0.10	-0.001	0.002	-0.015	
20	0.20	-0.92	2.66	0.94	0.02	0.9	12.2	-12.7	-54.8	-10.2	20	0.20	0.05	0.40	0.07	-0.001	0.001	-0.013	
25	0.25	-0.94	2.35	0.58	0.03	0.8	9.8	-11.3	-48.3	-12.3	25	0.25	0.03	0.35	0.05	-0.001	0.001	-0.010	
30	0.30	-0.95	2.24	0.33	0.03	0.9	7.1	-10.5	-39.4	-15.1	30	0.30	0.02	0.33	0.02	0.000	0.000	-0.008	
35	0.35	-0.91	2.18	0.07	0.04	0.9	4.2	-8.5	-34.8	-17.5	35	0.35	0.02	0.31	-0.00	0.000	0.000	-0.008	
40	0.40	-0.85	2.25	-0.17	0.04	0.9	0.7	-8.1	-33.3	-19.3	40	0.40	0.01	0.30	-0.02	0.000	0.000	-0.007	
45	0.45	-0.79	2.19	-0.26	0.05	0.8	-2.4	-6.5	-32.3	-19.2	45	0.45	0.00	0.29	-0.02	0.000	0.000	-0.006	
50	0.50	-0.75	2.07	-0.22	0.05	0.7	-4.4	-5.0	-31.9	-17.6	50	0.50	0.00	0.27	-0.02	0.000	0.000	-0.006	
55	0.55	-0.71	1.90	-0.16	0.05	0.8	-3.7	-4.8	-30.8	-16.0	55	0.55	0.00	0.27	-0.02	0.000	0.000	-0.006	
60	0.60	-0.67	1.72	-0.07	0.06	0.8	-1.1	-5.4	-29.8	-14.7	60	0.60	0.01	0.27	-0.01	0.000	0.000	-0.007	
65	0.65	-0.68	1.64	0.07	0.05	0.7	0.8	-3.5	-8.9	-30.0	-14.1	65	0.65	0.01	0.29	0.00	0.000	0.000	-0.008
70	0.70	-0.80	1.72	0.31	0.07	1.1	8.7	-8.9	-32.5	-13.4	70	0.70	0.02	0.32	0.02	-0.001	0.000	-0.009	
75	0.75	-0.99	2.04	0.63	0.08	1.5	13.5	-10.9	-37.6	-12.7	75	0.75	0.04	0.38	0.03	-0.001	0.000	-0.011	
80	0.80	-1.06	2.34	0.89	0.08	1.8	16.4	-12.7	-44.2	-11.7	80	0.80	0.05	0.38	0.05	-0.001	0.000	-0.012	
85	0.85	-1.07	2.64	1.37	0.09	2.1	18.2	-14.4	-50.6	-10.5	85	0.85	0.06	0.41	0.07	-0.001	0.000	-0.014	
90	0.90	-1.07	2.98	1.75	0.09	2.2	18.5	-15.8	-56.5	-9.1	90	0.90	0.06	0.41	0.09	-0.001	0.000	-0.014	
95	0.95	-1.04	3.15	1.92	0.09	2.2	18.3	-17.2	-60.1	-8.1	95	0.95	0.06	0.42	0.10	-0.001	0.000	-0.015	
100	1.00	-1.17	3.37	2.13	0.10	2.2	19.0	-20.0	-64.9	-8.1	100	1.00	0.07	0.44	0.12	-0.001	0.002	-0.016	

HUMERAL AND FOREARM ORIENTATION ANGLES (degrees):

% Intensity	FlexU			RoHt			FlexL			RoHt							
	Inter:	FlexU	RoHt	FlexL	RoHt	FlexL	RoHt	FlexL	RoHt	FlexL	RoHt						
0	0.00	-57	50	-24	107	0.00	-57	50	-24	107	0.00	-57	50	-24	107		
5	0.05	-57	46	-23	104	5	0.05	-57	46	-23	104	5	0.05	-57	46	-23	104
10	0.10	-55	44	-25	100	10	0.10	-55	44	-25	100	10	0.10	-55	44	-25	100
15	0.15	-49	43	-30	94	15	0.15	-49	43	-30	94	15	0.15	-49	43	-30	94
20	0.20	-43	40	-35	85	20	0.20	-43	40	-35	85	20	0.20	-43	40	-35	85
25	0.25	-37	37	-39	75	25	0.25	-37	37	-39	75	25	0.25	-37	37	-39	75
30	0.30	-33	33	-42	65	30	0.30	-33	33	-42	65	30	0.30	-33	33	-42	65
35	0.35	-31	28	-42	55	35	0.35	-31	28	-42	55	35	0.35	-31	28	-42	55
40	0.40	-30	24	-41	47	40	0.40	-30	24	-41	47	40	0.40	-30	24	-41	47
45	0.45	-30	22	-39	41	45	0.45	-30	22	-39	41	45	0.45	-30	22	-39	41
50	0.50	-31	20	-38	38	50	0.50	-31	20	-38	38	50	0.50	-31	20	-38	38
55	0.55	-31	21	-36	40	55	0.55	-31	21	-36	40	55	0.55	-31	21	-36	40
60	0.60	-31	24	-38	45	60	0.60	-31	24	-38	45	60	0.60	-31	24	-38	45
65	0.65	-32	29	-41	54	65	0.65	-32	29	-41	54	65	0.65	-32	29	-41	54
70	0.70	-33	34	-42	64	70	0.70	-33	34	-42	64	70	0.70	-33	34	-42	64
75	0.75	-37	39	-41	75	75	0.75	-37	39	-41	75	75	0.75	-37	39	-41	75
80	0.80	-41	42	-38	84	80	0.80	-41	42	-38	84	80	0.80	-41	42	-38	84
85	0.85	-47	45	-35	93	85	0.85	-47	45	-35	93	85	0.85	-47	45	-35	93
90	0.90	-52	47	-30	100	90	0.90	-52	47	-30	100	90	0.90	-52	47	-30	100
95	0.95	-56	48	-27	104	95	0.95	-56	48	-27	104	95	0.95	-56	48	-27	104
100	1.00	-57	50	-24	107	100	1.00	-57	50	-24	107	100	1.00	-57	50	-24	107

NORMALIZED MUSCLE ACTIVATION, ARM ELEVATION, GLENOID FOSSA FORCES AND JOINT MOMENTS
FOR A DYNAMIC PRESS-UP WITH JOINT STABILITY
SCAPULA ORIENTATION ESTIMATED FROM MEASURED STATIC SEQUENCES
File: PRESS03.WK1
Date: June 20, 1993

NORMALIZED MUSCLE FORCES (*body weight):		Coraco		Deltoid		Intra		Latisimus		Pectoralis		Sub		Supra		Teres		Triceps		Intensity				
%	Inter:	Biceps	SH	LH	Brac	Coraco	Brac	SH	LH	Brac	Coraco	Brac	SH	LH	Brac	Coraco	Brac	SH	LH	Brac	Coraco	Brac		
0	0.00	0.00	0.05	0.00	0.31	0.24	0.00	0.00	0.03	0.82	1.07	0.61	0.01	0.15	0.21	0.00	0.01	0.58	0.31	0.04	0.01	1.37	0.17	1.03
5	0.05	0.00	0.06	0.00	0.20	0.26	0.02	0.00	0.02	0.81	1.05	0.62	0.00	0.21	0.26	0.00	0.01	0.61	0.38	0.08	0.00	1.37	0.17	1.03
10	0.10	0.00	0.08	0.00	0.11	0.26	0.06	0.00	0.01	0.78	0.98	0.61	0.00	0.24	0.27	0.00	0.01	0.62	0.38	0.08	0.00	1.32	0.16	0.87
15	0.15	0.00	0.09	0.00	0.07	0.21	0.18	0.00	0.01	0.63	0.81	0.53	0.00	0.28	0.19	0.00	0.01	0.54	0.30	0.07	0.01	1.17	0.06	0.81
20	0.20	0.00	0.10	0.01	0.06	0.17	0.31	0.00	0.01	0.53	0.67	0.43	0.00	0.25	0.14	0.00	0.02	0.47	0.21	0.06	0.05	1.00	0.11	0.69
25	0.25	0.00	0.12	0.01	0.08	0.13	0.38	0.00	0.00	0.48	0.56	0.31	0.01	0.20	0.10	0.00	0.02	0.42	0.16	0.04	0.05	0.84	0.01	0.59
30	0.30	0.00	0.17	0.01	0.06	0.10	0.45	0.00	0.00	0.44	0.51	0.23	0.00	0.17	0.10	0.00	0.01	0.37	0.13	0.03	0.03	0.83	0.00	0.55
35	0.35	0.00	0.26	0.01	0.02	0.07	0.55	0.00	0.00	0.43	0.48	0.18	0.00	0.16	0.07	0.00	0.02	0.31	0.13	0.02	0.05	0.67	0.00	0.57
40	0.40	0.00	0.39	0.01	0.00	0.05	0.60	0.00	0.00	0.44	0.46	0.15	0.00	0.15	0.08	0.00	0.01	0.27	0.14	0.04	0.07	0.94	0.00	0.60
45	0.45	0.00	0.47	0.01	0.00	0.02	0.81	0.00	0.00	0.42	0.39	0.12	0.00	0.15	0.07	0.00	0.01	0.25	0.15	0.06	0.09	0.91	0.00	0.56
50	0.50	0.01	0.48	0.00	0.00	0.01	0.59	0.00	0.00	0.38	0.33	0.13	0.00	0.16	0.07	0.00	0.01	0.24	0.17	0.06	0.10	0.84	0.00	0.49
55	0.55	0.01	0.43	0.00	0.00	0.02	0.54	0.00	0.00	0.34	0.33	0.14	0.00	0.14	0.05	0.00	0.01	0.25	0.17	0.10	0.09	0.76	0.00	0.44
60	0.60	0.01	0.34	0.01	0.00	0.04	0.50	0.00	0.00	0.34	0.40	0.15	0.00	0.12	0.05	0.00	0.01	0.26	0.16	0.09	0.09	0.70	0.00	0.42
65	0.65	0.00	0.22	0.01	0.01	0.09	0.46	0.00	0.00	0.38	0.44	0.23	0.00	0.14	0.07	0.00	0.01	0.30	0.14	0.05	0.09	0.67	0.00	0.43
70	0.70	0.00	0.11	0.01	0.02	0.09	0.42	0.00	0.00	0.38	0.44	0.23	0.00	0.14	0.07	0.00	0.01	0.33	0.19	0.02	0.03	0.70	0.01	0.47
75	0.75	0.00	0.06	0.01	0.04	0.13	0.33	0.00	0.00	0.45	0.54	0.37	0.00	0.14	0.10	0.00	0.00	0.37	0.24	0.04	0.01	0.81	0.00	0.56
80	0.80	0.00	0.04	0.00	0.06	0.17	0.25	0.00	0.00	0.54	0.66	0.48	0.00	0.14	0.14	0.00	0.00	0.42	0.28	0.04	0.03	0.94	0.05	0.67
85	0.85	0.00	0.04	0.00	0.15	0.21	0.19	0.00	0.01	0.62	0.77	0.55	0.00	0.13	0.17	0.00	0.00	0.47	0.33	0.04	0.04	1.09	0.07	0.77
90	0.90	0.00	0.05	0.00	0.26	0.23	0.08	0.00	0.03	0.71	0.91	0.58	0.01	0.14	0.19	0.00	0.00	0.51	0.36	0.04	0.03	1.23	0.08	0.88
95	0.95	0.00	0.05	0.00	0.30	0.24	0.01	0.00	0.03	0.77	1.00	0.60	0.01	0.16	0.21	0.00	0.00	0.53	0.35	0.03	0.00	1.32	0.20	0.96
100	1.00	0.00	0.05	0.00	0.31	0.24	0.00	0.00	0.03	0.82	1.07	0.61	0.01	0.15	0.21	0.00	0.01	0.58	0.31	0.04	0.01	1.37	0.17	1.03

NORMALIZED GLENOID FOSSA FORCES (*body weight):		NORMALIZED JOINT MOMENTS (Nm):		HUMERAL AND FOREARM ORIENTATION ANGLES (degrees):		HAND FORCES AND MOMENTS (*body weight & (*body weight)m) wrt the lab.											
%	Inter:	Fxgl	Fzgl	Fxgl	Fzgl	FlexU	Inter:	Fx	Fy	Fz	Mx	My	Mz				
0	0.00	0.23	4.59	0.73	0	0.00	-55	49	-26	105	0.00	0.07	0.44	0.12	-0.001	0.002	-0.016
5	0.05	0.36	4.75	0.73	5	0.05	-57	47	-23	105	0.05	0.06	0.46	0.12	-0.001	0.002	-0.016
10	0.10	0.41	4.58	0.88	10	0.10	-56	45	-24	102	0.10	0.06	0.47	0.11	-0.001	0.002	-0.015
15	0.15	0.20	3.81	0.52	15	0.2	-49	43	-29	94	0.15	0.06	0.43	0.10	-0.001	0.002	-0.015
20	0.20	-0.01	3.29	0.33	20	0.2	-43	40	-35	85	0.20	0.05	0.40	0.07	-0.001	0.001	-0.013
25	0.25	-0.16	2.73	0.18	25	0.3	-37	38	-40	76	0.25	0.03	0.35	0.05	-0.001	0.001	-0.010
30	0.30	-0.27	2.53	0.07	30	0.3	-33	34	-42	65	0.30	0.02	0.31	0.02	0.000	0.000	-0.008
35	0.35	-0.37	2.54	-0.07	35	0.4	-30	33	-43	55	0.35	0.02	0.31	0.00	0.000	0.000	-0.008
40	0.40	-0.42	2.71	-0.20	40	0.4	-30	34	-41	47	0.40	0.01	0.30	-0.02	0.000	-0.002	-0.007
45	0.45	-0.43	2.69	-0.26	45	0.5	-32	34	-40	41	0.45	0.00	0.29	-0.02	0.000	-0.002	-0.008
50	0.50	-0.42	2.60	-0.24	50	0.5	-31	33	-41	38	0.50	0.00	0.27	-0.02	0.000	-0.002	-0.008
55	0.55	-0.39	2.45	-0.20	55	0.6	-31	33	-40	40	0.55	0.00	0.27	-0.02	0.000	-0.002	-0.008
60	0.60	-0.36	2.27	-0.15	60	0.6	-31	34	-40	45	0.60	0.01	0.27	-0.01	0.000	-0.001	-0.007
65	0.65	-0.32	2.13	-0.04	65	0.7	-30	33	-41	53	0.65	0.01	0.29	0.00	0.000	0.000	-0.008
70	0.70	-0.26	2.21	0.09	70	0.7	-33	33	-42	63	0.70	0.02	0.32	0.02	0.000	0.000	-0.009
75	0.75	-0.16	2.61	0.23	75	0.8	-37	33	-41	74	0.75	0.04	0.38	0.03	-0.001	-0.001	-0.011
80	0.80	-0.09	3.10	0.35	80	0.8	-43	33	-41	83	0.80	0.05	0.38	0.05	-0.001	-0.001	-0.012
85	0.85	0.01	3.60	0.47	85	0.9	-46	35	-42	92	0.85	0.06	0.41	0.07	-0.001	0.000	-0.014
90	0.90	0.01	4.09	0.60	90	0.9	-51	47	-41	98	0.90	0.06	0.41	0.09	-0.001	0.001	-0.014
95	0.95	0.13	4.37	0.70	95	1.0	-54	48	-41	103	0.95	0.06	0.42	0.10	-0.001	0.001	-0.015
100	1.00	0.23	4.59	0.73	100	1.0	-55	49	-41	105	1.00	0.07	0.44	0.12	-0.001	0.002	-0.016

Motion Analysis Study Chin-up Results

NORMALIZED MUSCLE ACTIVATION, ARM ELEVATION, GLENOID FOSSA FORCES AND JOINT MOMENTS
 FOR A DYNAMIC CHIN-UP WITHOUT JOINT STABILITY
 SCAPULA ORIENTATION ESTIMATED FROM MEASURED STATIC SEQUENCES
 Date: June 20, 1993
 File: CHINUP02.WK1

NORMALIZED MUSCLE FORCES (% body weight):		Deltoid		Infra		Latissimus		Pectoralis		Sub		Supra		Teres		Triceps		Intensity		
Inter: %		SH	UH	Coraco	Brac	Myo	Mth	Myh	Mzh	AbdH	RoH	FlexU	FlexU	FlexU	FlexU	FlexU	FlexU	FlexU	FlexU	
0	0.00	0.00	0.43	0.00	0.00	0.00	0.00	0.00	0.00	0.00	0.00	0.00	0.00	0.00	0.00	0.00	0.00	0.00	0.00	0.00
5	0.05	0.01	0.42	0.00	0.00	0.00	0.00	0.00	0.00	0.00	0.00	0.00	0.00	0.00	0.00	0.00	0.00	0.00	0.00	0.00
10	0.10	0.02	0.38	0.00	0.00	0.00	0.00	0.00	0.00	0.00	0.00	0.00	0.00	0.00	0.00	0.00	0.00	0.00	0.00	0.00
15	0.15	0.05	0.31	0.00	0.00	0.00	0.00	0.00	0.00	0.00	0.00	0.00	0.00	0.00	0.00	0.00	0.00	0.00	0.00	0.00
20	0.20	0.08	0.25	0.00	0.00	0.00	0.00	0.00	0.00	0.00	0.00	0.00	0.00	0.00	0.00	0.00	0.00	0.00	0.00	0.00
25	0.25	0.07	0.20	0.00	0.00	0.00	0.00	0.00	0.00	0.00	0.00	0.00	0.00	0.00	0.00	0.00	0.00	0.00	0.00	0.00
30	0.30	0.04	0.18	0.00	0.00	0.00	0.00	0.00	0.00	0.00	0.00	0.00	0.00	0.00	0.00	0.00	0.00	0.00	0.00	0.00
35	0.35	0.01	0.18	0.00	0.00	0.00	0.00	0.00	0.00	0.00	0.00	0.00	0.00	0.00	0.00	0.00	0.00	0.00	0.00	0.00
40	0.40	0.00	0.15	0.00	0.00	0.00	0.00	0.00	0.00	0.00	0.00	0.00	0.00	0.00	0.00	0.00	0.00	0.00	0.00	0.00
45	0.45	0.00	0.11	0.00	0.00	0.00	0.00	0.00	0.00	0.00	0.00	0.00	0.00	0.00	0.00	0.00	0.00	0.00	0.00	0.00
50	0.50	0.00	0.08	0.00	0.00	0.00	0.00	0.00	0.00	0.00	0.00	0.00	0.00	0.00	0.00	0.00	0.00	0.00	0.00	0.00
55	0.55	0.00	0.07	0.00	0.00	0.00	0.00	0.00	0.00	0.00	0.00	0.00	0.00	0.00	0.00	0.00	0.00	0.00	0.00	0.00
60	0.60	0.00	0.06	0.00	0.00	0.00	0.00	0.00	0.00	0.00	0.00	0.00	0.00	0.00	0.00	0.00	0.00	0.00	0.00	0.00
65	0.65	0.01	0.13	0.00	0.00	0.00	0.00	0.00	0.00	0.00	0.00	0.00	0.00	0.00	0.00	0.00	0.00	0.00	0.00	0.00
70	0.70	0.02	0.19	0.00	0.00	0.00	0.00	0.00	0.00	0.00	0.00	0.00	0.00	0.00	0.00	0.00	0.00	0.00	0.00	0.00
75	0.75	0.03	0.25	0.00	0.00	0.00	0.00	0.00	0.00	0.00	0.00	0.00	0.00	0.00	0.00	0.00	0.00	0.00	0.00	0.00
80	0.80	0.03	0.31	0.00	0.00	0.00	0.00	0.00	0.00	0.00	0.00	0.00	0.00	0.00	0.00	0.00	0.00	0.00	0.00	0.00
85	0.85	0.01	0.37	0.00	0.00	0.00	0.00	0.00	0.00	0.00	0.00	0.00	0.00	0.00	0.00	0.00	0.00	0.00	0.00	0.00
90	0.90	0.01	0.38	0.00	0.00	0.00	0.00	0.00	0.00	0.00	0.00	0.00	0.00	0.00	0.00	0.00	0.00	0.00	0.00	0.00
95	0.95	0.00	0.38	0.00	0.00	0.00	0.00	0.00	0.00	0.00	0.00	0.00	0.00	0.00	0.00	0.00	0.00	0.00	0.00	0.00
100	1.00	0.00	0.43	0.00	0.00	0.00	0.00	0.00	0.00	0.00	0.00	0.00	0.00	0.00	0.00	0.00	0.00	0.00	0.00	0.00

PCSA, [mm2]: 200 200 100 186 195 217 229 388 157 209 233 100 100 100 150 150 197 273 216 293 296 415 207 200 200 200

NORMALIZED GLENOID FOSSA FORCES (% body weight):		NORMALIZED JOINT MOMENTS (Nm):		HUMERAL AND FOREARM ORIENTATION ANGLES (degrees):		HAND FORCES AND MOMENTS (% body weight & (x body weight)(m) wrt the lab.															
Inter: %		Inter: %	Inter: Mxu Myu Mth Myh Mzh	Inter: %	Inter: FlexH AbdH RoH	FlexU	Inter: Fx Fy Fz Mx My Mz														
0	0.00	-0.26	4.43	-0.02	0	0.00	31	47	-43	80	0.00	-0.01	0.73	0.11	-0.002	0.000	0.007				
5	0.05	-0.24	4.27	0.04	5	0.05	37	40	-36	82	0.05	-0.03	0.69	0.11	-0.001	0.000	0.006				
10	0.10	-0.27	4.07	-0.01	10	0.1	0.3	-10.9	23.1	91.9	29.5	0.10	0.10	0.64	0.10	-0.001	0.000	0.006			
15	0.15	-0.43	3.77	-0.16	15	0.2	-0.0	-8.8	23.8	86.8	28.7	15	0.15	0.51	20	-9	92	0.000	0.000	0.005	
20	0.20	-0.56	3.61	-0.33	20	0.2	-0.6	-8.6	24.3	83.4	23.9	20	0.20	0.44	17	-5	99	0.000	0.000	0.004	
25	0.25	-0.69	3.41	-0.46	25	0.3	-1.0	-6.7	24.3	79.5	20.4	25	0.25	0.35	15	-3	106	0.001	-0.001	0.004	
30	0.30	-0.74	3.27	-0.54	30	0.3	-1.3	-3.9	23.6	75.6	16.2	30	0.30	0.30	28	14	-2	114	0.001	-0.001	0.003
35	0.35	-0.81	3.22	-0.57	35	0.4	-1.6	-0.4	23.1	71.9	12.7	35	0.35	0.35	22	13	-1	120	0.002	-0.001	0.003
40	0.40	-0.90	3.08	-0.62	40	0.4	-1.8	3.1	22.0	67.4	9.7	40	0.40	0.40	17	12	0	126	0.002	-0.001	0.003
45	0.45	-0.94	2.85	-0.61	45	0.5	-1.8	6.2	19.9	61.6	6.9	45	0.45	0.45	14	12	1	130	0.003	-0.001	0.003
50	0.50	-0.95	2.56	-0.57	50	0.5	-1.7	8.2	17.7	55.5	5.2	50	0.50	0.50	12	11	2	133	0.003	-0.001	0.003
55	0.55	-0.85	2.26	-0.50	55	0.6	-1.4	7.6	15.3	49.1	4.0	55	0.55	-0.02	0.35	0.04	0.003	0.000	0.002	0.000	
60	0.60	-0.77	2.09	-0.46	60	0.6	-1.2	5.6	14.2	46.3	3.7	60	0.60	-0.02	0.33	0.04	0.003	0.000	0.001	0.001	
65	0.65	-0.79	2.17	-0.45	65	0.7	-1.0	1.3	14.7	46.1	4.6	65	0.65	-0.02	0.33	0.04	0.003	0.000	0.002	0.000	
70	0.70	-0.78	2.43	-0.46	70	0.7	-0.9	-3.9	16.5	53.8	6.5	70	0.70	-0.02	0.43	0.06	0.001	-0.001	0.003	0.000	
75	0.75	-0.73	2.78	-0.44	75	0.8	-0.7	-8.0	18.4	61.9	9.7	75	0.75	-0.02	0.49	0.07	0.000	-0.001	0.004	0.000	
80	0.80	-0.62	3.32	-0.34	80	0.8	-0.5	-13.6	20.3	73.7	15.3	80	0.80	0.01	0.56	0.06	0.000	-0.001	0.005	0.000	
85	0.85	-0.43	3.67	-0.22	85	0.9	-0.3	-14.8	21.2	84.8	21.5	85	0.85	0.00	0.61	0.09	-0.001	-0.001	0.006	0.000	
90	0.90	-0.32	3.91	-0.13	90	0.9	-0.2	-12.1	20.7	90.9	25.9	90	0.90	0.00	0.64	0.09	-0.001	-0.001	0.007	0.000	
95	0.95	-0.27	4.00	-0.06	95	1.0	0.2	-6.3	18.7	95.5	27.8	95	0.95	0.00	0.67	0.10	-0.001	0.000	0.007	0.000	
100	1.00	-0.26	4.43	-0.02	100	1.0	0.1	-7.8	21.5	107.0	31.3	100	1.00	-0.01	0.73	0.11	-0.002	0.000	0.007	0.000	

APPENDIX G

This appendix contains listings of the programs used in modelling shoulder biomechanics and averaging and normalizing programs used for model results and EMG data.

The programs and units included in this appendix are:

MAIN1, This is the first program used on Vicon motion analysis data. From it is produced a set of subject kinematics and hand loading from reach frame of data. These results are stored to files of extension .EU1. Units called from this program include:

MAIN2, This is the second program of the shoulder biomechanical model. It uses the results of MAIN1 to calculate anatomical kinematics and joint moments, predict muscle activation and calculate joint forces. Units called from this program include:

FILEINT, used to integrate predicted model results

FILENORM, used to normalize integrated model results for the five activities.

EMGCONV, EMG processing program that rectified, magnitude normalized and integrated the EMG signal.

TIMENORM, used to normalize EMG data from EMGCONV for each activity

Units used by the main programs are listed alphabetically and include:

-ALIGN, calculates hand and arm position wrt Trunk Coordinate System, clavicle position wrt trunk, scapula position wrt trunk

-CONV, converts data from one coordinate system to another and muscle attachment data from individual bone to trunk coordinate system.

-CORRECT corrects humeral data so that muscle data lays on the surface of either the head or shaft

-CSALIGN, determines clavicle and scapula orientation

-EULEXP, calculates clinical (experimntal) segment orientation angles

-EULERS, given rotation angle and rotation axis calculates the accompanying Euler rotation matrix.

-FORCDIR, calculates muscle fibre direction vectors. These are normalized vectors.

-FORCEBAL, calculates the force equilibrium parameters for the Gleno Humeral joint in a coordinate system based on the Glenoid Fossa.

-LOAD, calculates shoulder and elbow loads (due to gravity and external

- MISCOPS, a unit containing various matrix and trig routines
- MUSMOMS, calculates the moments due to muscle action about the humeral/radial joint, the humeral/ulnar joint, and the glenoid/humeral joint.
- ORIENT, calculates segment direction cosine matrices
- READEXP, reads experimental vicon and subject data, and calculates hand forces and moments
- READINFO, reads subject and test information and workfiles used by this program. writes it to the
- SETVALS, sets limb, body and loading variables.
- SIMFMT, puts data into a format for optimization.
- SIMPLEX, optimization routine (simplex)
- VARIABLE, global variable declarations.
- VARSIMP, simplex optimization routine variables
- WRAPS, a procedure that corrects muscle insertions to account for wrapping around the first the humeral head and then the humeral shaft.

```

{*****}
{*****}
PROGRAM MAIN;
    {This program calculates body orientation
    Euler angles from experimental marker data.
    Scapula position is calculated twice, using
    experimental marker data and also by prediction.
    Scapula marker correction in this program
    version is normal to the plane of the scapula.

    Three data collection formats are supported by
    this program.
        FORMAT 1 uses 10 markers.
        FORMAT 2 uses 12 markers and was developed
        March 27 92 for the forthcoming lab session.
        requiring elbow flexion angles other than
        90 degrees.
        FORMAT 3 uses 15 markers and was developed
        in July 92 for use with the Hand Grip Pylon
        Transducer and FORMAT 2 subject markers.}

    USES CRT, PRINTER, CONV, CORRECT, MISCOPS, VARIABLE, READEXP, EULEXP, ORIENT;

{*****}
{*****}
BEGIN
    {Read subject information if required and store in a working file; WRKFILE3.PRN.}
    REXPER1(SUBJINFO);

    {Prompt for input file name, number of frames and data collection format of
    the file to be analysed. If required the Pylon correction matrix is inverted
    for use later on.}
    REXPER2(ANALOGUE, ANALOGRT, NANALOG, NFRAMES, NMARKERS, S3);

    {Output files can be initialized for later use.}
    S2:=S3+'.EUL';
    ASSIGN(FILEOUT12,S2); REWRITE(FILEOUT12);
    S2:=S3+'.EU2';
    ASSIGN(FILEOUT13,S2); REWRITE(FILEOUT13);

    {A workfile must be filled with the trunk to marker coord system transformation.
    This workfile need only be filled once for each test(ie for each marker
    placement).}
    WRITELN('For each test subject, a transformation must be defined for');
    WRITELN('conversion between the trunk and marker coord systems. ');
    WRITELN('The trunk coord sys must be parallel to the lab system for this');
    WRITELN('calculation. ');
    WRITELN('IS THE TRANSFORMATION TO BE CALCULATED, Y/<ret.> for NO');
    A:=WHEREY; A:=A-1; GOTOXY(60,A);
    READLN(S1);
    STATUS:=2;
    IF((S1='Y')OR(S1='y'))THEN STATUS :=1;

    {Scapula can be predicted from the Xs A-P plane angle to the Xt axis. If
    this is to be calculated then the integer variable PREDICT = 2
    otherwise PREDICT = 1, if no scapula orientation is required then PREDICT = 3}
    WRITELN('IS SCAPULA ORIENTATION TO BE CALCULATED? Y/<ret for N>');
    A:=WHEREY; A:=A-1; GOTOXY(60,A);
    READLN(S1);
    IF((S1='Y')OR(S1='y'))THEN
        BEGIN
            WRITELN('IS SCAPULA ORIENTATION TO BE PREDICTED? Y/<ret for N>');
            A:=WHEREY; A:=A-1; GOTOXY(60,A);
            READLN(S1);
            IF((S1='Y')OR(S1='y'))THEN PREDICT:=2 ELSE PREDICT:=1;
            END ELSE
            BEGIN
                PREDICT:=3;
                FOR A:= 1 TO 3 DO SPOS[A]:=0;
            END;

    {Rib cage information must be scaled and corrected for scapular position
    prediction. After this it can be stored to a matrix, in this case matrix MDT}
    IF(PREDICT=2)THEN
        BEGIN
            RCONV; {These lines were originally positioned before file declaration}
            ASSIGN(FILEIN5,'WRKFILES.PRN'); RESET(FILEIN5);
            FOR A:= 1 TO 10 DO FOR B:= 1 TO 20 DO FOR C:= 1 TO 3 DO MDT[B,A,1,C]:=0 ;
            MDT[B,A,2,C]:=0 ;

            READ(FILEIN5,E,F);
            FOR A:= 1 TO 10 DO FOR B:= 1 TO 20 DO READ(FILEIN5,MDT[B,A,1,1],
            MDT[B,A,1,2],MDT[B,A,1,3]);
            CLOSE(FILEIN5);
            END;

```

```

{Each frame can now be analysed. NFRAMES is the number of frames to be done and
FRAMENUM is the frame number currently being considered. NMARKERS is the number
of markers to be analysed in each frame. ANALOGUE is = 0 if no analogue channels
are being considered, if force plate 1 is used, then 8 analogue channels are
used and ANALOGUE = 1.}
FRAMENUM:=0;

{*****}
REPEAT
FRAMENUM:=FRAMENUM+1;
IF ((FRAMENUM=1) AND (STATUS=1)) THEN
BEGIN
STATUS:=1;
END ELSE
BEGIN
STATUS:=2;
END;

{Read experimental marker data, convert to metres and store in matrix "MARKERS".
Analogue data is read or calculated and converted to forces Fx, Fy & Fz stored in
VECT1.}
REXP3 (HNDFORCE, HNDMOMNT, SUBJINFO,
MARKERS, ANALOGUE, ANALOGRT, FRAMENUM, NANALOG, NMARKERS);

{A check must be made to the marker data. If no data was obtained for a
marker in a few frames then these frames should not be included in the analysis
that follows here. Therefore no further calculations are required for such a
frame.}
B:=1; C:=NMARKERS-3; {without pylon last 3 markers not required}
IF ((ANALOGUE=2) OR (ANALOGUE=3)) THEN C:=NMARKERS; {when using pylon all markers
are required}
IF (PREDICT<>3) THEN
FOR A:=1 TO C DO IF ((MARKERS[A,1]=0) AND (MARKERS[A,2]=0) AND
(MARKERS[A,3]=0)) THEN B:=2;
IF (PREDICT =3) THEN {scapula IA & MS markers are not required}
BEGIN
FOR A:= 1 TO 3 DO IF ((MARKERS[A,1]=0) AND (MARKERS[A,2]=0) AND
(MARKERS[A,3]=0)) THEN B:=2;
FOR A:= 6 TO C DO IF ((MARKERS[A,1]=0) AND (MARKERS[A,2]=0) AND
(MARKERS[A,3]=0)) THEN B:=2;
END;

IF (B=2) THEN
BEGIN
WRITELN(' '); WRITELN('FRAME NUMBER ', FRAMENUM:4, ' HAS MARKER DATA MISSING');
WRITELN(' ');
END;
IF (B=1) THEN
BEGIN

{Two major calculations are performed TORIENT. First, is to
calculate trunk coord sys orientation wrt the lab coord sys (STATUS=1). Second is
to convert all marker data so it is wrt the trunk coord systems and not the
lab's (STATUS=2) Note: The first procedure requires that the first frame being
analysed for any subject be collected when the trunk coord sys is parallel to
the lab system. That is facing in the +ve X direction, standing up straight.
Workfile, " WRKFILE1.PRN", is generated in this procedure and contains the
transformation matrix for marker coord to trunk coordinate systems.}
TORIENT (NMARKERS, PREDICT, STATUS, TROTMAT, MARKERS);

{Calculate orientation of Clavicle coord sys wrt the trunk coord sys}
CORIENT (ACCENT, CROTMAT, MARKERS);

{Calculate orientation of Scapula coord system wrt the trunk.}
IF (PREDICT<>3) THEN
SORIENT (ACCENT, SROTMAT, MARKERS);

{Calculate orientation of Humeral coord system wrt the trunk. Note, this
procedure is different whether FORMAT 1 OR FORMAT 2 is being used.}
HORIENT (NMARKERS, HROTMAT, MARKERS);

{*****}
{write to file}
write to file (fileout13, framenum:5,
hrotmat [1,1]:9:3, hrotmat [1,2]:9:3, hrotmat [1,3]:9:3,
hrotmat [2,1]:9:3, hrotmat [2,2]:9:3, hrotmat [2,3]:9:3);
{*****}
{Calculate orientation of forearm coord system wrt the trunk. Note, this
procedure is different whether FORMAT 1 OF FORMAT 2 is being used.}
RORIENT (NMARKERS, RROTMAT, MARKERS);

{Calculate trunk Euler orientation angles}
TEULER (TPOS, TROTMAT);

{Calculate Clavicle Euler orientation angles.}

```

```

CEULER (CPOS, CROTMAT);

{Calculate Scapula Euler orientation angles.}
IF (PREDICT<>3) THEN
  SEULER (SPOS, SROTMAT);

{Calculate Humeral Euler orientation angles.}
HEULER (HPOS, HROTMAT, HELEVA);

{Calculate scapular spine to VERTICAL angle in the AP plane}
IF (PREDICT<>3) THEN
  SPINHAP (HROTMAT, SROTMAT, THETA);

{Calculate Forearm Euler orientation angles.}
REULER (RPOS, HROTMAT, RROTMAT);

{Write orientation angles including calculated scapular angles to a file: .EU1
and to screen.}
  WRITELN (FILEOUT12, FRAMENUM:5,
    TPOS [1] :7:1, ' ', TPOS [2] :7:1, ' ', TPOS [3] :7:1,
    CPOS [1] :7:1, ' ', CPOS [2] :7:1, ' ', CPOS [3] :7:1,
    SPOS [1] :7:1, ' ', SPOS [2] :7:1, ' ', SPOS [3] :7:1,
    HPOS [1] :7:1, ' ', HPOS [2] :7:1, ' ', HPOS [3] :7:1,
    RPOS [1] :7:1, ' ', RPOS [2] :7:1, ' ', RPOS [3] :7:1,
    HNDFORCE [1] :7:1, HNDFORCE [2] :7:1, HNDFORCE [3] :7:1,
    HNDMOMNT [1] :7:1, HNDMOMNT [2] :7:1, HNDMOMNT [3] :7:1);

  WRITELN (' ');
  WRITELN ('CURRENT FRAME NUMBER', FRAMENUM:5);
  WRITELN ('EULER ORIENTATION ANGLES ARE AS FOLLOWS, (in deg.):');
  WRITELN ('Also Included: "Scapula Spine to vert. angle" & "Total Humeral Elev."');
  WRITELN ('TRUNK', TPOS [1] :5:1, ' ', TPOS [2] :5:1, ' ', TPOS [3] :5:1);
  WRITELN ('CLAVICLE', CPOS [1] :5:1, ' ', CPOS [2] :5:1, ' ', CPOS [3] :5:1);
  WRITELN ('CALCULATED SCAPULA', SPOS [1] :5:1, ' ', SPOS [2] :5:1, ' ', SPOS [3] :5:1,
    ', THETA:5:1);

{Predicting scapular orientation and writing to screen and working file:}
IF (PREDICT=2) THEN
  BEGIN
    SPORIE2 (ACCENT, MDT, SROTMAT, MARKERS);
    SEULER (SPOS, SROTMAT);
    SPINHAP (HROTMAT, SROTMAT, THETA);
    WRITELN ('2. PREDICTED SCAPULA', SPOS [1] :5:1, ' ', SPOS [2] :5:1, ' ', SPOS [3] :5:1,
    ', THETA:5:1);
    WRITELN (FILEOUT13, FRAMENUM:3,
      TPOS [1] :7:1, ' ', TPOS [2] :7:1, ' ', TPOS [3] :7:1,
      CPOS [1] :7:1, ' ', CPOS [2] :7:1, ' ', CPOS [3] :7:1,
      SPOS [1] :7:1, ' ', SPOS [2] :7:1, ' ', SPOS [3] :7:1,
      HPOS [1] :7:1, ' ', HPOS [2] :7:1, ' ', HPOS [3] :7:1,
      RPOS [1] :7:1, ' ', RPOS [2] :7:1, ' ', RPOS [3] :7:1,
      HNDFORCE [1] :7:1, HNDFORCE [2] :7:1, HNDFORCE [3] :7:1,
      HNDMOMNT [1] :7:1, HNDMOMNT [2] :7:1, HNDMOMNT [3] :7:1);

    END;

    WRITELN ('HUMERAL', HPOS [1] :5:1, ' ', HPOS [2] :5:1, ' ', HPOS [3] :5:1,
    ', HELEVA:5:1);
    WRITELN ('FOREARM', RPOS [1] :5:1, ' ', RPOS [2] :5:1, ' ', RPOS [3] :5:1);
  END;
  UNTIL (FRAMENUM=NFRAMES);
{*****}
  CLOSE (FILEIN10); CLOSE (FILEOUT12); CLOSE (FILEOUT13);
{*****}
END.
{*****}

```

```

{*****}
{*****}
PROGRAM MAIN2;      {FILE: This program is the main program to coordinate
                    the calculation of shoulder biomechanical
                    information from external load and anatomical
                    data.}

USES CRT, PRINTER,
    ALIGN, CONV, CORRECT, CSALIGN, FORCDIR, FORCEBAL, LOAD, MUSMOMS, SETVALS,
    SIMFMT, READINFO, VARIABLE, WRAPS; {simfmt, EULERS, MISCOPS}

    {The units used by this main program include:
    -READINFO, reads subject and test information and
    writes it to the workfiles used by this program.
    -SETVALS, sets limb, body and loading variables.
    -EULERS, given rotation angle and rotation axis
    calculates the accompanying Euler rotation matrix.
    -MISCOPS, a unit containing various matrix and
    vector routines including:
        -MATEMULT, a procedure to multiply two 3x3 matrices
        -VECTMULT, a procedure to multiply a 3x3 mat. and 3x1
vector
        -RMSERR, a function to find RMS error between
        two 3-D positions.
        -NORMALIZ, a procedure to normalize a 3-D vector
        -VECTCROS, a procedure returning the vector cross
        product of two vectors.
        -VECTDOT, a function returning the vector dot
        product of two vectors.
    -VARIABLE, global variable declarations.
    -ALIGN,
        -ALIGNMENT calculates hand and arm position wrt
        the Trunk Coordinate System.
    -CSALIGN
        -CALIGN calculates clavicle position wrt trunk
        coord. sys.
        -SALIGN calculates scapula position wrt trunk
        coord. sys.
    -LOAD, calculates shoulder and elbow loads (due to
    gravity and external
    -CORRECT
        -MDCOR, corrects humeral data so that muscle data
        lays on the surface of either the head or shaft
        -RCCOR, scales rib cage data to comply with
        muscle origin/insertion and clinical information.
    -CONV, converts data from one coordinate system
    to another
        -BTCONV, converts muscle attachment data from
        individual bone to trunk coordinate system.
        -RCCONV, reads in rib cage data from file: RCAGE3.PRN
        and converts it to SI units and the Trunk Coord
        system used throughout this program.
    -FORCDIR,
        -MUSD, calculates the muscle fibre direction
        vectors. These are normalized vectors.
        -COND, same as MUSD but calculates the contact
        force directions between scapula and trunk.
    -FORCEBAL,
        -GHFORBAL, calculates the force equilibrium
        parameters for the Gleno Humeral joint in a
        coordinate system based on the Glenoid Fossa.
        This info is used for ensuring GH stability
        during optimization.
    -MUSMOMS,
        -HRMUSCLE, calculates the moments due to muscle
        action about the humeral/radial joint.
        -HUMUSCLE, calculates the moments due to muscle
        action about the humeral/ulnar joint.
        -GHMUSCLE, calculates the moments due to muscle
        action about the glenoid/humeral joint.
        -CSMUSCLE, calculates the moments due to muscle
        action about the clavicle/scapular joint.
    -QSBFMT, contains procedures to convert joint
    moment information to the format required by
    the optimization program QSB.
        -FMT01, uses 10 moment equations and 55 force
        elements basically the whole shoulder.
        -FMT02, uses only 5 moment equations and only
        those force elements that cross the GH and
        elbow joints.
    -WRAPS,
        -WRAP1, a procedure that corrects muscle
        insertions to account for wrapping around the
        first the humeral head and then the humeral
        shaft.

```

```

}
{*****}
{*****}
BEGIN

{Read in subject information and store into file: WRKFILE3.PRN }
  READIN1;
{Prompt for Euler and hand load data input file, plus the number of frames to
analyse}
  READIN2 (NFRAMES, S3);
  FRAMENUM:=1;
{Open and initialize the files to be used for storing muscle moment information,
glenoid fossa shear force information, optimized muscle forces with stability
and without, and muscle origin and insertion coords wrt the trunk coord sys.
This coord info. includes the results of wrapping corrections.}
  S1:=S3+'.GFS';    ASSIGN(FILEOUT10,S1); REWRITE(FILEOUT10);
  S1:=S3+'.ANG';    ASSIGN(FILEOUT11,S1); REWRITE(FILEOUT11);
  S1:=S3+'.MOM';    ASSIGN(FILEOUT12,S1); REWRITE(FILEOUT12);
  S1:=S3+'.OP2';    ASSIGN(FILEOUT13,S1); REWRITE(FILEOUT13);
  S1:=S3+'.OP3';    ASSIGN(FILEOUT14,S1); REWRITE(FILEOUT14);
{*****}
{Repeat calculations on all required frames within the input data file.}
  REPEAT
{Read limb Euler orientation and hand load data from the input file and
store in file: WRKFILE2.PRN.}
  READIN3 (FRAMENUM);

  WRITELN(' ');

WRITELN('*****');
  WRITELN('          ANALYSIS FOR  FRAME NUMBER ',FRAMENUM:3);
WRITELN('*****');

{Calculate clavicle orientation, and SC and AC joint locations wrt the trunk
coordinate system and origin.}
  CALIGN (SCCENT, ACCENT, CROTMAT, CIROTMAT);

{Calculate scapula orientation, and Gh joint position wrt the trunk coord sys.}
  SALIGN (GHCENT, ACCENT, SROTMAT, SIROTMAT);

{Calculate anatomical bone alignment, humeral shaft centre, elbow centre
and hand centre wrt humeral head centre, given clinical limb alignment
and limb sizing parameters. True Euler orientation angles for the humerus
are stored to the working file, WRKFILE2.PRN.}
  ARMALIGN (GHCENT, HSCENT, ELCENT, HRCENT, HNDCENT, HROTMAT, HIROTMAT,
           EROTMAT, EIROTMAT, UROTMAT, UIROTMAT, RROTMAT, RIROTMAT);

{Using bone and joint information calculated above, trunk to lab orientation
and hand loading, joint forces and moments can be calculated.}
{Calculate 3-D elbow loads using LOAD.}
  HULOAD (ELCENT, HNDCENT, HUFLOAD, HUMLOAD, UROTMAT);

{Calculate 3-D radial coordinate system loads using unit: LOAD}
  HRLOAD (ELCENT, HRCENT, HNDCENT, HRFLOAD, HRMLoad, RROTMAT);

{Calculate 3-D gleno humeral loads using Unit LOAD.}
  GHLOAD (GHCENT, ELCENT, HNDCENT, GHFLOAD, GHMLoad, HROTMAT);

{Read muscle data from SETVAL1 and correct humeral origins & insertions so
coordinates lay on the humeral surface. This unit uses an assumed humeral
torsion value, HTORS, for G. J. average cadaver humeral torsion angle.
By using this angle, experimental HTORSION values can be used while rotator
cuff in addition to other humeral muscle insertion locations are maintained. }
  MDCOR (MD);

{Convert muscle data in matrix MD to trunk coordinate system and store in
matrix MDT. In addition, both MD and MDT are converted from mm to metres.}

  BTCONV (SCCENT, ACCENT, GHCENT, ELCENT, HRCENT,
         CIROTMAT, SIROTMAT, HIROTMAT, UIROTMAT, RIROTMAT, MD, MDT);

{Correct for muscle wrapping around locations on their respective bones.}
  WRAP1 (GHCENT, HSCENT, MDT, HROTMAT);

{*****}
{Calculate muscle fibre directions, using the origin and insertion
locations stored in matrix MDT. Note these have already been corrected
for wrapping around other locations on their respective bones.}
  MUSD (MDT, MDIR);

{*****}
{Muscle moment factors need to be calculated. These values correspond to the
moment arm times the appropriate normalized direction vector for moment balance

```

```

about the relevant coord. axis. }
HRMUSCLE (HRCENT,MDT,MDIR,RROTMAT,MOMFACTS);
HUMUSCLE (ELCENT,MDT,MDIR,UROTMAT,MOMFACTS);
GHMUSCLE (GHCENT,MDT,MDIR,HROTMAT,MOMFACTS);

{External moment factors can be added to array MOMFACTS}
MOMFACTS [1,56] :=HRMLOAD [1]; MOMFACTS [2,56] :=HUMLOAD [2];
MOMFACTS [3,56] :=GHMLOAD [1]; MOMFACTS [4,56] :=GHMLOAD [2];
MOMFACTS [5,56] :=GHMLOAD [3];
MOMFACTS [6,56] :=ACMLOAD [1]; MOMFACTS [7,56] :=ACMLOAD [2];
MOMFACTS [8,56] :=ACMLOAD [3];
MOMFACTS [9,56] :=SCMLOAD [2]; MOMFACTS [10,56] :=SCMLOAD [3];

{*****}
{For Gh joint stability forces must be summated for all muscle elements
crossing the joint, ext forces and gravity. This info is stored in a working
file: WRKFILE7, for use during optimization. In addition the forces are given
in terms of a coord system based on the Glenoid Fossa (see notes Feb 21 92).}
GHFORBAL (FRAMENUM,GHFLOAD,MDT,MDIR,SROTMAT,FORFACTS,S3);

{Data can now be converted to a format for optimization and then Optimized.}
{simplex:}
FMT02 (FRAMENUM, ICASE, MOMFACTS, FORFACTS); {NO STABILITY CONSTRAINT}
{ FMT03 (FRAMENUM, ICASE, MOMFACTS, FORFACTS); } {WITH STABILITY CONSTRAINT}

{If optimization successful then write shoulder and elbow alignment variables
to file ".ANG" and muscle moment factors to ".MOM." }
IF (ICASE=0) THEN
BEGIN
SETVAL3 (TPOS, CPOS, SPOS, HPOS, UPOS, RPOS);
FOR B:=1 TO 3 DO HPOS [B] :=HPOS [B] *57.3;
UPOS [1] :=UPOS [1] *57.3;
WRITELN (FILEOUT11, FRAMENUM:5, ' ', HPOS [1]:9:0, HPOS [2]:9:0,
HPOS [3]:9:0, ' ', UPOS [1]:9:0);

WRITELN (FILEOUT12, FRAMENUM:5, MOMFACTS [1,56]:8:2, MOMFACTS [2,56]:8:2,
MOMFACTS [3,56]:12:2, MOMFACTS [4,56]:8:2, MOMFACTS [5,56]:8:2);
END;

UNTIL (FRAMENUM>=NFRAMES);
CLOSE (FILEIN10);
CLOSE (FILEOUT10); CLOSE (FILEOUT11); CLOSE (FILEOUT12); CLOSE (FILEOUT13);
CLOSE (FILEOUT14);
sound (220); delay (200); nosound;
sound (440); delay (200); nosound;
sound (880); delay (200); nosound;

{*****}
{*****}
END.
{*****}
{*****}

```

```

{*****}
{*****}
PROGRAM FILEINT;
    {This program integrates the data within
    four files produced by MAIN2.PAS (.OP2,
    .ANG, .MOM & .GFS) simplifying data analysis.
    As a result of the upper arm flexion being
    defined as <=-90 and <90 degrees the other
    angles jump at the transition if the arm is
    abducted >90 degrees. This causes problems if
    the two formats are averaged so the format
    most common in the average interval will be
    used.

    Also this program calculates humeral elevation
    in the sagittal (flexion) and frontal (abduction)
    planes, saving the results to the a ".ELI"
    file.
    }
{*****}
{*****}
USES CRT, PRINTER, EULERS, MISCOPS, VARIABLE;

TYPE MATRIX21 = ARRAY[1..30] OF REAL;
TYPE MATRIX22 = ARRAY[1..5] OF REAL;

VAR A, B, C,
    AVGFACT,
    STATUS,
    STARTFRAME, ENDFRAME,
    FRAMENUM,
    ITERATIONA, ITERATIONB : INTEGER;
    AA, BB, CC, DD, EE, CUTOFF : REAL;
    RECOP2, SUMOP2, AVGOP2 : MATRIX21;
    RECANG, SUMANG1, AVGGANG,
        SUMANG2,
    RECGFS, SUMGFS, AVGGFS,
    RECMOM, SUMMOM, AVGMOM,
    RECELV, SUMELV, AVGELV : MATRIX22;
    FILEIN1, FILEIN2,
    FILEIN3, FILEIN4,
    FILEOUT1, FILEOUT2,
    FILEOUT3, FILEOUT4,
    FILEOUT5 : TEXT;
    S1 : STRING;

{*****}
{*****}
BEGIN
    CLRSCR; GOTOXY(1,20);
    REPEAT {until all subjects and acts have been completed}

        WRITE('FILENAME TO BE INTEGRATED, do not include an extension. ');
        READLN(S1);

        WRITE('INTEGRATION FACTOR TO BE USED, (ie No. of frames to avg): ');
        READLN(AVGFACT);
    {For this program a cut off is required so that if a group to be averaged has
    less than that number of records in it it will not be included in the final results.}
        CUTOFF:=AVGFACT*(40/100);

    {Initialize all the input and output files to be used}
        ASSIGN(FILEIN1, S1+'.OP3'); RESET(FILEIN1);
        ASSIGN(FILEIN2, S1+'.ANG'); RESET(FILEIN2);
        ASSIGN(FILEIN3, S1+'.GFS'); RESET(FILEIN3);
        ASSIGN(FILEIN4, S1+'.MOM'); RESET(FILEIN4);

        ASSIGN(FILEOUT1, S1+'.OPI'); REWRITE(FILEOUT1);
        ASSIGN(FILEOUT2, S1+'.ANI'); REWRITE(FILEOUT2);
        ASSIGN(FILEOUT3, S1+'.GFI'); REWRITE(FILEOUT3);
        ASSIGN(FILEOUT4, S1+'.MOI'); REWRITE(FILEOUT4);
        ASSIGN(FILEOUT5, S1+'.ELI'); REWRITE(FILEOUT5);

    {Set variables before calculations begin}
        ITERATIONA:=0; STATUS:=0;

        REPEAT {Until end of data file is found}

            FOR A:= 1 TO 30 DO SUMOP2[A]:=0;
            FOR A:= 1 TO 5 DO
                BEGIN
                    SUMANG1[A]:=0;
                    SUMANG2[A]:=0;
                    SUMGFS[A]:=0;

```



```

SUMMOM[A] :=0;
SUMELV[A] :=0;
END;

ITERATIONA:=ITERATIONA+1;
ITERATIONB:=0; B:=0; C:=0;
writeln('iterationa = ',iterationa:5);
{Read first framenummer }
IF(ITERATIONA=1) THEN
  BEGIN
    READ(FILEIN1,FRAMENUM);
    STARTFRAME:=FRAMENUM;
  END;

{Calculate the framenummer that corresponds to the end of the averaging group}
ENDFRAME:=(ITERATIONA*AVGFACT)+STARTFRAME-1;

{For each group to be averaged }
IF(FRAMENUM<=ENDFRAME) THEN
  BEGIN
    REPEAT
      ITERATIONB:=ITERATIONB+1;
      writeln(' ',iterationb:5);
    {Read data from the files}
    FOR A:= 1 TO 26 DO READ(FILEIN1,RECOP2[A]); READLN(FILEIN1,RECOP2[27]);

    READ(FILEIN2,AA); FOR A:= 1 TO 4 DO READ(FILEIN2,RECANG[A]);
    READ(FILEIN3,AA); FOR A:= 1 TO 3 DO READ(FILEIN3,RECGFS[A]);
    READ(FILEIN4,AA); FOR A:= 1 TO 5 DO READ(FILEIN4,RECMOM[A]);

    {*****}
    {Calculate the elevation angles using unit: HELEVATU.PAS}
    {convert angles to radians }
    BB:=RECANG[1]/57.3;
    CC:=RECANG[2]/57.3;
    DD:=RECANG[3]/57.3;

    {Calculate the inverse direction cosine matrix for the humerus}
    EULERY(MAT3,BB);
    EULERZ(MAT2,CC);
    EULERX(MAT1,DD);

    MATEMULT(MAT1,MAT2,MAT4);
    MATEMULT(MAT4,MAT3,MAT5);

    {Sagital (Xt-Zt) plane humeral elevation ie flexion is now:}
    BB:=SQRT(SQR(MAT5[1,1])+SQR(MAT5[1,3]));
    BB:=MAT5[1,1]/BB;

    IF(BB=1) THEN CC:=0;
    IF((BB>-1) AND (BB<1)) THEN
      deg)
      BEGIN
        BB:=ASIN(BB);
        CC:=-1*(BB-1.57);
      END ELSE
        DD:=0;

      IF(MAT5[1,3]>0) THEN CC:= -1 * CC;

    {Frontal (Xt-Yt) plane humeral elevation ie abduction is now:}
    BB:=SQRT(SQR(MAT5[1,1])+SQR(MAT5[1,2]));
    BB:=MAT5[1,1]/BB;

    IF(BB=1) THEN DD:=0;
    IF((BB>-1) AND (BB<1)) THEN
      BEGIN
        BB:=ASIN(BB);
        DD:=-1*(BB-1.57);
      END ELSE
        DD:=0;

      IF(MAT5[1,2]<0) THEN DD:= -1 * DD;

    {convert angles back into degrees}
    RECELV[1]:=CC*57.3;
    RECELV[2]:=DD*57.3;

    {*****}

    {Calculate the sums of each group to be averaged by column}
    FOR A:= 1 TO 27 DO SUMOP2[A]:=SUMOP2[A]+RECOP2[A];
    IF(RECANG[2]<=90) THEN
      BEGIN

```

```

        FOR A:= 1 TO 4 DO SUMANG1[A]:=SUMANG1[A]+RECANG[A];
        B:=B+1;
        END;
    IF (RECANG[2]> 90) THEN
        BEGIN
            FOR A:= 1 TO 4 DO SUMANG2[A]:=SUMANG2[A]+RECANG[A];
            C:=C+1;
            END;
        FOR A:= 1 TO 3 DO SUMGFS[A]:=SUMGFS[A]+RECGFS[A];
        FOR A:= 1 TO 5 DO SUMMOM[A]:=SUMMOM[A]+RECMOM[A];
        FOR A:= 1 TO 2 DO SUMELV[A]:=SUMELV[A]+RECELV[A];

{Read the next frame number in the data file but first check to ensure not EOF}
        IF Eof(FILEIN1) THEN
            BEGIN
                STATUS:=2;
            END ELSE
                READ(FILEIN1,FRAMENUM);

            UNTIL((STATUS=2) OR (FRAMENUM>ENDFRAME));

{Calculate averages for each column of data}
        IF (ITERATIONB>=CUTOFF) THEN
            BEGIN
                FOR A:= 1 TO 27 DO AVGOP2[A]:=SUMOP2[A]/ITERATIONB;

                IF (B>=C) THEN
                    FOR A:= 1 TO 4 DO AVGAN1[A]:=SUMANG1[A] / B;
                IF (B< C) THEN
                    FOR A:= 1 TO 4 DO AVGAN2[A]:=SUMANG2[A] / C;

                FOR A:= 1 TO 3 DO AVGGFS[A]:=SUMGFS[A]/ITERATIONB;
                FOR A:= 1 TO 5 DO AVGMOM[A]:=SUMMOM[A]/ITERATIONB;
                FOR A:= 1 TO 2 DO AVGELV[A]:=SUMELV[A]/ITERATIONB;

{Write averages to output file}
                WRITE(FILEOUT1,ITERATIONA:5);
            FOR A:= 1 TO 26 DO WRITE(FILEOUT1,AVGOP2[A]:7:0); WRITELN(FILEOUT1,AVGOP2[27]:9:3);

                WRITE(FILEOUT2,ITERATIONA:5);
            FOR A:= 1 TO 3 DO WRITE(FILEOUT2,AVGAN1[A]:9:0); WRITELN(FILEOUT2,AVGAN1[4]:9:0);

                WRITE(FILEOUT3,ITERATIONA:5);
            FOR A:= 1 TO 2 DO WRITE(FILEOUT3,AVGGFS[A]:9:0); WRITELN(FILEOUT3,AVGGFS[3]:9:0);

                WRITE(FILEOUT4,ITERATIONA:5);
            FOR A:= 1 TO 4 DO WRITE(FILEOUT4,AVGMOM[A]:9:2); WRITELN(FILEOUT4,AVGMOM[5]:9:2);

                WRITELN(FILEOUT5,ITERATIONA:5,AVGELV[1]:9:0, AVGELV[2]:9:0);
            END;
        END;
    UNTIL(STATUS=2);

    CLOSE(FILEIN1); CLOSE(FILEIN2); CLOSE(FILEIN3); CLOSE(FILEIN4);
    CLOSE(FILEOUT1); CLOSE(FILEOUT2); CLOSE(FILEOUT3); CLOSE(FILEOUT4);
    CLOSE(FILEOUT5);

    WRITE('DO YOU WISH TO CONTINUE, Y OR <ret for N> ');
    READLN(S1);
    IF ((S1='Y') OR (S1='y')) THEN STATUS:=1;

    UNTIL(STATUS<>1);

END.

```

```

{*****}
{*****}
PROGRAM FILENORM;          {This program normalizes cyclic data files with
                           respect to time and body weight. It
                           interpolates to find the overall average
                           signal values at intervals spaced at 5% of
                           the complete cycle. Data must be organized
                           in columns, with the first as a sequential
                           "record number". This version reads the
                           5 files (.OPI, .ANI, .GFI, .MOI, .ELI)
                           automatically. These files contain the
                           averaged or integrated output (calculated by using
program                               FILEINT.PAS) of the shoulder muscle model. }

{*****}
{*****}
USES CRT, PRINTER;

TYPE  MATRIX1 = ARRAY[1..30] OF REAL;
      MATRIX2 = ARRAY[1..20,1..30] OF REAL;
      MATRIX3 = ARRAY[1..20,1..5] OF REAL;
      MATRIX4 = ARRAY[1..200] OF REAL;
      MATRIX5 = ARRAY[1..20] OF STRING;

VAR   A, B, C,
      ACTNUM, ACTTOT,
      CYCTOT, CYCSTART,
      CURCYC, CURREC, CURINT,
      PASTREC,
      STATUS, ITERATION      : INTEGER;

      AA, BB, CC, DD, EE,
      RECINT, BODYWT        : REAL;

      NEWREC1, OLDREC1,
      NEWREC2, OLDREC2,
      NEWREC3, OLDREC3,
      NEWREC4, OLDREC4,
      NEWREC5, OLDREC5      : MATRIX1;

      AVGOPI, CNTOPI, SUMOPI : MATRIX2;

      AVGANI, CNTANI, SUMANI,
      AVGGFI, CNTGFI, SUMGFI,
      AVGMOI, CNTMOI, SUMMOI,
      AVGELI, CNTELI, SUMELI : MATRIX3;

      CYCEND                : MATRIX4;

      FILENAMES              : MATRIX5;

      FILEIN1, FILEIN2,
      FILEIN3, FILEIN4,
      FILEIN5, FILEIN6,
      FILEOUT1, FILEOUT2,
      FILEOUT3, FILEOUT4,
      FILEOUT5, FILEOUT6    : TEXT;
      S1, S2, S3            : STRING;

{*****}
{*****}
BEGIN
  STATUS:=0;
  CLRSCR;  GOTOXY(1,5);

  ASSIGN(FILEOUT6, 'WRKFILE6.PRN'); REWRITE(FILEOUT6);

  WRITE('How many acts to be included in normalization. '); READLN(ACTTOT);
  FOR ACTNUM:=1 TO ACTTOT DO
    BEGIN
      WRITELN('*****');
      WRITE('Data file name for act',ACTNUM:3,' (no extension) ');
      READLN(FILENAMES[ACTNUM]);
      WRITELN('*****');

      WRITELN('Subject body weight, if no weight normalization required enter 1. ');
      WRITE('Weight units should be the same as used for muscle force. ');
      READLN(BODYWT);
      WRITE(FILEOUT6, BODYWT:9:0);

      WRITE('Record number before start of cycle 1: '); READLN(CYCSTART);
      WRITE(FILEOUT6, CYCSTART:9);
    END
  ;

```

```

WRITE('Total number of cycles in the act: '); READLN(CYCTOT);
WRITE(FILEOUT6,CYCTOT:9);

WRITELN('Input last record number of each cycle ');
FOR A:=1 TO CYCTOT DO
  BEGIN
    WRITE(A:3,'. '); READLN(CYCEND[A]); WRITE(FILEOUT6,CYCEND[A]:9:0);
  END;
WRITELN(FILEOUT6,' '); WRITELN(' '); WRITELN(' ');
END;

CLOSE(FILEOUT6);
ASSIGN(FILEIN6,'WRKFILE6.PRN'); RESET(FILEIN6);

WRITE('Input the output data file name, (no extension): '); READLN(S1); WRITELN('
');
ASSIGN(FILEOUT1,S1+'.OPN'); REWRITE(FILEOUT1);
ASSIGN(FILEOUT2,S1+'.ANN'); REWRITE(FILEOUT2);
ASSIGN(FILEOUT3,S1+'.GPN'); REWRITE(FILEOUT3);
ASSIGN(FILEOUT4,S1+'.MON'); REWRITE(FILEOUT4);
ASSIGN(FILEOUT5,S1+'.ELN'); REWRITE(FILEOUT5);
{*****}
{Calculations}
{Zero averaging arrays }
FOR A:=1 TO 20 DO FOR B:=1 TO 30 DO AVGOPI[A,B]:=0;
FOR A:=1 TO 20 DO FOR B:=1 TO 5 DO AVGANI[A,B]:=0;
FOR A:=1 TO 20 DO FOR B:=1 TO 5 DO AVGGFI[A,B]:=0;
FOR A:=1 TO 20 DO FOR B:=1 TO 5 DO AVGMOI[A,B]:=0;
FOR A:=1 TO 20 DO FOR B:=1 TO 5 DO AVGELI[A,B]:=0;

FOR A:=1 TO 20 DO FOR B:=1 TO 30 DO SUMOPI[A,B]:=0;
FOR A:=1 TO 20 DO FOR B:=1 TO 5 DO SUMANI[A,B]:=0;
FOR A:=1 TO 20 DO FOR B:=1 TO 5 DO SUMGFI[A,B]:=0;
FOR A:=1 TO 20 DO FOR B:=1 TO 5 DO SUMMOI[A,B]:=0;
FOR A:=1 TO 20 DO FOR B:=1 TO 5 DO SUMELI[A,B]:=0;

FOR A:=1 TO 20 DO FOR B:=1 TO 30 DO CNTOPI[A,B]:=0;
FOR A:=1 TO 20 DO FOR B:=1 TO 5 DO CNTANI[A,B]:=0;
FOR A:=1 TO 20 DO FOR B:=1 TO 5 DO CNTGFI[A,B]:=0;
FOR A:=1 TO 20 DO FOR B:=1 TO 5 DO CNTMOI[A,B]:=0;
FOR A:=1 TO 20 DO FOR B:=1 TO 5 DO CNTELI[A,B]:=0;

{Repeat calculations for all the acts}
FOR ACTNUM:= 1 TO ACTTOT DO
  BEGIN
    CURCYC:=0;

{Read the current act information and optn the input files}
    READ(FILEIN6, BODYWT,CYCSTART,CYCTOT);

    FOR A:= 1 TO CYCTOT-1 DO READ(FILEIN6,CYCEND[A]);
    READLN(FILEIN6,CYCEND[CYCTOT]);

    S1:=FILENAMES[ACTNUM];
    ASSIGN(FILEIN1,S1+'.OPI'); RESET(FILEIN1);
    ASSIGN(FILEIN2,S1+'.ANI'); RESET(FILEIN2);
    ASSIGN(FILEIN3,S1+'.GFI'); RESET(FILEIN3);
    ASSIGN(FILEIN4,S1+'.MOI'); RESET(FILEIN4);
    ASSIGN(FILEIN5,S1+'.ELI'); RESET(FILEIN5);

{*****}

    REPEAT {until all cycles are completed}
      CURCYC:=CURCYC+1;
      ITERATION:=1;
      CURINT:=1;
      WRITELN(' ');
      writeln('Current act and cycle is: ',actnum:3,'. ',CURCYC);
{Calculate record spacing for current cycle}
      IF(CURCYC=1) THEN RECINT:= 1/ (CYCEND[1]-CYCSTART);
      IF(CURCYC>1) THEN RECINT:= 1/(CYCEND[CURCYC]-CYCEND[CURCYC-1]);

      REPEAT {until all records for each cycle are read}
        {The first record of any CYCLE is treated specially for storage purposes plus
        the input file may have records at the start that are not to be included
        in the normalization.}
        IF ((ITERATION=1)and(CURCYC=1))THEN
          BEGIN
            repeat
              READ(FILEIN1,CURREC);
              FOR A:= 1 TO 26 DO READ(FILEIN1,NEWREC1[A]); READLN(FILEIN1,NEWREC1[27]);
              READ(FILEIN2,AA);
              FOR A:= 1 TO 3 DO READ(FILEIN2,NEWREC2[A]); READLN(FILEIN2,NEWREC2[4]);

```

```

    READ(FILEIN3,AA);
    FOR A:= 1 TO 2 DO READ(FILEIN3,NEWREC3[A]); READLN(FILEIN3,NEWREC3[3]);
    READ(FILEIN4,AA);
    FOR A:= 1 TO 4 DO READ(FILEIN4,NEWREC4[A]); READLN(FILEIN4,NEWREC4[5]);
    READLN(FILEIN5,AA,NEWREC5[1],NEWREC5[2]);
until(currec>cycstart);

{Some data must be normalized wrt body weight of each subject}
FOR A:= 1 TO 26 DO NEWREC1[A]:=NEWREC1[A]/BODYWT;
FOR A:= 1 TO 3 DO NEWREC3[A]:=NEWREC3[A]/BODYWT;

END;

{A new record is read when the desired interval is to the rt to the
"new" record position. The only exception to this is when the final record
in the cycle has already been read.}
REPEAT
    FOR A:=1 TO 27 DO OLDREC1[A]:=NEWREC1[A];
    FOR A:=1 TO 4 DO OLDREC2[A]:=NEWREC2[A];
    FOR A:=1 TO 3 DO OLDREC3[A]:=NEWREC3[A];
    FOR A:=1 TO 5 DO OLDREC4[A]:=NEWREC4[A];
    FOR A:=1 TO 2 DO OLDREC5[A]:=NEWREC5[A];
    PASTREC:=CURREC;

    IF Eof(FILEIN1) THEN
        BEGIN
            WRITELN('ERROR in ACT, ',actnum:5,' MISSING SIGNAL DATA ');
            DELAY(2000);
            STATUS:=5;
        END ELSE
        BEGIN
            ITERATION:=ITERATION+1;

            read(filein1,currec);
            A:=WHEREY; WRITE('READING RECORD: ', CURREC:5); GOTOXY(1,A);

            FOR A:= 1 TO 26 DO READ(FILEIN1,NEWREC1[A]); READLN(FILEIN1,NEWREC1[27]);
            READ(FILEIN2,AA);
            FOR A:= 1 TO 3 DO READ(FILEIN2,NEWREC2[A]); READLN(FILEIN2,NEWREC2[4]);
            READ(FILEIN3,AA);
            FOR A:= 1 TO 2 DO READ(FILEIN3,NEWREC3[A]); READLN(FILEIN3,NEWREC3[3]);
            READ(FILEIN4,AA);
            FOR A:= 1 TO 4 DO READ(FILEIN4,NEWREC4[A]); READLN(FILEIN4,NEWREC4[5]);
            READLN(FILEIN5,AA,NEWREC5[1],NEWREC5[2]);

{Normalizing wrt body weight:}
            FOR A:= 1 TO 26 DO NEWREC1[A]:=NEWREC1[A]/BODYWT;
            FOR A:= 1 TO 3 DO NEWREC3[A]:=NEWREC3[A]/BODYWT;

            END;

            IF (CURCYC=1) THEN AA:=(CURREC-CYCSTART)*RECINT;
            IF (CURCYC>1) THEN AA:=(CURREC-CYCEND[CURCYC-1])*RECINT;
            UNTIL((CURINT*0.05)<=AA) OR (CURREC>=CYCEND[CURCYC]);

{Required interval is to the left of the final record position. The only possible
exception to this is if the final interval of a cycle is being analysed.
The current value is solved using an interpolation/extrapolation type routine}
            REPEAT
                IF (CURCYC=1) THEN AA:=PASTREC-CYCSTART;
                IF (CURCYC>1) THEN AA:=PASTREC-(CYCEND[CURCYC-1]);
                AA:=(CURINT*0.05)-(AA*RECINT);
                BB:=(CURREC-PASTREC)*RECINT;

{if too many records in any particular act then this cycle's interval should
not be included}
                IF (CC<3) THEN
                    BEGIN
                        FOR A:= 1 TO 27 DO
                            BEGIN
                                DD:=NEWREC1[A]-OLDREC1[A];
                                EE:=(DD/BB)*AA;
                                SUMOPI [CURINT,A] :=SUMOPI [CURINT,A] +(OLDREC1[A]+EE);
                                CNTOPI [CURINT,A] :=CNTOPI [CURINT,A] +1;
                            END;

                        FOR A:= 1 TO 4 DO
                            BEGIN
                                DD:=NEWREC2[A]-OLDREC2[A];
                                EE:=(DD/BB)*AA;
                                SUMANI [CURINT,A] :=SUMANI [CURINT,A] +(OLDREC2[A]+EE);
                                CNTANI [CURINT,A] :=CNTANI [CURINT,A] +1;
                            END;
                    END;
            REPEAT

```

```

FOR A:= 1 TO 3 DO
  BEGIN
  DD:=NEWREC3 [A] -OLDREC3 [A];
  EE:=(DD/BB)*AA;
  SUMGFI [CURINT,A]:=SUMGFI [CURINT,A]+(OLDREC3 [A]+EE);
  CNTGFI [CURINT,A]:=CNTGFI [CURINT,A]+1;
  END;

FOR A:= 1 TO 5 DO
  BEGIN
  DD:=NEWREC4 [A] -OLDREC4 [A];
  EE:=(DD/BB)*AA;
  SUMMOI [CURINT,A]:=SUMMOI [CURINT,A]+(OLDREC4 [A]+EE);
  CNTMOI [CURINT,A]:=CNTMOI [CURINT,A]+1;
  END;

FOR A:= 1 TO 2 DO
  BEGIN
  DD:=NEWREC5 [A] -OLDREC5 [A];
  EE:=(DD/BB)*AA;
  SUMELI [CURINT,A]:=SUMELI [CURINT,A]+(OLDREC5 [A]+EE);
  CNTELI [CURINT,A]:=CNTELI [CURINT,A]+1;
  END;

END;

CURINT:=CURINT+1;

IF (CURCYC=1) THEN AA:=(CURREC-CYCSTART)*RECINT;
IF (CURCYC>1) THEN AA:=(CURREC-CYCEND [CURCYC-1])*RECINT;

UNTIL(((CURINT*0.05)>AA) OR (CURINT>20));

UNTIL ( CURREC>=CYCEND [CURCYC] );
IF (CURINT>21) THEN WRITELN('ERROR IN CYCLE: ',CURCYC:4);

UNTIL ( CURCYC=CYCTOT );

{*****}

CLOSE (FILEIN1);   CLOSE (FILEIN2);
CLOSE (FILEIN3);   CLOSE (FILEIN4);
CLOSE (FILEIN5);
END;                {all acts have been completed}

{Averages for each interval can now be calculated}
FOR A:= 1 TO 20 DO
  BEGIN
  FOR B:= 1 TO 27 DO  AVGOPI [A,B]:= SUMOPI [A,B] / CNTOPI [A,B];
  FOR B:= 1 TO 4 DO  AVGANI [A,B]:= SUMANI [A,B] / CNTANI [A,B];
  FOR B:= 1 TO 3 DO  AVGGFI [A,B]:= SUMGFI [A,B] / CNTGFI [A,B];
  FOR B:= 1 TO 5 DO  AVGMOI [A,B]:= SUMMOI [A,B] / CNTMOI [A,B];
  FOR B:= 1 TO 2 DO  AVGELI [A,B]:= SUMELI [A,B] / CNTELI [A,B];
  END;

{To correct for any extrapolation errors on the first calculated interval,
it is averaged with the final interval and the second interval.}
FOR B:= 1 TO 27 DO  AVGOPI [1,B]:= (AVGOPI [1,B]+AVGOPI [2,B]+AVGOPI [20,B])/3;
FOR B:= 1 TO 4 DO  AVGANI [1,B]:= (AVGANI [1,B]+AVGANI [2,B]+AVGANI [20,B])/3;
FOR B:= 1 TO 3 DO  AVGGFI [1,B]:= (AVGGFI [1,B]+AVGGFI [2,B]+AVGGFI [20,B])/3;
FOR B:= 1 TO 5 DO  AVGMOI [1,B]:= (AVGMOI [1,B]+AVGMOI [2,B]+AVGMOI [20,B])/3;
FOR B:= 1 TO 2 DO  AVGELI [1,B]:= (AVGELI [1,B]+AVGELI [2,B]+AVGELI [20,B])/3;

{Write output to the appropriate files}
WRITE (FILEOUT1,0:5);
WRITE (FILEOUT2,0:5);
WRITE (FILEOUT3,0:5);
WRITE (FILEOUT4,0:5);
WRITE (FILEOUT5,0:5);
FOR B:=1 TO 26 DO WRITE (FILEOUT1,AVGOPI [20,B]:8:2);
WRITELN (FILEOUT1,AVGOPI [20,27]:8:3);
FOR B:=1 TO 4 DO WRITE (FILEOUT2,AVGANI [20,B]:8:0); WRITELN (FILEOUT2,' ');
FOR B:=1 TO 3 DO WRITE (FILEOUT3,AVGGFI [20,B]:8:2); WRITELN (FILEOUT3,' ');
FOR B:=1 TO 5 DO WRITE (FILEOUT4,AVGMOI [20,B]:8:2); WRITELN (FILEOUT4,' ');
FOR B:=1 TO 2 DO WRITE (FILEOUT5,AVGELI [20,B]:8:0); WRITELN (FILEOUT5,' ');
FOR A:=1 TO 20 DO
  BEGIN
  AA:=A/20;
  WRITE (FILEOUT1,AA:5:2);
  WRITE (FILEOUT2,AA:5:2);
  WRITE (FILEOUT3,AA:5:2);
  WRITE (FILEOUT4,AA:5:2);
  WRITE (FILEOUT5,AA:5:2);
  FOR B:=1 TO 26 DO WRITE (FILEOUT1,AVGOPI [A,B]:8:2);

```

```

WRITELN(FILEOUT1,AVGOPI[A,27]:8:3);
  FOR B:=1 TO 4 DO WRITE(FILEOUT2,AVGANI[A,B]:8:0); WRITELN(FILEOUT2,' ');
  FOR B:=1 TO 3 DO WRITE(FILEOUT3,AVGGFI[A,B]:8:2); WRITELN(FILEOUT3,' ');
  FOR B:=1 TO 5 DO WRITE(FILEOUT4,AVGMOI[A,B]:8:2); WRITELN(FILEOUT4,' ');
  FOR B:=1 TO 2 DO WRITE(FILEOUT5,AVGELI[A,B]:8:0); WRITELN(FILEOUT5,' ');
END;

CLOSE(FILEIN6);
CLOSE(FILEOUT1);   CLOSE(FILEOUT2);
CLOSE(FILEOUT3);   CLOSE(FILEOUT4);
CLOSE(FILEOUT5);
{*****}
END.
{*****}

```

```

{*****}
{*****}
PROGRAM EMGCONV;           {This program performs offset correction,
                           normalization, rectification and averaging
                           to EMG ASCII data files while performing only
                           offset correction and averaging to accompanying
                           ANALOGUE ASCII files.}

{*****}
{*****}

USES CRT, PRINTER;

TYPE  MATRIX1 = ARRAY[1..16] OF REAL;
      MATRIX2 = ARRAY[1..16] OF TEXT;

VAR   A,B,C,      D,
      EMGTOT,ANATOT,CHANTOT,
      INTFACT, STATUS,
      ITERATION           :INTEGER;
      AA,BB,CC           :REAL;
      NORMFACT,CALFACT,
      CAVG,BASEEMG       :MATRIX1;
      FILEIN             :MATRIX2;
      FILEOUT            :TEXT;
      S1,S2,S3,s4,s5,S6 :STRING;

{*****}
{*****}
BEGIN
  CLRSCR; GOTOXY(1,10);
  ITERATION:=0;

  WRITE('Input the number of EMG channels: '); READLN(EMGTOT); WRITELN(' ');
  WRITE('Input the number of Analogue channels: '); READLN(ANATOT); WRITELN(' ');

  CHANTOT:=EMGTOT+ANATOT;

  WRITE('Input data directory to be used: '); READLN(S1); WRITELN(' ');
  WRITE('Input the subject Number if using MYOSOFT 2000 output: ');
  READLN(S2); WRITELN(' ');
  WRITE('Input the test Number if using MYOSOFT 2000 output: ');
  READLN(S3); WRITELN(' ');

  S4:=S1+S2+'_'+S3+'_';

  WRITELN('Input the EMG ASCII file NUMBER: ');
  FOR C:=1 TO EMGTOT DO
    BEGIN
      WRITE(' ',C:1,'.',S4); A:=WHEREX; READLN(S5);
      A:=A+3; B:= WHEREY-1; GoToXY(A,B); WRITELN('.ASC');
      S6:=S4+S5+'.ASC';
      ASSIGN(FILEIN[C],S6); RESET(FILEIN[C]);
    END;

  WRITELN(' ');
  WRITELN('Input the ANALOGUE ASCII file names: ');
  FOR C:= EMGTOT+1 TO CHANTOT DO
    BEGIN
      WRITE(' ',C:1,'.',S4); A:=WHEREX; READLN(S5);
      A:=A+3; B:=WHEREY-1; GotoXY(A,B); WRITELN('.ASC');
      S6:=S4+S5+'.ASC';
      ASSIGN(FILEIN[C],S6); RESET(FILEIN[C]);
    END;

  WRITELN(' ');
  WRITELN('Input the EMG MAGNITUDE NORMALIZATION FACTORS. Note that for maximum');
  WRITELN('contraction OR baseline EMG files use a value of 1. ');
  FOR C:= 1 TO EMGTOT DO
    BEGIN
      WRITELN(' ',C:1,'. '); A:=WhereY; A:=A-1; GotoXY(8,A);
      READLN(NORMFACT[C]);
    END; WRITELN(' ');

  WRITE('Do yo wish to correct for Baseline EMG activity? [Y or <ret>]');
  READLN(S6); WRITELN(' ');
  FOR C:=1 TO EMGTOT DO BASEEMG[C]:=0;
  IF((S6='Y') OR (S6='y'))THEN
    BEGIN
      WRITELN('Enter baseline (non normalized)EMG levels for each channel. ');
      WRITELN('Note: The base EMG levels are subtracted from the Max EMG levels. ');
      FOR C:= 1 TO EMGTOT DO
        BEGIN
          WRITE(' ',C:3,'. '); READLN(BASEEMG[C]);
        END;
    END;
END;

```



```

        END;
    END;

    WRITELN('Input the ANALOGUE CALIBRATION FACTORS,{N/comp. unit etc.}: ');
    FOR C:= EMGTOT+1 TO CHANTOT DO
        BEGIN
            WRITE(' ',C:1,' '); READLN(NORMFACT[C]);
            END; WRITELN(' ');

    WRITELN('Input the data collection CALIBRATION VALUES: ');
    FOR C:= 1 TO CHANTOT DO
        BEGIN
            WRITE(' ',C:2,' '); READLN(CALFACT[C]);
            END; WRITELN(' ');

    WRITE('Input the INTEGRATION or averaging factor: ');
    READLN(INTFACT); writeln(' ');

    WRITE('Input the OUTPUT FILE name: '); READLN(S6);
    ASSIGN(FILEOUT,S6); REWRITE(FILEOUT);

    {*****}
    {*****}

    REPEAT

        ITERATION:=ITERATION+1;

        IF(ITERATION>1)THEN {read in required new data}
            BEGIN
                WRITE('Input the NEW "Act" number: ');
                READLN(S3); WRITELN(' ');

                S4:=S1+S2+'_'+S3+'_';

                WRITELN('Input the EMG ASCII file NUMBER: ');
                FOR C:=1 TO EMGTOT DO
                    BEGIN
                        WRITE(' ',C:1,' ',S4); A:=WHEREX; READLN(S5);
                        A:=A+3; B:=WHEREY -1; GoToXY(A,B); WRITELN(' .ASC');
                        S6:=S4+S5+' .ASC';
                        ASSIGN(FILEIN[C],S6); RESET(FILEIN[C]);
                        END;

                WRITELN(' ');
                WRITELN('Input the EMG ASCII file NUMBER: ');
                FOR C:= EMGTOT+1 TO CHANTOT DO
                    BEGIN
                        WRITE(' ',C:1,' ',S4); A:=WHEREX; READLN(S5);
                        A:=A+3; B:=WHEREY -1; GoToXY(A,B); WRITELN(' .ASC');
                        S6:=S4+S5+' .ASC';
                        ASSIGN(FILEIN[C],S6); RESET(FILEIN[C]);
                        END;

                WRITELN('Input the data collection CALIBRATION VALUES: ');
                FOR C:= 1 TO CHANTOT DO
                    BEGIN
                        WRITE(' ',C:2,' '); READLN(CALFACT[C]);
                        END; WRITELN(' ');

                WRITE('Input the INTEGRATION or averaging factor: ');
                READLN(INTFACT); writeln(' ');

                WRITE('Input the OUTPUT FILE name: '); READLN(S6);
                ASSIGN(FILEOUT,S6); REWRITE(FILEOUT);
                END;

    {*****}
    {*****}
    {Max EMG levels must be corrected to be wrt the BASE EMG levels BUT ONLY ONCE}

    IF(ITERATION=1)THEN
        FOR A:= 1 TO EMGTOT DO NORMFACT[A]:=NORMFACT[A]-BASEEMG[A];

    {*****}
    {*****}
    {Write calculation information to header of output file}

    WRITELN(FILEOUT, INTFACT:5);
    FOR A:= 1 TO CHANTOT-1 DO WRITE(FILEOUT, (NORMFACT[A]+BASEEMG[A]):9:3,' ');
    WRITELN(FILEOUT, (NORMFACT[CHANTOT]+BASEEMG[CHANTOT]):9:3);
    FOR A:= 1 TO EMGTOT-1 DO WRITE(FILEOUT, BASEEMG[A]:9:3,' ');
    WRITELN(FILEOUT, BASEEMG[EMGTOT]:9:3);

```

```

WRITELN(FILEOUT, ' ');

{*****}
{Calculations}
{*****}

WRITELN('Record being read: ');
STATUS:=0; D:=0;
REPEAT                                     {perform calculations until end of file
encountered}
D:=D+1;

FOR A:=1 TO INTFACT DO
BEGIN

IF(A=1)THEN FOR B:=1 TO 16 DO CAVG[B]:=0;

FOR B:=1 TO CHANTOT DO
BEGIN
if Eof(FILEIN[B])then
BEGIN
STATUS:=2; A:=INTFACT; B:=CHANTOT;
writeln('Input file completed!');
END;

IF(STATUS<2)THEN
BEGIN
c:=WHEREY; c:=c-1; GOTOXY(30,c); WRITELN(D:5, ' ',a:2, ' ',b:2);
READLN(FILEIN[B],AA);
AA:=AA-CALFACT[B];                                     {remove A-D offset}
IF(B<=EMGTOT) THEN
BEGIN
AA:=ABS(AA);                                         {rectify EMG channels}
AA:=AA-BASEEMG[B];                                   {remove baseline EMG activity}
AA:=AA/NORMFACT[B];                                  {normalize EMG channels}
END
ELSE AA:=AA*NORMFACT[B];                             {Convert A-D units to Newtons}
CAVG[B]:=CAVG[B]+(AA/INTFACT);                       {calculate ongoing AVG of each channel}
END;
END;

IF(STATUS=0)THEN                                     {write data to output file}
BEGIN
FOR B:=1 TO CHANTOT-1 DO WRITE(FILEOUT,CAVG[B]:9:3, ' ');
WRITELN(FILEOUT,CAVG[CHANTOT]:9:3);
END;

UNTIL(STATUS=2);

FOR A:= 1 TO CHANTOT DO CLOSE(FILEIN[A]);
CLOSE(FILEOUT);

WRITELN(' ');
WRITE('Repeat the procedure for the same subject? [Y or <ret> ');
READLN(S6); WRITELN(' ');

UNTIL ((S6<>'Y')AND(S6<>'y'))

{*****}
{*****}
END.
{*****}
{*****}

```

```

{*****}
{*****}
PROGRAM TIMENORM;           {This program normalizes cyclic data files with
                           respect to time. It interpolates to find the
                           overall average signal values at intervals
                           spaced at 5 % of the complete cycle. Data must
                           be organized in columns, with the first
                           as a sequential "record number".

                           The program has been modified to include hand
                           force normalization, March 21 93.}
{*****}
{*****}

USES CRT, PRINTER;

TYPE MATRIX1 = ARRAY[1..16] OF REAL;
MATRIX2 = ARRAY[1..20,1..16] OF REAL;
MATRIX3 = ARRAY[1..200] OF REAL;

VAR  A, B, C,
      CHNTOT, CYCTOT, ANATOT,
      CURCYC, CURREC, CURINT,
      STATUS, ITERATION      : INTEGER;

      AA, BB, CC, DD,
      RECINT                  : REAL;

      NEWREC, OLDREC         : MATRIX1;
      AVGSIG                 : MATRIX2;
      CYCEND, FORNORM        : MATRIX3;

      FILEIN1, FILEIN2,
      FILEOUT1               : TEXT;
      S1, S2, S3             : STRING;

{*****}
{*****}
BEGIN
  STATUS:=0;
  CLRSCR;  GOTOXY(1,10);

  WRITE('Input the SIGNAL data file name: ');  READLN(S1);      Writeln(' ');
  ASSIGN(FILEIN1,S1);  RESET(FILEIN1);

  WRITE('Input the output data file name: ');  READLN(S1);      Writeln(' ');
  ASSIGN(FILEOUT1,S1);  REWRITE(FILEOUT1);

  WRITE('Input the number of channels: ');      READLN(CHNTOT);  Writeln(' ');
  WRITE('Input the number of cycles: ');        READLN(CYCTOT);  Writeln(' ');

  WRITE('Input the cycle end points using a data file? [Y or <ret>]');
  READLN(S2);      Writeln(' ');
  IF((S2='Y')OR(S2='y'))THEN
    BEGIN
      WRITE('Input the end point file name: ');  READLN(S1);      Writeln(' ');
      ASSIGN(FILEIN2,S1);  RESET(FILEIN2);
      STATUS:=1;
    END;

  IF(STATUS=0)THEN  Writeln('Input the end points one at a time.');
```

```

FOR A:= 1 TO CYCTOT DO
  BEGIN
WRITE('Factor for cycle ',A:3,' is: ',AA:4,' <ret> for O.K. or C for change');
  READLN(S2);
  IF((S2='C')OR(S2='c'))THEN
    BEGIN
      WRITE('Input subject weight [N] for cycle: ',A:3,' : ');
      READLN(AA); WRITELN(' ');
      END;
    FORNORM[A]:=AA;
    END;
  END;

  IF (STATUS=1) THEN CLOSE(FILEIN2);
  {*****}
  {Write calculation information to header of output file}

  WRITELN(FILEOUT1, CYCTOT:5);
  WRITELN(FILEOUT1, ' ');

  {*****}
  {Calculations}
  CURCYC:=0;
  FOR A:=1 TO 20 DO FOR B:=1 TO CHNTOT DO AVGSIG[A,B]:=0;

  REPEAT                                     {until all cycles are completed}
    CURCYC:=CURCYC+1;
    ITERATION:=1;
    CURINT:=1;

  {Calculate record spacing for current cycle}
  IF(CURCYC=1) THEN RECINT:= 1/ CYCEND[1];
  IF(CURCYC>1) THEN RECINT:= 1/(CYCEND[CURCYC]-CYCEND[CURCYC-1]);

  {*****}
  REPEAT                                     {until all records for each cycle are read}

  {The first record of any cycle is treated specially for storage purposes}
  IF(ITERATION=1)THEN
    BEGIN
      READ(FILEIN1,CURREC);

      FOR A:= 1 TO CHNTOT DO
        BEGIN
          IF EoF(FILEIN1)THEN
            BEGIN
              WRITELN('ERROR, in record ',currec:5,' MISSING SIGNAL DATA ');
              STATUS:=5;
              END ELSE
                READ(FILEIN1,NEWREC[A]);

          IF((ANATOT>0)AND(A>=(CHNTOT-ANATOT+1)))THEN
            NEWREC[A]:=NEWREC[A]/FORNORM[CURCYC];
          END;
        END;

  {A new record is read when the desired interval is to the rt to the
  "new" record position. The only exception to this is when the final record
  in the cycle has already been read.}
  REPEAT
    FOR A:=1 TO CHNTOT DO OLDREC[A]:=NEWREC[A];

    READ(FILEIN1,CURREC);
    ITERATION:=ITERATION+1;
    A:=WHEREY; WRITE('CALCULATING RECORD: ', CURREC:5); GOTOXY(1,A);

    FOR A:= 1 TO CHNTOT DO
      BEGIN
        IF EoF(FILEIN1)THEN
          BEGIN
            WRITELN('ERROR in record, ',currec:5,' MISSING SIGNAL DATA ');
            STATUS:=5;
            END ELSE
              READ(FILEIN1,NEWREC[A]);

          IF((ANATOT>0)AND(A>=(CHNTOT-ANATOT+1)))THEN
            NEWREC[A]:=NEWREC[A]/FORNORM[CURCYC];
          END;
        UNTIL(((CURINT*0.05)<=(ITERATION*RECINT)) OR (CURREC=CYCEND[CURCYC]));

  {Required interval is to the left of the final record position. The only possible
  exception to this is if the final interval of a cycle is being analysed.

```

```

The current value is solved using an interpolation/extrapolation type routine}
REPEAT
  AA:=(CURINT*0.05)-((ITERATION-1)*RECINT);
  BB:=RECINT;
  FOR A:= 1 TO CHNTOT DO
    BEGIN
      DD:=NEWREC[A]-OLDREC[A];
      CC:=(DD/BB)*AA;
      AVGSIG[CURINT,A]:=AVGSIG[CURINT,A]+((OLDREC[A]+CC)/CYCTOT);
      {WRITELN(AVGSIG[CURINT,A]:3:3);}
    END;
  CURINT:=CURINT+1;
  UNTIL(((CURINT*0.05)>(ITERATION*RECINT))OR(CURINT>20));

  UNTIL(CURREC=CYCEND[CURCYC]);
  IF(CURINT>21)THEN WRITELN('ERROR IN CYCLE: ',CURCYC:4);

  UNTIL(CURCYC=CYCTOT);

{To correct for any extrapolation errors on the first calculated interval,
it is averaged with the final interval and the second interval.}
  FOR B:= 1 TO CHNTOT DO
    AVGSIG[1,B]:=(AVGSIG[1,B]+AVGSIG[2,B]+AVGSIG[20,B])/3;

  WRITE(FILEOUT1,0:5);
  FOR B:=1 TO CHNTOT DO WRITE(FILEOUT1,AVGSIG[20,B]:9:3); WRITELN(FILEOUT1,' ');
  FOR A:=1 TO 20 DO
    BEGIN
      AA:=A/20;
      WRITE(FILEOUT1,AA:5:2);
      FOR B:=1 TO CHNTOT DO WRITE(FILEOUT1,AVGSIG[A,B]:9:3); WRITELN(FILEOUT1,' ');
    END;

  CLOSE(FILEIN1);
  CLOSE(FILEOUT1);
{*****}
  END.
{*****}

```

```

{*****}
{*****}
UNIT ALIGN;          {FILE ALIGN03 This unit calculates actual bone alignment,
                    hand centre and elbow centre w.r.t. the Trunk
                    Ref. Sys. origin at the humeral head centre.
                    Clinical alignment and limb dimensional parameters
                    are required for the calculations. Forearm
                    rotation is included in this version.}

{*****}
{*****}
INTERFACE
USES CRT, PRINTER, EULERS, MISCOPS, VARIABLE, SETVALS;

PROCEDURE ARMALIGN (VAR GHCENT, HSCENT, ELCENT, HRCENT, HNDCENT: MATRIX1;
                   VAR HROTMAT, HIROTMAT, EROTMAT, EIROTMAT, UROTMAT,
                   UIROTMAT, RROTMAT, RIROTMAT: MATRIX3);

IMPLEMENTATION
{*****}
{*****}
{ Procedures and Functions used in calculating actual bone alignment }

{This procedure combines limb rotation matrices in the correct order to
predict radial coord. sys. position from the Trunk Ref. Sys. By inserting
identity matrices starting at mat8, ulnar or humeral coordinate system
orientation can be determined.}
PROCEDURE PROCED1 (VAR MAT1, MAT2, MAT3, MAT4, MAT5, MAT6, MAT7, MAT8, MAT15: MATRIX3);
BEGIN
  MATEMULT (MAT1, MAT2, MAT11);      MATEMULT (MAT3, MAT4, MAT12);
MATEMULT (MAT11, MAT12, MAT13);
  MATEMULT (MAT5, MAT6, MAT11);      MATEMULT (MAT7, MAT8, MAT12);
MATEMULT (MAT11, MAT12, MAT14);
  MATEMULT (MAT13, MAT14, MAT15);
END;

{This procedure prints the final bone alignment results to the screen. }
PROCEDURE PROCED2 (HPOS, UPOS: MATRIX1; HCARANG, UCARANG, ERR: REAL);
BEGIN
  HPOS [1] := HPOS [1] * 180 / Pi;    HPOS [2] := HPOS [2] * 180 / Pi;
HPOS [3] := HPOS [3] * 180 / Pi;
  HCARANG := HCARANG * 180 / Pi;      UCARANG := UCARANG * 180 / Pi;
UPOS [1] := UPOS [1] * 180 / Pi;
  A := WhereY; A := A - 3; GOTOXY (1, A);
  WRITELN ('GH Flexion, Abduction and Rotation are:      ');
HPOS [1] : 7:1, HPOS [2] : 7:1, HPOS [3] : 7:1);
  WRITELN ('Humeral Carrying Ang, Ulnar Flex & Carrying Ang are:
', HCARANG: 7:1, UCARANG [1] : 7:1, UCARANG: 7:1);
  WRITELN ('With these alignment parameters, RMS Error is:      ', ERR: 10:5);
END;

{*****}
{*****}
PROCEDURE ARMALIGN (VAR GHCENT, HSCENT, ELCENT, HRCENT, HNDCENT: MATRIX1;
                   VAR HROTMAT, HIROTMAT, EROTMAT, EIROTMAT, UROTMAT,
                   UIROTMAT, RROTMAT, RIROTMAT: MATRIX3);
BEGIN
{Begin by setting up an identity matrix for use later on.}
FOR A:=1 TO 3 DO FOR B:=1 TO 3 DO IF (A=B) THEN IDENTMAT [A,B] := 1 ELSE
IDENTMAT [A,B] := 0;

{Calculating CLINICAL UPPER ARM orientation wrt trunk sys.}
SETVAL3 (TPOS, CPOS, SPOS, HPOS, UPOS, RPOS);
SETVAL4 (TPARAMS, CPARAMS, SPARAMS, HPARAMS, UPARAMS, RPARAMS, HCARANG, UCARANG, HTORSION);

  EULERY (MAT3, HPOS [1]);            EULERZ (MAT2, HPOS [2]);          EULERX (MAT1, HPOS [3]);
  MATEMULT (MAT1, MAT2, MAT4);        MATEMULT (MAT4, MAT3, MAT5);

{*****}
{Actual upper arm orientation involves a correction in the X-Z plane to
account for the upper arm X-axis passing through the humeral epicondyles and
the humeral shaft X-axis not. The angle between the two X-axes is:}
SETVAL1 (MD);
THETA := ARCTAN (HPARAMS [3] / (HPARAMS [1] - MD [3, 1, 2, 1]));
EULERY (MAT4, THETA);
MATEMULT (MAT4, MAT5, HROTMAT);
MATEINV (HROTMAT, HIROTMAT);

{True Humeral shaft Euler angles can be calculated. See EULEXP.PAS FOR DETAILS}
VECT1 [1] := 1 ;   VECT1 [2] := 0 ;   VECT1 [3] := 0 ;
VECT2 [1] := 0 ;   VECT2 [2] := 1 ;   VECT2 [3] := 0 ;
VECT3 [1] := 0 ;   VECT3 [2] := 0 ;   VECT3 [3] := 1 ;

FOR A:= 1 TO 3 DO

```

```

BEGIN
  VECT4 [A] :=HROTMAT [1,A];
  VECT5 [A] :=HROTMAT [2,A];
  VECT6 [A] :=HROTMAT [3,A];
  END;
NORMALIZ (VECT1);          NORMALIZ (VECT2);          NORMALIZ (VECT3);
NORMALIZ (VECT4);          NORMALIZ (VECT5);          NORMALIZ (VECT6);
VECTCROS (VECT4,VECT2,VECT7) ;NORMALIZ (VECT7);
IF (VECT7 [3]<0) THEN FOR A:= 1 TO 3 DO VECT7 [A] := -1*VECT7 [A];

AA:=VECTDOT (VECT7,VECT1);    BB:=ASIN (AA);          HPOS [1] :=BB;
AA:=VECTDOT (VECT2,VECT4);    BB:=ASIN (AA);
IF (VECT4 [1]<0) THEN BB:=Pi-BB;
HPOS [2] :=BB;

EULERY (MAT1,HPOS [1]);
EULERZ (MAT2,HPOS [2]);
MATEMULT (MAT2,MAT1,MAT3);
FOR A:= 1 TO 3 DO VECT8 [A] :=MAT3 [2,A];
NORMALIZ (VECT8);
AA:=VECTDOT (VECT5,VECT8); AA:= ASIN (AA);
BB:=VECTDOT (VECT6,VECT8); BB:= ASIN (BB);

IF (AA>=0) THEN HPOS [3] :=-1*(BB);
IF (AA< 0) THEN HPOS [3] :=-1*(PI-BB);

{*****}
{Calculating elbow centre position wrt the apparent shoulder location}
VECT1 [1] :=HPARAMS [1];    VECT1 [2] :=0;          VECT1 [3] :=HPARAMS [3];
VECTMULT (HIROTMAT,VECT1,ELCENT);

{Calculate apparent forearm coordinate system orientation wrt trunk ref sys
This is accomplished by imposing app. elbow flexion on the humeral
coordinate system rot. matrix: HROTMAT}
EULERY (MAT1,UPOS [1]);
MATEMULT (MAT1,HROTMAT,UROTMAT);
MATEINV (UROTMAT,UIROTMAT);

{Calculating hand centre position wrt the apparent shoulder location}
VECT2 [1] :=RPARAMS [1];    VECT2 [2] :=0;          VECT2 [3] :=0;
VECTMULT (UIROTMAT,VECT2,VECT3);
HNDCENT [1] :=ELCENT [1]+VECT3 [1];
HNDCENT [2] :=ELCENT [2]+VECT3 [2];
HNDCENT [3] :=ELCENT [3]+VECT3 [3];

{*****}
{In this section, actual bone alignment is calculated. This accomplished by
using the apparent shoulder centre, elbow centre and hand centre generated
previously and iteratively solving for the actual alignment so as to
reproduce the apparent overall limb alignment. }

{Angle between ulnar coord. sys. and radial coord sys X-axes will be:}
BB:=-1*ARCTAN ( (2*UPARAMS [2])/UPARAMS [1] );

{Origin of radial coord sys wrt ulnar coord sys will be:}
VECT4 [1] :=UPARAMS [2] * (SIN (UCARANG)/COS (UCARANG));
VECT4 [2] :=UPARAMS [2];
VECT4 [3] :=0;

{Location of hand centre wrt radial coord sys, origin elbow centre, will be:}
VECT5 [1] :=RPARAMS [1] *COS (-1*BB);
VECT5 [2] :=RPARAMS [1] *SIN (-1*BB);
VECT5 [3] :=0;

{Location of hand centre wrt the radial coord. sys and origin is :}
FOR A:=1 TO 3 DO VECT5 [A] :=VECT5 [A]-VECT4 [A];

{Set all known rotation matrices,mat1-mat6 except for mat3 & mat5}
EULERY (MAT1,-1*HPOS [1]);
EULERZ (MAT2,-1*HPOS [2]);
EULERZ (MAT4,-1*HCARANG);
EULERZ (MAT6,-1*UCARANG);
EULERZ (MAT7,-1*BB);
EULERX (MAT8,-1*RPOS [3]);

{Set initial guess at humeral rotation,HPOS [3], (ignoring humeral head) and
elbow flex, UPOS [1], as the apparent (clinical) values as detailed in SETVALS3.}
{Set rotation matrices for initial guesses of humeral rotation and ulnar flex}
EULERX (MAT3,-1*HPOS [3]);
EULERY (MAT5,-1*UPOS [1]);

{Combine rotation matrices to give orientation of radial coord sys
orientation wrt the trunk coord. sys. MAT15 is the combined rotation matrix}

```

```

PROCED1 (MAT1, MAT2, MAT3, MAT4, MAT5, MAT6, MAT7, MAT8, MAT15);
{Hand centre location wrt the trunk coord sys, origin at the radial coord. sys.
origin (ie radial head) will be:}
VECTMULT (MAT15, VECT5, VECT6);

{Radial coord sys origin location wrt the elbow centre in the trunk coord sys
will be:}
PROCED1 (MAT1, MAT2, MAT3, MAT4, MAT5, MAT6, IDENTMAT, IDENTMAT, MAT15);
VECTMULT (MAT15, VECT4, VECT7);

{Hand centre location wrt the trunk coord sys and elbow centre is:}
FOR A:=1 TO 3 DO VECT1[A]:=VECT6[A]+VECT7[A];
NORMALIZ (VECT1);

{The actual direction vector joining the elbow to the hand will be:}
VECT2 [1]:=HNDCENT [1]-ELCENT [1];
VECT2 [2]:=HNDCENT [2]-ELCENT [2];
VECT2 [3]:=HNDCENT [3]-ELCENT [3];
NORMALIZ (VECT2);

{The error between these two direction vectors will be:}
ERR:=RMSERR (VECT1, VECT2);

WRITELN (' '); WRITELN ('BONE ALIGNMENT:');
WRITELN (' '); WRITELN (' '); WRITELN (' ');
PROCED2 (HPOS, UPOS, HCARANG, UCARANG, ERR);

{Iterative search can now be initiated to try and improve values of
ulnar flexion, UPOS[1], and humeral rotation, HPOS[3].
The first variable to be incremented is HROT, and both are incremented
twice in total. }
{Set iteration parameters }
ITERH:=0.01; ITERU:=0.01;
ERROLD:=ERR; HROTOLD:=HPCS [3] ; UFLEXOLD:=UPOS [1];
ITERSET:=1;

{Begin iteration }
REPEAT
IF (ITERSET=1) THEN HPOS [3]:=HROTOLD+ITERH;
IF (ITERSET=2) THEN UPOS [1]:=UFLEXOLD+ITERU;

{Calculate corresponding vector error for iteration parameters}
EULERX (MAT3, -1*HPOS [3]);
EULERY (MAT5, -1*UPOS [1]);
EULERZ (MAT7, -1*BB);
EULERX (MAT8, -1*RPOS [3]);
PROCED1 (MAT1, MAT2, MAT3, MAT4, MAT5, MAT6, MAT7, MAT8, MAT15);
VECTMULT (MAT15, VECT5, VECT6);
PROCED1 (MAT1, MAT2, MAT3, MAT4, MAT5, MAT6, IDENTMAT, IDENTMAT, MAT15);
VECTMULT (MAT15, VECT4, VECT7);
FOR A:= 1 TO 3 DO VECT1 [A]:=VECT6 [A]+VECT7 [A];
NORMALIZ (VECT1);
ERR:=RMSERR (VECT1, VECT2);
PROCED2 (HPOS, UPOS, HCARANG, UCARANG, ERR);

{Compare iteration results and decide on parameter changes to improve err.}
IF (ERR <= ERROLD) THEN
BEGIN
IF (ITERSET = 1) THEN ERROLD:=ERR; HROTOLD:=HPOS [3];
IF (ITERSET = 2) THEN ERROLD:=ERR; UFLEXOLD:=UPOS [1];
END ELSE
BEGIN
IF ((ITERSET = 2) AND (ITERU=-0.01)) THEN ITERSET:=3;
IF ((ITERSET = 2) AND (ITERU= 0.01)) THEN ITERU :=-0.01;
IF ((ITERSET = 1) AND (ITERH=-0.01)) THEN ITERSET:=2;
IF ((ITERSET = 1) AND (ITERH= 0.01)) THEN ITERH :=-0.01;
END;
UNTIL (ITERSET = 3);

HPOS [3]:=HROTOLD ; UPOS [1]:=UFLEXOLD; ERR:=ERROLD;

{The humeral shaft, elbow, ulnar and radial orientation rotation matrices wrt
the trunk coord sys are required.}
EULERY (MAT1, -1*HPOS [1]);
EULERZ (MAT2, -1*HPOS [2]);
EULERX (MAT3, -1*HPOS [3]);
PROCED1 (MAT1, MAT2, MAT3, IDENTMAT, IDENTMAT, IDENTMAT, IDENTMAT, HIROTMAT);
MATEINV (HIROTMAT, HROTMAT);

EULERZ (MAT4, -1*HPCARANG);
EULERY (MAT5, -1*UPOS [1]);
PROCED1 (MAT1, MAT2, MAT3, MAT4, MAT5, IDENTMAT, IDENTMAT, IDENTMAT, EIROTMAT);
MATEINV (EIROTMAT, EROTMAT);

```



```

EULERZ (MAT6, -1*UCARANG);
PROCED1 (MAT1, MAT2, MAT3, MAT4, MAT5, MAT6, IDENTMAT, IDENTMAT, UIROTMAT);
MATEINV (UIROTMAT, UROTMAT);

EULERZ (MAT7, -1*BB);
EULERX (MAT8, -1*RPOS [3]);
PROCED1 (MAT1, MAT2, MAT3, MAT4, MAT5, MAT6, MAT7, MAT8, RIROTMAT);
MATEINV (RIROTMAT, RROTMAT);

{Resultes can be written to the screen.}
PROCED2 (HPOS, UPOS, HCARANG, UCARANG, ERR);

{*****}
{Humeral head position is considered in this section. Humeral Head position
is found with respect to the coordinate system origin used above. Humeral
shaft, elbow, and hand centres can then be found in terms of the trunk
coordinate system.

The Humeral head coordinate system has an X-axis parallel with the humeral
long axis, Y-axis is in the plane of elbow flexion and origin at the humeral
head centre.}
{Humeral Coord. Sys. wrt the Trunk Coord. Sys. is: MAT10 }
EULERY (MAT3, HPOS [1]);
EULERZ (MAT2, HPOS [2]);
EULERX (MAT1, HPOS [3]);
MATEMULT (MAT1, MAT2, MAT9);
MATEMULT (MAT9, MAT3, MAT10);

{Humeral Head coord. sys. is related to the Humeral coord.sys. by an X-axis
rotation equal to -ve humeral torsion.}
AA:=-1*HTORSION;
EULERX (MAT4, AA);
MATEMULT (MAT4, MAT10, MAT5);
MATEINV (MAT5, MAT6);

{Humeral Head coordinates in the Humeral coordinate system can now be found.}
VECT1 [1]:=0; VECT1 [2]:=-1*HPARAMS [2]; VECT1 [3]:=0;
VECTMULT (MAT6, VECT1, VECT2);
{ WRITELN('Humeral head position with humeral shaft:
', VECT2 [1]:7:3, VECT2 [2]:7:3, VECT2 [3]:7:3);}

{Humeral shaft centre, elbow centre and hand centre locations can now
be corrected to be wrt the humeral head centre.}
HNDCENT [1]:=HNDCENT [1]-VECT2 [1];
HNDCENT [2]:=HNDCENT [2]-VECT2 [2];
HNDCENT [3]:=HNDCENT [3]-VECT2 [3];

ELCENT [1]:=ELCENT [1]-VECT2 [1];
ELCENT [2]:=ELCENT [2]-VECT2 [2];
ELCENT [3]:=ELCENT [3]-VECT2 [3];

HSCENT [1]:=-1*VECT2 [1];
HSCENT [2]:=-1*VECT2 [2];
HSCENT [3]:=-1*VECT2 [3];

{Glenoid humeral, elbow and hand centres can now be given in terms of the
trunk coordinate system.}
HNDCENT [1]:=HNDCENT [1]+GHCENT [1];
HNDCENT [2]:=HNDCENT [2]+GHCENT [2];
HNDCENT [3]:=HNDCENT [3]+GHCENT [3];

ELCENT [1]:=ELCENT [1]+GHCENT [1];
ELCENT [2]:=ELCENT [2]+GHCENT [2];
ELCENT [3]:=ELCENT [3]+GHCENT [3];

HSCENT [1]:=HSCENT [1]+GHCENT [1];
HSCENT [2]:=HSCENT [2]+GHCENT [2];
HSCENT [3]:=HSCENT [3]+GHCENT [3];

VECT1 [1]:=UPARAMS [2]*(SIN (UCARANG)/COS (UCARANG));
VECT1 [2]:=UPARAMS [2];
VECT3 [3]:=0;

VECTMULT (UIROTMAT, VECT1, HRCENT);
HRCENT [1]:=ELCENT [1]+HRCENT [1];
HRCENT [2]:=ELCENT [2]+HRCENT [2];
HRCENT [3]:=ELCENT [3]+HRCENT [3];

WRITELN(' '); WRITELN('WRT TO TRUNK COORDINATE SYSTEM: ');
WRITELN('GH centre is: ', GHCENT [1]:7:3, GHCENT [2]:7:3, GHCENT [3]:7:3);
WRITELN('Elbow centre is: ', ELCENT [1]:7:3, ELCENT [2]:7:3, ELCENT [3]:7:3);
WRITELN('Radial Head cent:', HRCENT [1]:7:3, HRCENT [2]:7:3, HRCENT [3]:7:3);
WRITELN('Hand centre is: ', HNDCENT [1]:7:3, HNDCENT [2]:7:3, HNDCENT [3]:7:3);

```

```

{Humeral head alignment wrt the trunk coord. sys will be:}
HHPOS[1]:=HPOS[1];
HHPOS[2]:=HPOS[2];
HHPOS[3]:=HPOS[3]-HTORSION;
AA:=HHPOS[1]*180/Pi; BB:=HHPOS[2]*180/Pi; CC:=HHPOS[3]*180/Pi;
WRITELN('Humeral head orientation wrt Trunk coord sys is: ',AA:7:1, BB:7:1, CC:7:1);
WRITELN(' ');

{*****}
{Euler orientation angles can now be stored to the Euler angle
working file:WRKFILE2}
ASSIGN(FILEIN2,'WRKFILE2.PRN'); RESET(FILEIN2);
READLN(FILEIN2,VECT1[1],VECT1[2],VECT1[3]);
READLN(FILEIN2,VECT2[1],VECT2[2],VECT2[3]);
READLN(FILEIN2,VECT3[1],VECT3[2],VECT3[3]);
READLN(FILEIN2,VECT4[1],VECT4[2],VECT4[3]);
READLN(FILEIN2,VECT5[1],VECT5[2],VECT5[3]);
READLN(FILEIN2,HNDFORCE[1],HNDFORCE[2],HNDFORCE[3]);
READLN(FILEIN2,HNDMOMNT[1],HNDMOMNT[2],HNDMOMNT[3]); CLOSE(FILEIN2);

FOR A:= 1 TO 3 DO VECT4[A]:=HPOS[A]*180/Pi;
VECT5[1]:=UPOS[1]*180/Pi; VECT5[2]:=0; VECT5[3]:=RPOS[3]*180/Pi;
ASSIGN(FILEOUT2,'WRKFILE2.PRN'); REWRITE(FILEOUT2);
WRITELN(FILEOUT2,VECT1[1],', ',VECT1[2],', ',VECT1[3]);
WRITELN(FILEOUT2,VECT2[1],', ',VECT2[2],', ',VECT2[3]);
WRITELN(FILEOUT2,VECT3[1],', ',VECT3[2],', ',VECT3[3]);
WRITELN(FILEOUT2,VECT4[1],', ',VECT4[2],', ',VECT4[3]);
WRITELN(FILEOUT2,VECT5[1],', ',VECT5[2],', ',VECT5[3]);
WRITELN(FILEOUT2,HNDFORCE[1],', ',HNDFORCE[2],', ',HNDFORCE[3]);
WRITELN(FILEOUT2,HNDMOMNT[1],', ',HNDMOMNT[2],', ',HNDMOMNT[3]);
CLOSE(FILEOUT2);
END;

{*****}
{*****}
END.
{*****}
{*****}

```

```

{*****}
{*****}
UNIT CONV;                                {File:CONV3, This unit contains procedures to
                                           convert information from one coordinate system
                                           another.
                                           BTCONV-Converts bone data in matrix MD
                                           to trunk coord. sys. and stores in MDT
                                           }
{*****}
{*****}

INTERFACE
USES CRT, EULERS, MISCOPS, SETVALS, VARIABLE;

PROCEDURE BTCONV(VAR SCCENT, ACCENT, GHCENT, ELCENT, HRCENT: MATRIX1;
                 VAR CIROTMAT, SIROTMAT, HIROTMAT, UIROTMAT, RIROTMAT: MATRIX3;
                 VAR MD, MDT: MATRIX2);

IMPLEMENTATION
{*****}
{*****}
PROCEDURE BTCONV(VAR SCCENT, ACCENT, GHCENT, ELCENT, HRCENT: MATRIX1;
                 VAR CIROTMAT, SIROTMAT, HIROTMAT, UIROTMAT, RIROTMAT: MATRIX3;
                 VAR MD, MDT: MATRIX2);

BEGIN
  {Zero MDT matrix }
  FOR A:=1 TO 20 DO FOR B:=1 TO 10 DO FOR C:=1 TO 2 DO FOR D:=1 TO 3 DO
    MDT[A,B,C,D]:=0;
  {Sort MD matrix and perform the appropriate conversion for data}
  FOR A:=1 TO 20 DO
    BEGIN
      FOR B:=1 TO 10 DO
        BEGIN
          FOR C:=1 TO 2 DO
            BEGIN
              {correct muscle origins}
              IF (C=1) THEN
                BEGIN
                  IF(( A=5 ) OR
                     ( A=6 ) OR
                     ( A=7 ) OR
                     ( A=8 ) OR
                     ( A=9 ) OR
                     ( A=10) OR
                     ( A=11) OR
                     ( A=16))
                    THEN                                     {Trunk data}
                      BEGIN
                        FOR D:= 1 TO 3 DO VECT1[D]:=MD[A,B,C,D];
                        IF((VECT1[1]<>0) OR (VECT1[2]<>0) OR (VECT1[3]<>0))
                          THEN
                            BEGIN
                              FOR D:= 1 TO 3 DO MDT[A,B,C,D]:=VECT1[D];
                            END;
                        END;
                    END;
                  IF((A=1 ) AND (B<3)) OR
                     ( A=2 ) OR
                     ((A=3 ) AND (B>2)) OR
                     ( A=4 ) OR
                     ( A=12) OR
                     ( A=13) OR
                     ( A=14) OR
                     ( A=15) OR
                     ((A=17) AND (B=1)) )
                    THEN                                     {Scapular data}
                      BEGIN
                        FOR D:= 1 TO 3 DO VECT1[D]:=MD[A,B,C,D];
                        IF((VECT1[1]<>0) OR (VECT1[2]<>0) OR (VECT1[3]<>0))
                          THEN
                            BEGIN
                              {Perform required rotations from scapula to trunk coord sys}
                              VECTMULT(SIROTMAT,VECT1,VECT2);
                              {Perform required translation from scapula to trunk coord. sys.}
                              FOR D:= 1 TO 3 DO MDT[A,B,C,D]:=VECT2[D]+ACCENT[D];
                            END;
                        END;
                    END;
                  IF( (A=3 )AND(B<3) )                       {Clavicular data}
                    THEN
                      BEGIN
                        FOR D:= 1 TO 3 DO VECT1[D]:=MD[A,B,C,D];
                        IF((VECT1[1]<>0) OR (VECT1[2]<>0) OR (VECT1[3]<>0))
                          THEN

```

```

BEGIN
  {Perform required rotations from clavicle to trunk coord sys}
  VECTMULT(CIROTMAT,VECT1,VECT2);
  {Perform required translation from clavicle to trunk coord.
sys.)
  FOR D:= 1 TO 3 DO MDT[A,B,C,D]:=VECT2[D]+SCCENT[D];
END;
END;

IF(((A=17)AND(B>1)) OR (Humeral data)
(A= 1)AND(B=3)))
THEN
BEGIN
FOR D:= 1 TO 3 DO VECT1[D]:=MD[A,B,C,D];
IF((VECT1[1]<>0)OR(VECT1[2]<>0)OR(VECT1[3]<>0))
THEN
BEGIN
  {Perform required rotations from humeral to trunk coord sys}
  VECTMULT(HIROTMAT,VECT1,VECT2);
  {Perform required translation from humeral to trunk coord. sys.}
  FOR D:= 1 TO 3 DO MDT[A,B,C,D]:=VECT2[D]+GHCENT[D];
  END;
END;
END;

{correct muscle INSERTIONS}
IF (C=2)THEN
BEGIN
  IF(( A=6 ) OR
(A=8 ) OR
(A=9 ) OR
(A=10) OR
(A=11) OR
(A=16) OR
(A=18) ) {Scapular data}
THEN
BEGIN
FOR D:= 1 TO 3 DO VECT1[D]:=MD[A,B,C,D];
IF((VECT1[1]<>0)OR(VECT1[2]<>0)OR(VECT1[3]<>0))
THEN
BEGIN
  {Perform required rotations from scapula to trunk coord sys}
  VECTMULT(SIROTMAT,VECT1,VECT2);
  {Perform required translation from scapula to trunk coord. sys.}
  FOR D:= 1 TO 3 DO MDT[A,B,C,D]:=VECT2[D]+ACCENT[D];
  END;
END;

IF((A=1 ) AND ( B=3 )) OR
(A=2 ) OR
(A=3 ) OR
(A=4 ) OR
(A=5 ) OR
(A=7 ) OR
(A=12) OR
(A=13) OR
(A=14) OR
(A=15)) {Humeral data}
THEN
BEGIN
FOR D:= 1 TO 3 DO VECT1[D]:=MD[A,B,C,D];
IF((VECT1[1]<>0)OR(VECT1[2]<>0)OR(VECT1[3]<>0))
THEN
BEGIN
  {Perform required rotations from humeral to trunk coord sys}
  VECTMULT(HIROTMAT,VECT1,VECT2);
  {Perform required translation from humeral to trunk coord. sys.}
  FOR D:= 1 TO 3 DO MDT[A,B,C,D]:=VECT2[D]+GHCENT[D];
  END;
END;

IF (( A=1 ) AND ( B<3 )) {Radial data}
THEN
BEGIN
FOR D:= 1 TO 3 DO VECT1[D]:=MD[A,B,C,D];
IF((VECT1[1]<>0)OR(VECT1[2]<>0)OR(VECT1[3]<>0))
THEN
BEGIN
  {Perform required rotations from radial to trunk coord sys}
  VECTMULT(RIROTMAT,VECT1,VECT2);
  {Perform required translation from radial to trunk coord. sys.}
  FOR D:= 1 TO 3 DO MDT[A,B,C,D]:=VECT2[D]+HRCENT[D];
  END;
END;

```

```

IF ( A=17)                                {Ulnar data}
  THEN
  BEGIN
  FOR D:= 1 TO 3 DO VECT1[D]:=MD[A,B,C,D];
  IF ((VECT1[1]<>0)OR(VECT1[2]<>0)OR(VECT1[3]<>0))
  THEN
  BEGIN
  {Perform required rotations from ulnar to trunk coord sys}
  VECTMULT(UIROTMAT,VECT1,VECT2);
  {Perform required translation from ulnar to trunk coord. sys.}
  FOR D:= 1 TO 3 DO MDT[A,B,C,D]:=VECT2[D]+ELCENT[D];
  END;
  END;
  END;
  END;
  END;
  END;
  {*****}
  {*****}
  END.
  {*****}
  {*****}

```

```

{*****}
{*****}
UNIT CORRECT;          {FILE CORRECT4 This unit contains one procedure
                        that corrects data for program use.

                        MDCOR, corrects muscle data in
                        matrix MD, so that coordinates that should lay
                        on the humeral surface, do. HTORS is the assumed
                        humeral torsion angle for the cadavers used to
                        obtain MD (muscle data) matrix.
                        }
{*****}
{*****}
INTERFACE
USES CRT,EULERS,MISCOPS,SETVALS,VARIABLE;

PROCEDURE MDCOR(VAR MD:MATRIX2);

IMPLEMENTATION
{*****}
{*****}
{This procedure retrieves subject information from workfile WRKFILE3.PRN}
PROCEDURE PROCED1(VAR SUBJINFO:MATRIX6);
BEGIN
  ASSIGN(FILEIN3,'WRKFILE3.PRN'); RESET(FILEIN3);
  READLN(FILEIN3,S1);
  FOR A:= 1 TO 3 DO
    BEGIN
      READLN(FILEIN3,AA);
      B:= A+1;
      SUBJINFO[B]:=AA;
    END;
  CLOSE(FILEIN3);
  END;

{*****}
{*****}
{This internal procedure corrects data coordinates for humeral head diameter
Humeral coordinate system origin is at the humeral head centre. The humeral
coordinate system origin is coincident with the humeral head centre.}
PROCEDURE HUMHEAD(VAR HHDIA,HTORS,HTORSION:REAL; VAR VECT3:MATRIX1);
BEGIN

{A correction has to be made for the difference between humeral
torsion value used experimentally and that assumed for the cadavers.}
  AA:=HTORSION-HTORS;
  EULERX(MAT1,AA);
  VECTMULT(MAT1,VECT3,VECT4);

{The coordinates can now be corrected so that they lay JUST OUTSIDE the sphere
of HH diameter.}
  CC:=SQRT(SQR(VECT4[1])+SQR(VECT4[2])+SQR(VECT4[3]));
  DD:=(HHDIA+0.001)/2/CC;
  FOR E:= 1 TO 3 DO VECT3[E]:=(VECT4[E] * DD);
  END;

{*****}
{*****}
{This internal procedure corrects data coordinates for humeral shaft diameter, so
that all coordinates that should lay on the humeral shaft surface, lay just
outside it. Humeral coordinate system origin is assumed to be coincident
with the humeral head centre. Note no correction is required in the X-axis
direction ie axially}
PROCEDURE HUMSHAFT(VAR HSDIA,HTORS,HTORSION:REAL; VAR HPARAMS,VECT3:MATRIX1);
BEGIN
  AA:=HPARAMS[2]*COS(HTORS);          BB:=HPARAMS[2]*SIN(HTORS)*-1;
  VECT4[2]:=0+AA;                     VECT4[3]:=0+BB;
  CC:=SQRT(SQR(VECT3[2]-VECT4[2])+SQR(VECT3[3]-VECT4[3]));
  DD:=(HSDIA+0.001)/2/CC;

  AA:=HPARAMS[2]*COS(HTORSION);      BB:=HPARAMS[2]*SIN(HTORSION)*-1;
  VECT5[2]:=0+AA;                     VECT5[3]:=0+BB;

  FOR E:= 2 TO 3 DO VECT3[E]:=VECT5[E] +((VECT3[E]-VECT4[E]) * DD);
  END;
{*****}
{*****}
{This procedure corrects coordiantes so that they lay on either the humeral shaft
or conversely on the humeral head sphere surface. HTORS is the assumed humeral
torsion angle for the cadavers used to obtain the MD (muscle data) matrix}

PROCEDURE MDCOR(VAR MD:MATRIX2);
BEGIN
  SETVAL1(MD);
  SETVAL4(TPARAMS,CPARAMS,SPARAMS,HPARAMS,UPARAMS,RPARAMS,

```

```

        HCARANG,UCARANG,HTORSION);
SETVAL6(ITGROOVE,HHDIA,HSDIA,HTORS);

{Divide muscle data by those that require H.head correction and those needing
H.shaft corrections.}
FOR A:= 1 TO 20 DO
  BEGIN
    FOR B:=1 TO 10 DO
      BEGIN
        FOR C:= 1 TO 3 DO VECT1[C]:=MD[A,B,1,C];
        FOR C:= 1 TO 3 DO VECT2[C]:=MD[A,B,2,C];

        IF(( A=4 ) OR
           ( A=12 ) OR
           ( A=13 ) OR
           ( A=15)) THEN
          BEGIN
            IF((VECT2[1]<>0)OR(VECT2[2]<>0)OR(VECT2[3]<>0)) THEN
              HUMHEAD(HHDIA,HTORS,HTORSION,VECT2);
              END;
              {only insertions at hum head}

              IF(( A=2 ) OR
                 ( A=3 ) OR
                 ( A=5 ) OR
                 ( A=7 ) OR
                 ( A=14 ) OR
                 ( A=15)) THEN
                 {humeral shaft insertions considered here}
                 {note: T. Minor is considered for both }
                 {H. head and shaft wrapping}
                 BEGIN
                   IF((VECT2[1]<>0)OR(VECT2[2]<>0)OR(VECT2[3]<>0)) THEN
                     HUMSHAFT(HSDIA,HTORS,HTORSION,HPARAMS,VECT2);
                     END;

                     IF(( A=17) AND ((B=2) OR (B=3)))THEN
                       HUMSHAFT(HSDIA,HTORS,HTORSION,HPARAMS,VECT1);
                       FOR C:= 1 TO 3 DO MD[A,B,1,C]:=VECT1[C];
                       FOR C:= 1 TO 3 DO MD[A,B,2,C]:=VECT2[C];
                       END;
                       {hum shaft origins }
                     END;

                     {The intertubercle groove must also be corrected for its location wrt the humeral
                     head}
                     HUMHEAD(HHDIA,HTORS,HTORSION,ITGROOVE);
                     {store intertubercle groove location in both the biceps fasicle 3 insertion and
                     origin locations}
                     FOR C:= 1 TO 3 DO
                       BEGIN
                         MD[1,3,1,C]:=ITGROOVE[C];
                         MD[1,3,2,C]:=ITGROOVE[C];
                       END;
                     END;

                     {*****}
                     {*****}
                     END.
                     {*****}
                     {*****}

```

```

{*****}
{*****}
UNIT CSALIGN;

INTERFACE
USES CRT, PRINTER, EULERS, VARIABLE, SETVALS, MISCOPS;

PROCEDURE CALIGN (VAR SCCENT, ACCENT: MATRIX1; VAR CROTMAT, CIROTMAT: MATRIX3);
PROCEDURE SALIGN (VAR GHCENT, ACCENT: MATRIX1; VAR SROTMAT, SIROTMAT: MATRIX3);

IMPLEMENTATION
{*****}
{*****}
{Procedure used to define clavicle orientation wrt the trunk coord. sys.}
PROCEDURE CALIGN (VAR SCCENT, ACCENT: MATRIX1; VAR CROTMAT, CIROTMAT: MATRIX3);
BEGIN
  SETVAL3 (TPOS, CPOS, SPOS, HPOS, UPOS, RPOS);      {get clinical alignment info.}

  {Reorientating trunk coord. sys. parallel to clavicle sys. requires a 90 deg.
  rotation}
  AA:=90*Pi/180;   BB:=CPOS [1];   CC:=CPOS [2];   DD:=CPOS [3];
  EULERZ (MAT4, AA);  EULERY (MAT3, BB);  EULERZ (MAT2, CC);  EULERX (MAT1, DD);

  MATEMULT (MAT1, MAT2, MAT8);
  MATEMULT (MAT3, MAT4, MAT9);
  MATEMULT (MAT8, MAT9, CROTMAT);
  MATEINV (CROTMAT, CIROTMAT);

  {For SC & AC joint centre locations wrt trunk coord. sys., bone parameters
  must be read}
  SETVAL4 (TPARAMS, CPARAMS, SPARAMS, HPARAMS, UPARAMS, RPARAMS, HCARANG, UCARANG,
  HTORSION);

  VECTMULT (CIROTMAT, CPARAMS, VECT1);

  FOR A:=1 TO 3 DO
  BEGIN
    SCCENT [A] :=TPARAMS [A];
    ACCENT [A] :=TPARAMS [A]+VECT1 [A];
  END;

  {*****}
  {*****}
  {Procedure used to define scapula orientation wrt the trunk coord. sys.}
  PROCEDURE SALIGN (VAR GHCENT, ACCENT: MATRIX1; VAR SROTMAT, SIROTMAT: MATRIX3);
  BEGIN
    SETVAL3 (TPOS, CPOS, SPOS, HPOS, UPOS, RPOS);      {get clinical position info.}

    {Reorientating trunk coord. sys. parallel to scapula sys. requires a 180 deg.
    rotation}
    AA:=Pi;   BB:=SPOS [1];   CC:=SPOS [2];   DD:=SPOS [3];
    EULERX (MAT4, AA);  EULERX (MAT3, BB);  EULERZ (MAT2, CC);  EULERY (MAT1, DD);

    MATEMULT (MAT1, MAT2, MAT8);
    MATEMULT (MAT3, MAT4, MAT9);
    MATEMULT (MAT8, MAT9, SROTMAT);
    MATEINV (SROTMAT, SIROTMAT);

    {For GH joint centre location wrt trunk coord. sys., bone parameters
    must be read}
    SETVAL4 (TPARAMS, CPARAMS, SPARAMS, HPARAMS, UPARAMS, RPARAMS, HCARANG, UCARANG,
    HTORSION);

    VECTMULT (SIROTMAT, SPARAMS, VECT1);
    FOR A:=1 TO 3 DO  GHCENT [A] :=ACCENT [A]+VECT1 [A];
  END;

  {*****}
  {*****}
  END.
  {*****}
  {*****}

```



```

UNIT EULERS ; {FILE EULERS2
              THIS PROGRAM CALCULATES AN EULER ROTATION MATRIX GIVEN THE}
              {ROTATION AXIS AND ANGLE}

```

```

INTERFACE
USES VARIABLE;

```

```

PROCEDURE EULERX (VAR MAT01: MATRIX3; AA: REAL);
PROCEDURE EULERY (VAR MAT01: MATRIX3; AA: REAL);
PROCEDURE EULERZ (VAR MAT01: MATRIX3; AA: REAL);

```

```

IMPLEMENTATION

```

```

PROCEDURE EULERX (VAR MAT01: MATRIX3; AA: REAL);
BEGIN
  MAT01 [1, 1] := 1 ; MAT01 [1, 2] := 0 ; MAT01 [1, 3] := 0 ;
  MAT01 [2, 1] := 0 ; MAT01 [2, 2] := COS (AA) ; MAT01 [2, 3] := SIN (AA) ;
  MAT01 [3, 1] := 0 ; MAT01 [3, 2] := -1 * SIN (AA) ; MAT01 [3, 3] := COS (AA) ;
END;

```

```

PROCEDURE EULERY (VAR MAT01: MATRIX3; AA: REAL);
BEGIN
  MAT01 [1, 1] := COS (AA) ; MAT01 [1, 2] := 0 ; MAT01 [1, 3] := -1 * SIN (AA) ;
  MAT01 [2, 1] := 0 ; MAT01 [2, 2] := 1 ; MAT01 [2, 3] := 0 ;
  MAT01 [3, 1] := SIN (AA) ; MAT01 [3, 2] := 0 ; MAT01 [3, 3] := COS (AA) ;
END;

```

```

PROCEDURE EULERZ (VAR MAT01: MATRIX3; AA: REAL);
BEGIN
  MAT01 [1, 1] := COS (AA) ; MAT01 [1, 2] := SIN (AA) ; MAT01 [1, 3] := 0 ;
  MAT01 [2, 1] := -1 * SIN (AA) ; MAT01 [2, 2] := COS (AA) ; MAT01 [2, 3] := 0 ;
  MAT01 [3, 1] := 0 ; MAT01 [3, 2] := 0 ; MAT01 [3, 3] := 1 ;
END;
END.

```

```

{*****}
{*****}
UNIT EULEXP;                                {Using transformation matrices calculated for
                                             each body segment, corresponding Euler Angles
                                             are defined by this unit. A Floating Axis technique
                                             as defined by Grood and Suntay is used for
                                             the calculations.}

{*****}
{*****}
INTERFACE
USES CRT, PRINTER,
      EULERS, MISCOPS, SETVALS, VARIABLE;

PROCEDURE TEULER (VAR TPOS: MATRIX1; VAR TROTMAT: MATRIX3);
PROCEDURE CEULER (VAR CPOS: MATRIX1; VAR CROTMAT: MATRIX3);
PROCEDURE SEULER (VAR SPOS: MATRIX1; VAR SROTMAT: MATRIX3);
PROCEDURE HEULER (VAR HPOS: MATRIX1; VAR HROTMAT: MATRIX3; VAR HELEVA: REAL);
PROCEDURE REULER (VAR RPOS: MATRIX1; VAR HROTMAT, RROTMAT: MATRIX3);
PROCEDURE SPINHAP (VAR HROTMAT, SROTMAT: MATRIX3; VAR THETA: REAL);

IMPLEMENTATION
{*****}
{*****}
{Lab to Trunk Euler angles are calculated here}
PROCEDURE TEULER (VAR TPOS: MATRIX1; VAR TROTMAT: MATRIX3);
BEGIN

{The lab coord system must be rearranged to be parallel with the trunk coord sys.}
FOR A:= 1 TO 3 DO FOR B:= 1 TO 3 DO MAT2[A,B]:= 0;
MAT2[1,2]:=-1; MAT2[2,3]:=1; MAT2[3,1]:=-1;

{Calculating Euler angles requires a "Floating Axis", VECT7, to be defined.}
FOR A:= 1 TO 3 DO
  BEGIN
    VECT1[A]:=MAT2[1,A];
    VECT2[A]:=MAT2[2,A];                                {STATIONARY OR LAB SYSTEM}
    VECT3[A]:=MAT2[3,A];
    VECT4[A]:=TROTMAT[1,A];
    VECT5[A]:=TROTMAT[2,A];                                {MOVING OR TRUNK SYSTEM}
    VECT6[A]:=TROTMAT[3,A];
  END;
  NORMALIZ(VECT1);   NORMALIZ(VECT2);   NORMALIZ(VECT3);
  NORMALIZ(VECT4);   NORMALIZ(VECT5);   NORMALIZ(VECT6);

  VECTCROS(VECT2,VECT4,VECT7);                {FLOATING AXIS}
  NORMALIZ(VECT7);

{Trunk flexion may be > 90 degrees, so a check and corresponding correction
must be made to allow the trigonometric functions to yield the correct answer.}
AA:= VECTDOT(VECT7,VECT1);
IF(VECT4[2]>0)THEN {flexion > 90 degrees}
  TPOS[1]:= Pi-ASIN(AA)
ELSE
  TPOS[1]:= ASIN(AA);

{Trunk abduction is now}
AA:= VECTDOT(VECT2,VECT4);
TPOS[2]:= ASIN(AA);

{Trunk rotation is now}
AA:= VECTDOT(VECT5,VECT7);
TPOS[3]:=-1*ASIN(AA);

{Converting Euler Angles, TPOS, to degrees from radians}
FOR A:= 1 TO 3 DO TPOS[A]:= TPOS[A]*(180/PI);

END;

{*****}
{*****}
{Trunk to Clavicle Euler angles are calculated here}
PROCEDURE CEULER (VAR CPOS: MATRIX1; VAR CROTMAT: MATRIX3);
BEGIN

{The Trunk coord system must be rearranged to be parallel with the Clavicle coord
sys.}
FOR A:= 1 TO 3 DO FOR B:= 1 TO 3 DO MAT2[A,B]:= 0;
MAT2[1,2]:=1; MAT2[2,1]:=-1; MAT2[3,3]:=1;

{Calculating Euler angles requires a "Floating Axis", VECT7, to be defined.}
FOR A:= 1 TO 3 DO
  BEGIN
    VECT1[A]:=MAT2[1,A];

```

```

    VECT2 [A] :=MAT2 [2,A];           {STATIONARY OR MODIFIED TRUNK SYSTEM}
    VECT3 [A] :=MAT2 [3,A];
    VECT4 [A] :=CROTMAT [1,A];
    VECT5 [A] :=CROTMAT [2,A];       {MOVING OR CLAVICLE SYSTEM}
    VECT6 [A] :=CROTMAT [3,A];
    END;
    NORMALIZ (VECT1);      NORMALIZ (VECT2);      NORMALIZ (VECT3);
    NORMALIZ (VECT4);      NORMALIZ (VECT5);      NORMALIZ (VECT6);

    VECTCROS (VECT4,VECT2,VECT7);     {FLOATING AXIS}
    NORMALIZ (VECT7);

    {Clavicle flexion is now}
    AA:= VECTDOT (VECT7,VECT1);
    CPOS [1]:= ASIN (AA);

    {Clavicle abbduction is now}
    AA:= VECTDOT (VECT2,VECT4);
    CPOS [2]:= ASIN (AA);

    {Clavicle rotation is now}
    AA:= VECTDOT (VECT5,VECT7);
    CPOS [3]:= -1*ASIN (AA);

    {Converting Euler Angles, CPOS, to degrees from radians}
    FOR A:= 1 TO 3 DO CPOS [A]:= CPOS [A]*(180/PI);

    END;

    {*****}
    {*****}
    {Trunk to Scapula Euler angles are calculated here}

    PROCEDURE SEULER (VAR SPOS: MATRIX1; VAR SROTMAT: MATRIX3);
    BEGIN

    {The Trunk coord system must be rearranged to be parallel with the Scapula coord
    sys.}
    AA:=Pi;
    EULERX (MAT2,AA);

    {Calculating Euler angles requires a "Floating Axis", VECT7, to be defined.}
    FOR A:= 1 TO 3 DO
    BEGIN
    VECT1 [A] :=MAT2 [1,A];
    VECT2 [A] :=MAT2 [2,A];           {STATIONARY OR MODIFIED TRUNK SYSTEM}
    VECT3 [A] :=MAT2 [3,A];
    VECT4 [A] :=SROTMAT [1,A];
    VECT5 [A] :=SROTMAT [2,A];       {MOVING OR SCAPULA SYSTEM}
    VECT6 [A] :=SROTMAT [3,A];
    END;
    NORMALIZ (VECT1);      NORMALIZ (VECT2);      NORMALIZ (VECT3);
    NORMALIZ (VECT4);      NORMALIZ (VECT5);      NORMALIZ (VECT6);

    { VECTCROS (VECT4,VECT2,VECT7);      }           {FLOATING AXIS}
    VECTCROS (VECT5,VECT1,VECT7);
    NORMALIZ (VECT7);

    {Scapula medial lateral rotation ie abduction (about Zs axis):}
    { AA:= VECTDOT (VECT2,VECT4); }
    FOR A:=1 TO 3 DO VECT8 [A] :=-1*VECT1 [A];
    AA:= VECTDOT (VECT8,VECT5);
    SPOS [2]:= ASIN (AA);

    {Scapula vertical tilting ie flexion (about the Ys axis)}
    { AA:= VECTDOT (VECT7,VECT1); }
    AA:= VECTDOT (VECT4,VECT7);
    SPOS [3]:= ASIN (AA);

    {Clavicle rotation ie rotation (about the Xs axis)}
    { AA:= VECTDOT (VECT5,VECT7); }
    AA:= VECTDOT (VECT2,VECT7);
    SPOS [1]:=ASIN (AA);

    {Converting Euler Angles, SPOS, to degrees from radians}
    FOR A:= 1 TO 3 DO SPOS [A]:= SPOS [A]*(180/PI);

    END;

    {*****}
    {*****}
    {trunk to upper arm Euler angles are calculated here}

```

```

PROCEDURE HEULER (VAR HPOS: MATRIX1; VAR HROTMAT: MATRIX3; VAR HELEVA: REAL);
BEGIN

{The stationary coord system is arranged parallel with base upper arm coord sys.}
  FOR A:= 1 TO 3 DO FOR B:= 1 TO 3 DO MAT2[A,B]:= 0;
  MAT2[1,1]:=1; MAT2[2,2]:=1; MAT2[3,3]:=1;

{Calculating Euler angles requires a "Floating Axis", VECT7, to be defined.}
  FOR A:= 1 TO 3 DO
    BEGIN
      VECT1[A]:=MAT2[1,A];
      VECT2[A]:=MAT2[2,A]; {STATIONARY OR trunk SYSTEM}
      VECT3[A]:=MAT2[3,A];
      VECT4[A]:=HROTMAT[1,A];
      VECT5[A]:=HROTMAT[2,A]; {MOVING OR upper arm SYSTEM}
      VECT6[A]:=HROTMAT[3,A];
    END;
  NORMALIZ(VECT1); NORMALIZ(VECT2); NORMALIZ(VECT3);
  NORMALIZ(VECT4); NORMALIZ(VECT5); NORMALIZ(VECT6);

{Due to mobility of upper arm coord sys, Floating axis is restricted
to lay in the +ve Ztrunk direction. This restriction limits humeral
to -90< flexion <90 degrees. This is to eliminate convention change problems
due to the upper arm centre line crossing over the VECT2 direction.}
  VECTCROS(VECT4,VECT2,VECT7); {FLOATING AXIS}
  NORMALIZ(VECT7);

  if(vect7[3]<0) then for a:= 1 to 3 do vect7[a]:=-1*vect7[a];

{Upper arm flexion is now}
  AA:= VECTDOT(VECT7,VECT1);
  BB:= ASIN(AA);
  HPOS[1]:=BB;

{Upper arm abdduction is now}
  AA:= VECTDOT(VECT2,VECT4);
  BB:= ASIN(AA);
  IF(VECT4[1]<0) THEN BB:=PI-BB;
  HPOS[2]:=BB;

{Upper arm rotation must be calculated differently that normal for the
floating axis technique. see notes Nov 24, 92 for details. The two orientation
angles calculated so far can give the centre line of the arm.}
  eulery(mat1,hpos[1]);
  eulerz(mat2,hpos[2]);
  matmult(mat2,mat1,mat3);

{The second row is the yh axis direction vector (VECT8) before arm
rotation is included. By comparing this to the expected Yh from
HROTMAT (VECT5), the required rotation correction angle can be calculated.}
  FOR A := 1 TO 3 DO VECT8[A]:=MAT3[2,A];
  NORMALIZ(VECT8);

  AA:=VECTDOT(VECT5,VECT8); BB:=VECTDOT(VECT6,VECT8);
  AA:=ASIN(AA); BB:=ASIN(BB);

  IF(AA>=0) THEN HPOS[3]:=-1*(BB);
  IF((AA< 0) and (BB< 0)) THEN HPOS[3]:=-1*((-1*PI)-BB);
  IF((AA< 0) AND (BB>=0)) THEN HPOS[3]:=-1*(PI)-BB);

{Converting Euler Angles, HPOS, to degrees from radians}
  FOR A:= 1 TO 3 DO HPOS[A]:= HPOS[A]*(180/PI);

{Total humeral elevation is:}
  AA:=VECTDOT(VECT4,VECT1);
  BB:=ASIN(AA);
  HELEVA:=((BB*180/PI)-90)*-1;

  END;
  {*****}
  {*****}
  {trunk to forearm Euler angles are calculated here}
  PROCEDURE REULER (VAR RPOS: MATRIX1; VAR HROTMAT, RROTMAT: MATRIX3);
  BEGIN

{The stationary coord system is the upper arm coord sys.}
  FOR A:= 1 TO 3 DO
    BEGIN
      VECT1[A]:=HROTMAT[1,A];
      VECT2[A]:=HROTMAT[2,A]; {STATIONARY OR upper arm SYSTEM}
      VECT3[A]:=HROTMAT[3,A];
      VECT4[A]:=RROTMAT[1,A];
      VECT5[A]:=RROTMAT[2,A]; {MOVING OR lower arm SYSTEM}
      VECT6[A]:=RROTMAT[3,A];
    END;

```

```

        END;
        NORMALIZ (VECT1);      NORMALIZ (VECT2);      NORMALIZ (VECT3);
        NORMALIZ (VECT4);      NORMALIZ (VECT5);      NORMALIZ (VECT6);

{Calculating Euler angles requires a "Floating Axis", VECT7, to be defined.}
        VECTCROS (VECT4, VECT2, VECT7);      {FLOATING AXIS}
        NORMALIZ (VECT7);

{Lower arm flexion is now}
        AA:= VECTDOT (VECT7, VECT3);
        BB:= ASIN (AA);
        bb:= (pi/2)-bb;
        RPOS [1] :=BB;

{Lower arm abbduction, should be zero but is calculated here }
        AA:= VECTDOT (VECT2, VECT4);
        BB:= ASIN (AA);
        RPOS [2] :=BB;

{Lower arm rotation is now}
        AA:= VECTDOT (VECT5, VECT7);
        BB:=ASIN (AA);
        if (bb<0) then
            begin
                {if bb <0 then use vect7 dot vect6 and add the difference}
                aa:=vectdot (vect6, vect7);
                bb:= asin(aa) - (pi/2);
            end;
        RPOS [3] :=BB;

{Converting Euler Angles, RPOS, to degrees from radians}
        FOR A:= 1 TO 3 DO RPOS [A] := RPOS [A] *(180/PI);
        END;
        {*****}
        {*****}
        {This procedure calculates the scapular spine to humeral angle as
        projected in the AP plane.}
        PROCEDURE SPINHAP (VAR HROTMAT, SROTMAT: MATRIX3; VAR THETA: REAL);
        BEGIN
            SETVAL1 (MD);

{Contact point 1 is the medial end of the spine now VECT1}
            FOR A:= 1 TO 3 DO VECT1 [A] :=MD [18, 1, 2, A];

{Converting to be wrt the trunk coord system}
            MATEINV (SROTMAT, SIROTMAT);
            VECTMULT (SIROTMAT, VECT1, VECT2);

{Spino vertical AP plane angle is now:}
            THETA:= (ARCTAN (VECT2 [1]/VECT2 [2]))+(Pi/2);
            THETA:=THETA*180/Pi;
            END;

        {*****}
        {*****}
        END.
        {*****}
        {*****}

```

```

{*****}
{*****}
UNIT FORCDIR;          {FILE FORCDIR3, This unit contains the procedure.
                        MDIR,  calculation of muscle fibre directions.

                        Since all muscle origin/insertion data is given
                        wrt the trunk coord. sys. (matrix MDT) then
                        calculating directions is simplified.}
{*****}
{*****}
INTERFACE
USES CRT,SETVALS,MISCOPS,VARIABLE;

PROCEDURE MUSD(VAR MDT,MDIR :MATRIX2);
IMPLEMENTATION

{*****}
{*****}
PROCEDURE MUSD(VAR MDT,MDIR :MATRIX2);
BEGIN
{zero muscle direction matrix}
FOR A:=1 TO 20 DO
  BEGIN
  FOR B:=1 TO 10 DO
    BEGIN
    FOR C:=1 TO 2 DO
      BEGIN
      FOR D:= 1 TO 3 DO
        BEGIN
          MDIR[A,B,C,D]:=0 ;
        END;
      END;
    END;
  END;
END;

{Origin and insertion data can now be sequencially examined to determine muscle
force directions.}
FOR A:=1 TO 20 DO
  BEGIN
  FOR B:=1 TO 10 DO
    BEGIN
    IF ( (MDT[A,B,1,1]<>0) OR (MDT[A,B,1,2]<>0) OR (MDT[A,B,1,3]<>0)
      OR (MDT[A,B,2,1]<>0) OR (MDT[A,B,2,2]<>0) OR (MDT[A,B,2,3]<>0)) THEN
      BEGIN

{Calculate direction of muscle forces at the origin and insertion of biceps.
Biceps fascicle 2 is unusual as it is split into two parts. The first uses
the origin and inserts into the corrected intertubercle groove location, the
second originates at the intertubercle groove and inserts into the radius.
see notes FEB 10 92}
      IF ((A=1)AND((B=2)OR(B=3))) THEN
        BEGIN
          IF (B=2) THEN
            BEGIN
              FOR C:= 1 TO 3 DO
                BEGIN
                  VECT2[C]:=MDT[1,3,2,C]-MDT[1,2,1,C];
                  VECT3[C]:=MDT[1,2,2,C]-MDT[1,3,1,C];
                END;
              NORMALIZ(VECT2);    NORMALIZ(VECT3);
              FOR C:= 1 TO 3 DO
                BEGIN
                  MDIR[A,B,1,C]:=VECT2[C];
                  MDIR[A,B,2,C]:=VECT3[C]*-1;
                END;
              END;
            END ELSE
            BEGIN
{Calculate direction of vector joining origina and insertion for
remaining muscle fascicles.}
              FOR C:= 1 TO 3 DO    VECT1[C]:=MDT[A,B,2,C]-MDT[A,B,1,C];
              NORMALIZ(VECT1);
              FOR C:= 1 TO 3 DO
                BEGIN
                  MDIR[A,B,1,C]:=VECT1[C];
                  MDIR[A,B,2,C]:=VECT1[C]*-1;
                END;
              END;
            END;
          END;
        END;
      END;
    END;
  END;
END;
END;
END;

```

```
{*****}  
{*****}  
END.  
{*****}  
{*****}
```

```

{*****}
{*****}
UNIT FORCEBAL;           {This unit calculates forces at a joint
                        due to external applied loads, gravity and
                        muscle forces. Results are written to working
                        files for use in determining joint stability etc.}
{*****}
{*****}
INTERFACE
USES CRT, PRINTER,
    EULERS, MISCOPS, SETVALS, VARIABLE;
PROCEDURE GHFORBAL (VAR FRAMENUM: INTEGER;
                   VAR GHFLOWD: MATRIX1; VAR MDT, MDIR: MATRIX2;
                   VAR SROTMAT: MATRIX3; VAR FORFACTS: MATRIX9; VAR S3: STRING );

IMPLEMENTATION
{*****}
{*****}
{This procedure calculates the parameters for performing a force balance
calculation at the Gleno Humeral joint. Output is sent to a file ext:.BAL and
workfile:"WRKFILE7.PRN". This information is with respect to a coordinate
system defined by the glenoid fossa as per notes Feb 22,92. The output
information is then used during optimization for ensuring the GH joint is
stable with the optimized forces. }
PROCEDURE GHFORBAL (VAR FRAMENUM: INTEGER;
                   VAR GHFLOWD: MATRIX1; VAR MDT, MDIR: MATRIX2;
                   VAR SROTMAT: MATRIX3; VAR FORFACTS: MATRIX9; VAR S3: STRING );

BEGIN
{Definition of a coordinate system based on the glenoid fossa is required. The
orientation of the fossa wrt the scapula coord system is given by two rotation
angles the first is a Zs-axis rotation, the second an Xs-axis rotation and the
third is not required yet.}
    SETVAL5 (GFPOS, GFDIA);
    AA:=GFPOS[1]*-1;
    EULERZ (MAT1, AA);
    AA:=GFPOS[2];
    EULERX (MAT2, AA);
    MATEMULT (MAT2, MAT1, MAT3);
    MATEMULT (MAT3, SROTMAT, MAT10);

{The procedure now sequentially looks at the muscles crossing the GH joint.
Force directions associated with each required muscle fascicle are converted
to the Glenoid Fossa coord system and stored to the working file.}
    C:= 2; G:=0;
    FOR A:= 1 TO 20 DO
        BEGIN
            FOR B:= 1 TO 10 DO
                BEGIN
                    {Only certain of the fascicles are used in the program and of these 55 only 24
                    are required for GH force balance.}
                    IF ((A= 1) AND (B<=2)) OR
                       ((A= 2) AND (B= 1)) OR
                       ((A= 3) AND (B<=5)) OR
                       ((A= 4) AND (B<=3)) OR
                       ((A= 5) AND (B<=3)) OR
                       ((A= 7) AND (B<=3)) OR
                       ((A=12) AND (B<=3)) OR
                       ((A=13) AND (B =1)) OR
                       ((A=14) AND (B =1)) OR
                       ((A=15) AND (B =1)) OR
                       joint)
                       ((A=17) AND (B =1)) ) THEN
                        BEGIN
                            G:=G+1;
                            FOR D:= 1 TO 3 DO
                                BEGIN
                                    VECT1 [D] :=MDIR [A, B, C, D];
                                    IF ((A=1) AND (B=2)) THEN VECT1 [D] :=-1*MDIR [1, 2, 1, D];
                                END;
                                VECTMULT (MAT10, VECT1, VECT2);
                                FOR D:= 1 TO 3 DO FORFACTS [D, G] :=VECT2 [D];
                            END;
                            IF ((A= 6) AND (B =1)) OR
                               ((A= 8) AND (B<=3)) OR
                               ((A= 9) AND (B<=5)) OR
                               ((A=10) AND (B =1)) OR
                               ((A=11) AND (B<=9)) OR
                               ((A=16) AND (B<=8)) OR
                               ((A=17) AND ((B= 2) OR (B=3))) OR
                               ((A=18) AND (B<=2)) ) THEN
                                {muscles not crossing the GH joint}
                                BEGIN
                                    FOR D:= 1 TO 3 DO VECT2 [D] := 0;
                                END;
                            END;
                        END;
                END;
            END;
        END;
    END;

```


{MAT10 can now be used to convert ext and gravity loads to the glenoid fossa coord system. These new values can be stored to the output working file.}

```
VECTMULT(MAT10,GHFLOAD,VECT1);
FOR D:= 1 TO 3 DO
  BEGIN
    FORFACTS[D,25]:=0.0;
    FORFACTS[D,26]:=0.0;
    FORFACTS[D,27]:=VECT1[D];
  END;
END;
{*****}
{*****}
END.
{*****}
{*****}
```

```

{*****}
{*****}
UNIT LOAD;                                {FILE ARMLOAD3
                                           This unit using anatomical bone position,
                                           load information, and trunk alignment info.
                                           calculates external forces and moments at
                                           various joints associated with the shoulder.
                                           -GHLOAD, external glenohumeral forces and moments
                                           -HULOAD, external elbow forces and moments
                                           -HRLOAD, external humeral ulnar forces and moments.)
{*****}
{*****}
INTERFACE
USES CRT, PRINTER, SETVALS, EULERS, MISCOPS, VARIABLE;

PROCEDURE HULOAD (VAR ELCENT, HNDCENT, HUFLOAD, HUMLOAD: MATRIX1; VAR UROTMAT: MATRIX3);
PROCEDURE HRLOAD (VAR ELCENT, HRCENT, HNDCENT, HRFLOAD, HRMLOAD: MATRIX1; VAR
RROTMAT: MATRIX3);
PROCEDURE GHLOAD (VAR GHCENT, ELCENT, HNDCENT, GHFLOAD, GHMLOAD: MATRIX1; VAR
HROTMAT: MATRIX3);
PROCEDURE ACLOAD (VAR ACCENT, GHCENT, ELCENT, HNDCENT, ACFLOAD, ACMLOAD: MATRIX1; VAR
SROTMAT: MATRIX3);
PROCEDURE SCLOAD (VAR SCCENT, GHCENT, ELCENT, HNDCENT, SCFLOAD, SCMLOAD: MATRIX1; VAR
CROTMAT: MATRIX3);

IMPLEMENTATION
{*****}
{*****}
PROCEDURE PROCED1 (VAR TPOS: MATRIX1; VAR MAT10: MATRIX3);
{Calculate rotation matrix for conversion of lab to trunk coord. sys. info.
The first step is to rearrange the lab coord sys so it is parallel to the
trunk coord sys when 0 deg. trunk flex, abd, and rot are imposed.}

BEGIN
  FOR A:=1 TO 3 DO FOR B:=1 TO 3 DO MAT4[A,B]:=0;
  MAT4[1,2]:=-1 ; MAT4[2,3]:=1 ; MAT4[3,1]:=-1;

  {The three Euler rotation matrices can now be calculated.}
  TPOS[1]:=(TPOS[1])*-1;
  EULERY (MAT3, TPOS[1]);
  EULERZ (MAT2, TPOS[2]);
  EULERX (MAT1, TPOS[3]);

  {Combining the rotation matrices to give the total rotation, MAT10.}
  MATEMULT (MAT1, MAT2, MAT8);
  MATEMULT (MAT8, MAT3, MAT9);
  MATEMULT (MAT9, MAT4, MAT10);
  END;
{*****}
{*****}
PROCEDURE HULOAD (VAR ELCENT, HNDCENT, HUFLOAD, HUMLOAD: MATRIX1; VAR UROTMAT: MATRIX3);
BEGIN

  {Set body alignment and load variables.}
  SETVAL2 (BHEIGHT, BWEIGHT, HNDFORCE, HNDMOMNT);
  SETVAL3 (TPOS, CPOS, SPOS, HPOS, UPOS, RPOS);

  {Calculate orientation of trunk coord sys wrt the lab coord sys.}
  PROCED1 (TPOS, MAT10);

  {Calculating gravity loads for the forearm/hand.}
  {Limb weights are calculated using Contini and Drillis(1966) data.}
  VECT2[1]:=0 ; VECT2[2]:=-1*(0.018+0.006)*BWEIGHT ; VECT2[3]:=0;

  {Converting hand loads and gravity effects to TRUNK coord. sys.}
  VECTMULT (MAT10, HNDFORCE, VECT5);
  FOR A:=1 TO 3 DO HNDFORCE[A]:=VECT5[A];

  VECTMULT (MAT10, HNDMOMNT, VECT5);
  FOR A:=1 TO 3 DO HNDMOMNT[A]:=VECT5[A];

  VECTMULT (MAT10, VECT2, VECT5);
  FOR A:=1 TO 3 DO VECT2[A]:=VECT5[A];

  {Calculating position of lower arm/hand centres of mass wrt the
ULNAR coord. sys. Note: coordinates are wrt trunk coordinate system.}
  DD:=HNDCENT[1]-ELCENT[1];
  EE:=HNDCENT[2]-ELCENT[2];
  FF:=HNDCENT[3]-ELCENT[3];

  VECT4[1]:=(DD*0.420);
  VECT4[2]:=(EE*0.420);

```

```

VECT4 [3] := (FF*0.420);

{Total elbow force load will then be:}
FOR A:=1 TO 3 DO HUFLOAD[A] := HNDFORCE[A] + VECT2[A];

{Total elbow moments will then be:}
VECT5 [1] := HNDMOMNT [1] + (HNDFORCE [3] * EE - HNDFORCE [2] * FF);
VECT5 [1] := VECT5 [1] + (VECT2 [3] * VECT4 [2] - VECT2 [2] * VECT4 [3]);

VECT5 [2] := HNDMOMNT [2] + (HNDFORCE [1] * FF - HNDFORCE [3] * DD);
VECT5 [2] := VECT5 [2] + (VECT2 [1] * VECT4 [3] - VECT2 [3] * VECT4 [1]);

VECT5 [3] := HNDMOMNT [3] + (HNDFORCE [2] * DD - HNDFORCE [1] * EE);
VECT5 [3] := VECT5 [3] + (VECT2 [2] * VECT4 [1] - VECT2 [1] * VECT4 [2]);

{Converting moments to ulnar coord. sys.}
VECTMULT (UROTMAT, VECT5, HUMLOAD);

{
WRITELN ('ELBOW LOADS, (N, WRT TRUNK):
', HUFLOAD [1] : 7:3, HUFLOAD [2] : 7:3, HUFLOAD [3] : 7:3);
WRITELN ('ELBOW MOMENTS, Nm:
', HUMLOAD [1] : 7:3, HUMLOAD [2] : 7:3, HUMLOAD [3] : 7:3);
}
END;

{*****}
PROCEDURE HRLOAD (VAR ELCENT, HRCENT, HNDCENT, HRFLOAD, HRMLOAD: MATRIX1; VAR
RROTMAT: MATRIX3);
BEGIN
{Set body alignment and load variables.}
SETVAL2 (BHEIGHT, BWEIGHT, HNDFORCE, HNDMOMNT);
SETVAL3 (TPOS, CPOS, SPOS, HPOS, UPOS, RPOS);
SETVAL4 (TPARAMS, CPARAMS, SPARAMS, HPARAMS, UPARAMS, RPARAMS, HCARANG, UCARANG, HTORSION);

{Calculate orientation of trunk coord sys wrt the lab coord sys.}
PROCEED1 (TPOS, MAT10);

{Calculating gravity loads for the forearm/hand.}
{Limb weights are calculated using Contini and Drillis (1966) data.}
VECT2 [1] := 0; VECT2 [2] := -1 * (0.018 + 0.006) * BWEIGHT; VECT2 [3] := 0;

{Converting hand loads and gravity effects to trunk coord. sys.}
VECTMULT (MAT10, HNDFORCE, VECT5);
FOR A:=1 TO 3 DO HNDFORCE[A] := VECT5[A];

VECTMULT (MAT10, HNDMOMNT, VECT5);
FOR A:=1 TO 3 DO HNDMOMNT[A] := VECT5[A];

VECTMULT (MAT10, VECT2, VECT5);
FOR A:=1 TO 3 DO VECT2[A] := VECT5[A];

{Calculating position of lower arm/hand centres of mass wrt the
trunk coord. sys. Note: coordinates are wrt trunk coordinate system.}

DD := HNDCENT [1] - HRCENT [1];
EE := HNDCENT [2] - HRCENT [2];
FF := HNDCENT [3] - HRCENT [3];

VECT4 [1] := (DD*0.420);
VECT4 [2] := (EE*0.420);
VECT4 [3] := (FF*0.420);

{Total force load about the radial coord sys origin will then be:}
FOR A:=1 TO 3 DO HRFLOAD[A] := HNDFORCE[A] + VECT2[A];

{Total moments about the radial coord sys origin will then be:}
VECT5 [1] := HNDMOMNT [1] + (HNDFORCE [3] * EE - HNDFORCE [2] * FF);
VECT5 [1] := VECT5 [1] + (VECT2 [3] * VECT4 [2] - VECT2 [2] * VECT4 [3]);

VECT5 [2] := HNDMOMNT [2] + (HNDFORCE [1] * FF - HNDFORCE [3] * DD);
VECT5 [2] := VECT5 [2] + (VECT2 [1] * VECT4 [3] - VECT2 [3] * VECT4 [1]);

VECT5 [3] := HNDMOMNT [3] + (HNDFORCE [2] * DD - HNDFORCE [1] * EE);
VECT5 [3] := VECT5 [3] + (VECT2 [2] * VECT4 [1] - VECT2 [1] * VECT4 [2]);

{Converting moments to radial coord. sys.}
VECTMULT (RROTMAT, VECT5, HRMLOAD);

{
WRITELN ('RADIAL LOADS, (N, WRT TRUNK):
', HRFLOAD [1] : 7:3, HRFLOAD [2] : 7:3, HRFLOAD [3] : 7:3);
WRITELN ('RADIAL MOMENTS, Nm:
', HRMLOAD [1] : 7:3, HRMLOAD [2] : 7:3, HRMLOAD [3] : 7:3);
}
END;

```

```

{*****}
{*****}
PROCEDURE GHLOAD (VAR GHCENT, ELCENT, HNDCENT, GHFLOW, GHMLOAD: MATRIX1; VAR
HROTMAT: MATRIX3);

{Set body alignment and load variables.}
BEGIN
  SETVAL2 (BHEIGHT, BWEIGHT, HNDFORCE, HNDMOMNT);
  SETVAL3 (TPOS, CPOS, SPOS, HPOS, UPOS, RPOS);

{Calculate orientation of trunk coord sys wrt the lab coord sys}
  PROCEDI (TPOS, MAT10);

{Calculating gravity loads for the upperarm and forearm/hand.}
{Limb weights are calculated using Contini and Drillis(1966) data.}
  VECT1 [1] := 0 ; VECT1 [2] := -1 * 0.0357 * BWEIGHT ; VECT1 [3] := 0;
  VECT2 [1] := 0 ; VECT2 [2] := -1 * (0.018 + 0.006) * BWEIGHT ; VECT2 [3] := 0;

{Converting hand loads and gravity effects to trunk coord. sys.}
  VECTMULT (MAT10, HNDFORCE, VECT5);
  FOR A := 1 TO 3 DO HNDFORCE [A] := VECT5 [A];

  VECTMULT (MAT10, HNDMOMNT, VECT5);
  FOR A := 1 TO 3 DO HNDMOMNT [A] := VECT5 [A];

  VECTMULT (MAT10, VECT1, VECT5);
  FOR A := 1 TO 3 DO VECT1 [A] := VECT5 [A];

  VECTMULT (MAT10, VECT2, VECT5);
  FOR A := 1 TO 3 DO VECT2 [A] := VECT5 [A];

{Calculating position of centres of mass for the upperarm and lowerarm/hand
wrt the trunk coord. sys. Note: coordinates ar wrt trunk coordinate system.}
  AA := ELCENT [1] - GHCENT [1]; DD := HNDCENT [1] - GHCENT [1];
  BB := ELCENT [2] - GHCENT [2]; EE := HNDCENT [2] - GHCENT [2];
  CC := ELCENT [3] - GHCENT [3]; FF := HNDCENT [3] - GHCENT [3];

  VECT3 [1] := AA * 0.461;
  VECT3 [2] := BB * 0.461;
  VECT3 [3] := CC * 0.461;

  VECT4 [1] := ((HNDCENT [1] - ELCENT [1]) * 0.420) + AA;
  VECT4 [2] := ((HNDCENT [2] - ELCENT [2]) * 0.420) + BB;
  VECT4 [3] := ((HNDCENT [3] - ELCENT [3]) * 0.420) + CC;

{Total shoulder force load will then be:}
  FOR A := 1 TO 3 DO GHFLOW [A] := HNDFORCE [A] + VECT1 [A] + VECT2 [A];

{Total shoulder moments will then be:}
  VECT5 [1] := HNDMOMNT [1] + (HNDFORCE [3] * EE - HNDFORCE [2] * FF);

  VECT5 [1] := VECT5 [1] + ((VECT1 [3] * VECT3 [2] - VECT1 [2] * VECT3 [3]) + (VECT2 [3] * VECT4 [2] - VECT2 [2]
* VECT4 [3]));

  VECT5 [2] := HNDMOMNT [2] + (HNDFORCE [1] * FF - HNDFORCE [3] * DD);

  VECT5 [2] := VECT5 [2] + ((VECT1 [1] * VECT3 [3] - VECT1 [3] * VECT3 [1]) + (VECT2 [1] * VECT4 [3] - VECT2 [3]
* VECT4 [1]));

  VECT5 [3] := HNDMOMNT [3] + (HNDFORCE [2] * DD - HNDFORCE [1] * EE);

  VECT5 [3] := VECT5 [3] + ((VECT1 [2] * VECT3 [1] - VECT1 [1] * VECT3 [2]) + (VECT2 [2] * VECT4 [1] - VECT2 [1]
* VECT4 [2]));

{Converting moments to HUMERAL coord. sys.}
  VECTMULT (HROTMAT, VECT5, GHMLOAD);

{
  WRITELN ('GLEN-HUM. LOADS, (N, WRT TRUNK):
', GHFLOW [1] : 7:3, GHFLOW [2] : 7:3, GHFLOW [3] : 7:3);
  WRITELN ('GLEN-HUM. MOMENTS, Nm:
', GHMLOAD [1] : 7:3, GHMLOAD [2] : 7:3, GHMLOAD [3] : 7:3);
}
END;
{*****}
{*****}
END.
{*****}
{*****}

```

```

{*****}
{*****}

```

```

UNIT MISCOPS; {FILE MISCOPS2
This unit contains Procedures and Functions to perform }
{operations required repeatedly in various locations in }
{other programs}

```

```

{It contains the following titles: }

```

```

-MATEMULT, a procedure used to multiply two 3x3 matrices}
order: [MAT01]*[MAT02]=[MAT03]
-VECTMULT, a procedure used to multiply a 3x3 matrix
and a position vector
order: [MAT01]*[VECT01]=[VECT03]
-NORMALIZ, a procedure to normalize a vector
order: n[VECT01]= [VECT01]
-RMSERR, a function to calculate the RMS Error between
two 3-D positions (or position vectors)
order: (VECT01^2 - VECT02^2)^0.5= RMSERR
-MATEINV, a procedure to find the inverse of a matrix
by simply switching rows for columns
order: inv[MAT01]=[MAT02]
-MATEINV2, a procedure to find the inverse of a matrix
order: inv[MAT01]=[MAT02]
-VECTCROS, a procedure calculating vector cross product}
order: [VECT01 x VECT02]= VECT03
-VECTDOT, A function returning the vector dot value
order: [VECT01 dot VECT02]
-ASIN, Arc Sin function
order: ASIN[ ]

```

```

{*****}
{*****}

```

```

INTERFACE
USES VARIABLE, CRT;

```

```

PROCEDURE MATEMULT (VAR MAT01, MAT02, MAT03: MATRIX3);
PROCEDURE VECTMULT (MAT01: MATRIX3; VAR VECT02, VECT03: MATRIX1);
PROCEDURE NORMALIZ (VAR VECT01: MATRIX1);
FUNCTION RMSERR (VECT01, VECT02: MATRIX1): REAL;
PROCEDURE MATEINV (VAR MAT01, MAT02: MATRIX3);
PROCEDURE MATEINV2 (VAR MAT01, MAT02: MATRIX3);
PROCEDURE VECTCROS (VAR VECT01, VECT02, VECT03: MATRIX1);
FUNCTION VECTDOT (VAR VECT01, VECT02: MATRIX1): REAL;
FUNCTION ASIN (VAR AA: REAL): REAL;

```

```

IMPLEMENTATION

```

```

{*****}
{*****}

```

```

{Some variables used by the procedures in this unit.}
TYPE MATRIX3A = ARRAY[1..3, 1..6] OF REAL;

```

```

VAR MATINV, MATCALC : MATRIX3A; {matirx inversion}
A2, B2, C2, D2, E2, F2 : INTEGER;
AA2, BB2, CC2, DD2 : REAL;

```

```

{*****}
{*****}

```

```

PROCEDURE MATEMULT (VAR MAT01, MAT02, MAT03: MATRIX3);

```

```

BEGIN
FOR A2:=1 TO 3 DO
BEGIN
FOR B2:=1 TO 3 DO
BEGIN
AA2:=0;
FOR C2:=1 TO 3 DO
BEGIN
AA2:=MAT01 [B2, C2] *MAT02 [C2, A2]+AA2;
END;
MAT03 [B2, A2] :=AA2;
END;
END;
END;

```

```

END;
{*****}
PROCEDURE VECTMULT (MAT01: MATRIX3; VAR VECT02, VECT03: MATRIX1);
BEGIN
    FOR B2:=1 TO 3 DO
        BEGIN
            AA2:=0;
            FOR C2:=1 TO 3 DO
                BEGIN
                    AA2:=MAT01 [B2, C2] *VECT02 [C2] +AA2;
                END;
            VECT03 [B2] :=AA2;
        END;
    END;
{*****}
PROCEDURE NORMALIZ (VAR VECT01: MATRIX1);
BEGIN
    AA2:=SQRT (SQR (VECT01 [1]) +SQR (VECT01 [2]) +SQR (VECT01 [3]));
    VECT01 [1] :=VECT01 [1] /AA2;
    VECT01 [2] :=VECT01 [2] /AA2;
    VECT01 [3] :=VECT01 [3] /AA2;
END;
{*****}
FUNCTION RMSERR (VECT01, VECT02: MATRIX1) :REAL;
BEGIN
    AA2:=0;
    FOR A2:=1 TO 3 DO
        BEGIN
            AA2:=SQR (VECT01 [A2] -VECT02 [A2]) + AA2;
        END;
    RMSERR:= SQRT (AA2);
END;
{*****}
PROCEDURE MATEINV (VAR MAT01, MAT02: MATRIX3);
BEGIN
    FOR A2:= 1 TO 3 DO
        BEGIN
            FOR B2:= 1 TO 3 DO
                BEGIN
                    MAT02 [B2, A2] := MAT01 [A2, B2];
                END;
            END;
        END;
END;
{*****}
PROCEDURE MATEINV2 (VAR MAT01, MAT02: MATRIX3);
BEGIN
    {Set up MATINV matrix }
    FOR A2:=1 TO 3 DO
        BEGIN
            FOR B2:=1 TO 3 DO
                BEGIN
                    MATINV [A2, B2] :=MAT01 [A2, B2];
                    C2:=B2+3;
                    IF (A2=B2) THEN MATINV [A2, C2] :=1 ELSE MATINV [A2, C2] :=0;
                END;
            END;
        END;
    {Perform iterative solution to solve for matrix inverse}
    FOR ITERSET:=1 TO 3 DO
        BEGIN
            D2:= 2*3+1-ITERSET;
            FOR B2:=2 TO D2 DO
                BEGIN
                    F2:= B2 - 1;
                    FOR A2:=2 TO 3 DO
                        BEGIN
                            E2:=A2 - 1;
                            MATCALC [E2, F2] :=MATINV [A2, B2] - ((MATINV [1, B2] *MATINV [A2, 1]) /MATINV [1, 1]);
                        END;
                    MATCALC [3, F2] :=MATINV [1, B2] /MATINV [1, 1];
                END;
            FOR A2:=1 TO 3 DO
                BEGIN
                    D2:=2*3 - ITERSET;
                    FOR B2:= 1 TO D2 DO
                        BEGIN
                            MATINV [A2, B2] :=MATCALC [A2, B2]
                        END;
                    END;
                END;
            FOR A2:= 1 TO 3 DO
                BEGIN
                    FOR B2:= 1 TO 3 DO

```

```

        BEGIN
        MAT02 [A2, B2] :=MATINV [A2, B2] ;
        END;
    END;
END;
{*****}
PROCEDURE VECTCROS (VAR VECT01, VECT02, VECT03 :MATRIX1);
BEGIN
    VECT03 [1] := (VECT01 [2] *VECT02 [3]) - (VECT01 [3] *VECT02 [2]) ;
    VECT03 [2] := (VECT01 [3] *VECT02 [1]) - (VECT01 [1] *VECT02 [3]) ;
    VECT03 [3] := (VECT01 [1] *VECT02 [2]) - (VECT01 [2] *VECT02 [1]) ;
END;
{*****}
FUNCTION VECTDOT (VAR VECT01, VECT02 :MATRIX1) :REAL;
BEGIN
    VECTDOT := (VECT01 [1] *VECT02 [1]) + (VECT01 [2] *VECT02 [2]) + (VECT01 [3] *VECT02 [3]) ;
END;
{*****}
FUNCTION ASIN (VAR AA :REAL) :REAL;
BEGIN
    ASIN := ARCTAN (AA / (SQRT (1 - SQR (AA)))) ;
END;
{*****}
{*****}
END .
{*****}
{*****}

```

```

{*****}
{*****}
UNIT MUSMOMS;          {File:MUSMOMS3
                      This unit contains procedures to calculate muscle
                      moment factors for the various shoulder and associated
                      joints. The muscle moment factors are the product of
                      multiplying the relevent moments and direction vectors
                      for the various muscles.
                      It contains the following procedures:

                      MUSCLE MOMENT FACTORS
                      -HRMUSCLE, calculates the humeral/radial factors
                      -HUMUSCLE, calculates the humeral/ulnar factors
                      -GHMUSCLE, calculates the glenoid/humeral factors}
{*****}
INTERFACE
USES VARIABLE, CRT, MISCOPS;

PROCEDURE HRMUSCLE (VAR HRCENT: MATRIX1; VAR MDT, MDIR: MATRIX2; VAR RROTMAT: MATRIX3; VAR
MOMFACTS: MATRIX5);
PROCEDURE HUMUSCLE (VAR ELCENT: MATRIX1; VAR MDT, MDIR: MATRIX2; VAR UROTMAT: MATRIX3; VAR
MOMFACTS: MATRIX5);
PROCEDURE GHMUSCLE (VAR GHCENT: MATRIX1; VAR MDT, MDIR: MATRIX2; VAR HROTMAT: MATRIX3; VAR
MOMFACTS: MATRIX5);

IMPLEMENTATION
{*****}
{*****}
{Note: only X-axis (radial coord sys) moments are balanced for humeral/radial
joint.}
PROCEDURE HRMUSCLE (VAR HRCENT: MATRIX1; VAR MDT, MDIR: MATRIX2; VAR RROTMAT: MATRIX3; VAR
MOMFACTS: MATRIX5);
  BEGIN
  {zero MOMFACTS matrix}
  FOR A:= 1 TO 10 DO   FOR B:= 1 TO 60 DO   MOMFACTS[A,B]:=0;

  {Only the 2 fascicles of biceps (Muscle number 1) are involved here}
  A:= 1;
  FOR B:= 1 TO 2 DO
  BEGIN

  {convert muscle insertion location to be wrt the radial coord sys }
  FOR C:= 1 TO 3 DO   VECT1[C]:= MDT[A,B,2,C]-HRCENT[C];
  VECTMULT(RROTMAT, VECT1, VECT2);

  {convert muscle insertion direction vector to be wrt the radial coord sys}
  FOR C:= 1 TO 3 DO   VECT1[C]:= MDIR[A,B,2,C];
  VECTMULT(RROTMAT, VECT1, VECT3);

  {now moment balance about the X-axis is: Sum of Mx=(y Fz - z Fy)  }
  D:= 1;
  D:=(D-1)+B;
  MOMFACTS[1,D]:= VECT2[2]*VECT3[3] - VECT2[3]*VECT3[2];
  END;
  END;
{*****}
{Only biceps and triceps (muscle 1 & 17) are considered for humeral ulnar
moment balance (ulnar Y-axis)}
PROCEDURE HUMUSCLE (VAR ELCENT: MATRIX1; VAR MDT, MDIR: MATRIX2; VAR UROTMAT: MATRIX3; VAR
MOMFACTS: MATRIX5);
  BEGIN
  FOR A:= 1 TO 20 DO
  BEGIN
  FOR B:= 1 TO 10 DO
  BEGIN
  IF( ((A=1) AND ((B=1) OR (B=2))) OR
      ((A=17) AND ((B=1) OR (B=2) OR (B=3))) ) THEN
  BEGIN

  {convert muscle insertion location to be wrt the ulnar coord sys }
  FOR C:= 1 TO 3 DO   VECT1[C]:= MDT[A,B,2,C]-ELCENT[C];
  VECTMULT(UROTMAT, VECT1, VECT2);

  {convert muscle insertion direction vector to be wrt the ulnar coord sys}
  FOR C:= 1 TO 3 DO   VECT1[C]:= MDIR[A,B,2,C];
  VECTMULT(UROTMAT, VECT1, VECT3);

  {now moment balance about the Y-axis is: Sum of My=(z Fx - x Fz)  }
  IF( A= 17) THEN D:= 51;
  IF( A= 1) THEN D:= 1;
  C:= (D-1)+B;
  MOMFACTS[2,C]:= VECT2[3]*VECT3[1] - VECT2[1]*VECT3[3];

```


{For triceps, if flexion is greater than about 120 degrees, the tendon will wrap around the joint, therefore a minimum moment distance is incurred.}

```

IF(A=17) THEN
  BEGIN
    AA:= SQRT( SQR(VECT3[1]) + SQR(VECT3[3]) );
    AA:=0.5 * AA * SQRT( SQR(VECT2[1]) + SQR(VECT2[3]) );
    BB:=ABS(MOMFACTS[2,C]);
    IF(BB<AA)THEN MOMFACTS[2,C]:=-1*AA;
  END;
END;
END;
END;
END;

```

{*****}

{Muscles crossing the Glenoid humeral joint include :

name	muscle No.	fascicle No.
biceps,	1	1 & 2
coraco	2	1
deltoid	3	1 - 5
infra spin	4	1 - 3
lat. dor.	5	1 - 3
pect maj	7	1 - 3
sub scap	12	1 - 3
supra spin	13	1
teres maj	14	1
teres min	15	1
triceps	17	1

PROCEDURE GHMUSCLE(VAR GHCENT: MATRIX1, VAR MDT, MDIR: MATRIX2; VAR HROTMAT: MATRIX3; VAR MOMFACTS: MATRIX5);

```

BEGIN
  FOR A:= 1 TO 20 DO
    BEGIN
      FOR B:= 1 TO 10 DO
        BEGIN
          IF( ((A=1 ) AND ( (B=1) OR (B=2) ) ) OR
              ((A=2 ) AND (B=1) ) OR
              ((A=3 ) AND ( (B=1) OR (B=2) OR (B=3) OR (B=4) OR (B=5) ) ) OR
              ((A=4 ) AND ( (B=1) OR (B=2) OR (B=3) ) ) OR
              ((A=5 ) AND ( (B=1) OR (B=2) OR (B=3) ) ) OR
              ((A=7 ) AND ( (B=1) OR (B=2) OR (B=3) ) ) OR
              ((A=12) AND ( (B=1) OR (B=2) OR (B=3) ) ) OR
              ((A=13) AND (B=1) ) OR
              ((A=14) AND (B=1) ) OR
              ((A=15) AND (B=1) ) OR
              ((A=17) AND (B=1) ) THEN
            BEGIN

```

{convert muscle insertion location to be wrt the GH coord. sys. }

```

FOR C:= 1 TO 3 DO
  BEGIN
    VECT1[C] := MDT[A,B,2,C] - GHCENT[C];
    IF((A=1) AND (B=2)) THEN VECT1[C] := MDT[1,3,2,C] - GHCENT[C];
  END;
  VECTMULT(HROTMAT, VECT1, VECT2);

  FOR C:= 1 TO 3 DO
    BEGIN
      VECT1[C] := MDIR[A,B,2,C];
      IF((A=1) AND (B=2)) THEN VECT1[C] := MDIR[1,2,1,C] * -1;
    END;
    VECTMULT(HROTMAT, VECT1, VECT3);

```

```

IF( A= 17) THEN D:= 51;
IF( A= 15) THEN D:= 42;
IF( A= 14) THEN D:= 41;
IF( A= 13) THEN D:= 40;
IF( A= 12) THEN D:= 37;
IF( A= 7) THEN D:= 16;
IF( A= 5) THEN D:= 12;
IF( A= 4) THEN D:= 9;
IF( A= 3) THEN D:= 4;
IF( A= 2) THEN D:= 3;
IF( A= 1) THEN D:= 1;
C:=(D-1)+B;

```

{now moment balance about the humeral X-axis is: Sum of $M_x = (y F_z - z F_y)$ }

```

MOMFACTS[3,C] := VECT2[2]*VECT3[3] - VECT2[3]*VECT3[2];

```

{now moment balance about the humeral Y-axis is: Sum of $M_y = (z F_x - x F_z)$ }

```

MOMFACTS[4,C] := VECT2[3]*VECT3[1] - VECT2[1]*VECT3[3];

```

{now moment balance about the humeral Z-axis is: Sum of $M_z = (x F_y - y F_x)$ }

```
      MOMFACTS[5,C] := VECT2[1]*VECT3[2] - VECT2[2]*VECT3[1];
      END;
    END;
  END;
{*****}
{*****}
END.
{*****}
{*****}
```

```

{*****}
{*****}
UNIT ORIENT;                                {This unit calculates body coord system
                                              orientations from experimental 3-D marker data.
                                              Orientations are returned to the program in matrix
                                              form and Inverse Direction Cosine format.
                                              In addition, the TORIENT procedure also converts
                                              all marker data to be wrt the Trunk coord sys
                                              as opposed to the lab coord system.
                                              Scapula marker correction in this program
                                              version is normal to the scapula plane.}

{*****}
{*****}
INTERFACE
USES CRT, PRINTER,
    EULERS, MISCOPS, SETVALS, VARIABLE;

PROCEDURE TORIENT (VAR NMARKERS, PREDICT, STATUS: INTEGER; VAR TROTMAT: MATRIX3; VAR
MARKERS: MATRIX8);
PROCEDURE CORIENT (VAR ACCENT: MATRIX1; VAR CROTMAT: MATRIX3; VAR MARKERS: MATRIX8);
PROCEDURE SORIENT (VAR ACCENT: MATRIX1; VAR SROTMAT: MATRIX3; VAR MARKERS: MATRIX8);
PROCEDURE SPORIE2 (VAR ACCENT: MATRIX1; VAR MDT : MATRIX2; VAR SROTMAT: MATRIX3;
    VAR MARKERS: MATRIX8);
PROCEDURE SPORIE3 (VAR ACCENT: MATRIX1; VAR MDT : MATRIX2; VAR SROTMAT: MATRIX3;
    VAR MARKERS: MATRIX8; VAR HELEVA: REAL);
PROCEDURE HORIENT (VAR NMARKERS: INTEGER; VAR HROTMAT: MATRIX3; VAR MARKERS: MATRIX8);
PROCEDURE RORIENT (VAR NMARKERS: INTEGER; VAR RROTMAT: MATRIX3; VAR MARKERS: MATRIX8);

IMPLEMENTATION
VAR
    MINX, MAXX : REAL;

{*****}
{*****}
{This procedure is used internally to recall subject information
details from the current working file, "WRKFILE3.PRN".}
PROCEDURE PROCED1 (VAR SUBJINFO: MATRIX6);
    BEGIN
        ASSIGN (FILEIN3, 'WRKFILE3.PRN'); RESET (FILEIN3);
        READLN (FILEIN3, S1);

        FOR A:= 1 TO 18 DO
            BEGIN
                READLN (FILEIN3, AA);
                B:= A+1;
                SUBJINFO[B] := AA;
            END;
        CLOSE (FILEIN3);
    END;

{*****}
{*****}
{Procedure used in predicting scapula position.}
{This procedure is used for determining the minimum distance between a
point (in trunk coord sys) and any rib cage node, from a digitized RC slice.}
PROCEDURE RCDIST (VAR VECT01: MATRIX1; VAR MDT: MATRIX2; VAR CC: REAL; VAR E, F: INTEGER);

    BEGIN
        {Set some iteration parameters}
        CC:=1.000; E:=0; F:=0;
        {Begin search by looking for the closest X level, ie slice to the pt of
        interest.}
        FOR A:= 1 TO 10 DO
            BEGIN
                DD:=ABS (VECT01[1]-MDT[1,A,1,1]);
                IF (DD<CC) THEN
                    BEGIN
                        E:=A;
                        CC:= DD;
                    END ELSE

                    BEGIN
                        A:=10;
                    END;
            END;

        {Begin search to find closest nodes, in the Y Z PLANE. }
        IF ((VECT01[1]<MDT[1,E,1,1]) AND (E>=2)) THEN E:= E-1;
        CC:=1.0;
        FOR B:= 1 TO 20 DO
            BEGIN
                DD:=SQRT ( SQR (MDT[B,E,1,2] -VECT01[2]) + SQR (MDT[B,E,1,3]-VECT01[3]));
                IF ( DD<CC ) THEN

```

```

        BEGIN
        CC:=DD;
        F:=B;
        END ELSE
        BEGIN
        B:= 20;
        END;
    END;

{Check the next slice as well}
E:=E+1;
FOR B:= 1 TO 20 DO
    BEGIN
    DD:=SQRT( SQR(MDT[B,E,1,2] -VECT01[2]) + SQR(MDT[B,E,1,3]-VECT01[3]));
    IF( DD<CC ) THEN
        BEGIN
        CC:=DD;
        F:=B;
        END ELSE
        BEGIN
        B:= 20;
        END;
    END;
END;

{*****}
{*****}
{This procedure calculates trunk orientation wrt the lab coord
sys. and converts marker data to be wrt the trunk coord system.}
PROCEDURE TORIENT(VAR NMARKERS,PREDICT,STATUS:INTEGER; VAR TROTMAT:MATRIX3; VAR
MARKERS:MATRIX8);
BEGIN
{Define marker coord system}
FOR A:= 1 TO 3 DO
    BEGIN
    VECT3[A]:= MARKERS[2,A]-MARKERS[1,A];           {Z AXIS}
    VECT4[A]:= MARKERS[10,A]-MARKERS[1,A];         {pseudo x axis}
    END;
    NORMALIZ(VECT3);
    NORMALIZ(VECT4);
    VECTCROS(VECT3,VECT4,VECT2);                   {Y AXIS}
    NORMALIZ(VECT2);
    VECTCROS(VECT2,VECT3,VECT1);                   {X AXIS}
    NORMALIZ(VECT1);

{Lab to marker transformation is now: ie Inverse Direction Cosine.}
FOR A:= 1 TO 3 DO
    BEGIN
    MAT2[1,A]:=VECT1[A];
    MAT2[2,A]:=VECT2[A];
    MAT2[3,A]:=VECT3[A];
    END;

{Several calculations are performed only once for each test subject. This next
section contains several procedures of this type, including:
1. calculation of marker to trunk coord sys transformation.
It is performed once, on the first frame of collected data,
for each subject, when lab and trunk coord systems are parallel.
This calculation is done if STATUS = 1 if it =2 then the normal procedure is
followed.
}

{ WRITELN('INPUT Is the trunk sys parallel to the lab sys? Y/N:');
A:=WhereY; A:=A-1; GOTOXY(60,A);
ReadLN(S2); WRITELN(' ');
IF((S2='Y')OR(S2='y'))THEN
}

IF(STATUS=1)THEN
    BEGIN
    ASSIGN(FILEOUT1,'WRKFILE1.PRN'); REWRITE(FILEOUT1);

{Lab to trunk coord transformation will be}
FOR A:= 1 TO 3 DO FOR B:= 1 TO 3 DO TROTMAT[A,B]:= 0;
TROTMAT[1,2]:=-1; TROTMAT[2,3]:=1; TROTMAT[3,1]:=-1;

{Marker to trunk coord transformation can now be calculated}
MATEINV(MAT2,MAT5);
MATEMULT(TROTMAT,MAT5,MAT4);

FOR A:= 1 TO 3 DO WRITELN(FILEOUT1, MAT4[A,1], ' ',MAT4[A,2], ' ',MAT4[A,3]);
CLOSE(FILEOUT1);
END ELSE

```

```

{This section calculates lab to trunk coord transformation for any trunk position.
To do this it uses the "marker to trunk trans matrix" calculated (above) for the
subject when their trunk coord sys was parallel to the lab system. To begin
the matrix must be read from a workfile.}
BEGIN
  ASSIGN(FILEIN1,'WRKFILE1.PRN'); RESET(FILEIN1);
  FOR A:= 1 TO 3 DO READ(FILEIN1,MAT4[A,1],MAT4[A,2],MAT4[A,3]);
  CLOSE(FILEIN1);
{Lab to TRUNDK coord sys transformation can now be calculated}
  MATEMULT(MAT4,MAT2,TROTMAT);
{Mat1 is now the Direction Cosine matrix for lab to trunk transformation}
  END;

{Converting Marker data to the trunk coord sys can now be done. The first
step in this conversion is to find the trunk coord system origin.
Trunk origin is in the Z axis direction from marker 1 a distance
equal to the IJ marker correction value.}

{Subject information is required here to for the 1st marker to trunk origin
correction distance.}
  PROCED1(SUBJINFO);
  AA:=SUBJINFO[12];
  BB:= SQRT( SQR(MARKERS[2,1]-MARKERS[1,1])
            +SQR(MARKERS[2,2]-MARKERS[1,2])
            +SQR(MARKERS[2,3]-MARKERS[1,3]));
  VECT1[1]:= MARKERS[1,1]+ ((AA/BB)*(MARKERS[2,1]-MARKERS[1,1]));
  VECT1[2]:= MARKERS[1,2]+ ((AA/BB)*(MARKERS[2,2]-MARKERS[1,2]));
  VECT1[3]:= MARKERS[1,3]+ ((AA/BB)*(MARKERS[2,3]-MARKERS[1,3]));

{Marker data origin can now be translated to the Trunk coord system origin.}
  FOR A:= 1 TO NMARKERS DO
    BEGIN
      IF((PREDICT<>3)OR((A<4)OR(A>5)))THEN
        BEGIN
          FOR B:= 1 TO 3 DO VECT2[B]:=MARKERS[A,B]-VECT1[B];

{Marker data can now converted to be wrt the trunk coord sys orientation.}
          VECTMULT(TROTMAT,VECT2,VECT3);
          FOR B:= 1 TO 3 DO MARKERS[A,B]:=VECT3[B];
        END;
      END;
    END;

{*****}
{Transformation of Clavicle coord system wrt the trunk is calculated in this
procedure}
  PROCEDURE CORIENT(VAR ACCENT:MATRIX1; VAR CROTMAT:MATRIX3; VAR MARKERS:MATRIX8);
  BEGIN

{Information on SC joint position wrt the trunk origin is located in SETVAL4.}
  SETVAL4(TPARAMS,CPARAMS,SPARAMS,HPARAMS,UPARAMS,RPARAMS,HCARANG,UCARANG,HTORSION);

{Subject information is required to know the 3rd marker to AC joint distance.}
  PROCED1(SUBJINFO);

{SC joint position is now:}
  FOR A:= 1 TO 3 DO SCCENT[A]:= TPARAMS[A];

{Marker correction wrt CLAVICLE coord sys, for marker 3 is :}
  VECT8[1]:=0; VECT8[2]:=-1*SUBJINFO[13]; VECT8[3]:=0;

{Marker correction wrt TRUNK coord sys for marker 3 is}
  VECT9[1]:=-1*VECT8[2]; VECT9[2]:=VECT8[1]; VECT9[3]:=VECT8[3];

{Iteration variable is now:}
  ITERSET:= 1; {iteration flag, 2 signals end of iteration}
  {*****}
  REPEAT

{AC joint position is now:}
  FOR A:= 1 TO 3 DO ACCENT[A]:=MARKERS[3,A]+VECT9[A];

{Define Clavicle coord system from JOINT CENTRES}
  FOR A:= 1 TO 3 DO VECT1[A]:= ACCENT[A]-SCCENT[A]; {X AXIS}
  NORMALIZ(VECT1);
  VECT4[1]:=-1; VECT4[2]:=0; VECT4[3]:=0; {pseudo y-axis}
  VECTCROS(VECT1,VECT4,VECT3); {Z AXIS}
  NORMALIZ(VECT3);
  VECTCROS(VECT3,VECT1,VECT2); {Y AXIS}
  NORMALIZ(VECT2);

{Trunk to Clavicle transformation is now: ie Inverse Direction Cosine.}
  FOR A:= 1 TO 3 DO

```

```

BEGIN
CROTMAT [1,A] :=VECT1 [A] ;
CROTMAT [2,A] :=VECT2 [A] ;
CROTMAT [3,A] :=VECT3 [A] ;
END;

{Marker correction vectors can now be updated so correction is perpendicular
to plane of scapula.}
MATEINV (CROTMAT, CIROTMAT) ;
VECTMULT (CIROTMAT, VECT8, VECT11) ;

{Check to see magnitude of correction over last iteration}
AA:=RMSERR (VECT9, VECT11) ;

IF (AA<0.002) THEN
BEGIN
ITERSET2:= 2; {correction not large enough for another iteration}
END ELSE

BEGIN
ITERSET2:= 1;
FOR A:= 1 TO 3 DO VECT9 [A] :=VECT11 [A] ;
END;

UNTIL (ITERSET2=2) ;
{*****}
END;

{*****}
{Transformation of Scapula coord system wrt the trunk is calculated in this
procedure}
PROCEDURE SORIENT (VAR ACCENT: MATRIX1; VAR SROTMAT: MATRIX3; VAR MARKERS: MATRIX8) ;
BEGIN

{Subject information is required to know marker to correction factors.}
PROCED1 (SUBJINFO) ;

{Define marker correction vectors for scapula}
FOR A:= 1 TO 3 DO
BEGIN
VECT7 [A] :=0; {vect7 is for marker 4, med scap}
VECT8 [A] :=0; {vect8 is for marker 5, inferior angle}
END;
VECT7 [3] :=SUBJINFO [14] ; {note corrections are in the Zs direction}
VECT8 [3] :=SUBJINFO [15] ; {which is assumed parallel to Zt direction here}

FOR A:= 1 TO 3 DO
BEGIN
VECT9 [A] := VECT7 [A] *-1; {note:-1's correct for opposite directs of Zs & Zt}
VECT10 [A] := VECT8 [A] *-1; {during iterations, SIROTMAT takes place of -1's}
END;

{Iteration variables are required}
C:= 0; {counter}
ITERSET2:= 1; {iteration flag, 2 signals end of iteration}
{*****}
REPEAT

{Coordinates of the medial scapula landmark will now be:}
FOR A:= 1 TO 3 DO VECT1 [A] :=MARKERS [4,A] +VECT9 [A] ;

{Coordinates of the Inferior angle landmark will now be:}
FOR A:= 1 TO 3 DO VECT2 [A] :=MARKERS [5,A] +VECT10 [A] ;

"Scapular" coord system from landmark locations. }
FOR A:= 1 TO 3 DO
BEGIN
VECT4 [A] := VECT2 [A] -ACCENT [A] ; { X AXIS}
VECT5 [A] := VECT1 [A] -ACCENT [A] ; {pseudo Y AXIS}
END;
NORMALIZ (VECT4) ; NORMALIZ (VECT5) ;
VECTCROS (VECT4, VECT5, VECT6) ; {Z AXIS}
NORMALIZ (VECT6) ;
VECTCROS (VECT6, VECT4, VECT5) ; {Y AXIS}
NORMALIZ (VECT5) ;

{Trunk to Scapula transformation is now: ie Inverse Direction Cosine.}
FOR A:= 1 TO 3 DO
BEGIN
SROTMAT [1,A] :=VECT4 [A] ;
SROTMAT [2,A] :=VECT5 [A] ;
SROTMAT [3,A] :=VECT6 [A] ;
END;

```

```

{Marker correction vectors can now be updated so correction is perpendicular
to plane of scapula.}
MATEINV(SROTMAT,SIROTMAT);
VECTMULT(SIROTMAT,VECT7,VECT11);
VECTMULT(SIROTMAT,VECT8,VECT12);

{Check to see magnitude of correction over last iteration}
AA:=RMSERR(VECT9,VECT11);

IF(AA<0.002)THEN
BEGIN
ITERSET2:= 2; {correction not large enough for another iteration}
END ELSE

BEGIN
ITERSET2:= 1;
C:=C+1;
FOR A:= 1 TO 3 DO
BEGIN
VECT9[A]:=VECT11[A];
VECT10[A]:=VECT12[A];
END;
END;

UNTIL(ITERSET2=2);
END;
{*****}
{Transformation of HUMERAL coord system wrt the trunk is calculated in this
procedure.
Humeral orientation calculations, here, define clinical orientation,ie based
on the upper arm visual centreline, and within the forearm flexion
plane. Actual bone orientation is determined in the main program. }
PROCEDURE HORIENT(VAR NMARKERS:INTEGER; VAR HROTMAT:MATRIX3; VAR MARKERS:MATRIX8);
BEGIN
PROCED1(SUBJINFO);

{If 10 MARKERS ARE being used, then ELCENT is calculated using a
correction vector pointing at the HNDCENT from marker 7. If 12 MARKERS ARE being
used then the correction vector is in the direction of marker 7 from marker
11, the distance of marker 7 from the epicondyles.}
IF NMARKERS = 10 THEN
FOR A:= 1 TO 3 DO VECT1[A] := (0.5*(MARKERS[8,A]+MARKERS[9,A]))-MARKERS[7,A];

IF ((NMARKERS=12) or (NMARKERS=15)) THEN
FOR A:= 1 TO 3 DO VECT1[A] := MARKERS[7,A]-MARKERS[11,A];

NORMALIZ(VECT1);
FOR A:= 1 TO 3 DO ELCENT[A] := MARKERS[7,A] + (VECT1[A]*SUBJINFO[17]);

{The forearm X-axis is now :}
FOR A:= 1 TO 3 DO VECT1[A] := (0.5*(MARKERS[8,A]+MARKERS[9,A]))-ELCENT[A];
NORMALIZ(VECT1);

{Coordinates of deltoid insertion marker and its distance to the clinical
humeral centre line are VECT11 and HH respectively.}
FOR A:= 1 TO 3 DO VECT11[A] := MARKERS[6,A];
HH:=SUBJINFO[16]; {note: marker correction is in the -Yh direction}

{A coord sys can be defined by the forearm axis, elbow centre and deltoid
insertion marker. Origin @ elbow centre, ELCENT, VECT1 as the X-axis.}
FOR A:= 1 TO 3 DO VECT2[A] := VECT11[A]-ELCENT[A];
NORMALIZ(VECT2); {pseudo Y-axis}
VECTCROS(VECT1,VECT2,VECT3); { Z-axis}
NORMALIZ(VECT3);
VECTCROS(VECT3,VECT1,VECT2); { Y-axis}
NORMALIZ(VECT2);

{The coord sys can be rotated around the X-axis by an angle THETA so the humeral
centre line will lay in the XY plane. To calculate THETA, the deltoid
insertion marker postion must be known wrt the coordinate system defined above.}
FOR A:= 1 TO 3 DO
BEGIN
VECT7[A] := VECT11[A]-ELCENT[A]; {VECT7 contains marker coords wrt elbow
centre}
MAT1[1,A] := VECT1[A];
MAT1[2,A] := VECT2[A]; {MAT1 contains inv dir cos fro trunk to
plane}
MAT1[3,A] := VECT3[A]; {conversion}
END;
VECTMULT(MAT1,VECT7,VECT8); {VECT8 contains marker coords wrt the above}
{ coord sys}
{THETA is now equal to the arcsin of marker correction distance, HH, divided by

```

```

the marker's Y coord value wrt the coord sys defined above, (-ve for convention).)
  AA:=HH/VECT8[2];
  IF(AA>1)THEN theta:=1.57 ELSE THETA:=-1*ASIN(AA);

{Matrix transformation from the coord sys defined above to that with humeral
centre line laying in the XY plane will be MAT2.}
  EULERX(MAT2,THETA);

{Deltoid insertion coordinates wrt the new coord sys should be VECT9:}
  VECTMULT(MAT2,VECT8,VECT9);

{Coords of humeral centre line as is passes beneath the deltoid insertion marker
will be VECT9 but with zero Z-axis coord:}
  VECT9[3]:=0;

{The transformation matrix from the new coord sys to trunk coord sys will
be MAT4}
  MATEMULT(MAT2,MAT1,MAT3);
  MATEINV(MAT3,MAT4);

{Coords of humeral centre line as is passes beneath the deltoid insertion marker
wrt the trunk coord sys will be VECT10:}
  VECTMULT(MAT4,VECT9,VECT10);

{Upper arm coord sys can now be defined: X-axis from VECT10 through elbow centre;
Y-axis equal cross product of X-axis and forearm centreline. }
  for a:= 1 to 3 do vect4[a]:=vect10[a] * -1;          {X-AXIS}
  NORMALIZ(VECT4);
  VECTCROS(VECT4,VECT1,VECT5);
  NORMALIZ(VECT5);          {Y-AXIS}
  VECTCROS(VECT4,VECT5,VECT6);
  NORMALIZ(VECT6);          {Z-AXIS}

{Humeral rotation matrix, HROTMAT, is :}
  FOR A:= 1 TO 3 DO
    BEGIN
      HROTMAT[1,A]:=VECT4[A];
      HROTMAT[2,A]:=VECT5[A];
      HROTMAT[3,A]:=VECT6[A];
    END;
  END;

{*****}
{*****}
{Transformation of FOREARM coord system wrt the trunk is calculated in this
procedure.
Forearm orientation calculations, here, define clinical orientation, and
include elbow flexion and forearm rotation. }

PROCEDURE RORIENT(VAR NMARKERS:INTEGER; VAR RROTMAT:MATRIX3; VAR MARKERS:MATRIX8);
BEGIN
  PROCED1(SUBJINFO);

{Hand centre, is calculated by taking the mid way point between markers 8 & 9.}
  FOR A:= 1 TO 3 DO
    BEGIN
      HNDCENT[A]:=0.5*(MARKERS[8,A]+MARKERS[9,A]);
      VECT6[A]:= MARKERS[8,A]-MARKERS[9,A];          {vector directed dorsally from
palm}
    END;
  NORMALIZ(VECT6);

{For 10 marker format, Elbow centre is found by moving the correction distance
from the marker towards the hand centre. With 12 marker format elbow centre
is found by moving in the direction of marker 7 from marker 11.}
  IF NMARKERS = 10 THEN          FOR A:= 1 TO 3 DO
    VECT1[A]:=HNDCENT[A]-MARKERS[7,A];
  IF ((NMARKERS=12)or(NMARKERS=15)) THEN FOR A:= 1 TO 3 DO
    VECT1[A]:=MARKERS[7,A]-MARKERS[11,A];

  NORMALIZ(VECT1);
  FOR A:= 1 TO 3 DO  ELCENT[A]:= MARKERS[7,A]+(VECT1[A]*SUBJINFO[17]);

{Forearm coord sys is defined as origin at elbow centre, X-axis through
hand centre and Y-axis the cross product of vect6 and X-axis.}
  FOR A:= 1 TO 3 DO  VECT4[A]:=HNDCENT[A]-ELCENT[A];  {X-AXIS}
  NORMALIZ(VECT4);
  VECTCROS(VECT6,VECT4,VECT5);          {Y-AXIS}
  NORMALIZ(VECT5);
  VECTCROS(VECT4,VECT5,VECT6);          {Z-AXIS}
  NORMALIZ(VECT6);

{Forearm rotation matrix, HROTMAT, is :}
  FOR A:= 1 TO 3 DO
    BEGIN

```



```
RROTMAT [1, A] := VECT4 [A] ;
RROTMAT [2, A] := VECT5 [A] ;
RROTMAT [3, A] := VECT6 [A] ;
END ;
END ;
{*****}
{*****}
END .
{*****}
{*****}
```

```

{*****}
{*****}
UNIT READEXP;          {This unit:
                      1. Prompts for and stores subject information
                        in a working file and also a subject file.
                        This allows a subjects details to be input
                        once and then recalled later if required.
                      2. Prompts for Vicon data file name, number of
                        of frames to be analysed and marker format
                        being used. Header information from vicon
                        file is read so that frame information
                        can be read with the last procedure.
                      3. Reads marker information obtained experimentally,
                        converts it to standard SI format and stores
                        it to matrix "MARKERS".
                      }
{*****}
{*****}

```

INTERFACE

USES CRT,EULERS,MISCOPS,VARIABLE;

```

PROCEDURE REXPER1 (VAR SUBJINFO:MATRIX6);
PROCEDURE REXPER2 (VAR ANALOGUE,ANALOGRT,NANALOG,NFRAMES,NMARKERS:INTEGER; VAR
S3:STRING);
PROCEDURE REXPER3 (VAR VECT1,VECT2:MATRIX1; VAR SUBJINFO:MATRIX6;
VAR MARKERS:MATRIX8; VAR
ANALOGUE,ANALOGRT,FRAMENUM,NANALOG,NMARKERS:INTEGER);

```

IMPLEMENTATION

```

{*****}
{*****}
PROCEDURE REXPER1 (VAR SUBJINFO:MATRIX6);
BEGIN
{Subject information can be input, or recalled if necessary.}
REPEAT
  CLRSCR;
  GOTOXY(1,2);
  WRITELN('INPUT SUBJECT DETAILS? (Y/N/" "),( <ret> for no change)');
  A:= Wherey; A:=A-1; GOTOXY(60,A);
  READLN(S1); WRITELN(' ');
  IF ((S1='Y') OR (S1='y')) THEN
    BEGIN
      WRITELN('INPUT NAME OF SUBJECT RECORD FILE WITH EXTENSION:');
      READLN(S2);
      ASSIGN(FILEOUT1,S2); REWRITE(FILEOUT1);
      ASSIGN(FILEOUT2,'WRKFILE3.PRN'); REWRITE(FILEOUT2);
      WRITELN('SUBJECT NAME?');
      READLN(S3);
      WRITELN(FILEOUT1,S3); WRITELN(FILEOUT2,S3);
      WRITELN('HEIGHT:');
      READLN(AA);
      WRITELN(FILEOUT1,AA); WRITELN(FILEOUT2,AA);
      WRITELN('WEIGHT :');
      READLN(AA);
      WRITELN(FILEOUT1,AA); WRITELN(FILEOUT2,AA);
      WRITELN('T1 - T12 DISTANCE:');
      READLN(AA);
      WRITELN(FILEOUT1,AA); WRITELN(FILEOUT2,AA);
      WRITELN('RIB CAGE WIDTH UNDER THE ARMS:');
      READLN(AA);
      WRITELN(FILEOUT1,AA); WRITELN(FILEOUT2,AA);
      WRITELN('RIB CAGE DEPTH FROM MANUBRIOSTERNAL JOINT TO T4:');
      READLN(AA);
      WRITELN(FILEOUT1,AA); WRITELN(FILEOUT2,AA);
      WRITELN('CLAVICLE LENGTH:');
      READLN(AA);
      WRITELN(FILEOUT1,AA); WRITELN(FILEOUT2,AA);
      WRITELN('SCAPULAR AC - INFERIOR ANGLE LENGTH:');
      READLN(AA);
      WRITELN(FILEOUT1,AA); WRITELN(FILEOUT2,AA);
    END
  UNTIL (S1='N') OR (S1='n') OR (S1='');

```

```

WRITELN('HUMERAL CONDYLES TO HUMERAL HEAD TOP:');
READLN(AA);
WRITELN(FILEOUT1,AA); WRITELN(FILEOUT2,AA); {9}

WRITELN('BACK OF ELBOW TO WRIST CENTRE DISTANCE FOR A FLEXED ARM:');
READLN(AA);
WRITELN(FILEOUT1,AA); WRITELN(FILEOUT2,AA); {10}

WRITELN('WRIST WIDTH:');
READLN(AA);
WRITELN(FILEOUT1,AA); WRITELN(FILEOUT2,AA); {11}

WRITELN('MARKER 1 CORRECTION:');
READLN(AA);
WRITELN(FILEOUT1,AA); WRITELN(FILEOUT2,AA); {12}

WRITELN('MARKER 3 CORRECTION:');
READLN(AA);
WRITELN(FILEOUT1,AA); WRITELN(FILEOUT2,AA); {13}

WRITELN('MARKER 4 CORRECTION:');
READLN(AA);
WRITELN(FILEOUT1,AA); WRITELN(FILEOUT2,AA); {14}
WRITELN('MARKER 5 CORRECTION:');
READLN(AA);
WRITELN(FILEOUT1,AA); WRITELN(FILEOUT2,AA); {15}
WRITELN('MARKER 6 CORRECTION:');
READLN(AA);
WRITELN(FILEOUT1,AA); WRITELN(FILEOUT2,AA); {16}
WRITELN('MARKER 7 CORRECTION:');
READLN(AA);
WRITELN(FILEOUT1,AA); WRITELN(FILEOUT2,AA); {17}
WRITELN('MARKER 8 CORRECTION:');
READLN(AA);
WRITELN(FILEOUT1,AA); WRITELN(FILEOUT2,AA); {18}
WRITELN('MARKER 9 CORRECTION:');
READLN(AA);
WRITELN(FILEOUT1,AA); WRITELN(FILEOUT2,AA); {19}

WRITELN(' ');
WRITELN('*****');
WRITELN('          SUBJECT INFORMATION HAS BEEN STORED AS FILE: ',S2);
WRITELN('          AND ALSO THE CURRENT WORKING FILE');
WRITELN('*****');
WRITELN(' ');
CLOSE(FILEOUT1); CLOSE(FILEOUT2); DELAY(5000); CLRSCR;
END;

IF ((S1='N') OR (S1='n')) THEN
  BEGIN
  WRITELN('INPUT SUBJECT INFORMATION FILE TO BE USED:');
  A:=WhereY; A:=A-1; GOTOXY(60,A);
  READLN(S2); WRITELN(' ');

  ASSIGN(FILEIN1,S2); RESET(FILEIN1);
  ASSIGN(FILEOUT2,'WRKFILE3.PRN'); REWRITE(FILEOUT2);

  READLN(FILEIN1,S3);
  WRITELN(FILEOUT2,S3);
  FOR A:= 2 TO 19 DO
    BEGIN
      READLN(FILEIN1,AA);
      WRITELN(FILEOUT2,AA);
    END;
  CLOSE(FILEIN1); CLOSE(FILEOUT2);
  END;

IF ((S1<>'Y') AND (S1<>'N')) THEN
  BEGIN
  ASSIGN(FILEIN1,'WRKFILE3.PRN'); RESET(FILEIN1);
  READLN(FILEIN1,S3);
  FOR A:= 2 TO 19 DO READLN(FILEIN1,SUBJINFO[A]);
  CLOSE(FILEIN1);
  END;

WRITELN('IS THE SETUP SATISFACTORY? (Y/N)');
A:=WhereY; A:=A-1; GOTOXY(60,A);
READLN(S1); WRITELN(' ');
UNTIL((S1='Y') OR (S1='y'));
END;
{*****}
{*****}
{Data input file can be declared and set}

```

```

PROCEDURE REXPER2 (VAR ANALOGUE,ANALOGRT,NANALOG,NFRAMES,NMARKERS:INTEGER; VAR
S3:STRING);
BEGIN
  WRITELN('INPUT NAME OF VICON FILE CONTAINING MARKER DATA, ');
  WRITELN('DO NOT INCLUDE AN EXTENSION AS ".A3D" IS ASSUMED:');
  A:=WhereY; A:=A-1; GOTOXY(60,A);
  READLN(S3); WRITELN(' ');
  S2:=S3+'.A3D';
  ASSIGN(FILEIN10,S2); RESET(FILEIN10);

{Header information can be read from the input file.}
  READLN(FILEIN10,NMARKERS,S1);
  READLN(FILEIN10,NFRAMES,S1);
  READLN(FILEIN10,NANALOG,S1);
  IF (NANALOG=0) THEN READLN(FILEIN10,S1); {no analogue then a blank
line}
  ANALOGRT:=1;
  IF (NANALOG>0) THEN READLN(FILEIN10,ANALOGRT,S1); {analogue then read analogue
to video rate}

  REPEAT

  WRITELN('DO YOU WISH TO ANALYSE ALL ',NFRAMES:5,' FRAMES? <ret for Y>/N');
  A:=WhereY; A:=A-1; GOTOXY(60,A);
  READLN(S1);
  IF (S1='N') OR (S1='n') THEN
    BEGIN
      WRITELN('INPUT THE NUMBER OF FRAMES TO ANALYSE:');
      A:=WhereY; A:= A-1; GOTOXY(60,A);
      READLN(nframes);
      END;

  IF (NANALOG=0) THEN ANALOGUE:=0
  ELSE
    BEGIN
      WRITELN('ARE HAND FORCES TO BE CALCULATED? <ret for Y>/N');
      A:=WhereY; A:=A-1; GOTOXY(60,A);
      READLN(S1);
      IF ((S1='N') OR (S1='n')) THEN ANALOGUE:= 0
      ELSE BEGIN
        WRITELN('USING THE HAND GRIP PYLON TRANSDUCER? <ret for Y>/N');
        A:=WhereY; A:= A-1; GOTOXY(60,A);
        READLN(S1);
        IF (S1='') OR (S1='y') OR (S1='Y') THEN
          BEGIN
            WRITELN('USE THE FIRST 5 FRAMES AS A REFERENCE TO ');
            WRITELN(' CORRECT FOR PYLON SIGNAL DRIFT? <ret for Y>/N');
            A:=WhereY; A:=A-1; GOTOXY(60,A);
            READLN(S1);
            IF (S1='N') OR (S1='n') THEN ANALOGUE:=2;
            IF (S1='') OR (S1='y') OR (S1='Y') THEN ANALOGUE:=3;
            END ELSE

            BEGIN
              WRITELN('USING THE FORCE PLATE DATA? <ret for Y>/N');
              A:= WhereY; A:= A-1; GOTOXY(60,A);
              READLN(S1);
              IF (S1='') OR (S1='Y') OR (S1='y') THEN ANALOGUE:= 1
              ELSE BEGIN
                WRITELN('USING CofG ACCELERATION IS NOT RECOMMENDED START AGAIN');
                WRITELN(' '); DELAY(5000);
                END;
              END;
            END;
          END;

  WRITELN('CONTINUE? <ret for Y>/ N');
  A:= WhereY; A:= A-1; GOTOXY(60,A);
  READLN(S2);

  UNTIL (S2='') OR (S2='Y') OR (S2='y');
  END;

{*****}
{Data can now be stored to a matrix,"MARKERS". Data is read from the Vicon data
file and was assigned and reset in the above procedure as FILEIN1. For this
version number of markers markers is given and marker data is in mm not m.
In addition, analogue data can be read if required. 8 analogue channels fit
on each data line.}
PROCEDURE REXPER3 (VAR VECT1,VECT2:MATRIX1; VAR SUBJINFO:MATRIX6;
VAR MARKERS:MATRIX8; VAR
ANALOGUE,ANALOGRT,FRAMENUM,NANALOG,NMARKERS:INTEGER);
BEGIN

```

```

READLN(FILEIN10,S1);
IF (S1='') THEN READLN(FILEIN10,S1); {sometimes there is an extra blank line}
FOR A:= 1 TO 2 DO
  BEGIN
  READLN(FILEIN10,S1); {junk in input file}
  END;

FOR A:= 1 TO NMARKERS DO {marker coordinate data}
  BEGIN
  READLN(FILEIN10, B, MARKERS[A,1], MARKERS[A,2], MARKERS[A,3], AA, BB);
  FOR B:= 1 TO 3 DO MARKERS[A,B] := MARKERS[A,B]/1000;
  END;

IF (ANALOGUE = 0) THEN {hand forces = 0}
  BEGIN
  FOR A:= 1 TO ANALOGR T DO FOR B:= 1 TO 3 DO READLN(FILEIN10,S1);
  FOR A:= 1 TO 3 DO VECT1[A] := 0;
  FOR A:= 1 TO 3 DO VECT2[A] := 0;
  END;

IF (ANALOGUE = 1) THEN {FORCE PLATE data is the hand load}
  BEGIN
  FOR B:= 1 TO 8 DO MFORCE[2,B] := 0; {zero array places }
  FOR A:= 1 TO ANALOGR T DO {repeat for No. of analogue collections per
video)
  BEGIN
  READLN(FILEIN10,S1); {blank line before analogue
data)
  FOR B:= 1 TO 7 DO READ(FILEIN10,MFORCE[1,B]);
  READLN(FILEIN10,MFORCE[1,8]); {force plate always 1st 8
channels)
  READLN(FILEIN10,S1); {blank or unwanted analogue
data line)
  FOR B:= 1 TO 8 DO MFORCE[2,B] := MFORCE[2,B] + MFORCE[1,B];
  END;
  AA := ((MFORCE[2,1]/ANALOGR T) - 2048) * 0.31252;
  BB := ((MFORCE[2,2]/ANALOGR T) - 2048) * 0.31252;
  CC := ((MFORCE[2,3]/ANALOGR T) - 2048) * -0.31381;
  DD := ((MFORCE[2,4]/ANALOGR T) - 2048) * -0.31381;
  EE := ((MFORCE[2,5]/ANALOGR T) - 2048) * 0.63356;
  FF := ((MFORCE[2,6]/ANALOGR T) - 2048) * 0.63356;
  GG := ((MFORCE[2,7]/ANALOGR T) - 2048) * 0.63356;
  HH := ((MFORCE[2,8]/ANALOGR T) - 2048) * 0.63356;

  VECT1[1] := CC+DD; {Fx}
  VECT1[2] := EE+FF+GG+HH; {Fy}
  VECT1[3] := AA+BB; {Fz}
  VECT2[1] := 0.12*(-FF-GG+EE+HH) ; {Mx,plate}
  VECT2[2] := 0.20*(BB-AA)+0.12*(-CC+DD); {My,plate}
  VECT2[3] := 0.20*(EE+FF-GG-HH) ; {Mz,plate}
  if (vect1[2] <> 0) then
  begin
  AA := ( VECT2[3] + (VECT1[1] * +0.057)) / VECT1[2]; {Xcp}
  BB := (-1*VECT2[1] + (VECT1[3] * +0.057)) / VECT1[2]; {Zcp}
  VECT2[1] := 0; {Mx}
  VECT2[2] := VECT2[2] - (VECT1[1]*BB) + (VECT1[3]*AA); {My}
  VECT2[3] := 0; {Mz}
  end else
  begin
  vect2[1] := 0; vect2[2] := 0; vect2[3] := 0;
  end;

END;

{If the pylon transducer is used to calculate hand loads, orientation of the
transducer must be calculated from MARKER data. Transducer data must be
corrected for cross sensitivity and hand grip centre offset. Due to signal
drift, the option is included to use the signal average over the first 2
frames as a reference point for measuring signal magnitude during the remainder
of the collection.}

IF (ANALOGUE=2) OR (ANALOGUE=3) THEN {pylon transducer data is hand load}
  BEGIN
  FOR B := 1 TO 6 DO MFORCE[8,B] := 0; {zero array
used later)
  FOR A:= 1 TO ANALOGR T DO
  BEGIN
  READLN(FILEIN10,S1); {blank line}
  IF (NANALOG=14) THEN FOR B:= 1 TO 8 DO READ(FILEIN10,AA); {USELESS F/P}

```

```

DATA)      FOR B:= 1 TO 5 DO READ(FILEIN10,MFORCE[7,B]);
           READLN(FILEIN10,MFORCE[7,6]);           {6 pylon
chans.)    IF(NANALOG=6) THEN READLN(FILEIN10,S1); {blank line
if no F.P. analogue data}
           FOR B:= 1 TO 6 DO MFORCE[8,B]:=MFORCE[8,B]+MFORCE[7,B];
           END;

           FOR B:= 1 TO 6 DO MFORCE[7,B]:=MFORCE[8,B]/ANALOGRT; {average for
each video frame}

{To remove drift from the pylon input signal, data can be compared with the
average signals over the first two frames. This calculation is conducted
when ANALOGUE = 3. If ANALOGUE = 2 then pylon signals are taken as absolute
values and this section is skipped.}
           IF(ANALOGUE=3)THEN
           BEGIN
           if(framenum=1)then for b:= 1 to 6 do mforce[9,b]:=0;
           if(framenum<=5)then for b:= 1 to 6 do mforce[9,b]:=mforce[9,b]+mforce[7,b];
           if(framenum<=5)then for b:= 1 to 6 do mforce[7,b]:=0;
           if(framenum=5)then for b:= 1 to 6 do mforce[9,b]:=mforce[9,b]/5;
           if(framenum>5)then for b:= 1 to 6 do
mforce[7,b] :=(mforce[7,b]-mforce[9,b])*0.0048828;
           end;

           {
           IF(FRAMENUM=1)THEN FOR B:= 1 TO 6 DO MFORCE[9,B]:=MFORCE[7,B];
           IF(FRAMENUM=2)THEN FOR B:= 1 TO 6 DO
MFORCE[9,B] :=(MFORCE[7,B]+MFORCE[9,B])/2;
           IF(FRAMENUM<3)THEN FOR B:= 1 TO 6 DO MFORCE[7,B]:=0;
           IF(FRAMENUM>2)THEN FOR B:= 1 TO 6 DO
MFORCE[7,B] :=(MFORCE[7,B]-MFORCE[9,B])*0.0048828;
           END; } {204 steps per volt, from calibration (old
one 0.00443114)}

           IF(ANALOGUE=2)THEN FOR B:= 1 TO 6 DO
MFORCE[7,B] :=(MFORCE[7,B]-2048)*0.0048828;

{An inverse cross sensitivity matrix must be used it is defined
here and stored in the matrix MFORCE for space reasons.}
           IF(FRAMENUM=1)THEN
           BEGIN
MFORCE[1,1]:=-229.6; MFORCE[1,2]:= 1.0; MFORCE[1,3]:= -7.5;
MFORCE[1,4]:=-14.7; MFORCE[1,5]:= 0.2; MFORCE[1,6]:= 8.7;

MFORCE[2,1]:= 0.2; MFORCE[2,2]:= 389.3; MFORCE[2,3]:= -3.5;
MFORCE[2,4]:= -0.1; MFORCE[2,5]:=-27.7; MFORCE[2,6]:= -0.9;

MFORCE[3,1]:= -8.3; MFORCE[3,2]:= -3.5; MFORCE[3,3]:= 226.1;
MFORCE[3,4]:= 7.8; MFORCE[3,5]:= -4.3; MFORCE[3,6]:= 9.5;

MFORCE[4,1]:= 0.1; MFORCE[4,2]:= 0.0; MFORCE[4,3]:= -0.2;
MFORCE[4,4]:=-20.5; MFORCE[4,5]:= 0.2; MFORCE[4,6]:= -0.3;

MFORCE[5,1]:= 0.1; MFORCE[5,2]:= 0.1; MFORCE[5,3]:= 0.0;
MFORCE[5,4]:= -0.1; MFORCE[5,5]:=-32.8; MFORCE[5,6]:= 0.0;

MFORCE[6,1]:= 0.0; MFORCE[6,2]:= 0.0; MFORCE[6,3]:= -0.1;
MFORCE[6,4]:= -0.2; MFORCE[6,5]:= -0.2; MFORCE[6,6]:= 20.5;
           END;

{Multiplying the six analogue channels by the above correction matrix will yield
the hand forces wrt the transducer centre and coord sys. VECT1 & VECT2 are the
forces and moments respectively.}
           FOR A:= 1 TO 6 DO
           BEGIN
MFORCE[8,A]:=0;
           FOR B:= 1 TO 6 DO MFORCE[8,A]:= MFORCE[8,A] + MFORCE[A,B]*MFORCE[7,B];
           END;

           VECT1[1]:=MFORCE[8,1]; {X direction pylon force }
           VECT1[2]:=MFORCE[8,2]; {Y direction pylon force }
           VECT1[3]:=MFORCE[8,3]; {Z direction pylon force }

           VECT2[1]:=MFORCE[8,4]; {X direction pylon moment }
           VECT2[2]:=MFORCE[8,5]; {Y direction pylon moment }
           VECT2[3]:=MFORCE[8,6]; {Z direction pylon moment }

{To calculate hand moments the OFFSET between the hand and transducer centres
must be corrected for.}
           VECT2[1]:=VECT2[1]- VECT1[3]* 0.13575;
           VECT2[2]:=VECT2[2];

```

```

VECT2[3]:=VECT2[3]+ VECT1[1]* 0.13575;

{The hand forces and moments must now be converted to be wrt the
lab coordinate system. This procedure begins by defining the
marker coordinate system VECT4,5&6.}
FOR A:= 1 TO 3 DO VECT5[A]:=MARKERS[14,A]-MARKERS[13,A]; {y-axis marker}
FOR A:= 1 TO 3 DO VECT7[A]:=MARKERS[15,A]-MARKERS[13,A]; {x'-axis
marker}

IF ((VECT5[1]<>0)OR(VECT5[2]<>0)OR(VECT5[3]<>0))THEN NORMALIZ(VECT5);
IF ((VECT7[1]<>0)OR(VECT7[2]<>0)OR(VECT7[3]<>0))THEN NORMALIZ(VECT7);

VECTCROS(VECT7,VECT5,VECT6); {z-axis
marker}
VECTCROS(VECT5,VECT6,VECT4); {x-axis
marker}

IF ((VECT4[1]<>0)OR(VECT4[2]<>0)OR(VECT4[3]<>0))THEN NORMALIZ(VECT4);
IF ((VECT6[1]<>0)OR(VECT6[2]<>0)OR(VECT6[3]<>0))THEN NORMALIZ(VECT6);

MAT1[1,1]:=VECT4[1]; MAT1[1,2]:=VECT5[1]; MAT1[1,3]:=VECT6[1]; {direction
cosine matrix}
MAT1[2,1]:=VECT4[2]; MAT1[2,2]:=VECT5[2]; MAT1[2,3]:=VECT6[2];
MAT1[3,1]:=VECT4[3]; MAT1[3,2]:=VECT5[3]; MAT1[3,3]:=VECT6[3];

{A -47.2 deg, Y axis rotation is required to convert between the marker
and pylon coord systems (see Nov 6 92 notes). Note the marker used for this format
are: 13 on -ve Xp axis, 14 on +ve Yp direction from 13, and 15 on +ve Zp axis}
EULERY(MAT2,-0.8238);

{Conversion between lab and pylon coordinate systems can now be calculated}
MATEMULT(MAT1,MAT2,MAT3);

{Hand forces and moments wrt the lab are now:}
VECTMULT(MAT3,VECT1,VECT3);
VECTMULT(MAT3,VECT2,VECT4);
FOR A:= 1 TO 3 DO VECT1[A]:= VECT3[A];
FOR A:= 1 TO 3 DO VECT2[A]:= VECT4[A];
END;
END;
{*****}
{*****}
END.
{*****}
{*****}

```

```

{*****}
{*****}
UNIT READINFO;
{This unit:
1. Reads subject information and stores it into
workfile: WRKFILE3.PRN.
2. Reads Euler orientation information and stores
it to workfile: WRKFILE2.PRN }
{*****}
{*****}
INTERFACE
USES CRT, PRINTER, VARIABLE;
PROCEDURE READIN1;
PROCEDURE READIN2 (VAR NFRAMES:INTEGER; VAR S3:STRING);
PROCEDURE READIN3 (VAR FRAMENUM:INTEGER);

IMPLEMENTATION
{*****}
{*****}
PROCEDURE READIN1;
BEGIN

{Subject information to be stored in a workfile can be reread by supplying
the file name containing the information or the workfile can simply
be reused if it has been used immediately before.}
REPEAT
CLRSCR;
GOTOXY(1,2);
WRITELN('DEFINE SUBJECT INFO FILE? (Y/ <ret> for no change)');
A:=WhereY; A:=A-1; GOTOXY(60,A);
READLN(S1); WRITELN(' ');

IF ((S1='Y') OR (S1='y')) THEN
BEGIN
WRITELN('INPUT SUBJECT INFORMATION FILE TO BE USED:');
A:=WhereY; A:=A-1; GOTOXY(60,A);
READLN(S2); WRITELN(' ');

ASSIGN(FILEIN1, S2); RESET(FILEIN1);
ASSIGN(FILEOUT2, 'WRKFILE3.PRN'); REWRITE(FILEOUT2);

READLN(FILEIN1, S3);
WRITELN(FILEOUT2, S3);
FOR A:= 2 TO 19 DO
BEGIN
READLN(FILEIN1, AA);
WRITELN(FILEOUT2, AA);
END;
CLOSE(FILEIN1); CLOSE(FILEOUT2);
END;

WRITELN('IS THE SETUP SATISFACTORY? (Y/N)');
A:=WhereY; A:=A-1; GOTOXY(60,A);
READLN(S1); WRITELN(' ');
UNTIL((S1='Y') OR (S1='y'));
END;

{*****}
{*****}
This procedure prompts for and initializes input file information }
PROCEDURE READIN2 (VAR NFRAMES:INTEGER; VAR S3:STRING);
BEGIN
{Euler orientation data is read from a file.}
WRITELN('NAME OF FILE CONTAINING EULER DATA (NO EXT.), ');
A:=WhereY; A:=A-1; GOTOXY(48,A);
READLN(S3);
WRITELN('INPUT FILE EXTENSION, ');
A:=WhereY; A:=A-1; GOTOXY(48,A);
READLN(S2); WRITELN(' ');
S1:= S3+'.'+S2;
ASSIGN(FILEIN10, S1); RESET(FILEIN10);

WRITELN('HOW MANY FRAMES DO YOU WANT TO ANALYSE?');
A:=WhereY; A:=A-1; GOTOXY(48,A);
READLN(NFRAMES);
END;

{*****}
{*****}
This procedure reads info frame by frame and stores it to a working file
in the format of Euler angles followed by hand loads.}
PROCEDURE READIN3 (VAR FRAMENUM:INTEGER);
BEGIN
{This data can now be read and stored in workfile: WRKFILE2.PRN}
ASSIGN(FILEOUT2, 'WRKFILE2.PRN'); REWRITE(FILEOUT2);

```



```
READ(FILEIN10,FRAMENUM);
FOR A:= 1 TO 7 DO      {5 sets of Euler angles and 2 sets of hand loads}
  BEGIN
    READ(FILEIN10, AA, BB, CC);
    WRITELN(FILEOUT2,AA,' ',BB,' ',CC);
  END;

CLOSE(FILEOUT2);
END;
{*****}
{*****}
END.
{*****}
{*****}
```

```

{*****}
{*****}
UNIT SETVALS;
      {FILE SETVALS4
      This unit sets variable values used throughout
      the programs associated with shoulder biomechanics.
      Different variables are used by each section of the
      program with some overlapping of the information.}

      {NOTE:SETVAL1 uses muscle origin/insertion data from
      both dry bone studies and G. Johnson. The dry bone
      data was collected February 10, 1993 and details can
      be found in the notes.
      G.J.'s data renumbered to agree with the format
      of Anterior->Posterior and Superior->Inferior. For
      example, Deltoid Fascicles are numbered from anterior
      to posterior and Trapezius is numbered from Superior
      to inferior.
      The scapular coord sys used in the program is
      defined as follows: origin at AC joint; x-axis through
      inferior angle; y-axis laying in plane defined by AC
      joint, inferior angle and medial spinal root; and
      z-axis begin perpendicular to x and y.}

{*****}
{*****}
INTERFACE
USES CRT,VARIABLE,EULERS,MISCOPS;

PROCEDURE SETVAL1(VAR MD:MATRIX2);
PROCEDURE SETVAL2(VAR BHEIGHT,BWEIGHT:REAL; VAR HNDFORCE,HNDMOMNT:MATRIX1);
PROCEDURE SETVAL3(VAR TPOS,CPOS,SPOS,HPOS,UPOS,RPOS:MATRIX1);
PROCEDURE SETVAL4(VAR TPARAMS,CPARAMS,SPARAMS,HPARAMS,UPARAMS,RPARAMS:MATRIX1;
      VAR HCARANG,UCARANG,HTORSION:REAL);
PROCEDURE SETVAL5(VAR GFPOS:MATRIX1; VAR GFDIAM:REAL);
PROCEDURE SETVAL6(VAR ITGROOVE:MATRIX1; VAR HHDIA,HSDIA,HTORS:REAL);

IMPLEMENTATION
VAR
  A1,B1,C1,D1 :INTEGER;
  AA1,BB1,CC1,DD1 :REAL;
{*****}
{*****}
PROCEDURE PROCED1(VAR SUBJINFO:MATRIX6);
BEGIN
  ASSIGN(FILEIN3,'WRKFILE3.PRN'); RESET(FILEIN3);
  READLN(FILEIN3,S1);

  FOR A:= 1 TO 18 DO
    BEGIN
      READLN(FILEIN3,AA);
      B:= A+1;
      SUBJINFO[B]:=AA;
    END;
  CLOSE(FILEIN3);
  END;

{*****}
{*****}
{This procedure sets muscle information}
PROCEDURE SETVAL1(VAR MD:MATRIX2);
BEGIN
  {Get scaling factors required in this procedure from PROCED1}
  PROCED1(SUBJINFO);
  TSCALEH:=0.808*SUBJINFO[4]; {T1-T12 distance corrected to agree with GJ data}
  TSCALEW:=SUBJINFO[5];      {rib cage width under arms}
  TSCALED:=SUBJINFO[6];      {rib cage depth}
  CSCALE :=SUBJINFO[7];      {clavicle length}
  SSCALE :=SUBJINFO[8];
  HSCALE :=SUBJINFO[9];
  USCALE :=SUBJINFO[10];

  {Zero muscle data matrices}
  FOR A1 := 1 TO 20 DO FOR B1:= 1 TO 10 DO
    FOR C1:= 1 TO 2 DO FOR D1:= 1 TO 3 DO MD[A1,B1,C1,D1]:=0;

  {*****}
  {BICEPS, #1}
      {SCAPULAR ATTACHMENTS}
  MD[1,1,1,1]:= 0.099 ; MD[1,1,1,2]:=-0.042 ; MD[1,1,1,3]:= 0.196 ; {JR DATA}
  MD[1,2,1,1]:= 0.134 ; MD[1,2,1,2]:=-0.011 ; MD[1,2,1,3]:= 0.056 ; {JR DATA}

      {RADIAL INSERTIONS}

```

```

MD[1,1,2,1]:=0.166 ; MD[1,1,2,2]:=-0.013 ; MD[1,1,2,3]:=-0.037 ; {JR DATA}
MD[1,2,2,1]:=0.166 ; MD[1,2,2,2]:=-0.013 ; MD[1,2,2,3]:=-0.037 ; {JR DATA}

{*****}
{CORACOBRACHIALIS, #2}
      {SCAPULAR ATTACHMENTS}
MD[2,1,1,1]:= 0.099 ; MD[2,1,1,2]:=-0.042 ; MD[2,1,1,3]:= 0.196 ; {JR DATA}
      {HUMERAL INSERTION}
MD[2,1,2,1]:= 0.426 ; MD[2,1,2,2]:=-0.006 ; MD[2,1,2,3]:=-0.031 ; {JR DATA}

{*****}
{DELTOID, #3}
      {CLAVICLE ATTACHMENTS}
MD[3,1,1,1]:=0.607 ; MD[3,1,1,2]:= 0.040 ; MD[3,1,1,3]:=-0.040 ; {anterior}
MD[3,2,1,1]:=0.837 ; MD[3,2,1,2]:= 0.019 ; MD[3,2,1,3]:=-0.019 ; {middle anterior}
      {SCAPULAR ATTACHMENTS}
MD[3,3,1,1]:=-0.039 ; MD[3,3,1,2]:=-0.078 ; MD[3,3,1,3]:=-0.021 ; {JR DATA}
MD[3,4,1,1]:= 0.096 ; MD[3,4,1,2]:=-0.070 ; MD[3,4,1,3]:=-0.169 ; {middle}
MD[3,5,1,1]:= 0.329 ; MD[3,5,1,2]:= 0.198 ; MD[3,5,1,3]:=-0.115 ; {middle posterior}
      {HUMERAL INSERTION}
      {posterior}

FOR A:= 1 TO 5 DO
  .. BEGIN
    MD[3,A,2,1]:= 0.380 ; MD[3,A,2,2]:= 0.046 ; MD[3,A,2,3]:=-0.033 ;
  END;
{*****}
{INFRASPINATUS, #4}
      {SCAPULAR ATTACHMENTS}
MD[4,1,1,1]:= 0.529 ; MD[4,1,1,2]:= 0.289 ; MD[4,1,1,3]:=-0.022 ; {JR DATA}
MD[4,2,1,1]:= 0.663 ; MD[4,2,1,2]:= 0.192 ; MD[4,2,1,3]:=-0.031 ; {superior}
MD[4,3,1,1]:= 0.842 ; MD[4,3,1,2]:= 0.082 ; MD[4,3,1,3]:=-0.027 ; {middle}
      {HUMERAL INSERTIONS}
      {inferior}

FOR A:= 1 TO 3 DO
  BEGIN
    MD[4,A,2,1]:=-0.018 ; MD[4,A,2,2]:= 0.074 ; MD[4,A,2,3]:= 0.033 ;
  END;
{*****}
{LATISSIMUS DORSI, #5}
      {TRUNK ATTACHMENTS}
MD[5,1,1,1]:= 0.570 ; MD[5,1,1,2]:= 0 ; MD[5,1,1,3]:= 0.620 ; {JR DATA}
superior}
MD[5,2,1,1]:= 0.710 ; MD[5,2,1,2]:= 0.480 ; MD[5,2,1,3]:= 0.240 ; {JR DATA middle}
MD[5,3,1,1]:= 1.520 ; MD[5,3,1,2]:= 0.310 ; MD[5,3,1,3]:= 0.620 ; {JR DATA}
inferior}

      {HUMERAL INSERTION}

FOR A:= 1 TO 3 DO
  BEGIN
    MD[5,A,2,1]:= 0.201 ; MD[5,A,2,2]:= 0.015 ; MD[5,A,2,3]:=-0.045 ; {JR DATA}
  END;
{*****}
{LEVATOR SCAPULAE, #6}
      {TRUNK ATTACHMENTS}
MD[6,1,1,1]:=-0.520 ; MD[6,1,1,2]:= 0 ; MD[6,1,1,3]:= 0.480 ; {JR DATA}
      {SCAPULAR INSERTIONS}
MD[6,1,2,1]:= 0.353 ; MD[6,1,2,2]:= 0.368 ; MD[6,1,2,3]:= 0.034; {JR DATA}

{*****}
{PECTORALIS MAJOR, #7}
      {TRUNK ATTACHMENTS}
MD[7,3,1,1]:= 0.228 ; MD[7,3,1,2]:= 0.207 ; MD[7,3,1,3]:=-0.112 ; {inferior}
MD[7,2,1,1]:=-0.059 ; MD[7,2,1,2]:= 0.045 ; MD[7,2,1,3]:=+0.016 ; {middle}
MD[7,1,1,1]:=-0.256 ; MD[7,1,1,2]:= 0.021 ; MD[7,1,1,3]:=+0.065 ; {superior}
      {HUMERAL INSERTION}

FOR A:=1 TO 3 DO
  BEGIN
    MD[7,A,2,1]:= 0.270 ; MD[7,A,2,2]:= 0.042 ; MD[7,A,2,3]:=-0.048 ;
  END;
{*****}
{PECTORALIS MINOR, #8}
      {TRUNK ATTACHMENTS}
MD[8,3,1,1]:= 0.325 ; MD[8,3,1,2]:= 0.496 ; MD[8,3,1,3]:=+0.001 ; {inferior}
MD[8,2,1,1]:= 0.262 ; MD[8,2,1,2]:= 0.391 ; MD[8,2,1,3]:=+0.021 ; {middle}
MD[8,1,1,1]:= 0.156 ; MD[8,1,1,2]:= 0.290 ; MD[8,1,1,3]:=+0.027 ; {superior}
      {SCAPULAR INSERTIONS}

FOR A:=1 TO 3 DO

```

```

BEGIN
MD[8,A,2,1]:= 0.130 ; MD[8,A,2,2]:= 0.048 ; MD[8,A,2,3]:= 0.170 ; {JR DATA}
END;
{*****}
{RHOMBOID MAJOR, #9}
      {TRUNK ATTACHMENTS}
MD[9,1,1,1]:=-0.277 ; MD[9,1,1,2]:= 0.000 ; MD[9,1,1,3]:=+0.742 ; {superior}
MD[9,2,1,1]:=-0.217 ; MD[9,2,1,2]:= 0.000 ; MD[9,2,1,3]:=+0.712 ; {I}
MD[9,3,1,1]:=-0.137 ; MD[9,3,1,2]:= 0.000 ; MD[9,3,1,3]:=+0.745 ; {I}
MD[9,4,1,1]:= 0.000 ; MD[9,4,1,2]:= 0.000 ; MD[9,4,1,3]:=+0.792 ; {I}
MD[9,5,1,1]:= 0.104 ; MD[9,5,1,2]:= 0.000 ; MD[9,5,1,3]:=+0.825 ; {inferior}
      {data for 1 st fascicle missing so copied from the 2 nd}

      {SCAPULAR INSERTIONS}
MD[9,1,2,1]:= 0.592 ; MD[9,1,2,2]:= 0.347 ; MD[9,1,2,3]:=-0.016 ; {JR DATA}
MD[9,2,2,1]:= 0.667 ; MD[9,2,2,2]:= 0.289 ; MD[9,2,2,3]:=-0.012 ; {superior}
MD[9,3,2,1]:= 0.765 ; MD[9,3,2,2]:= 0.234 ; MD[9,3,2,3]:=-0.016 ; {I}
MD[9,4,2,1]:= 0.856 ; MD[9,4,2,2]:= 0.177 ; MD[9,4,2,3]:=-0.016 ; {I}
MD[9,5,2,1]:= 0.939 ; MD[9,5,2,2]:= 0.086 ; MD[9,5,2,3]:=-0.014 ; {inferior}
{*****}
{RHOMBOID MINOR, #10}
      {TRUNK ATTACHMENTS}
MD[10,1,1,1]:=-0.277 ; MD[10,1,1,2]:= 0 ; MD[10,1,1,3]:= 0.742 ; {JR DATA}

      {SCAPULAR INSERTIONS}
MD[10,1,2,1]:= 0.529 ; MD[10,1,2,2]:= 0.382 ; MD[10,1,2,3]:=-0.012 ; {JR DATA}
{*****}
{SERRATUS ANTERIOR, #11}
      {TRUNK ATTACHMENTS}
MD[11,1,1,1]:=-0.254 ; MD[11,1,1,2]:= 0.380 ; MD[11,1,1,3]:=+0.331 ; {superior}
MD[11,2,1,1]:=-0.188 ; MD[11,2,1,2]:= 0.450 ; MD[11,2,1,3]:=+0.222 ; {I}
MD[11,3,1,1]:= 0.055 ; MD[11,3,1,2]:= 0.508 ; MD[11,3,1,3]:=+0.179 ; {I}
MD[11,4,1,1]:= 0.215 ; MD[11,4,1,2]:= 0.522 ; MD[11,4,1,3]:=+0.107 ; {I}
MD[11,5,1,1]:= 0.356 ; MD[11,5,1,2]:= 0.544 ; MD[11,5,1,3]:=+0.075 ; {I}
MD[11,6,1,1]:= 0.472 ; MD[11,6,1,2]:= 0.583 ; MD[11,6,1,3]:=+0.102 ; {I}
MD[11,7,1,1]:= 0.581 ; MD[11,7,1,2]:= 0.624 ; MD[11,7,1,3]:=+0.180 ; {I}
MD[11,8,1,1]:= 0.681 ; MD[11,8,1,2]:= 0.621 ; MD[11,8,1,3]:=+0.193 ; {I}
MD[11,9,1,1]:= 0.801 ; MD[11,9,1,2]:= 0.626 ; MD[11,9,1,3]:=+0.270 ; {inferior}

      {SCAPULAR INSERTIONS}
MD[11,1,2,1]:= 0.312 ; MD[11,1,2,2]:= 0.372 ; MD[11,1,2,3]:= 0.084 ; {JR DATA}
MD[11,2,2,1]:= 0.430 ; MD[11,2,2,2]:= 0.403 ; MD[11,2,2,3]:= 0.034 ; {superior}
MD[11,3,2,1]:= 0.486 ; MD[11,3,2,2]:= 0.372 ; MD[11,3,2,3]:= 0.007 ; {I}
MD[11,4,2,1]:= 0.653 ; MD[11,4,2,2]:= 0.303 ; MD[11,4,2,3]:= 0.001 ; {I}
MD[11,5,2,1]:= 0.746 ; MD[11,5,2,2]:= 0.241 ; MD[11,5,2,3]:= 0.001 ; {I}
MD[11,6,2,1]:= 0.832 ; MD[11,6,2,2]:= 0.193 ; MD[11,6,2,3]:= 0.001 ; {I}
MD[11,7,2,1]:= 0.925 ; MD[11,7,2,2]:= 0.102 ; MD[11,7,2,3]:= 0.003 ; {I}
MD[11,8,2,1]:= 0.962 ; MD[11,8,2,2]:= 0.008 ; MD[11,8,2,3]:= 0.015 ; {I}
MD[11,9,2,1]:= 0.876 ; MD[11,9,2,2]:=-0.061 ; MD[11,9,2,3]:= 0.027 ; {inferior}
{*****}
{SUBSCAPULARIS, #12}
      {SCAPULAR ATTACHMENTS}
MD[12,1,1,1]:= 0.472 ; MD[12,1,1,2]:= 0.318 ; MD[12,1,1,3]:=-0.017 ; {JR DATA}
MD[12,2,1,1]:= 0.592 ; MD[12,2,1,2]:= 0.262 ; MD[12,2,1,3]:=-0.005 ; {superior}
MD[12,3,1,1]:= 0.815 ; MD[12,3,1,2]:= 0.072 ; MD[12,3,1,3]:=-0.012 ; {middle}
{inferior}

      {HUMERAL INSERTIONS}
FOR A:=1 TO 3 DO
  BEGIN
    MD[12,A,2,1]:=-0.012 ; MD[12,A,2,2]:= 0.015 ; MD[12,A,2,3]:=-0.083 ;
  END;
{*****}
{SUPRASPINATUS, #13}
      {SCAPULAR ATTACHMENT}
MD[13,1,1,1]:= 0.394 ; MD[13,1,1,2]:= 0.293 ; MD[13,1,1,3]:= 0.007 ; {JR DATA}

      {HUMERAL INSERTION}
MD[13,1,2,1]:=-0.052 ; MD[13,1,2,2]:= 0.072 ; MD[13,1,2,3]:=-0.018 ;
{*****}
{TERES MAJOR, #14}
      {SCAPULAR ATTACHMENTS}
MD[14,1,1,1]:= 0.837 ; MD[14,1,1,2]:=-0.071 ; MD[14,1,1,3]:=-0.015 ; {JR DATA}

      {HUMERAL INSERTIONS}
MD[14,1,2,1]:= 0.201 ; MD[14,1,2,2]:=+0.015 ; MD[14,1,2,3]:=-0.045 ;
{*****}
{TERES MINOR, #15}
      {SCAPULAR ATTACHMENTS}
MD[15,1,1,1]:= 0.673 ; MD[15,1,1,2]:=-0.052 ; MD[15,1,1,3]:= -0.032 ; {JR DATA}

```

```

                                {HUMERAL INSERTIONS}
MD[15,1,2,1]:= 0.020 ; MD[15,1,2,2]:= 0.048 ; MD[15,1,2,3]:= 0.053 ;

{*****}
{TRAPEZIUS, #16}
                                {TRUNK ATTACHMENTS}
MD[16,1,1,1]:=-0.368 ; MD[16,1,1,2]:= 0.000 ; MD[16,1,1,3]:=+0.627 ; {superior}
MD[16,2,1,1]:=-0.283 ; MD[16,2,1,2]:= 0.000 ; MD[16,2,1,3]:=+0.670 ; {I}
MD[16,3,1,1]:=-0.217 ; MD[16,3,1,2]:= 0.000 ; MD[16,3,1,3]:=+0.712 ; {I}
MD[16,4,1,1]:=-0.137 ; MD[16,4,1,2]:= 0.000 ; MD[16,4,1,3]:=+0.745 ; {I}
MD[16,5,1,1]:= 0.000 ; MD[16,5,1,2]:= 0.000 ; MD[16,5,1,3]:=+0.792 ; {I}
MD[16,6,1,1]:= 0.104 ; MD[16,6,1,2]:= 0.000 ; MD[16,6,1,3]:=+0.825 ; {I}
MD[16,7,1,1]:= 0.208 ; MD[16,7,1,2]:= 0.000 ; MD[16,7,1,3]:=+0.840 ; {I}
MD[16,8,1,1]:= 0.354 ; MD[16,8,1,2]:= 0.000 ; MD[16,8,1,3]:=+0.849 ; {inferior}

                                {SCAPULAR INSERTIONS}
MD[16,1,2,1]:=-0.001 ; MD[16,1,2,2]:= 0.005 ; MD[16,1,2,3]:=-0.023 ; {JR DATA}
MD[16,2,2,1]:= 0.051 ; MD[16,2,2,2]:= 0.021 ; MD[16,2,2,3]:=-0.075 ; {superior}
MD[16,3,2,1]:= 0.136 ; MD[16,3,2,2]:= 0.067 ; MD[16,3,2,3]:=-0.106 ; {I}
MD[16,4,2,1]:= 0.211 ; MD[16,4,2,2]:= 0.117 ; MD[16,4,2,3]:=-0.107 ; {I}
MD[16,5,2,1]:= 0.274 ; MD[16,5,2,2]:= 0.165 ; MD[16,5,2,3]:=-0.109 ; {I}
MD[16,6,2,1]:= 0.338 ; MD[16,6,2,2]:= 0.218 ; MD[16,6,2,3]:=-0.097 ; {I}
MD[16,7,2,1]:= 0.391 ; MD[16,7,2,2]:= 0.252 ; MD[16,7,2,3]:=-0.079 ; {I}
MD[16,8,2,1]:= 0.455 ; MD[16,8,2,2]:= 0.291 ; MD[16,8,2,3]:=-0.058 ; {inferior}
{*****}
{TRICEPS, #17}
                                {SCAPULAR ATTACHMENT}
MD[17,1,1,1]:= 0.331 ; MD[17,1,1,2]:=-0.104 ; MD[17,1,1,3]:=-0.008 ; {JR DATA}

                                {HUMERAL ATTACHMENTS}
MD[17,2,1,1]:= 0.379 ; MD[17,2,1,2]:= 0.031 ; MD[17,2,1,3]:= 0.006 ; {JR DATA}
MD[17,3,1,1]:= 0.385 ; MD[17,3,1,2]:=-0.010 ; MD[17,3,1,3]:= 0.006 ; {JR DATA}

                                {ULNAR INSERTIONS}
FOR A:=1 TO 3 DO
  BEGIN
    MD[17,A,2,1]:=-0.062 ; MD[17,A,2,2]:= 0 ; MD[17,A,2,3]:= 0.045 ; {JR DATA}
  END;
{*****}
{SCAPULAR CONTACT WITH RIB CAGE, 18}
                                {SCAPULAR CONTACT LOCATIONS (INSERTIONS)}
MD[18,1,2,1]:=0.529; MD[18,1,2,2]:=0.382; MD[18,1,2,3]:=0; {superior, taken as
rhom. min. ins.}
MD[18,2,2,1]:=1.0 ; MD[18,2,2,2]:=0 ; MD[18,2,2,3]:=0; {inferior}

{*****}
{Scale all muscle data according to scaling factors outlined in procedure PROCEDI
Trunk scaling is complicated because G Johnson's data only used a vertical
scaling factor, TSCALEH. This proved to be unacceptable for our purposes.
Trunk width, TSCALEW, and depth, TSCALEL, scaling factors were added. Depth
scale measurement is taken from the Sternum horizontally back to the T4 spinoeus
process. This should be equal to the T4 fascicle insertion Z coord of trapezius.
Fascicle numbered 5 is attached to T4. Regarding width scaling, few muscles are
inserted on the trunk anywhere but centrally. Therefore, width scaling has little
effect on their values. Since a scale factor cannot be calculated for width
because no estimate of rib cage width was given for the muscle data used,
height scale factor is used.}

AA1:=TSCALEL/ MD[16,5,1,3];

FOR A1:=1 TO 20 DO
  BEGIN
    FOR B1:=1 TO 10 DO
      BEGIN
        FOR C1:=1 TO 2 DO
          BEGIN
            FOR D1:= 1 TO 3 DO
              BEGIN
                {correct muscle origins}
                IF (C1=1)THEN
                  BEGIN
                    IF(( A1=5 ) OR
( A1=6 ) OR
( A1=7 ) OR
( A1=8 ) OR
( A1=9 ) OR
( A1=10) OR
( A1=11) OR
( A1=16)) THEN
                      BEGIN
                        IF (D1=1)THEN MD[A1,B1,C1,D1]:=MD[A1,B1,C1,D1]*TSCALEH;
                        IF (D1=2)THEN MD[A1,B1,C1,D1]:=MD[A1,B1,C1,D1]*TSCALEH;

```

```

        IF(D1=3) THEN MD[A1,B1,C1,D1]:=MD[A1,B1,C1,D1]*AA1;
        END;

        IF(( A1=1 ) OR
           ( A1=2 ) OR
           ((A1=3 ) AND (B1>2)) OR
           ( A1=4 ) OR
           ( A1=12) OR
           ( A1=13) OR
           ( A1=14) OR
           ( A1=15) OR
           ((A1=17) AND (B1=1)) ) THEN MD[A1,B1,C1,D1]:=MD[A1,B1,C1,D1]*SSCALE;

        IF( (A1=3 )AND(B1<3) ) THEN MD[A1,B1,C1,D1]:=MD[A1,B1,C1,D1]*CSCALE;

        IF( (A1=17)AND(B1>1) ) THEN MD[A1,B1,C1,D1]:=MD[A1,B1,C1,D1]*HSCALE;
        END;

{correcting muscle insertions and scapular/rib cage contact points}
        IF (C1=2)THEN
        BEGIN
        IF(( A1=6 ) OR
           ( A1=8 ) OR
           ( A1=9 ) OR
           ( A1=10) OR
           ( A1=11) OR
           ( A1=16) OR
           ( A1=18)) THEN MD[A1,B1,C1,D1]:=MD[A1,B1,C1,D1]*SSCALE;

        IF(( A1=2 ) OR
           ( A1=3 ) OR
           ( A1=4 ) OR
           ( A1=5 ) OR
           ( A1=7 ) OR
           ( A1=12) OR
           ( A1=13) OR
           ( A1=14) OR
           ( A1=15)) THEN MD[A1,B1,C1,D1]:=MD[A1,B1,C1,D1]*HSCALE;

        IF(( A1=1 ) OR
           ( A1=17)) THEN MD[A1,B1,C1,D1]:=MD[A1,B1,C1,D1]*USCALE;
        END;
        END;
        END;
        END;
        end;
        {*****}
        {*****}
        {This procedure sets parameters required for limb loading calculations}
        {Note:loads are in terms of a lab coord sys ie X-forward, Y-up, Z to right}
        PROCEDURE SETVAL2(VAR BHEIGHT,BWEIGHT:REAL; VAR HNDFORCE,HNDMOMNT:MATRIX1);
        BEGIN
        {Body height(in mm), weight(in Kg)is retrieved using PROCED1}
        PROCED1(SUBJINFO);
        BHEIGHT:=SUBJINFO[2]; {in m}
        BWEIGHT:=SUBJINFO[3]*9.81; {in Newtons}
        {Hand loads for each Frame are stored after the Euler angle info in
        WRKFILE2.PRN}
        ASSIGN(FILEIN2,'WRKFILE2.PRN'); RESET(FILEIN2);
        FOR A1:=1 TO 5 DO READLN(FILEIN2,AA,BB,CC); {Euler angle info}

        {External force on the hand in Newtons.}
        READLN(FILEIN2,HNDFORCE[1],HNDFORCE[2],HNDFORCE[3]);
        {External moment on the hand in Newton meters.}
        READLN(FILEIN2,HNDMOMNT[1],HNDMOMNT[2],HNDMOMNT[3]);
        CLOSE(FILEIN2);
        END;

        {*****}
        {*****}
        {This procedure sets apparent bone position variables. }
        PROCEDURE SETVAL3(VAR TPOS,CPOS,SPOS,HPOS,UPOS,RPOS:MATRIX1);

        BEGIN
        ASSIGN(FILEIN2,'WRKFILE2.PRN'); RESET(FILEIN2);

        {Trunk flexion,abduction, and external rotation wrt the ground}
        READLN(FILEIN2, TPOS[1], TPOS[2], TPOS[3]);

        {Apparent (ie clinical) clavicle protraction, abbduction and rotation(=0)wrt the
        trunk}

```

```

READLN(FILEIN2, CPOS[1], CPOS[2], CPOS[3]);
{Apparent (ie clinical) scapula Xs axis, Zs axis (med/lat) and Ys axis wrt the trunk}
READLN(FILEIN2, SPOS[1], SPOS[2], SPOS[3]);
{Apparent (ie clinical) upper arm flexion, abbduction and ext. rot. wrt the trunk}
READLN(FILEIN2, HPOS[1], HPOS[2], HPOS[3]);
{Apparent (ie clinical) ulnar flexion and forearm supnation wrt the humerus.}
READLN(FILEIN2, UPOS[1], UPOS[2], RPOS[3]);
{Forearm orientation angles that are always equal to zero. }
UPOS[3]:=0 ; RPOS[1]:=0 ; RPOS[2]:=0 ;

CLOSE(FILEIN2);

BB1:=(Pi/180);
FOR A1:=1 TO 3 DO
  BEGIN
    TPOS[A1]:=TPOS[A1]*BB1;
    CPOS[A1]:=CPOS[A1]*BB1;
    SPOS[A1]:=SPOS[A1]*BB1;
    HPOS[A1]:=HPOS[A1]*BB1;
    UPOS[A1]:=UPOS[A1]*BB1;
    RPOS[A1]:=RPOS[A1]*BB1;
  END;
END;

{*****}
{*****}
{In this procedure, the translations from one coordinate system to another are
given. For example, TPARAMS give the clavicle origin location wrt the trunk
coordinate system and origin, using x,y,z dimensions. The only exceptions to
this are in HPARAMS, UPARAMS AND RPARAMS. In HPARAMS, "y" is the humeral head
offset distance. In UPARAMS, "x" is the elbow centre to ulnar head distance, "y"
is the distance to the radial centre line and "z" is not used. In RPARAMS, "x"
is the elbow centre to hand centre distance and "y" and "z" are not used.}

PROCEDURE SETVAL4 (VAR TPARAMS,CPARAMS,SPARAMS,HPARAMS,UPARAMS,RPARAMS:MATRIX1;
VAR HCARANG,UCARANG,HTORSION:REAL);

BEGIN

  TPARAMS[1]:=-0.20 ; TPARAMS[2]:= 0.075 ; TPARAMS[3]:= 0.14 ;
  CPARAMS[1]:= 1.0 ; CPARAMS[2]:= 0 ; CPARAMS[3]:= 0 ;
  SPARAMS[1]:= 0.223; SPARAMS[2]:=-0.056 ; SPARAMS[3]:= 0.042 ;{Glenoid Fossa
Centre}
  HPARAMS[1]:= 0.925; HPARAMS[2]:= 0.034 ; HPARAMS[3]:=-0.047 ;
  UPARAMS[1]:= 0.934; UPARAMS[2]:= 0.078 ; UPARAMS[3]:= 0 ;
  RPARAMS[1]:= 1.125; RPARAMS[2]:= 0 ; RPARAMS[3]:= 0 ;

  HCARANG:=5*Pi/180 ; {These three values may be changed}
  UCARANG:= 5*Pi/180;
  HTORSION:=25*Pi/180; {to study their effects on the predictions.}

{Some of these values must now be combined with appropriate scaling factors}

  PROCED1 (SUBJINFO);
  TSCALEH:=SUBJINFO[4]*0.808; {G.J's TSCALE value wasn't T1-T12 so correction of
0.808 is used}
  TSCALEW:=SUBJINFO[5];
  TSCALE:=SUBJINFO[6];
  CSCALE :=SUBJINFO[7];
  SSCALE :=SUBJINFO[8];
  HSCALE :=SUBJINFO[9];
  USCALE :=SUBJINFO[10];

  FOR B1:= 1 TO 3 DO
    BEGIN
      TPARAMS[B1]:=TPARAMS[B1]*TSCALEH; {only small effect of using only trunk
height}
      CPARAMS[B1]:=CPARAMS[B1]*CSCALE; { scaling factor}
      SPARAMS[B1]:=SPARAMS[B1]*SSCALE;
      HPARAMS[B1]:=HPARAMS[B1]*HSCALE;
      UPARAMS[B1]:=UPARAMS[B1]*USCALE;
      RPARAMS[B1]:=RPARAMS[B1]*USCALE; {Note: radial parameters use ulnar scaling
factor}
    END;

  {SPARAMS value gives the Glenoid Fossa Centre wrt ACCENT and so to give the
Humeral Head centre position a small calculation is performed. It is assumed
that the H.Head, Glenoid Fossa Centre and Rhomboid Minor insertion all lay on
a line. The distance separating tyhe H.Head centre and Glenoid Fossa Centre is
1/2 H.Head Diameter. Notes from Feb 14,92 detail the calculation of the

```

```

direction vector used here.)
  SETVAL1(MD); HHDIA:=0.044;
  FOR A1:= 1 TO 3 DO VECT01[A1] :=SPARAMS[A1]-MD[10,1,2,A1];
  NORMALIZ(VECT01);
  FOR A1:= 1 TO 3 DO SPARAMS[A1]:=SPARAMS[A1]+(VECT01[A1]*0.5* HHDIA);
END;
{*****}
{*****}
{Information required for determining GH joint stability. }
PROCEDURE SETVAL5(VAR GFPOS:MATRIX1; VAR GFDIAM:REAL);
BEGIN
  GFPOS[1]:=40.0; {Lateral rotation of Glenoid Fossa about Zs axis in deg.}
  GFPOS[2]:=-7.0; {Retrotilt (+ve posteriorly) of Fossa about Xs' axis in deg.}
  GFPOS[3]:= 0.0; {not used yet}

  GFDIAM :=
0.025{*****}
{*****}
;{Glenoid fossa mean diameter}

  FOR A1:= 1 TO 3 DO GFPOS[A1]:=GFPOS[A1]*Pi/180;
  END;

{*****}
{*****}
{Various data is required for muscle wrapping calculations. This data is
stored here.}
PROCEDURE SETVAL6(VAR ITGROOVE:MATRIX1; VAR HHDIA,HSDIA,HTORS:REAL);
BEGIN
  ITGROOVE[1]:=-0.027;
  ITGROOVE[2]:= 0.049;
  ITGROOVE[3]:=-0.053;

  PROCED1(SUBJINFO);
  HSCALE:=SUBJINFO[9];
  FOR A1:= 1 TO 3 DO ITGROOVE[A1]:=ITGROOVE[A1]*HSCALE;

  HHDIA:= 0.044; {m} {If changing, change here AND in SETVAL4}
  HSDIA:= 0.020; {m}

  HTORS:= 25 *Pi/180; {cadaver humeral torsion angle given
in deg. and converted to rads.}
END;
{*****}
{*****}
END.
{*****}
{*****}

```



```

{*****}
{*****}
UNIT SIMFMT;
{From file: converts information
calculated by the Main program into SIMPLEX
format and calls optimization routine.
FMT02, (Format 2, only GH and elbow joint muscles)
-Input info from file PCSA1.PRN and array MOMFACTS
-5 moment equations, 4 are "=" and 1 is >= as
discussed in March 9,92 notes.
-26 force (muscle) elements are considered.
-format details are:
-moment parameters rounded and given in 1/100's m.
-ext moments rounded to 10 N/mm given in Nmm.
-PCSA's rounded to and given in 100's mm^2.
-all data given to at least 1 decimal place.
FMT03, (Format 2, only GH and elbow joint muscles)
-GH joint stability considered.
-Input info is file PCSA1.PRN, arrays MOMFACTS
and FORFACTS.
-5 moment equations, 4 are "=", and 1 >= as
described in March 12 92 notes.
-1 GH joint stability equation (see notes Feb 21 92)
-26 force (muscle) elements are considered.
-format details are:
-moment parameters rounded and given in 1/100's m.
-ext moments rounded to 10 N/mm given in Nmm.
-PCSA's rounded to and given in 100's mm^2.
-all data given to at least 1 decimal place.}
{*****}
{*****}
INTERFACE
USES CRT, PRINTER,
MISCOPS, SETVALS, SIMPLEX, VARIABLE, VARSIMP;

PROCEDURE FMT03 (VAR FRAMENUM, ICASE:INTEGER; VAR MOMFACTS:MATRIX5; VAR
FORFACTS:MATRIX9);
PROCEDURE FMT02 (VAR FRAMENUM, ICASE:INTEGER; VAR MOMFACTS:MATRIX5; VAR
FORFACTS:MATRIX9);

IMPLEMENTATION
{*****}
{*****}
{This internal procedure sorts the optimized muscle forces into ascending order}
PROCEDURE PROCED1 (VAR OPTA:RealArrayMPbyNP; VAR IPOSV:IntegerArrayM; N:integer);
LABEL 10;
BEGIN
FOR C:= 2 TO M DO
BEGIN
A := IPOSV[C];
BB:= OPTA[C,1];
FOR D:= C-1 DOWNT0 1 DO
BEGIN
IF IPOSV[D] <= A THEN GOTO 10;
IPOSV[D+1] := IPOSV[D];
OPTA[D+1,1] := OPTA[D,1]
END;
D := 0;
10: IPOSV[D+1] := A;
OPTA[D+1,1] := BB
END
END;

{*****}
{*****}
{This procedure is very similar to FMT02 it introduces a stability
equation to the optimization. Only those muscles crossing the GH joint and
elbow are considered in this analysis.}
PROCEDURE FMT03 (VAR FRAMENUM, ICASE:INTEGER; VAR MOMFACTS:MATRIX5; VAR
FORFACTS:MATRIX9);
BEGIN

{open and initialize the muscle X-section data input file AND OPT matrix file}
ASSIGN(FILEIN2, 'PCSA1.PRN'); RESET(FILEIN2);
STATUS:=0;

{For stability, the ratio of Glenoid fossa diameter to humeral head dia. must
calculated. Information required for this calculation is stored in SETVAL5 for
calculation details see notes Feb 21 92. Also, since a true resultant shear
force cannot be calculated, the stability ratio is reduced by 0.707 so that
in a worse case, the true resultant shear force will not cause instability.}
SETVAL5 (GFPOS, GFDIA);
SETVAL6 (ITGROOVE, HHDIA, HSDIA, HTORS);
AA:=(GFDIA/2) /HHDIA;
AA:=ASIN(AA);

```

```

AA:=HHDIA*COS(AA);
GG:=0.01*ROUND(100*0.707*(GFDIA/AA));           {stability ratio}

{Read the PCSA constraint equation parameters. Read information from
muscle X-section data input file, round to mm^2 and units of 100's mm^2.}
F:=0; G:=0;
FOR D:= 1 TO 60 DO      {55}
  BEGIN
  F:=F+1;
  IF ((D<=14) OR (D=16) OR (D=17) OR (D=18) OR (D=37) OR (D=38) OR (D=39) OR (D=40)
      OR (D=41) OR (D=42) OR (D=51) OR (D=52) OR (D=53)) THEN
    BEGIN
    G:=G+1;
    READ(FILEIN2,AA);
    PCSA[G]:=(10*ROUND(0.1*AA)) /1000;
    END
  ELSE
    READ(FILEIN2,AA);
  END;
CLOSE(FILEIN2);

REPEAT

{Zero optimization matrix}
FOR A:= 1 TO mp DO FOR B:= 1 TO np DO OPTA[A,B]:=0.0;

for a:= 1 to mp do iposv[a]:=0;
for a:= 1 to np do izrov[a]:=0;

{Write the objective equation to the output ARRAY}
IF (STATUS=0) THEN BEGIN
FOR A:= 1 TO 27 DO OPTA[1,A]:= 0.0;
OPTA[1,28]:=-1.0; END
ELSE
FOR A:= 2 TO 27 DO OPTA[1,A]:=-1.0;

{Write PCSA infor to the optimization array}
IF (STATUS=0) THEN BEGIN
FOR A:= 2 TO 27 DO
  BEGIN
  C:= A-1;
  AA:=-1/PCSA[C];
  BB:= PCSA[C];
  FOR B:= 2 TO 27 DO
    IF (A=B) THEN OPTA[A,B]:=-1;
  OPTA[A,28]:=BB;
  OPTA[A, 1]:=0;
  END;
END
ELSE BEGIN
FOR A:= 2 TO 27 DO
  BEGIN
  C:= A-1;
  BB:=pcsa[c]*(ff+0.000001); {0.01+(0.01*ROUND(100*PCSA[C]*FF));}
  FOR B:= 2 TO 27 DO
    IF (A=B) THEN OPTA[A,B]:=-1;
  OPTA[A,1]:=BB;
  OPTA[A,28]:=0;
  END;
END;

{Write the 4 stability constraint equations}
D:=0; E:=27; F:=0; H:=33; {33 OR 32}

BB:=(-1*FORFACTS[1,27]-(GG*FORFACTS[2,27]));
AA:=0.01*ROUND(10*BB);
IF BB>=0 THEN BEGIN
F:= F+1; G:=H-F;
BB:=1; CC:=STATUS*-0.02;
END
ELSE BEGIN
D:= D+1; G:=E+D;
BB:=-1; CC:=STATUS* 0.02;
END;
OPTA[G,1]:=BB*AA; OPTA[G,28]:=0;
FOR B:= 1 TO 26 DO
OPTA[G,B+1]:=CC+BB*-0.1*ROUND(100*(FORFACTS[1,B] + (GG*FORFACTS[2,B])));

BB:= (FORFACTS[1,27]-(GG*FORFACTS[2,27]));
AA:=0.01*ROUND(10*BB);
IF BB>=0 THEN BEGIN
F:= F+1; G:=H-F;
BB:=1; CC:=STATUS*-0.02;
END

```

```

ELSE BEGIN
  D:= D+1; G:=E+D;
  BB:=-1; CC:=STATUS* 0.02;
  END;
OPTA[G,1]:=BB*AA; OPTA[G,28]:=0;
FOR B:= 1 TO 26 DO
  OPTA[G,B+1]:=CC+BB*-0.1*ROUND(100*((-1*FORFACTS[1,B])+(GG*FORFACTS[2,B])));

BB:=(-1*FORFACTS[3,27]-(GG*FORFACTS[2,27]));
AA:=0.01*ROUND(10*BB);
IF BB>=0 THEN BEGIN
  F:= F+1; G:=H-F;
  BB:=1; CC:=STATUS*-0.02;
  END
ELSE BEGIN
  D:= D+1; G:=E+D;
  BB:=-1;CC:=STATUS* 0.02;
  END;
OPTA[G,1]:=BB*AA; OPTA[G,28]:=0;
FOR B:= 1 TO 26 DO OPTA[G,B+1]:=CC+BB*-0.1*ROUND(100*((
FORFACTS[3,B])+(GG*FORFACTS[2,B])));

BB:=( FORFACTS[3,27]-(GG*FORFACTS[2,27]));
AA:=0.01*ROUND(10*BB);
IF BB>=0 THEN BEGIN
  F:= F+1; G:=H-F;
  BB:=1; CC:=STATUS*-0.02;
  END
ELSE BEGIN
  D:= D+1; G:=E+D;
  BB:=-1; CC:=STATUS* 0.02;
  END;
OPTA[G,1]:=BB*AA; OPTA[G,28]:=0;
FOR B:= 1 TO 26 DO
  OPTA[G,B+1]:=CC+BB*-0.1*ROUND(100*((-1*FORFACTS[3,B])+(GG*FORFACTS[2,B])));

{Read moment eqn paramters from moment data input ARRAY, round to 1/100's m
and units of 1/100's m. Write the moment constraint equations. Note only first
five are used as the remaining 5 are for AC and SC joints. Due to problem
encountered April 29 92 moment balance for the humeral/radial joint has been
removed. To effect this change, M1 =31-f from M1=30-f and a=2 to 5 from
a= 1 to 5.}

M1:=31-F; M2:=F;

FOR A:= 2 TO 5 DO
  BEGIN
  AA:=MOMFACTS[A,56];
  IF( AA<0 ) THEN BB:= -1 ELSE BB:=1;
  IF(( AA<0 ) AND ( A=1 ))THEN
    BEGIN
    M2:=M2+1;
    F:=33-M2;
    END;
  IF(( AA>=0 ) AND ( A=1 ))THEN
    BEGIN
    M1:=M1+1;
    F:=M1+1;
    END;
  IF A> 1 THEN
    F:=A+31; G:= 0; {31 OR 29 }
  FOR D:= 1 TO 60 DO
    BEGIN
    IF((D<=14)OR(D=16)OR(D=17)OR(D=18)OR(D=37)OR(D=38)OR(D=39)OR(D=40)
OR(D=41)OR(D=42)OR(D=51)OR(D=52)OR(D=53))THEN
      BEGIN
      G:=G+1;
      OPTA[F,G+1]:=0.1*ROUND(1000*MOMFACTS[A,D])*BB;
      IF((A<=2)AND((D=1)OR(D=2)))THEN OPTA[F,G+1]:=OPTA[F,G+1]*2;
      END;
    END;
  OPTA[F,1]:=0.01*ROUND(100*MOMFACTS[A,56])*BB;
  END;

  M1:=31-M2 ; M3:=4;
  SIMPLX(OPTA,m,n,m1,m2,m3,icase,izrov,iposv);

  IF ICASE = +1 THEN Writeln('FMT 3 OPTIMIZATION UNSUCCESSFUL, OBJECTIVE FUNCTION
UNBOUNDED');
  IF ICASE = -1 THEN Writeln('FMT 3 OPTIMIZATION UNSUCCESSFUL, NO POSSIBLE
SOLUTION');
  IF ICASE <>0 THEN BEGIN
  {
  Writeln(FILEOUT14,FRAMENUM:3,' ');
  STATUS:=2;
  }

```

```

SOUND(80); DELAY(200); NOSOUND;
END;

IF((ICASE = 0)AND(STATUS=0))THEN FF:=-1*OPTA[1,1];

STATUS:=1; {if double optimization required, then remove this line}

IF((ICASE = 0)AND(STATUS>0))THEN {solution can be sorted and written to OP2}
BEGIN
WRITELN('FMT 3 OPTIMIZATION SUCCESSFUL');
OPTA[27,2]:=FF; {1st row gives intensity}
FOR A:= 1 TO M DO OPTA[A,1]:=OPTA[A+1,1]; {remove 1st row}
PROCED1(OPTA,IPOSV,N); {sort}
D:= 0;A:=1;
REPEAT {use 2nd column of OPTA}
D:= D+1; {to store the sorted muscle}
IF (IPOSV[A]=D)THEN {forces with 0's added as
required}
BEGIN
OPTA[D,2]:=OPTA[A,1];
A:= A+1
END ELSE
OPTA[D,2]:=0;
UNTIL( D=26 );
{The solution can be written to a working file that is rewritten for each frame.}
{The solution can be written to the file .OP3 that keeps track of all frame results.}
FOR A:= 1 TO 26 DO OPTA[A,2]:=OPTA[A,2]*100;
WRITELN(FILEOUT14,FRAMENUM:3,
OPTA[ 1,2]:7:1,OPTA[ 2,2]:7:1,OPTA[ 3,2]:7:1,OPTA[ 4,2]:7:1,OPTA[
5,2]:7:1,
OPTA[ 6,2]:7:1,OPTA[ 7,2]:7:1,OPTA[ 8,2]:7:1,OPTA[
9,2]:7:1,OPTA[10,2]:7:1,
OPTA[11,2]:7:1,OPTA[12,2]:7:1,OPTA[13,2]:7:1,OPTA[14,2]:7:1,OPTA[15,2]:7:1,
OPTA[16,2]:7:1,OPTA[17,2]:7:1,OPTA[18,2]:7:1,OPTA[19,2]:7:1,OPTA[20,2]:7:1,
OPTA[21,2]:7:1,OPTA[22,2]:7:1,OPTA[23,2]:7:1,OPTA[24,2]:7:1,OPTA[25,2]:7:1,
OPTA[26,2]:7:1,OPTA[27,2]:9:3);

{The optimized muscle forces can now be used with the information in array
FORFACTS, to compute the forces being transmitted through the Glenoid Fossa.}
FOR A:= 1 TO 3 DO
BEGIN
AA:=0.0;
FOR B:= 1 TO 26 DO AA:=AA+OPTA[B,2]*FORFACTS[A,B]; {muscle forces}
VECT1[A]:=AA+FORFACTS[A,27]; {external forces}
END;
WRITELN(FILEOUT10,FRAMENUM:3,VECT1[1]:8:1,VECT1[2]:8:1,VECT1[3]:8:1);
END;
IF(STATUS=1)THEN STATUS:=2;
IF(STATUS=0)THEN STATUS:=1;
UNTIL(STATUS=2);
END;

{*****}
{This procedure although using the same working files as FMT01 actually sets
up experimental data for optimization of only those muscles crossing the
GH joint and elbow. The procedure uses a double optimization format, that is
it finds the minimum possible overall muscle intensity and then repeats the
optimization sequence minimizing the overall total muscle force. The variable
STATUS marks which is being done.}
PROCEDURE FMT02(VAR FRAMENUM,ICASE:INTEGER; VAR MOMFACTS:MATRIX5; VAR
FORFACTS:MATRIX9);
BEGIN
STATUS:=0;

{open and initialize the muscle X-section data input file AND opt matrix file}
ASSIGN(FILEIN2,'PCSA1.PRN'); RESET(FILEIN2);
{ ASSIGN(FILEOUT1,'JUNKOUT1.PRN'); REWRITE(FILEOUT1);}

{Read the PCSA constraint equation parameters. Read information from
muscle X-section data input file, round to mm^2 and units of 100's mm^2.}
F:=0; G:=0;
FOR D:= 1 TO 60 DO
BEGIN
F:=F+1;
IF((D<=14)OR(D=16)OR(D=17)OR(D=18)OR(D=37)OR(D=38)OR(D=39)OR(D=40)
OR(D=41)OR(D=42)OR(D=51)OR(D=52)OR(D=53))THEN
BEGIN
G:=G+1;
READ(FILEIN2,AA);
PCSA[G]:=(10*ROUND(0.1*AA))/1000;

```

```

        END
    ELSE
        READ(FILEIN2,AA);
    END;
CLOSE(FILEIN2);

REPEAT
    M2:=0;

{Zero optimization matrix}
FOR A:= 1 TO mp DO FOR B:= 1 TO np DO OPTA[A,B]:=0.0;
FOR A:= 1 TO MP DO IPOSV[A]:=0;
FOR A:= 1 TO NP DO IZROV[A]:=0;

{Write the objective equation to the output ARRAY}
IF (STATUS=0) THEN BEGIN
    FOR A:= 1 TO 27 DO OPTA[1,A] := 0.0;
    OPTA[1,28] := -1.0; END
ELSE
    FOR A:= 2 TO 27 DO OPTA[1,A] := -1.0;

{Write PCSA infor to the optimization array}
IF (STATUS=0) THEN BEGIN
    FOR A:= 2 TO 27 DO
        BEGIN
            C:= A-1;
            AA:=-1/PCSA[C];
            BB:= PCSA[C];
            FOR B:= 2 TO 27 DO
                IF (A=B) THEN OPTA[A,B] := -1;
            OPTA[A,28] := BB;
            OPTA[A,1] := 0;
        END;
    END
ELSE BEGIN
    FOR A:= 2 TO 27 DO
        BEGIN
            C:= A-1;
            BB:= PCSA[C]*(FF+0.000001);
            FOR B:= 2 TO 27 DO
                IF (A=B) THEN OPTA[A,B] := -1;
            OPTA[A,1] := BB;
            OPTA[A,28] := 0;
        END;
    END;

{Write 4 BOGUS equations so that format3 optimization can use the
same optimizing unit.}
FOR A:= 28 TO 31 DO FOR B:= 1 TO 28 DO OPTA[A,B] := 0;

{Read moment eqn paramters from moment data input ARRAY, round to 1/100's m
and units of 1/100's m. Write the moment constraint equations. Note only first
five are used as the remaining 5 are for AC and SC joints.}
{***** Due to problem encountered on April 29, 92 moment balance for the
humeral-radial joint has been removed from the optimization. This problem
due to uncorrected wrapping about the radius. To remove this equation, M1
set to 31 from 30 and A= 2 to 5 instead of A = 1 to 5}
M1:=31; M2:=0;
FOR A:= 2 TO 5 DO {3}
    BEGIN
        AA:=MOMFACTS[A,56];
        IF ( AA<0 ) THEN BB:= -1 ELSE BB:=1;
        IF (( AA<0 ) AND ( A=1 )) THEN
            BEGIN
                M2:=M2+1;
                F:=33-M2;
            END;
        IF (( AA>=0 ) AND ( A=1 )) THEN
            BEGIN
                M1:=M1+1;
                F:=M1+1;
            END;
        IF A> 1 THEN
            F:=A+31; G:= 0; {31 OR 25 OR 29}
        FOR D:= 1 TO 60 DO
            BEGIN
                IF ((D<=14) OR (D=16) OR (D=17) OR (D=18) OR (D=37) OR (D=38) OR (D=39) OR (D=40)
                    OR (D=41) OR (D=42) OR (D=51) OR (D=52) OR (D=53) ) THEN
                    BEGIN
                        G:=G+1;
                        OPTA[F,G+1] := 0.1*ROUND(1000*MOMFACTS[A,D])*BB;
                        IF ((A<=2) AND ((D=1) OR (D=2))) THEN OPTA[F,G+1] := OPTA[F,G+1]*2;
                    END;
            END;
        END;

```

```

OPTA[F,1]:=0.01*ROUND(100*MOMFACTS[A,56])*BB;
END;

{ FOR A:= 1 TO MP-1 DO
  WRITELN(FILEOUT1,
    OPTA[A,1]:7:3,OPTA[A,2]:7:3,OPTA[A,3]:7:3,OPTA[A,4]:7:3,OPTA[A,5]:7:3,
    OPTA[A,6]:7:3,OPTA[A,7]:7:3,OPTA[A,8]:7:3,OPTA[A,9]:7:3,OPTA[A,10]:7:3,
OPTA[A,11]:7:3,OPTA[A,12]:7:3,OPTA[A,13]:7:3,OPTA[A,14]:7:3,OPTA[A,15]:7:3,
OPTA[A,16]:7:3,OPTA[A,17]:7:3,OPTA[A,18]:7:3,OPTA[A,19]:7:3,OPTA[A,20]:7:3,
OPTA[A,21]:7:3,OPTA[A,22]:7:3,OPTA[A,23]:7:3,OPTA[A,24]:7:3,OPTA[A,25]:7:3,
  OPTA[A,26]:7:3,OPTA[A,27]:7:3,OPTA[A,28]:7:3);}

  M3:=4; M1:=35-M2-M3;
  { WRITELN(M1:3,M2:3,M3:3);}
  SIMPLX(OPTA,m,n,m1,m2,m3,icase,izrov,iposv);
  { FOR A:= 1 TO M+1 DO WRITELN(FILEOUT1,IPOSV[A-1]:3,OPTA[A,1]);}

  IF ICASE = +1 THEN WRITELN('FMT 2 OPTIMIZATION UNSUCCESSFUL, OBJECTIVE FUNCTION
UNBOUNDED');
  IF ICASE = -1 THEN WRITELN('FMT 2 OPTIMIZATION UNSUCCESSFUL, NO POSSIBLE
SOLUTION');
  IF ICASE <> 0 THEN BEGIN
  { WRITELN(FILEOUT13,FRAMENUM:3, ' ');}
  STATUS:=2;
  SOUND(80);DELAY(200);NOSOUND;
  END;
  IF((ICASE = 0)AND(STATUS=0))THEN FF:=-1*OPTA[1,1];
  IF((ICASE = 0)AND(STATUS>0))THEN {solution can be sorted and written to .OP2}
  BEGIN
  WRITELN('FMT 2 OPTIMIZATION SUCCESSFUL');
  OPTA[27,2]:=FF; {1st row gives intensity}
  FOR A:= 1 TO M DO OPTA[A,1]:=OPTA[A+1,1]; {remove 1st row}
  PROCED1(OPTA,IPOSV,N); {sort}
  D:= 0;A:=1;
  REPEAT {use 2nd column of OPTA}
  D:=D+1; {to store the sorted muscle}
  IF (IPOSV[A]=D)THEN {forces with 0's added as
required}
  BEGIN
  OPTA[D,2]:=OPTA[A,1];
  A:= A+1
  END ELSE
  OPTA[D,2]:=0;
  UNTIL( D=26 );
  {The solution can be written to a working file that is rewritten for each frame.}
  {The solution can be written to the file .OP2 that keeps track of all frame results.}
  FOR A:= 1 TO 26 DO OPTA[A,2]:=OPTA[A,2]*100;
  { WRITELN(FILEOUT1, ' 0 ');}
  WRITELN(FILEOUT13,FRAMENUM:3,
    OPTA[ 1,2]:7:1,OPTA[ 2,2]:7:1,OPTA[ 3,2]:7:1,OPTA[ 4,2]:7:1,OPTA[
5,2]:7:1,
    OPTA[ 6,2]:7:1,OPTA[ 7,2]:7:1,OPTA[ 8,2]:7:1,OPTA[
9,2]:7:1,OPTA[10,2]:7:1,
OPTA[11,2]:7:1,OPTA[12,2]:7:1,OPTA[13,2]:7:1,OPTA[14,2]:7:1,OPTA[15,2]:7:1,
OPTA[16,2]:7:1,OPTA[17,2]:7:1,OPTA[18,2]:7:1,OPTA[19,2]:7:1,OPTA[20,2]:7:1,
OPTA[21,2]:7:1,OPTA[22,2]:7:1,OPTA[23,2]:7:1,OPTA[24,2]:7:1,OPTA[25,2]:7:1,
  OPTA[26,2]:7:1,OPTA[27,2]:9:3);
  {The optimized muscle forces can now be used with the information in array
FORFACTS, to compute the forces being transmitted through the Glenoid Fossa.}
  FOR A:= 1 TO 3 DO
  BEGIN
  AA:=0.0;
  FOR B:= 1 TO 26 DO AA:=AA+OPTA[B,2]*FORFACTS[A,B]; {muscle forces}
  VECT1[A]:=AA+FORFACTS[A,27]; {external forces}
  END;
  WRITELN(FILEOUT10,FRAMENUM:3,VECT1[1]:8:1,VECT1[2]:8:1,VECT1[3]:8:1);
  END;
  IF(STATUS=1)THEN STATUS:=2;
  IF(STATUS=0)THEN STATUS:=1;
  UNTIL(STATUS=2);
  { CLOSE(FILEOUT1);}
  END;
  {*****}
  {*****}
  END.
  {*****}
  {*****}

```

```

{*****}
{*****}
UNIT SIMPLX;          {from Numerical Recipes in Pascal, Press et al, 1990}

INTERFACE
USES VARSIMP;
PROCEDURE SIMPLX(VAR opta:RealArrayMPbyNP;
                 m,n,m1,m2,m3:integer;
                 VAR  icase:integer;
                 VAR  izrov:integerArrayN;
                 VAR  iposv:integerArrayM);

IMPLEMENTATION
{*****}
{*****}

PROCEDURE SIMPLX(VAR opta:RealArrayMPbyNP;
                 m,n,m1,m2,m3:integer;
                 VAR  icase:integer;
                 VAR  izrov:integerArrayN;
                 VAR  iposv:integerArrayM);

LABEL 1,2,3,4,5,99;
CONST
  eps = 1.0e-9;
VAR
  n12,n11,m12,kp,kh,k,is,ir,ip,i:integer;
  q1,bmax:real;
  l1: ^IntegerArrayNP;
  l2,l3: ^IntegerArrayM;

PROCEDURE simpl(VAR opta:realArrayMPbyNP;
                mm:integer;
                VAR l1:integerArrayNP;
                n11,iabf:integer;
                VAR kp:integer;
                VAR bmax:real);

VAR
  k: integer;
  test: real;
BEGIN
  kp := l1[l1];
  bmax := opta[mm+1,kp+1];
  FOR k := 2 TO n11 DO BEGIN
    IF iabf = 0 THEN
      test := opta[mm+1,l1[k]+1]-bmax
    ELSE
      test := abs(opta[mm+1,l1[k]+1])-abs(bmax);
    IF test > 0.0 THEN BEGIN
      bmax := opta[mm+1,l1[k]+1];
      kp := l1[k]
    END
  END
END;

PROCEDURE simp2(VAR opta:RealArrayMPbyNP;
                m,n:integer;
                VAR l2:IntegerArrayM;
                n12:integer;
                VAR ip:integer;
                kp:integer;
                VAR q1:real);

LABEL 1,2,99;
CONST
  eps = 1.0e-9;
VAR
  k,ii,i:integer;
  qp,q0,q:real;
BEGIN
  ip := 0;
  FOR i := 1 TO n12 DO
    IF opta[l2[i]+1,kp+1] < -eps THEN GOTO 1;
  GOTO 99;
1: q1 := -opta[l2[i]+1,1]/opta[l2[i]+1,kp+1];
  ip := l2[i];
  FOR i := i+1 TO n12 DO BEGIN
    ii := l2[i];
    IF opta[ii+1,kp+1] < -eps THEN BEGIN
      q := -opta[ii+1,1]/opta[ii+1,kp+1];
      IF q < q1 THEN BEGIN
        ip := ii;
        q1 := q
      END
    ELSE IF q = q1 THEN BEGIN
      FOR k := 1 TO n DO BEGIN
        qp := -opta[ip+1,k+1]/opta[ip+1,kp+1];

```

```

                q0 := -opta[ii+1,k+1]/opta[ii+1,kp+1];
                IF q0 <> qp THEN GOTO 2
            END;
        2:      IF q0 < qp THEN ip :=ii
            END
            END
            END;
99:
END;

PROCEDURE simp3(VAR opta:RealArrayMPbyNp;    {Matrix operation to exchange lft & rt
hnd variables}
                i1,k1,ip,kp:integer);
VAR
    kk,ii:integer;
    piv:real;
BEGIN
    piv :=1.0/opta[ip+1,kp+1];
    FOR ii := 1 TO i1+1 DO BEGIN
        IF ii-1 <> ip THEN BEGIN
            opta[ii,kp+1] := opta[ii,kp+1]*piv;
            FOR kk :=1 TO k1+1 DO
                IF kk-1 <> kp THEN
                    opta[ii,kk] := opta[ii,kk] -opta[ip+1,kk]*opta[ii,kp+1]
            END
        END;
        FOR kk := 1 TO k1+1 DO
            IF kk-1 <>kp THEN
                opta[ip+1,kk] := -opta[ip+1,kk]*piv;
            opta[ip+1,kp+1] := piv
        END;
    END;

BEGIN
    IF m <> m1+m2+m3 THEN BEGIN
        Writeln('pause in routine SIMPLX');
        Writeln('bad input constraint counts');
        readln
    END;
    new(l1);
    new(l2);
    new(l3);
    n11 := n;
    FOR k := 1 TO n DO BEGIN
        l1^ [k] := k;
        izrov[k] := k
    END;
    n12 := m;
    FOR i := 1 TO m DO BEGIN
        IF opta[i+1,1] < 0.0 THEN BEGIN
            writeln('pause in routine SIMPLX');
            writeln('bad input tableau');
            readln
        END;
        l2^ [i] := i;
        iposv[i] := n+i
    END;
    FOR i := 1 TO m2 DO l3^ [i] := 1;
    ir := 0;
    IF m2+m3 = 0 THEN
        GOTO 5;
    ir := 1;
    FOR k :=1 TO n+1 DO BEGIN
        q1 :=0.0;
        FOR i:= m1+1 TO m DO
            q1 := q1+opta[i+1,k];
        opta[m+2,k] := -q1
    END;
3:  simp1(opta,m+1,l1^,n11,0,kp,bmax);
    IF (bmax <= eps) AND (opta[m+2,1] < -eps) THEN BEGIN
        icense := -1;
        GOTO 99
    END
    ELSE IF (bmax<=eps)
        AND (opta[m+2,1] <=eps) THEN BEGIN
        m12 := m1+m2+1;
        IF m12 <= m THEN BEGIN
            FOR ip :=m12 TO m DO BEGIN
                IF iposv[ip] = ip+n THEN BEGIN
                    simp1(opta,ip,l1^,n11,1,kp,bmax);
                    IF bmax >0.0 THEN GOTO 1
                END
            END
        END
    END;
END;

```



```

    ir := 0;
    m12 := m12-1;
    IF m1+1 > m12 THEN GOTO 5;
    FOR i := m1+1 TO m12 DO
        IF l3^[i-m1] = 1 THEN
            FOR k := 1 TO n+1 DO opta[i+1,k] := -opta[i+1,k];
        GOTO 5
    END;
    simp2(opta,m,n,l2^,n12,ip,kp,q1);
    IF ip = 0 THEN BEGIN
        icense := -1;
        GOTO 99
    END;
1: simp3(opta,m+1,n,ip,kp);
    IF iposv[ip] >= n+m1+m2+1 THEN BEGIN
        FOR k := 1 TO n11 DO
            IF l1^[k] = kp THEN GOTO 2;
2:    n11 := n11-1;
        FOR is := k TO n11 DO l1^[is] := l1^[is+1]
    END
    ELSE BEGIN
        IF iposv[ip] < n+m1+1 THEN GOTO 4;
        kh := iposv[ip]-m1-n;
        IF l3^[kh] = 0 THEN GOTO 4;
        l3^[kh] := 0
    END;
    opta[m+2,kp+1] := opta[m+2,kp+1]+1.0;
    FOR i := 1 TO m+2 DO opta[i,kp+1] := -opta[i,kp+1];
4: is := izrov[kp];
    izrov[kp] := iposv[ip];
    iposv[ip] := is;
    IF ir <> 0 THEN
        GOTO 3;
5: simpl(opta,0,l1^,n11,0,kp,bmax);
    IF bmax <= 0.0 THEN BEGIN
        icense := 0;
        GOTO 99
    END;
    simp2(opta,m,n,l2^,n12,ip,kp,q1);
    IF ip = 0 THEN BEGIN
        icense := 1;
        GOTO 99
    END;
    simp3(opta,m,n,ip,kp);
    GOTO 4;
99:    dispose(l3);
        dispose(l2);
        dispose(l1)
END;
END.

```

```

{*****}
{*****}
UNIT VARIABLE;                                {FILE VARIABLE3}
INTERFACE
TYPE
  MATRIX1 = ARRAY[1..3] OF REAL;
  MATRIX2 = ARRAY[1..20,1..10,1..2,1..3] OF REAL;
  MATRIX3 = ARRAY[1..3,1..3] OF REAL;
  MATRIX4 = ARRAY[1..20,1..10] OF REAL;
  MATRIX5 = ARRAY[1..10,1..100] OF REAL;
  MATRIX6 = ARRAY[1..60] OF REAL;
  MATRIX7 = ARRAY[1..25,1..3] OF REAL;
  MATRIX8 = ARRAY[1..15,1..3] OF REAL;
  MATRIX9 = ARRAY[1..3, 1..30] OF REAL;
VAR
{*****}
{VARIOUS MATRICES USED FOR CALCULATIONS}
{*****}
  IDENTMAT,                                {IDENTITY MATRIX}
  MAT1, MAT2, MAT3, MAT4, MAT5,            {UNDEFINED MATRICES}
  MAT6, MAT7, MAT8, MAT9, MAT10,
  MAT11, MAT12, MAT13, MAT14, MAT15,
  MAT01, MAT02, MAT03, MAT04, MAT05,

{COORDINATE SYSTEM TRANSFORMATION MATRICES}
  TROTMAT,                                {GROUND TO TRUNK}
  CROTMAT,                                {TRUNK TO CLAVICLE}
  SROTMAT,                                {TRUNK TO SCAPULA}
  HROTMAT,                                {TRUNK TO HUMERUS}
  EROTMAT,                                {TRUNK TO ELBOW}
  UROTMAT,                                {TRUNK TO ULNA}
  RROTMAT,                                {TRUNK TO RADIUS}
  TIROTMAT,                               {TRUNK TO GROUND}
  CIROTMAT,                               {CLAVICLE TO TRUNK}
  SIROTMAT,                               {SCAPULA TO TRUNK}
  HIROTMAT,                               {HUMERUS TO TRUNK}
  EIROTMAT,                               {ELBOW TO TRUNK}
  UIROTMAT,                               {ULNAR TO TRUNK}
  RIROTMAT                                :MATRIX3;    {RADIUS TO TRUNK}

{*****}
{VARIOUS VECTORS USED FOR CALCULATIONS}
{*****}
  VECT1, VECT2, VECT3, VECT4, VECT5,
  VECT6, VECT7, VECT8, VECT9, VECT10, VECT11, VECT12,
  VECT01, VECT02, VECT03, VECT04, VECT05,

{LIMB DIMENSIONS}
  TPARAMS,                                {TRUNK ORIGIN TO CLAVICLE ORIGIN}
  CPARAMS,                                {CLAVICLE ORIGIN TO SCAPULA ORIGIN}
  SPARAMS,                                {SCAPULA ORIGIN TO HUMERAL HEAD CENTRE}
  HPARAMS,                                {HUMERAL HEAD TO ELBOW CENTRE}
  UPARAMS,                                {ULNAR PARAMETERS}
  RPARAMS,                                {ELBOW TO HAND CENTRE INFORMATION}

{POSITIONING}
  TPOS,                                    {TRUNK FLEXION, ABB. AND ROTATION}
  CPOS,                                    {CLAVICLE -----"-----}
  SPOS,                                    {SCAPULA -----"-----}
  HPOS,                                    {HUMERAL -----"-----}
  HHPOS,                                   {HUMERAL HEAD -----"-----}
  UPOS,                                    {ULNAR FLEXION}
  RPOS,                                    {FOREARM ROTATION}
  GFPOS,                                   {GLENOID FOSSA ORIENT. WRT SCAP COORD SYS}

{JOINT AND HAND CENTRES, FOR TRANSLATING CLINICAL TO ANATOMICAL ALIGNMENT}
  ELCENT,                                  {ELBOW}
  HRCENT,                                  {HUMERAL RADIAL JOINT CENTRE}
  HNDCENT,                                 {HAND}
  HSCENT,                                  {HUMERAL SHAFT CENTRE}
  SCCENT,                                  {STERNAL CLAVIULAR JOINT CENTRE}
  ACCENT,                                  {ACROMIAL CLAVICULAR JOINT CENTRE}
  GHCENT,                                  {GLENOHUMERAL JOINT CENTRE LOCATION}

{EXTERNAL LOADS}
  GHFLOAD, GHMLOAD,                       {FORCE & MOMENT @HUMERAL HEAD DUE TO EXT
LOADS}
  HUFLOAD, HUMLOAD,                       {FORCE & MOMENT @ELBOW DUE TO EXT LOADS}
  HRFLOAD, HRMLoad,                       {FORCE & MOMENT FOR RADIAL COORD SYS DUE TO
EXT LOADS}
  ACFLoad, ACMLOAD,                       {FORCE & MOMENT FOR ACCROM-CLAV. DUE TO EXT.
LOADS }
  SCFLoad, SCMLOAD,                       {----- " ----- STERN -CLAV ----- "
----- }

```

```

HNDFORCE,                {EXTERNAL FORCE @ THE HAND}
HNDMOMNT,                 {EXTERNAL MOMENT @ THE HAND}

{MISC}
ITGROOVE                  :   MATRIX1; {INTERTUBERCLE GROOVE LOCATION ON THE
HUMERUS}

MFORCE                    :   MATRIX4; {MUSCLE FORCE PER VESICLE ALSO USED FOR PYLON
CHANNEL MATH}
FORFACTS                  :   MATRIX9; {MUSCLE FORCE FACTS FOR GLEN. FOSSA EQUIL}
                                {Also body positions used for hand load calcs}

from accel}
MOMFACTS                  :   MATRIX5; {MUSCLE MOMENT FACTORS }
SUBJINFO,                 {EXPERIMENTAL SUBJECT INFORMATION}
PCSA                      :   MATRIX6; {MUSCLE X-SECTION AREA IN CM }
RC                        :   MATRIX7; {RIB NODAL POINTS USED FOR RIB CAGE SHAPE
DESCRIPTION}
MARKERS                   :   MATRIX8; {3-D EXPERIMENTAL MARKER DATA}

{*****}
{MUSCLE ORIGIN AND INSERTION DATA}
{*****}
MDT,                      {MUSCLE DATA WRT TRUNK COORD SYS ORIENTATION}
                                {AND LOCAL COORD SYS ORIGIN }
MD,                       {MUSCLE (DATA) ATTACHMENTS}
                                { @1,@2,@3,@4) -@1 muscle number
                                -@2 vescicle number
                                -@3 1-origin, 2-insertion
                                -@4 xyz coordinates in
                                terms of the local bone
                                coord sys.}

{*****}
{MUSCLE FORCE INFORMATION}
{*****}
MDIR                      :   MATRIX2; {DIRECTION OF ORIGIN AND INSERTION MUSCLE
FIBRES}

{*****}
{SIMPLE VARIABLES}
{*****}

GFDIA,                    {MEAN GLENOID FOSSA DIAMETER}
HTORSION,                 {EXPERIMENTAL HUMERAL TORISON }
HTORS,                   {HUMERAL TORSION ASSUMED FOR MEASURED
CADAVERS}
HHDIA,                    {HUMERAL HEAD DIAMETER}
HSDIA,                    {HUMERAL SHAFT DIAMETER}
HROTOLD,                  {HROT OLD VALUE USED FOR ITERATIVE
SOLUTION}
HCARANG,UCARANG,          {HUMERAL & ULNAR CARRING ANGLES}
TSCALEH,                  {TRUNK HEIGHT SCALING FACTOR}
TSCALEW,                  {TRUNK WIDTH SCALING FACTOR}
TSCALED,                  {TRUNK DEPTH SCALING FACTOR}
CSCALE,                   {CLAVICLE SCALING FACTOR}
SSCALE,                   {SCAPULA SCALING FACTOR}
HSCALE,                   {HUMERUS SCALING FACTOR}
USCALE,                   {ULNAR AND RADIAL SCALING FACTOR}
UFLEXOLD,                 {UFLEX OLD VALUE USED FOR ITERATIVE
SOLUTION}
BHEIGHT,BWEIGHT,          {BODY HEIGHT AND WEIGHT}
RCWIDTH,                  {RIB CAGE WITDTH, MEASURED CLINICALLY}
MAX,                      {5th RIB NODE WITH LARGEST "Y" VALUE}
THETA,                    {ITERATION VALUE USED FOR SCAPULAR
POSITIONING}
HELEVA,                   {HUMERAL ELEVATION FROM VERTICAL}
ERR,ERROLD,ERRNEW,STEP,  {ERROR VALUES FOR ITERATIVE SOLUTION}
ITERH,ITERU,              {ITERATIVE SEARCH PARAMETERS}
AA,BB,CC,DD,EE,FF,GG,HH : REAL; {CALCULATION VARIABLES}

A,B,C,D,E,F,G,H,I,J,K,   {CALCULATION VARIABLES}
ITERSET,ITERSET2,        {ITERATIVE SEARCH PARAMETERS}
ICASE,                    {SIMPLEX OPT SOLUTION INDEX}
{ FORMAT, }              {MARKER FORMAT USED FOR DATA
COLLECTION}
FRAMENUM,                 {CURRENT FRAME NUMBER}
NFRAMES,                  {TOTAL NUMBER OF FRAMES TO BE ANALYSED}
NMARKERS,                 {NUMBER OF MARKERS USED DURING DATA
COLLECTION}
PREDICT,                  {IF SCAP ORIENT. PREDICTED THEN = 2
OTHERWISE =1}
ANALOGUE,                 {HAND FORCE SOURCE USED: 0-NONE, 1 F/P, 2

```

```

PYLON, 3 CofG ACCEL}
ANALOGRT,                               {RATIO OF ANALOGUE TO VIDEO DATA
COLLECTION}
NANALOG,                                {NUMBER OF ANALOGUE DATA CHANNELS}
STATUS, STATUS2                          :INTEGER; {ITERATIVE SEARCH STATUS}

FILEIN1, FILEIN2, FILEIN3,              {INPUT FILES FOR PROGRAM}
FILEIN4, FILEIN5, FILEIN6, FILEIN7,
FILEOUT1, FILEOUT2, FILEOUT3,
FILEOUT4, FILEOUT5, FILEOUT6,
FILEOUT7, FILEOUT8, FILEOUT9,          {OUTPUT FILES FOR PROGRAM}
FILEIN10, FILEOUT10,
FILEOUT11,
FILEOUT12,
FILEOUT13,
FILEOUT14                               :TEXT;

S1, S2, S3, S4                           :STRING; {INPUT VARIABLE FOR SCREEN COMMANDS}
{*****}
IMPLEMENTATION
BEGIN
END.
{*****}

```

```

{*****}
{*****}
UNIT VARSIMP;
{*****}
{*****}
INTERFACE
CONST
  N = 27;
  M = 35; {29OR 33 OR 35}
  NP = 28;
  MP = 37;

TYPE
  RealArrayMPbyNp = ARRAY[1..MP,1..NP] OF REAL;
  INTEGERARRAYN = ARRAY[1..N] OF INTEGER;
  INTEGERARRAYM = ARRAY[1..M] OF INTEGER;
  INTEGERARRAYNP = ARRAY[1..NP] OF INTEGER;
VAR
  OPTA :RealArrayMPbyNp;
  m1,m2,m3,icase :integer;
  izrov :IntegerArrayN;
  iposv :IntegerArrayM;

IMPLEMENTATION
BEGIN
END.

```

```

{*****}
{*****}
UNIT WRAPS ;                               {Contained in this unit are the procedures
                                           adjusting muscle lines of action because
                                           of wrapping.}

{*****}
{*****}

INTERFACE
USES CRT, PRINTER,
    EULERS, MISCOPS, SETVALS, VARIABLE;

VAR INTEXT          :INTEGER;              {factor -lorl for int or ext rot}
    SLOPE, INTER, RADIU :REAL;

PROCEDURE WRAP1(VAR GHCENT, HSCENT:MATRIX1; VAR MDT:MATRIX2; VAR HROTMAT:MATRIX3);

IMPLEMENTATION
{*****}
{*****}
{This internal procedure calculates if there is an intersection between a line
joining muscle origin and insertion and a circle, radius given. Within this
procedure the claculations are purely planer as both Humeral Shaft and Head
wrapping procedures have reduced the problem to a planar state before calling
this procedure. The analysis plane used in this procedure is the Z-Y plane
as designated in both the H. Shaft and H. Head procedures. VECT1 AND VECT2
coordiantes are given wrt the circle centre.}

PROCEDURE PROCED1(VAR A, ITERSET, STATUS, INTEXT:INTEGER;
    VAR VECT1, VECT2, VECT3:MATRIX1;
    VAR RADIU:REAL);

    BEGIN
        FOR B:= 1 TO 3 DO VECT3[B]:=VECT2[B];
        {Check to see if the humeral shaft passes between the origin and insertion
        indicating that wrapping is occurring. This calculation is done by looking
        at the O/I and humeral shaft in the Y-Z plane of the humeral shaft. A line is
        drawn between O and I using slope intercept technique. This equation is
        combined with the HS circle equation and roots are sought. If no roots then no
        intersection, 1 root means the line touches the circle and two roots indicates
        the line and circle interset in two places. If intersecion is indicated then
        the intersection is checked to see if it exists between the O & I.}

        IF ((STATUS=0) AND (VECT2[2]=VECT1[2])) THEN {O/I line parallel to Z axis}
            BEGIN
                AA:= ABS(VECT2[2]); BB:=RADIU;
                IF (AA>BB) THEN
                    BEGIN
                        STATUS:=1 {no intersection}
                    END
                ELSE
                    BEGIN {check if intersection is between O & I}
                        FF:=VECT2[2]; GG:=SQRT(SQR(BB)-SQR(FF));
                        IF ((VECT1[3]<=GG) AND (GG<=VECT2[3])) OR
                            ((VECT1[3]>=GG) AND (GG>=VECT2[3])) THEN
                            BEGIN
                                IF (AA=BB) THEN STATUS:=2;
                                IF (AA<BB) THEN STATUS:=3;
                            END;
                        END;
                    END;
            END;

        IF ((STATUS=0) AND (VECT2[3]=VECT1[3])) THEN {O/I line parallel to Y axis}
            BEGIN
                AA:= ABS(VECT2[3]); BB:=RADIU;
                IF (AA>BB) THEN
                    BEGIN
                        STATUS:=1; {no intersection}
                    END ELSE
                    BEGIN {check if intersection is between O & I}
                        GG:=VECT2[3]; FF:=SQRT(SQR(BB)-SQR(GG));
                        IF ((VECT1[2]<=FF) AND (FF<=VECT2[2])) OR
                            ((VECT1[2]>=FF) AND (FF>=VECT2[2])) THEN
                            BEGIN
                                IF (AA=BB) THEN STATUS:=2;
                                IF (AA<BB) THEN STATUS:=3;
                            END;
                        END;
                    END;
            END;

        IF (STATUS=0) THEN {O/I line has slope and intersept}
            BEGIN
                SLOPE:=(VECT2[3]-VECT1[3])/(VECT2[2]-VECT1[2]); {slope of O/I line }
            END;
    END;

```

```

INTER:=VECT1[3] - (SLOPE*VECT1[2]);           {intersept of O/I line}
AA:=SQR(SLOPE)+1;
BB:=2*INTER*SLOPE;                            {binomial parameter A}
CC:=SQR(INTER) - SQR(RADIU);                  {-----"----- B}
                                                {-----"----- C}

DD:=4*AA*CC;
EE:=SQR(BB);
FF:=EE-DD;

IF(FF< 0 ) THEN
  BEGIN
    STATUS:=1;
  END ELSE

  BEGIN
    VECT4[2] := (-1*BB+ SQR(EE-DD))/(2*AA);    {location of intersections}
    IF ((VECT1[2] <= VECT4[2]) AND (VECT4[2] <= VECT2[2]) OR
        ((VECT1[2] >= VECT4[2]) AND (VECT4[2] >= VECT2[2]))) THEN
      BEGIN
        IF(EE=DD) THEN STATUS:=2;
        IF(EE>DD) THEN STATUS:=3;
      END ELSE

      BEGIN
        STATUS:=1;
      END
    END;
  END;

{It has now been determined what is the muscle fascicle status. Action can now
be taken.}
IF(STATUS<0) THEN WRITELN('***** ERROR 1, WRAPPING MUSCLE:
',ITERSET:3,',',A:3,' *****');

{ IF(STATUS=0) THEN WRITELN('ERROR 2, WRAPPING MUSCLE: ',ITERSET:3,',',A:3);}
{ IF(STATUS=1) THEN WRITELN('NO WRAPPING FOR MUSCLE: ',ITERSET:3,',',A:3);}
{ IF(STATUS=2) THEN WRITELN('MUSCLE WAS TOUCHING, NO CHG',ITERSET:3,',',A:3);}

IF(STATUS=3) THEN
  BEGIN
    B:=WhereY; B:=B-1; GOTOXY(1,B);
    WRITELN('Muscle',ITERSET:3,',',A:3,' was wrapped and is now corrected. ');
    AA:=RADIU;
    BB:=SQR(SQR(VECT1[2])+SQR(VECT1[3]));
    CC:=SQR(SQR(AA)+SQR(BB));
    DD:=(Pi/2)-ARCTAN(AA/CC);
    EE:=ARCTAN(VECT1[3]/VECT1[2]);

    IF(VECT1[2]>0) THEN
      BEGIN
        EE:=ARCTAN(VECT1[3]/VECT1[2]);
        IF(INTEXT=-1) THEN FF:=EE+DD;
        IF(INTEXT= 1) THEN GG:=EE-DD;
      END;

    IF(VECT1[2]=0) THEN
      BEGIN
        IF(VECT1[3]>0) THEN EE:=(Pi/ 2);
        IF(VECT1[3]<0) THEN EE:=(Pi/-2);
        IF(INTEXT=-1) THEN FF:=EE+DD;
        IF(INTEXT= 1) THEN GG:=EE-DD;
      END;

    IF(VECT1[2]<0) THEN
      BEGIN
        EE:=ARCTAN(VECT1[3]/VECT1[2]);
        IF(INTEXT=-1) THEN FF:=Pi+EE+DD;
        IF(INTEXT= 1) THEN GG:=Pi+EE-DD;
      END;

{The variables FF & GG now contain the angles for new insertion position
corresponding to internal and external rotating muscle types respectively.
The correct angle for each muscle can now be chosen.}

{New insertion position will be;}
IF(INTEXT=-1) THEN
  BEGIN
    VECT3[1] := 0.0;
    VECT3[2] := (RADIU)*COS(FF);
    VECT3[3] := (RADIU)*SIN(FF);
  END;

```

```

IF (INTEXT= 1) THEN
  BEGIN
    VECT3 [1] := 0.0;
    VECT3 [2] := (RADIU)*COS (GG);
    VECT3 [3] := (RADIU)*SIN (GG);
  END;
END;
END;

{*****}
{*****}
{This procedure corrects Deltoid muscle wrapping. The procedure corrects any
fascicles wrapped around the humeral head using a dominant muscle plane whose
rotation axis is parallel to the humeral Y-axis. Any fascicles not wrapped
around the humeral head are corrected if they are wrapped around the
humeral shaft as was done in "WRAP1". }
PROCEDURE WRAP1 (VAR GHCENT, HSCENT: MATRIX1; VAR MDT: MATRIX2; VAR HROT MAT: MATRIX3);

BEGIN
  SETVAL3 (TPOS, CPOS, SPOS, HPOS, UPOS, RPOS);
  SETVAL4 (TPARAMS, CPARAMS, SPARAMS, HPARAMS, UPARAMS, RPARAMS,
    HCARANG, UCARANG, HTORSION);
  SETVAL6 (VECT1, HHDIA, HSDIA, HTORS); {VECT1 IS JUNK INFO HERE}

  {Repeat calculations, once for each muscle. ITERSET holds the muscle
  number for each repeat, and STATUS contains information regarding wrapping
  type: 0 - initial start value,
  -1 - origin lays inside humeral shaft circle when viewed in Y-Zhs plane.
  1 - no intersection
  2 - single intersection
  3 - double intersection }

  ITERSET:=1; {biceps is first}
  REPEAT
    C:=3; {num of fascicles per muscle}
  IF ((ITERSET=1) OR (ITERSET=13) OR (ITERSET=14) OR (ITERSET=15)) THEN C:=1;
  IF (ITERSET=3) THEN C:=5;

  FOR A:= 1 TO C DO
    BEGIN
      IF (ITERSET=1) THEN A:=2;
      STATUS:=0; STATUS2:=1;
      {Define origin and insertion of fascicle as VECT1 AND VECT2.}
      {Define VECT3 as a vector passing from insertion through origin in trunk sys.}
      FOR B:= 1 TO 3 DO
        BEGIN
          VECT1 [B] :=MDT [ITERSET, A, 1, B];
          VECT2 [B] :=MDT [ITERSET, A, 2, B];
          IF (ITERSET=1) THEN VECT2 [B] :=MDT [1, 3, 2, B];
          VECT3 [B] :=VECT1 [B] -VECT2 [B];
        END;

        {Define dominant muscle plane as containing VECT3 and Humeral Head Z axis
        for all but the middle fascicle of Deltoid, Supraspinatus and biceps
        long head. These fascicles use a dominant plane parallel to the
        humeral head X-axis. }
        AA:=-1*HTORSION;
        EULERX (MAT1, AA);
        MATEMULT (MAT1, HROT MAT, MAT2);

        {If long axis of humerus is pointing superiorly, then the factor stating
        whether internal or external rotating muscle is being corrected must
        be multiplied by -1.}
        FOR B:= 1 TO 3 DO
          BEGIN
            VECT6 [B] := MAT2 [3, B];
            VECT5 [B] :=-1*VECT3 [B];
            IF ((ITERSET=1) OR (ITERSET=13) OR ((ITERSET=3) AND (A=3))) THEN VECT6 [B] :=-1*MAT2 [1, B];
          END;
          NORMALIZ (VECT5); NORMALIZ (VECT6);
          VECTCROS (VECT5, VECT6, VECT4); NORMALIZ (VECT4);

          {A check must be made to ensure that the muscle plane normal, VECT4, is
          pointing in the correct direction. It should always point in approx the
          direction that the vector (Yt cross Zh) would point.
          To perform this check, we take Zh from HROT MAT and cross it with the Yt
          vector. The resulting vector and VECT4 can be
          compared and if not in the same direction then VECT4 and VECT5 can be
          REDEFINED.}
          IF ((ITERSET=1) OR (ITERSET=13) OR ((ITERSET=3) AND (A=3))) THEN
            ELSE
              BEGIN
                FOR B:= 1 TO 3 DO VECT7 [B] :=HROT MAT [3, B];
                VECT8 [1] := 0; VECT8 [2] :=1; VECT8 [3] :=0;

```



```

    VECTCROS (VECT8,VECT7,VECT9);  NORMALIZ (VECT9);
    AA:=VECTDOT (VECT9,VECT4);
    IF (AA<0) THEN FOR B:= 1 TO 3 DO  VECT4 [B] :=-1*VECT4 [B];
    END;

    VECTCROS (VECT6,VECT4,VECT5);  NORMALIZ (VECT5);

{A Coord Sys that describes the dominant muscle plane wrt the trunk coord
sys is now:}
    FOR B:= 1 TO 3 DO
        BEGIN
            MAT3 [1,B] :=VECT4 [B];
            MAT3 [2,B] :=VECT5 [B];
            MAT3 [3,B] :=VECT6 [B];
        END;

{ A problem occurs if the humeral X-axis rises above the dominant muscle
plane.  For example, Anterior Deltoid acts as an internal rotator until
abduction reaches about 120 degrees then it starts to act as an external
rotator.  To correct the problem, STATUS2 is set to -1 when the D.M.plane
rises above the GHCENT.  STATUS2 is then used to change the rotation
convention of the muscle's H.shaft wrapping calculation.}

{Muscle origin, insertion, and humeral head centre can now be
given wrt this coord sys origin at the muscle insertion}
    FOR B:= 1 TO 3 DO
        BEGIN
            VECT1 [B] :=VECT1 [B] -VECT2 [B];
            VECT3 [B] :=GHCENT [B] -VECT2 [B];
            VECT4 [B] :=HSCENT [B] -VECT2 [B];
            VECT2 [B] :=VECT2 [B] -VECT2 [B];
        END;
        VECTMULT (MAT3,VECT1,VECT10);  FOR B:=1 TO 3 DO VECT1 [B] :=VECT10 [B];
        VECTMULT (MAT3,VECT2,VECT10);  FOR B:=1 TO 3 DO VECT2 [B] :=VECT10 [B];
        VECTMULT (MAT3,VECT3,VECT10);  FOR B:=1 TO 3 DO VECT3 [B] :=VECT10 [B];
        VECTMULT (MAT3,VECT4,VECT10);  FOR B:=1 TO 3 DO VECT4 [B] :=VECT10 [B];

    IF (VECT3 [1] >0) THEN
        BEGIN
            IF ((ITERSET=3) AND ((A=3) OR (A=4) OR (A=5))) THEN
                BEGIN
                    STATUS2:=1;
                END ELSE

                BEGIN
                    STATUS2:=-1;
                END;
            END;

{*****}
{Latisimus Dorsi and Teres Major are two muscles that require special treatment.
Once abduction becomes large, their paths no longer are well approximated with
the Dominant Muscle plane technique used for the other muscles.  Instead, if the
D.M. Plane passes above the H. Head centre the plane is "hinged" at the Humeral
head centre.  The new plane containing the H.H centre and muscle origin with
rotation axis parallel to the Z humeral head axis can then be used to determine
a new muscle insertion position.}
            IF ((VECT3 [1] >0) AND ((ITERSET=5) OR (ITERSET=14))) THEN
                BEGIN
                    FOR B:= 1 TO 3 DO
                        BEGIN
                            VECT1 [B] :=MDT [ITERSET,A,1,B];
                            VECT2 [B] :=0.0;
                            VECT5 [B] :=GHCENT [B] -VECT1 [B];
                        END;
                    NORMALIZ (VECT5);
                    VECTCROS (VECT5,VECT6,VECT4);  NORMALIZ (VECT4);

{As above, a check must be made to ensure that the Xp axis is pointing in the
same direction as the Xh axis after arm flexion but before abduction and rotation}
                    FOR B:= 1 TO 3 DO  VECT7 [B] :=HROTMAT [3,B];
                    VECT8 [1] := 0;  VECT8 [2] :=1;  VECT8 [3] :=0;
                    VECTCROS (VECT8,VECT7,VECT9);  NORMALIZ (VECT9);
                    AA:=VECTDOT (VECT9,VECT4);
                    IF (AA<0) THEN FOR B:= 1 TO 3 DO  VECT4 [B] :=-1*VECT4 [B];

                    VECTCROS (VECT6,VECT4,VECT5);  NORMALIZ (VECT5);

{A Coord Sys that describes the NEW dominant muscle plane wrt the trunk coord
sys is now:}
                    FOR B:= 1 TO 3 DO
                        BEGIN
                            MAT3 [1,B] :=VECT4 [B];
                            MAT3 [2,B] :=VECT5 [B];
                            MAT3 [3,B] :=VECT6 [B];
                        END;

```

```

{Muscle origin, wrt the humeral head centre and new D.M. plane can now be given.}
FOR B:= 1 TO 3 DO VECT1[B]:=VECT1[B]-GHCENT[B];
VECTMULT(MAT3,VECT1,VECT10); FOR B:=1 TO 3 DO VECT1[B]:=VECT10[B];

{Some parameters that are required by PROCED1 are:}
INTEXT:=-1;
RADIU:=(HHDIA+0.01)/2;
STATUS:=3;
PROCED1(A,ITERSET,STATUS,INTEXT,VECT1,VECT2,VECT3,RADIU);
END;
{Now the new insertion position is known wrt the H.head and the D.M.plane as
described by MAT3. STATUS=3 so no further new insertion positions will be
calculated. }

{*****}

{If H.H. sphere intersects the dominant muscle plane the radius of
this circle can be calculated. The muscle may or may not wrap
around this circle and PROCED1 will determine this. If the H.head
circle doesn't intersect the D.muscle plane then no wrapping
around the H.head can occur.}
AA:=ABS(VECT3[1]);
RADIU:=(HHDIA)/2;
IF((ITERSET=3)OR(ITERSET=5)OR(ITERSET=7)OR(ITERSET=14))THEN
RADIU:=(HHDIA+0.01)/2;
IF((AA<=RADIU)AND(STATUS=0))THEN
BEGIN
AA:=AA/RADIU;
BB:=ASIN(AA);
RADIU:=RADIU*COS(BB);

{To allow the internal procedure PROCED1 to be used, muscle O/I and intersection
circle centre coords must be given wrt the circle centre and plane
coord sys.}
FOR B:= 2 TO 3 DO
BEGIN
VECT1[B]:=VECT1[B]-VECT3[B];
VECT2[B]:=VECT2[B]-VECT3[B];
END;

{Several parameters must now be set so that PROCED1 can be used to correct for
any wrapping that is occurring.}

IF(ITERSET= 1) THEN INTEXT:= 1;
IF(ITERSET= 4) THEN INTEXT:= 1;
IF(ITERSET= 5) THEN INTEXT:=-1;
IF(ITERSET= 7) THEN INTEXT:=-1;
IF(ITERSET=12) THEN INTEXT:=-1;
IF(ITERSET=13) THEN INTEXT:= 1;
IF(ITERSET=14) THEN INTEXT:=-1;
IF(ITERSET=15) THEN INTEXT:= 1;
IF(ITERSET= 3) THEN
BEGIN
IF(A=1)THEN INTEXT:=-1;
IF(A=2)THEN INTEXT:=-1;
IF(A=3)THEN INTEXT:= 1;
IF(A=4)THEN INTEXT:= 1;
IF(A=5)THEN INTEXT:= 1;
END;
PROCED1(A,ITERSET,STATUS,INTEXT,VECT1,VECT2,VECT3,RADIU);
END;

{If a new insertion position has been chosen, it can now be converted back
to being wrt the trunk coord sys.}
IF(STATUS=3)THEN
BEGIN
WRITELN('MUSCLE',ITERSET:3,A:3,' FROM (wrt H HEAD):',VECT2[1]:5:3,' ',VECT2[2]:5:3,'
',VECT2[3]:5:3);}
WRITELN(' TO :',VECT3[1]:5:3,' ',VECT3[2]:5:3,'
',VECT3[3]:5:3);}
FOR B:= 1 TO 3 DO VECT3[B]:=VECT3[B]-VECT1[B];
MATEINV(MAT3,MAT4);
VECTMULT(MAT4,VECT3,VECT4);
FOR B:= 1 TO 3 DO
BEGIN
VECT1[B]:=MDT[ITERSET,A,1,B];
IF(ITERSET>1)THEN MDT[ITERSET,A,2,B]:=VECT1[B]+VECT4[B];
IF(ITERSET=1)THEN MDT[ITERSET,3,2,B]:=VECT1[B]+VECT4[B];
END;
END;
{*****}
{If humeral head wrapping was indicated, ie STATUS=3 then this next section is
not required. If humeral head wrapping was not required then humeral shaft
wrapping must be checked for. Only those muscles that may be wrapped around

```

```

the shaft are considered.)
{*****}
{Redefine VECT1 and VECT2}
  IF ((STATUS=0) AND ((ITERSET=3) OR (ITERSET=5) OR (ITERSET=7) OR
    (ITERSET=14) OR (ITERSET=15))) THEN
    BEGIN
      FOR B:= 1 TO 3 DO
        BEGIN
          VECT1[B] :=MDT[ITERSET,A,1,B];           {origin}
          VECT2[B] :=MDT[ITERSET,A,2,B];           {insertion}
          IF (ITERSET=1) THEN VECT2[B] :=MDT[1,3,2,B];
        END;
    }
{Convert O/I to humeral HEAD coord system origin at the H. shaft centre.}
  FOR B:= 1 TO 3 DO
    BEGIN
      VECT3[B] :=VECT1[B] -HSCENT[B];
      VECT4[B] :=VECT2[B] -HSCENT[B];
    END;
    VECTMULT(MAT2,VECT3,VECT1);
    VECTMULT(MAT2,VECT4,VECT2);
}
{Wrapping can now be checked for and corrected if necessary. Some parameters
required for the internal procedure PROCED1 are:}
  RADIU:=HSDIA/2;

  IF(ITERSET= 1) THEN INTEXT:= 1;
  IF(ITERSET= 4) THEN INTEXT:= 1;
  IF(ITERSET= 5) THEN INTEXT:=-1;
  IF(ITERSET= 7) THEN INTEXT:=-1;
  IF(ITERSET=12) THEN INTEXT:=-1;
  IF(ITERSET=13) THEN INTEXT:= 1;
  IF(ITERSET=14) THEN INTEXT:=-1;
  IF(ITERSET=15) THEN INTEXT:= 1;
  IF(ITERSET= 3) THEN
    BEGIN
      IF(A=1) THEN INTEXT:=-1;
      IF(A=2) THEN INTEXT:=-1;
      IF(A=3) THEN INTEXT:= 1;
      IF(A=4) THEN INTEXT:= 1;
      IF(A=5) THEN INTEXT:= 1;
    END;
    INTEXT:=INTEXT*STATUS2;
}
  IF (STATUS2=-1) THEN WRITELN('STATUS2 = -1'); }
  PROCED1(A,ITERSET,STATUS,INTEXT,VECT1,VECT2,VECT3,RADIU);

{Teris major and Latisimus dorsi are both strong internal rotators. When
humeral external rotation increases, there is a possibility that the origin
and insertion of these muscles may become "visible" to each other. When this
happens, no muscle wrapping corrections will be conducted although the muscle
is actually wrapping extensively. To correct for this situation, both
muscles are considered wrapped if the humerus is externally rotated. If they
are truly not wrapped, the error resulting from this correction will be small.
On the other hand, for the most part it is an improvement.}
  {
    IF ((HPOS[3]>0) AND ((ITERSET=5) OR (ITERSET=14))) THEN
      BEGIN
        STATUS:=3;
        PROCED1(A,ITERSET,STATUS,INTEXT,VECT1,VECT2,VECT3,RADIU);
      END;
}

{If a new insertion position has been chosen, the corresponding X-axis
coordinate must also be calculated.}

  IF ((VECT2[2] <> VECT3[2]) OR (VECT2[3] <> VECT3[3])) THEN
    BEGIN
      {origin to new insertion position in Yz plane is}
      AA:=SQRT(SQR(VECT1[2]-VECT3[2])+SQR(VECT1[3]-VECT3[3]));

      {Angle of insertion to the Y axis in the YZ plane is:}
      IF (VECT2[2]>0) THEN BB:=ARCTAN(VECT2[3]/VECT2[2]);
      IF ((VECT2[2]=0) AND (VECT2[3]>0)) THEN BB:=Pi/ 2;
      IF ((VECT2[2]=0) AND (VECT2[3]<0)) THEN BB:=-Pi/2;
      IF (VECT2[2]<0) THEN BB:=Pi+ ARCTAN(VECT2[3]/VECT2[2]);

      {To find the actual wrapping angle an iterative search is used}
      FOR B:= 1 TO 3 DO
        BEGIN
          VECT5[B] :=VECT2[B];
          VECT6[B] :=VECT3[B];
        END;
        ERROLD:=SQRT(SQR(VECT5[2]-VECT6[2])+SQR(VECT5[3]-VECT6[3]));
        STEP:=0;           {INTEXT gives proper direction to step}
        STATUS:=0;
    }

```

```

REPEAT
STEP:=STEP+((-2*Pi/180)*INTEXT);
EULERX(MAT3,STEP);
VECTMULT(MAT3,VECT5,VECT7);
ERRNEW:=SQRT(SQR(VECT7[2]-VECT6[2])+SQR(VECT7[3]-VECT6[3]));

IF(ERRNEW<ERROLD)THEN
BEGIN
ERROLD:=ERRNEW;
STATUS:=0
END;
IF(ERRNEW>ERROLD)THEN
BEGIN
IF(ERRNEW>=0.005)THEN STATUS:=0;
IF(ERRNEW< 0.005)THEN
BEGIN
STATUS:=1;
STEP:=STEP-((2*Pi/180)*INTEXT);
END;
END;
UNTIL(STATUS=1);

{
WRITELN('WRAP ANGLE IS: ',STEP:5:3);}

{Wrap length is:}
AA:=ABS(STEP*HSDIA); { ie (theta/Pi)* Pi*Diameter }
{Total muscle length in YZ plane is}
BB:=AA+ SQRT(SQR(VECT1[2]-VECT3[2])+SQR(VECT1[3]-VECT3[3]));
{Total X axis displacement between origin and insertion is}
CC:=VECT1[1]-VECT2[1];
{X coordinate of new insertion position will be}
VECT3[1]:=VECT2[1]+ (CC*(AA/BB));

{Check this new X value to be sure it lays on the humeral shaft. If it
doesn't then restrict it to.}
AA:=(0.02+HHDIA)/4;
IF(VECT3[1]<AA) THEN VECT3[1]:=AA;

{New insertion position can now be given wrt the trunk coord sys and stored
in matrix MDT in place of the original insertion position.}
{WRITELN('MUSCLE',ITERSET:3,A:3,' FROM (wrt H shaft):',VECT2[1]:5:3,'
',VECT2[2]:5:3,' ',VECT2[3]:5:3);}
{WRITELN('
',VECT3[1]:5:3,' ' ',VECT3[2]:5:3,'
',VECT3[3]:5:3);}
MATEINV(MAT2,MAT3);
VECTMULT(MAT3,VECT3,VECT2);
FOR B:= 1 TO 3 DO MDT[ITERSET,A,2,B]:=VECT2[B]+HSCENT[B];
END;
END;
IF(ITERSET=1)THEN A:=1;
END;
IF(ITERSET=15)THEN ITERSET:=25;
IF(ITERSET=14)THEN ITERSET:=15;
IF(ITERSET=13)THEN ITERSET:=14;
IF(ITERSET=12)THEN ITERSET:=13;
IF(ITERSET= 7)THEN ITERSET:=12;
IF(ITERSET= 5)THEN ITERSET:= 7;
IF(ITERSET= 4)THEN ITERSET:= 5;
IF(ITERSET= 3)THEN ITERSET:= 4;
IF(ITERSET= 1)THEN ITERSET:= 3;

UNTIL(ITERSET=25);
END;
{*****}
END.
{*****}

```